Targeting p53 and its domains for cancer gene therapy

Dissertation
zur
Erlangung des Doktorgrades
der Naturwissenschaften
(Dr. rer. nat.)

dem

Fachbereich
der Philipps-Universität Marburg
vorgelegt von
Karina Julia Matissek
aus Krakau (Polen)

Marburg/Lahn 2014

Vom Fachbereich Pharmazie der Philipps-Universität Marburg als Dissertation am 04.04.2014 angenommen.

Erstgutachter: Prof. Dr. Carol S. Lim
Zweitgutachter: Prof. Dr. Thomas Kissel
Drittgutachter: Prof. Dr. Roland Hartmann

Tag der mündlichen Prüfung: 07.04.2014

Zusammenfassung

Der Tumorsuppressor p53 ist eines der am häufigsten mutierten Proteine in humanen Krebsarten und wird daher umfassend für seinen Nutzen in der Krebstherapie erforscht. Dies führte in China zur Markteinführung von Wildtyp-p53 zur Therapie von Kopf-Hals-Karzinomen.

p53 fungiert in der Zelle hauptsächlich als Transkriptionsfaktor und stimuliert eine Vielzahl von Genen, die im intrinsischen und extrinsischen Apoptosemechanismus involviert sind. In Krebszellen treten Mutationen normalerweise in der DNA-Bindungsdomäne von p53 auf, wohingegen die Tetramerizationsdomäne (TD) des Tumorsuppressors intakt bleibt. Dies führt intrazellular zur Bildung von Heterotetrameren von Wildtyp-p53 und seiner mutierten Form, was die Transkriptionsaktivität erheblich beeinträchtigt und einen dominant negativen Effekt ergibt.

Während transkriptionell aktives p53 als Gentherapeutikum genutzt wird, ist das therapeutische Potential für den Einsatz von mitochondrialem p53 noch nicht vollständig ermittelt. Wenn p53 zum Mitochondrium *getargeted* wird, interagiert es mit pro- und anti-apoptotischen Proteinen, die sich in der mitochondrialen Außenmembran befinden. Für diese Interaktion reicht die monomere Form von p53 aus, was bedeutet, dass es nicht durch mutiertes p53 inaktiviert werden kann.

In dieser Arbeit wurde die Funktion von mitochondrialem p53 charakterisiert, indem es zu verschiedenen mitochondrialen Kompartimenten *getargeted* wurde: der mitochondrialen Außenmembran, der Innenmembran und der Matrix. Es konnte nachgewiesen werden, dass mitochondriale *Targeting* Sequenzen (MTS) in der mitochondrialen Außenmembran optimal für eine p53-spezifische Aktivierung geeignet sind. Auch konnte gezeigt werden, dass als minimalste Domäne von p53 die DNA-Bindungsdomäne (DBD) ausreicht, um Apoptose zu induzieren. Weitere Untersuchungen haben ergeben, dass das Vereinigen von p53 oder nur seiner DBD mit der MTS von Bcl-XL, eine Bcl-XL spezifische Apoptose hervorruft, während eine Vereinigung der Segmente mit Bak auf p53/Bak spezifische Apoptose zurückzuführen ist. Dies hebt hervor, dass mitochondriales *Targeting* von p53 stark von der benutzten MTS abhängig ist. Außerdem haben *in vitro*-Studien gezeigt, dass die Bindung von p53 oder DBD an die MTS von Bcl-XL eine dominant negative

Inhibition überwinden kann, aber auβerstande ist dominant negative MDA-MB-468 Tumore in einem orthotopischen Maus-Tumor-Model für das gewählte Dosisschema zu reduzieren.

Die Thematik dieser Dissertation war die Entwicklung Apoptose-induzierender Proteine basierend auf p53 und seinen Bindungsdomänen, um eine modifizierte Version von p53 zu generieren. Der Schwerpunkt lag sowohl auf der Optimierung eines mitochondrial *getargeten* p53 für mögliche Krebstherapien als auch in der Neugestaltung der TD von p53, um den dominant negativen Effekt der Transkriptionsaktivität zu überwinden. Dafür wurde die Oligomerizationsdomäne von p53 mit der Coiled-Coil (CC) Domäne von BCR ersetzt, damit der dominant negative Effekt von mutiertem p53 ausgeschaltet wird. Experimente zeigen, dass das chimäre p53 (p53-CC) in den Nukleus transloziert, Gene transaktiviert und Apoptose in ähnlicher Form wie Wildtyp-p53 auslöst. *In vitro*- und *in vivo*-Studien haben gezeigt, dass im Gegensatz zu Wildtyp-p53, das neu generierte p53-CC nicht mit endogen mutiertem p53 interagiert und seine apoptotische Aktivität in Krebszellen, die dominant negatives mutiertes p53 enthalten, beibehält.

Zusammenfassend liegt der Forschungsschwerpunkt dieser Dissertation in der Entwicklung neuartiger p53-Gentherapeutika, die das Potential haben derzeitige Einschränkungen einer Wildtyp-p53 Therapie zu überwinden.

Abstract

The tumor suppressor p53 is one of the most frequently mutated proteins in human cancer and has been extensively targeted for cancer therapy. This resulted in wild type p53 gene therapeutic approval for the treatment of head and neck cancer in China. p53 mainly functions as a transcription factor and stimulates a variety of genes involved in the intrinsic and extrinsic apoptotic pathway by binding to p53 responsive elements as a tetramer. In cancer cells, mutations in p53 typically occur in its DNA binding domain (DBD), while its tetramerization domain remains intact. Therefore, mutant p53 can heterotetramerize with *wt* p53 and abolish its transcriptional activity (dominant negative effect).

While transcriptionally active *wt* p53 is used for gene therapy, mitochondrial p53 has not been fully exploited yet. Targeting p53 to the mitochondria causes a direct rapid apoptotic response by directly interacting with pro-and anti- apoptotic proteins at the mitochondrial outer membrane. Because the monomeric from is sufficient to interact with pro-and anti-apoptotic proteins, mitochondrial p53 is not affected by the dominant negative inactivation. To ensure mitochondrial targeting of p53, we targeted p53 to different mitochondrial compartments; mitochondrial outer membrane, inner membrane and matrix. We have demonstrated that MTSs from the mitochondrial outer membrane are optimal for p53-specific activation. In addition, we discovered the minimal domain of p53, its DNA binding domain (DBD), which is needed for apoptosis induction. Further studies have shown that fusing p53 or DBD to MTS from Bcl-XL causes p53/Bcl-XL specific apoptosis while fusing them to Bak results in p53/Bak specific apoptosis, emphasizing that mitochondrial targeting of p53 is highly dependent on the MTS used. Further, we have shown that DBD fused to the MTS from Bcl-XL can overcome dominant negative inhibition *in vitro*, but it was unable to shrink dominant negative MDA-MB-468 tumors in an orthotopic mouse model at one dosing regimen attempted.

The main theme of this thesis was to design apoptotic proteins based on p53 domains to create modified versions of p53. We focused mainly on optimizing mitochondrial targeting of p53 for cancer therapy but also redesigned the TD of p53 to overcome the dominant negative effect. We substituted the oligomerization domain of p53 with the coiled-coil (CC) domain from BCR to bypass dominant

negative inhibition of mutant p53. Our chimeric p53 (p53-CC) can translocate into the nucleus, transactivate genes and cause apoptosis in a similar manner as *wt* p53. Unlike *wt* p53, p53-CC does not interact with endogenous mutant p53 and retains apoptotic activity in cancer cells harboring dominant negative mutant p53 *in vitro* and *in vivo*. In summary this dissertation focuses on new p53 gene therapeutics, with the potential to overcome current limitations with *wt* p53 therapy.

Publications

Peer-Reviewed Publications

First Author Publications

- **Matissek K.J.,** Okal, A., Mossalam M., Lim C.S. Delivery of a monomeric p53 subdomain with mitochondrial targeting signals from pro-apoptotic Bak or Bax, Pharm Res., minor revisions.

- **Matissek K.J.,** Mossalam M., Okal A., Lim C.S. The DNA binding domain of p53 is sufficient to trigger a potent apoptotic response at the mitochondria. Mol Pharm. 2013 Oct 7;10(10):3592-602.

- **Matissek K.J.*,** Mossalam M.*** (*co-first authors)** Okal A., Constance J.E., Lim C.S. Direct induction of apoptosis using an optimal mitochondrially targeted p53. Mol Pharm. 2012 May 7;9(5):1449-58.

- **Matissek K.J.,** Bender R.R., Davis J.R., Lim C.S. Choosing Targets for Gene Therapy in the book Targets for Gene Therapy. Intech Open Access Publisher, 2011 July, ISBN 978-953-307-540-2.

Co-Author Publications

- Okal A., Mossalam M., **Matissek K.J.,** Dixon A.S., Moos P.J., Lim C.S. A chimeric p53 evades mutant p53 transdominant inhibition in cancer cells. Mol Pharm. 2013 Oct 7;10(10):3922-33.

- Constance J.E., Woessner D.W., **Matissek K.J.,** Mossalam M., Lim C.S. Enhanced and selective killing of chronic myelogenous leukemia cells with an engineered BCR-ABL binding protein and imatinib. Mol Pharm. 2012 Nov 5;9(11):3318-29.

- Okal A., **Matissek, K.J.,** Matissek S.J., Price R., Salama M., Janát-Amsbury M.M., Lim C.S. Re-engineered p53 activates apoptosis in vivo and causes primary tumor regression in a dominant negative breast cancer xenograft model. submitted to Gene Ther. 2014 Feb 5;

- Okal A., Matissek S.J., **Matissek K.J.,** Cornillie S., Cheatham T. E. III, Lim C.S. Towards Super p53: A Re-engineered Tumor Suppressor with Enhanced Homo-oligomerization and Increased Apoptotic Activity. In preparation, 2014.

Table of Contents

1. Introduction

1.1 The p53 protein

The tumor suppressor p53 is one of the most widely studied proteins. Over the last 30 years it has been shown that p53 is involved in a wide network of signaling pathways that involves tumorgenesis, cellular senescence, metabolism and DNA damage preventing tumorgenesis (1). Since its discovery, p53 has been of great interest because it is mutated in almost 50% of all human cancers (2). Mutations in p53 are crucial for cancer development and therefore make it an interesting target for cancer therapy (3).

1.2 Structure of *wt* p53

The 393 amino acid p53 protein is encoded by the *TP53* gene (4). It contains a N-terminus, a DNA binding domain (DBD) and a C-terminal region as shown in figure 1. The N-terminus consists of the transactivation domain (TA) and the proline rich domain (PRD) (4). The TA can be further divided into MDM2 binding domain (MBD) (5) and a nuclear export signal (E) (6). The C-terminus contains three nuclear localization signals (NLS)s (7), one nuclear export signal (E) (8) and the tetramerization domain (TD) as depicted in figure 1 (9).

The TA is essential for either the transcriptional activity of p53 (10, 11) or for its degradation (12) depending on post-transcriptional modifications occurring in the TA. When no transcriptional modifications occur, p53 is ubiquitinated via MDM2 and MDMX and degraded via the ubiquitin-dependent proteasomal pathway (12). On the other hand, when Thr 18 is phosphorylated, the affinity of TAD for transcriptional cofactors such as p300/CBP and its various subdomains is highly increased and p53 can exhibit its function as a transcription factor (13).

The PRD has a predominantly structural role (14). It allows for the TA to interact with transcription cofactors and components of the basal transcription machinery. The DBD, as the name implies, binds directly to DNA sequences and triggers gene transcription (15).

The C-terminus undergoes various posttranslational modifications and can adopt different secondary structures. Modifications on this region play complex roles so that it can interact with numerous partner proteins (16). The three NLSs within the C-terminus are important for localization to the nucleus where p53 exhibits its function as a transcription factor (7). Tetramer formation is essential for the majority of its transcriptional activity (17). The p53 tetramer is formed via a dimeric intermediate (18). Primary dimers are stabilized by an intermolecular β-sheet and helix-packing interactions. The hydrophobic helix interfaces of two such dimers form a tightly packed tetramer, which is highly thermodynamically stable (19).

Figure 1: Structure of *wt* p53. The amino terminus contains the transactivation domain (TA), a nuclear export signal (E) and the MDM2 binding domain (M). The DNA binding domain (DBD) is between amino acids 94 and 294. The C-terminus consists of three nuclear localization signals (NLS) and the tetramerization domain (TD).

1.3 Degradation of p53

p53 is known as a transcription factor which inhibits tumor growth. It is capable of transactivating a variety of genes responsible for apoptosis, cell cycle arrest and DNA repair (20). Since p53 induces cell-cycle arrest and apoptosis, it has an

inhibitory effect on cellular growth. Therefore, p53 needs to be regulated so normal development can take place. The major regulator of p53 is the E3 ubiquitin ligase MDM2 (21). Even though other p53 E3 ligases have been discovered over the last couple of years, MDM2 still appears to be the physiological and primary E3 ligase regulating p53 (12). MDM2 and p53 form an autoregulatory feedback loop in which p53 transactivates MDM2 and influences its own degradation (22). p53 is degraded via different degradation pathways which all eventually result in polyubiquitination and eliminations by the 26S proteasome (Fig. 2) (23). In the nucleus, p53 binds directly to the MDM2 binding domain, monoubiquinates it and initiates nuclear export (24). Cytoplasmic mono-ubiquitinated p53 then gets polyubiquitinated by E4 factors (USE4B) or E4-like molecules (Cul4-DDB complex), and MDM2 is then sent to the proteasome for degradation (Fig. 2) (12). Additionally, other E-ligases (Pirh2) can facilitate polyubiquitination and proteasomal degradation of p53 with no involvement of MDM2 (25). Furthermore, it has been reported that MDM2 can form a heterodimer with another protein MDMX facilitating polyubiquitination and proteasomal degradation (Fig. 2) (26). MDMX and MDM2 show low amino acid sequence overlap but a nearly identical p53 binding domain located at their N-terminus and a C-terminal RING domain (12). Heterodimer formation occurs through this RING domain. MDMX alone does not have significant E3 ligase activity, but has been shown to modulate p53 via modulation of its transcriptional activity (12, 27).

The regulatory effect of MDM2 on p53 can also result in negative outcomes. The MDM2 gene is amplified or overexpressed in many human cancers, consequently inactivating p53. These cancers have been associated with poor prognosis (28). Therefore, the interaction of p53 and MDM2 provides an interesting target for cancer therapy.

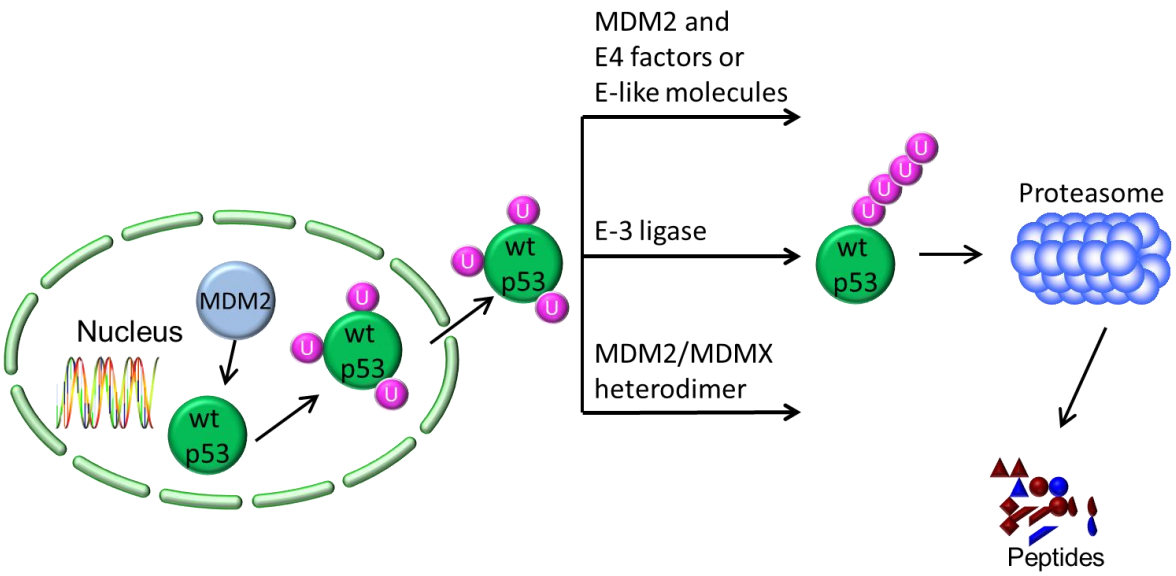

Figure 2: Proteasomeal degradation pathway of *wt* p53: MDM2 monoubiquitinates p53 in the nucleus; cytoplasmic monoubiquitinated p53 can either get polyubiquitinated via MDM2 and E4 factors, E-like molecules, via other E-ligases, or via MDM2/MDMX heterodimers. Polyubiquitinated p53 is targeted to the proteasome and degraded into peptides.

1.4 Regulation of gene transcription: cell cycle arrest or apoptosis?

p53 positively and negatively regulates the expression of responsive genes. Depending on the severity of damage to the cell, p53 decides the fate of the cell. p53 response elements (REs) are located within a few thousand nucleotides upstream or downstream from the transcription start site (29). It has been shown that binding affinity of p53 for its specific REs differs dramatically. Growth arrest-related genes have high affinity sites for p53 whereas proapoptotic genes are mostly associated with low affinity sites (30). Additionally, some REs exist in open occupied states while others do not (31). Since recognition of elements in *Mdm2* and *p21* promoters depend on non-B-DNA conformation, conformation of the DNA may also be important (32). Taken together these findings suggest that not all targeted genes are

equally responsive to p53 and that levels of p53 protein may determine which genes to turn on or off.

Mild damage to a cell is often reparable. Basal or low levels of p53 usually turn on cell cycle genes. Additionally, p53 undergoes pro-arrest modifications by ubiquitination of the Lys 320. Pro-apoptotic cofactors such as Brn3a reduce the ability of p53 to transactivate pro-apoptotic *Bax* whereas stimulating transcription of *p21*, results in cell cycle arrest (33). Transient cell cycle arrest allows for sufficient time to repair DNA damage and re-entry into the normal cell cycle.

When severe damage occurs, p53 levels rise dramatically and promote transactivation of pro-apoptotic genes due to pro-apoptotic posttranslational modification of the protein, such as acetylation of K120 (34), K320 (35) and phosphorylation of S46 in the p53 protein (36). DNA damage activates ASSP1 and 2 which interact with DBD of p53 and activate pro-apoptotic *Bax* and *PIG3* genes but do not promote transcription of pro-arrest genes such as *p21* or regulatory genes such as *Mdm2* (37). Another example is the crosstalk between p53 and the NF-KB subunit p52 leading to repression of the cell cycle activator *p21* and activation of proapoptotic *DR5* and *PUMA* resulting again in apoptosis (38).

1.5 p53 activates the intrinsic and extrinsic apoptotic pathway

Apoptosis proceeds through intrinsic and extrinsic pathways. p53 is capable of activating both apoptotic pathways. p53 induces genes encoding the transmembrane proteins FAS, DR5 and PERP (also called death receptors) which are essential for activating the extrinsic apoptotic pathway (Fig. 3) (39). Death receptors recruit adapter molecules such as FADD, which in turn, recruit procaspase-8 monomers. Dimerization and interchain cleavage of procaspase-8 facilitates the activation of caspase-8 (40). Caspase 8 then leads to cleavage of the inactive procaspase-3 dimer and the inactive procaspase-7 dimer via intramolecular rearrangements

resulting in active caspase-3 and caspase-7 dimers leading to apoptosis (Fig. 3) (41). However, cross talk between intrinsic and extrinsic apoptotic pathway occurs via BID which is truncated to tBid via caspase-8 (42).

The intrinsic apoptotic pathway occurs as a result of mitochondrial outer membrane permeabilization (MOMP) which releases various proteins from the mitochondrial intermembrane space such as cytochrome c (43). p53 targets a key subset of Bcl-2 family genes *BAX*, *NOXA* and *PUMA* which once transcribed and translated into proteins promote cytochrome c release and facilitate caspase-9 activation (Fig. 3) (44). Binding of cytochrome c and apoptotic protease-activating factor 1 (APAF1) assembles into a heptameric, wheel-like structure known as the apoptosome. The apoptosome activates the initiator caspase-9, which then initiates the executioner apoptotic caspases, caspase-3 and caspase-7 (Fig. 3) (45). Additionally, mitochondrial release of second mitochondrial derived activator of caspase (SMAC) and OMI neutralize the caspase inhibitory function of X-linked inhibitor of apoptosis protein (XIAP). XIAP is known to bind and inactivate caspases (46). All of these processes contribute to DNA fragmentation and eventually apoptosis (47).

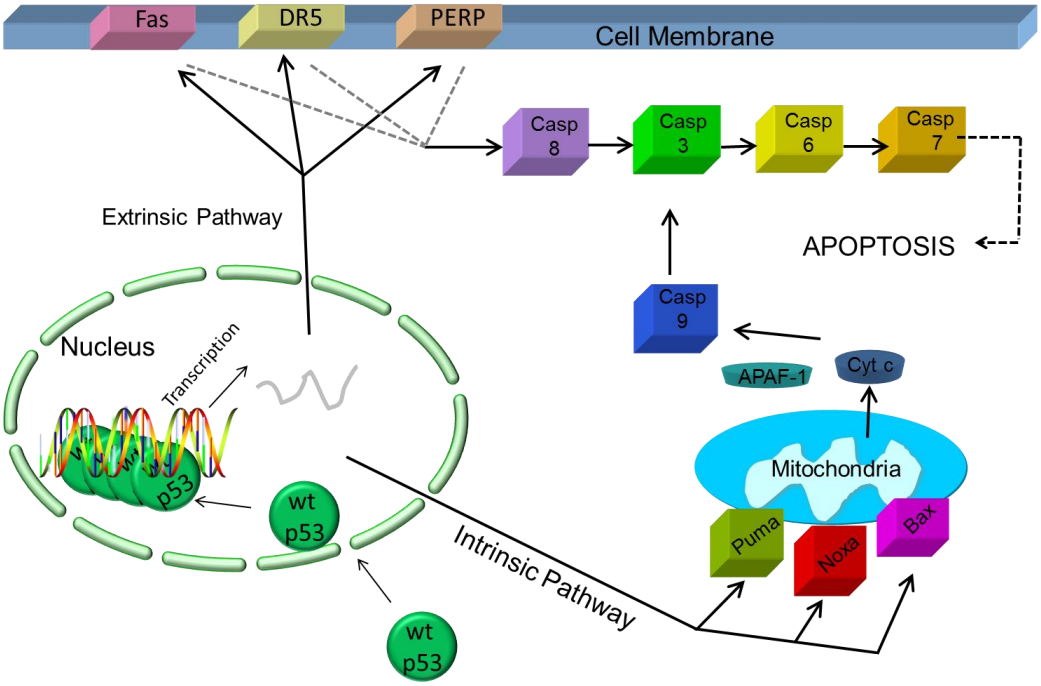

Figure 3: Transcriptional activity of *wt* p53: *wt* p53 translocates to the nucleus, forms a tetramer, binds to DNA and activates gene transactivation. Extrinsic pathway is facilitated via the death receptors Fas, Dr5 and PERP which trigger caspase-8 induction resulting in apoptosis. The intrinsic pathway is initiated via Puma, Noxa and Bax resulting in MOMP, cytochrome c release, caspase-9, and eventually triggers apoptosis.

1.6 Regulation of the intrinsic apoptotic pathway via the Bcl-2 protein family

In healthy cells, anti-apoptotic B cell lymphoma 2 (Bcl-2) family members form heterodimers with pro-apoptotic proteins resulting in their inactivation (48). However, when an apoptotic stimuli occurs such as DNA damage or ER stress, anti-apoptotic Bcl-2 proteins are released from the inhibitory complexes and homooligomerize resulting in MOMP (49).

The Bcl-2 family members are localized on the outer surface of the mitochondrial outer membrane. As listed in table 1, the Bcl-2 family of proteins are divided into three groups based on the Bcl-2 homology (BH) domain (50); anti-apoptotic Bcl-2 proteins such as Bcl-2, Bcl-w, Bcl-XL, A1 and Mcl-1 consists of four BH domains (BH1-4) and a transmembrane (TM) domain (51). The BH domain is responsible for their anti-apoptotic function while the TM domain is for the insertion into the mitochondrial outer membrane (51-53). Pro-apoptotic Bcl-2 proteins are divided into effectors and enhancers (50). The effectors are Bcl-2-associated X protein (Bax), Bcl-2 antagonist or killer (Bak) and Bcl-2-related ovarian killer protein (Bok) (54). They contain three BH domains (BH1-3) and the TM domain for membrane insertion (54, 55). Unlike other Bcl-2 proteins the pro-apoptotic enhancers BCL-2 antagonist of cell death (BAD), BH3-interacting domain death agonist (BID), BCL-2-interacting killer (BIK), BCL-2-interacting mediator of cell death (BIM), BCL-2-modifying factor (BMF), BCL-2 and adenovirus E1B 19 kDa protein-interacting protein 3(BNIP3),

hara-kiri (HRK), p53 upregulated modulator of apoptosis (PUMA) consist of only the BH3 domain and therefore do not insert themselves into the mitochondrial outer membrane (56).

Class	**Members**	**Structural domains**
Anti-apoptotic	Bcl-2, Bcl-w, Bcl-XL, A1, Mcl-1	BH1, BH2, BH3, BH4, TM
Pro-apoptotic: effectors	Bak, Bax, Bok	BH1, BH2, BH3, TM
Pro-apoptotic: enhancers	BAD, BID, BIK, BIM, BMF, BNIP3, HRK, Puma	BH3

Table 1: Classification of the different Bcl-2 protein family members with representative members and structural domains.

1.7 Transcriptional-independent activation of the intrinsic apoptotic pathway by p53

Aside from transactivating *Bax*, *NOXA* and *PUMA*, p53 can also directly activate the intrinsic apoptotic pathway by translocating to the mitochondria upon severe stress signal induction such as radiation (57). Unlike other mitochondrial proteins, p53 does not contain a mitochondrial targeting signal. It has been hypothesized that nuclear p53 gets mono-ubiquitinated and exported into the cytoplasm. Cytoplasmic monoubiquitinated p53 is imported into the mitochondria via the herpes virus-associated ubiquitin-specific protease (HAUSP) (58, 59). At the mitochondrial outer membrane p53 interacts directly with pro-and anti-apoptotic Bcl-2 family members (Fig. 4) (60-62). The DBD of p53 are essential for the electrostatic interaction with anti-apoptotic Bcl-XL and Bcl-2 and pro-apoptotic Bak (60, 61). The positively charged basic surface of the DBD interacts with the negatively charged BH4 domain and the loops between alpha 4/5 and 5/6 of Bcl-XL and Bcl-2 (61, 63, 64). The affinity of the positively charged DBD to bind pro-apoptotic Bak is 10 times less than

to Bcl-XL and Bcl-2 (61, 64, 65). The lower interaction is due to the differences in structure between Bcl-2, Bcl-XL and Bak. While Bcl-XL and Bcl-2 contain a very acidic protein surface and a BH4 domain, Bak does not have a very acidic protein surface nor a BH4 domain and therefore its binding affinity to the positively charged DBD of p53 is decreased. Bax on the other hand has been shown to be activated by p53, but no actual interaction has been detected yet (66). Since p53 has to directly bind to and sequester Bcl-XL and Bcl-2 to liberate Bak and Bax (60, 61), the affinity towards these proteins has to be higher than to Bak and Bax, while the pro-apoptotic Bcl-2 proteins Bak and Bax only need to be activated and can then form homo-oligomers. Additionally, the higher affinity towards Bcl-2 and Bcl-XL suggests a sequential mechanism. First p53 binds to Bcl-2 and Bcl-XL and then it binds to Bak and Bax (65). Therefore, p53 is considered a super BH3-only protein because it acts as an enabler and as an activator of pro- and anti-apoptotic mitochondrial proteins (67). All of these functions eventually result in MOMP and activation of the intrinsic apoptotic pathway (65).

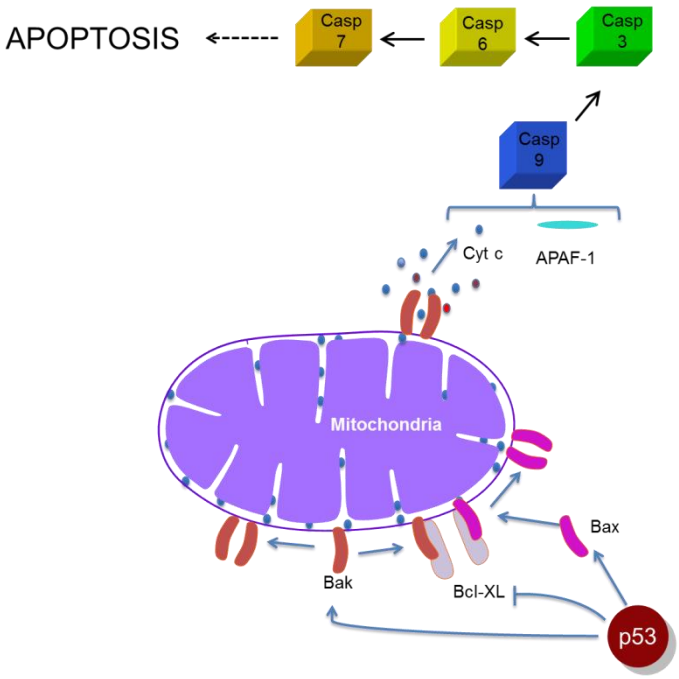

Figure 3: Mitochondrial p53 directly activates the intrinsic apoptotic pathway through a sequential mechanism: First mitochondrial p53 interacts with anti- (Bcl-XL) and then binds to pro- (Bak; Bax) Bcl-2 proteins. Bak or Bax form homo-oligomers causing MOMP and cytochrome c release, activation of caspase 9 and eventually apoptosis.

1.8 p53 and its function in metabolism and cell growth

Besides its well characterized functions of cell cycle arrest and apoptosis, p53 has a clear role in glycolysis, autophagy, cell survival and regulation of oxidative stress, invasion and motility, cellular senescence, angiogenesis, differentiation and bone remodeling (68). Unlike for transactivation of apoptotic genes where high concentrations of p53 are required, low levels of p53 have been shown to be essential for normal growth, development and metabolism (68).

p53 has multiple functions in cellular metabolism. It is a negative regulator of glycolysis and lowers gene expression of glucose transporters, inhibits NF-KB and represses the insulin receptor promoter (69). Additionally, *TP53*-induced glycolysis and apoptosis regulator (TIGAR) lowers the glycolysis rate and promotes the pentose phosphate pathway (70). On the other hand, p53 promotes the more efficient tricarboxylic acid (TCA) cycle by enhancing transcription of cytochrome c oxidase 2, subunit1 of complex IV and AIF (essential for complex I function) (71). Taken together the negative regulation of glycolysis and the promotion of the TCA cycle oppose the Warburg effect (aerobic glycolysis) which promotes cancer cells proliferation and is an additional proof for p53 tumor suppressor activity. Concerning oxidative stress, p53 has an ambivalent role. Under mild stress p53 plays an anti-oxidative role. It promotes transcription of GPX1, MnSOD, ALDH4 and TPP53INP1 all of which are antioxidant targets. Under severe stress, p53 promotes ROS which then triggers apoptosis through cytochrome c oxidation (69, 72).

1.9 Negative activity of p53

Besides the functions of p53 that prevent tumorgenesis (DNA-repair, cell cycle arrest, apoptosis and metabolism), the apoptotic function of p53 can also result in unfavorable outcome. p53-dependent apoptosis is the major contributor to radiation and chemotherapy induced sickness (68). Furthermore, the shortage of glucose and oxygen caused by ischemia results in p53 activation. This can cause stroke and myocardial infarct (73, 74). Finally, in neurodegenerative diseases, p53 causes cell death in neurons and therefore worsens Parkinson's (75), Alzheimer's (76) and Huntington's (77) disease. Small molecules such as pifithrin α have therefore been developed which block p53-dependent transcriptional activity while protecting healthy cells from genotoxic stress caused by most chemotherapeutics. Pifithrin α can also protect neuronal cell death (78).

1.10 Inactivation of p53 in cancer via mutations

When p53 was discovered in 1979, it was first thought to be an oncogene. The observation that many tumors produce high levels of p53 while normal cells harbor low or undetectable levels suggested that this hypothesis was true. Ten years after its discovery, it was finally determined that p53 is a tumor suppressor (1). The first assumption of p53 being an oncogene is not surprising since p53 is mutated in around 50% of all tumors, and mutated p53 has oncogenic potential that differs completely from wild type activity. The mutations occurring in p53 are unique among tumor suppressors. While most tumor suppressors are inactivated by deletion or truncating mutations, *TP*53 is inactivated in 74% of cases by a single monoallelic missense mutation resulting in formation of a stable full length protein (79).

Mutations in *TP*53 differ in their frequency depending on the type of cancer. In hematopoietic malignancies about 10% (80) and in breast cancer about 30% of p53 shows mutations (81). However, in ovarian (82), colorectal (83) and head and neck (84) cancers, p53 is mutated 50% to 70% of the time. The majority of *TP*53

mutations take place in the DNA-binding domain of p53 (85, 86). The tetramerization domain of p53 is usually not mutated; therefore mutated p53 can form heteroteramers with *wt* p53 and inactivate *wt* p53 function: this is referred to as the dominant negative effect (87-89). Additionally, p53 mutants can also inactivate p53 family members p63 and p73, which are usually not mutated in human cancer (90, 91).

In general, *TP*53 mutations can be classified as conformational and DNA contact mutations. Conformational mutations either cause local (R249S; G245S) or global (R175H; R282W) disruptions of the protein structure (79). DNA contact mutants obliterate p53 binding to specific DNA-sequences and therefore abolish its transcriptional activity (92). Additionally, these contact mutants cause dominant negative inhibition and are responsible for new oncogenic functions such as drug-resistance, survival and metastasis. The mechanism of mutant p53 function is multifaceted: binding to DNA, altering gene expression, binding to transcription factors to enhance or prevent their function, or interacting with proteins to alter their function directly (93).

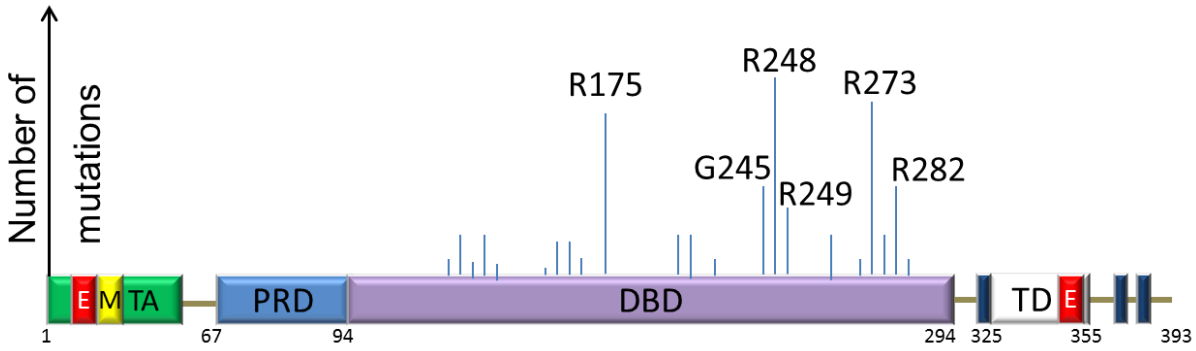

Figure 5: Frequency of *TP53* mutations with the most frequent mutations outlined in the DBD. Line length indicates the number of mutations (79).

1.11 p53 therapeutics

Targeting p53 for cancer therapy is either achieved by directly reintroducing *wt* p53 into cancer cells via gene therapy, activating p53 and its family members via small molecules and peptides, or using immunotherapy.

1.11.1 p53 gene therapy

The following paragraph is exerted from: Matissek KJ BR, Davis JR, Lim CS. Choosing Targets for Gene Therapy. Targets for Gene Therapy 2011 July.

"The first p53 based gene therapy in humans was conducted in 1996. This trial used a retroviral vector containing wild type p53 with an actin promoter for the treatment of non-small cell lung carcinoma. In this study three patients showed tumor regression and three other patients showed tumor growth stabilization (Roth et al. 1996). China was the first country which approved a p53 adenovirus for gene therapy, Gendicine™ SiBiono, in combination with radiotherapy for head and neck squamous cell cancer in 2004 (Shi & Zheng 2009). Gendicine™ is a recombinant serotype 5 adenovirus with the E1 region replaced by the p53 expressing cassette (with a Rous sarcoma virus promoter). The adenovirus particles infect tumor target cells carrying therapeutic p53 (Peng 2005). Clinical trials for Gendicine™ showed that in combination with radiation therapy it caused partial or complete tumor regression (Peng 2005; Xin 2006). There were also some clinical trials for Gendicine™ in advanced liver cancer, lung cancer and other advanced solid tumors (Peng 2005). It should be kept in mind that China's State Food and Drug Administration (SFDA) has different standards for the approval of a cancer drug compared to the U.S. FDA and the European Medicine Agency (EMA). Gendicine™ was approved in China on the basis of tumor shrinkage. The U.S. FDA and the EMA require novel cancer drugs to extend the lifetime of the treated patients (Guo & Xin 2006). Another p53 product is Gendicine™ from Shanghai SunwayBiotech, an oncolytic virus. Gendicine™ was approved for the treatment of head and neck cancer in China in 2006 (Yu & Fang

2007). It is a replicative adenovirus 2/adenovirus 5 hybrid with deletion in E1B55K and E3B (Raty et al. 2008). This oncolytic virus was expected to infect and lyse cancer cells only and not affect normal cells (Guo et al. 2008). Even though clinical studies showed that it was not specific for cancer cells, it did, however, kill tumor cells preferentially (Garber 2006). Phase I/II trials showed little dose-limiting toxicity (Lockley et al. 2006) and the combination of Gendicine^{TM} with chemotherapy showed greater tumor shrinkage in patients with head and neck cancer, compared to chemotherapy alone. It should be kept in mind that like Gendicine^{TM}, Oncorine^{TM} was also approved by the SFDA based on objective response rate, not on survival (Garber 2006). Nevertheless, all the available data concerning p53 and its proven function as tumor suppressor qualifies it as an adjuvant treatment with radiotherapy or chemotherapy." (20)

1.11.2 Activating *wt* p53

About 50% of all tumors retain wild-type p53 function that is inhibited by increased degradation or proteins that interact with p53. The most famous example is the cis-imidazoline compound Nutlin-3a. It interacts with the p53 binding pocket of MDM2 and consequently disrupts the p53-MDM2 interaction resulting in p53 activation and tumor shrinkage (94). On the other hand, the small molecule RITA (reactivation of p53 and induction of tumor cell apoptosis) binds directly to p53, preventing MDM2 binding and promoting a strong apoptotic effect on tumors (95).

Furthermore, several siRNA approaches have been investigated for *wt* p53 activation. The viral E6 protein from the human papilloma virus binds and targets p53 for inactivation and degradation. SiRNA targeting of E6 inactivates E6 and triggers p53 mediated response (96). SiRNA targeting of MDM2 can also stabilize and activate p53 (97).

Another way to stabilize *wt* p53 is through post transcriptional modifications. Acetylated p53 is more stable and cannot be degraded via the MDM2 degradation

pathway. Therefore, inhibiting protein-deacetylating activities of proteins such as SirT1 and SirT2 (members of the sirtuin family) could stabilize p53. The small molecule inhibitor Tenovin-1 and its more water-soluble analog Tenovin-6 both prevent protein-deacetylating activities of SirT1 and SirT2 (98).

1.11.3 Reactivating p53 mediated response in cancers with mutated p53 status

The challenge in targeting mutant p53 is that it is a heterogeneous target because of the broad range of mutations occurring in human tumors. Drugs developed in the last couple of years mainly focused on reactivating specific variants of mutant p53 to achieve *wt* p53 like function. One such drug is the carbazole derivative PhiKa083, which binds only to the unstable Y220C mutant, raises its melting temperature and reactivates its function. The Y220C mutation accounts for 75000 patients per year (99). On the other hand contact and conformational mutants can both be rescued via an ellipticine derivate, 9-hydroxy-ellipticine, which induces G1 arrest and triggers G1 phase-restricted apoptosis in a mutant p53-dependent manner (100).

The small molecules PRIMA (p53 reactivation and induction of massive apoptosis) and MIRA (mutant p53-dependent induction of rapid apoptosis) both can reactivate mutant p53. PRIMA rescues DNA contact mutants and structural mutants by forming adducts with thiols in mutant p53 core domain. This covalent modification reactivates mutant p53 and induces apoptosis in tumor cells (101, 102). MIRA restores *wt* conformation and function of mutant p53 and is more potent than PRIMA (103). The maleimide group in MIRA reacts with thiol and amino groups in proteins and stabilizes the native fold of p53 (102, 103).

Further, p53-mediated response in tumors containing mutated p53 can be activated not by restoring p53, but instead by its family member p73. In human cancers, p73 is usually not mutated. The small molecule RETRA (reactivation of transcriptional reporter activity) releases p73 from the inhibitory p73/p53mut complex which produces a p53-like tumor suppressor response. Therefore, RETRA increases p21

and PUMA transcription and eventually triggers a delay of tumor formation in xenograft tumor model (104).

In summary, many different approaches have been used to target the p53 pathway for cancer therapy. However, all have critical disadvantages. When reintroducing *wt* p53 via gene therapy into cancer cells that harbor mutant p53, endogenous *wt* p53 will face dominant negative inhibition and oncogenic gain of function of mutant p53. This is also the reason why small molecules such as Nutlin-3 that attempt to reactivate functional *wt* p53 could be indirectly inactivated by mutant p53. Therefore, this approach is only beneficial for patients with *wt* p53. Additionally, p53 is a very heterogeneous target, and some drugs such as PhiKa083 only work for a very small subset of patients. The function of all the drugs listed in this section is highly dependent on the p53 status of the cancer, which require personalized medicine in treating each cancer patient individually.

We propose to target p53 directly to the mitochondria using an optimal mitochondrial targeting signal (MTS). Since p53 exhibits its rapid, direct apoptotic function at the mitochondria in its monomeric form, regardless of p53 status, we hypothesis that it will be effective under any circumstances.

Therapeutic		**Mechanism of action**	**Application dependent on p53 status**	**Ref:**
gene	Gendicine™	Similar to endogenous *wt* p53	*wt* p53, p53 null	(20)
	Oncorine™	Similar to endogenous wt p53	*wt* p53, p53 null	(20)

siRNA	siRNA to E6	Inactivates E6; p53 mediated apoptosis	*wt* p53	(96)
	siRNA to MDM2	Prevents p53 degradation	*wt* p53	(97)
Small molecule	Nutlin-3a	Binds to MDM2; stabilizes	*wt* p53	(94)
	RITA	Binds to p53; stabilizes p53	*wt* p53	(95)
	Tenovin-1 or 6	Inhibits p53 deacetylation: stabilizes p53	*wt* p53	(98)
	PhiKa 083	Binds to p53Y220Cmut; raises melting temperature	p53Y220Cmut	(99)
	Ellipticine derivate	Induces G1 arrest; G1 restricted apoptosis	p53mut	(100)
	PRIMA	Forms thiol adducts with p53mut core domain; stabilizes folding	p53mut	(101)
	MIRA	Maleimide group reactivates thiols and amines in p53 mut; stabilizes its folding	p53mut	(103)
	RETRA	Releases p73 from inhibitory p73/p53mut complex	p53mut	(104)

Table 2: Summary of p53 therapeutics with their mechanism of action and p53 status

1.12 Mitochondrial targeting of p53 for cancer therapy

Wild type p53 has been used almost for a decade in cancer gene therapy. It was approved for the treatment of head and neck cancer in China under the trade name Gendacine® and Oncorine® (20). In the U.S., there are several clinical trials ongoing with wild-type p53 mostly in combination with other chemotherapeutics (105). All these gene therapy approaches have focused mainly on p53's role as a transcription factor (20, 105, 106). Moll and colleagues have attempted targeting p53 to the mitochondria for cancer therapy but did not achieve clinical translation (107-109). For better understanding of mitochondrial targeting, we discuss the mitochondrial compartment in section 1.13.

As mentioned before, p53 does not contain a mitochondrial targeting signal. Moll and colleagues suggested that MDM2 triggers monoubiquitination of p53 which results in nuclear export. Cytoplasmic monoubiquitinated p53 is imported into the mitochondrial via the herpes virus-associated ubiquitin-specific protease (58, 59). At the mitochondria p53 triggers the intrinsic apoptotic pathway by interacting with anti- (Bcl-XL, Mcl-1) and pro- (Bak, Bax) apoptotic Bcl-2 protein family members (57, 65, 66, 110). At the mitochondrial outer membrane, p53 interacts first with anti-apoptotic Bcl-2 proteins by sequestering them. Then it activates pro-apoptotic Bak and Bax, triggers their homo-oligomerization, resulting in cytochrome c release, caspase activation and eventually apoptosis (65).

In this thesis, we evaluated different mitochondrial targeting signals (MTS)s for their ability to induce p53-mediated apoptosis. The Moll group has already demonstrated that p53 can be targeted to the mitochondria via the MTS from the ornithine transcarbamylase (OTC) (58, 59). However, we have shown that OTC has internal toxicity and therefore identified non-toxic MTS from XL as optimal for mitochondrial

targeting. Further, we investigated if a p53 subdomain is sufficient to trigger apoptosis at the mitochondria through p53-specific interaction with anti-apoptotic Bcl-XL and pro-apoptotic Bak.

Mitochondrial p53 is superior to wild type p53 in three ways. First, mitochondrial p53 directly interacts with pro-and anti-apoptotic proteins at the mitochondrial outer membrane and triggers the intrinsic apoptotic pathway. *wt* p53 usually acts as a transcription factor and needs to transactivate its targeted genes first. Therefore, mitochondrially targeted p53 causes a more rapid apoptotic response compared to wild type p53 (57, 107). Second, mitochondrial p53 solely induces apoptosis while *wt* p53 has the ability to transactivate genes involved in cell cycle arrest, DNA repair and metabolism which might not have a beneficial effect in cancer therapy. Third, transcriptional activity of p53 is highly dependent on tetramer formation (111, 112). In cancer cells, p53 mutations occur in the DNA binding domain of p53 while the tetramerization domain (TD) remains active forming *wt*/mut heterotetramers (described previously as dominant negative effect) (87-89). In contrast to tetrameric transcriptionally active p53, mitochondrial p53 is mostly monomeric and may be unaffected by dominant negative inhibition. Another approach to overcome dominant negative inhibition by mutant p53 is discussed in section 1.14.

1.13 The mitochondrial compartment and its import machinery

The mitochondria is known to be involved in the synthesis of ATP and in numerous other metabolic processes including biosynthesis of vitamin cofactors, amino acids, fatty acids, and iron- sulfur clusters (113, 114). Additionally, mitochondria are also known as the central regulator of the intrinsic apoptotic pathway (115, 116). The mitochondrion consists of an outer membrane surrounding an inner membrane and two aquosis compartments intermembrane space (IMS) and matrix (117). IMS harbors cytotoxic proteins such as cytochrome c and SMAC/diabolo while the matrix is essential for citric acid cycle and fatty acid-oxidation (118). Even though the

mitochondrion encloses their own genome (119, 120), most of the mitochondrial polypeptides are encoded in the nuclear genome (121). Mitochondrial proteins are synthesized in the cytosol and imported into the mitochondria (122). For proper translocation and membrane insertion of these proteins, the mitochondrial membranes contain specific machinery for mitochondrial import. The two mitochondrial membranes contain two major import receptors (123). The translocase of the outer mitochondrial membrane (TOM) complex is localized as the name implies in the mitochondrial membrane. It contains seven different subunits, the receptors Tom20, Tom22, Tom70; the channel-forming protein Tom40 and the small Tom proteins Tom5, Tom6, Tom7 (124-126). The Tom 20 receptor recognizes the mitochondrial targeting signal (MTS) of the mitochondrial protein, guides it to Tom22 which than targets it to the translocase of the inner membrane (TIM) (127, 128). The TIM complex consists of two functional modules the membrane-integrated translocase unit (Tim23, Tim17, Tim50) and the presequence-translocase-assoiated import-motor complex (PAM complex) (129, 130). The ATP-powered PAM complex is a multiprotein complex consisting of mitochondrial heat-shock protein-70 (mtHsp70) and its essential cofactors (130).

There are two main classes of mitochondrial targeting signals, N-terminal presequences and tail-anchored sequences (131-133). Most of the matrix and some of the inner and intermembrane space proteins have the N-terminal presequences consisting of 10-30 amino acids which form an α- helix (134). One side of the helix has a hydrophobic surface and the other side is positively charged (135). The MTSs are recognized and imported by the TOM complex and the TIM complex. Once they reach the matrix, matrix-localized processing peptidase cleave the MTS from the remaining protein (136). Tail-anchored proteins are usually found on the mitochondrial outer membrane. They consist of a signal membrane insertion sequence at their C-terminus and display a large N-terminal portion to the cytosol (55, 137). Examples of tail-anchored proteins are the pro-and anti-apoptotic Bcl-2 proteins such as Bcl-XL, MCl-1, Bcl-2, Bak and Bax to mention a few (133, 138).

1.14 Replacing TD of p53 to overcome dominant negative inhibition

To avoid dominant negative inhibition by mutant p53, we substituted the TD of p53 with an oligomerization domain of break point cluster region (Bcr) a 72 amino acid coiled-coil (CC) named p53-CC (139). Superficially, these two oligomerization domains might appear structurally different, but both contain a main α-helix that forms antiparallel dimers of dimers. One other group has replaced the TD with an oligomerization domain that forms parallel dimers of dimers (111, 140). However, their construct only showed marginal success, which might be due to the parallel tetramer formation of their p53 construct. We hypothesis that p53-CC will solely homotetramerize with itself while causing p53-dependent apoptosis in dominant negative breast cancer *in vitro* and *in vivo*. We plane on delivering mitochondrial targeted p53 and p53-CC by using adenoviral drug delivery.

1.15 Adenoviral drug delivery

Since p53 delivered by adenovirus is already approved as a drug and has been used in various clinical trials (141-144), we chose adenovirus for delivery as well. There are two major types of gene delivery vehicles: viral and non-viral vectors. Non-viral gene delivery is potentially a safer approach but limited due to inefficiency (145, 146). Conversely, viral vectors allow efficient gene transfer with some safety risks (147). Two viral vectors are used in clinical trials; retrovirus and adenovirus (144). Retrovirus has the advantage of having a permanent effect on the infected cells since the gene-load is inserted in the genome of the host cells. This advantage represents a double-edged sword: on one hand it is highly efficient but on the other hand it integrates randomly into the patient's genome and can therefore cause additional malignancies (147). Since we do not need a permanent genomic change and only want to cause cancer cell apoptosis, we decided to proceed with adenoviral drug delivery which only has an immediate effect and therefore does not integrate into the host's genome (148). The disadvantage of adenoviral drug delivery is the

development of antibodies against the virus (149). Since we are targeting a local tumor in breast cancer, intratumoral injections can be used for adenoviral gene therapy *in vivo* (150). Further hypothesis and specific aims will be introduced.

1.16 Statement of objectives

The long term objective of this project this project is to develop re-engineered p53 constructs for effective treatment of cancer.

Hypothesis I: Targeting p53 to the mitochondria using an optimal mitochondrial targeting signal (MTS) will achieve rapid and efficient apoptosis of cancer cells.

Aim 1: *Investigate an optimal mitochondrial targeting signal to facilitate p53 compartmentalization to the mitochondria.*

Aim 2: *Determine which subdomain of p53 is responsible for interacting with anti-apoptotic Bcl-XL and pro-apoptotic Bak or Bax.*

Aim 3*: Validate that designed constructs from Aim 1 and Aim 2 delivered using an adenovirus vector will eradicate or reduce breast cancer in an orthotopic breast cancer model.*

Hypothesis II: Replacing the tetramerization domain of *wt* p53 with the coiled-coil (CC) domain from Bcr (breakpoint cluster region) maintains similar transcribtional activity as *wt* p53 while escaping dominant negative inhibition of mutant p53.

This project I was co-author on, with Abood Okal as the primary author.

Aim 1: *Validate that p53-CC will still retain the tumor suppressor activity of p53 and additionally preclude the formation of hetero-oligomers.*

Aim 2: *Demonstrate that designed constructs from Aim 1 delivered using an adenovirus vector will eradicate or reduce breast cancer in an orthotopic breast cancer model.*

Hypothesis and Aims will be discussed in chapter 2-6. Thereby hypothesis I represents mainly the foundation of this thesis with aims 1-3 decribed in chapter 2 through 5. Hypothesis II is described in chapter 6.

1.17 References

1. Levine AJ, Oren M. The first 30 years of p53: growing ever more complex. Nat Rev Cancer. 2009 Oct;9(10):749-58.
2. Olivier M, Hollstein M, Hainaut P. TP53 mutations in human cancers: origins, consequences, and clinical use. Cold Spring Harb Perspect Biol. 2010 Jan;2(1):a001008.
3. Jackson JG, Lozano G. The mutant p53 mouse as a pre-clinical model. Oncogene. 2013 Sep 12;32(37):4325-30.
4. Joerger AC, Fersht AR. The tumor suppressor p53: from structures to drug discovery. Cold Spring Harb Perspect Biol. 2010 Jun;2(6):a000919.
5. Kussie PH, Gorina S, Marechal V, Elenbaas B, Moreau J, Levine AJ, et al. Structure of the MDM2 oncoprotein bound to the p53 tumor suppressor transactivation domain. Science. 1996 Nov 8;274(5289):948-53.
6. Zhang Y, Xiong Y. A p53 amino-terminal nuclear export signal inhibited by DNA damage-induced phosphorylation. Science. 2001 Jun 8;292(5523):1910-5.
7. Shaulsky G, Goldfinger N, Ben-Ze'ev A, Rotter V. Nuclear accumulation of p53 protein is mediated by several nuclear localization signals and plays a role in tumorigenesis. Mol Cell Biol. 1990 Dec;10(12):6565-77.
8. Stommel JM, Marchenko ND, Jimenez GS, Moll UM, Hope TJ, Wahl GM. A leucine-rich nuclear export signal in the p53 tetramerization domain: regulation of

subcellular localization and p53 activity by NES masking. EMBO J. 1999 Mar 15;18(6):1660-72.

9. Lee W, Harvey TS, Yin Y, Yau P, Litchfield D, Arrowsmith CH. Solution structure of the tetrameric minimum transforming domain of p53. Nat Struct Biol. 1994 Dec;1(12):877-90.

10. Thut CJ, Chen JL, Klemm R, Tjian R. p53 transcriptional activation mediated by coactivators TAFII40 and TAFII60. Science. 1995 Jan 6;267(5194):100-4.

11. Lill NL, Grossman SR, Ginsberg D, DeCaprio J, Livingston DM. Binding and modulation of p53 by p300/CBP coactivators. Nature. 1997 Jun 19;387(6635):823-7.

12. Wang X, Jiang X. Mdm2 and MdmX partner to regulate p53. FEBS Lett. 2012 May 21;586(10):1390-6.

13. Ferreon JC, Lee CW, Arai M, Martinez-Yamout MA, Dyson HJ, Wright PE. Cooperative regulation of p53 by modulation of ternary complex formation with CBP/p300 and HDM2. Proc Natl Acad Sci U S A. 2009 Apr 21;106(16):6591-6.

14. Toledo F, Lee CJ, Krummel KA, Rodewald LW, Liu CW, Wahl GM. Mouse mutants reveal that putative protein interaction sites in the p53 proline-rich domain are dispensable for tumor suppression. Mol Cell Biol. 2007 Feb;27(4):1425-32.

15. Pavletich NP, Chambers KA, Pabo CO. The DNA-binding domain of p53 contains the four conserved regions and the major mutation hot spots. Genes Dev. 1993 Dec;7(12B):2556-64.

16. Toledo F, Wahl GM. Regulating the p53 pathway: in vitro hypotheses, in vivo veritas. Nat Rev Cancer. 2006 Dec;6(12):909-23.

17. Kitayner M, Rozenberg H, Kessler N, Rabinovich D, Shaulov L, Haran TE, et al. Structural basis of DNA recognition by p53 tetramers. Mol Cell. 2006 Jun 23;22(6):741-53.

18. Mateu MG, Sanchez Del Pino MM, Fersht AR. Mechanism of folding and assembly of a small tetrameric protein domain from tumor suppressor p53. Nat Struct Biol. 1999 Feb;6(2):191-8.

19. Mateu MG, Fersht AR. Nine hydrophobic side chains are key determinants of the thermodynamic stability and oligomerization status of tumour suppressor p53 tetramerization domain. EMBO J. 1998 May 15;17(10):2748-58.
20. Matissek KJ BR, Davis JR, Lim CS. Choosing Targets for Gene Therapy. Targets for Gene Therapy 2011 July.
21. Marine JC, Lozano G. Mdm2-mediated ubiquitylation: p53 and beyond. Cell Death Differ. 2010 Jan;17(1):93-102.
22. Barak Y, Juven T, Haffner R, Oren M. mdm2 expression is induced by wild type p53 activity. EMBO J. 1993 Feb;12(2):461-8.
23. Brooks CL, Gu W. p53 ubiquitination: Mdm2 and beyond. Mol Cell. 2006 Feb 3;21(3):307-15.
24. Li M, Brooks CL, Wu-Baer F, Chen D, Baer R, Gu W. Mono- versus polyubiquitination: differential control of p53 fate by Mdm2. Science. 2003 Dec 12;302(5652):1972-5.
25. Hakem A, Bohgaki M, Lemmers B, Tai E, Salmena L, Matysiak-Zablocki E, et al. Role of Pirh2 in mediating the regulation of p53 and c-Myc. PLoS Genet. 2011 Nov;7(11):e1002360.
26. Tanimura S, Ohtsuka S, Mitsui K, Shirouzu K, Yoshimura A, Ohtsubo M. MDM2 interacts with MDMX through their RING finger domains. FEBS Lett. 1999 Mar 19;447(1):5-9.
27. Shvarts A, Steegenga WT, Riteco N, van Laar T, Dekker P, Bazuine M, et al. MDMX: a novel p53-binding protein with some functional properties of MDM2. EMBO J. 1996 Oct 1;15(19):5349-57.
28. Onel K, Cordon-Cardo C. MDM2 and prognosis. Mol Cancer Res. 2004 Jan;2(1):1-8.
29. Aylon Y, Oren M. Living with p53, dying of p53. Cell. 2007 Aug 24;130(4):597-600.
30. Inga A, Storici F, Darden TA, Resnick MA. Differential transactivation by the p53 transcription factor is highly dependent on p53 level and promoter target sequence. Mol Cell Biol. 2002 Dec;22(24):8612-25.

31. Braastad CD, Han Z, Hendrickson EA. Constitutive DNase I hypersensitivity of p53-regulated promoters. J Biol Chem. 2003 Mar 7;278(10):8261-8.

32. Kim E, Deppert W. The complex interactions of p53 with target DNA: we learn as we go. Biochem Cell Biol. 2003 Jun;81(3):141-50.

33. Budram-Mahadeo V, Morris PJ, Latchman DS. The Brn-3a transcription factor inhibits the pro-apoptotic effect of p53 and enhances cell cycle arrest by differentially regulating the activity of the p53 target genes encoding Bax and p21(CIP1/Waf1). Oncogene. 2002 Sep 5;21(39):6123-31.

34. Sykes SM, Mellert HS, Holbert MA, Li K, Marmorstein R, Lane WS, et al. Acetylation of the p53 DNA-binding domain regulates apoptosis induction. Mol Cell. 2006 Dec 28;24(6):841-51.

35. Le Cam L, Linares LK, Paul C, Julien E, Lacroix M, Hatchi E, et al. E4F1 is an atypical ubiquitin ligase that modulates p53 effector functions independently of degradation. Cell. 2006 Nov 17;127(4):775-88.

36. Shmueli A, Oren M. Mdm2: p53's lifesaver? Mol Cell. 2007 Mar 23;25(6):794-6.

37. Sullivan A, Lu X. ASPP: a new family of oncogenes and tumour suppressor genes. Br J Cancer. 2007 Jan 29;96(2):196-200.

38. Schumm K, Rocha S, Caamano J, Perkins ND. Regulation of p53 tumour suppressor target gene expression by the p52 NF-kappaB subunit. EMBO J. 2006 Oct 18;25(20):4820-32.

39. Attardi LD, Reczek EE, Cosmas C, Demicco EG, McCurrach ME, Lowe SW, et al. PERP, an apoptosis-associated target of p53, is a novel member of the PMP-22/gas3 family. Genes Dev. 2000 Mar 15;14(6):704-18.

40. Boatright KM, Renatus M, Scott FL, Sperandio S, Shin H, Pedersen IM, et al. A unified model for apical caspase activation. Mol Cell. 2003 Feb;11(2):529-41.

41. Boatright KM, Salvesen GS. Mechanisms of caspase activation. Curr Opin Cell Biol. 2003 Dec;15(6):725-31.

42. Roy S, Nicholson DW. Cross-talk in cell death signaling. J Exp Med. 2000 Oct 16;192(8):F21-5.

43. Desagher S, Martinou JC. Mitochondria as the central control point of apoptosis. Trends Cell Biol. 2000 Sep;10(9):369-77.
44. Haupt S, Berger M, Goldberg Z, Haupt Y. Apoptosis - the p53 network. J Cell Sci. 2003 Oct 15;116(Pt 20):4077-85.
45. Riedl SJ, Salvesen GS. The apoptosome: signalling platform of cell death. Nat Rev Mol Cell Biol. 2007 May;8(5):405-13.
46. Martins LM, Iaccarino I, Tenev T, Gschmeissner S, Totty NF, Lemoine NR, et al. The serine protease Omi/HtrA2 regulates apoptosis by binding XIAP through a reaper-like motif. J Biol Chem. 2002 Jan 4;277(1):439-44.
47. Janicke RU, Sprengart ML, Wati MR, Porter AG. Caspase-3 is required for DNA fragmentation and morphological changes associated with apoptosis. J Biol Chem. 1998 Apr 17;273(16):9357-60.
48. Zha H, Aime-Sempe C, Sato T, Reed JC. Proapoptotic protein Bax heterodimerizes with Bcl-2 and homodimerizes with Bax via a novel domain (BH3) distinct from BH1 and BH2. J Biol Chem. 1996 Mar 29;271(13):7440-4.
49. Antonsson B, Montessuit S, Sanchez B, Martinou JC. Bax is present as a high molecular weight oligomer/complex in the mitochondrial membrane of apoptotic cells. J Biol Chem. 2001 Apr 13;276(15):11615-23.
50. Chipuk JE, Moldoveanu T, Llambi F, Parsons MJ, Green DR. The BCL-2 family reunion. Mol Cell. 2010 Feb 12;37(3):299-310.
51. Willis SN, Adams JM. Life in the balance: how BH3-only proteins induce apoptosis. Curr Opin Cell Biol. 2005 Dec;17(6):617-25.
52. Zheng JY, Tsai YC, Kadimcherla P, Zhang R, Shi J, Oyler GA, et al. The C-terminal transmembrane domain of Bcl-xL mediates changes in mitochondrial morphology. Biophys J. 2008 Jan 1;94(1):286-97.
53. Reed JC. Double identity for proteins of the Bcl-2 family. Nature. 1997 Jun 19;387(6635):773-6.
54. Chipuk JE, Green DR. How do BCL-2 proteins induce mitochondrial outer membrane permeabilization? Trends Cell Biol. 2008 Apr;18(4):157-64.

55. Ferrer PE, Frederick P, Gulbis JM, Dewson G, Kluck RM. Translocation of a Bak C-terminus mutant from cytosol to mitochondria to mediate cytochrome C release: implications for Bak and Bax apoptotic function. PLoS One. 2012;7(3):e31510.

56. Tait SW, Green DR. Mitochondria and cell death: outer membrane permeabilization and beyond. Nat Rev Mol Cell Biol. 2010 Sep;11(9):621-32.

57. Mihara M, Erster S, Zaika A, Petrenko O, Chittenden T, Pancoska P, et al. p53 has a direct apoptogenic role at the mitochondria. Mol Cell. 2003 Mar;11(3):577-90.

58. Marchenko ND, Wolff S, Erster S, Becker K, Moll UM. Monoubiquitylation promotes mitochondrial p53 translocation. EMBO J. 2007 Feb 21;26(4):923-34.

59. Marchenko ND, Moll UM. The role of ubiquitination in the direct mitochondrial death program of p53. Cell Cycle. 2007 Jul 15;6(14):1718-23.

60. Hagn F, Klein C, Demmer O, Marchenko N, Vaseva A, Moll UM, et al. BclxL changes conformation upon binding to wild-type but not mutant p53 DNA binding domain. J Biol Chem. 2010 Jan 29;285(5):3439-50.

61. Tomita Y, Marchenko N, Erster S, Nemajerova A, Dehner A, Klein C, et al. WT p53, but not tumor-derived mutants, bind to Bcl2 via the DNA binding domain and induce mitochondrial permeabilization. J Biol Chem. 2006 Mar 31;281(13):8600-6.

62. Perfettini JL, Kroemer RT, Kroemer G. Fatal liaisons of p53 with Bax and Bak. Nat Cell Biol. 2004 May;6(5):386-8.

63. Petros AM, Gunasekera A, Xu N, Olejniczak ET, Fesik SW. Defining the p53 DNA-binding domain/Bcl-x(L)-binding interface using NMR. FEBS Lett. 2004 Feb 13;559(1-3):171-4.

64. Sot B, Freund SM, Fersht AR. Comparative biophysical characterization of p53 with the pro-apoptotic BAK and the anti-apoptotic BCL-xL. J Biol Chem. 2007 Oct 5;282(40):29193-200.

65. Vaseva AV, Moll UM. The mitochondrial p53 pathway. Biochim Biophys Acta. 2009 May;1787(5):414-20.

66. Chipuk JE, Kuwana T, Bouchier-Hayes L, Droin NM, Newmeyer DD, Schuler M, et al. Direct activation of Bax by p53 mediates mitochondrial membrane permeabilization and apoptosis. Science. 2004 Feb 13;303(5660):1010-4.
67. Wolff S, Erster S, Palacios G, Moll UM. p53's mitochondrial translocation and MOMP action is independent of Puma and Bax and severely disrupts mitochondrial membrane integrity. Cell Res. 2008 Jul;18(7):733-44.
68. Vousden KH, Prives C. Blinded by the Light: The Growing Complexity of p53. Cell. 2009 May 1;137(3):413-31.
69. Maddocks OD, Vousden KH. Metabolic regulation by p53. J Mol Med (Berl). 2011 Mar;89(3):237-45.
70. Bensaad K, Tsuruta A, Selak MA, Vidal MN, Nakano K, Bartrons R, et al. TIGAR, a p53-inducible regulator of glycolysis and apoptosis. Cell. 2006 Jul 14;126(1):107-20.
71. Shen L, Sun X, Fu Z, Yang G, Li J, Yao L. The fundamental role of the p53 pathway in tumor metabolism and its implication in tumor therapy. Clin Cancer Res. 2012 Mar 15;18(6):1561-7.
72. Vousden KH, Ryan KM. p53 and metabolism. Nat Rev Cancer. 2009 Oct;9(10):691-700.
73. Watanabe H, Ohta S, Kumon Y, Sakaki S, Sakanaka M. Increase in p53 protein expression following cortical infarction in the spontaneously hypertensive rat. Brain Res. 1999 Aug 7;837(1-2):38-45.
74. Liu P, Xu B, Cavalieri TA, Hock CE. Pifithrin-alpha attenuates p53-mediated apoptosis and improves cardiac function in response to myocardial ischemia/reperfusion in aged rats. Shock. 2006 Dec;26(6):608-14.
75. Bretaud S, Allen C, Ingham PW, Bandmann O. p53-dependent neuronal cell death in a DJ-1-deficient zebrafish model of Parkinson's disease. J Neurochem. 2007 Mar;100(6):1626-35.
76. Culmsee C, Landshamer S. Molecular insights into mechanisms of the cell death program: role in the progression of neurodegenerative disorders. Curr Alzheimer Res. 2006 Sep;3(4):269-83.

77. Bae BI, Xu H, Igarashi S, Fujimuro M, Agrawal N, Taya Y, et al. p53 mediates cellular dysfunction and behavioral abnormalities in Huntington's disease. Neuron. 2005 Jul 7;47(1):29-41.

78. Culmsee C, Zhu X, Yu QS, Chan SL, Camandola S, Guo Z, et al. A synthetic inhibitor of p53 protects neurons against death induced by ischemic and excitotoxic insults, and amyloid beta-peptide. J Neurochem. 2001 Apr;77(1):220-8.

79. Brosh R, Rotter V. When mutants gain new powers: news from the mutant p53 field. Nat Rev Cancer. 2009 Oct;9(10):701-13.

80. Peller S, Rotter V. TP53 in hematological cancer: low incidence of mutations with significant clinical relevance. Hum Mutat. 2003 Mar;21(3):277-84.

81. Coles C, Condie A, Chetty U, Steel CM, Evans HJ, Prosser J. p53 mutations in breast cancer. Cancer Res. 1992 Oct 1;52(19):5291-8.

82. Schuijer M, Berns EM. TP53 and ovarian cancer. Hum Mutat. 2003 Mar;21(3):285-91.

83. Iacopetta B. TP53 mutation in colorectal cancer. Hum Mutat. 2003 Mar;21(3):271-6.

84. Blons H, Laurent-Puig P. TP53 and head and neck neoplasms. Hum Mutat. 2003 Mar;21(3):252-7.

85. Hollstein M, Sidransky D, Vogelstein B, Harris CC. p53 mutations in human cancers. Science. 1991 Jul 5;253(5015):49-53.

86. Kim E, Deppert W. The versatile interactions of p53 with DNA: when flexibility serves specificity. Cell Death Differ. 2006 Jun;13(6):885-9.

87. Milner J, Medcalf EA, Cook AC. Tumor suppressor p53: analysis of wild-type and mutant p53 complexes. Mol Cell Biol. 1991 Jan;11(1):12-9.

88. Milner J, Medcalf EA. Cotranslation of activated mutant p53 with wild type drives the wild-type p53 protein into the mutant conformation. Cell. 1991 May 31;65(5):765-74.

89. Sigal A, Rotter V. Oncogenic mutations of the p53 tumor suppressor: the demons of the guardian of the genome. Cancer Res. 2000 Dec 15;60(24):6788-93.

90. Bergamaschi D, Gasco M, Hiller L, Sullivan A, Syed N, Trigiante G, et al. p53 polymorphism influences response in cancer chemotherapy via modulation of p73-dependent apoptosis. Cancer Cell. 2003 Apr;3(4):387-402.
91. Lang GA, Iwakuma T, Suh YA, Liu G, Rao VA, Parant JM, et al. Gain of function of a p53 hot spot mutation in a mouse model of Li-Fraumeni syndrome. Cell. 2004 Dec 17;119(6):861-72.
92. Cho Y, Gorina S, Jeffrey PD, Pavletich NP. Crystal structure of a p53 tumor suppressor-DNA complex: understanding tumorigenic mutations. Science. 1994 Jul 15;265(5170):346-55.
93. Muller PA, Vousden KH. p53 mutations in cancer. Nat Cell Biol. 2013 Jan;15(1):2-8.
94. Vassilev LT, Vu BT, Graves B, Carvajal D, Podlaski F, Filipovic Z, et al. In vivo activation of the p53 pathway by small-molecule antagonists of MDM2. Science. 2004 Feb 6;303(5659):844-8.
95. Issaeva N, Bozko P, Enge M, Protopopova M, Verhoef LG, Masucci M, et al. Small molecule RITA binds to p53, blocks p53-HDM-2 interaction and activates p53 function in tumors. Nat Med. 2004 Dec;10(12):1321-8.
96. Jiang M, Milner J. Selective silencing of viral gene expression in HPV-positive human cervical carcinoma cells treated with siRNA, a primer of RNA interference. Oncogene. 2002 Sep 5;21(39):6041-8.
97. Yu Y, Sun P, Sun LC, Liu GY, Chen GH, Shang LH, et al. Downregulation of MDM2 expression by RNAi inhibits LoVo human colorectal adenocarcinoma cells growth and the treatment of LoVo cells with mdm2siRNA3 enhances the sensitivity to cisplatin. Biochem Biophys Res Commun. 2006 Jan 6;339(1):71-8.
98. Lain S, Hollick JJ, Campbell J, Staples OD, Higgins M, Aoubala M, et al. Discovery, in vivo activity, and mechanism of action of a small-molecule p53 activator. Cancer Cell. 2008 May;13(5):454-63.
99. Wiman KG. Pharmacological reactivation of mutant p53: from protein structure to the cancer patient. Oncogene. 2010 Jul 29;29(30):4245-52.

100. Sugikawa E, Hosoi T, Yazaki N, Gamanuma M, Nakanishi N, Ohashi M. Mutant p53 mediated induction of cell cycle arrest and apoptosis at G1 phase by 9-hydroxyellipticine. Anticancer Res. 1999 Jul-Aug;19(4B):3099-108.

101. Piantino CB, Reis ST, Viana NI, Silva IA, Morais DR, Antunes AA, et al. Prima-1 induces apoptosis in bladder cancer cell lines by activating p53. Clinics (Sao Paulo). 2013;68(3):297-303.

102. Saha MN, Qiu L, Chang H. Targeting p53 by small molecules in hematological malignancies. J Hematol Oncol. 2013;6:23.

103. Bykov VJ, Issaeva N, Zache N, Shilov A, Hultcrantz M, Bergman J, et al. Reactivation of mutant p53 and induction of apoptosis in human tumor cells by maleimide analogs. J Biol Chem. 2005 Aug 26;280(34):30384-91.

104. Kravchenko JE, Ilyinskaya GV, Komarov PG, Agapova LS, Kochetkov DV, Strom E, et al. Small-molecule RETRA suppresses mutant p53-bearing cancer cells through a p73-dependent salvage pathway. Proc Natl Acad Sci U S A. 2008 Apr 29;105(17):6302-7.

105. Lane DP, Cheok CF, Lain S. p53-based cancer therapy. Cold Spring Harb Perspect Biol. 2010 Sep;2(9):a001222.

106. Suzuki K, Matsubara H. Recent advances in p53 research and cancer treatment. J Biomed Biotechnol. 2011;2011:978312.

107. Palacios G, Crawford HC, Vaseva A, Moll UM. Mitochondrially targeted wild-type p53 induces apoptosis in a solid human tumor xenograft model. Cell Cycle. 2008 Aug 15;7(16):2584-90.

108. Palacios G, Moll UM. Mitochondrially targeted wild-type p53 suppresses growth of mutant p53 lymphomas in vivo. Oncogene. 2006 Oct 5;25(45):6133-9.

109. Talos F, Petrenko O, Mena P, Moll UM. Mitochondrially targeted p53 has tumor suppressor activities in vivo. Cancer Res. 2005 Nov 1;65(21):9971-81.

110. Erster S, Moll UM. Stress-induced p53 runs a direct mitochondrial death program: its role in physiologic and pathophysiologic stress responses in vivo. Cell Cycle. 2004 Dec;3(12):1492-5.

111. Jeffrey PD, Gorina S, Pavletich NP. Crystal structure of the tetramerization domain of the p53 tumor suppressor at 1.7 angstroms. Science. 1995 Mar 10;267(5203):1498-502.
112. Okal A, Mossalam M, Matissek KJ, Dixon AS, Moos PJ, Lim CS. A chimeric p53 evades mutant p53 transdominant inhibition in cancer cells. Mol Pharm. 2013 Oct 7;10(10):3922-33.
113. Mackenzie S, McIntosh L. Higher plant mitochondria. Plant Cell. 1999 Apr;11(4):571-86.
114. Bowsher CG, Tobin AK. Compartmentation of metabolism within mitochondria and plastids. J Exp Bot. 2001 Apr;52(356):513-27.
115. Jones A. Does the plant mitochondrion integrate cellular stress and regulate programmed cell death? Trends Plant Sci. 2000 May;5(5):225-30.
116. Youle RJ, Karbowski M. Mitochondrial fission in apoptosis. Nat Rev Mol Cell Biol. 2005 Aug;6(8):657-63.
117. Logan DC. The mitochondrial compartment. J Exp Bot. 2007;58(1):1225-43.
118. Fulda S, Galluzzi L, Kroemer G. Targeting mitochondria for cancer therapy. Nat Rev Drug Discov. 2010 Jun;9(6):447-64.
119. Leaver CJ, Hack E, Forde BG. Protein synthesis by isolated plant mitochondria. Methods Enzymol. 1983;97:476-84.
120. Gray MW, Burger G, Lang BF. Mitochondrial evolution. Science. 1999 Mar 5;283(5407):1476-81.
121. Unseld M, Marienfeld JR, Brandt P, Brennicke A. The mitochondrial genome of Arabidopsis thaliana contains 57 genes in 366,924 nucleotides. Nat Genet. 1997 Jan;15(1):57-61.
122. Whelan J, Glaser E. Protein import into plant mitochondria. Plant Mol Biol. 1997 Mar;33(5):771-89.
123. Wiedemann N, Frazier AE, Pfanner N. The protein import machinery of mitochondria. J Biol Chem. 2004 Apr 9;279(15):14473-6.

124. Hill K, Model K, Ryan MT, Dietmeier K, Martin F, Wagner R, et al. Tom40 forms the hydrophilic channel of the mitochondrial import pore for preproteins [see comment]. Nature. 1998 Oct 1;395(6701):516-21.
125. Kunkele KP, Heins S, Dembowski M, Nargang FE, Benz R, Thieffry M, et al. The preprotein translocation channel of the outer membrane of mitochondria. Cell. 1998 Jun 12;93(6):1009-19.
126. van Wilpe S, Ryan MT, Hill K, Maarse AC, Meisinger C, Brix J, et al. Tom22 is a multifunctional organizer of the mitochondrial preprotein translocase. Nature. 1999 Sep 30;401(6752):485-9.
127. Abe Y, Shodai T, Muto T, Mihara K, Torii H, Nishikawa S, et al. Structural basis of presequence recognition by the mitochondrial protein import receptor Tom20. Cell. 2000 Mar 3;100(5):551-60.
128. Brix J, Dietmeier K, Pfanner N. Differential recognition of preproteins by the purified cytosolic domains of the mitochondrial import receptors Tom20, Tom22, and Tom70. J Biol Chem. 1997 Aug 15;272(33):20730-5.
129. Geissler A, Chacinska A, Truscott KN, Wiedemann N, Brandner K, Sickmann A, et al. The mitochondrial presequence translocase: an essential role of Tim50 in directing preproteins to the import channel. Cell. 2002 Nov 15;111(4):507-18.
130. Rehling P, Brandner K, Pfanner N. Mitochondrial import and the twin-pore translocase. Nat Rev Mol Cell Biol. 2004 Jul;5(7):519-30.
131. Endo T, Kohda D. Functions of outer membrane receptors in mitochondrial protein import. Biochim Biophys Acta. 2002 Sep 2;1592(1):3-14.
132. Kemper C, Habib SJ, Engl G, Heckmeyer P, Dimmer KS, Rapaport D. Integration of tail-anchored proteins into the mitochondrial outer membrane does not require any known import components. J Cell Sci. 2008 Jun 15;121(Pt 12):1990-8.
133. Wattenberg B, Lithgow T. Targeting of C-terminal (tail)-anchored proteins: understanding how cytoplasmic activities are anchored to intracellular membranes. Traffic. 2001 Jan;2(1):66-71.

134. Bohni PC, Daum G, Schatz G. Import of proteins into mitochondria. Partial purification of a matrix-located protease involved in cleavage of mitochondrial precursor polypeptides. J Biol Chem. 1983 Apr 25;258(8):4937-43.
135. von Heijne G. Mitochondrial targeting sequences may form amphiphilic helices. EMBO J. 1986 Jun;5(6):1335-42.
136. Roise D, Schatz G. Mitochondrial presequences. J Biol Chem. 1988 Apr 5;263(10):4509-11.
137. Schinzel A, Kaufmann T, Schuler M, Martinalbo J, Grubb D, Borner C. Conformational control of Bax localization and apoptotic activity by Pro168. J Cell Biol. 2004 Mar 29;164(7):1021-32.
138. Wilfling F, Weber A, Potthoff S, Vogtle FN, Meisinger C, Paschen SA, et al. BH3-only proteins are tail-anchored in the outer mitochondrial membrane and can initiate the activation of Bax. Cell Death Differ. 2012 Aug;19(8):1328-36.
139. Zhao X, Ghaffari S, Lodish H, Malashkevich VN, Kim PS. Structure of the Bcr-Abl oncoprotein oligomerization domain. Nat Struct Biol. 2002 Feb;9(2):117-20.
140. Taylor CM, Keating AE. Orientation and oligomerization specificity of the Bcr coiled-coil oligomerization domain. Biochemistry. 2005 Dec 13;44(49):16246-56.
141. Yu W, Fang H. Clinical trials with oncolytic adenovirus in China. Curr Cancer Drug Targets. 2007 Mar;7(2):141-8.
142. Shi J, Zheng D. An update on gene therapy in China. Curr Opin Mol Ther. 2009 Oct;11(5):547-53.
143. Li Y, Li LJ, Zhang ST, Wang LJ, Zhang Z, Gao N, et al. In vitro and clinical studies of gene therapy with recombinant human adenovirus-p53 injection for oral leukoplakia. Clin Cancer Res. 2009 Nov 1;15(21):6724-31.
144. Ginn SL, Alexander IE, Edelstein ML, Abedi MR, Wixon J. Gene therapy clinical trials worldwide to 2012 - an update. J Gene Med. 2013 Feb;15(2):65-77.
145. Al-Dosari MS, Gao X. Nonviral gene delivery: principle, limitations, and recent progress. AAPS J. 2009 Dec;11(4):671-81.
146. Nayerossadat N, Maedeh T, Ali PA. Viral and nonviral delivery systems for gene delivery. Adv Biomed Res. 2012;1:27.

147. Thomas CE, Ehrhardt A, Kay MA. Progress and problems with the use of viral vectors for gene therapy. Nat Rev Genet. 2003 May;4(5):346-58.

148. Vorburger SA, Hunt KK. Adenoviral gene therapy. Oncologist. 2002;7(1):46-59.

149. Cotrim AP, Baum BJ. Gene therapy: some history, applications, problems, and prospects. Toxicol Pathol. 2008 Jan;36(1):97-103.

150. Rein DT, Breidenbach M, Curiel DT. Current developments in adenovirus-based cancer gene therapy. Future Oncol. 2006 Feb;2(1):137-43.

2. Direct Induction of Apoptosis Using an Optimal Mitochondrially Targeted p53

Mossalam M.[*], Matissek K.J.[*](*co-first author), Okal A., Constance J.E., Lim C.S.

Molecular Pharmaceutics, March 1, 2012

Co-first author contribution:

Research design: 35%

Experimental work: 45%

Data analysis and evaluation: 40%

Manuscript writing: 40%

2.1 Abstract

Targeting the tumor suppressor p53 to the mitochondria triggers a rapid apoptotic response as efficiently as transcription-dependent p53.(1, 2) p53 forms a complex with the anti-apoptotic Bcl-XL, which leads to Bak and Bax oligomerization resulting in apoptosis via mitochondrial outer membrane permeabilization.(3, 4) Although p53 performs its main role in the mitochondrial outer membrane it also interacts with different proteins in the mitochondrial inner membrane and matrix.(5, 6) To further investigate mitochondrial activity of p53, EGFP-p53 was fused to different mitochondrial targeting signals (MTSs) directing it to the mitochondrial outer membrane ("XL-MTS" from Bcl-XL; "TOM-MTS" from TOM20), the inner membrane ("CCO-MTS" from cytochrome c oxidase) or matrix ("OTC-MTS" from ornithine transcarbamylase). Fluorescence microscopy and a p53 reporter dual luciferase assay demonstrated that fusing MTSs to p53 increased mitochondrial localization and nuclear exclusion depending on which MTS was used. To examine if the MTSs initiate mitochondrial damage, we fused each individual MTS to EGFP (a non-toxic protein) as negative controls. We performed caspase-9, TUNEL, Annexin-V, and 7-AAD apoptosis assays on T47D breast cancer cells transfected with mitochondrial constructs. Except for EGFP-XL, apoptotic potential was observed in all MTS-EGFP-p53 and MTS-EGFP constructs. In addition, EGFP-p53-XL showed the greatest significant increase in programmed cell death compared to its non-toxic MTS control (EGFP-XL). The apoptotic mechanism for each construct was further investigated using pifithrin-α (an inhibitor of p53 transcriptional activity), pifithrin-μ (a small molecule that reduces binding of p53 to Bcl-2 and Bcl-XL), and over-expressing the anti-apoptotic Bcl-XL. Unlike the MTSs from TOM, CCO, and OTC, which showed different apoptotic mechanisms, we conclude that p53 fused to the MTS from Bcl-XL performs its apoptotic potential exclusively through p53/Bcl-XL specific pathway.

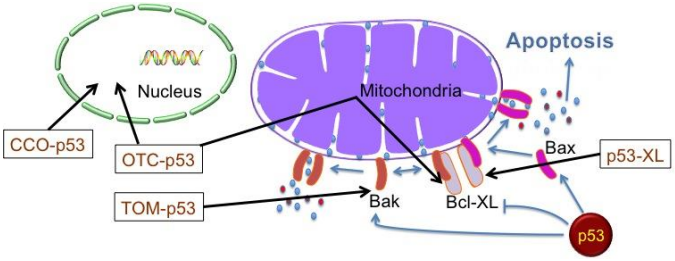

2.2 Introduction

The tumor suppressor p53 stimulates a wide network of signals involved in DNA repair, cell cycle arrest, senescence and apoptosis.(7-9) Although most of these effects can be linked to its role as a transcription factor, recent work has clearly demonstrated that p53 can cause apoptosis through its transcription-independent mitochondrial pathway.(3, 10) A small but highly reproducible fraction of p53 translocates to the mitochondria at the onset of p53-dependent apoptosis.(10) Translocation of p53 to the mitochondrial outer membrane triggers the release of cytochrome c and procaspase-3 activation. The DNA binding domain of p53 (DBD, residues 239-248) forms inhibitory complexes with anti-apoptotic Bcl-XL and Bcl-2 proteins (Figure 1), which are located in the mitochondrial outer membrane.(11) This induces oligomerization of Bak and Bax allowing them to form supramolecular pores.(4, 12, 13) In addition, p53 activates, directly binds to, and induces oligomerization of Bak and Bax.(4, 13, 14) The formation of permeability transition pores causes outer membrane rupture and releases cytochrome c from the intramembranous space into the cytosol triggering apoptosis via the apoptosome formation (Figure 1).(15-17) In addition, targeting p53 to the mitochondria triggers apoptosis faster than the transcription-dependent nuclear pathway.(1, 2) In most cancer cells, p53 is not able to bind to Bcl-2 proteins due to missense mutations in the DBD of p53, demonstrating the importance of the DBD in mitochondrial apoptosis.(11)

The therapeutic effect of pharmaceutical agents such as p53 may differ depending on their intracellular delivery (18). Precise compartmentalization and sub-

compartmentalization of proteins are essential for their biological activity. The majority of endogenous mitochondrial p53 localizes to the outer surface of the mitochondria,(19) which occurs after either DNA damage or hypoxic stress.(10) A detailed mechanism on how p53 translocates into the mitochondria is still under investigation since it is a nuclear protein due to its nuclear localization signals.(20) A study has shown that Bad (Bcl-2 antagonist of cell death) physically interacts with cytoplasmic p53 directing it to the surface of the mitochondria.(21, 22) Moll has suggested that p53 is imported via mtHsp70 targeting the membranous compartments.(10) The interaction with mtHsp70 and Hsp60 is increased with the R72P polymorphism in p53 due to elevation in nuclear export of p53.(23) MDM2 protein is responsible for the nuclear exclusion and ubiquitination of p53. The monoubiquitylated p53 is targeted to the mitochondria under stress, which disrupts the p53/MDM2 complex (24).

Despite what is known, exogenous mitochondrial targeting of p53 is still under investigation. To improve apoptosis via the p53/Bcl-XL pathway, p53 was delivered to different mitochondrial compartments. In this study, p53 was fused to different mitochondrial targeting signals (MTSs) targeting the mitochondrial outer membrane [MTS from Bcl-XL and MTS from the translocase of the outer membrane (TOM 20)], inner membrane (MTS from cytochrome c oxidase subunit VIII) and matrix (MTS from ornithine transcarbamylase) (Figure 1). These MTSs (Table 1) are generally thought to form α-helices, and are important for their recognition by translocation machineries in the mitochondrial outer (TOM complex) and inner (TIM complex) membranes.(25-28) Since MTSs are mainly found on the amino terminus of mitochondrial proteins.(25) All MTSs used were cloned on the amino terminus except for XL, which is inherently found on the carboxy terminus.(29) XL targets the outer surface of the mitochondria(29-32) while TOM is inserted into the outer membrane;(29) CCO translocates the outer membrane and then becomes imbedded into the inner membrane(33, 34) while the OTC crosses both membranes and

translocates to the matrix.(3, 35) The purpose of this work is to determine the ideal MTS for p53 mitochondrial targeting to induce the intrinsic apoptotic pathway.

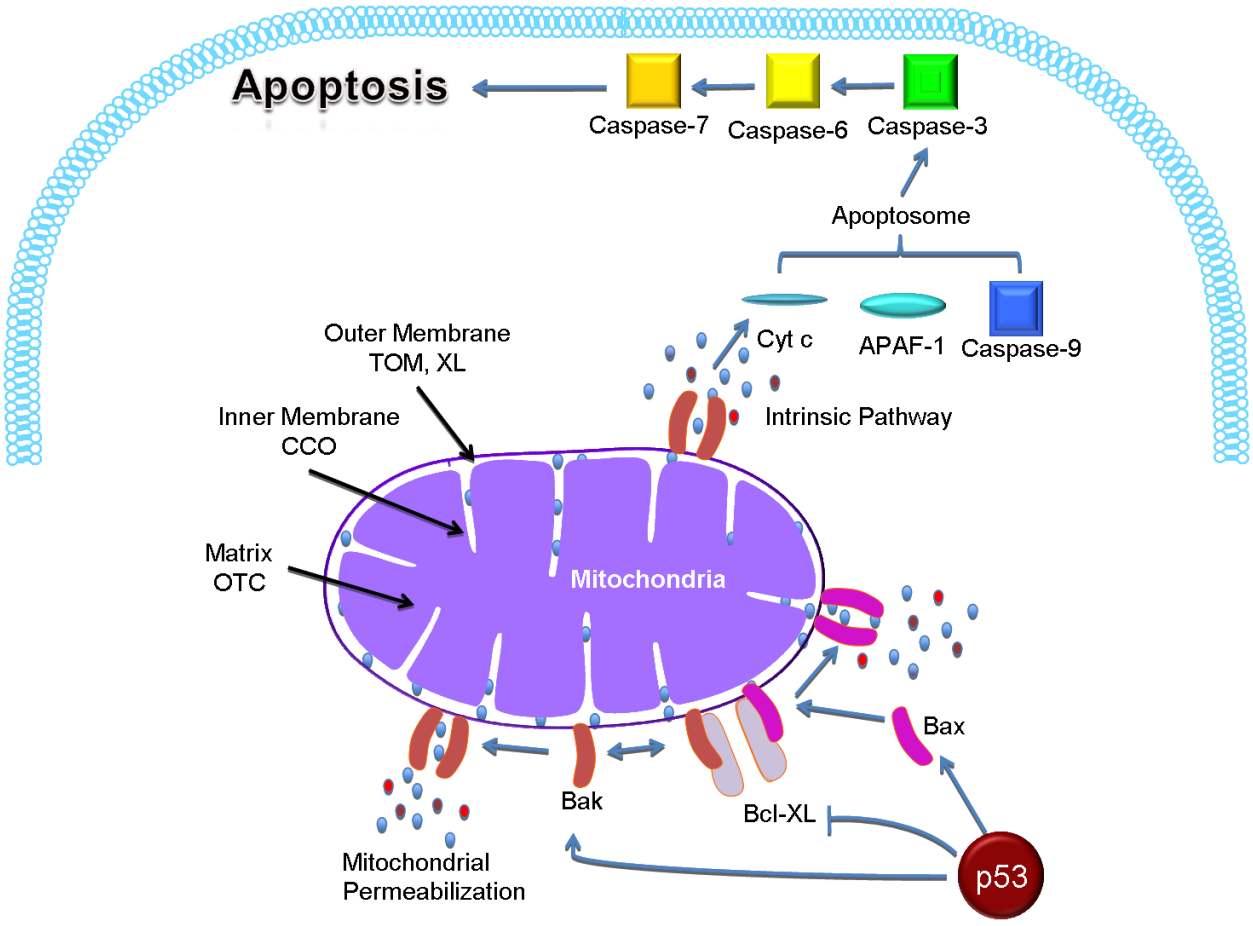

Figure 1. The mitochondrial apoptotic pathway of p53. When p53 is targeted to the mitochondria, it interacts with anti-apoptotic Bcl-XL, enables Bax and Bak oligomerization, and activates the intrinsic apoptotic pathway. The apoptosome (cytochrome c, APAF-1 and caspase-9) is triggered, leading to apoptosis via activation of caspases-3, -6, and -7. The left side of the diagram indicates the mitochondrial signals (MTSs) used and the different subsections of the mitochondria targeted, including the outer membrane ("XL-MTS" from Bcl-XL; "TOM-MTS" from TOM20), the inner membrane ("CCO-MTS" from cytochrome c oxidase), and the matrix ("OTC-MTS" from ornithine transcarbamylase).

Protein	Compartment	MTS Sequence
XL	Outer Membrane	RKGQERFNRWFLTGMTVAGVVLLGSLFSRK
TOM	Outer Membrane	MVGRNSAIAAGVCGALFIGYCIYFDRKRRSDPN
CCO	Inner Membrane	MSVLTPLLLRGLTGSARRLPVPRAKIHSL
OTC	Matrix	MLFNLRILLNNAAFRNGHNFMVRNFRCGQPLQNKVQ

Table 1. A list of the mitochondrial targeting signals used in this paper. TOM and XL target the mitochondrial outer membrane, CCO translocates to the mitochondrial inner membrane, and the OTC localizes to the mitochondrial matrix.

2.3 Materials and Methods

2.3.1 Plasmid Construction

EGFP-p53 Plasmid (pEGFP-p53). The DNA encoding p53 was amplified through PCR from pCMV-p53 wt (a generous gift from Dr. S. J. Baker, Addgene, Cambridge, MA) using the primers 5′-GCGCGCGCGCTCCGGAGCCATGGAGGAGCCGCAGT-3′ and 5′- GCGCGCGCGCGGTACCTCAGTCTGAGTCAGGCCCTTCTGTC-3′. This was subcloned into the BspEI and KpnI restriction enzyme sites in pEGFP-C1 (Clontech, Mountain View, CA).

pOTC-EGFP-p53 Plasmid. An oligonucleotide encoding the mitochondrial targeting signal from OTC (including the Kozak region), 5′-CCGGTCGCCACCATGCTGTTTAATCTGAGGATCCTGTTAAACAATGCAGCTTTTAGAAATGGTCACAACTTCATGGTTCGAAATTTTCGGTGTGGACAACCACTACAAAATAAAGTGCAGCGA-3′ was annealed to its complementary strand. This was then cloned at the amino terminus of EGFP-p53 at the AgeI site.

pTOM-EGFP-p53 and pCCO-EGFP-p53 Plasmids. The OTC region from pOTC-EGFP-p53 was replaced with annealed oligonucleotides encoding the mitochondrial

targeting signal from the TOM20 complex (TOM) at the AgeI site, 5′-GATCCCCGGTCGCCACCATGGTGGGTCGGAACAGCGCCATCGCCGCCGGTGTATGCGGGGCCCTTTTCATTGGGTACTGCATCTACTTCGACCGCAAAAGACGAAGTGACCCCAACCGA-3′ and its reverse complement, or with oligonucleotides encoding the mitochondrial targeting signal from the cytochrome c oxidase (CCO) at the AgeI site, 5′-CCGGTCGCCACCATGTCCGTCCTGACGCCGCTGCTGCTGCGGGGCTTGACAGGCTCGGCCCGGCGGCTCCCAGTGCCGCGCGCCAAGATCCATTCGTTGA-3′ and its reverse complement.

pEGFP-p53-XL Plasmid. The mitochondrial signal from Bcl-XL was fused to the carboxy terminus of EGFP-p53 using the BamHI restriction site as follows. The XL oligonucleotide 5′-AGAAAGGGCCAGGAGAGATTCAACAGATGGTTCCTGACCGGCATGACCGTGGCCGGCGTGGTGCTGCTGGGCAGCCTGTTCAGCAGAAAGTGA-3′ was annealed to its complimentary strand (with BamHI sticky ends). The p53 stop codon was then mutated (TGA to TTA) in pEGFP-p53-XL using the primers 5′-GAAGGGCCTGACTCAGACTTAGGTACCGCGGGCCCGGGAT-3′ and the reverse complement.

pEGFP Constructs with MTSs. Plasmids encoding OTC-EGFP, TOM-EGFP, CCO-EGFP, and EGFP-XL were constructed using the same oligonucleotides and restriction sites mentioned above but inserted in pEGFP-C1 instead of pEGFP-p53.

MTS-EGFP-p53NLSmut. Mutations (K319T and K320T) in the nuclear localization signal (NLS) of p53 were introduced in all mitochondrial p53 constructs via QuikChange II XL Site-Directed Mutagenesis Kit (Agilent, Santa Clara, CA) using the primers 5′- CTCTCCCCAGCCAACGACGAAACCACTGG -3′ and its reverse complement.

2.3.2 Cell Lines and Transient Transfections.

1471.1 murine adenocarcinoma cells (gift of G. Hager, NCI, NIH), MCF-7 human breast adenocarcinoma cells (ATCC, Manassas, VA), and T47D human ductal breast epithelial tumor cells (ATCC) were grown as monolayers in DMEM (1471.1) or RPMI (MCF-7 and T47D) (Invitrogen, Carlsbad, CA), supplemented with 10% fetal bovine serum (Invitrogen), 1% penicillin-streptomycin-glutamine (Invitrogen), and 0.1% gentamicin (Invitrogen). In addition, T47D and MCF-7 media was supplemented with 4 mg/L insulin (Sigma, St. Louis, MO). The cells were maintained in a 5% CO_2 incubator at 37ºC. 7.5×10^4 cells for 1471.1 and 3.0×10^5 cells for MCF-7 and T47D were seeded in 6-well plates (Greiner Bio-One, Monroe, NC) or 2-well live cell chambers (Nalgene Nunc, Rochester, NY). Transfections were carried out 24 hours after seeding using Lipofectamine 2000 (Invitrogen) following the manufacturer's recommendations. Unless otherwise indicated, 1 pmol DNA was transfected per well for all assays.

2.3.3 Mitochondrial Staining, Microscopy, and Image Analysis.

Prior to live-cell imaging and mitochondrial staining, media in live cell chambers was replaced with phenol red-free DMEM (Invitrogen) for 1471.1 cells or phenol red-free RPMI (Invitrogen) for T47D and MCF-7 cells containing 10% charcoal-stripped fetal bovine serum (CS-FBS, Invitrogen). Cells were incubated with 250 nM MitoTracker Red FM (Invitrogen) for 15 min at 37˚C and protected from light. Images were acquired as previously (36), using an Olympus IX71F fluorescence microscope (Scientific Instrument Company, Aurora, CO) with high-quality narrow band GFP filter (ex: HQ480/20 nm, me: HQ510/20 nm) and HQ: TRITC filter (ex: HQ545/30, me: HQ620/60) from Chroma Technology (Brattleboro, VT) with a 40X PlanApo oil immersion objective (NA 1.00) on an F-View Monochrome CCD camera. Images were analyzed for mitochondrial stain overlap with EGFP fusion constructs using Image software and the Jacopo plugin (37). Jacopo was used to generate the localization statistic [i.e., Pearson's correlation coefficient (PCC) post Costs'

automatic threshold algorithm] (38, 39), as we have done before (40). PCC evaluates correlation between pairs of individual pixels from EGFP and MitoTracker stained cells. The higher the PCC value the higher the correlation. For increased visual clarity of mitochondrial localization of the EGFP-fused constructs, spatial representations of pixel intensity correlation have been generated using Colocalization Color map (ImageJ).(41) Microscopy was repeated in triplicate (n=3) and 10 cells were analyzed for each construct.

2.3.4 Luciferase Assay

All constructs (3.5 µg of DNA) were co-transfected with 3.5 µg of p53-Luc Cis-Reporter (encoding for firefly luciferase, Agilent) in T47D and MCF-7 cells. To normalize for transfection efficiency, 0.35 µg of pRL-SV40 plasmid (encoding for renilla luciferase, gift from Dr. Philip Moos, University of Utah) was co-transfected. The Dual-Glo Luciferase Assay System (Promega, Madison, WI) was used to determine firefly luciferase activity and renilla luciferase per manufacturer's instructions. Luciferase activity was detected 24 hours after transfection using PlateLumino (Stratec Biomedical Systems, Birkenfeld, Germany). Firefly luciferase values were normalized for renilla luciferase. EGFP-p53 served as a positive control and EGFP as a negative control. The Dual-Glo Luciferase Assay was run three times independently, each in triplicate.

2.3.4 Caspase-9 Assay

T47D cells were probed 19 hours after transfection using CaspaLux®9-M_2D_2 kit (OncoImmunin, Inc., Gaithersburg, MD) per manufacturer's recommendations. The cells were then suspended in flow cytometry buffer (OncoImmunin, Inc.) and analyzed via the FACSAria-II (BD-BioSciences, University of Utah Core Facility) utilizing 488 nm (for EGFP) and 563 nm (for cleaved caspase 9 substrate) lasers. FACSDiva software was used as an evaluation tool. Only EGFP transfected cells at

507 nm emission were analyzed. All constructs were gated at the same EGFP intensity levels to ensure equal expression of proteins. The samples were detected in the PE (phycoerythrin) channel with the 580 nm emission peak. Each construct was assayed three times (n=3).

2.3.6 TUNEL Assay

T47D cells were prepared 48 hours after transfection using In Situ Death Detection Kit, TMR red (Roche, Mannheim, Germany) per the company's protocol. The kit, labels the DNA single strand breaks (TUNEL reaction) in apoptotic cells. The FACSAria-II was used to analyze the cells suspended in PBS (Invitrogen). The same FACS settings mentioned above with the caspase-9 assay were used. Only EGFP positive cells were analyzed for DNA segmentation. Each construct was analyzed three times (n=3).

2.3.6 Annexin-V Assay

At 48 hours post transfection, T47D cells were assayed for Annexin-V binding. The cells were suspended in 100 µl Annexin binding buffer (Invitrogen) and incubated with 5 µl Annexin-APC (Annexin-V conjugated to allophycocyanin, Invitrogen) for 15 minutes. The incubated cells were then diluted in 400 µl Annexin binding buffer and analyzed using the FACSCanto-II (BD-BioSciences, University of Utah Core Facility) with FACSDiva software. EGFP was excited at 488 nm wavelength and detected at 507 nm. APC was excited with 635 nm laser and detected at 660 nm. Analysis was based on EGFP positive cells. All constructs were gated at the same EGFP intensity levels. Each construct was tested three times (n=3).

2.3.7 7-AAD Assay

T47D and MCF-7 cells were stained with 7-aminoactinomycin D (7-AAD, Invitrogen) according to manufacturer's instructions 48 hours after transfection. The samples were analyzed using the FACSCanto-II (BD-BioSciences). Analyzed cells were gated for EGFP (as mentioned in Annexin-V assay). In addition, EGFP and 7-AAD were excited with the 488 nm laser. EGFP and 7-AAD were detected at 507 nm and 660 nm, respectively. Each construct was assayed three times (n=3).

2.3.8 Rescue Experiment Using Pifithrin-α.

Six hours after transfection, T47D cells were incubated with previously optimized concentration of 40 μM pifithrin-α (Cayman Chemical, Ann Arbor, MI) for 42 hours and compared to transfected cells without pifithrin-α. At the 48 hour time point, the 7-AAD assay was performed as above.

2.3.9 Rescue Experiment Using Pifithrin-μ

Six hours after transfection, T47D cells were incubated with previously optimized concentration of 5 nM pifithrin-μ (Tocris Bioscience, Ellisville, MO) for 42 hours and compared to transfected cells without pifithrin-μ. At the 48 hour time point, the 7-AAD assay was performed as detailed above.

2.3.10 Rescue Experiment Using Bcl-XL

T47D Cells were co-transfected with 1 pmol of MTS constructs and 1 pmol of pBcl-XL (Addgene). After 48 hours, cells were pelleted and assayed with 7-AAD as described above.

2.3.11 Statistical Analysis

All experiments were repeated in triplicate (n=3). The data were presented as the mean ± standard error. Statistical differences between each MTS-EGFP-p53 and its MTS-EGFP were resolved via unpaired t-test using GraphPad Prism software. The MTS-EGFP controls were compared to EGFP by one-way ANOVA with Tukey's post test. The degree of colocalization was analyzed using odds ratio with Pearson's Chi-square. A p value <0.05 was considered significant.

2.4 Results

2.4.1 Mitochondrial localization of MTS-EGFP-p53

Mitochondrial targeting of all constructs was verified using fluorescence microscopy. Figure 2A shows representative 1471.1 cells, which are larger in size, spread well, and are generally easier to visualize versus T47D or MCF-7 cells. However, irrespective of the cell line, similar microscopy results were observed in T47D and MCF-7 cells (data not shown). To better illustrate the colocalization of the EGFP fused constructs, PCC values were generated and graphed for each construct (Figure 2B). PCC values range from +1 to -1; perfect correlation is represented by +1, anti-correlation by -1, and a PCC value of zero denotes random distribution (37). Following the example of Bolte and Cordelières, a PCC of 0.6 or greater will define colocalization or co-compartmentalization (Figure 2B) (37, 40). Fusing different MTSs to EGFP and p53 showed a high degree of colocalization with the mitochondria. EGFP-C1 served as negative control for colocalization analysis and as expected, there was no colocalization between EGFP alone and the mitochondria. EGFP and p53 tagged to TOM and XL targeted the mitochondria better than CCO-EGFP-p53 and OTC-EGFP-p53. CCO and OTC were the "weakest" MTSs since there was some nuclear targeting of both CCO-EGFP-p53 and OTC-EGFP-p53. Therefore we mutated K319T and K320T in the nuclear localization signal (NLS) of p53 (20) which resulted in increased mitochondrial targeting for CCO-EGFP-p53 and

OTC-EGFP-p53. For easier visualization of colocalization among constructs, a spatial depiction of pixel overlap and intensity correlation are provided in the 'Color Map' column (Figure 2A). The Color Map spectrum moves from cold to warm colors as pixel correlation increases (41).

2.4.2 Testing the transcriptional activity of MTS-EGFP-p53

To demonstrate the lack of transcriptional activity of these p53 constructs, a p53 reporter dual luciferase assay was performed in T47D (Figure 3A) and MCF-7 cells (Figure 3B). T47D cells contain a mutation in p53 (in the DBD which renders it inactive) that is also localized in the cytoplasm(42, 43) while MCF-7 cells express wild-type p53 mislocalized to the cytoplasm.(44) TOM and XL fused to EGFP-p53 showed no nuclear activity in either cell lines. CCO-EGFP-p53 expressed similar transcriptional activity to EGFP-p53 (positive control) in T47D (Figure 3A) and significant activity in MCF-7 (Figure 3B) compared to the EGFP negative control. Introducing NLS mutations (K3319T and K320T) in CCO-EGFP-p53 resulted in major reduction of nuclear activity in both cell lines. OTC-EGFP-p53 showed low transcriptional activity in MCF-7 (Figure 3B) and a significant activation in T47D cells (Figure 3A). Surprisingly, introduction of NLS mutations into OTC-EGFP-p53 did not result in any changes in nuclear activity in either cell line (Figures 3A and B).

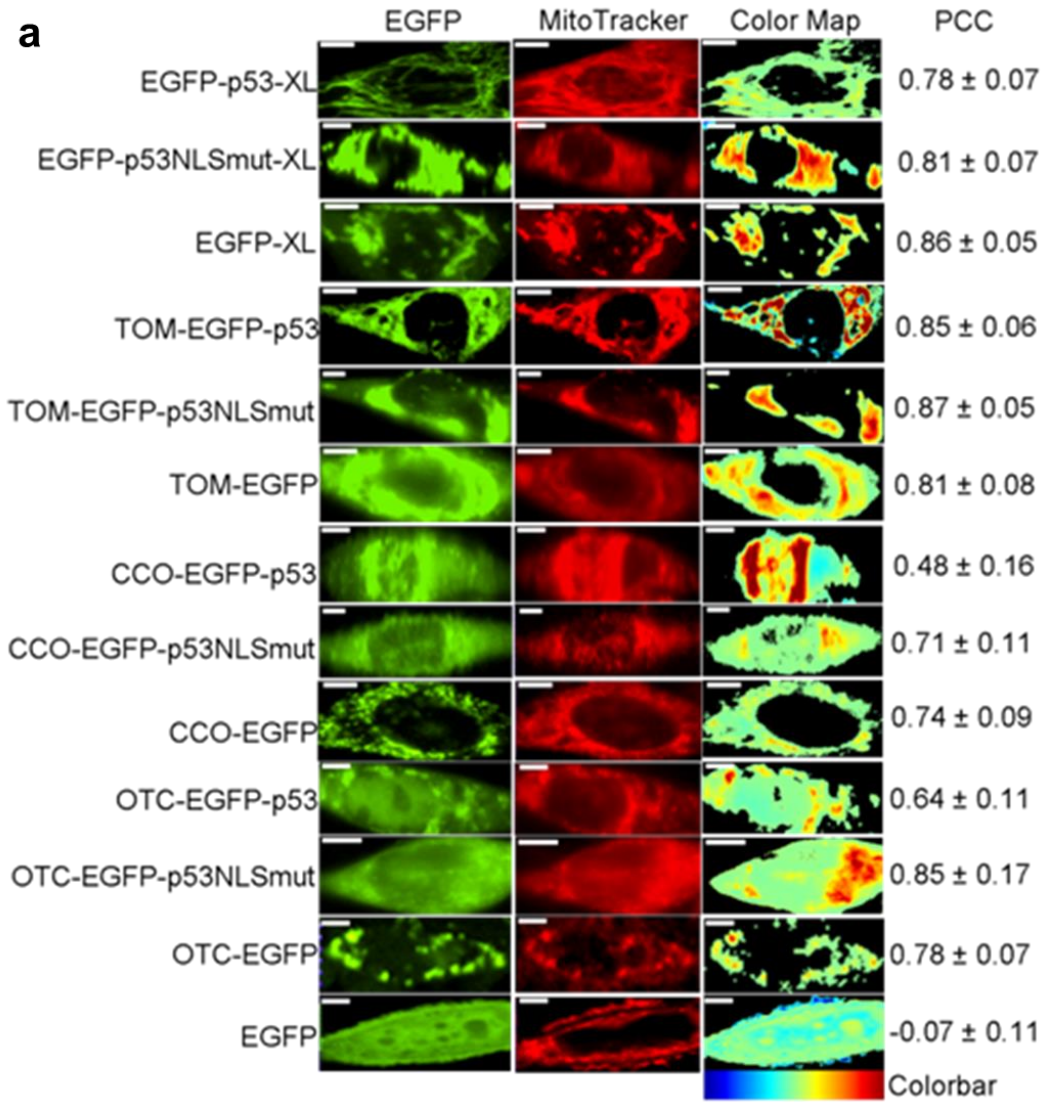
a
EGFP
MitoTracker
Color Map
PCC
EGFP-p53-XL
0.78 ± 0.07
EGFP-p53NLSmut-XL
0.81 ± 0.07
EGFP-XL
0.86 ± 0.05
TOM-EGFP-p53
0.85 ± 0.06
TOM-EGFP-p53NLSmut
0.87 ± 0.05
TOM-EGFP
0.81 ± 0.08
CCO-EGFP-p53
0.48 ± 0.16
CCO-EGFP-p53NLSmut
0.71 ± 0.11
CCO-EGFP
0.74 ± 0.09
OTC-EGFP-p53
0.64 ± 0.11
OTC-EGFP-p53NLSmut
0.85 ± 0.17
OTC-EGFP
0.78 ± 0.07
EGFP
-0.07 ± 0.11
Colorbar

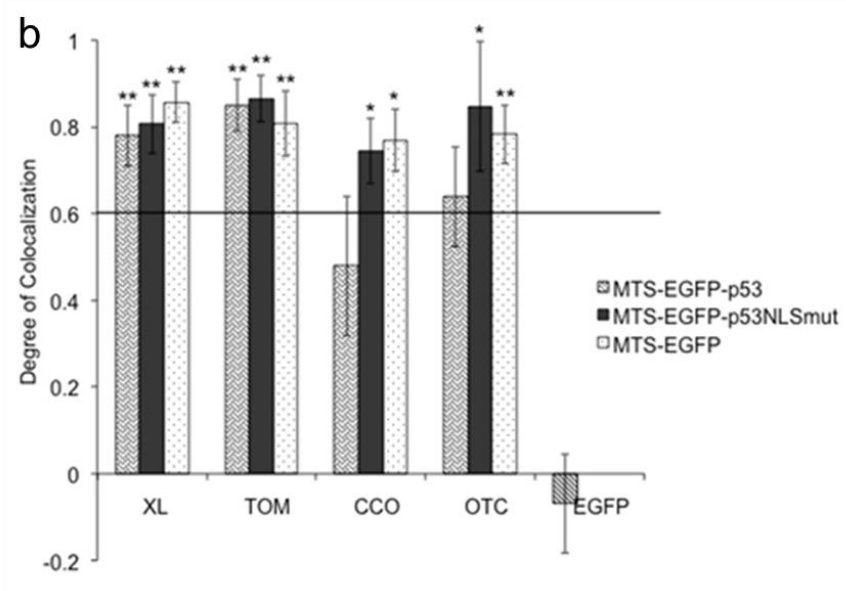
b
Degree of Colocalization
1
0.8
0.6
0.4
0.2
0
-0.2
XL
TOM
CCO
OTC
EGFP
MTS-EGFP-p53
MTS-EGFP-p53NLSmut
MTS-EGFP

Figure 2. Colocalization of MTS constructs and MitoTracker Red mitochondrial stain in 1471.1 cells. A) Representative images of MTS-EGFP-p53, MTS-EGFP-p53 NLS mutation, MTS-EGFP and EGFP-C1 are shown in the left column with images of MitoTracker Red distribution in the middle column. The 'EGFP' and 'MitoTracker' columns have been false colored green and red, respectively. Enhanced visualization of colocalized pixels is rendered in the 'Color Map' column. Warm colors depict pixels with highly correlated intensity and spatial overlap while cool colors are indicative of anti- or random correlation (color bar for interpretation is shown below column). Corresponding PCC values are shown in the right column. White scale bars are all 10 μm. B) The degree of colocalization is represented by PCC following Costes' approach. (38, 39) All constructs with values higher than 0.6 are considered highly colocalized with mitochondrial stain MitoTracker Red. Statistical analysis was performed by using odds ratio with Pearson's Chi-square. The adjusted odds ratio for PCC value of 0.6 were compared with each sample. *$p<0.05$, and **$p<0.01$ comparing odds ratio of lowest value for samples with odds ratio of 1 for PCC of 0.6.

2.4.3 The effect of MTS-EGFP-p53 on early apoptosis (caspase-9)

In this paper we focused on T47D cells because they are more resistant to apoptosis compared to MCF-7 (45). The apoptotic potential of p53 fused to different MTSs targeting the mitochondrial matrix, outer, and inner membranes was evaluated via caspase-9, TUNEL, Annexin-V and 7-AAD assays. Caspases are a group of proteolytic enzymes that are directly involved in apoptosis by cleaving proteins such as lamin and PARP. Its inactive form procaspase-9 is activated through cytochrome c release and APAF-1 which occurs after mitochondrial outer membrane disruption (known as the intrinsic apoptotic pathway).(46) Caspase-9 itself cleaves the peptide sequence LEHD, which was used in the caspase-9 assay to measure the intrinsic apoptotic pathway.(47) Only EGFP-p53-XL ($p<0.05$) and OTC-EGFP-p53 ($p<0.05$)

were significantly different from their corresponding MTS-EGFP controls as shown in figure 4.

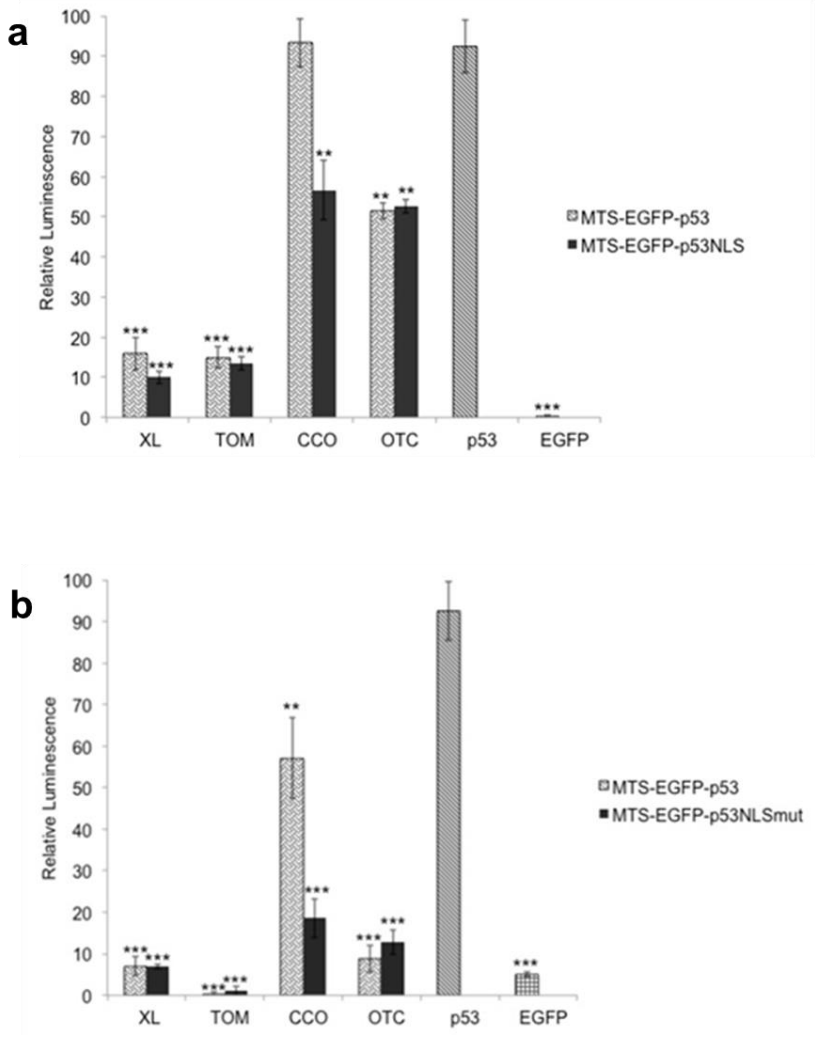

Figure 3. Luciferase assay: All MTS-EGFP-p53 and MTS-EGFP-p53 NLS mutation constructs were tested for their ability to activate a p53 reporter in A) T47D cells and B) MCF-7 cells. EGFP-p53 serves as a positive control and EGFP as a negative control. All constructs were corrected to EGFP-p53 control, which is set at 100%.

Statistical analysis was performed by using one-way ANOVA with Tukey's post test. **p<0.005 and ***p<0.0005 compared to EGFP-p53.

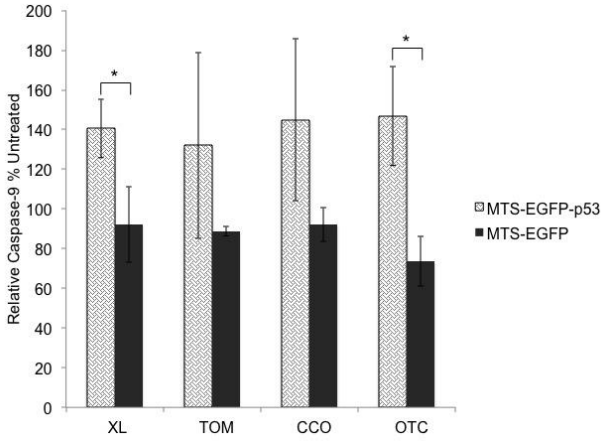

Figure 4. The activation of caspase-9 was analyzed 19 hours following transfection of T47D cells. All constructs were corrected to untreated control, which is set at 100%. Statistical analysis was performed by using unpaired t-test. * p<0.05 for MTS-EGFP-p53 compared to its MTS-EGFP.

2.4.4 The effect of MTS-EGFP-p53 on DNA fragmentation

Terminal deoxynucleotidyl transferase dUTP nick end labeling (TUNEL) was measured to detect DNA fragmentation by labeling the terminal end of nucleic acids. DNA fragmentation is a hallmark of apoptosis and is generated by caspase cleavage (48). Figure 5 illustrates that EGFP-p53-XL and CCO-EGFP-p53 are the only constructs that were statistically significant from their control MTS-EGFP. Constructs with mutations in the NLS of p53 did not differ from constructs without mutation (see the supporting information: S1). Staurosporine, which activates caspase-3/7 and leads to DNA fragmentation (45), served as a positive control.

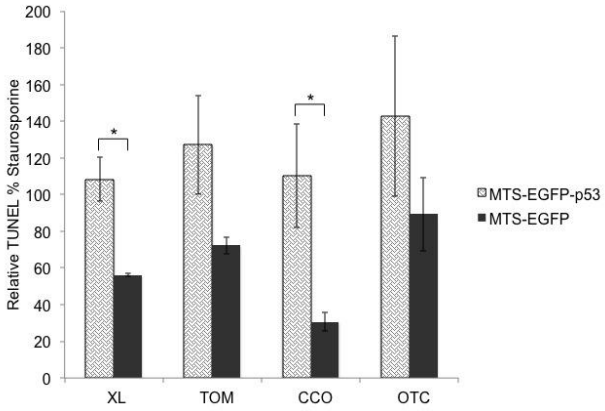

Figure 5. T47D cells were tested 48 hours following transfection. DNA fragmentation was analyzed with the TUNEL assay. All constructs were corrected to staurosporine positive control, which is set at 100%. Statistical analysis was performed by unpaired t-test. * $p<0.05$ for MTS-EGFP-p53 compared to its MTS-EGFP.

2.4.5 The effect of MTS-EGFP-p53 on plasma membrane

The effects of the mitochondrial constructs were further explored by analyzing externalization of phosphatidylserine and cell membrane rupture. Annexin-V was used to detect the externalization of phosphatidylserine on the cell surface of apoptotic cells via flow cytometry.(49, 50) In the majority of healthy cells, the plasma membrane expresses phosphatidylserine on the cytosolic surface while in apoptotic cells, the phosphatidylserine is transported to the outer surface, which allows labeled Annexin-V to bind.(51) All MTS-EGFP-p53 constructs showed a significant effect on inducing apoptosis compared to their corresponding MTS-EGFP controls in T47D cells (Figure 6). In addition, EGFP-XL was the only construct that showed minimal activity similar to the non-toxic EGFP negative control (Figure 6).

To further validate the effect of mitochondrial p53 on late apoptosis, the 7-AAD assay was performed via flow cytometry (Figure 7). The 7-AAD fluorescent marker cannot stain the DNA in healthy cells due to inability to penetrate an intact cell membrane (52). However, it is able to stain the DNA in apoptotic and necrotic cells because of their disrupted membrane.(53) Similar to Annexin-V results, all mitochondrial p53 constructs showed significant 7-AAD intercalation with DNA compared to their MTS-EGFP controls (Figure 7A). In addition, EGFP-XL was the only construct that showed similar activity to EGFP alone (Figure 7A). In a cell line that is less resistant to apoptosis such as MCF-7 (45), EGFP-p53-XL is the only construct that was significantly different than its MTS-EGFP control (Figure 7B). In MCF-7 cells, there was no statistical difference between p53 fused to TOM, CCO or OTC and their respective MTS-EGFP controls (Figure 7B). Mutating the NLS of p53 in MTS-EGFP-p53 had no effect on 7-AAD permeation in both cell lines except with CCO-EGFP-p53 in T47D (see the supporting information: S2). In addition, EGFP-XL showed no activity similar to EGFP alone in MCF-7 (Figure 7B). Similar to Annexin V, EGFP-XL was also the only construct with minimum activity as EGFP alone in T47D cells (Figure 7A).

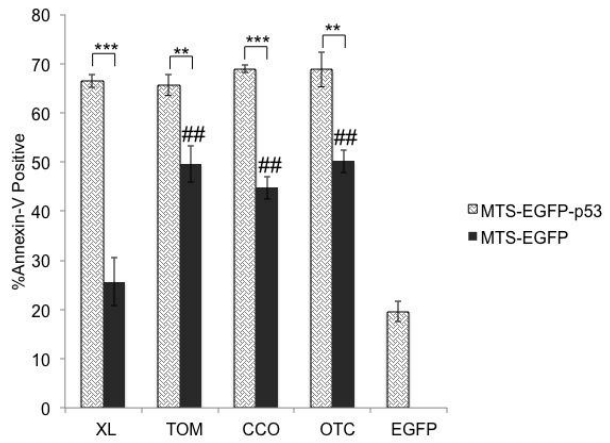

Figure 6. Annexin-V assay was conducted in T47D cells 48 hours after transfection. Statistical analysis was performed by one-way ANOVA with Tukey's post test. **p<0.005 and ***p<0.0005 comparing MTS-EGFP-p53 to their MTS-EGFP controls. The negative controls (MTS-EGFP) were compared to EGFP-C1 using one-way ANOVA with Tukey's post test ##p<0.005.

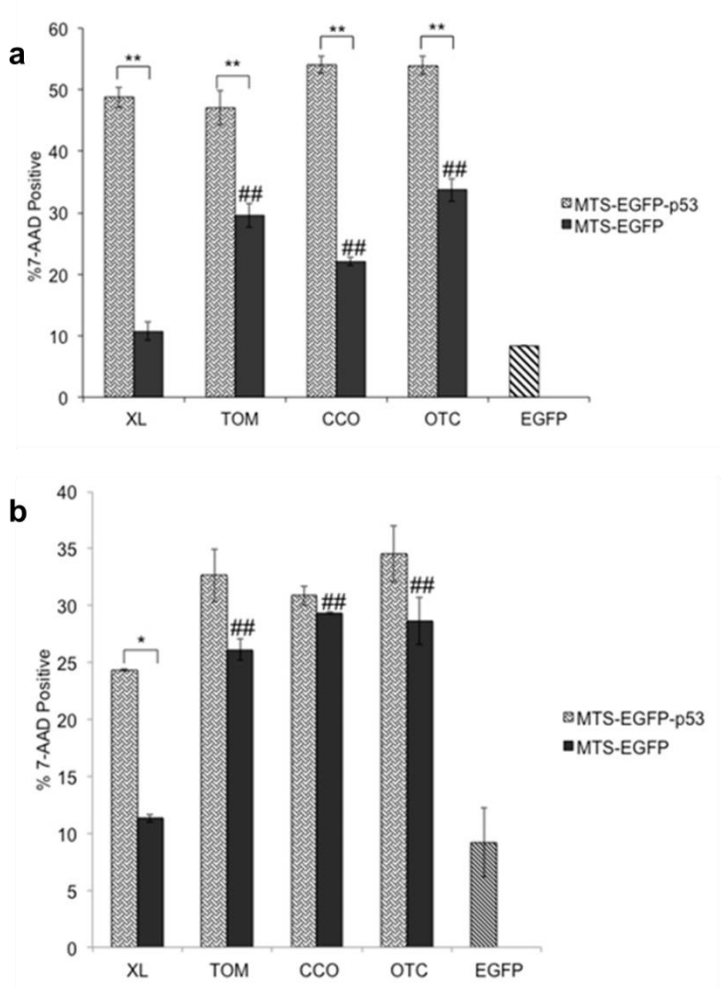

Figure 7. The 7-AAD assay was tested in (A) T47D and (B) MCF-7 cells 48 hours after transfection. Statistical analysis was performed by one-way ANOVA with

Tukey's post test. * $p<0.05$, ** $p<0.005$ comparing MTS-EGFP-p53 to their MTS-EGFP controls. The controls (MTS-EGFP) were compared to EGFP-C1 using one-way ANOVA with Tukey's post test ## $p<0.005$.

2.4.6 Investigating the apoptotic mechanism

Apoptosis resulting from p53 transcriptional activity of our mitochondrial p53 constructs was examined via a pifithrin-α rescue experiment. Pifithrin-α is a small molecule, which inhibits p53-mediated transcriptional activity (54, 55). The effect of pifithrin-α was measured in a 7-AAD assay (Figure 8A). As expected from the transcriptional activity data, the apoptotic effect of EGFP-p53 fused to either CCO or OTC was reduced significantly after pifithrin-α treatment. In addition, there was no impact on the apoptotic potential of EGFP-p53 fused to either XL or TOM (Figure 8A).

In order to investigate p53's apoptotic mechanism in the mitochondria, pifithrin-μ was used in a rescue experiment in the 7-AAD assay. Pifithrin-μ is a compound that reduces the binding affinity of p53 to the anti-apoptotic proteins, Bcl-2 and Bcl-XL (56, 57). Pifithrin-μ had a significant impact on the apoptotic potential of p53 fused to both XL and OTC (Figure 8B). However, apoptosis caused by p53 fused to either TOM or CCO was not rescued by pifithrin-μ. In addition, all the MTS-EGFP controls were not altered in this rescue experiment (see the supporting information: S3A).

The apoptotic mechanism was further explored by over-expression of the anti-apoptotic protein, Bcl-XL. The cells were then analyzed in the 7-AAD assay via flow cytometry. Bcl-XL had a significant effect on reducing 7-AAD positive cells treated with EGFP-p53 fused to TOM, XL, and OTC (Figure 8C). Cells treated with EGFP-p53-XL showed the most significant reduction in 7-AAD when co-transfected with Bcl-XL. Meanwhile, Bcl-XL had no effect on cells transfected with CCO-EGFP-p53. In addition, all the MTS-EGFP controls were not altered in this rescue experiment (see the supporting information: S3B).

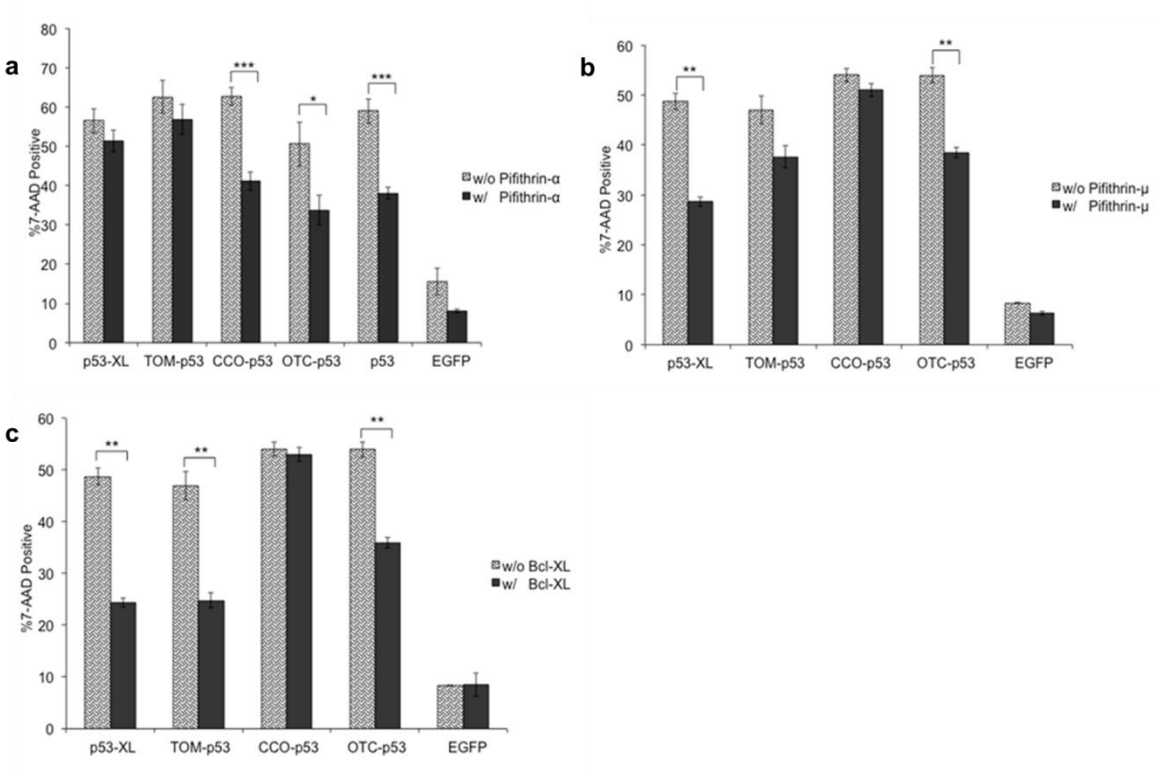

Figure 8. Rescue experiments using (A) pifithrin-α, (B) pifithrin-μ, or (C) Bcl-XL. 7-AAD assay was performed 48 hours after transfection in T47D cells. All constructs were fused to EGFP. Statistical analysis was performed by unpaired t-test. * $p<0.05$, ** $p<0.005$, *** <0.0005 comparing treated (with pifithrin-α, pifithrin-μ, or Bcl-XL) to untreated (no drug or Bcl-XL added).

2.5 Discussion

The tumor suppressor p53 was targeted with different MTSs in order to investigate its optimal mitochondrially triggered apoptotic pathway. We hypothesized that it might be possible that sending any protein (even EGFP) to mitochondria could be "toxic" to cells by disruption of mitochondrial function. Fusing p53 to MTSs targeting the mitochondrial outer membrane, inner membrane, and matrix did indeed result in apoptosis. However, sending even EGFP to the mitochondrial matrix (OTC), the inner membrane (CCO), or the TOM complex (TOM) perturbed mitochondrial

stability as evidenced by the apoptotic assays. Only p53-XL was capable of inducing mitochondrial apoptosis exclusively via mitochondrial p53/Bcl-XL pathway.

Directing EGFP to the matrix and inner membrane via OTC and CCO, respectively, resulted in late stage apoptosis. This shows that fusing EGFP to OTC or CCO has a toxic effect on the mitochondria. We speculate that sending EGFP to the mitochondrial matrix and inner membrane could cause an imbalance in the sensitive mitochondrial system due to import through mitochondrial membranes. On the other hand, targeting EGFP to the mitochondrial outer membrane using TOM and XL shows minimal toxicity with XL but significant toxicity with TOM. Since EGFP-XL is directed towards Bcl-XL (58) on the surface of the outer membrane (29-31), it is not expected to become imbedded into the mitochondrial membrane. Conversely, the TOM-EGFP may interfere with TOM20 involved in mitochondrial import machinery (18, 59). The TOM complex is responsible for importing proteins across the mitochondrial outer membrane. TOM20 is one of the receptor subunits in the TOM complex (60, 61). Perhaps fusing any protein to the MTS from TOM20 might affect the sensitive import mechanism.

As p53 is a nuclear protein, the MTS fused to it will compete with the protein's nuclear localization signals (NLSs). p53 contains three NLSs; the most active of them is located at residues 305-322 (20). The nuclear import of large proteins is dependent on the availability of a NLS (62-64). To prevent the nuclear targeting of our constructs, we introduced mutations (K319T and K320T) in the strongest NLS of p53.(20) Colocalization data and p53 transcriptional activity assay showed an increase in mitochondrial targeting and a decrease in p53 nuclear activity after the introduction of the NLS mutations in CCO-p53. According to our colocalization data, CCO-EGFP showed the lowest mitochondrial targeting compared to the other MTS-EGFP (Figure 2). The weak mitochondrial CCO signal explains the high transcriptional activity when fused to p53 without NLS mutations (Figure 3). The strong NLS in p53 competes with the relatively weak MTS from CCO and shifts the distribution to the nucleus. After mutating the strong NLS, the CCO MTS was also in

competition with the other weak NLSs in p53 (20), which may explain why the CCO-p53 NLS mutation still showed transcriptional activity (Figure 3). However, the mutations did not have any effect on the mitochondrial targeting or nuclear activity of the TOM, XL, and OTC constructs. EGFP-p53 fused to TOM and XL showed minimal nuclear p53 activity presumably due to their strong mitochondrial signals. Introducing NLS mutations to p53 fused to TOM or XL did not show any reduction on the already low transcriptional activity (Figure 3). On the other hand, OTC-p53 showed significant p53 nuclear activity but was not reduced upon NLS mutation (Figure 3).

In addition, the nuclear activity of MTS-p53 differed between MCF-7 and T47D. These differences might be due to variability in proteins involved with p53 transcriptional activity, mitochondrial shuttling, or number of mitochondria in each cell line. In MCF-7, all MTS-p53 constructs (with or without NLS mutations) showed minimum transcriptional activity except for the CCO-p53, which had half the activity of wild type p53 (Figure 3B). However, in T47D cells all MTS-p53 constructs showed generally higher nuclear activity than in MCF-7, especially CCO-p53, which showed the same nuclear activity as wild type p53. CCO-p53 NLS mutation and OTC-p53 (with and without NLS mutation) showed fifty percent transcriptional activity in T47D (Figure 3A).

Even though the NLS mutations increased mitochondrial targeting of the CCO-p53 construct, it did not have any effect on increasing the apoptotic potential. This was also the case for NLS mutations in all other constructs (see the supporting information: S1 and S2). CCO-p53 was significant compared to its CCO-EGFP control in TUNEL, Annexin-V, and 7-AAD assays. Since CCO-EGFP showed cytotoxicity, the increase in apoptosis when attached to p53 was likely due to nuclear p53 activity. This is reflected in our luciferase assay (Figure 3) and the rescue experiments with pifithrin-α, pifithrin-μ and Bcl-XL (Figure 8). The apoptotic activity of CCO-p53 was reduced in the pifithrin-α (an inhibitor of p53 transcriptional activity) rescue experiment. However, it was not rescued by either over-expression with the

anti-apoptotic Bcl-XL or incubation with pifithrin-μ (an inhibitor of p53 binding to Bcl-2 and Bcl-XL) (56, 57). This demonstrates that CCO-p53 does not initiate p53/Bcl-XL specific apoptosis.

OTC-p53 also showed transcriptional activity. In addition, OTC-p53 exhibited significant caspase-9 induction, and late stage apoptosis compared to its cytotoxic OTC-EGFP control. To examine if the increase of activity was due to nuclear or mitochondrial p53, the rescue experiments (with pifithrin-μ and Bcl-XL) were conducted and showed reduction in programmed cell death (Figure 8). This indicates that apoptosis was likely initiated through p53 binding to Bcl-XL and Bcl-2. In addition, the transcriptional activity data demonstrates that OTC-p53 has activity in both the nucleus (rescued by pifithrin-α) and the mitochondria (rescued by pifithrin-μ and Bcl-XL). Even though OTC directs p53 to the mitochondrial matrix, p53 is still able to interact with Bcl-XL and Bcl-2 proteins on the outer membrane. This could be due to cleavage of the MTS by endopeptidase, which enables p53 to target the outer membrane (3, 10).

Instead of targeting the protein to the matrix then translocating it to the outer membrane, as was the case for OTC, we fused EGFP-p53 to TOM to directly target the outer membrane. Direct targeting of the outer membrane with TOM-p53 was able to initiate apoptosis (Annexin-V and 7-AAD) robustly compared to its TOM-EGFP control. Interestingly this increase in apoptosis was only rescued when Bcl-XL was co-transfected but not when pifithrin-α or pifithrin-μ were added (Figure 8). The pifithrin-α rescue experiment indicates that TOM-p53 has no transcriptional activity. We speculate that TOM-EGFP-p53 is binding to pro-apoptotic Bak and enhancing its oligomerization, which disrupts the mitochondrial outer membrane.(13, 14) Bcl-XL forms a heterodimer with Bak and prevents Bak homodimerization.(14, 65, 66) Therefore, when Bcl-XL is over-expressed, it competes with TOM-p53 in binding with Bak and hence reduces apoptosis. Since pifithrin-μ reduces the binding of p53 to anti-apoptotic Bcl-XL and Bcl-2 and has no effect on binding to Bak, it did not show reduction in programmed cell death for TOM-p53.

In an effort to directly target the p53/Bcl-XL pathway, we fused XL to EGFP-p53. Directing p53 to the mitochondria via XL showed significant caspase-9, TUNEL, 7-AAD, and Annexin-V activity compared to its EGFP-XL control. This apoptotic response was not due to transcriptional activity of p53 as shown in the luciferase assay data (Figure 3) and the pifithrin-α rescue experiment (Figure 8A). However, the apoptotic response was due to p53/Bcl-XL pathway. To confirm this interaction, rescue experiments using pifithrin-μ and Bcl-XL were conducted and showed reduction in apoptosis (Figure 8B and C). In addition, the EGFP-XL control showed no toxicity compared to the other MTS-EGFP controls especially in MCF-7 cells (Figure 6 and 7). This data demonstrates that sending p53 to a specific protein (Bcl-XL) in the mitochondrial outer membrane causes p53 specific apoptosis. Table 2 is a summary of the results and speculation from this work.

MTS	XL	TOM	CCO	OTC
Mitochondrial compartment	Outer surface of outer membrane	Outer membrane	Inner membrane	Matrix
Relative MTS Strength*	Strong	Strong	Weak	Medium/Strong
Intrinsic mito-toxicity of MTS-EGFP	Non-toxic	Toxic	Toxic	Toxic
p53 apoptotic response	Caspase-9, TUNEL, Annexin-V, and 7-AAD	Annexin-V, and 7-AAD	TUNEL, Annexin-V, and 7-AAD	Caspase-9, Annexin-V, and 7-AAD
Speculated apoptotic mechanism	May interact with Bcl-XL	May interact with Bak	Transcriptional p53	Transcriptional p53 and may interact with Bcl-XL

Table 2. A summary of collected data and speculated mechanism. The table compares the four MTSs in mitochondrial localization, strength (*based on colocalization), mito-toxicity of MTS-EGFP, apoptotic response of MTS-p53 compared to MTS-EGFP, and speculated apoptotic mechanism.

In summary, efficiency in targeting the mitochondria depends on the strength of the MTS. In the case of targeting proteins containing relatively strong NLSs such as p53 (residues 305-322) (20), mitochondrial targeting can best be achieved by using strong MTSs to counter the NLS. In this study, relatively weaker MTSs are not efficient enough to compete with the strong NLS in p53. In addition, protein targeting to the mitochondria disrupts the sensitive balance in the mitochondria, which initiates intrinsic apoptosis. Except for EGFP-XL, all mitochondrial constructs had apoptotic effects. We conclude that p53-XL was the most specific to p53/Bcl-XL mitochondrial pathway. Our data shows that not all mitochondrial targeting signals are optimal for mitochondrial induction of apoptosis with p53. In conclusion, specific binding of p53 to mitochondrial Bcl-XL (and hence apoptotic activity) is best achieved by directly targeting p53 to Bcl-XL via the XL MTS. This work therefore provides a mechanistic explanation and provides additional speculation towards the understanding of mitochondrial p53 apoptosis. Our future goal is to employ the p53-XL construct as a therapeutic *in vivo* using viral delivery. Ultimately, p53-XL gene therapy is expected to be beneficial for other types of progressive cancers that currently have no effective therapy

2.6 Supporting Information

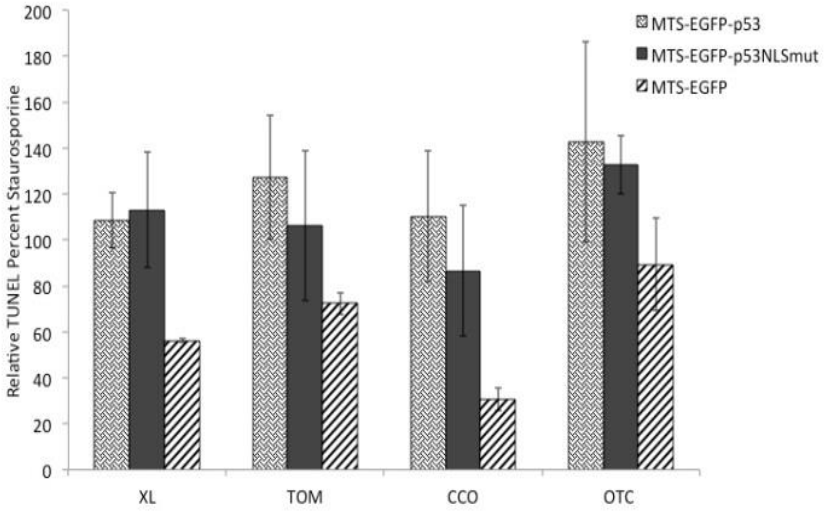

Figure S1: T47D cells were tested 48 hours following transfection. DNA fragmentation was analyzed with the TUNEL assay. All constructs were corrected to staurosporine positive control, which is set at 100%. Statistical analysis comparing MTS-EGFP-p53 NLS mutation to MTS-EGFP-p53 was performed by unpaired t-test.

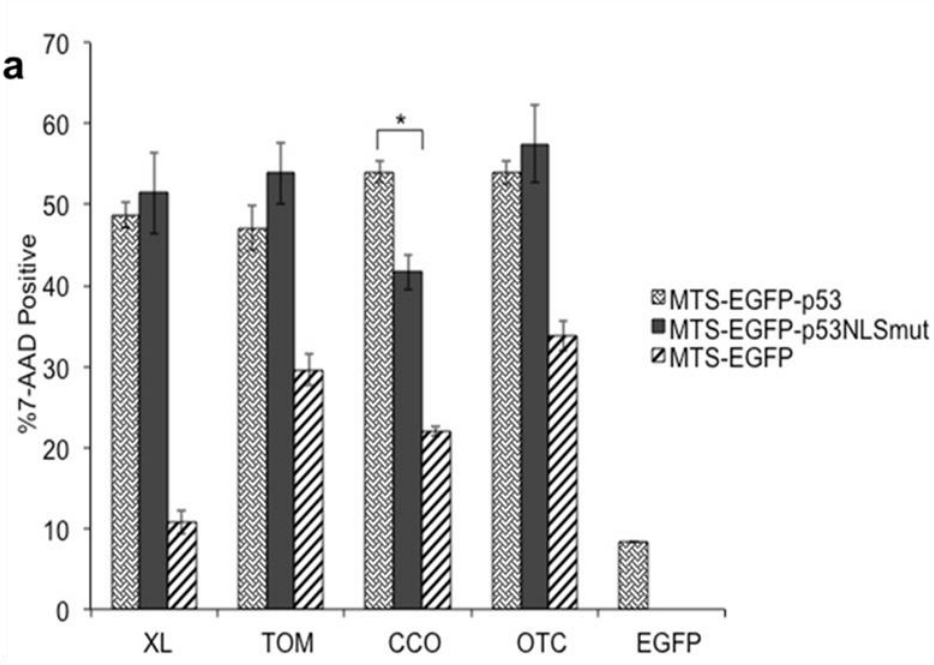

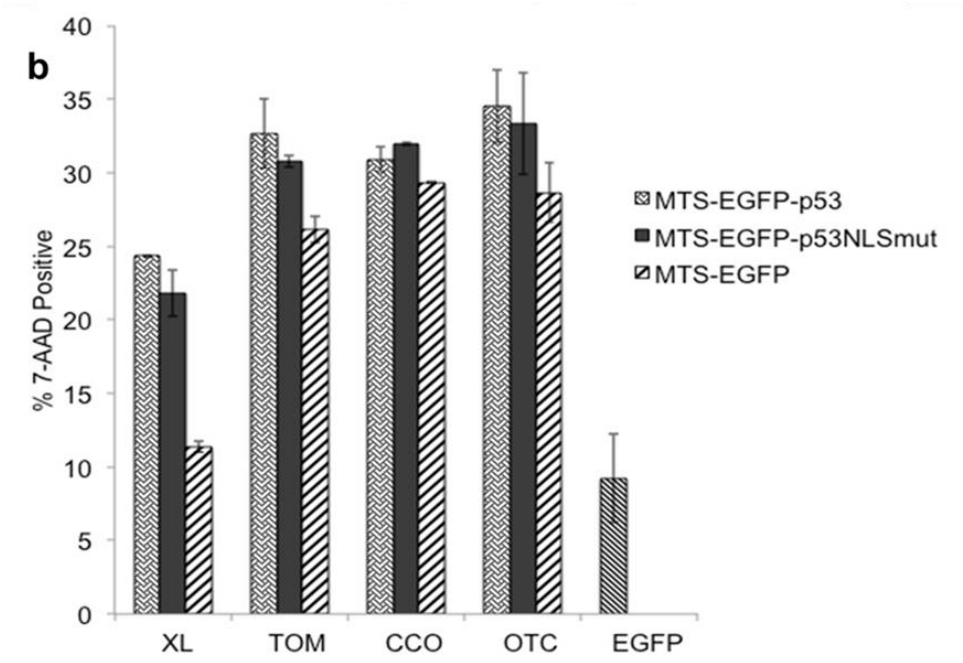

Figure S2. The 7-AAD assay was tested in (A) T47D and (B) MCF-7 cells 48 hours after transfection. Statistical analysis was performed by unpaired t-test. * $p<0.05$ for MTS-EGFP-p53 NLS mutation compared to its MTS-EGFP-p53. Except for CCO-EGFP-p53 NLS mutation in T47D cells all constructs with NLS mutation were not statistically significant from constructs without mutations. The T47D data is consistent with luciferase assay (Figure 3A) and pifithrin-α rescue experiment (Figure 8A).

2.7 Acknowledgements

This work was funded by NIH R01-CA151847. We acknowledge Katharina Opper, Geoff Miller, Andy Dixon, Ben Bruno, Rian Davis, David Woessner, and Shams Reaz for scientific discussions.

2.8 References

1. Erster S, Mihara M, Kim RH, Petrenko O, Moll UM. In vivo mitochondrial p53 translocation triggers a rapid first wave of cell death in response to DNA damage that can precede p53 target gene activation. Mol Cell Biol. 2004 Aug;24(15):6728-41.

2. Erster S, Moll UM. Stress-induced p53 runs a transcription-independent death program. Biochem Biophys Res Commun. [Review]. 2005 Jun 10;331(3):843-50.

3. Mihara M, Erster S, Zaika A, Petrenko O, Chittenden T, Pancoska P, et al. p53 has a direct apoptogenic role at the mitochondria. Mol Cell. 2003 Mar;11(3):577-90.

4. Chipuk JE, Kuwana T, Bouchier-Hayes L, Droin NM, Newmeyer DD, Schuler M, et al. Direct activation of Bax by p53 mediates mitochondrial membrane permeabilization and apoptosis. Science. 2004 Feb 13;303(5660):1010-4.

5. Zhao Y, Chaiswing L, Velez JM, Batinic-Haberle I, Colburn NH, Oberley TD, et al. p53 translocation to mitochondria precedes its nuclear translocation and targets mitochondrial oxidative defense protein-manganese superoxide dismutase. Cancer Res. 2005 May 1;65(9):3745-50.

6. Canugovi C, Maynard S, Bayne AC, Sykora P, Tian J, de Souza-Pinto NC, et al. The mitochondrial transcription factor A functions in mitochondrial base excision repair. DNA Repair. 2010 Oct 5;9(10):1080-9.

7. Vogelstein B, Lane D, Levine AJ. Surfing the p53 network. Nature. 2000 Nov 16;408(6810):307-10.

8. El-Deiry WS, Harper JW, O'Connor PM, Velculescu VE, Canman CE, Jackman J, et al. WAF1/CIP1 is induced in p53-mediated G1 arrest and apoptosis. Cancer Res. 1994 Mar 1;54(5):1169-74.

9. Harris SL, Levine AJ. The p53 pathway: positive and negative feedback loops. Oncogene. 2005 Apr 18;24(17):2899-908.

10. Marchenko ND, Zaika A, Moll UM. Death signal-induced localization of p53 protein to mitochondria. A potential role in apoptotic signaling. J Biol Chem. 2000 May 26;275(21):16202-12.

11. Tomita Y, Marchenko N, Erster S, Nemajerova A, Dehner A, Klein C, et al. WT p53, but not tumor-derived mutants, bind to Bcl2 via the DNA binding domain and induce mitochondrial permeabilization. J Biol Chem. 2006 Mar 31;281(13):8600-6.

12. Chipuk JE, Maurer U, Green DR, Schuler M. Pharmacologic activation of p53 elicits Bax-dependent apoptosis in the absence of transcription. Cancer Cell. 2003 Nov;4(5):371-81.

13. Leu JI, Dumont P, Hafey M, Murphy ME, George DL. Mitochondrial p53 activates Bak and causes disruption of a Bak-Mcl1 complex. Nat Cell Biol. 2004 May;6(5):443-50.

14. Pietsch EC, Leu JI, Frank A, Dumont P, George DL, Murphy ME. The tetramerization domain of p53 is required for efficient BAK oligomerization. Cancer Biol Ther. [Research Support, N.I.H., Extramural]. 2007 Oct;6(10):1576-83.

15. Green DR, Reed JC. Mitochondria and apoptosis. Science. 1998 Aug 28;281(5381):1309-12.

16. Reed JC. Cytochrome c: can't live with it--can't live without it. Cell. 1997 Nov 28;91(5):559-62.

17. Green DR, Evan GI. A matter of life and death. Cancer Cell. 2002 Feb;1(1):19-30.

18. Mossalam M, Dixon AS, Lim CS. Controlling subcellular delivery to optimize therapeutic effect. Ther Deliv. 2010 Jul 1;1(1):169-93.

19. Mihara M, Moll UM. Detection of mitochondrial localization of p53. Methods Mol Biol. 2003;234:203-9.

20. Shaulsky G, Goldfinger N, Ben-Ze'ev A, Rotter V. Nuclear accumulation of p53 protein is mediated by several nuclear localization signals and plays a role in tumorigenesis. Mol Cell Biol. 1990 Dec;10(12):6565-77.

21. Jiang P, Du W, Heese K, Wu M. The Bad guy cooperates with good cop p53: Bad is transcriptionally up-regulated by p53 and forms a Bad/p53 complex at the mitochondria to induce apoptosis. Mol and Cel Biol. 2006 Dec;26(23):9071-82.

22. Sansome C, Zaika A, Marchenko ND, Moll UM. Hypoxia death stimulus induces translocation of p53 protein to mitochondria. Detection by immunofluorescence on whole cells. FEBS Lett. 2001 Jan 19;488(3):110-5.

23. Dumont P, Leu JI, Della Pietra AC, 3rd, George DL, Murphy M. The codon 72 polymorphic variants of p53 have markedly different apoptotic potential. Nat Genet. 2003 Mar;33(3):357-65.

24. Marchenko ND, Wolff S, Erster S, Becker K, Moll UM. Monoubiquitylation promotes mitochondrial p53 translocation. EMBO J. 2007 Feb 21;26(4):923-34.

25. Von Heijne G. Mitochondrial targeting sequences may form amphiphilic helices. EMBO J. 1986 Jun;5(6):1335-42.

26. Koehler CM. New developments in mitochondrial assembly. Annu Rev Cell Dev Biol. 2004;20:309-35.

27. Roise D, Schatz G. Mitochondrial presequences. J Biol Chem. 1988 Apr 5;263(10):4509-11.

28. Wiedemann N, Frazier AE, Pfanner N. The protein import machinery of mitochondria. J Biol Chem. [Review]. 2004 Apr 9;279(15):14473-6.

29. Kaufmann T, Schlipf S, Sanz J, Neubert K, Stein R, Borner C. Characterization of the signal that directs Bcl-x(L), but not Bcl-2, to the mitochondrial outer membrane. J Cell Biol. 2003 Jan 6;160(1):53-64.

30. Pollack M, Leeuwenburgh C. Apoptosis and aging: role of the mitochondria. J Gerontology. 2001 Nov;56(11):B475-82.

31. Lindsay J, Esposti MD, Gilmore AP. Bcl-2 proteins and mitochondria--specificity in membrane targeting for death. Biochim Biophys Acta. [Review]. 2011 Apr;1813(4):532-9.

32. Rehling P, Brandner K, Pfanner N. Mitochondrial import and the twin-pore translocase. Nat Rev Mol Cell Biol. 2004 Jul;5(7):519-30.

33. Power SD, Lochrie MA, Patterson TE, Poyton RO. The nuclear-coded subunits of yeast cytochrome c oxidase. II. The amino acid sequence of subunit VIII and a model for its disposition in the inner mitochondrial membrane. J Biol Chem. 1984 May 25;259(10):6571-4.

34. Fabrizi GM, Sadlock J, Hirano M, Mita S, Koga Y, Rizzuto R, et al. Differential expression of genes specifying two isoforms of subunit VIa of human cytochrome c oxidase. Gene. 1992 Oct 1;119(2):307-12.

35. Isaya G, Fenton WA, Hendrick JP, Furtak K, Kalousek F, Rosenberg LE. Mitochondrial import and processing of mutant human ornithine transcarbamylase precursors in cultured cells. Mol Cell Biol. 1988 Dec;8(12):5150-8.

36. Dixon AS, Kakar M, Schneider KM, Constance JE, Paullin BC, Lim CS. Controlling subcellular localization to alter function: Sending oncogenic Bcr-Abl to the nucleus causes apoptosis. J Control Release.. 2009 Dec 16;140(3):245-9.

37. Bolte S, Cordelieres FP. A guided tour into subcellular colocalization analysis in light microscopy. J Microscopy. 2006 Dec;224(Pt 3):213-32.

38. Costes SV, Daelemans D, Cho EH, Dobbin Z, Pavlakis G, Lockett S. Automatic and quantitative measurement of protein-protein colocalization in live cells. Biophysical J.. 2004 Jun;86(6):3993-4003.

39. Adler J, Parmryd I. Quantifying colocalization by correlation: the Pearson correlation coefficient is superior to the Mander's overlap coefficient. Cytometry A. Aug;77(8):733-42.

40. Dixon AS, Miller GD, Bruno BJ, Constance JE, Woessner DW, Fidler TP, et al. Improved coiled-coil design enhances interaction with bcr-abl and induces apoptosis. Mol Pharm. 2012 Jan 1;9(1):187-95.

41. Jaskolski F, Mulle C, Manzoni OJ. An automated method to quantify and visualize colocalized fluorescent signals. J Neuroscience Methods. 2005 Jul 15;146(1):42-9.

42. Schafer JM, Lee ES, O'Regan RM, Yao K, Jordan VC. Rapid development of tamoxifen-stimulated mutant p53 breast tumors (T47D) in athymic mice. Clin Cancer Res. 2000 Nov;6(11):4373-80.

43. Alkhalaf M, El-Mowafy AM. Overexpression of wild-type p53 gene renders MCF-7 breast cancer cells more sensitive to the antiproliferative effect of progesterone. J Endocrinol. 2003 Oct;179(1):55-62.

44. Takahashi K, Sumimoto H, Suzuki K, Ono T. Protein synthesis-dependent cytoplasmic translocation of p53 protein after serum stimulation of growth-arrested MCF-7 cells. Mol Carcinog. 1993;8(1):58-66.

45. Mooney LM, Al-Sakkaf KA, Brown BL, Dobson PR. Apoptotic mechanisms in T47D and MCF-7 human breast cancer cells. Br J Cancer. 2002 Oct 7;87(8):909-17.

46. Chowdhury I, Tharakan B, Bhat GK. Caspases - an update. Comp Biochem Physiol B Biochem Mol Biol [Review]. 2008 Sep;151(1):10-27.

47. Yin Q, Park HH, Chung JY, Lin SC, Lo YC, da Graca LS, et al. Caspase-9 holoenzyme is a specific and optimal procaspase-3 processing machine. Mol Cell. 2006 Apr 21;22(2):259-68.

48. Loo DT, Rillema JR. Measurement of cell death. Meth Cell Biol. [Review]. 1998;57:251-64.

49. Koopman G, Reutelingsperger CP, Kuijten GA, Keehnen RM, Pals ST, van Oers MH. Annexin V for flow cytometric detection of phosphatidylserine expression on B cells undergoing apoptosis. Blood. 1994 Sep 1;84(5):1415-20.

50. Vermes I, Haanen C, Steffens-Nakken H, Reutelingsperger C. A novel assay for apoptosis. Flow cytometric detection of phosphatidylserine expression on early apoptotic cells using fluorescein labelled Annexin V. J Immun Meth. 1995 Jul 17;184(1):39-51.

51. Metkar SS, Wang B, Catalan E, Anderluh G, Gilbert RJ, Pardo J, et al. Perforin rapidly induces plasma membrane phospholipid flip-flop. PLoS One. 2011;6(9):e24286.

52. Schmid I, Krall WJ, Uittenbogaart CH, Braun J, Giorgi JV. Dead cell discrimination with 7-amino-actinomycin D in combination with dual color immunofluorescence in single laser flow cytometry. Cytometry. 1992;13(2):204-8.

53. Serrano MJ, Sanchez-Rovira P, Algarra I, Jaen A, Lozano A, Gaforio JJ. Evaluation of a gemcitabine-doxorubicin-paclitaxel combination schedule through flow cytometry assessment of apoptosis extent induced in human breast cancer cell lines. Jap J Cancer Res. 2002 May;93(5):559-66.

54. Komarov PG, Komarova EA, Kondratov RV, Christov-Tselkov K, Coon JS, Chernov MV, et al. A chemical inhibitor of p53 that protects mice from the side effects of cancer therapy. Science. 1999 Sep 10;285(5434):1733-7.

55. Liu X, Chua CC, Gao J, Chen Z, Landy CL, Hamdy R, et al. Pifithrin-alpha protects against doxorubicin-induced apoptosis and acute cardiotoxicity in mice. Am J Physiol. 2004 Mar;286(3):H933-9.

56. Hagn F, Klein C, Demmer O, Marchenko N, Vaseva A, Moll UM, et al. BclxL changes conformation upon binding to wild-type but not mutant p53 DNA binding domain. J Biol Chem. 2010 Jan 29;285(5):3439-50.

57. Strom E, Sathe S, Komarov PG, Chernova OB, Pavlovska I, Shyshynova I, et al. Small-molecule inhibitor of p53 binding to mitochondria protects mice from gamma radiation. Nat Chem Biol. 2006 Sep;2(9):474-9.

58. Vaseva AV, Moll UM. The mitochondrial p53 pathway. Biochim Biophys Acta. 2009 May;1787(5):414-20.

59. Schmidt O, Pfanner N, Meisinger C. Mitochondrial protein import: from proteomics to functional mechanisms. Nat Rev Mol Cell Biol. 2010 Sep;11(9):655-67.

60. Endo T, Kohda D. Functions of outer membrane receptors in mitochondrial protein import. Biochim Biophys Acta. 2002 Sep 2;1592(1):3-14.

61. Dolezal P, Likic V, Tachezy J, Lithgow T. Evolution of the molecular machines for protein import into mitochondria. Science. 2006 Jul 21;313(5785):314-8.

62. Mattaj IW, Englmeier L. Nucleocytoplasmic transport: the soluble phase. Annu Rev Biochem. 1998;67:265-306.

63. Gorlich D, Kutay U. Transport between the cell nucleus and the cytoplasm. Annu Rev Cell Dev Biol. 1999;15:607-60.

64. Davis JR, Kakar M, Lim CS. Controlling protein compartmentalization to overcome disease. Pharm Res. 2007 Jan;24(1):17-27.

65. Sattler M, Liang H, Nettesheim D, Meadows RP, Harlan JE, Eberstadt M, et al. Structure of Bcl-xL-Bak peptide complex: recognition between regulators of apoptosis. Science. 1997 Feb 14;275(5302):983-6.

66. Galluzzi L, Morselli E, Kepp O, Tajeddine N, Kroemer G. Targeting p53 to mitochondria for cancer therapy. Cell Cycle. 2008 Jul 1;7(13):1949-55.

3. The DNA binding domain of p53 is sufficient to trigger a potent apoptotic response at the mitochondria

Karina J. Matissek, Mohanad Mossalam, Abood Okal, Carol S. Lim

Molecular Pharmaceutics, August 23, 2013

First author contribution:

Research design: 85%

Experimental work: 80%

Data analysis and evaluation: 85%

Manuscript writing: 90%

3.1 Abstract

The tumor suppressor p53 is one of the most studied proteins in human cancer (1-3). While nuclear p53 has been utilized for cancer gene therapy, mitochondrial targeting of p53 has not been fully exploited to date (4, 5). In response to cellular stress, p53 translocates to the mitochondria and directly interacts with Bcl-2 family proteins including anti-apoptotic Bcl-XL and Bcl-2 and pro-apoptotic Bak and Bax (6). Anti-apoptotic Bcl-XL forms inhibitory complexes with pro-apoptotic Bak and Bax preventing their homo-oligomerization (7). Upon translocation to the mitochondria, p53 binds to Bcl-XL, releases Bak and Bax from the inhibitory complex and enhances their homo-oligomerization (8). Bak and Bax homo-tetramer formation disrupts the mitochondrial outer membrane, releases anti-apoptotic factors such as cytochrome c and triggers a rapid apoptotic response mediated by caspase induction (9). It is still unclear if the MDM2 binding domain (MBD), the proline-rich domain (PRD) and/or DNA binding domain (DBD) of p53 are the domains responsible for interaction with Bcl-XL (10-17). The purpose of this work is to determine if a smaller functional domain of p53 is capable of inducing apoptosis similarly to full length p53. To explore this question, different domains of p53 (MBD, PRD, DBD) were fused to the mitochondrial targeting signal (MTS) from Bcl-XL to ensure Bcl-XL specific targeting (18). The designed constructs were tested for apoptotic activity (TUNEL, Annexin-V, and 7-AAD) in 3 different breast cancer cell lines (T47D, MCF-7, MDA-MB-231), in a cervical cancer cell line (HeLa) and in non-small cell lung adenocarcinoma cells H1373. Our results indicate that DBD-XL (p53 DBD fused to the Bcl-XL MTS) reproduces (in T47D cells) or demonstrates increased apoptotic activity (in MCF-7, MDA-MB-231, and HeLa cells) compared to p53-XL (full length p53 fused to Bcl-XL MTS). Additionally, mitochondrial dependent apoptosis assays (TMRE, caspase-9), co-IP and over-expression of Bcl-XL in T47D cells suggest that DBD fused to XL MTS may bind to and inhibit Bcl-XL. Taken together, our data demonstrates for the first time that the DBD of p53 may be the minimally necessary domain for achieving apoptosis at the mitochondria in multiple cell lines. This work

highlights the role of small functional domains of p53 as a novel cancer biologic therapy.

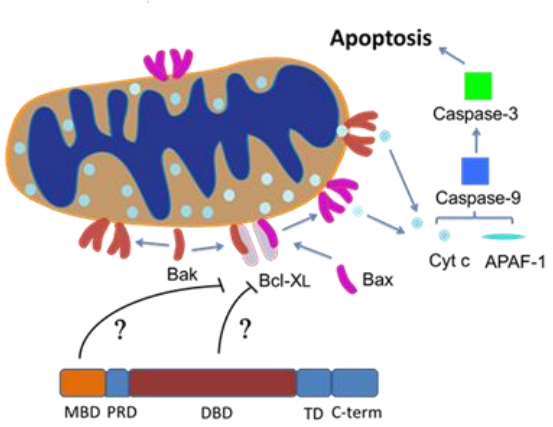

3.2 Introduction

The tumor suppressor p53 is one of the most commonly mutated genes in all cancers (1-3). Although nuclear-mediated transcriptional activity has been extensively characterized, mitochondrial targeting of p53 has yet to be fully exploited as a therapeutic approach (4, 5). The main advantage of targeting p53 to the mitochondria is its ability to trigger a rapid apoptotic response, while in the nucleus p53 first has to form a tetramer, bind to DNA, and initiate transcription of various apoptotic genes. As a consequence of stress, p53 translocates to the mitochondria and initiates apoptosis through mitochondrial outer membrane permeabilization (MOMP) (6). Mitochondrial p53 directly interacts with anti- and pro-apoptotic members of the Bcl-2 family of proteins located in the mitochondrial outer membrane. In apoptosis resistant cells, the anti-apoptotic members, Bcl-XL, Bcl-2 and Mcl-1 form heterodimers with pro-apoptotic proteins Bak and Bax, preventing apoptosis (7). To trigger MOMP, p53 binds to Bcl-XL, Bcl-2 and Mcl-1 and frees pro-apoptotic Bak and Bax allowing them to oligomerize (8). Homo-tetramer formation of Bak and Bax in the mitochondrial outer membrane triggers the release of various

pro-apoptotic proteins such as cytochrome c. APAF-1 and cytochrome c form the apoptosome and activate caspase-9 that can initiate the caspase cascade resulting in programmed cell death (9).

It is unclear which domains of p53 are directly responsible for triggering apoptosis at the mitochondria, presumably by interacting with anti-apoptotic Bcl-XL (11-15). The structure of p53 can be divided into amino terminus, DNA binding domain (DBD) and C-terminal region (Fig. 1A) (10). The amino terminus consists of the MDM2 binding domain (MBD) and the proline-rich domain (PRD). The C-terminal region encloses the tetramerization domain (TD) and three nuclear localization signals (NLS) (Fig. 1A) (10). It has been reported that the DBD binds to anti-apoptotic Bcl-XL in the mitochondrial outer membrane and the PRD functions as an enhancer that improves this binding (11-13). However, the MBD has been also proposed as a binding partner for Bcl-XL which is enhanced by the PRD (14-17).

To our knowledge, no one has attempted to target different domains of p53 to the mitochondria. Therefore, the purpose of this study is to determine if a smaller domain of p53 is capable of inducing apoptosis similar to full length p53 when targeted to the mitochondria. This will be achieved by fusing different domains of p53 (MBD, PRD, DBD, TD) to the mitochondrial targeting signal (MTS) from Bcl-XL (abbreviated XL) to ensure mitochondrial targeting (Fig. 1B) (18). This information will provide details on which domain is responsible for the rapid apoptotic response at the mitochondria. In addition to answering this mechanistic question, an overall goal is to decrease the size of the p53 construct for gene therapy purposes.

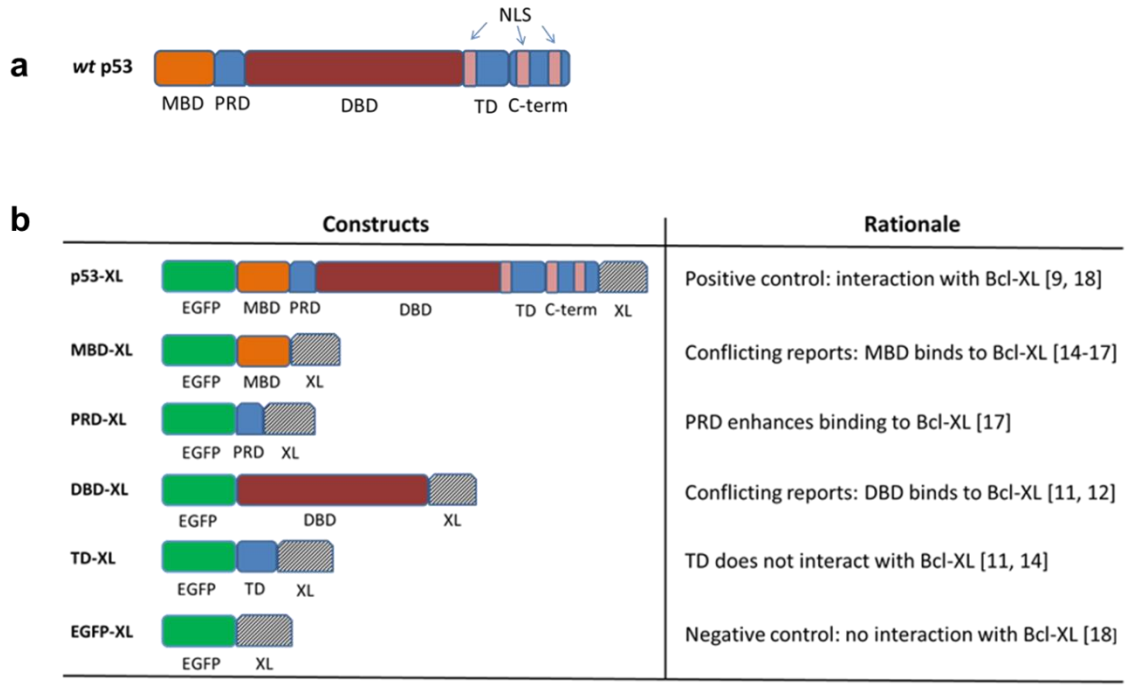

Figure 1: a: Schematic representation of wild type p53 (*wt* p53). The 393 amino acids of p53 are divided into amino terminus, DNA binding domain (DBD), and C-terminal region. The MDM2 binding domain (MBD) and proline-rich domain (PRD) are located in the amino terminus. The tetramerization (TD) domain and the nuclear localization signals (NLSs) are located in the C-terminus. b: Schematic representation of the main experimental constructs and controls including the rational for design. p53-XL shows the structure of full length p53 with the enhanced green fluorescence protein EGFP on the amino terminus and the MTS from Bcl-XL (XL) on the C-terminus. All the other constructs contain various combinations of the different domains of p53, in addition to EGFP and XL. The negative control (E-XL) consists of only EGFP and XL.

3.3 Materials and Methods

3.3.1 Cell Lines and Transient Transfections

1471.1 murine adenocarcinoma cells (gift of G. Hager, NCI, NIH), T47D human ductal breast epithelial tumor cells (ATCC, Manassas, VA), MCF-7 human breast adenocarcinoma cells (ATCC) (18), MDA-MB-231 human breast adenocarcinoma cells (a generous gift from Dr. David Bearss, University of Utah), HeLa human epithelial cervical adenocarcinoma cells (ATCC), and H1373 human non-small lung carcinoma cells (a kind gift from Dr. Andrea Bild, University of Utah) were grown as monolayers in DMEM (1471.1) and RPMI (T47D, MCF-7, MDA-MB-231, HeLa, H1373) (Invitrogen, Carlsbad, CA) supplemented with 10% FBS (Invitrogen), 1% penicillin-streptomycin (Invitrogen), 1% glutamine (Invitrogen) and 0.1% gentamycin (Invitrogen). T47D and MCF-7 cells were additionally supplemented with 4 mg/L insulin (Sigma, St. Louis, MO). Cells were maintained in a 5% CO2 incubator at 37ºC. 3.0 x 10^5 cells for T47D and MCF-7 cells, 1.0 x 10^5 cells for MDA-MB-231 and HeLa, 2.0 x 10^5 for H1373 were seeded in 6-well plates (Greiner Bio-One, Monroe, NC). Different amounts of cells were plated to account for varying cell growth rates in order to maximize transfection efficiency. Approximately 24 h after seeding, transfection was performed using 1 pmol of DNA per well and Lipofectamine 2000 (Invitrogen) following the manufacturer's recommendations.

3.3.2 Plasmid Construction

The main plasmids used in this work are depicted in Fig 1B.

pEGFP-p53ΔC-XL (p53ΔC-XL): The DNA encoding p53ΔC (amino acids 1-322), a truncated version of *wt* p53 that lacks the C-terminus, was amplified via PCR with the primers 5'-GCGCGCGCGCTCCGGAATGGAGGAGCCGCAGTCA-3' and 5'-GCGCGCGCGCGGTACCTCATGGTTTCTTCTTTGGCTGGGG-3' using previously

subcloned pEGFP-p53 (18) as the template DNA. p53ΔC was cloned into pEGFP-XL (E-XL) (18) using BspEI and KpnI sites.

pEGFP-DBD-XL (DBD-XL): The DNA encoding the DBD was amplified via PCR from pEGFP-p53-XL (p53-XL) (18) using 5'-CCGGGCCCGCGGTCCGGAACCTACCAGGGCAGCTACG-3' and 5'-CCGGGCCCGCGGGGTACCTTTCTTGCGGAGATTCTCTTCCT and cloned into E-XL (18) using BspEI and KpnI sites.

pEGFP-PRD-DBD-XL (PRD-DBD-XL): The DNA encoding the PRD-DBD was amplified using PCR from p53-XL (18) with the primers 5'-GCGCGCGCGCGGTACCGCTCCCAGAATGCCAGAGGC-3' and 5'-GCGCGCGCGCGGATCCTTTCTTGCGGAGATTCTCTT and cloned into E-XL (18) at the KpnI and BamHI site.

pEGFP-TD-XL (TD-XL): The DNA encoding the TD was amplified via PCR from previously subcloned p53-XL (18) using 5'-GCGCGCGCGCGGGATCCGGCTGGATGGAGAATATTTCACCCTTCA-3' and 5'-GCGCGCGCGCGGGAtCCTCACCCAGCCTGGGCATCCTT-3' and cloned into E-XL (18) at the BamHI site.

pEGFP-MBD-PRD-XL (MBD-PRD-XL): Previously subcloned p53-XL (18) was mutated via site-directed mutagenesis using the QuikChange II XL Site directed Mutagenesis Kit (Agilent, Santa Clara, CA) using 5' TCCCTTCCCAGAAAAGGTACCAGGGCAGCTACGGT-3' and its reverse complement to introduce an additional KpnI site (mutations underlined). Then the DBD and C-terminus were digested out using KpnI. Additionally, a frame shift mutation was corrected (one base pair deletion) by mutating the cloned plasmid using 5'-TCGAGCTATGGAAACATTTTCAGACCTATGGAAACTACTTCCTGAACGGAATTCTG-3' and its complementary strand via site-directed mutagenesis.

pEGFP-PRD-XL (PRD-XL): MBD-PRD-XL was mutated via site-directed mutagenesis using 5’ TTCACTGAAGACCCAGGTCCATCCGGAGCTCCCAGAATGCCAGA-3’ and its complementary strand to introduce an additional BspEI site. The MBD was cut out with BspEI to create PRD-XL

pEGFP-CC (E-CC): pEGFP-CC was subcloned as before (19).

pBFP-Bcl-XL (BFP-Bcl-XL): Bcl-XL was digested out from pSFFV-neo-Bcl-XL (gift from Dr. S. Korsmeyer, Addgene, Cambridge, MA) with EcoRI and cloned into the EcoRI site of the pTagBFP-C vector (Evrogen, Moscow, Russia). A frame shift mutation was conducted (one base pair addition) by mutating the cloned plasmid using 5’- TCTCGAGCTCAAGCTTCGAATTCATTGGACAATGG-3’ and its complementary strand via site-directed mutagenesis.

3.3.3 Mitochondrial Staining, Microscopy, and Image Analysis

Before live-cell imaging and mitochondrial staining of transfected cells was performed, media in live cell chambers was replaced with phenol red-free DMEM (Invitrogen) for 1471.1 cells or phenol red-free RPMI (Invitrogen) for T47D and MCF-7 cells containing 10% charcoal stripped fetal bovine serum (CS-FBS, Invitrogen). Cells were incubated with 150 nM MitoTracker Red FM (Invitrogen) for 15 min at 37 °C and protected from light. As previously, images were acquired using an Olympus IX71F fluorescence microscope (Scientific Instrument Company, Aurora, CO) with high quality (HQ) narrow band GFP filter (ex, HQ480/20 nm; em, HQ510/20 nm) and HQ:TRITC filter (ex, HQ545/30; em, HQ620/60) from Chroma Technology (Brattleboro, VT) with a 40× PlanApo oil immersion objective (NA 1.00) on an F-View Monochrome CCD camera (19-21).

ImageJ software and JACoP plugin was used to analyze images for mitochondrial stain overlap with EGFP fusion constructs (18, 22-24). As previously, JACoP was

used to generate the colocalization statistic [i.e., Pearson's correlation coefficient (PCC) post Costes' automatic threshold algorithm] (23-27). PCC evaluates correlation between pairs of individual pixels from EGFP and MitoTracker stained cells. The higher the PCC value, the higher the correlation. According to Costes a PCC value of 0.6 or greater determines colocalization between a cellular compartment and the designed protein (25). Spatial representations of pixel intensity correlation have been generated using Colocalization Color map (ImageJ) for increased visual clarity of mitochondrial localization of the EGFP-fused constructs (28). Microscopy was repeated in triplicate (n = 3), and 10 cells were analyzed for each construct.

3.3.4 7- AAD Assay

Transfected T47D, MCF-7, MDA-MB-231, HeLa and H1373 cells were pelleted and resuspended in 500 µL PBS (Invitrogen) containing 1 µM 7-aminoactinomycin D (7-AAD) (Invitrogen) for 30 min prior to analysis following the recommended protocol from the manufacturer. The assay was performed 48 h after transfection for T47D (18), MCF-7 (18) and H1373 and 24 h after transfection for MDA-MB-231 and HeLa. Only EGFP positive cells were analyzed by using the FACS Canto-II (BD-BioSciences, University of Utah Core Facility) with FACS Diva software. EGFP and 7-AAD were excited with the 488 nm laser, and were detected at 507 nm and 660 nm, respectively. Independent transfections of each construct were tested three times (n=3).

3.3.5 Annexin V Assay

48 h after transfection, T47D cells were pelleted and resuspended in 400 µL of annexin-V binding buffer (Invitrogen) and incubated with 5 µL of annexin-APC (annexin-V conjugated to allophycocyanin, Invitrogen) for 15 min as before (18). Only transfected cells were analyzed as mentioned in 7-AAD assay. EGFP and APC

were excited at 488 nm and 635 nm wavelengths, respectively and detected at their corresponding 507 nm and 660 nm wavelengths. Independent transfections of each construct were tested three times (n=3).

3.3.6 TUNEL Assay

T47D cells were harvested 48 h after transfection. In situ Death Detection Kit, TMR red (Roche, Mannheim, Germany) was used following manufacturer's recommendations as before (18, 24). Cells were resuspended in PBS (Invitrogen) and analyzed via the FACSAria-II (BD-Biosciences, University of Utah Core Facility). EGFP and TMR red were excited at 488 nm and 563 nm, respectively, and FACSDiva software was used to analyze the data. Independent transfections of each construct were tested three times (n=3).

3.3.7 Colony Forming Assay (CFA)

Transfected T47D cells were harvested 24h post transfection and resuspended in RPMI (Invitrogen) at a concentration of 3.0 x 10^5 cells/mL. The Cytoselect® 96-well cell transformation assay (Cell Biolabs, San Diego, CA) was used following manufacturer's recommendations. Equal amount of 1.2% Agar Solution, 2X DMEM/20% FBS media, and cell suspension (1:1:1) were mixed and 75 µL of the mixture was added to a 96-well plate containing a solidified base agar layer (50 µL of previously solidified1.2% Agar Solution), and allowed to solidify at 4ºC for 15 min. The following steps were performed according to the manufacture's recommendations. A Spectra Max M2 plate reader (Molecular Devices, Sunnyvale, CA) was used to detect fluorescence using a 485/520 nm filter set. Independent transfections of each construct were tested three times (n=3).

3.3.8 TMRE Assay

36 h after transfection T47D cells were incubated with 100 nM tetramethylrhodamineethylester (TMRE) (Invitrogen) for 30 min at 37ºC (29). T47D cells were pelleted and resuspended in 300 µL annexin-V binding buffer (1X) (Invitrogen). Only EGFP positive cells were analyzed by using the FACS Canto-II (BD- BioSciences, University of Utah Core Facility) with FACS Diva software. EGFP was excited with the 488 nm laser with emission filter 530/35 and TMRE was excited with the 561 nm laser with the emission filter 585/15. Mitochondrial depolarization (loss in TMRE intensity) correlates with an increase in MOMP. Independent transfections of each construct were tested three times (n=3).

3.3.9 Caspase-9 Assay

T47D cells were probed 48 h after transfection using SR FLICA Caspase-9 Assay Kit (Immunochemistry Technologies, Bloomington, MN) (30, 31). Cells were incubated with SR FLICA Caspase-9 reagent for 60 min per manufacturer's recommendations, pelleted and resuspended in 300 µL 1X wash buffer (Immunochemistry Technologies). Only EGFP positive cells were analyzed by using the FACS Canto-II (BD- BioSciences, University of Utah Core Facility) with FACS Diva software. EGFP and FLICA were excited with the 488 nm (emission filter 530/35) and the 561 laser (emission filter 585/15), respectively. Independent transfections of each construct were tested three times (n=3).

3.3.10 Co-Immunoprecipitation (Co-IP)

Anti-GFP antibody (ab290, Abcam) was coupled to dynabeads using Dynabeads Antibody Coupling Kit (Invitrogen). 24 h post transfection, T47D cells were prepared using the Dynabeads Co-Immunoprecipitation Kit (Invitrogen). Cell pellets were lysed using extraction buffer B (1 x IP, 100 nM NaCl, 2 mM MgCl2, 1 mM DTT, 1% protease inhibitor). The lysate was incubated for 30 min at 4ºC with 1.5 mg of

dynabeads coupled with anti-GFP antibody, and co-IP was performed per the company's protocol. The final protein complex was denatured and western blot was performed (19) by using Bcl-XL antibody (ab 2568, Abcam).

3.3.11 Rescue Experiment using BFP-Bcl-XL

T47D cells were co-transfected with 1 pmol of EGFP constructs and 1 pmol of BFP-Bcl-XL (BFP tag is necessary for gating Bcl-XL transfected cells). 48 h after transfection the 7-AAD assay was performed as described above. FACSCanto-II (BioSciences, University of Utah Core Facility) and FACSDiva software were used for EGFP and BFP gating. Excitation was set at 488 nm, and detected at 507 nm and 660 nm for EGFP and 7-AAD, respectively. BFP was excited at 405 nm and detected at 457 nm. Independent transfections of each construct were tested three times (n=3).

3.3.12 Statistical Analysis

All experiments were conducted in a triplicate (n=3). Statistical significance was determined by one-way analysis of variance (ANOVA) with Tukey's or Bonferroni's post test as indicated in figure legends; Student t-test was used to analyze the rescue experiment data. The degree of colocalization was analyzed using odds ratio with Pearson's Chi-square. A p value <0.05 was considered significant.

3.4 Results

3.4.1 Mitochondrial localization of single domain constructs

Different domains of p53 (Fig. 1B) were fused to the MTS from Bcl-XL (abbreviated XL) (18) and tested for their mitochondrial localization. Mitochondrial targeting of these constructs (Fig. 1) was determined by fluorescence microscopy as previously

(18, 23, 24). Figure 2A illustrates representative 1471.1 cells, which are large in size, spread well, and are optimal for microscopy. However, similar microscopy results were observed in T47D cells (data not shown). Figure 2B shows colocalization of the EGFP fused constructs with mitochondria which were generated using Pearson's correlation coefficient (PCC) following the example of Bolte and Cordelières and graphed for each construct (22, 25, 26). PCC values range from +1 (perfect correlation) to -1 (anticorrelation), and a PCC value of zero represents random distribution (22). Costes et al. have shown that a PCC of 0.6 or greater defines colocalization, or co-compartmentalization (Figure 2B) (25). Figure 2 shows that all designed single domain constructs translocate into the mitochondria, as expected. EGFP served as negative control for colocalization analysis, and there was no colocalization between EGFP alone and the mitochondria. Even though p53 is a nuclear protein containing three nuclear localization signals (NLSs), the XL MTS is strong enough to overcome nuclear targeting and directs p53-XL to the mitochondria (Fig. 1 and ref. (18)).

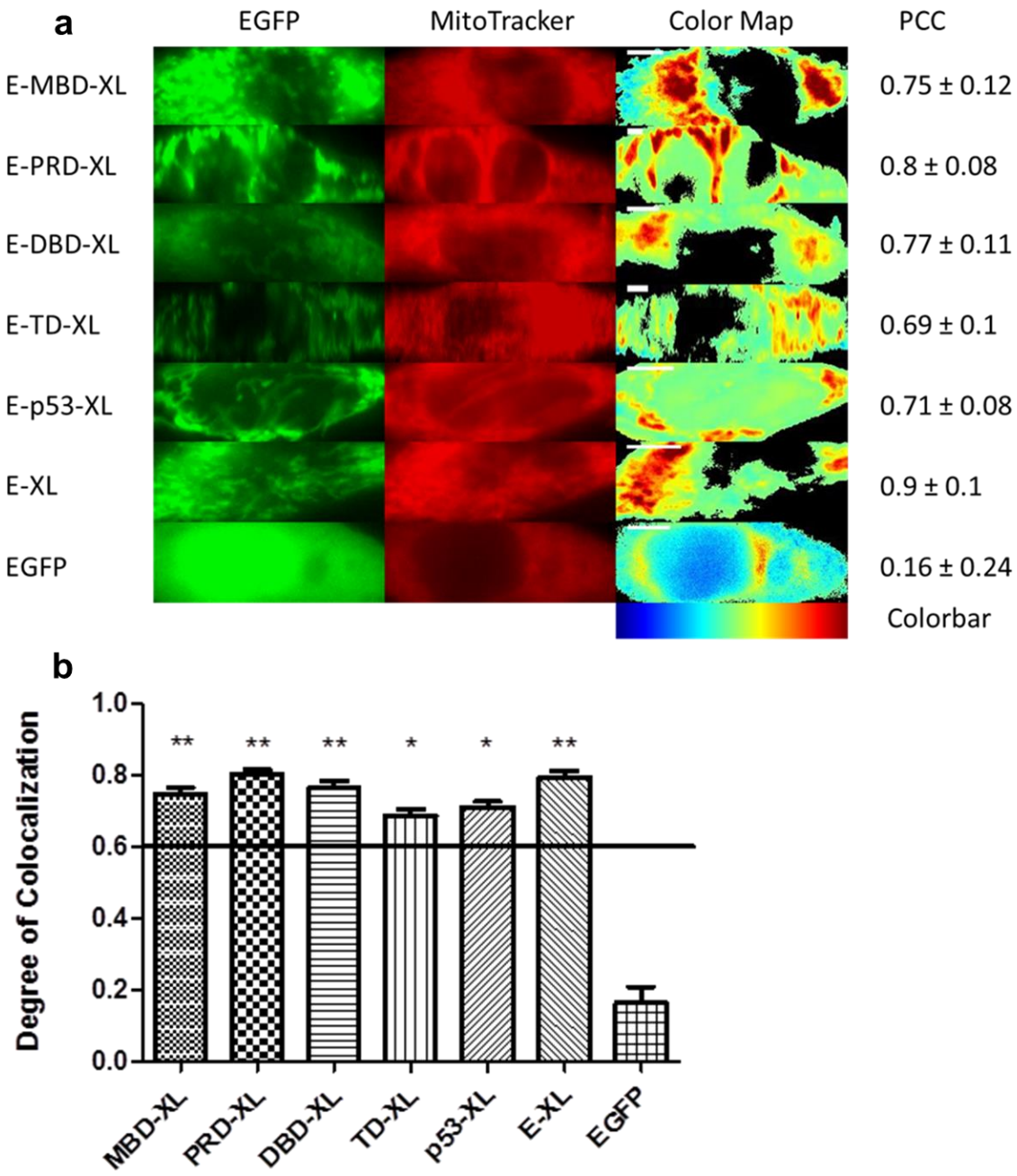

Figure 2: Colocalization of EGFP constructs and MitoTracker Red mitochondrial stain in 1471.1 cells. (A) Representative images of MBD-XL, PRD-XL, DBD-XL, TD-XL, p53-XL, E-XL and EGFP are shown in the left column with images of MitoTracker Red distribution in the middle column. The “EGFP” and “MitoTracker”

columns have been false colored green and red, respectively. Enhanced visualization of colocalized pixels is rendered in the “Color Map” column. Warm colors depict pixels with highly correlated intensity and spatial overlap while cool colors are indicative of anticorrelation or random correlation (color bar for interpretation is shown below column). Corresponding PCC values are shown in the right column. White scale bars are all 10 μm. (B) The degree of colocalization is represented by PCC following Costes’ approach. All constructs with values higher than 0.6 are considered highly colocalized with mitochondrial stain MitoTracker Red. Statistical analysis was performed by using odds ratio with Pearson’s Chi-square. The adjusted odds ratio for PCC value of 0.6 was compared with each sample. *$p < 0.05$, and **$p < 0.01$comparing odds ratio of lowest value for samples with odds ratio of 1 for PCC of 0.6.

3.4.2 Screening the mitochondrial activity of different p53 domains via 7-AAD

To determine if a subdomain of p53 was capable of evoking a similar apoptotic activity as wild type p53, different domains of p53 (Fig. 1B) fused to XL and combinations of them were tested for apoptosis using the 7-AAD viability assay in T47D human breast cancer cells. 7-AAD is a late apoptosis/necrosis assay which allows for distinguishing between apoptotic/necrotic (ruptured plasma membrane) and healthy (intact plasma membrane) cells. If the plasma membrane is disrupted, the 7-AAD dye intercalates with nuclear DNA of apoptotic/necrotic cells (32, 33). Figure 3 demonstrates that all constructs containing DBD (PRD-DBD-XL, DBD-XL, and p53ΔC-XL) are statistically higher than the negative control E-XL. Additionally, these three constructs are not statistically different from p53-XL (positive control) indicating that all constructs containing the DBD show similar apoptotic potential to p53-XL (Fig. 3). Further, MBD-XL, MBD-PRD-XL, and PRD-XL are not statistically significant from the negative control E-XL suggesting no apoptotic activity (Fig. 3). Interestingly, TD-XL is statistically different from the negative controls but is also significantly lower than p53-XL (Fig. 3).

Data from figure 3 illustrate that there is no difference in activity between the single domains (MBD-, PRD-, DBD-, TD; 1st, 3rd, 5th, 6th bars, respectively) versus combinations of the domains (MBD-PRD, PRD-DBD, p53ΔC; 2nd, 4th, 7th bars, respectively) when fused to XL. Therefore, we proceeded with the single domain constructs (i.e. MBD-XL, PRD-XL, DBD-XL, and TD-XL) for the remaining experiments.

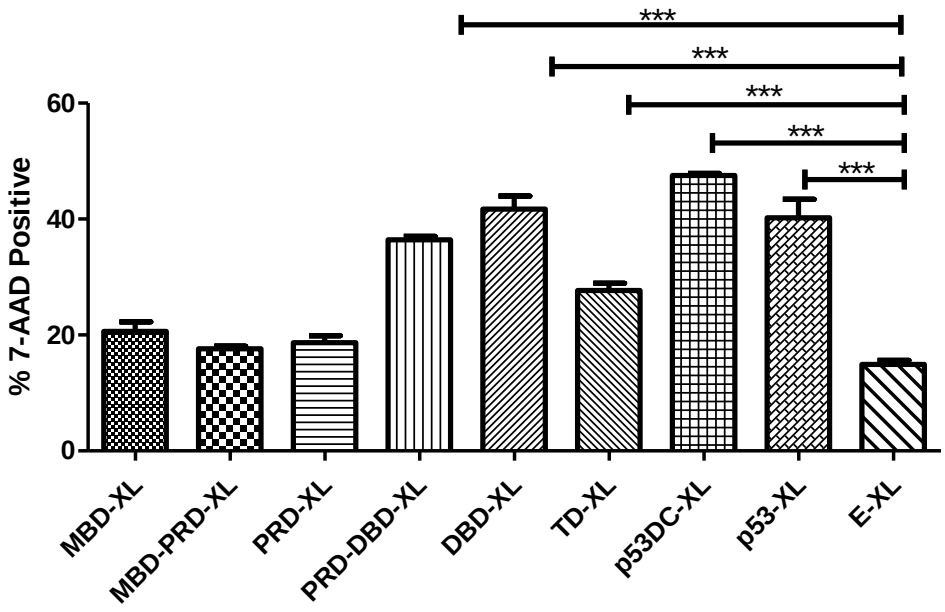

Figure 3: The 7-AAD assay was analyzed in T47D cells 48 h after transfection. Statistical analysis were conducted by one-way ANOVA with Tukey's post test. ***p < 0.001. PRD-DBD-XL, DBD-XL, p53ΔC-XL and p53-XL were not statistically significant from each other. MBD-XL, MBD-PRD-XL, PRD-XL, and TD-XL are statistically significantly lower than p53-XL.

3.4.3 Exploring the apoptotic potential of designed constructs

To test the apoptotic potential of our designed single domain constructs (Fig. 1B), the externalization of phoshatidylserine on the cell surface of apoptotic cells was measured via annexin V staining 48 h after transfection (18, 34). DBD-XL showed a

significantly higher apoptotic response than p53-XL (Fig 4A). Additionally, both constructs were significantly higher than the negative control E-XL whereas MBD-XL, PRD-XL and TD-XL were not statistically significant from the negative control (Fig 4A).

Further, the fragmentation of nuclear DNA was measured utilizing terminal deoxynucleotidyl transferase dUTP labeling (TUNEL) which tags the terminal end of nucleic acids. DNA fragmentation occurs when a cell is undergoing apoptosis, and the cellular DNA is cleaved by caspases (35). The TUNEL assay was conducted 48 h after transfection. Figure 4B shows that both p53-XL and DBD-XL have similar activities and are significantly higher than E-XL while MBD-XL, PRD-XL and TD-XL are not statistically different from the negative control.

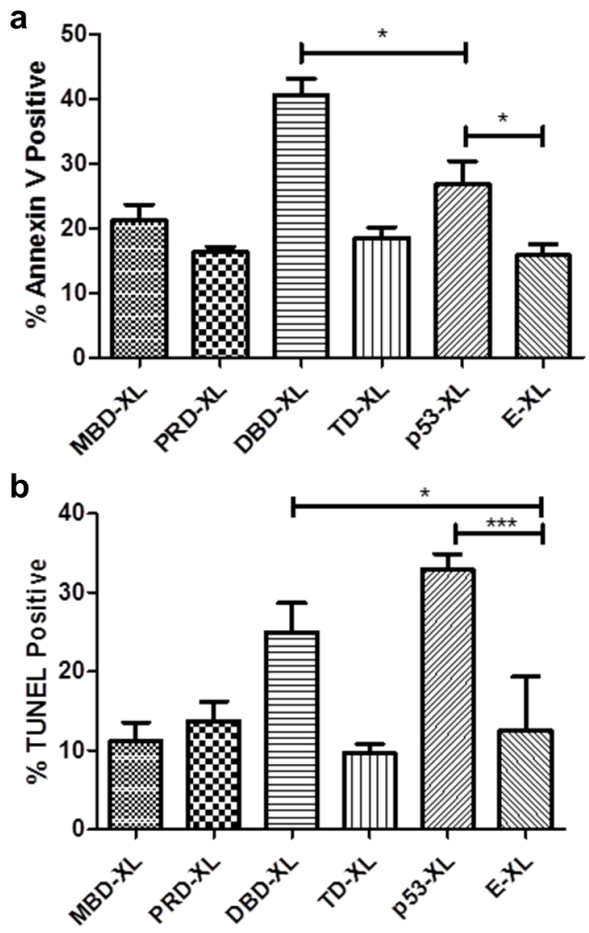

Figure 4: (A) Apoptotic potential was tested in T47D cells 48 h after transfection via annexin V assay. Statistical analysis was performed using one-way ANOVA with Tukey's post test with * $p < 0.05$. (B) Apoptotic potential was tested in T47D cells 48 h after transfection via TUNEL-assay. Statistical analysis was performed using one-way ANOVA with Tukey's post test with * $p < 0.05$, *** $p < 0.001$. p53-XL and DBD-XL were not statistically significant from each other. MBD-XL, PRD-XL, and TD-XL are statistically significantly lower than p53-XL.

3.4.4 Testing the oncogenic potential

To test the potential of designed constructs to inhibit the transforming ability of cancer cells, a colony forming assay was carried out in T47D cells eight days after treatment. As expected, p53-XL and DBD-XL showed significant decrease in transformative ability of T47D cells represented by fewer colonies (reduction in relative fluorescence units) compared to E-XL (Fig. 5). All the other small domain constructs failed to reduce cell proliferation similar to the negative control E-XL.

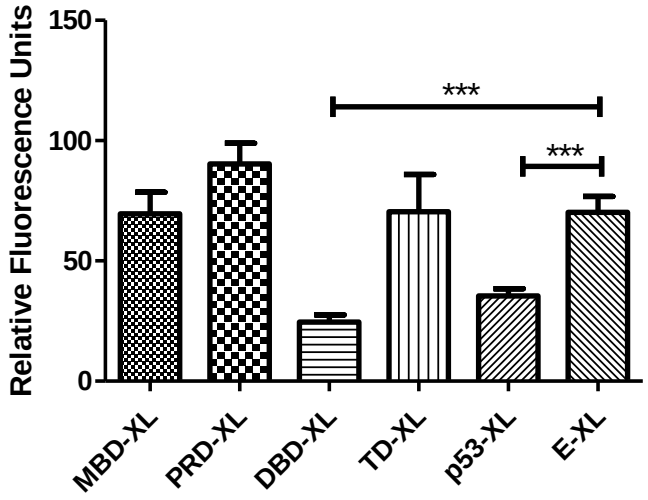

Figure 5: Transformative ability of T47D cells was determined 8 d after transfection of T47D cells via colony forming assay. Statistical analysis was accompanied using one-way ANOVA with Tukey's post test *** $p < 0.001$.

3.4.5 The ability of DBD-XL to induce late stage apoptosis is not cell line specific

To ensure that the ability of DBD-XL to induce apoptosis is not cell line- or cancer cell type specific, a 7-AAD assay was conducted in breast cancer cells (MCF-7, MDA-MB-231), cervical adenocarcinoma cells (HeLa) and human non-small cell lung adenocarcinoma (H1373). T47D and MDA-MB-231 both express mutant p53, with the mutations restricted to the DBD (L194F in T47D (36) and R280L in MDA-MB-231 (37)). These mutations reduce the activity of tumor suppressor activity substantially and cause these cells to be more resistant to apoptosis than MCF-7 and HeLa (38). Additionally, MCF-7 harbor mislocalized p53 in the cytoplasm (38), HeLa have endogenous *wt* p53 (39) and H1373 are p53 null (40).

Since MDA-MB-231 and HeLa are highly proliferating cells, both cell lines were assayed 24 h after transfection while T47D, MCF-7 and H1373 cells were assayed 48 h post transfection (optimal time points determined empirically).

Interestingly, DBD-XL showed significantly higher apoptotic activity compared to p53-XL in MCF-7 (Fig. 6A), MDA-MB-231(Fig. 6B) and H1373 (Fig. 6D). In HeLa cells, DBD-XL (and PRD-XL) were both statistically significant from p53-XL (Fig. 5C). These results are consistent with the apoptosis data from T47D cells (Figs. 3, 4A, and 4B) and show that DBD-XL is capable of inducing late stage apoptosis in four cell lines which differ in their endogenous p53 status, similarly to p53-XL.

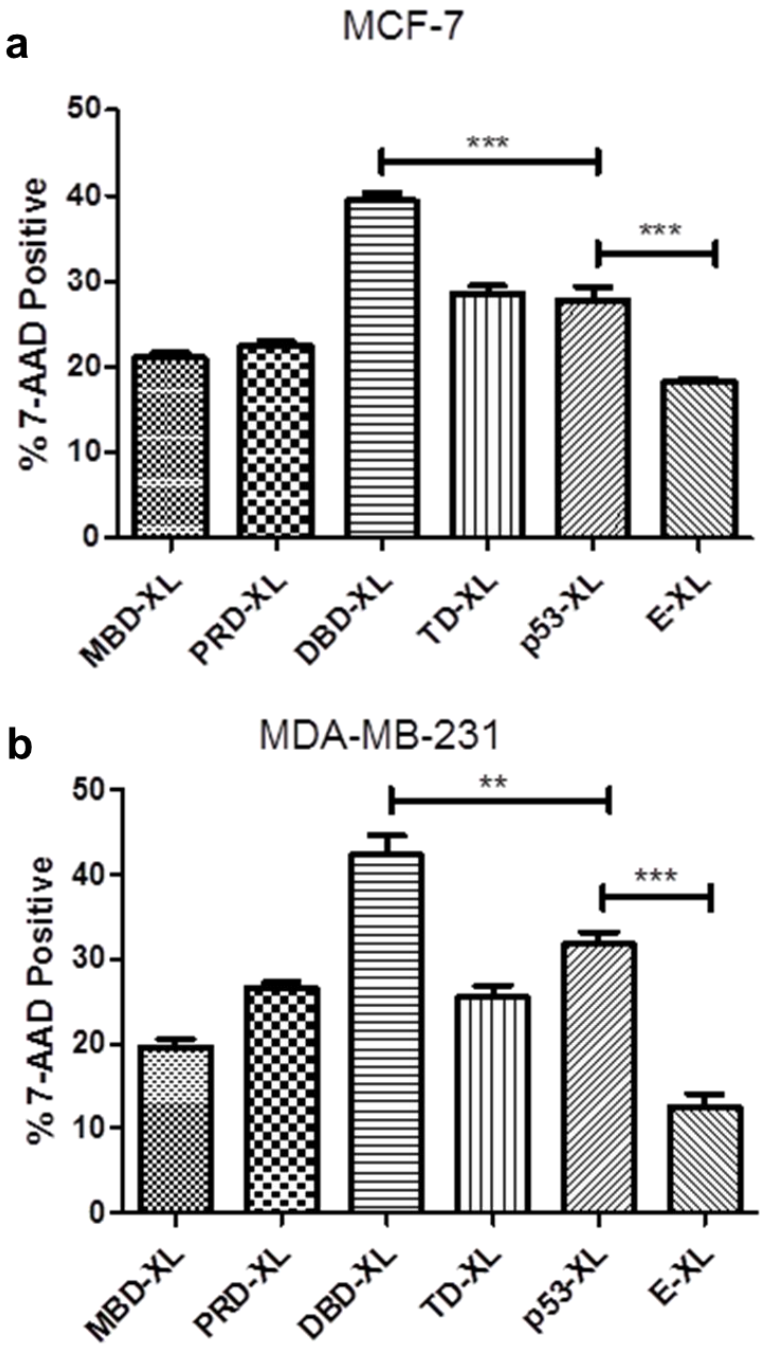
a
MCF-7
% 7-AAD Positive
50
40
30
20
10
0
***
***
MBD-XL
PRD-XL
DBD-XL
TD-XL
p53-XL
E-XL
b
MDA-MB-231
% 7-AAD Positive
50
40
30
20
10
0
**
***
MBD-XL
PRD-XL
DBD-XL
TD-XL
p53-XL
E-XL

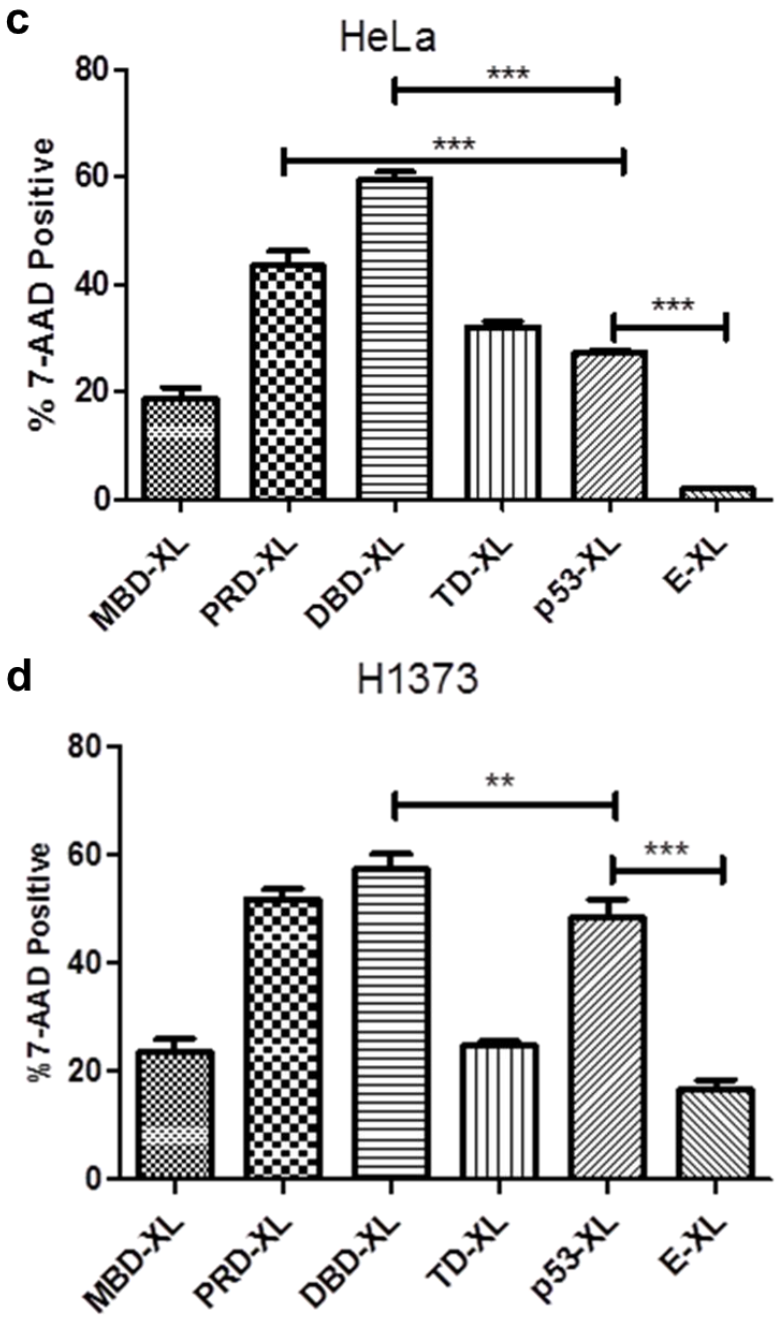

Figure 6: 7-AAD assay was conducted in (A) MCF-7, (B) MDA-MB-231, (C) HeLa and (D) H1373. Statistical analysis was performed using one-way ANOVA with Tukey's post test ** $p < 0.01$ and *** $p < 0.001$.

3.4.6 The apoptotic activity of DBD-XL is triggered via the mitochondrial/ intrinsic pathway

To determine that constructs-induced apoptotic effects are through the mitochondria TMRE and caspase-9 assays were performed. The DBD-XL was the only single domain construct that showed the same or higher apoptotic potential as p53-XL consistently in all tested cell lines. Therefore, we proceeded to investigate only the mechanism for DBD-XL compared to p53-XL for our further studies.

To ensure that DBD-XL causes MOMP in the same manner as p53-XL, the TMRE assay (analogous to the JC-1 assay) was used (41). TMRE is a cell-permeant, cationic, red-orange fluorescent dye that rapidly accumulates in mitochondria of living cells due to the negative mitochondrial membrane potential ($\Delta\Psi m$) of intact mitochondria compared to cytosol (29, 42, 43). Mitochondrial depolarization results in a loss of TMRE from mitochondria and a decrease in mitochondrial fluorescence intensity (FI) (42). The mitochondrial membrane permeabilization (loss of FI) was illustrated as %MOMP induction on the y-axis. DBD-XL and p53-XL have similar activity and are significantly higher than E-XL (Fig. 7A).

Further the activation of caspase-9 was measured. Caspase-9 is only triggered through the intrinsic apoptotic pathway. Once cytochrome c is released from the mitochondria, caspase-9 is the first effector caspase downstream of cytochrome c (44). Caspase-9 itself cleaves the peptide sequence leucine-glutamic acid-histidine-aspartic acid (LEHD) which is used in the caspase-9 assay to measure the intrinsic apoptotic pathway (45). DBD-XL and p53-XL show higher caspase-9 activation than E-XL (Fig. 7B). However, p53-XL triggers caspase-9 activation significantly more than DBD-XL (Fig. 7B). A proposed explanation for this effect will be explained further in the discussion.

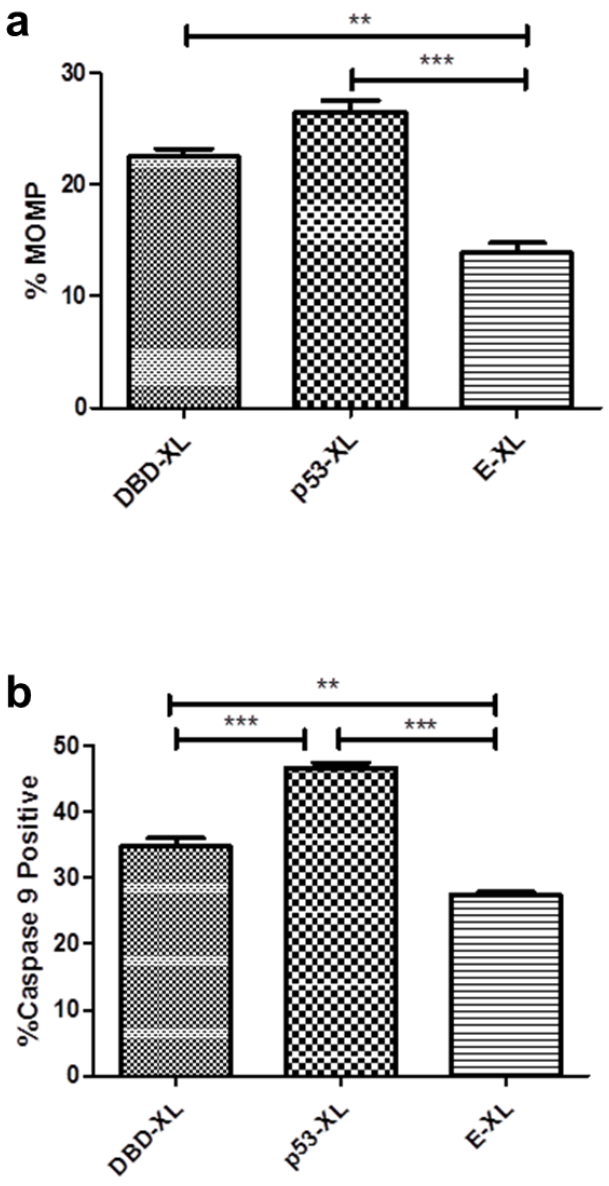

Figure 7: (A) Mitochondrial depolarization correlates with an increase in MOMP (as measured by TMRE). T47D cells were transfected with mitochondrial constructs and assayed using TMRE 36 h post transfections. (B) The activation of caspase-9 was analyzed 48 h following transfection of T47D cells. Statistical analysis was performed by using one-way ANOVA with Bonferroni's post test ** $p < 0.01$ and *** $p < 0.001$.

3.4.7 Investigating the apoptotic mechanism via co-IP and overexpression of Bcl-XL

To explore the apoptotic mechanism of our constructs, a co-IP was conducted (Fig. 8A). p53-XL, E-XL and E-CC (a negative control that does not contain the XL signal (19)) were transfected into T47D cells. T47D cells express the highest amount of endogenous Bcl-XL protein compared to MCF-7, MDA-MB-231 and HeLa (see the Supporting Information: S1). Approximately 24 h after transfection cells were lysed and incubated with anti-GFP antibody. A western blot was performed against EGFP (which is fused to all the constructs) and against Bcl-XL. Endogenous Bcl-XL (26 kDa) was expected to co-immunoprecipitate with exogenous p53-XL (75 kDa) due to its ability to induce apoptosis, while Bcl-XL should not co-immunoprecipitate with the negative control E-XL. Surprisingly, Bcl-XL co-immunoprecipitated with E-XL (32 kDa) just as p53-XL did (Fig. 8A, lane 1 and 2). To address if the binding is due to the mitochondrial targeting signal which was originally taken from the Bcl-XL protein, another negative control E-CC was used, which does not contain a MTS. EGFP (27 kDa) could not be used as a negative control because it is too close in size to Bcl-XL (26 kDa) and would not be distinguishable on the gel. Bcl-XL did not co-immunoprecipitate with E-CC (Fig 8A, lane 3) implying that the binding of E-XL to Bcl-XL was due to the XL mitochondrial targeting signal.

To further explore the apoptotic mechanism of DBD-XL and p53-XL at the mitochondria, Bcl-XL was overexpressed in T47D cells. The apoptotic activity was measured by 7-AAD. Cells transfected with just p53-, DBD-, or E-XL were compared to cells cotransfected with either of these constructs and with BFP-Bcl-XL. It was expected that the apoptotic potential of the constructs that are undergoing apoptosis through the p53/Bcl-XL pathway would be rescued by Bcl-XL overexpression. Indeed, DBD-XL and p53-XL apoptotic activities were significantly reduced when BFP-Bcl-XL was cotransfected (Fig. 8B). However, E-XL was not rescued by cotransfection of BFP-Bcl-XL (Fig. 8B).

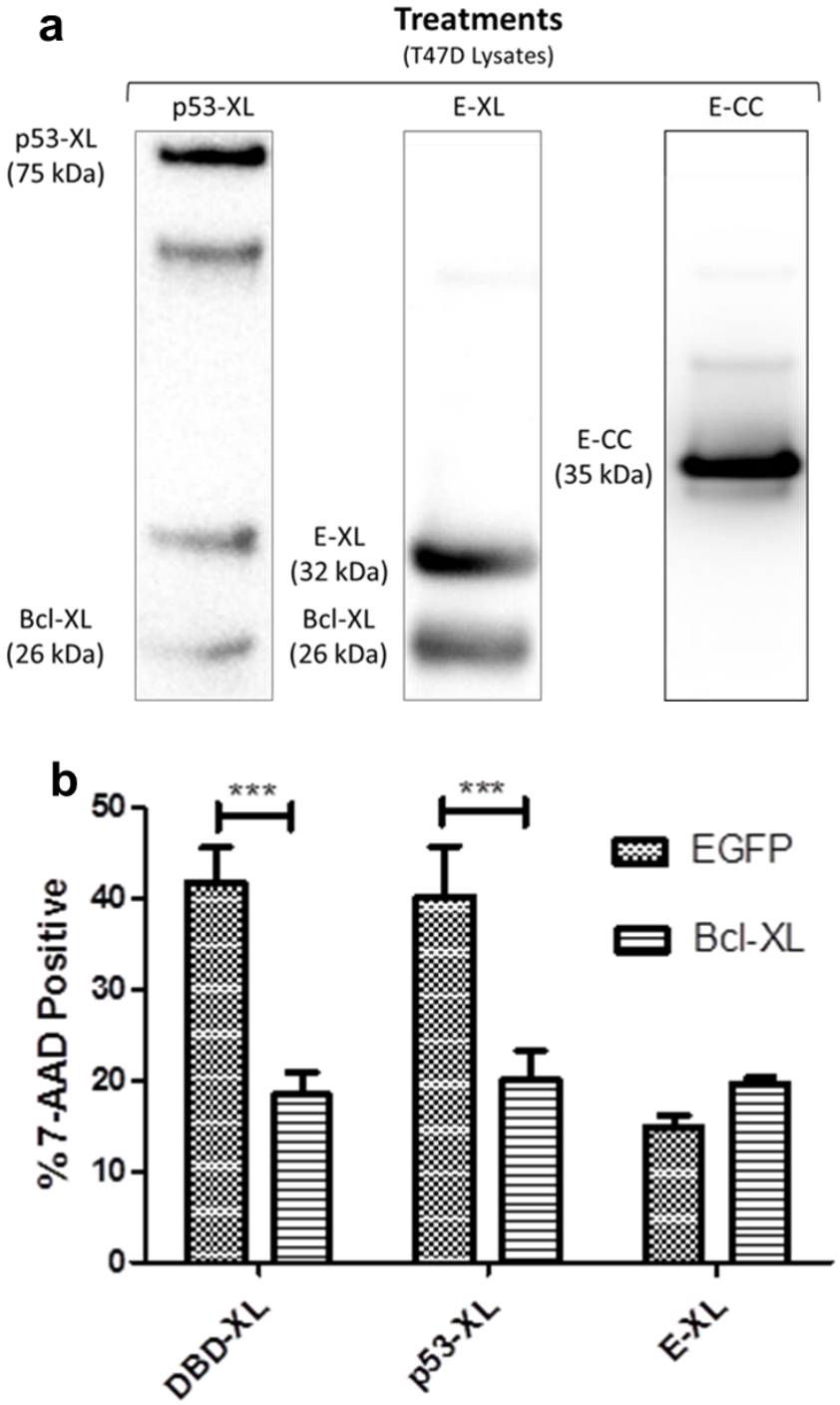

Figure 8: (A) Representative cropped western blot of protein complexes co-immunoprecipitated using anti-GFP antibody. Lane 1, exogenous p53-XL (75 kDa)

which was transfected into T47D cells co-immunoprecipitates with endogenous Bcl-XL (26 kDa). Lane 2, exogenous E-XL (32 kDa) co-immunoprecipitates with exogenous Bcl-XL (26 kDa). Lane 3 exogenous E-CC (35 kDa) fails to co-immunoprecipitate with endogenous Bcl-XL. Unlabeled bands are nonspecific binding. (B) Rescue experiment using Bcl-XL. 7-AAD assay was conducted 48 h post transfection in T47D cells. Statistical analysis was tested via unpaired t-test ** $p < 0.01$ and *** $p < 0.001$.

3.5 Discussion

Our laboratory has previously shown that targeting p53 to anti-apoptotic Bcl-XL is best achieved by using the MTS from Bcl-XL (18). Additionally, we validated that the XL signal is the only MTS that has no inherent toxicity by itself since it is targeting the outer surface of the mitochondrial outer membrane (18). Mitochondrial targeting of proteins to this region does not disrupt the sensitive balance of the mitochondria as reported with other MTSs (46-49). As an approach to determine which domain of p53 is capable of inducing apoptosis similar to p53-XL, different domains of p53 were fused to XL. To our knowledge, this is the first attempt to target different domains of p53 to the mitochondria.

Here, we have shown that our designed constructs translocate to the mitochondria (Fig. 2) and that any construct that contains the DBD of p53 is capable of inducing apoptosis similar to *wt* p53 (Fig. 3). It has been suggested that a combination of different domains of p53 is necessary for its apoptotic function and interaction with Bcl-XL at the mitochondria (11-13). For instance, the PRD is thought to enhance the binding of p53 to Bcl-XL (17). However, our data (Fig. 3) clearly validates that the DBD region without the PRD region of p53 is sufficient to induce the full mitochondrial apoptotic function of p53. Even though the PRD was reported to enhance the binding of MBD and DBD to Bcl-XL, it did not have any effect on

increasing the apoptotic potential. Hence, individual domains of p53 (Fig.1B) instead of combinations of domains were used in the remaining apoptotic assays.

Since the 7-AAD assay (Fig. 3) does not distinguish between apoptotic and necrotic cells, early apoptosis assays (annexin V and TUNEL) were conducted to verify that our designed constructs are causing cell death via apoptosis and not necrosis. Indeed, DBD-XL showed the same (Fig. 4B) or higher (Fig. 4A) apoptotic activity compared to p53-XL in human breast cancer cells (T47D). To further validate the tumor suppressor function of our constructs and their ability to inhibit proliferation, a colony forming assay was conducted. As expected, DBD-XL showed similar reduction in transformative ability as p53-XL in T47D breast carcinoma cells (Fig. 5).

To ensure that the increase in apoptotic activity is not cell line, cancer type or p53 status dependent, four different cancer cell lines (MCF-7, MDA-MB-231, HeLa, H1373) were tested. Surprisingly, DBD-XL induces late stage apoptosis significantly higher than p53-XL in all tested cell lines except T47D (Fig. 6). The p53/MDM2 pathway might offer an explanation to why DBD-XL shows higher apoptotic activity compared to p53-XL. MDM2, an ubiquitin ligase (E3) binds to the MBD domain of p53 and helps to transfer ubiquitin from E2 to lysine residues on the carboxy terminus of p53. Ubiquinated p53 is dragged to the proteasome for degradation (50, 51). DBD-XL may evade degradation by MDM2 since it lacks the MBD and C-terminal domain, allowing for higher stability and consequently increased apoptotic activity. Hagn et al. showed that the amino acids of p53 responsible for interacting with Bcl-XL are located in the DBD of p53 (Gly117, Ser121, Cys176, His178, Asn239, Met243, Arg248, Gly279, and Arg280) and the contact sites on Bcl-XL are residues Ser18, Tyr22, Ser23, Gln26, and Ser28 in helix 1 and 2, Ile114 between helix 3 and 4, and Val155, Asp156, and Glu158 in helix 5 (11). Consequently, DBD-XL contains the residues important for interaction with Bcl-XL while lacking the domains responsible for degradation.

Alternatively, the anti- oxidative role of p53 might offer an explanation to why p53-XL shows lower apoptotic activity compared to DBD-XL. In healthy cells, basal p53 expression limits oxidative stress and promotes cell survival (52). p53 upregulates the expression of genes involved in the oxidative stress survival pathways such as GPX1 (53), SOD2 (53), ALDH4A1 (54), INP1 (55), TIGAR (56), Hi95 (57) and PA26 (57). Even though all designed constructs translocate into the mitochondria (Fig 2), a small fraction could still enter the nucleus. Our previous publication shows that p53-XL remains some residual transcriptional activity (18). Unlike p53-XL which contains full length p53, DBD-XL is not capable of transcribing genes because it lacks the TD to form the transcriptionally active tetrameric p53 and the PRD which enhances transcription of various genes. This could provide another explanation why DBD-XL (which does not activate gene expression) shows higher apoptosis than p53-XL (which could upregulate the expression of genes involved in preventing oxidative stress).

Furthermore, the “mitochondrial priming theory” suggests that some cancer cells such as MCF-7 cells are inherently more sensitive to cytotoxic drugs than other cells (38, 58, 59). This response correlates with the sensitive balance of anti- and pro-apoptotic Bcl-2 family members at the mitochondrial outer membrane (58, 59). It is known that T47D (60), MCF-7 (61, 62), MDA-MB-231 (62) and HeLa (61) express anti-apoptotic Bcl-XL. Therefore, we compared the expression levels of Bcl-XL in T47D (60), MCF-7 (61, 62), MDA-MB-231 (62) and HeLa (61) (see the Supporting Information: S1). Indeed, T47D cells had the highest expression level of Bcl-XL confirming that they are “less primed” and more resistant to apoptosis.

Since the DBD-XL shows similar or higher apoptotic activity (measured by TUNEL, annexin V and 7-AAD) compared to p53-XL consistently in every tested cell line (Fig. 3, 4, and 6), we wanted to examine if the effect on cell death is due to a mitochondrial dependent mechanism. DBD-XL triggers more caspase-9 activation than the negative control E-XL (Fig. 7B) but surprisingly less caspase-9 induction than p53-XL (Fig. 7B). Even though p53-XL caspase activity is higher, this is a

transient effect that is not reflected in the more “final” apoptotic assays (Fig. 3,4,6). Additionally, a certain threshold of caspase 9 activation achieved by DBD-XL may be sufficient to induce cell death. Furthermore, DBD-XL induces MOMP to the same extent as p53-XL, suggesting that DBD-XL dependent apoptosis occurs through the intrinsic apoptotic pathway and might be through a direct interaction with Bcl-XL (Fig 7A). As described above, p53-XL could possibly be degraded via the proteasome. Once MDM-2, an ubiquitin ligase, binds to the MBD of p53, the C-terminal region of p53 becomes ubiquitinated and p53 is dragged into the proteasome for degradation (50, 51). This could explain why initially p53-XL causes more caspase-9 activation (Fig. 7A) but this difference in activity is not reflected in the more “final” apoptosis assays where DBD-XL shows even higher apoptosis activity compared to p53-XL (Fig. 6).

In an effort to determine if the apoptotic potential of our designed constructs is due to their interaction with Bcl-XL or if it is independent of the p53/Bcl-XL pathway, we conducted a co-IP and a rescue experiment achieved by overexpressing Bcl-XL. Interestingly, Bcl-XL co-immunoprecipitated with the "negative control" E-XL in the same manner as p53-XL (Fig. 8A). We hypothesize that the interaction with Bcl-XL is independent of p53 and it is mainly due to the XL MTS which will directly target every protein that contains XL to Bcl-XL. To investigate this hypothesis, E-CC (a negative control lacking the XL signal) was created. As expected, E-CC did not bind to Bcl-XL (Fig.8A), confirming that the XL signal is responsible for the interaction with Bcl-XL.

To prove indirectly that the apoptotic mechanism of p53- and DBD-XL are through direct interaction of p53 and DBD with Bcl-XL, a rescue experiment using overexpressed Bcl-XL was conducted. As expected the apoptotic activity of MBD-, PRD- and E-XL was not altered by Bcl-XL overexpression (see the Supporting Information: S2). However, DBD-XL, p53-XL (and even TD-XL) demonstrated reduction in apoptotic potential, further demonstrating the necessity of Bcl-XL for apoptosis initiation (Fig 8B, S2). Even though TD-XL showed significantly lower cell death compared to p53-XL, it was still significantly higher than the negative control

E-XL, and was still rescued by Bcl-XL (S2). It could be speculated that TD-XL binds to endogenous, mutant p53 through its TD and drags it to the mitochondria where it potentially interacts with Bcl-XL and triggers marginal apoptosis (63). Even though endogenous, mutant p53 is transcriptionally inactive in T47D cells due to the presence of the L194F mutation, this mutant p53 could still be active at the mitochondria, since the L194 residue is not involved in the interaction between p53 and Bcl-XL (11).

In summary, DBD-XL shows the same (T47D) or higher (MCF-7, MDA-MB-231, HeLa, H1373) apoptotic activity compared to p53-XL. Mechanistic studies suggest that DBD-XL may bind and trigger apoptosis similar to p53 through the Bcl-XL dependent pathway. Our data highlights that DBD (about half the size of full length p53) can be used instead of p53 for achieving apoptosis at the mitochondria when fused to the MTS from Bcl-XL. The benefit of decreasing the overall size of p53 by half while still maintaining full apoptotic activity allows for better drug delivery options. The next goal is to use DBD-XL as a therapeutic *in vivo* using adenoviral drug delivery. In conclusion, we show for the first time that DBD-XL can be used to trigger a potent, rapid apoptotic response in various cancer cell lines (including breast, cervical and lung carcinomas) with different p53 status, and is an alternative to *wt* p53 gene therapy. Importantly, the mechanism of DBD-XL-mediated apoptosis is distinctly different from conventional wild type p53 and represents a novel approach for cancer therapy.

3.6 Supporting Information

Additional figures depicting different endogenous expression levels of Bcl-XL can be found in Supplementary Figure 1. Rescue experiment including MBD-, PRD-, DBD-, TD-, p53- and E-XL can be found in Supplementary Figure 2.

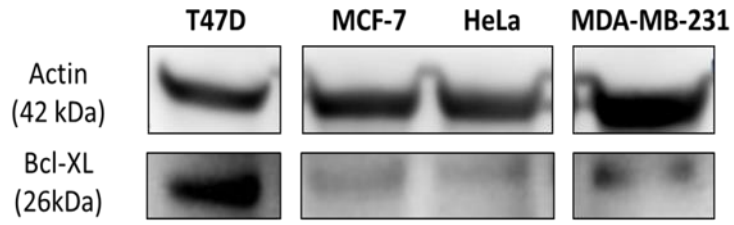

S1 Expression levels of Bcl-XL in T47D, MCF-7, HeLa and MDA-MB231 determined by western blot.

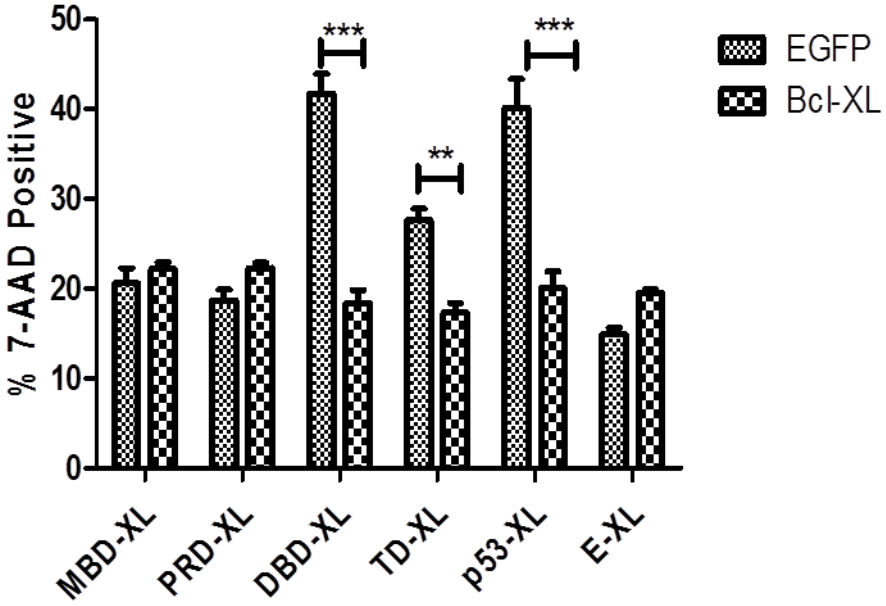

S2 Rescue experiment: T47D cells transfected either with or without Bcl-XL and MBD-XL, PRD-XL, DBD-XL, TD-XL, p53-XL and E-XL. 48 h post transfection 7-AAD assay was conducted. Statistical analysis was performed by using two-way ANOVA with Bonferroni's post test; ** $p < 0.01$, *** $p < 0.001$.

3.7 Acknowledgements

We would like to thank Christian Raab, David Woessner, Shams Reaz, Geoff Miller, and Ben Bruno for scientific discussions. We acknowledge the use of DNA/Peptide Core and Flow Cytometry Core (NCI Cancer Center Support Grant P30 CA042014, Huntsman Cancer Institute). Research reported in this publication was supported by the National Cancer Institute of the National Institutes of Health under award number R01-CA151847. This work was funded by NIH R01-CA151847.

3.8 References

1. Goh AM, Coffill CR, Lane DP. The role of mutant p53 in human cancer. J Pathol. 2011 Jan;223(2):116-26.

2. Sherr CJ. Principles of tumor suppression. Cell. 2004 Jan 23;116(2):235-46.

3. Martins CP, Brown-Swigart L, Evan GI. Modeling the therapeutic efficacy of p53 restoration in tumors. Cell. 2006 Dec 29;127(7):1323-34.

4. Xin H. Chinese gene therapy. Gendicine's efficacy: hard to translate. Science. 2006 Nov 24;314(5803):1233.

5. Peng Z. Current status of gendicine in China: recombinant human Ad-p53 agent for treatment of cancers. Hum Gene Ther. 2005 Sep;16(9):1016-27.

6. Palacios G, Crawford HC, Vaseva A, Moll UM. Mitochondrially targeted wild-type p53 induces apoptosis in a solid human tumor xenograft model. Cell Cycle. 2008 Aug 15;7(16):2584-90.

7. Fuster JJ, Sanz-Gonzalez SM, Moll UM, Andres V. Classic and novel roles of p53: prospects for anticancer therapy. Trends Mol Med. 2007 May;13(5):192-9.

8. Perfettini JL, Kroemer RT, Kroemer G. Fatal liaisons of p53 with Bax and Bak. Nat Cell Biol. 2004 May;6(5):386-8.

9. Vaseva AV, Moll UM. The mitochondrial p53 pathway. Biochim Biophys Acta. 2009 May;1787(5):414-20.

10. Joerger AC, Fersht AR. The tumor suppressor p53: from structures to drug discovery. Cold Spring Harb Perspect Biol. 2010 Jun;2(6):a000919.

11. Hagn F, Klein C, Demmer O, Marchenko N, Vaseva A, Moll UM, et al. BclxL changes conformation upon binding to wild-type but not mutant p53 DNA binding domain. J Biol Chem. 2010 Jan 29;285(5):3439-50.

12. Petros AM, Gunasekera A, Xu N, Olejniczak ET, Fesik SW. Defining the p53 DNA-binding domain/Bcl-x(L)-binding interface using NMR. FEBS Lett. 2004 Feb 13;559(1-3):171-4.

13. Tomita Y, Marchenko N, Erster S, Nemajerova A, Dehner A, Klein C, et al. WT p53, but not tumor-derived mutants, bind to Bcl2 via the DNA binding domain and induce mitochondrial permeabilization. J Biol Chem. 2006 Mar 31;281(13):8600-6.

14. Bharatham N, Chi SW, Yoon HS. Molecular basis of Bcl-X(L)-p53 interaction: insights from molecular dynamics simulations. PLoS One. 2011;6(10):e26014.

15. Chipuk JE, Maurer U, Green DR, Schuler M. Pharmacologic activation of p53 elicits Bax-dependent apoptosis in the absence of transcription. Cancer Cell. 2003 Nov;4(5):371-81.

16. Ha JH, Won EY, Shin JS, Jang M, Ryu KS, Bae KH, et al. Molecular mimicry-based repositioning of nutlin-3 to anti-apoptotic Bcl-2 family proteins. J Am Chem Soc. 2011 Feb 9;133(5):1244-7.

17. Xu H, Tai J, Ye H, Kang CB, Yoon HS. The N-terminal domain of tumor suppressor p53 is involved in the molecular interaction with the anti-apoptotic protein Bcl-Xl. Biochem Biophys Res Commun. 2006 Mar 24;341(4):938-44.

18. Mossalam M, Matissek KJ, Okal A, Constance JE, Lim CS. Direct induction of apoptosis using an optimal mitochondrially targeted p53. Mol Pharm. 2012 May 7;9(5):1449-58.

19. Dixon AS, Pendley SS, Bruno BJ, Woessner DW, Shimpi AA, Cheatham TE, 3rd, et al. Disruption of Bcr-Abl coiled coil oligomerization by design. J Biol Chem. 2011 Aug 5;286(31):27751-60.

20. Dixon AS, Miller GD, Bruno BJ, Constance JE, Woessner DW, Fidler TP, et al. Improved coiled-coil design enhances interaction with Bcr-Abl and induces apoptosis. Mol Pharm. 2012 Jan 1;9(1):187-95.

21. Dixon AS, Kakar M, Schneider KM, Constance JE, Paullin BC, Lim CS. Controlling subcellular localization to alter function: Sending oncogenic Bcr-Abl to the nucleus causes apoptosis. J Control Release. 2009 Dec 16;140(3):245-9.

22. Bolte S, Cordelieres FP. A guided tour into subcellular colocalization analysis in light microscopy. J Microsc. 2006 Dec;224(Pt 3):213-32.

23. Constance JE, Despres SD, Nishida A, Lim CS. Selective targeting of c-Abl via a cryptic mitochondrial targeting signal activated by cellular redox status in leukemic and breast cancer cells. Pharm Res. 2012 Aug;29(8):2317-28.

24. Constance JE, Woessner DW, Matissek KJ, Mossalam M, Lim CS. Enhanced and selective killing of chronic myelogenous leukemia cells with an engineered BCR-ABL binding protein and imatinib. Mol Pharm. 2012 Nov 5;9(11):3318-29.

25. Costes SV, Daelemans D, Cho EH, Dobbin Z, Pavlakis G, Lockett S. Automatic and quantitative measurement of protein-protein colocalization in live cells. Biophys J. 2004 Jun;86(6):3993-4003.

26. Adler J, Parmryd I. Quantifying colocalization by correlation: the Pearson correlation coefficient is superior to the Mander's overlap coefficient. Cytometry A. 2010 Aug;77(8):733-42.

27. Davis JR, Mossalam M, Lim CS. Controlled access of p53 to the nucleus regulates its proteasomal degradation by MDM2. Mol Pharm. 2013 Apr 1;10(4):1340-9.

28. Jaskolski F, Mulle C, Manzoni OJ. An automated method to quantify and visualize colocalized fluorescent signals. J Neurosci Methods. 2005 Jul 15;146(1):42-9.

29. Krohn AJ, Wahlbrink T, Prehn JH. Mitochondrial depolarization is not required for neuronal apoptosis. J Neurosci. 1999 Sep 1;19(17):7394-404.

30. Grabarek J, Amstad P, Darzynkiewicz Z. Use of fluorescently labeled caspase inhibitors as affinity labels to detect activated caspases. Hum Cell. 2002 Mar;15(1):1-12.

31. Grabarek J, Darzynkiewicz Z. In situ activation of caspases and serine proteases during apoptosis detected by affinity labeling their enzyme active centers with fluorochrome-tagged inhibitors. Exp Hematol. 2002 Sep;30(9):982-9.

32. Schmid I, Krall WJ, Uittenbogaart CH, Braun J, Giorgi JV. Dead cell discrimination with 7-amino-actinomycin D in combination with dual color immunofluorescence in single laser flow cytometry. Cytometry. 1992;13(2):204-8.

33. Serrano MJ, Sanchez-Rovira P, Algarra I, Jaen A, Lozano A, Gaforio JJ. Evaluation of a gemcitabine-doxorubicin-paclitaxel combination schedule through flow cytometry assessment of apoptosis extent induced in human breast cancer cell lines. Jpn J Cancer Res. 2002 May;93(5):559-66.

34. Vermes I, Haanen C, Steffens-Nakken H, Reutelingsperger C. A novel assay for apoptosis. Flow cytometric detection of phosphatidylserine expression on early apoptotic cells using fluorescein labelled Annexin V. J Immunol Methods. 1995 Jul 17;184(1):39-51.

35. Loo DT, Rillema JR. Measurement of cell death. Methods Cell Biol. 1998;57:251-64.

36. Nigro JM, Baker SJ, Preisinger AC, Jessup JM, Hostetter R, Cleary K, et al. Mutations in the p53 gene occur in diverse human tumour types. Nature. 1989 Dec 7;342(6250):705-8.

37. Bartek J, Iggo R, Gannon J, Lane DP. Genetic and immunochemical analysis of mutant p53 in human breast cancer cell lines. Oncogene. 1990 Jun;5(6):893-9.

38. Mooney LM, Al-Sakkaf KA, Brown BL, Dobson PR. Apoptotic mechanisms in T47D and MCF-7 human breast cancer cells. Br J Cancer. 2002 Oct 7;87(8):909-17.

39. Goodrum FD, Ornelles DA. p53 status does not determine outcome of E1B 55-kilodalton mutant adenovirus lytic infection. J Virol. 1998 Dec;72(12):9479-90.

40. Bodner SM, Minna JD, Jensen SM, D'Amico D, Carbone D, Mitsudomi T, et al. Expression of mutant p53 proteins in lung cancer correlates with the class of p53 gene mutation. Oncogene. 1992 Apr;7(4):743-9.

41. Jayaraman S. Flow cytometric determination of mitochondrial membrane potential changes during apoptosis of T lymphocytic and pancreatic beta cell lines: comparison of tetramethylrhodamineethylester (TMRE), chloromethyl-X-rosamine (H2-CMX-Ros) and MitoTracker Red 580 (MTR580). J Immunol Methods. 2005 Nov 30;306(1-2):68-79.

42. O'Reilly CM, Fogarty KE, Drummond RM, Tuft RA, Walsh JV, Jr. Quantitative analysis of spontaneous mitochondrial depolarizations. Biophys J. 2003 Nov;85(5):3350-7.

43. Ricci JE, Gottlieb RA, Green DR. Caspase-mediated loss of mitochondrial function and generation of reactive oxygen species during apoptosis. J Cell Biol. 2003 Jan 6;160(1):65-75.

44. Chowdhury I, Tharakan B, Bhat GK. Caspases - an update. Comp Biochem Physiol B Biochem Mol Biol. 2008 Sep;151(1):10-27.

45. Yin Q, Park HH, Chung JY, Lin SC, Lo YC, da Graca LS, et al. Caspase-9 holoenzyme is a specific and optimal procaspase-3 processing machine. Mol Cell. 2006 Apr 21;22(2):259-68.

46. Mihara M, Erster S, Zaika A, Petrenko O, Chittenden T, Pancoska P, et al. p53 has a direct apoptogenic role at the mitochondria. Mol Cell. 2003 Mar;11(3):577-90.

47. Power SD, Lochrie MA, Patterson TE, Poyton RO. The nuclear-coded subunits of yeast cytochrome c oxidase. II. The amino acid sequence of subunit VIII and a model for its disposition in the inner mitochondrial membrane. J Biol Chem. 1984 May 25;259(10):6571-4.

48. Mossalam M, Dixon AS, Lim CS. Controlling subcellular delivery to optimize therapeutic effect. Ther Deliv. 2010 Jul;1(1):169-93.

49. Schmidt O, Pfanner N, Meisinger C. Mitochondrial protein import: from proteomics to functional mechanisms. Nat Rev Mol Cell Biol. 2010 Sep;11(9):655-67.

50. Nalepa G, Rolfe M, Harper JW. Drug discovery in the ubiquitin-proteasome system. Nat Rev Drug Discov. 2006 Jul;5(7):596-613.

51. Haupt Y, Maya R, Kazaz A, Oren M. Mdm2 promotes the rapid degradation of p53. Nature. 1997 May 15;387(6630):296-9.

52. Maddocks OD, Vousden KH. Metabolic regulation by p53. J Mol Med (Berl). 2011 Mar;89(3):237-45.

53. Hussain SP, Amstad P, He P, Robles A, Lupold S, Kaneko I, et al. p53-induced up-regulation of MnSOD and GPx but not catalase increases oxidative stress and apoptosis. Cancer Res. 2004 Apr 1;64(7):2350-6.

54. Yoon KA, Nakamura Y, Arakawa H. Identification of ALDH4 as a p53-inducible gene and its protective role in cellular stresses. J Hum Genet. 2004;49(3):134-40.

55. Cano CE, Gommeaux J, Pietri S, Culcasi M, Garcia S, Seux M, et al. Tumor protein 53-induced nuclear protein 1 is a major mediator of p53 antioxidant function. Cancer Res. 2009 Jan 1;69(1):219-26.

56. Bensaad K, Tsuruta A, Selak MA, Vidal MN, Nakano K, Bartrons R, et al. TIGAR, a p53-inducible regulator of glycolysis and apoptosis. Cell. 2006 Jul 14;126(1):107-20.

57. Budanov AV, Karin M. p53 target genes sestrin1 and sestrin2 connect genotoxic stress and mTOR signaling. Cell. 2008 Aug 8;134(3):451-60.

58. Ni Chonghaile T, Sarosiek KA, Vo TT, Ryan JA, Tammareddi A, Moore Vdel G, et al. Pretreatment mitochondrial priming correlates with clinical response to cytotoxic chemotherapy. Science. 2011 Nov 25;334(6059):1129-33.

59. Constance JE, Lim CS. Targeting malignant mitochondria with therapeutic peptides. Ther Deliv. 2012 Aug;3(8):961-79.

60. Yamashita H, Nishio M, Fujii Y, Iwase H. Dominant-negative Stat5 inhibits growth and induces apoptosis in T47D-derived tumors in nude mice. Cancer Sci. 2004 Aug;95(8):662-5.

61. Shi J, Zhou Y, Huang HC, Mitchison TJ. Navitoclax (ABT-263) accelerates apoptosis during drug-induced mitotic arrest by antagonizing Bcl-xL. Cancer Res. 2011 Jul 1;71(13):4518-26.

62. Li H, Piao L, Xu P, Ye W, Zhong S, Lin SH, et al. Liposomes containing (-)-gossypol-enriched cottonseed oil suppress Bcl-2 and Bcl-xL expression in breast cancer cells. Pharm Res. 2011 Dec;28(12):3256-64.

63. Jeffrey PD, Gorina S, Pavletich NP. Crystal structure of the tetramerization domain of the p53 tumor suppressor at 1.7 angstroms. Science. 1995 Mar 10;267(5203):1498-502.

4. Delivery of a monomeric p53 subdomain with mitochondrial targeting signals from pro-apoptotic Bak or Bax

Matissek K.J., Okal A., Mossalam M., Lim C.S

Pharmaceutical Research, February 2014, minor revisions

First author contribution:

Research design: 85%

Experimental work: 80%

Data analysis and evaluation: 85%

Manuscript writing: 90%

4.1 Abstract

p53 targeted to the mitochondria is the fastest and most direct pathway for executing p53 death signaling. The purpose of this work was to determine if mitochondrial targeting signals (MTSs) from pro-apoptotic Bak and Bax are capable of targeting p53 to the mitochondria and inducing rapid apoptosis.

p53 and its DNA-binding domain (DBD) were fused to MTSs from Bak (p53-BakMTS, DBD-BakMTS) or Bax (p53-BaxMTS, DBD-BaxMTS). Mitochondrial localization was tested via fluorescence microscopy in 1471.1 cells, and apoptosis was detected via 7-AAD in breast (T47D), non-small cell lung (H1373), ovarian (SKOV-3) and cervical (HeLa) cancer cells. To determine that apoptosis is via the intrinsic apoptotic pathway, TMRE and caspase-9 assays were conducted. Finally, the involvement of p53/Bak specific pathway was tested.

MTSs from Bak and Bax are capable of targeting p53 to the mitochondria, and p53-BakMTS and p53-BaxMTS cause apoptosis through the intrinsic apoptotic pathway. Additionally, p53-BakMTS, DBD-BakMTS, p53-BaxMTS and DBD-BaxMTS caused apoptosis in T47D, H1373, SKOV-3 and HeLa cells. The apoptotic mechanism of p53-BakMTS and DBD-BakMTS was Bak dependent.

Our data demonstrates that p53-BakMTS (or BaxMTS) and DBD-BakMTS (or BaxMTS) cause apoptosis at the mitochondria and can be used as a potential gene therapeutic in cancer.

4.2 Introduction

The tumor suppressor p53 exhibits distinct functions at the cytoplasm, the nucleus and the mitochondria (1). Under normal conditions, the E3 ligase murine double minute 2 (MDM2) binds to the MDM2 binding domain (MBD) of p53 prompting polyubiquitination of terminal lysines on the C-terminus of p53, which marks p53 for proteasomal degradation (2). Upon stress induction, such as DNA damage or ER

stress, cytoplasmic p53 translocates either to the nucleus (3) or to the mitochondria (4). Three nuclear localization signals (NLS) in the C-terminus of p53 are responsible for p53 nuclear localization (5). In the nucleus, p53 forms a tetramer via its tetramerization domain (TD) (3) allowing its DNA binding domain (DBD) to bind to DNA activating various genes that are involved in apoptosis, DNA repair and cell cycle arrest (1).

Although p53 does not contain a mitochondrial targeting signal (MTS), it can still translocate to the mitochondria. Machenko et al. postulated that MDM2 triggers dimer formation and mono-ubiquitination of cytoplasmic p53 resulting in mitochondrial import via herpes virus-associated ubiquitin-specific protease (6). At the mitochondrial outer membrane, p53 directly interacts with pro-apoptotic (Bak or Bax) (7, 8) and anti-apoptotic Bcl-2 family members (Bcl-XL, Bcl-2, Mcl-1, Bcl-w, and A1) (9-11) through a sequential mechanism first binding anti-apoptotic Bcl-2 proteins followed by binding to pro-apoptotic Bak (Fig. 1) or Bax (12). Activation of Bak (Fig. 1) or Bax leads to homotetramer formation, which causes cytochrome c release from the intermembrane space (13). Binding of cytochrome c to APAF-1 stimulates the assembly of a hepameric, wheel-like structure known as the apoptosome (13). The apoptosome activates the initiator caspase-9 which initiates the executioner apoptotic caspase-3 and caspase-7 (Fig. 1) (14). Their proteolytic activity leads to nuclear fragmentation, chromatin condensation and cell shrinking, also known as programed cell death or apoptosis (4).

In cancer cells, overexpression of Bcl-2, Bcl-XL and Mcl-1 correlates with more aggressive phenotypes and leads to chemotherapy resistance (15-17). Many agents have been identified to target the anti-apoptotic Bcl-2 family members such as navitoclax (inhibits Bcl-2, Bcl-XL, and Bcl-w) and ABT-199 (inhibits Bcl-2) (17). These therapeutics initiate apoptosis by neutralizing anti-apoptotic proteins at the mitochondria thus allowing the pro-apoptotic Bcl-2 family members Bak or Bax to homo-oligomerize leading to apoptosis (18). However, these inhibitors do not inactivate anti-apoptotic Mcl-1 (17). Overexpression of Mcl-1 is linked to reduced

response to chemotherapy and poor prognosis which limits the therapeutic options for navitoclax and ABT-199 (17). Mcl-1 (and to a certain extent Bcl-XL) is the main inhibitor of Bak (9, 19) while Bax is mainly inhibited by Bcl-2 and Bcl-w (20). Our approach is to directly activate pro- apoptotic Bak and Bax by targeting p53 to the mitochondria using Bak's or Bax's own MTSs (Fig. 2). Targeting p53 to the mitochondria executes the shortest apoptotic pathway for p53. *wt* p53 mostly translocates to the nucleus due to its NLS, forms a tetramer, binds to DNA, produces mRNA which then is then translated to proteins and after that these proteins need to translocate to their designated compartment. On the other hand mitochondrially targeted p53 directly interacts with pro- and anti- apoptotic proteins at the mitochondria resulting directly in apoptosis.

The MTSs of Bak or Bax are located on the C-terminal hydrophobic regions of these proteins. The C-terminus contains the transmembrane domain (TM) and the C-segment (CS) (21, 22). The C-terminus contains the transmembrane domain (TM) and the C-segment (CS) (21, 22). The Amino acid sequence of the MTSs from Bax are as follows GTPTWQTVTIFVAGVLTASLTIWKKMG and from Bak as follows GNGPILNVLVVLGVVLLGQFVVRRFFKS with italic representing the TM domain and underlined illustrating the CS base pairs. The TM inserts both proteins into the mitochondrial outer membrane (tail anchored proteins) with at least two of the basic amino acids in the CS being necessary for the insertion (Fig. 2) (22). Bax, which is in the cytoplasm, sequesters its TM in its hydrophobic surface groove. Once an apoptotic stimuli occurs, the TM gets externalized, targets Bax to the mitochondria, and inserts itself into the mitochondrial outer membrane (Fig.3) (21, 23). However, Bak is always present at the mitochondrial outer membrane sequestered by Mcl-1 (and Bcl-XL) (Fig. 1; 3) (19).

As mentioned before *wt* p53 does not contain a MTS. Therefore, our approach is to achieve mitochondrial targeting of p53 by fusing the MTSs from Bak or Bax to p53. Murphy and colleagues have reported that *wt* p53 is required to be in a dimeric or tetrameric form in order to activate pro-apoptotic Bak (24). In addition, the DBD has

been reported to interact with pro-apoptotic Bak (25) and inhibit anti-apoptotic Bcl-XL (10) and Bcl-2 (11). Here, we show our finding that the DBD in isolation with a MTS from Bak or Bax is sufficient to induce apoptosis in different cancer cells.

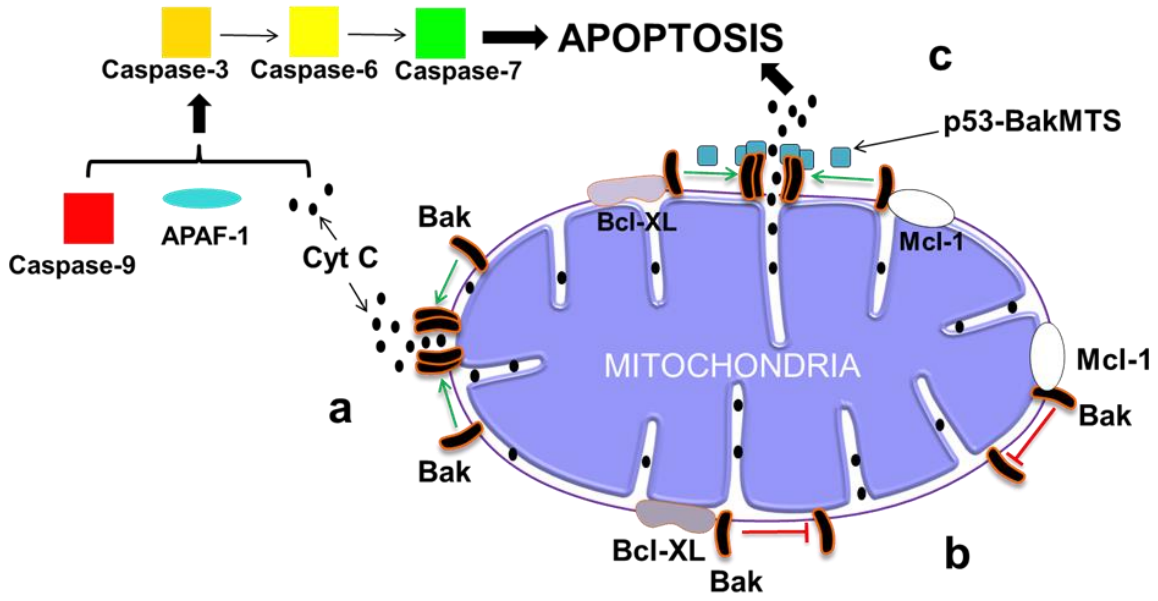

Fig. 1 Intrinsic mitochondrial pathway (a) Upon apoptotic stimuli, Bak homo-oligomerization allows pore formation and cytochrome c release. (b) Mcl-1 and Bcl-XL sequester Bak and do not allow homo-oligomerization (c) p53-BakMTS binds Bak, releases Bak from both Mcl-1 and Bcl-XL, and allows homo-oligomerization and cytochrome c release which results in apoptosis. On the other hand, Bax is sequestered by Bcl-2 and Bcl-w. p53-BaxMTS binds to Bax, releases Bax from Bcl-2 and Bcl-w and causes apoptosis (pathway for Bax not shown).

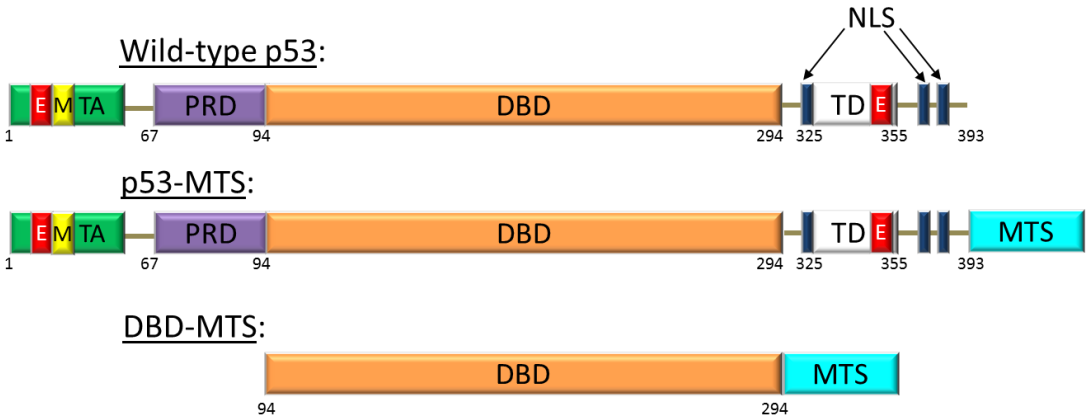

Fig. 2 Schematic representation of experimental constructs: Wild-type p53 is divided into N-terminus, DNA binding domain (DBD) and C-terminal region. The N-terminus consists of a transactivation domain (TA), nuclear export signal (E), MDM2 binding domain (M) and proline-rich domain (PRD). The C-terminus contains three nuclear localization signals (NLS), nuclear export signal (E) and tetramerization domain (TD). p53-MTS wild-type p53 was fused to the mitochondrial targeting signal (MTS) from Bak or Bax. DBD-MTS DNA-binding domain of p53 was fused to the MTS from Bak or Bax.

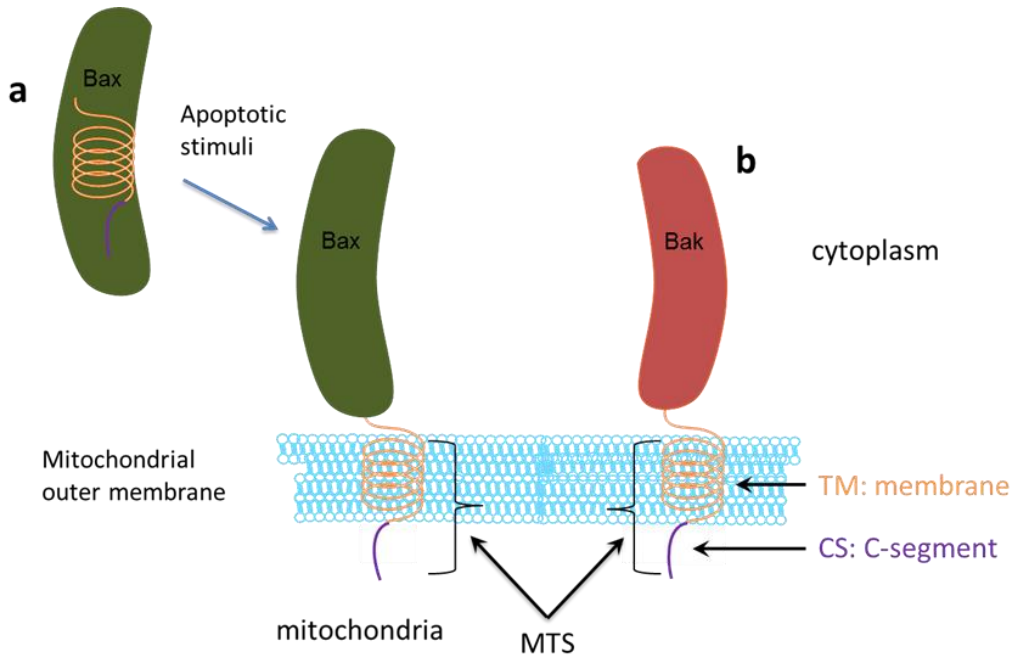

Fig. 3 Structure of the Bak and Bax mitochondrial targeting signals (MTSs) (a) The Bax protein is mainly found in the cytoplasm of healthy cells. Upon apoptotic stimuli, it translocates to the mitochondrial outer membrane. The MTS of the Bax protein, consisting of the transmembrane domain (TM) and the C-segment (CS), becomes exposed for integration into the mitochondrial outer membrane. (b) Unlike Bax, Bak is always present at the mitochondrial outer membrane via its TM and CS.

4.3 Material and Methods

4.3.1 Cell Lines and Transient Transfections

1471.1 murine adenocarcinoma cells (a kind gift of G. Hager, NCI, NIH), T47D human ductal breast epithelial tumor cells (ATCC, Manassas, VA), H1373 human non-small cell lung carcinoma cells (a kind gift from Dr. Andrea Bild, University of Utah), SKOV-3 human ovarian adenocarcinoma cells (a kind gift from Dr. Margit Janat-Amsbury, University of Utah) and HeLa human epithelial cervical adenocarcinoma cells (ATCC) were grown as monolayers in DMEM (1471.1, SKOV-3) or RPMI (T47D, H1373, HeLa) (Invitrogen, Carlsbad, CA) supplemented with 10% FBS (Invitrogen), 1% penicillin-streptomycin (Invitrogen), 1% glutamine (Invitrogen) and 0.1% gentamycin (Invitrogen) and maintained in a 5% CO2 incubator at 37ºC. T47D media was additionally supplemented with 4 mg/L insulin (Sigma, St. Louis, MO). For microscopy 7.5 x 10^4 cells for 1471.1 cells were seeded in a 2 well live cell chamber. For apoptosis assays 3.0 x 10^5 cells for T47D, 1.0 x 10^5 cells for HeLa, 2.0 x 10^5 for H1373 and SKOV-3 were seeded in 6-well plates (Greiner Bio-One, Monroe, NC). To account for varying cell growth rates, different amounts of cells were plated in live cell chambers and 6-well plates. Following the manufacturer's recommendations 24 h after seeding, transfections were performed using 1 pmol of DNA per well (unless otherwise indicated) and Lipofectamine 2000 (Invitrogen).

4.3.2 Plasmid Construction

pEGFP-p53-BakMTS (p53-BakMTS): An oligonucleotide encoding the MTS from Bak (5'-GATCCGGCAATGGTCCCATCCTGAACGTGCTGGTGGTTCTGGGTGTGGTTCTGTTGGGCCAGTTTGTGGTACGAAGATTCTTCAAATCATGAG-3') was annealed to its reverse complementary strand and fused to the C-terminus of EGFP-p53 (26) using the BamHI restriction sites (NEB, Ipswich, MA).

pEGFP-BakMTS (E-BakMTS): The annealed oligonucleotide encoding the MTS from Bak was fused to the C-terminus of EGFP-C1 vector (Clontech, Mountain View, CA) (26) using the BamHI (NEB) restriction sites.

pEGFP-DBD-BakMTS (DBD-BakMTS): The DNA encoding the DBD was amplified via PCR from previously subcloned pEGFP-p53 (26) using 5'-CCGGGCCCGCGGTCCGGAACCTACCAGGGCAGCTACG-3' and 5'-CCGGGCCCGCGGGGTACCTTTCTTGCGGAGATTCTCTTCCT and cloned between EGFP and Bak MTS into the multiple cloning site of E-BakMTS using BspEI (NEB) and KpnI (NEB) sites.

pEGFP-p53 K120A, R248A, R273A, R280A, E285A, E287A-Bak (p53m6-BakMTS) and pEGFP-DBD K120A, R248A, R273A, R280A, E285A, E287A-Bak (DBDm6-BakMTS): K120A, R248A, R273A, R280A, E285A, and E287A mutations were introduced in p53-BakMTS and DBD-BakMTS using the QuickChange II XL Site-Directed Mutagenesis Kit (Agilent, Santa Clara, CA). The primers listed below and their reverse complements were used to introduce the K120A mutation 5'-CATTCTGGGACAGCCGCGTCTGTGACTTGCAC-3'; the R248A mutation 5'-CAGTTCCTGCATGGGCGGCATGAACGCGAGGCCCATCCT-3'; the R273A mutation 5'-GGGACGGAACAGCTTTGAGGTGGCTGTTTGTGCCTGTCCT-3'; the R280A mutation 5'-TTTGTGCCTGTCCTGGGGCAGACCGGCGCACA-3'; and the E285A, E287A mutations 5'-ACCGGCGCACAGCGGAAGCGAATCTCCGC-3' (underlined sequence indicate mutation sites).

pEGFP-p53K120E-BakMTS (p53K120E-BakMTS) and pEGFP-DBDK120E-BakMTS (DBDK120E-BakMTS): The K120E mutation was introduced into p53-BakMTS and DBD-BakMTS via QuickChange II XL Site-Directed Mutagenesis Kit (Agilent) using 5'- GCATTCTGGGACAGCCGAGTCTGTGACTTGCACGTA-3' and its reverse complement.

pEGFP-p53-BaxMTS (p53-BaxMTS): An oligonucleotide encoding the MTS from Bax 5'-GATCCTCCTACTTTGGGACGCCCACGTGGCAGACCGTGACCATCTTTGTGG

CGGGAGTGCTCACCGCCTCACTCACCATCTGGAAGAAGATGGGCTGAG-3' was annealed to its reverse complementary strand and fused to the C-terminus of EGFP-p53 (26) using the BamHI (NEB) restriction sites.

pEGFP-BaxMTS (E-BaxMTS): The annealed oligonucleotide encoding the MTS from Bax was fused to the C-terminus of EGFP-C1 vector (Clontech) (26) using the BamHI (NEB) restriction sites.

pEGFP-DBD-BaxMTS (DBD-BaxMTS): The DNA encoding the DBD was amplified as mentioned above and cloned between EGFP and BaxMTS into the multiple cloning site of E-Bax using BspEI (NEB) and KpnI (NEB) sites.

4.3.3 Mitochondrial Staining and Microscopy

Prior to microscopy, media in live cell chambers was replaced with media containing 10% charcoal stripped fetal bovine serum (CS-FBS, Invitrogen). To stain the mitochondria, cells were incubated with 150 nM of MitoTracker Red FM (Invitrogen) for 15 min at 37°C and protected from light prior to imaging. All images of 1471.1 and T47D live cells were acquired as previously (26, 27) with an Olympus IX71F fluorescence microscope (Scientific Instrument Company, Aurora, CO) with high quality (HQ) narrow band GFP filter (ex, HQ480/20 nm; em, HQ510/20 nm) and HQ:TRITC filter (ex, HQ545/30; em, HQ620/60) from Chroma Technology

(Brattleboro, VT) with a 40× PlanApo oil immersion objective (NA 1.00) on an F-View Monochrome CCD camera.

4.3.4 Image Analysis

Images were analyzed by using JACoP plugin in ImageJ software (28). PCC values were generated using Pearson's correlation coefficient (PCC) with post Costes' automatic threshold algorithm. PCC depends on both the pixel intensity and overlap of signals. A PCC of +1 represents complete colocalization of EGFP constructs with mitochondria; a PCC of -1 represents anti-correlation, and PCC of 0 correlates to random distribution (29). Bolte and Cordelières defined PCC values equal to 0.6 or above to be colocalized (30). For images analysis, experiments were performed three times (n=3) with 10 cells analyzed per n and per construct.

4.3.5 7- AAD Assay

Transfected T47D, H1373, SKOV-3 and HeLa cells were pelleted and resuspended in 500 µL PBS (Invitrogen) containing 1 µM 7-aminoactinomycin D (7-AAD) (Invitrogen) for 30 min prior to analysis (26, 27). T47D and H1373 cells were analyzed 48 h after transfection, while SKOV-3 and HeLa cells were analyzed 24 h after transfection (time points optimized empirically). Only EGFP positive cells were assayed using the FACS Canto-II (BD- BioSciences, University of Utah Core Facility) with FACS Diva software as previously (26, 27). EGFP and 7-AAD were excited at 488 nm, and detected at 507 nm and 660 nm, respectively. Independent transfections of each construct were assayed three times (n=3). The highest value (EGFP positive cells stained with 7-AAD) was set at 100%, and the lowest at 0% (relative 7-AAD) as previously (31).

4.3.6 Reporter Gene Assay

3.5 µg of p53-BakMTS, E-BakMTS, p53-BaxMTS, E-BaxMTS, *wt* p53 or EGFP were co-transfected with 3.5 µg of p53-Luc Cis-Reporter (Agilent Technologies) encoding the firefly luciferase gene and 0.35 µg of pRL-SV40 plasmid encoding Renilla luciferase (Promega, Madison, WI) to normalize for transfection efficiency in T47D cells using the Dual-Glo Luciferase assay system as previously (26, 31). Luminescence was detected 24 h post transfection using PlateLumino (Stratec Biomedical Systems, Birkenfeld, Germany). Independent transfections of each constructs were assayed three times (n=3). The highest value was set at 100% and lowest value (untreated cells) was set as 0% (relative luminescence) as before (26, 31).

4.3.7 TMRE Assay

As previously (27), 36 h after transfection T47D cells were incubated with 100 nM tetramethylrhodamine, ethyl ester (TMRE) (Invitrogen) for 30 min at 37ºC, pelleted and resuspended in 300 µL annexin-V binding buffer (1X) (Invitrogen). The FACS Canto-II with FACS Diva software was used to analyze only EGFP positive cells (excited at 488 nm with emission 530/35) stained with TMRE (excited at 561 nm laser with the emission 585/15). Loss in TMRE intensity represents mitochondrial depolarization, which correlates with an increase in mitochondrial outer membrane permeabilization (MOMP). Independent transfections of each construct were assayed three times (n=3). The highest MOMP value was set as 100% and the lowest as 0% (relative MOMP) as before (27).

4.3.8 Caspase-9 Assay

As previously described (27), 48 h after transfection, T47D cells were tested with SR FLICA Caspase-9 Assay Kit (Immunochemistry Technologies, Bloomington, MN). Cells were incubated with SR FLICA Caspase-9 reagent for 60 min, pelleted and

resuspended in 300 µL 1X wash buffer (Immunochemistry Technologies). The FACS Canto-II with FACS Diva software was used to analyzed only EGFP positive cells stained with caspase-9, both were excited with the 488 nm (emission filter 530/35) and the 561 nm laser (emission filter 585/15), respectively. Independent transfections of each construct were assayed three times (n=3). The highest value (EGFP positive cells stained with caspase-9) was set as 100% and the lowest as 0% (relative caspase-9) as before (27).

4.3.9 Statistical Analysis

All experiments were done in triplicate (n=3). One-way analysis of variance (ANOVA) with Bonferroni's post test was used to determine statistical significance as indicated in figure legend. To determine the degree of colocalization odds ratio with Pearson's Chi-square was applied comparing each PCC value with PCC of 0.6. A p value of < 0.6 was considered significant (26, 27).

4.4 Results

4.4.1 Colocalization of designed constructs with the mitochondria

Since all designed constructs are tagged to EGFP, their mitochondrial localization was determined using fluorescence microscopy in murine adenocarcinoma cells (1471.1). Figure 4a illustrates representative pictures of 1471.1 cells transfected with p53-BakMTS, E-BakMTS, p53-BaxMTS, E-BaxMTS and EGFP. The mitochondrial compartment was stained by MitoTracker red. 1471.1 cells were chosen for the microscopy study because their large size allows for clear distinction between nucleus, cytoplasm and mitochondria. Similar results have been observed for T47D cells (data not shown).

Colocalization of EGFP tagged constructs with the mitochondrial compartment was illustrated by graphing the generated PCC values for each construct as shown in Figure 4b. PCC values of 0.6 or greater represent colocalization of EGFP tagged constructs with mitochondria (26-28). p53-BakMTS, E-BakMTS, p53-BaxMTS and E-BaxMTS have a significantly higher PCC value than 0.6. The negative control EGFP shows random distribution (PCC=0.29) (Fig. 4b). Since *wt* p53 is a transcription factor containing three nuclear localization signals (NLSs) (5), the main fraction of *wt* p53 localizes to the nucleus as we (31) and others (5) have shown before. However, MTSs derived from the pro-apoptotic Bak or Bax protein are capable of overcoming the three NLSs. These Bak and Bax MTSs are capable of targeting EGFP fused to p53 to the mitochondria (Fig. 4).

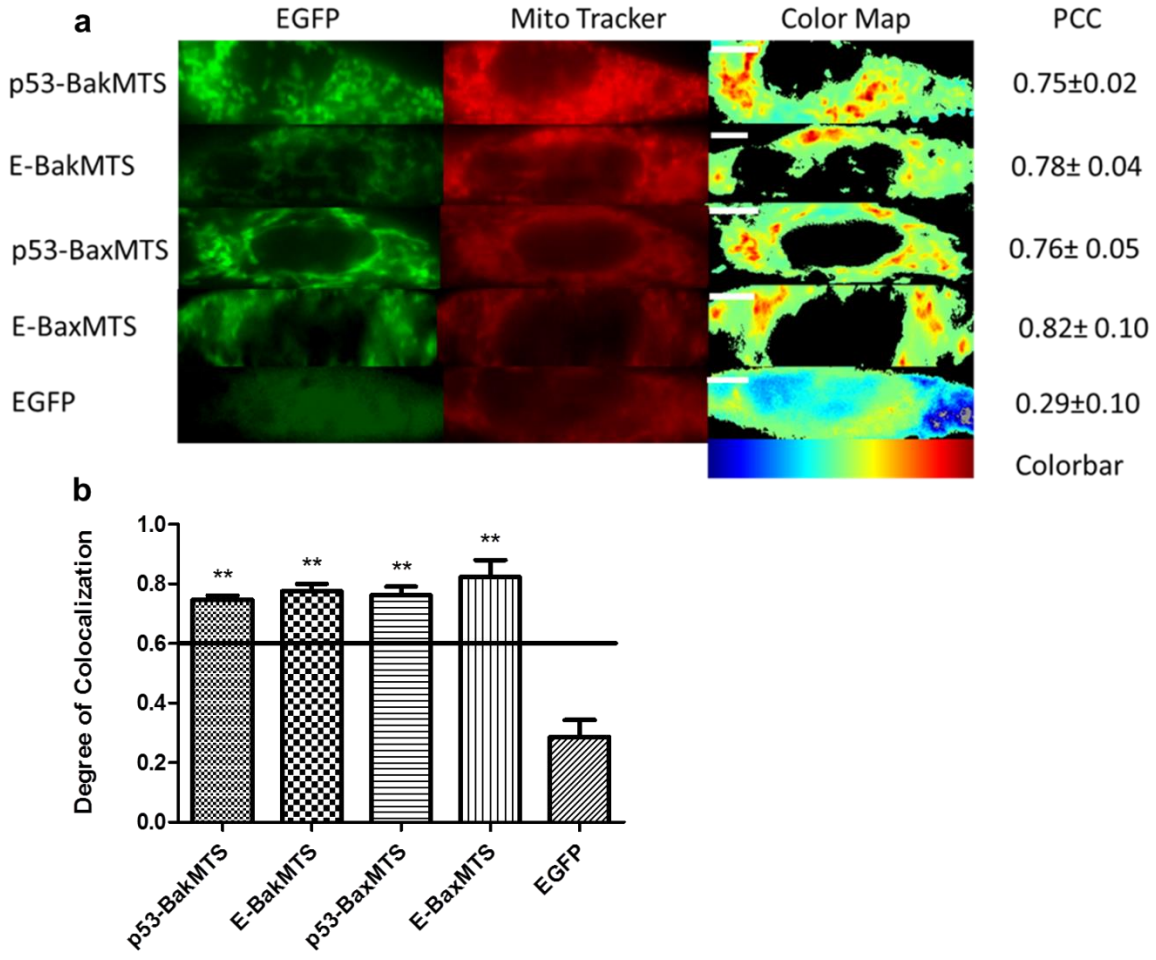

Fig. 4 Mitochondrial localization. (a) Representative images of 1471.1 cells transfected with p53-BakMTS, E-BakMTS, p53-BaxMTS, E-BaxMTS and EGFP. Left column shows EGFP tagged constructs, middle column mitochondria stained with MitoTracker red and right column depicts colocalization color map. Warm colors (red) are considered highly colocalized versus cold colors (blue) which represent anti-correlation (see color bars). White scale bars are all 10 μm (b) PCC values were graphed for each construct. PCC value equal to 0.6 and above is considered to be colocalized. Statistical analysis was performed using odds ratio with Pearson's Chi-square. The adjusted odds ratio for PCC value of 0.6 was compared with each sample (**$p < 0.01$).

4.4.2 p53-BakMTS and p53-BaxMTS induce late stage apoptosis

The ability of p53-BakMTS and p53-BaxMTS to induce apoptosis was tested via 7-AAD assay in T47D breast cancer cells. The 7-AAD dye intercalates into double-stranded DNA of apoptotic/necrotic cells which have a disrupted cell membrane. However, it is not capable of penetrating the intact cell membrane of living cells (32). p53-BakMTS, p53-BaxMTS and *wt* p53 (Fig. 5; compare 1st, 3rd, and 5th bars) show a significant apoptotic effect compared to their corresponding negative controls E-BakMTS, E-BaxMTS and EGFP respectively (Fig. 5; compare 2nd,4th, and 6th bars).

The apoptotic response induced by p53-BakMTS and p53-BaxMTS is similar to *wt* p53 (Fig. 5; compare 1st, 3rd, and 5th bars). Additionally, MTS negative controls, E-BakMTS and E-BaxMTS, show minimal activity similar to the nontoxic EGFP negative control (Fig 5; compare 2nd,4th, and 6th bars), which indicates no inherent mitochondrial toxicity for these MTSs by themselves.

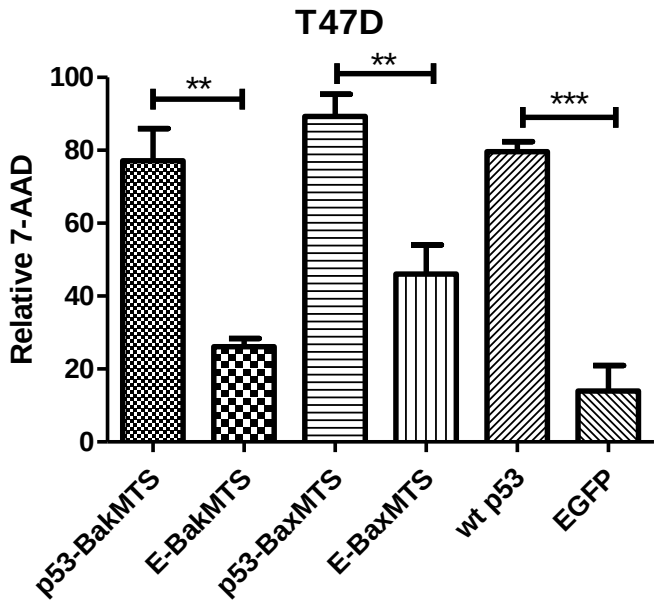

Fig. 5 7-AAD assay in T47D cells, 48 h after transfection. Statistical analysis was performed using one-way ANOVA with Bonferroni's post test; **p < 0.01, ***p < 0.001. Error bars represent standard deviations from at least three independent experiments (n=3).

4.4.3 p53-BakMTS and p53-BaxMTS do not trigger apoptosis through the nuclear but through the mitochondrial apoptotic pathway

To validate that the apoptotic activity of p53-BakMTS and p53-BaxMTS is not due to transcriptional activity at the nucleus, a p53 reporter dual luciferase assay was conducted in T47D cells. The cis reporter system relies on a synthetic promoter which consists of repeats of the transcription recognition consensus for p53 (TGCCTGGACTTGCCTGG)14 (33). Nuclear activity was represented as relative luminescence. Endogenous p53 is a nuclear protein and exhibits most of its tumor suppressor functions as a transcription factor. As expected, *wt* p53 shows high transcriptional activity (Fig. 6a; 5th bar). p53-BakMTS, E-BakMTS, p53-BaxMTS, E-BaxMTS (Fig. 6a; compare 1st, 2nd, 3rd, and 4th bars) show no nuclear activity

similar to that of the negative control EGFP (Fig. 6a; 6th bar). This suggests that the induction of apoptosis of the mitochondrial constructs p53-BakMTS and p53-BaxMTS seen in Fig. 5 (5th bar) is not due to transcriptionally active p53.

To explore if p53-BakMTS and p53-BaxMTS initiate apoptosis through the intrinsic apoptotic pathway, two major hallmarks for the mitochondrial apoptotic pathway (27, 34), mitochondrial outer membrane permeabilization (MOMP) and caspase-9 induction, were measured.

The TMRE assay is a direct measurement of MOMP. Homo-oligomerization of Bak or Bax triggers MOMP (7, 8) which results in a decrease in mitochondrial membrane potential (35). Cationic dyes such as TMRE accumulate in the mitochondria of healthy cells due to the higher negative charge seen in the mitochondria compared to cytoplasm (27). MOMP results in a loss of TMRE from mitochondria and can be measured via flow cytometry (27). Apoptotic cells are identified by a loss of TMRE fluorescence intensity and are represented as %MOMP induction on and y-axis (Fig. 6b).

The ability of caspase-9 to cleave the peptide sequence leucine-glutamic acid-histidine-aspartic acid determines caspase-9 activity in apoptotic cells (36). When the mitochondrial outer membrane ruptures, cytochrome c is released from the intermembrane space (13). Cytochrome c and Apaf-1 form the apoptosome and activate caspase-9 as shown in Figure 1 (13). Caspase-9 activation was measured via the caspase-9 assay.

p53-BakMTS, p53-BaxMTS and *wt* p53 (Fig. 6b, and c; compare 1st, 3rd, and 5th bars) show a significant effect on MOMP and caspase-9 activation compared to their corresponding controls E-BakMTS, E-BaxMTS and EGFP (Fig. 6 b, and c; compare 2nd, 4rd, and 6th bars). The negative controls E-BakMTS and E-BaxMTS show higher MOMP and caspase-9 activation compared to non-toxic EGFP (Fig. 6b, and c; compare 2nd, 4rd, and 6th bars).

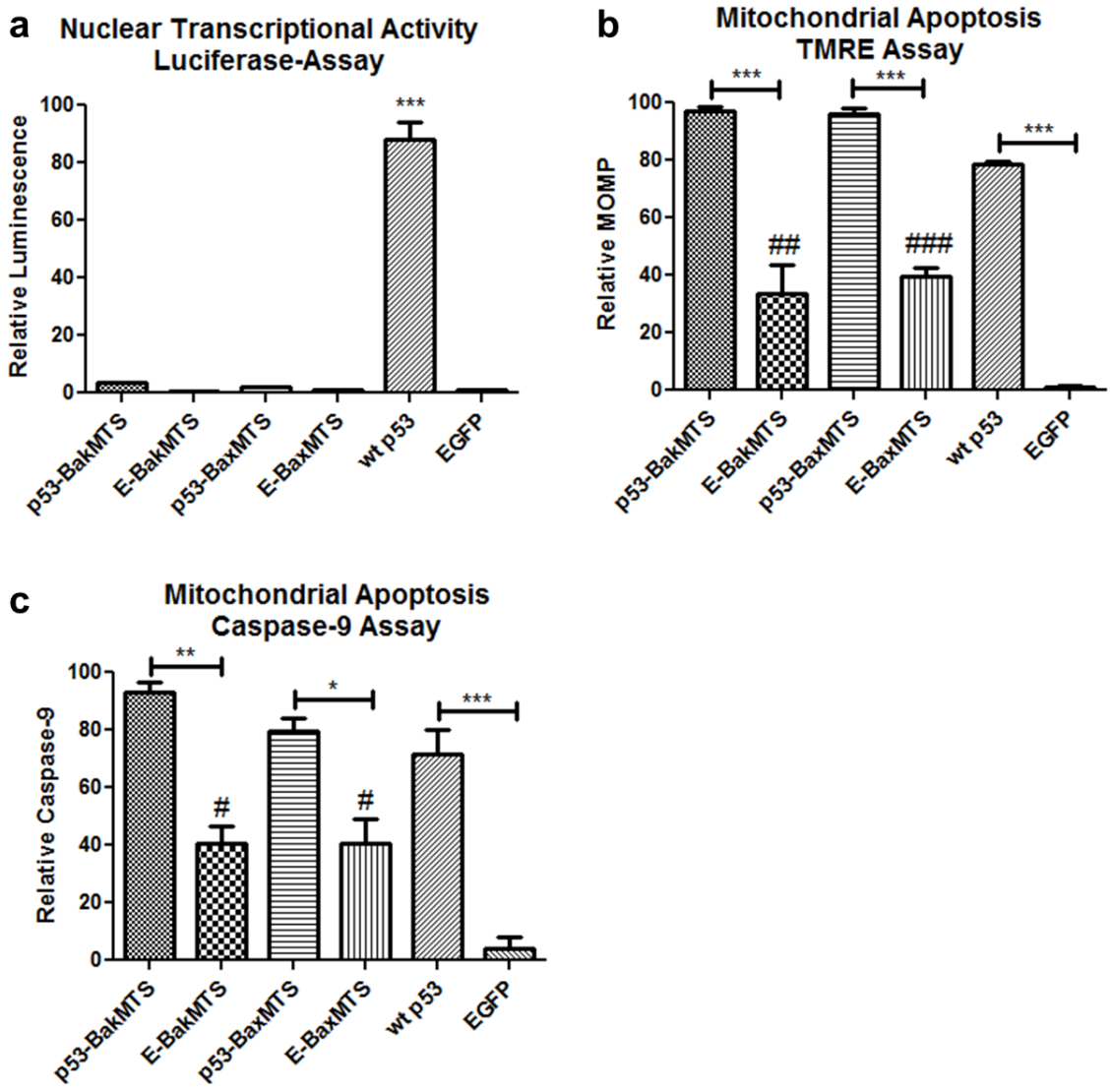

Fig. 6 (a) Nuclear transcriptional activity: p53 reporter gene assay: all MTS constructs were tested for their ability to activate p53-Luc Cis-Reporter in T47D cells. *Wt* p53 was used as a positive control and EGFP was considered a negative control. (b) Mitochondrial apoptosis: TMRE assay: all constructs were assayed in T47D cells. Mitochondrial depolarization correlates with an increase in MOMP (measured as loss of TMRE fluorescence). (c) Mitochondrial apoptosis: Caspase-9 activation was analyzed in T47D cells. All statistical analysis for a, b, and c were performed by using one-way ANOVA with Bonferroni's post test; *p< 0.05, **p < 0.01, ***p < 0.001.

Error bars represent standard deviations from at least three independent experiments (n=3). For b and c negative controls E-BakMTS and E-BaxMTS were compared to EGFP using one-way ANOVA with Bonferroni's post test; #p< 0.05, ##p < 0.01, ###p < 0.001. p53-BakMTS and p53-BaxMTS were not significantly higher from *wt* p53.

4.4.4 DBD-BakMTS and DBD-BaxMTS induce late stage apoptosis in a similar manner as p53-BakMTS and p53-BaxMTS

Pietsch et al. showed that p53 must form a dimer or a tetramer to activate Bak oligomerization (24). Additionally, the DBD has been reported to interact with pro-apoptotic Bak (25) and inhibit anti-apoptotic Bcl-XL (10) and Bcl-2 (11). We wanted to test if fusing DBD to MTS from Bak or Bax is sufficient to trigger apoptosis.

Similar levels of 7-AAD positive staining (apoptosis) were detected between cells transfected with DBD-BakMTS compared to p53-BakMTS (Fig. 7a), and cells transfected with DBD-BaxMTS and p53-BaxMTS (Fig. 7b). Additionally, all of these constructs had significantly higher apoptosis compared to cells transfected with MTS negative controls (E-BakMTS, E-BaxMTS) (Figs. 7a and b). DBD fused to Bak or Bax MTS induces a similar apoptotic response as full length p53 fused to these MTSs (Figs. 7a and b).

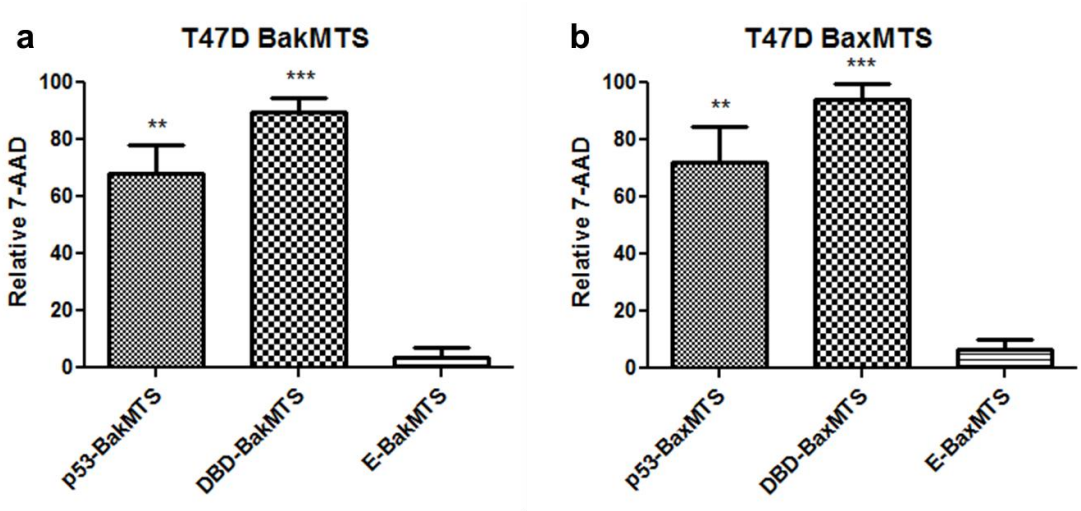

Fig. 7 7-AAD assay in T47D cells: Apoptotic potential of DBD-BakMTS and DBD-BaxMTS were tested. Statistical analysis was performed by using one-way ANOVA with Bonferroni's post test; **p < 0.01, ***p < 0.001 compared to negative controls. Error bars represent standard deviations from at least three independent experiments (n=3).

4.4.5 The activity of our re-engineered mitochondrially targeted p53 constructs in different cancer cell types

To confirm that the apoptotic potential of our designed constructs causes apoptosis in other cell lines besides T47D breast cancer cells (which express mutant p53 with a L194F point mutation in the DBD of p53) (37), a 7-AAD assay was conducted in non-small cell lung cancer cells (H1373), ovarian cancer cells (SKOV-3) and cervical carcinoma cells (HeLa). H1373 (38) and SKOV-3 cells are p53 null (39) while HeLa cells have endogenous *wt* p53 (40).

In H1373 cells, both p53-BakMTS and DBD-BakMTS apoptotic activities were statistically higher from their negative control E-BakMTS (Fig. 8a; compare 1st, 2nd, and 3rd bars). As expected, *wt* p53 showed significantly higher apoptosis compared to EGFP (Fig. 8a and b; compare 4st, and 5st bars). However, only DBD-BaxMTS

activity was significantly higher than E-BaxMTS (Fig. 8b; compare 2nd and 3rd bars) and there was no significant difference between p53-BaxMTS and E-BaxMTS (Fig. 8b; compare 1st and 3rd bars). Additionally, DBD-BakMTS and DBD-BaxMTS had significantly higher activities compared to their positive controls p53-BakMTS and p53-BaxMTS (Fig. 8a and b; compare 1st and 2nd bars).

In SKOV-3 cells, p53-BakMTS and DBD-BakMTS activities were significantly higher than their negative control E-BakMTS (Fig. 8c; compare 1st, 2nd, and 3rd bars). p53-BaxMTS and DBD-BaxMTS activities were only significant when compared to EGFP but no to E-BaxMTS (Fig 8d; compare 1st, 2nd, 3rd, and 5th bars). The activity of *wt* p53 was similar to nontoxic EGFP in SKOV-3 cells (Fig. 8c and d; compare 4th and 5th bars).

In HeLa cells, p53-BakMTS, DBD-BakMTS (Fig. 8e; compare 1st and 2nd bars), p53-BaxMTS, DBD-BaxMTS (Fig. 8f; compare 1st, and 2nd bars) and *wt* p53 (Fig. 8e and f; 4th bars) apoptotic activities were significant from their corresponding negative controls E-BakMTS (Fig. 8e; 3rd bar), E-BaxMTS (Fig. 8f; 3rd bar) and EGFP (Fig. 8e, and f; 5th bar) respectively. DBD-BakMTS showed a trend of higher apoptotic activity in HeLa cells compared to p53-BakMTS (Fig. 8e; compare 1st and 2nd bars). In addition, DBD-BaxMTS was significantly higher than p53-BaxMTS (Fig.8f; compare 1st and 2nd bars).

p53 is known to induce a conformational change in Bax that triggers its oligomerization and mitochondrial permeabilization through a hit-and-run type mechanism (7). However, this p53 interaction with Bax is transient, and the specific interacting residues are not known (7, 8, 12). On the other hand, it is known that p53 interacts with the Bak protein via amino acids K120, R248, R273, R280, E285 and E287 in p53 (25). Therefore these residues will be mutated to determine if this is a Bak specific interaction. Since p53-BakMTS and DBD-BakMTS showed consistently higher apoptotic activities than their MTS control in all tested cell lines (Figs. 7a, 8a,

c, e; compare 1st, 2nd, and 3rd bars), we proceeded to examine the apoptotic mechanism of the Bak MTS constructs.

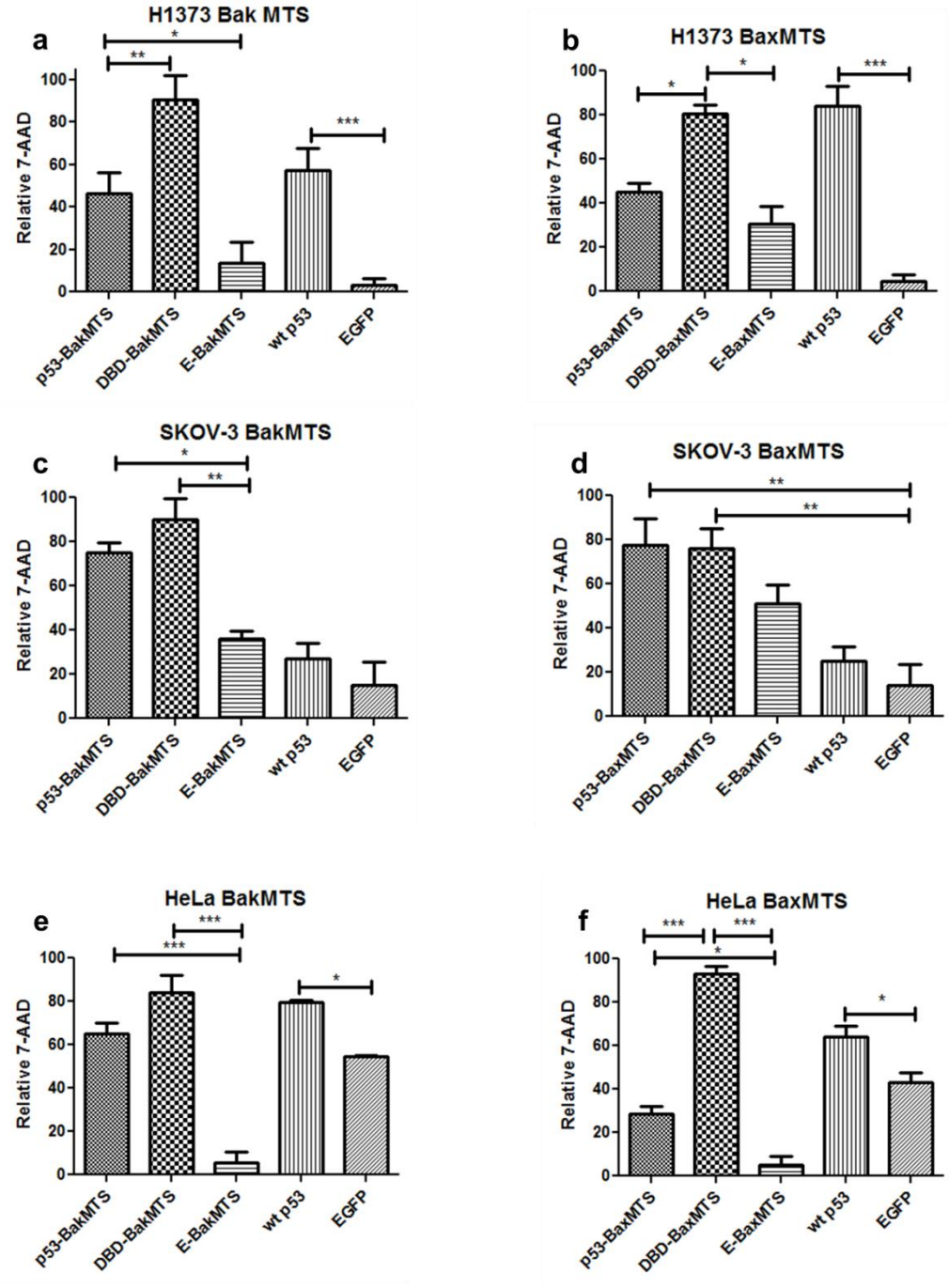

Fig. 8 7-AAD assay was conducted in (a) and (b) H1373, (c) and (d) SKOV-3, (e) and (f) HeLa cells. Statistical analysis was performed by using one-way ANOVA with Bonferroni's post test;* $p < 0.05$, **$p < 0.01$, ***$p < 0.001$. Error bars represent standard deviations from at least three independent experiments (n=3).

4.4.6 Exploring the interaction between p53-BakMTS, DBD-BakMTS and pro-apoptotic Bak protein

It has been reported that p53 interacts with pro-apoptotic Bak protein via amino acids K120, R248, R273, R280, E285 and E287, all of which are found in the DBD of p53 (25). To verify that the apoptotic potential of p53-BakMTS and DBD-BakMTS is through the p53/Bak specific pathway, all sites of p53 (K120A, R248A, R273A, R280A, E285A, E287A) (25) that contact the pro-apoptotic Bak protein were mutated to alanine. The constructs with these six mutations were named p53m6-BakMTS and DBDm6-BakMTS.

Mutating all six of these residues in p53-BakMTS to eliminate binding to pro-apoptotic Bak protein resulted in a complete loss of p53-BakMTS activity (Fig. 9a; 4th bar). p53m6-BakMTS and DBDm6-BakMTS activities are not significantly different from their negative control E-BakMTS suggesting Bak dependent apoptosis (Fig. 9a; compare 3rd, 4th, and 5th bars).

As mentioned above p53 interacts with Bak via its DBD (residues K120, R248, R273, R280, E285, E287). However, p53 also interacts with anti-apoptotic Bcl-XL through the following residues G117, S121, C176, H178, N239, M243, R248, G279, and R280 (10). Therefore, R248 and R280 localized in the DBD of p53 can interact with Bak and Bcl-XL. To exclude any Bcl-XL specific interaction of our designed constructs, only K120 was mutated in the p53-BakMTS and DBD-BakMTS plasmid to glutamic acid. The K120 residue only interacts with Bak not with Bcl-XL (10, 25).

Mutating the positively charged lysine 120 to negatively charged glutamic acid (K120E) in p53-BakMTS and DBD-BakMTS resulted in complete loss of apoptotic activity (Fig. 9b; 4th and 5th bars). p53K120E-BakMTS and DBDK120E-BakMTS activities are not statistically significant from the negative control E-BakMTS (Fig. 9b; compare 3rd, 4th, and 5th bars), suggesting a p53/Bak dependent apoptotic mechanism.

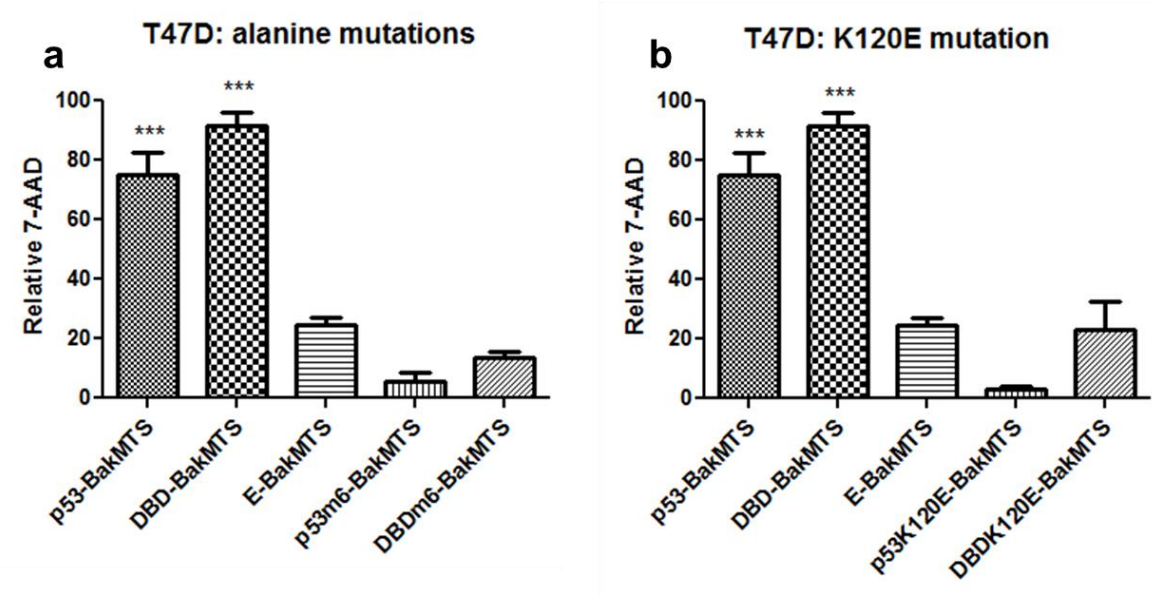

Fig. 9 Decrease in apoptotic potential caused by (a) K120A, R248A, R273A, R280A, E285A, E287A (m6) mutations and (b) K120E mutation was measured via 7-AAD assay in T47D cells. Statistical analysis was performed by using one-way ANOVA with Bonferroni's post test; **p < 0.01, ***p < 0.001 compared to E-BakMTS. Error bars represent standard deviations from at least three independent experiments (n=3).

4.5 Discussion

We and others have shown that targeting p53 to the mitochondria is sufficient to trigger a rapid apoptotic response (4, 26, 27, 41). Previously, our focus was to target p53 to different mitochondrial compartments concluding that targeting it to the outer surface of the mitochondrial membrane is the only compartment that leads to p53-dependent apoptosis (26), rather than non-specific mitochondrial toxicity. So far, only anti-apoptotic binding partners (such as Bcl-XL and Bcl-2) on the outer membrane have been addressed for p53 specific targeting. These constructs sequester anti-apoptotic Bcl-2 family members and therefore indirectly activate Bak and Bax (26). Here, our approach is to target p53 directly to Bak and Bax proteins. To our knowledge, this is the first attempt to target p53 to these pro-apoptotic proteins.

Fusing p53 to the MTSs derived from the pro-apoptotic Bak (p53-BakMTS) or Bax (p53-BaxMTS) proteins resulted in localization of these constructs to the mitochondria (Fig. 4) and induction of apoptosis (Figs. 5; 6b and c; 7). The tumor suppressor p53 is a nuclear protein containing three NLSs (5). When targeting p53 to the mitochondria, the chosen MTS must counteract these NLSs. Previously, our lab has targeted p53 with the MTSs from ornithine transcarbamylase (OTC), cytochrome c oxidase (CCO), translocase of the outer membrane (TOM) and Bcl-XL (XL) (26). We have shown that strong MTSs from TOM and XL are capable of overcoming the NLSs in the p53 protein while the weak MTS from CCO and the medium strength MTS from OTC are not strong enough to ensure entire mitochondrial targeting (26). Here, we show that MTSs from Bak and Bax are capable of counteracting the three NLSs in *wt* p53 and can be considered to be strong MTSs (Fig. 4). Additionally, EGFP fused to MTSs from Bak (E-BakMTS) or Bax (E-BaxMTS) showed minimal inherent toxicity which suggests that apoptotic activity of p53-BakMTS and p53-BaxMTS are p53 dependent and not due to MTS toxicity (Fig. 5).

Since we confirmed mitochondrial localization and apoptotic potential of p53-BakMTS and p53-BaxMTS, we wanted to examine if the apoptotic response occurs mainly through the mitochondrial pathway or through residual nuclear activity. As expected, *wt* p53 showed high nuclear activity, while p53-BakMTS and p53-BaxMTS showed no transcriptional activity, suggesting that the apoptotic function of p53-BakMTS and p53-BaxMTS is transcriptionally independent (Fig. 6a).

Further, we demonstrated that the apoptotic activity of p53-BakMTS and p53-BaxMTS is through the intrinsic apoptotic pathway. Mitochondrial outer membrane permeabilization (MOMP) and caspase-9 activation can only be initiated via the intrinsic apoptotic pathway (13). In fact, p53-BakMTS and p53-BaxMTS triggered permeabilization of the mitochondrial outer membrane and induced caspase-9 activation confirming the involvement of the intrinsic apoptotic pathway (Fig. 6b and c).

Negative controls E-BakMTS and E-BaxMTS showed some MOMP and caspase-9 activation which was higher than EGFP but still significantly lower than p53-BakMTS and p53-BaxMTS (Fig. 6b and c). However, this is not reflected in the more final apoptosis assay 7-AAD (Fig. 5) (32). It has been reported that can recover from mitochondrial outer membrane permeabilization (MOMP) which is measured by TMRE; cells can also recover from caspase-9 activation (13). Therefore, sending GFP to the mitochondria is slightly toxic to the cells reflected by TMRE and caspase-9 assay (Fig. 6) but does not translate into final cell death measured by 7-AAD assay (Fig. 5 and 8).

Next, we wanted to examine if a single domain of p53 (DBD) is sufficient to trigger apoptosis or if full length p53 is essential for cell death induction. Although the TD was reported to be essential for *wt* p53 function to exert its apoptotic effect via Bak oligomerization (24), we note our important discovery, that the DBD in isolation with a MTS from Bak or Bax is sufficient to induce apoptosis (Fig. 7). Murphy and colleagues reported that p53 must form a dimer or a tetramer for initiating Bak

oligomerization (24). However, our data is consistent with our previous finding (27) and other reports (10, 11) that monomeric p53 or just the DBD is sufficient to trigger mitochondrial dependent apoptosis. Moreover, the DBD of p53 (specifically through residues L120, R248, R273, R280, G285 and G287) has been shown to be the domain responsible for binding to Bak (25). An possible explanation to why DBD fused to MTS is sufficient to trigger apoptosis could be that since *wt* p53 does not have a MTS, mitochondrial import of *wt* p53 is only possible through dimerization and monoubiquitination via MDM2 (6). We postulate that forcing the DBD of p53 to be in close proximity to Bak via the Bak targeting signal may trigger an interaction with Bak via the previously reported residues in the DBD region leading to activation of the apoptotic pathway (25). In *wt* p53 the lack of a Bak MTS does not allow the interaction to take place. These results suggest that the Bak MTS fused to DBD can replace MBD and TD for mitochondrial import and is sufficient to cause Bak homo-oligomerization and apoptosis.

To ensure that this finding is not a T47D cell specific effect, we tested the DBD-BakMTS and DBD-BaxMTS in three different cancer cell lines (Fig. 8; Tbl. 2). In fact, DBD-BakMTS showed even significantly higher (Fig. 8a) or trending higher (Figs. 7a, 8c and e) activity compared to p53-BakMTS. A possible reason for the higher activity of DBD-BakMTS over full length p53-BakMTS is that DBD-BakMTS is lacking the MBD and C-terminus which are essential for the p53 degradation pathway. MDM2 binds to MBD of p53 and initiates polyubiquitination of the C-terminus causing proteasomal degradation (42, 43). As DBD-BakMTS lacks the MBD and C-terminus, it may avoid polyubiquitination and subsequent proteasomal degradation, thus making it more stable than p53-BakMTS.

Unlike constructs fused to Bak MTS, Bax tagged constructs showed inconsistent apoptotic activity profiles (Fig. 7 and 8). In SKOV-3, p53-BaxMTS and DBD-BaxMTS activities were not significantly different from their negative control E-BaxMTS (Fig. 8d), and in H1373 p53-BaxMTS did not show higher activity than E-BaxMTS (Fig. 8b). A possible explanation for this is that Bax is constantly shuttled between

cytoplasm and mitochondria (Fig. 3) (44, 45) . Mitochondrial p53 might lack the ability to activate cytoplasmic Bax while the fraction of Bax which is present at the mitochondria might not be sufficient to induce apoptosis in certain cell lines. This might offer an explanation why p53-BaxMTS and DBD-BaxMTS show inconsistent results (Fig. 7a; 8b,d, and f). Unlike Bax, Bak is mainly present at the mitochondria and sequestered by anti-apoptotic Mcl-1 and to a certain extent by Bcl-XL (19).

As our ultimate goal is to find a construct capable of robust apoptosis, we proceeded with BakMTS constructs for further studies. The apoptotic mechanism of p53-BakMTS and DBD-BakMTS was then investigated. p53-BakMTS causes apoptosis through a p53/Bak specific pathway, which was confirmed by mutating amino acids of p53 DBD (K120, R248, R273, R280, E285, E287) that are known to interact with the pro-apoptotic Bak protein to abolish any p53/Bak specific interactions (25). In fact, mutating these amino acids showed a complete loss of p53-BakMTS and DBD-BakMTS function (Fig. 9a).

Besides pro-apoptotic Bak, p53 also interacts with anti-apoptotic Bcl-XL through its DBD (residues G117, S121, C176, H178, N239, M243, R248, G279, and R280) (10). p53 interacts through amino acids R248 and R280 with Bak and Bax. To further validate that the apoptotic mechanism is mainly dependent on pro-apoptotic Bak protein and not Bcl-XL, the p53K120E-BakMTS and DBDK120E-BakMTS were created. This K120 residue is known to be significant and specific for the p53/Bak interaction (25). K120E mutation in p53-BakMTS and DBD-BakMTS resulted in dramatic loss of activity suggesting involvement of Bak/specific p53 pathway (Fig. 9b).

Our mitochondrially targeted p53 could potentially have additive or synergistic apoptotic effects with endogenous *wt* p53. *wt* p53 mainly translocates to the nucleus and triggers transactivation of genes responsible for the extrinsic and intrinsic pathway. While mitochondrial p53 might trigger the first wave of intrinsic apoptosis, *wt* p53 might additively or synergically enhance apoptosis via activation of the

extrinsic and intrinsic pathway. This situation would occur only if endogenous *wt* p53 was activated under stress conditions such as radiation or chemotherapy treatment.

In summary, our data shows that fusing p53 to MTSs from Bak or Bax results in mitochondrial localization and activation of an intrinsic apoptotic response. DBD-BakMTS and p53-BakMTS show apoptosis in breast, non-small cell lung, ovarian and cervical carcinomas in a p53/Bak dependent manner. Our next step is to test p53-BakMTS and DBD-BakMTS using adenoviral drug delivery in orthotopic breast cancer and ovarian cancer models to validate this *in vitro* work. Ultimately, correction of the p53 pathway and activation of apoptosis may be a universal approach. Mitochondrially targeted p53, which does not dimerize nor activate genes in the nucleus, simply has a direct apoptotic effect. Therefore, functional, mitochondrially targeted monomeric p53 re-introduced into cancer cells would act as a "sledgehammer," effective under any circumstances regardless of genetics or the pathway upon which the cancer develops.

4.6 Acknowledgements

Research reported in this publication was supported by the National Cancer Institute of the National Institutes of Health under award number R01-CA151847. The authors would also like to acknowledge Christian Raab for his technical work. We also would like to thank Ben Bruno and Geoff Miller for reviewing the manuscript. We acknowledge the use of DNA/Peptide Core and Flow Cytometry Core (NCI Cancer Center Support Grant P30 CA042014, Huntsman Cancer Institute).

4.7 References

1. Haupt S, Berger M, Goldberg Z, Haupt Y. Apoptosis - the p53 network. J Cell Sci. 2003 Oct 15;116(Pt 20):4077-85.

2. Davis JR, Mossalam M, Lim CS. Controlled access of p53 to the nucleus regulates its proteasomal degradation by MDM2. Mol Pharm. 2013 Apr 1;10(4):1340-9.

3. Weinberg RL, Freund SM, Veprintsev DB, Bycroft M, Fersht AR. Regulation of DNA binding of p53 by its C-terminal domain. J Mol Biol. 2004 Sep 17;342(3):801-11.

4. Mihara M, Erster S, Zaika A, Petrenko O, Chittenden T, Pancoska P, et al. p53 has a direct apoptogenic role at the mitochondria. Mol Cell. 2003 Mar;11(3):577-90.

5. Shaulsky G, Goldfinger N, Ben-Ze'ev A, Rotter V. Nuclear accumulation of p53 protein is mediated by several nuclear localization signals and plays a role in tumorigenesis. Mol Cell Biol. 1990 Dec;10(12):6565-77.

6. Marchenko ND, Wolff S, Erster S, Becker K, Moll UM. Monoubiquitylation promotes mitochondrial p53 translocation. EMBO J. 2007 Feb 21;26(4):923-34.

7. Perfettini JL, Kroemer RT, Kroemer G. Fatal liaisons of p53 with Bax and Bak. Nat Cell Biol. 2004 May;6(5):386-8.

8. Chipuk JE, Kuwana T, Bouchier-Hayes L, Droin NM, Newmeyer DD, Schuler M, et al. Direct activation of Bax by p53 mediates mitochondrial membrane permeabilization and apoptosis. Science. 2004 Feb 13;303(5660):1010-4.

9. Leu JI, Dumont P, Hafey M, Murphy ME, George DL. Mitochondrial p53 activates Bak and causes disruption of a Bak-Mcl1 complex. Nat Cell Biol. 2004 May;6(5):443-50.

10. Hagn F, Klein C, Demmer O, Marchenko N, Vaseva A, Moll UM, et al. BclxL changes conformation upon binding to wild-type but not mutant p53 DNA binding domain. J Biol Chem. 2010 Jan 29;285(5):3439-50.

11. Tomita Y, Marchenko N, Erster S, Nemajerova A, Dehner A, Klein C, et al. WT p53, but not tumor-derived mutants, bind to Bcl2 via the DNA binding domain and induce mitochondrial permeabilization. J Biol Chem. 2006 Mar 31;281(13):8600-6.

12. Chipuk JE, Fisher JC, Dillon CP, Kriwacki RW, Kuwana T, Green DR. Mechanism of apoptosis induction by inhibition of the anti-apoptotic BCL-2 proteins. Proc Natl Acad Sci U S A. 2008 Dec 23;105(51):20327-32.

13. Tait SW, Green DR. Mitochondria and cell death: outer membrane permeabilization and beyond. Nat Rev Mol Cell Biol. 2010 Sep;11(9):621-32.

14. Chowdhury I, Tharakan B, Bhat GK. Caspases - an update. Comp Biochem Physiol B Biochem Mol Biol. 2008 Sep;151(1):10-27.

15. Minn AJ, Rudin CM, Boise LH, Thompson CB. Expression of bcl-xL can confer a multidrug resistance phenotype. Blood. 1995 Sep 1;86(5):1903-10.

16. Yoshino T, Shiina H, Urakami S, Kikuno N, Yoneda T, Shigeno K, et al. Bcl-2 expression as a predictive marker of hormone-refractory prostate cancer treated with taxane-based chemotherapy. Clin Cancer Res. 2006 Oct 15;12(20 Pt 1):6116-24.

17. Green DR, Walczak H. Apoptosis therapy: driving cancers down the road to ruin. Nat Med. 2013 Feb;19(2):131-3.

18. Kang MH, Reynolds CP. Bcl-2 inhibitors: targeting mitochondrial apoptotic pathways in cancer therapy. Clin Cancer Res. 2009 Feb 15;15(4):1126-32.

19. Willis SN, Chen L, Dewson G, Wei A, Naik E, Fletcher JI, et al. Proapoptotic Bak is sequestered by Mcl-1 and Bcl-xL, but not Bcl-2, until displaced by BH3-only proteins. Genes Dev. 2005 Jun 1;19(11):1294-305.

20. Ku B, Liang C, Jung JU, Oh BH. Evidence that inhibition of BAX activation by BCL-2 involves its tight and preferential interaction with the BH3 domain of BAX. Cell Res. 2011 Apr;21(4):627-41.

21. Schinzel A, Kaufmann T, Schuler M, Martinalbo J, Grubb D, Borner C. Conformational control of Bax localization and apoptotic activity by Pro168. J Cell Biol. 2004 Mar 29;164(7):1021-32.

22. Ferrer PE, Frederick P, Gulbis JM, Dewson G, Kluck RM. Translocation of a Bak C-terminus mutant from cytosol to mitochondria to mediate cytochrome C release: implications for Bak and Bax apoptotic function. PLoS One. 2012;7(3):e31510.

23. Nechushtan A, Smith CL, Hsu YT, Youle RJ. Conformation of the Bax C-terminus regulates subcellular location and cell death. EMBO J. 1999 May 4;18(9):2330-41.

24. Pietsch EC, Leu JI, Frank A, Dumont P, George DL, Murphy ME. The tetramerization domain of p53 is required for efficient BAK oligomerization. Cancer Biol Ther. 2007 Oct;6(10):1576-83.

25. Pietsch EC, Perchiniak E, Canutescu AA, Wang G, Dunbrack RL, Murphy ME. Oligomerization of BAK by p53 utilizes conserved residues of the p53 DNA binding domain. J Biol Chem. 2008 Jul 25;283(30):21294-304.

26. Mossalam M, Matissek KJ, Okal A, Constance JE, Lim CS. Direct induction of apoptosis using an optimal mitochondrially targeted p53. Mol Pharm. 2012 May 7;9(5):1449-58.

27. Matissek KJ, Mossalam M, Okal A, Lim CS. The DNA Binding Domain of p53 Is Sufficient To Trigger a Potent Apoptotic Response at the Mitochondria. Mol Pharm. 2013 Sep 6.

28. Constance JE, Woessner DW, Matissek KJ, Mossalam M, Lim CS. Enhanced and selective killing of chronic myelogenous leukemia cells with an engineered BCR-ABL binding protein and imatinib. Mol Pharm. 2012 Nov 5;9(11):3318-29.

29. Costes SV, Daelemans D, Cho EH, Dobbin Z, Pavlakis G, Lockett S. Automatic and quantitative measurement of protein-protein colocalization in live cells. Biophys J. 2004 Jun;86(6):3993-4003.

30. Bolte S, Cordelieres FP. A guided tour into subcellular colocalization analysis in light microscopy. J Microsc. 2006 Dec;224(Pt 3):213-32.

31. Okal A, Mossalam M, Matissek KJ, Dixon AS, Moos PJ, Lim CS. A Chimeric p53 Evades Mutant p53 Transdominant Inhibition in Cancer Cells. Mol Pharm. 2013 Sep 9.

32. Schmid I, Krall WJ, Uittenbogaart CH, Braun J, Giorgi JV. Dead cell discrimination with 7-amino-actinomycin D in combination with dual color immunofluorescence in single laser flow cytometry. Cytometry. 1992;13(2):204-8.

33. Yahagi N, Shimano H, Matsuzaka T, Najima Y, Sekiya M, Nakagawa Y, et al. p53 Activation in adipocytes of obese mice. J Biol Chem. 2003 Jul 11;278(28):25395-400.

34. Wurstle ML, Laussmann MA, Rehm M. The central role of initiator caspase-9 in apoptosis signal transduction and the regulation of its activation and activity on the apoptosome. Exp Cell Res. 2012 Jul 1;318(11):1213-20.

35. Darzynkiewicz Z, Bruno S, Del Bino G, Gorczyca W, Hotz MA, Lassota P, et al. Features of apoptotic cells measured by flow cytometry. Cytometry. 1992;13(8):795-808.

36. Yin Q, Park HH, Chung JY, Lin SC, Lo YC, da Graca LS, et al. Caspase-9 holoenzyme is a specific and optimal procaspase-3 processing machine. Mol Cell. 2006 Apr 21;22(2):259-68.

37. Nigro JM, Baker SJ, Preisinger AC, Jessup JM, Hostetter R, Cleary K, et al. Mutations in the p53 gene occur in diverse human tumour types. Nature. 1989 Dec 7;342(6250):705-8.

38. Bodner SM, Minna JD, Jensen SM, D'Amico D, Carbone D, Mitsudomi T, et al. Expression of mutant p53 proteins in lung cancer correlates with the class of p53 gene mutation. Oncogene. 1992 Apr;7(4):743-9.

39. Yaginuma Y, Westphal H. Abnormal structure and expression of the p53 gene in human ovarian carcinoma cell lines. Cancer Res. 1992 Aug 1;52(15):4196-9.

40. Goodrum FD, Ornelles DA. p53 status does not determine outcome of E1B 55-kilodalton mutant adenovirus lytic infection. J Virol. 1998 Dec;72(12):9479-90.

41. Erster S, Moll UM. Stress-induced p53 runs a direct mitochondrial death program: its role in physiologic and pathophysiologic stress responses in vivo. Cell Cycle. 2004 Dec;3(12):1492-5.

42. Nalepa G, Rolfe M, Harper JW. Drug discovery in the ubiquitin-proteasome system. Nat Rev Drug Discov. 2006 Jul;5(7):596-613.

43. Haupt Y, Maya R, Kazaz A, Oren M. Mdm2 promotes the rapid degradation of p53. Nature. 1997 May 15;387(6630):296-9.

44. Schellenberg B, Wang P, Keeble JA, Rodriguez-Enriquez R, Walker S, Owens TW, et al. Bax exists in a dynamic equilibrium between the cytosol and mitochondria to control apoptotic priming. Mol Cell. 2013 Mar 7;49(5):959-71.

45. Edlich F, Banerjee S, Suzuki M, Cleland MM, Arnoult D, Wang C, et al. Bcl-x(L) retrotranslocates Bax from the mitochondria into the cytosol. Cell. 2011 Apr 1;145(1):104-16.

5. Delivery of a monomeric p53 with mitochondrial targeting signals from anti-apoptotic Bcl-XL to overcome dominant negative inhibition of mutant p53

5.1 Abstract

The tumor suppressor p53 is mutated in 60-88% of triple negative breast cancers, the most deadly form of breast cancer. Most of these mutations occur in the DNA binding domain (DBD) of p53 while the tetramerization domain (TD) remains active. This mutant p53 can heterotetramerize with exogenous *wt* p53 which is known as dominant negative inhibition. Unlike *wt* p53 which is only transcriptionally active as a tetramer, mitochondrial p53 performs its apoptotic function as a monomer. Targeting p53 to the mitochondria causes a rapid apoptotic response through direct interaction with pro-and anti-apoptotic Bcl-2 protein family members. To investigate if mitochondrially targeted p53 is capable of overcoming dominant negative inhibition, we tested p53 and its DBD tagged to the mitochondrial targeting signal (MTS) from anti-apoptotic Bcl-XL, *in vitro* and *in vivo*. We wanted to verify if mitochondrial p53 is affected by mutant p53 status *in vitro*, first by overexpressing R248W mutant p53 in p53 null non-small cell lung cancer cells (H1373 cells), and second, by conducting apoptosis assays in MDA-MB-468 triple negative breast cancer cells which harbor R273H mutant p53. While DBD fused to MTS from Bcl-XL (DBD-XL) was capable of overcoming dominant negative inhibition by mutant p53, it was unable to shrink MDA-MB-468 tumors in an orthotopic mouse model.

5.2 Introduction

The tumor suppressor p53 has been the focus of intensive cancer-based research in laboratories around the world for more than three decades. This resulted in adenovirally delivered *wt* p53 being approved for gene therapy in China under the trade names Gendicine and Oncorine (1, 2). Additionally, there are various clinical

trials for p53 based cancer therapy around the world (3). However, limitations of its use are due to dominant negative inactivation of *wt* p53 by endogenous mutant p53 (4, 5). Mutations in the p53 gene typically occur in the DNA binding domain (DBD) of p53, while the tetramerization (TD) domain usually remains active (6, 7). Therefore, *wt* p53 can form heterotetramers with mutant p53 which abolishes the transcriptional activity of the *wt* p53/mutp53 heterotetramer complex (5, 8, 9). This is, for example, a problem in triple negative breast cancer (TNBC) where 60-88% of TNBC have mutated p53 and would exhibit dominant negative inhibition if *wt* p53 was reintroduced (10). Mitochondrial p53 could circumvent this problem, and would represent a major advancement in treatment of TNBC.

We and others have shown that p53 targeted to the mitochondria interacts with pro- and anti-apoptotic Bcl-2 proteins at the mitochondrial outer membrane and causes a rapid apoptotic response (11-13). Our lab was the first to show that the DBD of p53 delivered to the mitochondria by a mitochondrial targeting signal is sufficient to cause apoptosis (14). Since DBD lacks the TD which is essential for tetramer formation, p53 initiates apoptosis at the mitochondria likely without tetamerization (e.g., as a monomer). We hypothesis that monomeric p53 will evade dominant negative inhibition of endogenous mutant p53. Our approach is to deliver p53-XL and DBD-XL adenovirally and show apoptosis *in vitro* and *in vivo*.

Since p53 delivered by adenovirus is already approved as a drug and has been used in various clinical trials (1, 2, 15, 16), we chose adenovirus for delivery as well. Nielsen et al. have already attempted to use adenovirally delivered *wt* p53 to treat xenografted triple negative breast cancer MDA-MB-468 tumors in mice (17, 18). However, due to the dominant negative inhibition of mutant p53, *wt* p53 was unable to cause tumor shrinkage and only resulted in tumor growth inhibition (17). Our approach is to use intratumorally injected adenoviral p53-XL and DBD-XL in an orthotopic breast cancer mouse model. We hypothesized that this would result in cell apoptosis and tumor shrinkage since our constructs will not be affected by dominant negative inhibition by mutant p53.

5.3 Methods

5.3.1 Cell Lines

H1373 human non-small cell lung carcinoma cells (a kind gift from Dr. Andrea Bild, University of Utah) were grown as monolayers in RPMI (Invitrogen, Carlsbad, CA) supplemented with 10% fetal bovine serum (Invitrogen), 1% penicillin-streptomycin-glutamine (Invitrogen), and 0.1% gentamicin (Invitrogen). HEK293 human embryonic kidney (ATCC) and MDA-MB-468 human breast adenocarcinoma cells (ATCC) were grown as monolayers in DMEM (Invitrogen) supplemented with 10% fetal bovine serum, 1% penicillin-streptomycin-glutamine, and 0.1% gentamicin. MDA-MB-468 cells were also supplemented with 1% MEM non-essential amino acids (Invitrogen). All cells were incubated in 5% CO2 at 37ºC. The cells were seeded for transduction at a density of 3.0×10^5 cells in 6-well plates (Greiner Bio-One, Monroe, NC). Viral transductions were carried out immediately after seeding the cells.

5.3.2 Recombinant Adenovirus Production

As previously (19), replication-deficient recombinant adenovirus serotype 5 (Ad) constructs were created by inserting PCR amplified p53-XL (Ad-p53-XL) or DBD-XL (Ad-DBD-XL) into a cassette under the control of the CMV promoter. Prior to insertion, these constructs were PCR amplified with primers containing 15 base pair homology with a linearized pAdenoX vector (Clontech) based on an In-Fusion® HD Cloning Kit (Clontech). Empty vector served as negative control (Ad-ZsGreen). For visualization the Adeno-X® Adenoviral Expression System 3 contains a separate CMV promoter for ZsGreen1 expression. The adenoviral vector plasmids containing our constructs were transformed into Stellar® competent cells (Clontech). For packaging and amplification, viral DNA was purified linearized and transfected into HEK293 cells. Viral particles were isolated from HEK293 cells by freeze-thawing, purified using Adeno-X® Mega Purification Kit (Clontech), and dialyzed against storage and proper tonicity buffer (2.5% glycerol (w/v), 25 mM NaCl, and 20 mM

Tris-HCl, pH 7.4). Following the manufacturer's recommendation, flow cytometry was used to determine the viral titer.

5.3.3 Overexpression of Mutant p53 using Lipofectamine Transfection

H1373 cells were cotransfected with 1 pmol of the transdominant mutant pTagBFP-mut-p53 (R248W) and 1 pmol of previously designed plasmids *wt* p53, p53-XL, E-XL or EGFP (19). To create pTagBFP-mut-p53 (R248W) the following primers were used 5′-CTGCATGGGCGGCATGAACTGGAGGCCCATCCTCACCA-3′ and 5′-TGGTGAGGATGGGCCTCCAGTTCATGCCGCCCATGCAG-3′. p53-XL was designed by cloning *wt* p53 and MTS from anti-apoptotic Bcl-XL into EGFP-C1 vector. E-XL was created by inserting MTS from XL into EGFP-C1 vector (13). Lipofectamine was used as the transfection reagent as before (13, 19, 20). 48 h post transfection, cells were stained as described in the 7-AAD assay and gated for EGFP and BFP using the FACSCanto-II (BD-BioSciences, University of Utah Core Facility) and FACSDiva software. Excitation for BFP was set at 405 nm and detected at 457 nm. The means from three separate experiments (n=3) were analyzed using two-way ANOVA with Bonferroni's post hoc test.

5.3.4 7-AAD Assay

As previously (13, 19, 20), 48 h after transfection MDA-MB-468 cells were stained with 7-aminoactinomycin D (7-AAD, Invitrogen). Excitation was set at 488 nm and detected at 507 nm and 780 nm for ZsGreen1 and 7-AAD, respectively using the FACSCanto-II (BD-BioSciences, University of Utah Core Facility) and FACSDiva software. The means from three separate experiments (n=3) were analyzed using one-way ANOVA with Bonferroni's post hoc test.

5.3.5 Western Blotting

MDA-MB-468 were harvested 24 h post infection, pelleted and resuspended in 200 µL lysis buffer (62.5 mM Tris-HCl, 2% w/v SDS, 10% glycerol, 1 % protease inhibitor). Standard western blotting procedures (19) were followed using primary antibodies to detect caspase-9, and actin as a loading control. The primary antibodies anti-caspase-9 (#7237P, Cell Signaling Technology) and anti-actin (rabbit, ab1801, Abcam) were detected with anti-rabbit (#7074S, Cell Signaling Technology) antibodies before the addition of SuperSignal West Pico chemiluminescent substrate (Thermo Scientific, Waltham, MA). The FluorChem FC2 imager and software (Alpha Innotech, Santa Clara, CA) was used to detect the signal.

5.3.6 *In Vivo* Experiments

Female nu/nu athymic mice (4-6 weeks old, Jackson Laboratories) were injected subcutaneously into the mammary fat pad with human MDA-MB-468 cells ($1x10^7$ cells/mouse in 100 µl of serum-free RPMI-1640 medium). After tumors reached the mean size of 50 mm^3, Ad-p53-XL, Ad-DBD-XL and Ad-ZsGreen1 were intratumorally injected on days 0-4 and 7-11. A dose of $5.0X10^8$ pfu in 50 µL volume was administrated (18). Tumor volumes were measured daily using Vernier calipers along the longest width (W) and the corresponding perpendicular length (L) using $V= (L \times (0.5W)^2)$ to calculate tumor volume. Mice were sacrificed and tumors and organs were harvested 24 h after the last injection. All procedures were approved by Institutional Animal Care and Use Committee (IACUC) at the University of Utah and performed according to established NIH and University of Utah Animal Care Committee guidelines.

5.4 Results

5.4.1 Mitochondrial p53 can bypass dominant negative inhibition *in vitro*

To determine if mitochondrial targeted p53-XL and DBD-XL can escape the dominant negative effect of *wt* p53, we first conducted a rescue experiment in H1373, and second, tested MDA-MB-468 cells that naturally harbor a dominant negative mutant p53 (R273H mutation).

We designed a mutant p53 construct with R248W mutation (called p53R248Wmut) which is known to exhibit a strong dominant negative effect (21, 22). We transfected human non-small cell lung carcinoma cells H1373 (p53 null) (23) with our constructs (p53-XL, DBD-XL, E-XL, *wt* p53, or EGFP), with or without the p53R248Wmut, and conducted a 7-AAD assay on these groups. In the absence of p53R248Wmut, p53-XL, DBD-XL and *wt* p53 showed significantly higher apoptosis compared to their negative controls E-XL and EGFP (Fig. 1A, white set of bars). When co-transfected with p53R248Wmut, p53-XL and DBD-XL are capable of rescuing apoptotic activity while the apoptotic activity of *wt* p53 is dramatically impaired (Fig. 1A, black set of bars) suggesting that mitochondrial targeting of p53 can overcome dominant negative inhibition of mutant p53.

To determine if mitochondrial p53 is capable of inducing apoptosis in a cell line that naturally harbors a dominant negative mutation, we infected MDA-MB-468 cells with our designed viral constructs and conducted a 7-AAD assay and a caspase-3/7 western blot. Triple negative breast cancer cells MDA-MB-468 harbor the R273H mutation which is considered to have a strong dominant negative effect on *wt* p53 (24, 25). For the H1373 rescue experiment, we used lipofectamine transfection of plasmid DNA. However, MDA-MB-468 are resistant to lipofectamine transfection. Therefore, we constructed Ad-p53-XL, Ad-DBD-XL and Ad-ZsGreen1 adenoviral constructs. For our previous plasmids (non-viral plasmids), EGFP was directly fused to our construct; for adenoviral constructs, ZsGreen1 is co-expressed with our protein of interest.

When MDA-MB-468 cells were infected with Ad-p53-XL, Ad-DBD-XL and Ad-ZsGreen1, only Ad-DBD-XL showed higher activity than Ad-ZsGreen1 in the 7-AAD assay (Fig. 1B). Surprisingly Ad-p53-XL was not significantly different from Ad-ZsGreen1 control.

To determine if the induced apoptotic effect of Ad-DBD-XL is though the mitochondrial/ intrinsic apoptotic pathway, caspase-9 was detected in MDA-MB-468 cells via western blotting. Caspase-9 can only be activated via the intrinsic apoptotic pathway (26). A representative cropped image of the western blot is shown in figure 1C. Ad-DBD-XL showed caspase-9 induction while Ad-p53-XL only shows a faint band and negative controls Ad-ZsGreen1 and untreated MDA-MB-468 cells did not show caspase-9 activity.

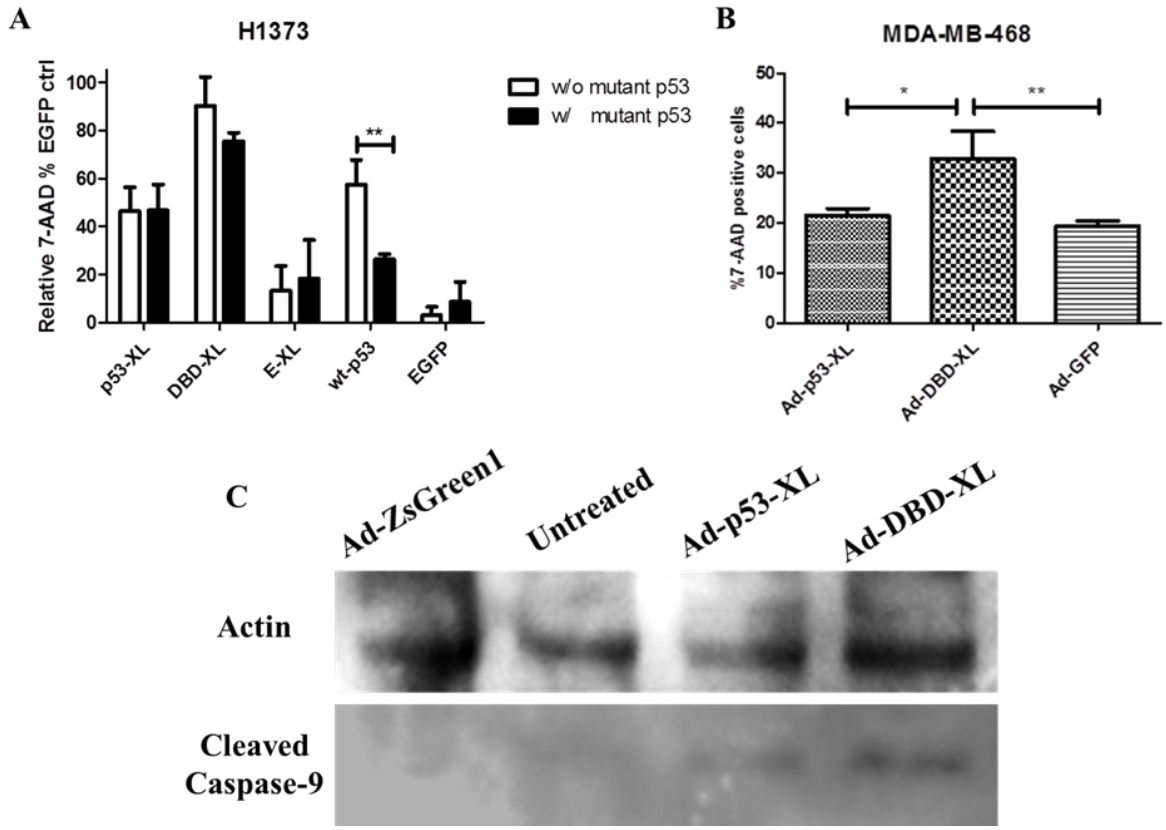

Figure 1: (A) rescue experiment: p53 null H1373 cells transfected either with or without p53R248Wmut and p53-XL, DBD-XL, E-XL, *wt* p53 and EGFP. 48 h post transfection 7-AAD assay was conducted. Statistical analysis was performed by using two-way ANOVA with Bonferroni's post test; ** $p < 0.01$ (B) MDA-MB-468 were infected with Ad-p53-XL, Ad-DBD-XL and Ad-ZsGreen. 72 h post infection, 7-AAD assay was conducted. Statistical analysis was performed by using one-way ANOVA with Bonferroni's post test; * $p < 0.05$ and ** $p < 0.01$. Error bars represent standard deviations from three different independent experiments (n=3). (C) Representative cropped western blot of MDA-MB-468 cell lysates 24 h post infection with Ad-ZsGreen, untreated, Ad-p53-XL and Ad-DBD-XL.

5.4.2 Testing the effect of mitochondrial p53 in an orthotopic breast cancer model*, in vivo*

We injected MDA-MB-468 cells into the mouse mammary fat pad, and allowed tumors to grow to 50 mm3. 5.0 X 10^8 pfu of Ad-p53-XL, Ad-DBD-XL and Ad-ZsGreen were then injected intratumorally on day 0-4 and 7-11 (18). Figure 2A shows a representative picture of a tumor-bearing mouse (black arrow indicates tumor site). The tumors were harvested 24 hours after the last treatment. Excised tumors of Ad-p53-XL, Ad-DBD-XL, untreated and Ad-ZsGreen1 are shown in figure 2B.

Although Ad-p53-XL and Ad-DBD-XL tumors appear smaller than the controls, their tumor sizes were smaller to begin with. In fact, tumor size measurements in figure 2C revealed that there were no difference between treatment groups and untreated showing that mitochondrial p53 is unable to evade dominant negative inhibition in this model.

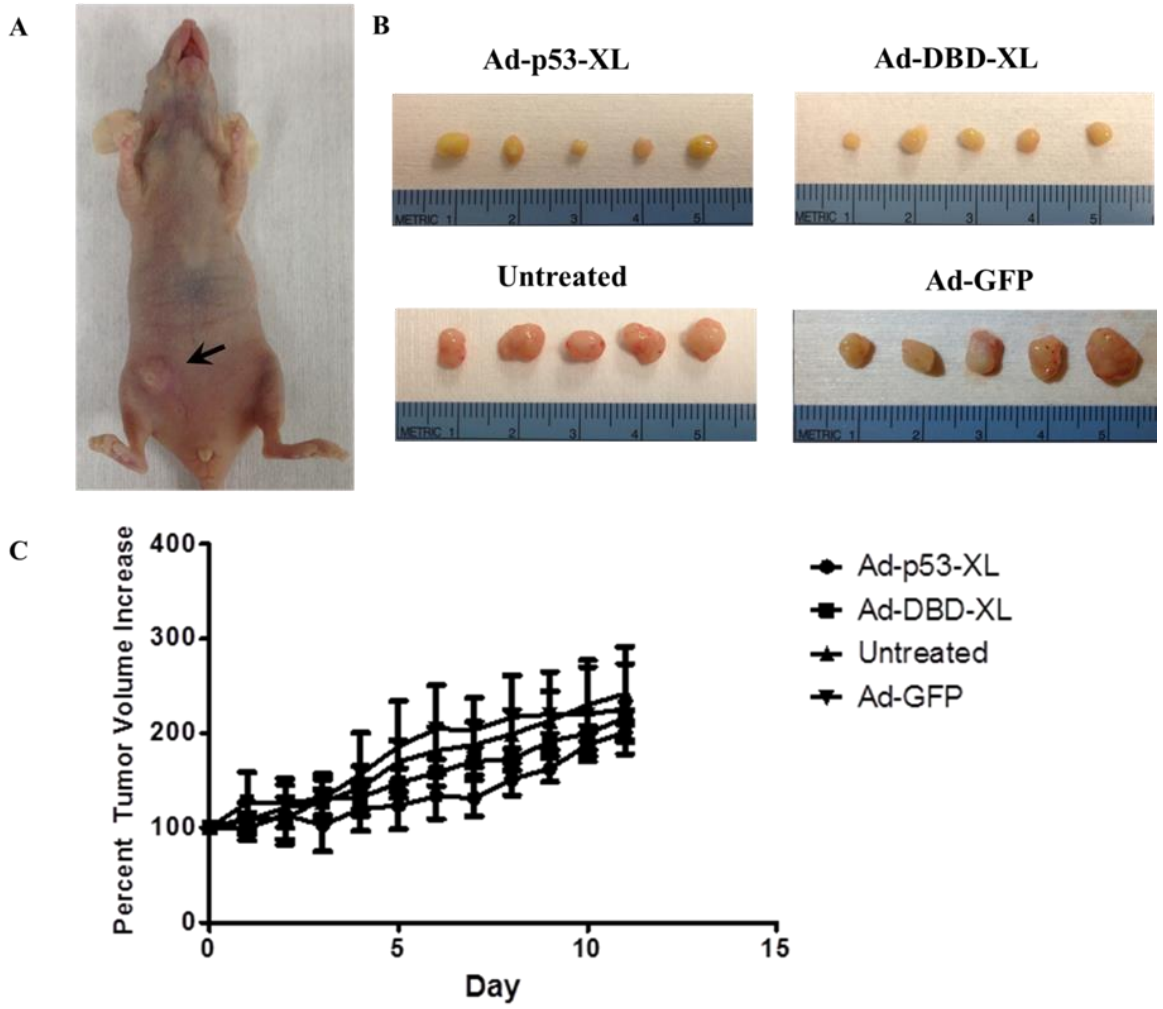

Figure 2: (A) generated tumor model: SQ injection of MDA-MB-468 human breast cancer cells into inguinal area of female nu/nu athymic mouse. $5X10^8$ pfu was injected intratumorally on days 0-4 and 7-11 (18). Black arrow indicates tumor location. (B) Tumors harvested from mice after treatment. (C) Tumor size reduction. Statistical analysis was performed by using one-way ANOVA with Bonferroni's post test. Error bars represent standard deviations from at least three independent experiments (n=5).

5.5 Discussion

Our lab and others have previously shown that targeting p53 to the mitochondria results in apoptosis in a variety of cancer cells (13, 20, 27). We were the first to show that the DBD of p53 is sufficient to cause apoptosis at the mitochondria (20). Here we wanted to test if mitochondrially targeted p53 is capable of overcoming dominant negative inhibition of endogenous mutant p53 *in vitro* and *in vivo*.

Therefore, we first overexpressed dominant mutant p53R248W in p53 null H1373 cells (Fig. 1A) and then conducted apoptosis assays in triple negative MDA-MB-468 cells (Fig. 1B, C) that naturally harbor dominant negative R273H mutant (25). In H1373 cells, p53-XL and DBD-XL retain the same apoptotic activity with or without overexpressing the dominant negative mutant, while apoptotic activity of *wt* p53 is dramatically decreased (Fig 1A). However, only Ad-DBD-XL was active in the dominant negative MDA-MB-468 cell line while Ad-p53-XL showed the same inactivity as the negative control Ad-ZsGreen1 (Fig. 1B). It might be speculated that p53-XL is sequestered via its TD by endogenous p53 in MDA-MB-468 cells. Unlike p53-XL, DBD-XL does not contain a TD and is therefore not inhibited by endogenous p53.

Further, we wanted to examine if apoptotic activity of DBD-XL is through the intrinsic apoptotic pathway. Thus, we chose to determine caspase-9 induction which can only be activated through the intrinsic apoptotic pathway (26). Again, Ad-DBD-XL showed caspase-9 activation while Ad-p53-XL only showed minimal capsase-9 activity (Fig. 1C). In summary, these results suggest that DBD-XL can bypass dominant negative inhibition of mutant p53.

Even though *in vitro* results looked promising, mitochondrial p53 was not capable of reducing MDA-MB-468 tumor size (Fig. 2C). It seems that the p53-specific intrinsic apoptotic response by p53-XL and DBD-XL in MDA-MB-468 cells is not sufficient to result in inhibition of tumor growth or tumor shrinkage in this particular mouse breast cancer model. The dosing regimen might be the reason for the treatment failure. At

day 5-6 when no drug was injected tumors started to grow again suggesting a transient effect of apoptosis by mitochondrial p53 (Fig. 2C). The dose used in this study is the same as for *wt* p53 therapy in MDA-MB-468 (18, 28). However, *wt* p53 and mitochondrial p53 have different apoptotic profiles. While mitochondrial p53 induces apoptosis solely through intrinsic apoptotic pathway (12, 13, 29), *wt* p53 activates the intrinsic and extrinsic pathway (30). Because mitochondrial p53 only induces the intrinsic apoptotic pathway, the effective dose may need to be higher than *wt* p53 therapy. In addition, the R273H mutant expressed in MDA-MB-468 has a very aggressive cancer profile. In fact, knock-in mice harboring this mutation (p53R273H/-mice) develop more carcinomas and have more invasive and metastatic properties than p53 knock-out mice (31). Due to differences in apoptotic mechanism and aggressiveness of MDA-MB-468 the dose of mitochondrial p53 should be increased and given more frequently, or combined with another cancer therapeutic.

It has been shown that in response to chemotherapy or radiation treatment p53-mediated apoptosis causes tumor regression (32) and transfecting these cell lines with *wt* p53 increases the sensitivity to chemotherapy (18). The potency of mitochondrial p53 can be enhanced by combination with a chemotherapeutic that targets the nucleus and intercalates with nuclear DNA (antracycline), interferes with DNA replication (alkylanting agent) or abolishes DNA/RNA synthesis (antimetabolite). The current treatment plan of breast cancer already involves a variety of cytotoxic drugs such as antracycline (doxorubicin, epirubicin), alkylating agents (cyclophosphamide, methotrexate) and antimetabolites (fluorouracil) (35). A dual approach combining mitochondrial p53 with antracycline, alkylating agent or antimetabolite has the advantage of targeting two cellular organelles which are highly involved in apoptosis resulting in higher apoptosis induction (18, 33).

However, the most promising approach is to further optimize mitochondrial targeting of p53 by fusing it to MTS from pro-apoptotic Bak. As previously shown, the MTS is responsible for directing p53 specifically to the protein where the MTS is taken from. We demonstrated that every protein that is tagged to XL will translocate to anti-

apoptotic Bcl-XL (20) while p53 fused to BakMTS will translocate to pro-apoptotic Bak (chapter IV). When p53 is targeted to Bcl-XL, it will primary inhibit Bcl-XL and is less effective on other anti-apoptotic proteins such as Bcl-2 and Mcl-1. In cells mainly expressing Bcl-XL with low Bcl-2 and Mcl-1 levels, neutralizing Bcl-XL will results in Bak homooligomerization and apoptosis. However, in aggressive cancers, Bcl-2, Bcl-XL and Mcl-1 are often overexpressed (34-37). Therefore, the amount of p53-XL and DBD-XL might not be efficient enough to sequester anti-apoptotic Bcl-2 proteins and to ensure Bak and Bax homo-oligomerization. This again suggests the need to increase the dose of p53-XL and DBD-XL.

Directly targeting the pro-apoptotic Bak or Bax might be therefore superior over targeting Bcl-XL. Bak and Bax are directly responsible for pore formation at the mitochondria. While anti-apoptotic Bcl-2 proteins such as Bcl-XL need to be sequestered, pro-apoptotic Bak or Bax just needs to be activated by a transient interaction and then can form pores at mitochondrial outer membrane. We have shown in chapter IV that targeting p53 to the mitochondria by using the MTS from Bak is superior to Bax. We speculate that this is due to differences in subcellular localization of these proteins. Bax is constantly shuttled between mitochondria and cytoplasm (38, 39). Therefore the amount present at the mitochondria might be not sufficient to initiate apoptosis. Bak on the other hand is always present at the mitochondria (40) and is activated when p53 is targeted to the mitochondria with MTS from Bak, triggering caspase activation and apoptosis.

In fact, we have shown that p53 or DBD fused to the MTS from pro-apoptotic Bak was superior over *wt* p53 and our chimeric p53 construct named p53-CC (unpublished data) in p53 null ovarian cancer cells SKOV-3 (Chapter IV). This might be due to a defect in the transcriptional apoptotic pathway of p53 in SKOV-3 cells. Targeting p53 to the mitochondria for ovarian cancer therapy will be further discussed in the future directions section (Chapter VII).

5.6 References

1. Yu W, Fang H. Clinical trials with oncolytic adenovirus in China. Curr Cancer Drug Targets. 2007 Mar;7(2):141-8.

2. Shi J, Zheng D. An update on gene therapy in China. Curr Opin Mol Ther. 2009 Oct;11(5):547-53.

3. Lane DP, Cheok CF, Lain S. p53-based cancer therapy. Cold Spring Harb Perspect Biol. 2010 Sep;2(9):a001222.

4. Sigal A, Rotter V. Oncogenic mutations of the p53 tumor suppressor: the demons of the guardian of the genome. Cancer Res. 2000 Dec 15;60(24):6788-93.

5. Milner J, Medcalf EA, Cook AC. Tumor suppressor p53: analysis of wild-type and mutant p53 complexes. Mol Cell Biol. 1991 Jan;11(1):12-9.

6. Hollstein M, Sidransky D, Vogelstein B, Harris CC. p53 mutations in human cancers. Science. 1991 Jul 5;253(5015):49-53.

7. Kim E, Deppert W. The versatile interactions of p53 with DNA: when flexibility serves specificity. Cell Death Differ. 2006 Jun;13(6):885-9.

8. Srivastava S, Wang S, Tong YA, Hao ZM, Chang EH. Dominant negative effect of a germ-line mutant p53: a step fostering tumorgenesis. Cancer Res. 1993 Oct 1;53(19):4452-5.

9. Kern SE, Pietenpol JA, Thiagalingam S, Seymour A, Kinzler KW, Vogelstein B. Oncogenic forms of p53 inhibit p53-regulated gene expression. Science. 1992 May 8;256(5058):827-30.

10. Turner N, Moretti E, Siclari O, Migliaccio I, Santarpia L, D'Incalci M, et al. Targeting triple negative breast cancer: is p53 the answer? Cancer Treat Rev. 2013 Aug;39(5):541-50.

11. Palacios G, Crawford HC, Vaseva A, Moll UM. Mitochondrially targeted wild-type p53 induces apoptosis in a solid human tumor xenograft model. Cell Cycle. 2008 Aug 15;7(16):2584-90.

12. Vaseva AV, Moll UM. The mitochondrial p53 pathway. Biochim Biophys Acta. 2009 May;1787(5):414-20.

13. Mossalam M, Matissek KJ, Okal A, Constance JE, Lim CS. Direct induction of apoptosis using an optimal mitochondrially targeted p53. Mol Pharm. 2012 May 7;9(5):1449-58.

14. Matissek KJ, Mossalam M, Okal A, Lim CS. The DNA Binding Domain of p53 Is Sufficient To Trigger a Potent Apoptotic Response at the Mitochondria. Mol Pharm. 2013 Sep 6.

15. Li Y, Li LJ, Zhang ST, Wang LJ, Zhang Z, Gao N, et al. In vitro and clinical studies of gene therapy with recombinant human adenovirus-p53 injection for oral leukoplakia. Clin Cancer Res. 2009 Nov 1;15(21):6724-31.

16. Ginn SL, Alexander IE, Edelstein ML, Abedi MR, Wixon J. Gene therapy clinical trials worldwide to 2012 - an update. J Gene Med. 2013 Feb;15(2):65-77.

17. Nielsen LL, Dell J, Maxwell E, Armstrong L, Maneval D, Catino JJ. Efficacy of p53 adenovirus-mediated gene therapy against human breast cancer xenografts. Cancer Gene Ther. 1997 Mar-Apr;4(2):129-38.

18. Nielsen LL, Lipari P, Dell J, Gurnani M, Hajian G. Adenovirus-mediated p53 gene therapy and paclitaxel have synergistic efficacy in models of human head and neck, ovarian, prostate, and breast cancer. Clin Cancer Res. 1998 Apr;4(4):835-46.

19. Okal A, Mossalam M, Matissek KJ, Dixon AS, Moos PJ, Lim CS. A chimeric p53 evades mutant p53 transdominant inhibition in cancer cells. Mol Pharm. 2013 Oct 7;10(10):3922-33.

20. Matissek KJ, Mossalam M, Okal A, Lim CS. The DNA binding domain of p53 is sufficient to trigger a potent apoptotic response at the mitochondria. Mol Pharm. 2013 Oct 7;10(10):3592-602.

21. Di Como CJ, Gaiddon C, Prives C. p73 function is inhibited by tumor-derived p53 mutants in mammalian cells. Mol Cell Biol. 1999 Feb;19(2):1438-49.

22. Brachova P, Thiel KW, Leslie KK. The consequence of oncomorphic TP53 mutations in ovarian cancer. Int J Mol Sci. 2013;14(9):19257-75.

23. Bodner SM, Minna JD, Jensen SM, D'Amico D, Carbone D, Mitsudomi T, et al. Expression of mutant p53 proteins in lung cancer correlates with the class of p53 gene mutation. Oncogene. 1992 Apr;7(4):743-9.

24. Lim LY, Vidnovic N, Ellisen LW, Leong CO. Mutant p53 mediates survival of breast cancer cells. Br J Cancer. 2009 Nov 3;101(9):1606-12.

25. Wang W, Cheng B, Miao L, Mei Y, Wu M. Mutant p53-R273H gains new function in sustained activation of EGFR signaling via suppressing miR-27a expression. Cell Death Dis. 2013;4:e574.

26. Chowdhury I, Tharakan B, Bhat GK. Caspases - an update. Comp Biochem Physiol B Biochem Mol Biol. 2008 Sep;151(1):10-27.

27. Mihara M, Erster S, Zaika A, Petrenko O, Chittenden T, Pancoska P, et al. p53 has a direct apoptogenic role at the mitochondria. Mol Cell. 2003 Mar;11(3):577-90.

28. Ding Y, Wen Y, Spohn B, Wang L, Xia W, Kwong KY, et al. Proapoptotic and antitumor activities of adenovirus-mediated p202 gene transfer. Clin Cancer Res. 2002 Oct;8(10):3290-7.

29. Perfettini JL, Kroemer RT, Kroemer G. Fatal liaisons of p53 with Bax and Bak. Nat Cell Biol. 2004 May;6(5):386-8.

30. Haupt S, Berger M, Goldberg Z, Haupt Y. Apoptosis - the p53 network. J Cell Sci. 2003 Oct 15;116(Pt 20):4077-85.

31. Olive KP, Tuveson DA, Ruhe ZC, Yin B, Willis NA, Bronson RT, et al. Mutant p53 gain of function in two mouse models of Li-Fraumeni syndrome. Cell. 2004 Dec 17;119(6):847-60.

32. El-Deiry WS. The role of p53 in chemosensitivity and radiosensitivity. Oncogene. 2003 Oct 20;22(47):7486-95.

33. Gurnani M, Lipari P, Dell J, Shi B, Nielsen LL. Adenovirus-mediated p53 gene therapy has greater efficacy when combined with chemotherapy against human head and neck, ovarian, prostate, and breast cancer. Cancer Chemother Pharmacol. 1999;44(2):143-51.

34. Minn AJ, Rudin CM, Boise LH, Thompson CB. Expression of bcl-xL can confer a multidrug resistance phenotype. Blood. 1995 Sep 1;86(5):1903-10.

35. Perego P, Righetti SC, Supino R, Delia D, Caserini C, Carenini N, et al. Role of apoptosis and apoptosis-related proteins in the cisplatin-resistant phenotype of human tumor cell lines. Apoptosis. 1997;2(6):540-8.

36. Reed JC. Bcl-2-family proteins and hematologic malignancies: history and future prospects. Blood. 2008 Apr 1;111(7):3322-30.

37. Yoshino T, Shiina H, Urakami S, Kikuno N, Yoneda T, Shigeno K, et al. Bcl-2 expression as a predictive marker of hormone-refractory prostate cancer treated with taxane-based chemotherapy. Clin Cancer Res. 2006 Oct 15;12(20 Pt 1):6116-24.

38. Schellenberg B, Wang P, Keeble JA, Rodriguez-Enriquez R, Walker S, Owens TW, et al. Bax exists in a dynamic equilibrium between the cytosol and mitochondria to control apoptotic priming. Mol Cell. 2013 Mar 7;49(5):959-71.

39. Edlich F, Banerjee S, Suzuki M, Cleland MM, Arnoult D, Wang C, et al. Bcl-x(L) retrotranslocates Bax from the mitochondria into the cytosol. Cell. 2011 Apr 1;145(1):104-16.

40. Willis SN, Chen L, Dewson G, Wei A, Naik E, Fletcher JI, et al. Proapoptotic Bak is sequestered by Mcl-1 and Bcl-xL, but not Bcl-2, until displaced by BH3-only proteins. Genes Dev. 2005 Jun 1;19(11):1294-305.

6. Re-engineered p53 avoids the dominant negative effect in cancer cells *in vivo* and *in vitro*

The following two manuscripts have been summarize. The methods and figures are directly taken from the manuscripts.

"**A chimeric p53 evades mutant p53 transdominant inhibition in cancer cells** " Okal A, Mossalam M, Matissek KJ, Dixon AS, Moos PJ, Lim CS, Mol Pharm. 2013 Oct 7

Co-Author Contribution:

Research design: 20%

Experimental work: 30%

Data evaluation: 20%

Manuscript writing: 5%

"**Re-engineered p53 activates apoptosis *in vivo* and causes primary tumor regression in a dominant negative breast cancer xenograft model**" Okal, A., Matissek, K.J., Matissek, S.J., Price, R., Salama, M., Janát-Amsbury, M.M., Lim, C.S. submitted to Gene Therapy 2014 February 5

Co-Author Contribution:

Research design: 20%

Experimental work: 30%

Data evaluation: 20%

Manuscript writing: 5%

6.1 Abstract

The tumor suppressor p53 is mutated in more than 50% of all cancers. While most of the mutations occur in the DNA binding domain (DBD) of p53, the tetramerization domain (TD) remains intact. This allows for *wt*p53/mutp53 heterotetramer formation, abolishing the transcriptional activity of p53 and reducing its tumor suppressor activity. To overcome this dominant negative inhibition, we re-engineered p53. The TD in *wt* p53 was removed and replaced with the coil-coiled (CC) oligomerization domain from breakpoint cluster region (BCR). CC in BCR tetramerizes in similar fashion to the TD in p53. Our designed p53-CC translocates to the nucleus (fluorescence microscopy) and shows the same apoptotic potential (TUNEL-, Annexin V-, and 7-AAD assay) as *wt* p53 in breast cancer cells T47D which do not exhibit a strong dominant negative effect. Unlike *wt* p53, our p53-CC does not interact with endogenous mutant p53 (co-IP). p53-CC remains active when dominant negative mutant p53 (R175H, R248W and R273H) is overexpressed and also causes apoptosis in triple negative MDA-MB-468 cells which harbor the R273H all dominant negative mutation (7-AAD assay). *In vivo*, intratumorally injection of adenoviral p53-CC results in tumor shrinkage. Analysis of the tumor tissue showed that p53-CC and *wt* p53 were highly expressed in MDA-MB-468 tumors and *wt* p53 caused more p21 expression than p53-CC (DAP staining). Additionally, p53-CC had higher necrotic potential (H&E staining) than *wt* p53 suggesting tumor shrinkage was due to cell death occurring through necrosis. In summary, we have shown that p53-CC can circumvent dominant negative mutant p53 *in vitro* and *in vivo* and therefore can be used for cancer gene therapy.

6.2 Introduction

The TP53 gene is mutated in more than 50% of all cancers (1-4). Mutations in the TP53 gene occur typically by a single monoallelic missense mutation (5) frequently affecting the DNA binding domain (DBD) of p53 which often prevents binding of p53

to specific DNA-sequences, abolishing its transcriptional activity (6, 7). The amino terminus and the C-terminus (containing the tetramerization domain or TD) of p53 are usually not mutated (7). Therefore, mutant p53 is capable of forming heterotetramers with *wt* p53 via its intact TD resulting in transcriptional inactivation of the entire p53 tetramer (8-10). This is the main disadvantage of *wt* p53 based gene therapy. While introducing *wt* p53 into cancers that are p53 null or harbor low levels of endogenous *wt* p53 results in apoptosis, exogenous *wt* p53 introduced into tumors with dominant negative mutant p53 face the dominant negative inhibition by endogenous mutant p53.

Thus, we proposed to replace the TD in p53 by a structurally similar tetramerization domain. The p53 tetramer is formed via a dimeric intermediate (11). The highly thermodynamically stable tetramer is formed by hydrophobic helix interaction of two dimers (12).

Only one other group has attempted replacing the TD before (13). Waterman et al. replaced the TD with an oligomerization domain which led to parallel tetramer formation and resulted in significant reduction in p53 transcriptional activity (13). We chose the oligomerization domain from breakpoint cluster region (Bcr) protein, a 72 amino acid coiled-coil (CC) which consists of two α helices. CC tetramerizes as two dimers of two antiparallel oriented monomers, in a similar fashion to the TD of *wt* p53 (14, 15). We hypothesized that our chimeric p53-Bcr fusion (named p53-CC) will solely tetramerize with itself when introduced into cancer cells harboring mutant p53. Therefore, our chimeric p53 is capable of escaping the dominant negative effect and cause apoptosis in mutant p53 cell lines.

6.3 Materials and methods

6.3.1 Construction of Plasmids

To construct pEGFP-p53-CC (p53-CC), a truncated version of *wt* p53 that lacks the tetramerization domain (amino acids 1-322) was amplified via PCR with primers 5'-GCGCGCGCGCTCCGGAATGGAGGAGCCGCAGTCA-3' and 5'-GCGCGCGCGCTCCGGATGGTTTCTTCTTTGGCTGGGGAGA-3' using the previously cloned pEGFP-p53 (*wt* p53) as the template DNA (16). The PCR product was then subcloned into the BspEI site of pEGFP-CC (CC).

To design pTagBFP-mut-p53, *wt* p53 was amplified via PCR with primers 5'-GCGCGCGCGCTCCGGAGCCATGGAGGAGCCGCAGT-3', and 5'-GCGCGCGCGCGGTACCTCAGTCTGAGTCAGGCCCTTCTGTC-3' using pEGFP-p53 as a template. This insert was then subcloned into the digested pTagBFP-C vector (Evrogen, Moscow, Russia) at the BspEI and KpnI sites. Three hot spot mutations (R175H, R248W, and R273H) were then introduced into pTagBFP-p53 via QuikChange II XL Site- Directed Mutagenesis Kit (Agilent, Santa Clara, CA). The following primers were used: for the R175H mutation, 5'-TGACGGAGGTTGTGAGGCACTGCCCCCACCATGAGCGC-3' and 5'-GCGCTCATGGTGGGGGCAGTGCCTCACAACCTCCGTCA-3'; for R248W, 5′-CTGCATGGGCGGCATGAACTGGAGGCCCATCCTCACCA-3′ and 5'-TGGTGAGGATGGGCCTCCAGTTCATGCCGCCCATGCAG-3'; and for R273H, 5'-GGAACAGCTTTGAGGTGCATGTTTGTGCCTGTCCTGGG-3' and 5'-CCCAGGACAGGCACAAACATGCACCTCAAAGCTGTTCC-3'.

6.3.2 Cell Lines and Transient Transfection

T47D human ductal breast epithelial tumor cells (ATCC, Manassas, VA), (ATCC) and H1373 human non-small cell lung carcinoma cells (a kind gift from Dr. Andrea Bild, University of Utah) were grown as monolayers in RPMI (Invitrogen, Carlsbad,

CA) supplemented with 10% fetal bovine serum (Invitrogen), 1% penicillin-streptomycin-glutamine (Invitrogen), 0.1% gentamicin (Invitrogen). T47D were also supplemented with 4 mg/L insulin (Sigma, St. Louis, MO). 1471.1 murine breast adenocarcinoma cells (gift of Dr. Gordon Hager, NCI, NIH), HEK293 human embryonic kidney (ATCC), MDA-MB-468 human breast adenocarcinoma cells (ATCC) were grown as monolayers in DMEM (Invitrogen) supplemented with 10% fetal bovine serum (Invitrogen), 1% penicillin-streptomycin-glutamine (Invitrogen), and 0.1% gentamicin (Invitrogen). MDA-MB-468 cells were also supplemented with 1% MEM non-essential amino acids (Invitrogen). All cells were incubated in 5% CO2 at 37ºC. The cells were seeded at a density of 7.5×10^4 cells (for 1471.1) and 3.0×10^5 cells (T47D, MDA-MB-468 and H1373 cells) in 6-well plates (Greiner Bio-One, Monroe, NC). Transfections of 1 pmol DNA were carried out 24 h after seeding using Lipofectamine 2000 (Invitrogen) following the manufacturer's recommendations.

6.3.3 Microscopy

All microscopy was performed using 1471.1 cells due to their ideal microscopic morphology (16). 24 h post transfection, media in 2-well live-cell chambers (Nalgene Nunc, Rochester, NY) was replaced with phenol red-free DMEM (Invitrogen). Cells were then incubated with 2 µg/mL Hoechst 33342 nuclear stain (Invitrogen) for 30 minutes at 37ºC. Images were taken using an Olympus IX71F fluorescence microscope (Scientific Instrument Company, Aurora, CO) with high-quality narrow band GFP filter (excitation, HQ480/20 nm; emission, HQ510/ 20 nm) to detect EGFP and cyan GFP v2 filter (excitation HQ436/20 nm, emission HQ480/40 nm, with beam splitter 455dclp) to detect H33342 as previously described (17).

6.3.4 TUNEL Assay

As previously described (16), T47D cells were prepared 48 h after transfection using In Situ Death Detection Kit, TMR red (Roche, Mannheim, Germany). Cells were

EGFP gated and analyzed using FACSAria-II (BD-BioSciences, University of Utah Core Facility) and FACSDiva software. EGFP and TMR red were excited at 488 nm and 563 nm wavelengths and detected at 507 nm and 580 nm, respectively. The TUNEL assay was repeated three times (n=3) and analyzed using one-way ANOVA with Bonferroni's post test.

6.3.5 Annexin-V Assay

The annexin-V assay was performed as before (16). Briefly, 48 h post transfection, T47D cells were suspended in 400 µl annexin binding buffer (Invitrogen) and incubated with 5 µl annexin-APC (annexin-V conjugated to allophycocyanin, Invitrogen) for 15 minutes. The incubated cells were EGFP gated and analyzed using FACSCanto-II. EGFP and APC were excited at 488 nm and 635 nm wavelengths and detected at 507 nm and 660 nm, respectively. Each construct was tested three times (n=3) and analyzed using one-way ANOVA with Bonferroni's post hoc test.

6.3.6 7-AAD Assay

As before (16), following manufacturer's instructions, T47D, H1373, and MDA-MB-468 cells were stained with 7-aminoactinomycin D (7-AAD, Invitrogen) 48 h after transfection. Cells were analyzed and gated for EGFP (with same fluorescence intensity to ensure equal expression of proteins) using the FACSCanto-II (BD-BioSciences, University of Utah Core Facility) and FACSDiva software. Excitation was set at 488 nm and detected at 507 nm and 660 nm for EGFP and 7-AAD, respectively. The means from three separate experiments (n=3) were analyzed using one-way ANOVA with Bonferroni's post test.

6.3.7 Co-Immunoprecipitation (co-IP)

The co-IP was performed using Dynabeads co-IP Kit (Invitrogen). T47D cells transfected with either EGFP-*wt*-p53 or EGFP-p53-CC were collected and weighed out (0.05 g) 20 h post transfection. Anti-GFP antibody (ab290, Abcam) was coupled to magnetic beads using Dynabeads Antibody Coupling Kit (Invitrogen). Approximately 0.2 g of cell pellet was lysed in 1.8 ml extraction buffer B (1x IP, 100 mM NaCl, 2 mM MgCl2, 1 mM DTT, 1 % protease inhibitor). The lysate was incubated for 30 min at 4°C with 1.5 mg of the dynabeads coupled with anti-GFP antibody. The immune complexes were then collected by a magnet and washed three times with extraction buffer B and one time with last wash buffer (1x LWB, 0.02% Tween 20). Immune complexes were then eluted using 60 µl elution buffer. Finally, the eluted complexes were denatured and blotted using anti-p53 antibody HRP-conjugated (sc-126 HRP, Santa Cruz Biotechnology, Santa Cruz, CA).

6.3.8 Overexpression of Mutant p53

H1373 cells were cotransfected with 1 pmol of the transdominant mutant pTagBFP-mut-p53 (R175H, R248W, and R273H) and 1 pmol of *wt* p53, p53-CC, or CC fused to EGFP. 48 h post transfection, cells were stained as in the 7-AAD assay above and gated for EGFP and BFP using the FACSCanto-II (BD-BioSciences, University of Utah Core Facility) and FACSDiva software. Excitation for BFP was set at 405 nm and detected at 457 nm. The means from three separate experiments (n=3) were analyzed using one-way with Bonferroni's post hoc test and unpaired t test.

6.3.9 Recombinant Adenovirus Production

Replication-deficient recombinant adenovirus serotype 5 (Ad) constructs were generated using the Adeno-X® Adenoviral Expression System 3 (Clontech). Either *wt* p53 or p53-CC was inserted into a cassette under the control of the CMV promoter. A separate CMV promoter controls the expression of ZsGreen1 for visualization. The

empty virus (vector) was used as a negative control. *wt* p53 and p53-CC were PCR amplified with primers containing 15 base pair homology with a linearized pAdenoX vector (Clontech) based on an In-Fusion® HD Cloning Kit (Clontech). Stellar® competent cells (Clontech) were transformed with the adenoviral vector plasmids containing our constructs. Viral DNA was then purified, linearized and transfected into HEK293 cells for packaging and amplification. Viral particles were isolated from HEK293 cells by freeze-thawing, purified using Adeno-X® Mega Purification Kit (Clontech), and dialyzed against storage and proper tonicity buffer (2.5% glycerol (w/v), 25 mM NaCl, and 20 mM Tris-HCl, pH 7.4). The viral titer was determined using flow cytometry per the manufacturer's recommendation.

6.3.10 *In Vivo* Study

The experimental protocol was approved by the Institutional Animal Care and Use Committee (IACUC) at the University of Utah. All experiments were performed in female nu/nu athymic mice (4-6 weeks old, Jackson Laboratories, Bar Harbor, ME). Human MDA-MB-468 cells ($1x10^7$ cells/mouse in 100ul of serum-free RPMI-1640 medium) were injected subcutaneously into a mammary fat pad. When tumors reached the mean size of 50 mm^3, peritumoral injections of adenoviral constructs ($5.0X10^8$ pfu) in a 50 µl volume were made on days 0-4 and 7-11 (18). 24 h after the last injection the mice were sacrificed and the organs were harvested for analyses. Tumor volumes were measured daily using a Vernier caliper along the longest width (W) and the corresponding perpendicular length (L). The tumor volume was calculated using $V= (L \times (0.5W)^2)$. All procedures were performed according to established NIH and University of Utah Animal Care Committee guidelines.

6.3.11 Histology

Animal tumor tissue samples and organs were fixated in 10% formalin for 24 h followed by dehydration in alcohol and embedded in paraffin. Embedded tissues were then sectioned to cut at 4 µm thick sections and mounted on plus slides. Slides from each tumor tissue from all mice in the three treatment groups as well as the untreated group were stained using hematoxylin and eosin and p21 immunohistochemistry stain. Tissue and histological slide preparation was conducted by ARUP Laboratories (Salt Lake City, Utah).

6.4 Results

6.4.1 p53-CC localizes to the nucleus

When engineering p53-CC, amino acids 323 to 393 were removed which accounts for most of the C-terminal domain including not only the TD, but also two of the three nuclear localization signals in *wt* p53. However, one strong NLS remains intact (aa 305-322) in p53-CC. The two NLSs (370-376 aa and 380-386 aa) which have been removed in p53-CC are considered weak NLSs (16, 19). Figure 1 demonstrates that the one strong NLS in p53-CC is capable of targeting p53-CC to the nucleus in a similar manner as *wt* p53 in murine adenocarcinoma cells 1471.1 (Fig. 1). 1471.1 cells were chosen for this experiment because they are larger in size, spread well, and are generally easier to visualize than T47D cells. However, similar results were observed in T47D breast cancer cells (20).

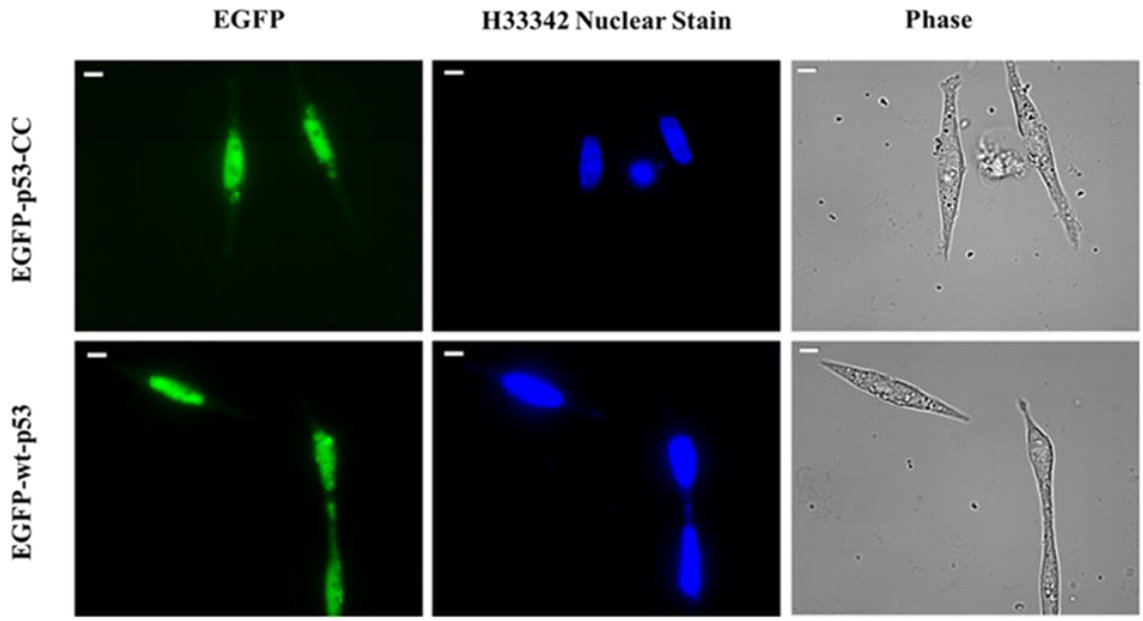

Figure 1: Representative images of p53-CC and *wt* p53 both tagged to EGFP are shown in the left column with images of nuclear stain H33342 in the middle column. The “EGFP” and “H33342 Nuclear Stain” columns have been false colored green and blue, respectively. The left column shows the phase contrast images. White scale bars on the top left corners are 10 μm.

6.4.2 Exploring the apoptotic potential of p53-CC

The apoptotic activity of p53-CC was determined via TUNEL, Annexin-V and 7-AAD assays in T47D human breast cancer cells. The L194F mutation which is present in T47D cells does not exhibit a strong transdominant effect (21).

When cells undergo apoptosis, the nuclear DNA is cleaved by caspases. DNA fragments can be detected by labeling the terminal end of nucleic acids (TUNEL assay) (22). Another hallmark of apoptosis is the externalization of phosphatidylserine to the outer surface of the plasma membrane, while in healthy cells, phosphatidylserine is typically found on the cytosolic surface (annexin-V assay) (23). Additionally, rupture of the plasma membrane of dying cells can be measured

by 7-AAD. The 7-AAD dye enters the apoptotic/ necrotic cell (ruptured cell membrane) and intercalates with nuclear DNA while healthy cells, which have an intact plasma membrane, remain unstained (24).

wt p53 and p53-CC have similar apoptotic activities in TUNEL (Fig. 2A), Annexin V (Fig. 2B) and 7-AAD (Fig. 2B) assays. Additionally, figure 2 showed that *wt* p53 and p53-CC induce significantly higher apoptosis compared to their negative controls CC and EGFP.

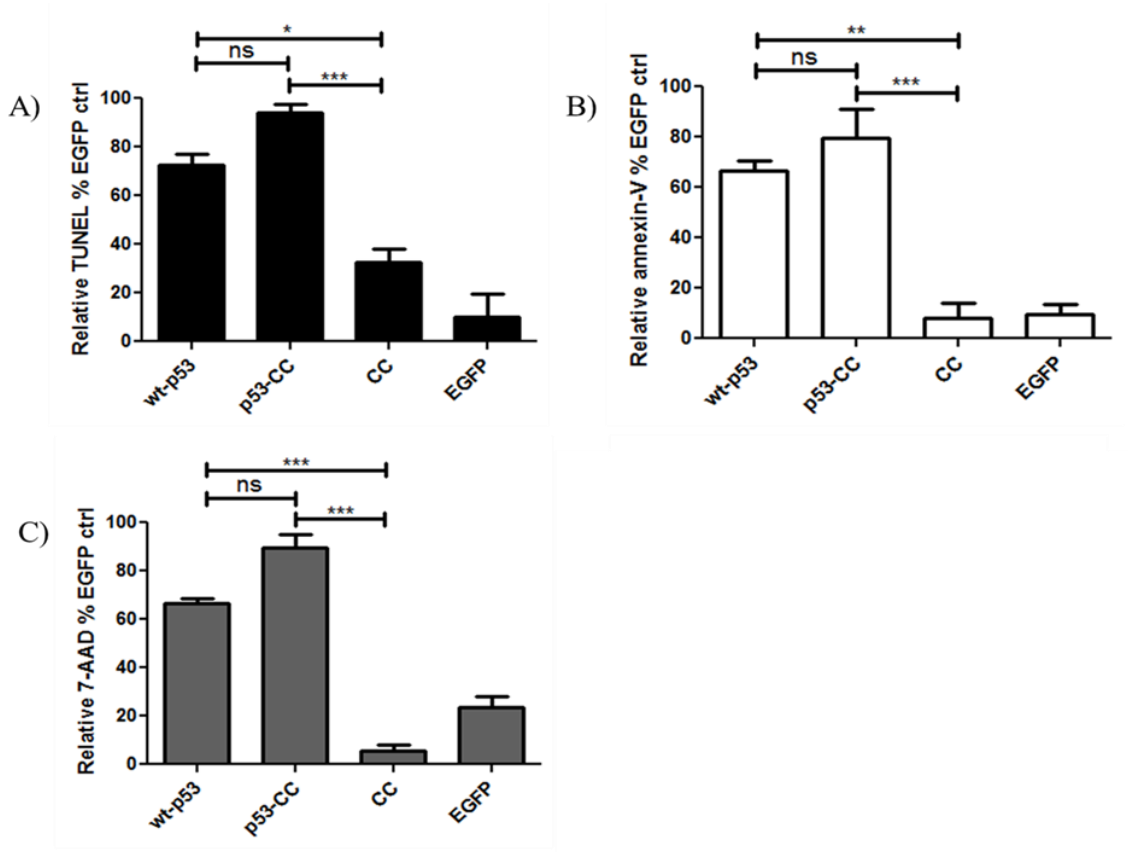

Figure 2: apoptotic potential of p53-CC: (A) TUNEL, (B) Annexin-V and (C) 7-AAD assay was carried out 24h for (A) and 48 h for (B) and (C) after transfection. Statistical analysis was performed by using one-way ANOVA with Bonferroni's post test; * $p < 0.05$, ** $p < 0.01$, and *** $p < 0.001$. Error bars represent standard deviations from at least three independent experiments (n=3).

6.4.3 p53-CC does not heterotetramerize with endogenous p53

To explore if p53-CC solely forms homotetramers or also interacts with mutant p53, we conducted a co-IP. *wt* p53 and p53-CC (both fused to EGFP) were transfected into T47D cells; cells were then lysed approximately 20 h after transfection and incubated with anti-GFP antibody. A western blot was done using antibodies against EGFP and against p53. Since exogenous *wt* p53 and p53-CC are fused to EGFP, their size is different from endogenous p53. Endogenous p53 (53 kDa) was expected to co-immunoprecipitate with exogenous *wt* p53 tagged to EGFP (70 kDa) due to having the same TD (Fig. 3 left lane). Exogenous p53-CC tagged to EGFP (71 kDa) did not co-immunoprecipitate with endogenous mutant p53 (Fig. 3 right lane) due to their different oligomerization domains, implying that p53-CC is capable of overcoming dominant negative inhibition.

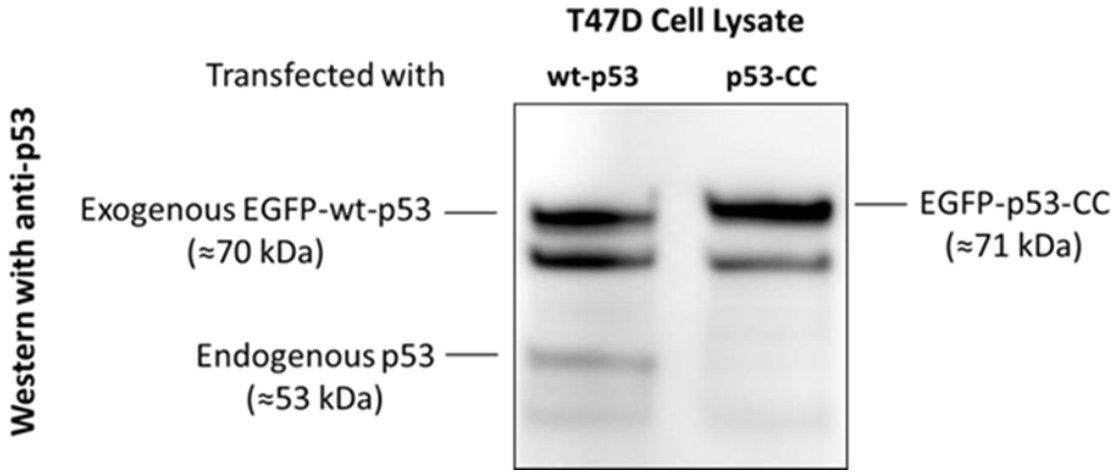

Fig. 3: Representative cropped western blot of protein complexes co-immunoprecipitated using anti-GFP antibody. Lane 1, exogenous *wt* p53 tagged to EGFP (70 kDa) which was transfected into T47D cells co-immunoprecipitates with endogenous *wt* p53 (53 kDa). Lane 2, exogenous p53-CC tagged to EGFP (71 kDa) does not co-immunoprecipitates with endogenous *wt* p53 (53 kDa). Unlabeled bands are nonspecific binding.

6.4.4 p53-CC evades dominant negative inhibition *in vitro*

To verify if p53-CC can avoid dominant negative inhibition, we first conducted a rescue experiment in H1373 cells, and second infected MDA-MB-468 which harbor the dominant negative mutant R273H (25) with our designed constructs.

For the rescue experiment, we transfected p53 null human non-small cell lung carcinoma cells H1373 (26) with *wt* p53, p53-CC and CC. This showed significant induction of apoptosis for *wt* p53 and p53-CC while negative control CC showed minimal activity (Fig. 4A first set of bars). Additionally, we designed a transdominant mutant p53 by combining three hotspot mutations (R175H, R248W, and R273H) that are known to exhibit a dominant negative effect and co-transfected this construct with *wt* p53, p53-CC or CC (27, 28). As expected, figure 4A (black set of bars) showed that p53-CC, but not *wt* p53, was still capable of inducing apoptosis in the presence of mutant p53 (R175H, R248W, and R273H).

To further demonstrate that p53-CC can overcome the dominant negative effect of mutant p53, triple negative breast cancer cells MDA-MB-468 were infected with adenovirus containing *wt* p53, p53-CC, or Zsgreen1. Lipofectamine 2000, which was used for all our previous studies (Fig.1- 4A), was not capable of transfecting this cell line, therefore we created the Ad-*wt*-p53, Ad-p53-CC and Ad-Zsgreen1 adenoviral constructs. In our non-viral plasmids EGFP was directly fused to our constructs. For the adenoviral construct ZsGreen1 is co-expressed with our protein of interest. Ad-p53-CC induces significantly higher apoptosis in MDA-MB-468 than Ad-*wt*-p53 and negative control Ad-Zsgreen1, suggesting again that p53-CC is not affected by dominant negative inhibition (Fig. 4B). On the other hand, Ad-*wt*-p53 shows the same minimal activity as negative control Ad-Zsgreen1 (Fig. 4B).

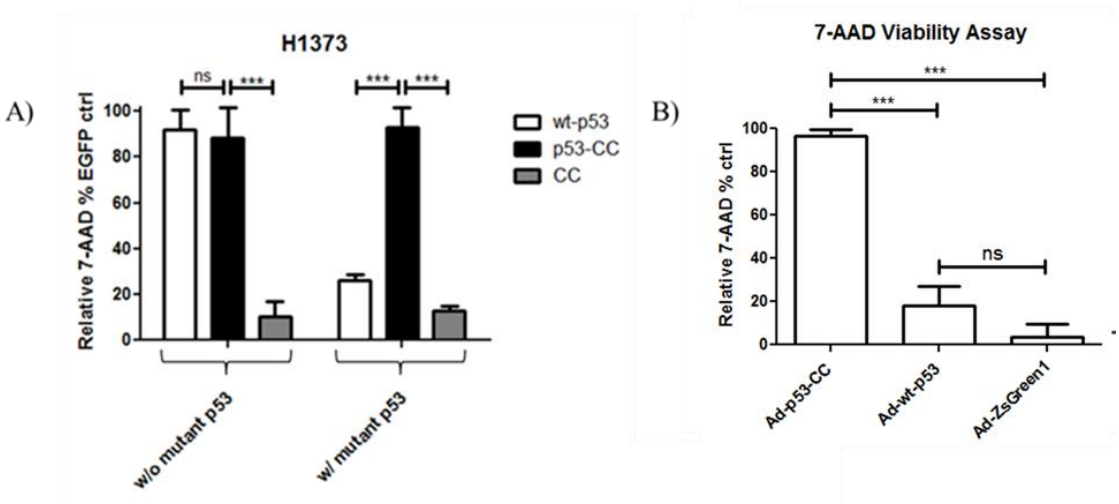

Fig. 4: p53-CC evades dominant negative inhibition: (A) rescue experiment: p53 null H1373 cells were transfected with *wt* p53, p53-CC and CC (left set of bars) or with *wt* p53, p53-CC, CC and cotransfected with mutant p53 (R175H, R248W, and R273H). (B) MDA-MB-468 cells were infected with Ad-*wt*-p53, Ad-p53-CC and Ad-Zsgreen and apoptotic potential was determined via 7-AAD assay. Statistical analysis was performed by using one-way ANOVA with Bonferroni's post test; ** < p 0.01, and *** p < 0.001. Error bars represent standard deviations from three independent experiments (n=3).

6.4.5. p53-CC bypasses dominant negative inhibition *in vivo*

To verify that p53-CC can evade dominant negative inhibition *in vivo,* injected MDA-MB-468 cells were injected into the mouse mammary fat pad to form orthotopic tumors. Once the tumors reached 50 mm3, we intratumorally injected 5.0 X 10^8 pfu of Ad-p53-CC, Ad-*wt*-p53 and Ad-ZsGreen1 (or no treatment) on days 0-4 and 7-11 (18). A representative picture of the generated tumor model is shown in figure 5A. We harvested all the tumors from each treatment group. Figure 5B depicts images of representative excised tumors for Ad-p53-CC, Ad-wt-p53, Ad-ZsGreen1 and the untreated group. We also noticed that negative controls Ad-ZsGreen1 and untreated

tumors are more vascularized and bloody than tumors treated with Ad-p53-CC and Ad-wt-p53 (Fig. 5B).

Ad-p53-CC had greater reduction in mean tumor size that is significant compared to Ad-wt-p53, Ad-ZsGreen1 and untreated (Fig. 5C). Ad-wt-p53 inhibited tumor growth but was not significantly different from Ad-ZsGreen1 and untreated (Fig 5C). To monitor overall animal health, we measured animal body weight. Figure 5D shows that there is no difference in the weights among the groups suggesting no toxicity from the virus.

There were no abnormalities or signs of pathology for liver, kidney, spleen, heart, or lungs. However, metastasis of tumors were noticed in two mice of the Ad-ZsGreen1 group and three of the mice in the untreated group.

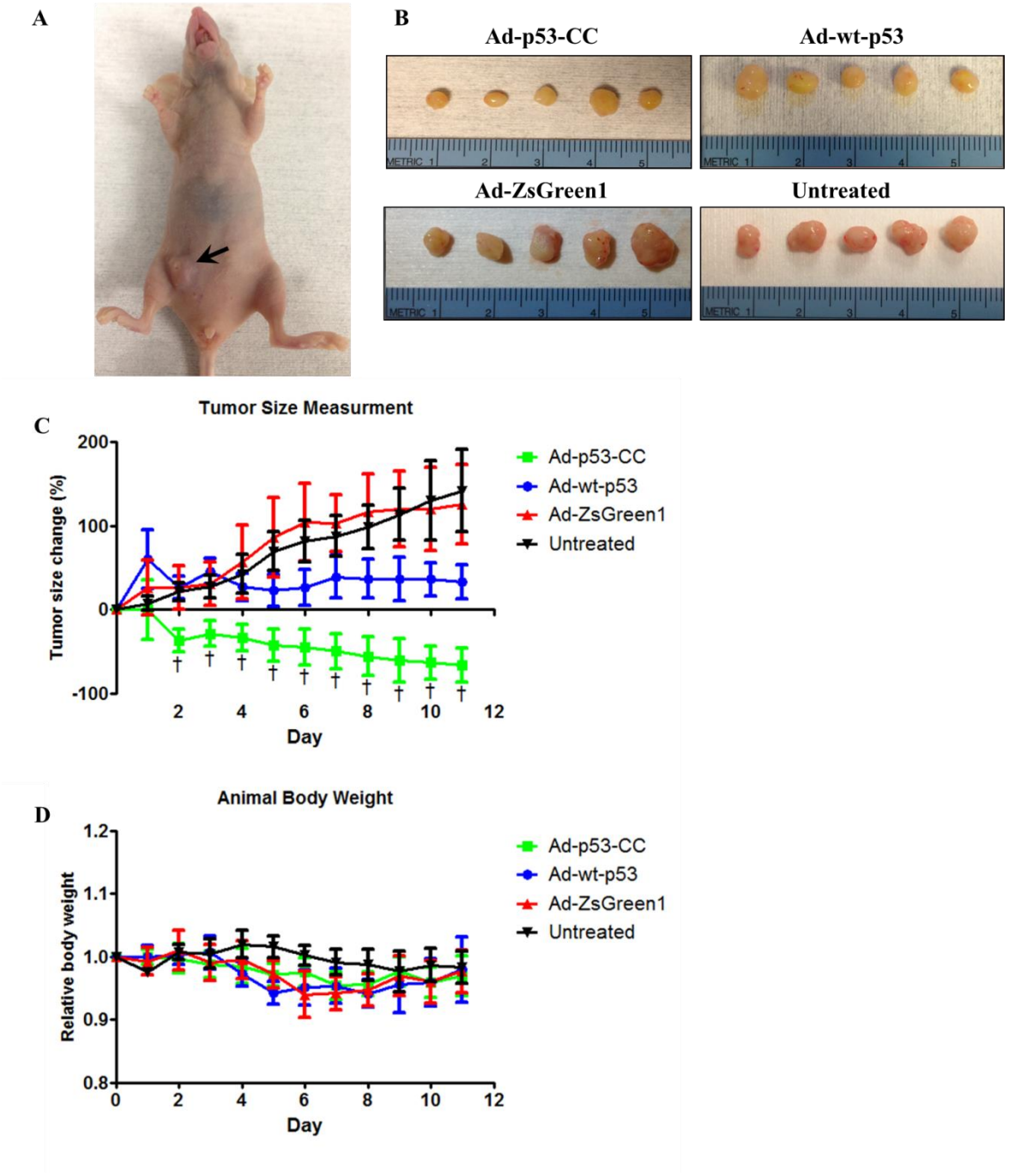

Figure 5: p53-CC evades dominant negative inhibition *in vivo*: (A) representative picture of MDA-MB-468 based orthotopic mouse model. MDA-MB-468 cells were subcutaneously injected into the mammary fat pad. When tumors reached 50 mm3, they were intratumorally injected with 5 X 10^8 pfu per each construct on days 0-4 and

7-11. (B) images of represented excised tumors of different treatment groups. (C) tumor size reduction (D) tumor weights of different treatment groups. Statistical analysis was performed by using one-way ANOVA with Bonferroni's post test † $p < 0.001$. Error bars represent standard deviations from at least three independent experiments (n=6).

6.4.6 Detection of p53 pathway specific markers

To verify that our constructs are expressed in tumors and can induce p53-dependent activity, we carried out immunohistochemistry staining using hematoxylin and eosin staining (H&E) depicted in figure 6A left column, p21 staining in figure 6A middle column and ZsGreen staining figure 6A right column. ZsGreen1 is co-expressed with our protein of interest *in vivo* (Fig 6A, right column). Ad-p53-CC, Ad-*wt*-p53 and Ad-ZsGreen1 showed significant expression of the construct in tumor tissue (Fig. 6 right column), while untreated, as expected, did not show any expression of ZsGreen1. Figure 6A left column shows H&E staining with solid arrows used to highlight necrosis while open arrows highlight non-necrotic areas. p53-CC had higher levels of necrosis in all tumor tissue from mice injected with Ad-p53-CC compared to Ad-*wt*-p53, Ad-ZsGreen1, or untreated. Since the necrotic potential was only significantly higher in the Ad-p53-CC group, while Ad-*wt*-p53, Ad-ZsGreen1 and untreated showed about the same necrotic potential (Fig. 6B), detected necrosis may be due to tumor suppressor activity of p53-CC and not hypoxia or injection site damage. p21 was detected using 3,3'-diaminobenzidine (DAP) staining of photomicrographs which stains nuclei of p21- positive cells brown. As expected Ad-ZsGreen1 and untreated showed no p21 expression (Fig. 6A and C). Ad-*wt*-p53 has significantly more p21 expression than Ad-p53-CC (Fig 6C). This observation will further be explained in the discussion section.

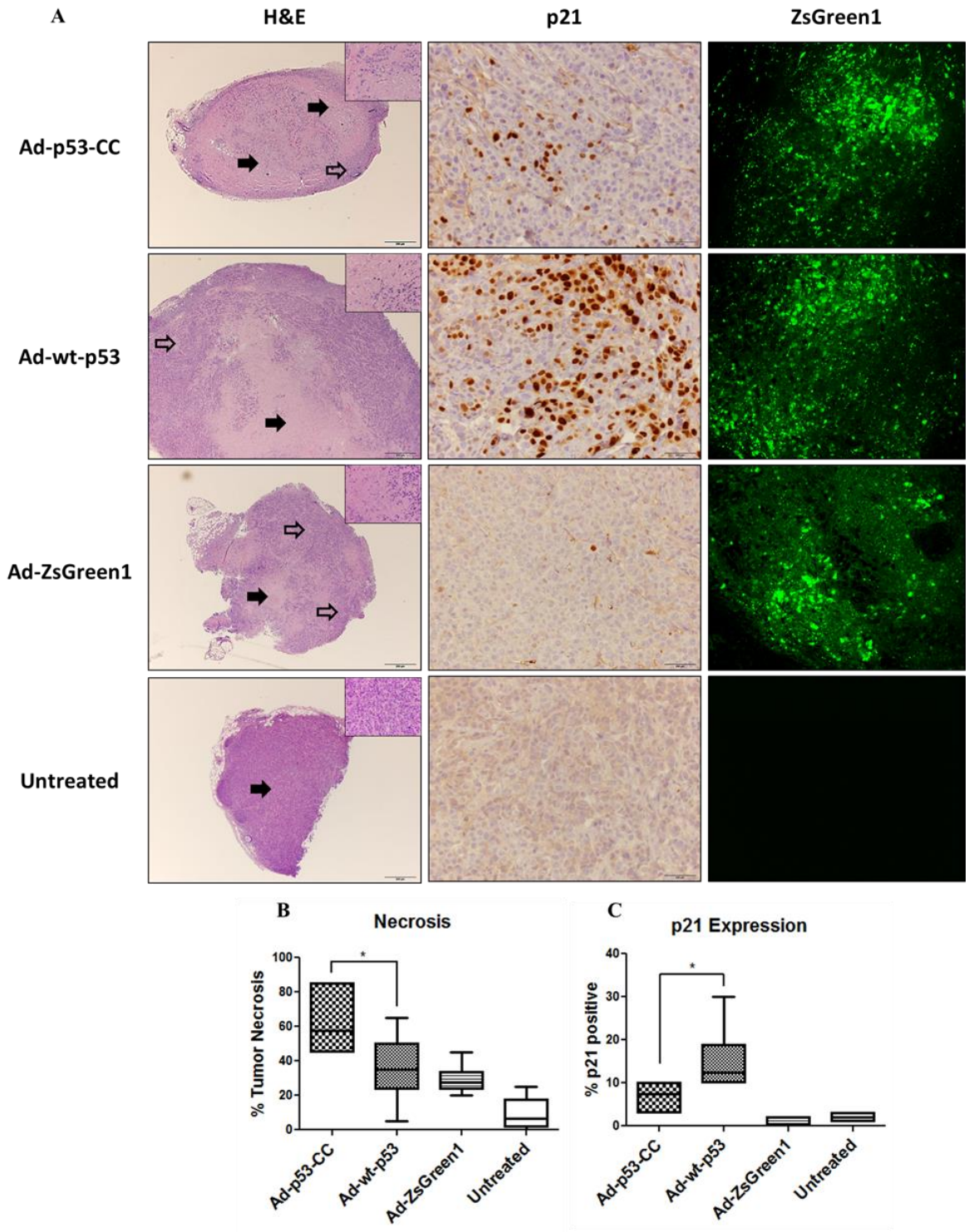

Figure 6 immunohistochemistry representative pictures (A) (left column) H&E, (middle column) p21 and (right column) ZsGreen1 expression levels (B) and (C)

semi-quantitative histoscore analysis of tumor (B) necrosis and (C) p21 upregulation in excised tumors from all groups. Statistical analysis was performed by using one-way ANOVA with Bonferroni's post test; * $p < 0.05$, ** $p < 0.01$, and *** $p < 0.001$. Error bars represent standard deviations from at least three independent experiments (n=6).

6.5. Discussion

We are the first group to successfully re-engineer p53 by replacing its TD with the oligomerization domain of Bcr while still retain apoptotic activity. In the past, only one group has attempted swapping out the TD with a four-stranded coiled coil (13). The weakness of their oligomerization domain is that it forms parallel dimers of dimers while the TD in p53 naturally forms anti-parallel dimers of dimers (14, 15, 29). Therefore, Waterman et al. had limited success with p53 regulated transcriptional and apoptotic activity of their construct (13).

We chose the oligomerization domain of Bcr because similar to the TD it also forms anti-parallel dimers of dimers (14). By constructing p53-CC, we replaced most of the C-terminus (starting from 322 aa) by CC and lost two out of the three NLSs. However, the two NLSs removed in p53-CC are considered to be weak NLSs, while p53-CC still harbors the strong NLS (305- 322 aa) (19). Even though p53-CC lacks the two weak NLSs it was still capable of translocating into the nucleus which is essential for its function as a transcription factor (Fig. 1).

Since we have proven nuclear localization, we wanted to examine if p53-CC retains the same apoptotic potential as *wt* p53. p53-CC is capable of inducing apoptosis similar to *wt* p53 shown in three different apoptosis assays in breast cancer cells which do not contain dominant negative mutant p53 (Fig. 2). Therefore, our p53-CC is superior to the Waterman construct (13) which showed low activity in colony forming assay compared to *wt* p53 in osteosarcoma Saos-2 cells in which the p53

gene is entirely deleted (30). Thus, our CC can replace the TD of p53 and emphasizes that the TD has mostly a structural role in forming p53 tetramers, and its regulatory roles are negligible. Even though post translational modifications in the C-terminus are important for transcriptional activity (31), we show that p53-CC has the same transcriptional and apoptotic activity as *wt* p53 although it lacks the entire C-regulatory domain.

Further, CC has a clear advantage over TD because unlike TD, CC does not heterotetramerize with endogenous *wt* p53 (Fig. 3). In summary, p53-CC retains *wt* p53 transcriptional and apoptotic activity (Fig. 2) and does not interact with endogenous *wt* p53 (Fig. 3) which could be beneficial in a dominant negative cell line. On the other hand p53-CC could potentially interact with endogenous Bcr via its CC. Bcr is a phosphotransferase protein that is suspected to have a role in the inflammatory pathway and in cell proliferation (32). However, this interaction is unlikely because Bcr is found in the cytoplasm (33) and p53-CC as shown via fluorescence microscopy (Fig. 1) translocates to the nucleus. We are further addressing p53-CC and Bcr interaction by introducing mutations in p53-CC to favor homotetramerization (manuscript in preparation: Towards super p53: A Re-engineered Tumor Suppressor with Enhanced Homo-oligomerization and Increased Apoptotic Activity).

Since we have verified homotetramerization, we wanted to examine if p53-CC is superior over *wt* p53 in evading the dominant negative effect first *in vitro* and then *in vivo*. Thus, we tested the ability of p53-CC to bypass the dominant negative effect with transdominant mutant p53 overexpression and by MDA-MB-468 that harbor dominant negative mutant p53 (Fig. 4). Both experiments verified that the apoptotic activity of p53-CC is unaffected by the presence of dominant negative mutant p53 while *wt* p53 mostly loses its activity (Fig. 4). To further validate if this is still the case *in vivo*, we used an orthotopic mouse breast cancer model using triple negative dominant negative MDA-MB-468 cells (34). Remarkably, p53-CC was capable of shrinking tumors while *wt* p53 only stopped tumor growth (Fig. 5C). This finding

correlates with Nielsen and colleagues who showed that *wt* p53 introduced into a xenograft MDA-MB-468 model inhibits tumor growth but does not cause tumor shrinkage (34). Our data emphasizes that p53-CC is capable of overcoming the dominant negative effect of *wt* p53 *in vivo* (Fig. 5C).

Next, we wanted to determine if tumor size reduction was due to p53-specific induction or due to p53-independent response. First, we verified that all our adenoviral constructs were highly expressed in tumor tissue (Fig. 6A right column). Second, we observed that p53-CC showed higher levels of necrosis compared to *wt* p53 (Fig. 6A left column; Fig. 6B) and negative controls ZsGreen1 and untreated, implying that the detected necrosis is due to p53-CC specific activity causing cell death which contributes to tumor reduction.

Finally, p21 is one of the best characterized p53 cell cycle genes (35). Ad-ZsGreen1 and untreated showed no p21 expression verifying that p21 expression was due to p53 specific response (Fig. 6A middle column; Fig. 6C). Ad-*wt*-p53 showed higher expression of p21 than Ad-p53-CC (Fig. 6A middle column; Fig. 6C). This might be due to structural and stability differences in p53-CC and *wt* p53. The melting temperature (Tm) for CC is about 83ºC (36) while Tm for TD is about 75ºC at physiological pH (37). Therefore, p53-CC can form more stable tetramers than wt p53. Additionally, it is known that mutant p53 sequesters *wt* p53 and forces it to form inactive hetero-oligomers with endogenous mutant p53 (9). The lower stability of *wt* p53 tetramers and sequestration of *wt* p53 results in low levels of *wt* p53 tetramers compared to high levels of p53-CC homotetramers. Basal or low levels of endogenous p53 typically turns on pro-arrest genes such as p21, while higher levels of p53 protein usually turn on pro-apoptotic genes such as Bax (38, 39). In breast cancer p53 activity has been linked to p21-dependent and-independent growth arrest and cellular senescence instead of cell death, resulting in minimal tumor regression and early relapse of breast cancer patients (40). Since Ad-*wt*-p53 induces more p21 than Ad-p53-CC this might provide an explanation to why Ad-*wt*-p53 only inhibits

tumor growth while Ad-p53-CC shrinks the tumors. Further testing needs to be done to verify how exactly p53 causes tumor shrinking.

In summary, we re-engineered p53 by replacing its TD with the CC from Bcr to bypass dominant negative inhibition by mutant p53. Our p53-CC has been shown to overcome dominant negative inhibition *in vitro* and *in vivo*. Therefore, our p53-CC which still remains its function in a dominant negative cancer is clearly superior over *wt* p53 gene therapy and can be used for a variety of cancers aside from breast cancer that currently have no cure.

6.6 References

1. Schuijer M, Berns EM. TP53 and ovarian cancer. Hum Mutat. 2003 Mar;21(3):285-91.

2. Peller S, Rotter V. TP53 in hematological cancer: low incidence of mutations with significant clinical relevance. Hum Mutat. 2003 Mar;21(3):277-84.

3. Coles C, Condie A, Chetty U, Steel CM, Evans HJ, Prosser J. p53 mutations in breast cancer. Cancer Res. 1992 Oct 1;52(19):5291-8.

4. Muller PA, Vousden KH. p53 mutations in cancer. Nat Cell Biol. 2013 Jan;15(1):2-8.

5. Brosh R, Rotter V. When mutants gain new powers: news from the mutant p53 field. Nat Rev Cancer. 2009 Oct;9(10):701-13.

6. Hollstein M, Sidransky D, Vogelstein B, Harris CC. p53 mutations in human cancers. Science. 1991 Jul 5;253(5015):49-53.

7. Kim E, Deppert W. The versatile interactions of p53 with DNA: when flexibility serves specificity. Cell Death Differ. 2006 Jun;13(6):885-9.

8. Milner J, Medcalf EA, Cook AC. Tumor suppressor p53: analysis of wild-type and mutant p53 complexes. Mol Cell Biol. 1991 Jan;11(1):12-9.

9. Srivastava S, Wang S, Tong YA, Hao ZM, Chang EH. Dominant negative effect of a germ-line mutant p53: a step fostering tumorigenesis. Cancer Res. 1993 Oct 1;53(19):4452-5.

10. Kern SE, Pietenpol JA, Thiagalingam S, Seymour A, Kinzler KW, Vogelstein B. Oncogenic forms of p53 inhibit p53-regulated gene expression. Science. 1992 May 8;256(5058):827-30.

11. Mateu MG, Sanchez Del Pino MM, Fersht AR. Mechanism of folding and assembly of a small tetrameric protein domain from tumor suppressor p53. Nat Struct Biol. 1999 Feb;6(2):191-8.

12. Mateu MG, Fersht AR. Nine hydrophobic side chains are key determinants of the thermodynamic stability and oligomerization status of tumour suppressor p53 tetramerization domain. EMBO J. 1998 May 15;17(10):2748-58.

13. Waterman MJ, Waterman JL, Halazonetis TD. An engineered four-stranded coiled coil substitutes for the tetramerization domain of wild-type p53 and alleviates transdominant inhibition by tumor-derived p53 mutants. Cancer Res. 1996 Jan 1;56(1):158-63.

14. Wichmann C, Becker Y, Chen-Wichmann L, Vogel V, Vojtkova A, Herglotz J, et al. Dimer-tetramer transition controls RUNX1/ETO leukemogenic activity. Blood. 2010 Jul 29;116(4):603-13.

15. Jeffrey PD, Gorina S, Pavletich NP. Crystal structure of the tetramerization domain of the p53 tumor suppressor at 1.7 angstroms. Science. 1995 Mar 10;267(5203):1498-502.

16. Mossalam M, Matissek KJ, Okal A, Constance JE, Lim CS. Direct induction of apoptosis using an optimal mitochondrially targeted p53. Mol Pharm. 2012 May 7;9(5):1449-58.

17. Dixon AS, Kakar M, Schneider KM, Constance JE, Paullin BC, Lim CS. Controlling subcellular localization to alter function: Sending oncogenic Bcr-Abl to the nucleus causes apoptosis. J Control Release. 2009 Dec 16;140(3):245-9.

18. Nielsen LL, Lipari P, Dell J, Gurnani M, Hajian G. Adenovirus-mediated p53 gene therapy and paclitaxel have synergistic efficacy in models of human head and neck, ovarian, prostate, and breast cancer. Clin Cancer Res. 1998 Apr;4(4):835-46.

19. Shaulsky G, Goldfinger N, Ben-Ze'ev A, Rotter V. Nuclear accumulation of p53 protein is mediated by several nuclear localization signals and plays a role in tumorigenesis. Mol Cell Biol. 1990 Dec;10(12):6565-77.

20. Mooney LM, Al-Sakkaf KA, Brown BL, Dobson PR. Apoptotic mechanisms in T47D and MCF-7 human breast cancer cells. Br J Cancer. 2002 Oct 7;87(8):909-17.

21. Nigro JM, Baker SJ, Preisinger AC, Jessup JM, Hostetter R, Cleary K, et al. Mutations in the p53 gene occur in diverse human tumour types. Nature. 1989 Dec 7;342(6250):705-8.

22. Loo DT, Rillema JR. Measurement of cell death. Methods Cell Biol. 1998;57:251-64.

23. Koopman G, Reutelingsperger CP, Kuijten GA, Keehnen RM, Pals ST, van Oers MH. Annexin V for flow cytometric detection of phosphatidylserine expression on B cells undergoing apoptosis. Blood. 1994 Sep 1;84(5):1415-20.

24. Schmid I, Krall WJ, Uittenbogaart CH, Braun J, Giorgi JV. Dead cell discrimination with 7-amino-actinomycin D in combination with dual color immunofluorescence in single laser flow cytometry. Cytometry. 1992;13(2):204-8.

25. Lim LY, Vidnovic N, Ellisen LW, Leong CO. Mutant p53 mediates survival of breast cancer cells. Br J Cancer. 2009 Nov 3;101(9):1606-12.

26. Bodner SM, Minna JD, Jensen SM, D'Amico D, Carbone D, Mitsudomi T, et al. Expression of mutant p53 proteins in lung cancer correlates with the class of p53 gene mutation. Oncogene. 1992 Apr;7(4):743-9.

27. Di Como CJ, Gaiddon C, Prives C. p73 function is inhibited by tumor-derived p53 mutants in mammalian cells. Mol Cell Biol. 1999 Feb;19(2):1438-49.

28. Dong P, Tada M, Hamada J, Nakamura A, Moriuchi T, Sakuragi N. p53 dominant-negative mutant R273H promotes invasion and migration of human endometrial cancer HHUA cells. Clin Exp Metastasis. 2007;24(6):471-83.

29. Lee W, Harvey TS, Yin Y, Yau P, Litchfield D, Arrowsmith CH. Solution structure of the tetrameric minimum transforming domain of p53. Nat Struct Biol. 1994 Dec;1(12):877-90.

30. Chandar N, Billig B, McMaster J, Novak J. Inactivation of p53 gene in human and murine osteosarcoma cells. Br J Cancer. 1992 Feb;65(2):208-14.

31. Toledo F, Wahl GM. Regulating the p53 pathway: in vitro hypotheses, in vivo veritas. Nat Rev Cancer. 2006 Dec;6(12):909-23.

32. Alexis JD, Wang N, Che W, Lerner-Marmarosh N, Sahni A, Korshunov VA, et al. Bcr kinase activation by angiotensin II inhibits peroxisome-proliferator-activated receptor gamma transcriptional activity in vascular smooth muscle cells. Circ Res. 2009 Jan 2;104(1):69-78.

33. Maru Y, Witte ON. The BCR gene encodes a novel serine/threonine kinase activity within a single exon. Cell. 1991 Nov 1;67(3):459-68.

34. Nielsen LL, Dell J, Maxwell E, Armstrong L, Maneval D, Catino JJ. Efficacy of p53 adenovirus-mediated gene therapy against human breast cancer xenografts. Cancer Gene Ther. 1997 Mar-Apr;4(2):129-38.

35. Giono LE, Manfredi JJ. Mdm2 is required for inhibition of Cdk2 activity by p21, thereby contributing to p53-dependent cell cycle arrest. Mol Cell Biol. 2007 Jun;27(11):4166-78.

36. Dixon AS, Pendley SS, Bruno BJ, Woessner DW, Shimpi AA, Cheatham TE, 3rd, et al. Disruption of Bcr-Abl coiled coil oligomerization by design. J Biol Chem. 2011 Aug 5;286(31):27751-60.

37. Galea C, Bowman P, Kriwacki RW. Disruption of an intermonomer salt bridge in the p53 tetramerization domain results in an increased propensity to form amyloid fibrils. Protein Sci. 2005 Dec;14(12):2993-3003.

38. Budram-Mahadeo V, Morris PJ, Latchman DS. The Brn-3a transcription factor inhibits the pro-apoptotic effect of p53 and enhances cell cycle arrest by differentially regulating the activity of the p53 target genes encoding Bax and p21(CIP1/Waf1). Oncogene. 2002 Sep 5;21(39):6123-31.

39. Aylon Y, Oren M. Living with p53, dying of p53. Cell. 2007 Aug 24;130(4):597-600.

40. Jackson JG, Pant V, Li Q, Chang LL, Quintas-Cardama A, Garza D, et al. p53-mediated senescence impairs the apoptotic response to chemotherapy and clinical outcome in breast cancer. Cancer Cell. 2012 Jun 12;21(6):793-806.

7. Conclusions and Future Directions

7.1 Conclusions

7.1.1 Activity of mitochondrially targeted p53 is dependent on the mitochondrial targeting signal (Chapters 2 and 4)

Targeting p53 to the mitochondria results in a rapid apoptotic response due to the direct interaction between p53 and pro-and anti-apoptotic Bcl-2 protein family members (1, 2). We attached p53 to different mitochondrial targeting signals (MTSs) from the mitochondrial matrix (ornithine transcarbomylase: OTC), inner membrane (cytochrome c oxidase: CCO), outer membrane (TOM20 complex: TOM) and outer surface of the outer membrane (anti-apoptotic Bcl-XL: XL; pro-apoptotic Bak: BakMTS; pro-apoptotic Bax: BaxMTS).

To function as a transcription factor nuclear localization is required. p53 contains three nuclear localization signals (NLS) one strong NLS and two weak NLSs to ensure nuclear translocation (3). However, mitochondrial translocation only occurs upon severe stress induction. Since it is known that monoubiquitinated p53 is shuttled out of the nucleus into the cytoplasm, Moll and colleagues speculated that monoubiquitinated p53 can be shuttled into the mitochondrial through HAUSP (4, 5).

To ensure mitochondrial localization of p53, different mitochondrial targeting signals were used. We showed that all the MTSs tested taken from proteins embedded in the mitochondrial outer membrane (XL, BakMTS, BaxMTS) are capable of targeting p53 to the mitochondria despite the three NLSs in the p53 protein. On the other hand, inner membrane (CCO) and matrix (OTC) MTSs were not capable of completely overcoming the NLSs. The mitochondrial localization of our p53-MTS constructs was determined using fluorescence microscopy and the degree of colocalization with the mitochondrial compartment was determined by Pearson's correlation coefficient following Coste's approach (6-8). As expected, all constructs that colocalized with the mitochondria, showed minimum transcriptional activity (p53

fused to XLMTS, BakMTS, BaxMTS). On the other hand constructs showing low mitochondrial localization (CCO-p53, OTC-p53) showed transcription activity. In fact, CCO-p53 showed the same and OTC-p53 showed half the transcription activity compared to *wt* p53. Further, mutating the strong NLS in p53 dramatically improved mitochondrial localization of the weak MTS CCO, and decreased its transcriptional activity.

When conducting various apoptosis assays (TUNEL, Annexin V, 7-AAD assay), we discovered the inherent toxicity of some MTSs. The matrix signal OTC, inner membrane signal CCO and the outer membrane signal TOM all caused p53-indepenten apoptosis when fused to non-toxic EGFP. We speculate that, EGFP fused to OTC or CCO could cause an imbalance in the sensitive mitochondrial system possibly interfering with proteins involved in the TCA cycle or other energy mechanism. On the other hand, TOM-EGFP could be interfering with the TOM complex which is the main import machinery for proteins into the mitochondria as discussed previously in the introduction section (Chapter 1) and might affect the sensitive import machinery (9). However, only the outer membrane signals from Bcl-XL, Bak and Bax which are thought to localize to the outer surface of the mitochondrial outer membrane, do not contain inherent MTS toxicity.

Furthermore, it is important that the pro (Bak, Bax)- or anti (Bcl-XL)- Bcl-2 protein from which the MTS is used is always present at the mitochondrial outer membrane. Bax is constantly shuttled between cytoplasm and mitochondria (10, 11). Mitochondrially targeted p53 which is fused to BaxMTS is not capable of activating cytoplasmic Bax, and the amount of mitochondrial Bax might not be sufficient for apoptosis induction. This results in unpredictable activity profiles varying from cell line to cell line for Bax. However, Bak is always present at the mitochondria and therefore consistent in its induction of apoptosis (12).

As discussed above, only MTSs from the mitochondrial outer membrane lack inherent toxicity to the mitochondria and therefore offer specific mitochondrial

apoptosis that is p53 dependent. Targeting p53 to the mitochondria via MTS from its anti- (Bcl-XL) and pro- (Bak) binding partners results in p53 dependent apoptosis. p53 fused to the mitochondrial targeting signal from anti-apoptotic Bcl-XL has been shown to interact with anti-apoptotic Bcl-2 proteins, in particular anti-apoptotic Bcl-XL at the mitochondria. On the other hand, targeting p53 with the MTS from the pro-apoptotic Bak protein verified Bak mediated apoptosis.

Therefore, mitochondrial targeting of p53 is highly dependent on the MTS used. The optimal MTS for p53 specific mitochondrial targeting is a MTS from a p53 interacting partner which is always present at the mitochondrial outer membrane (Bcl-XL, Bak) and is strong enough to ensure mitochondrial localization while overcoming the NLSs in p53 (XL, BakMTS).

7.1.2 Solely the DNA binding domain of p53 fused to a specific MTS is sufficient to trigger apoptosis (Chapter 3 and 4)

We are the first group to discover that the DNA binding domain (DBD) when fused to a MTS from anti- apoptotic Bcl-XL or pro-apoptotic Bak or Bax is sufficient to activate the intrinsic apoptotic pathway.

The MDM2 binding domain (MBD), the proline rich domain (PRD) and the DBD have been reported to play an important role for Bcl-XL interaction. We verified that solely the DBD fused to MTS from Bcl-XL (XL) is necessary for apoptosis induction while MBD, PRD, TD or combinations of these domains have the same impact on cell death as non-toxic EGFP fused to XL. Further, we showed that DBD-XL and p53-XL cause disruption of the mitochondrial membrane (TMRE assay) and activation of the intrinsic apoptotic pathway (caspase-9 assay). The initiation of the intrinsic apoptotic pathway is due to p53 or DBD interacting with anti-apoptotic Bcl-XL protein at the mitochondrial outer membrane (Bcl-XL rescue experiment).

For pro-apoptotic Bak, Murphy and colleagues reported that p53 must form a dimer or a tetramer to trigger Bak homo-oligomerization. On the other hand residues localized in the DBD (K120, R248, R273, R280, E285, E287) have been outlined to interact with pro-apoptotic Bak protein. We confirmed that DBD targeted with the MTS from Bak is capable of inducing the intrinsic apoptotic pathway. To illustrate that p53-BakMTS and DBD-BakMTS apoptotic activity is Bak protein specific, we mutated residues mentioned above in both constructs. Indeed, p53-BakMTS and DBD-BakMTS activity is completely lost when these residues are mutated, therefore indicating that p53-BakMTS and DBD-BakMTS cause Bak-specific apoptosis.

The potential of DBD fused to the different MTSs to cause apoptosis in different cell and cancer lines was examined using a late stage apoptosis assay, 7-AAD, in mammary ductal carcinoma (T47D), breast adenocarcinoma (MDA-MB-231), non-small lung carcinoma (H1373), ovarian adenocarcinoma (SKOV-3) and cervical carcinoma (HeLa) cells. In all tested cell lines, DBD fused to MTS from Bcl-XL or Bak had the same or even higher apoptotic potential than full length p53 fused to this MTSs. The p53/MDM2 degradation pathway as discussed earlier in the introduction could provide a valid explanation to why DBD shows higher activity than full length p53. The E-3 ligase MDM2 binds to the MBD of p53 and along with E4 factors, E like molecules or MDMX facilitates its polyubiquitination and proteasomal degradation (13). Unlike p53, DBD does not contain the MBD or the C-terminus and is therefore more stable than full length p53. This possible lack of degradation may explain the higher apoptotic activity of DBD-XL.

In summary, we demonstrate that the DBD when fused to MTSs from Bcl-XL or Bak is sufficient to trigger a rapid apoptotic respond at the mitochondria. Therefore, we decided to test our constructs delivered by adenovirus in an orthotropic breast cancer model.

7.1.3 Targeting monomeric p53 or its DBD fused to the MTS from Bcl-XL *in vivo* (Chapter 5)

We wanted to investigate if p53 or DBD targeted to the mitochondria is capable of overcoming dominant negative inhibition by mutant p53. In cancer cells, most of the mutations in p53 occur in its DNA binding domain while the TD remains active. Therefore, mutant p53 can heterotetramerize with *wt* p53 via their TD (dominant negative effect). While wild type p53 has to form a tetramer in order to be transcriptionally active and transactivate pro-apoptotic genes, mitochondrial p53 as we and others have demonstrated before (1, 14, 15) causes apoptosis at the mitochondria as a monomer.

To investigate if p53 and DBD both fused to the MTS from Bcl-XL (p53-XL, DBD-XL) can bypass dominant negative inhibition, we overexpressed dominant mutant p53 containing the R248W mutant (called p53R248Wmut) in p53 null H1373 non-small cell lung cancer cell. p53-XL and DBD-XL maintained the same apoptotic activity with or without overexpressing the p53R248Wmut, while *wt* p53 activity dramatically decreased when p53R248Wmut was present suggesting that p53-XL and DBD-XL have the potential to overcome dominant negative inhibition. Further, we tested if this is also true in MDA-MB-468 cells which naturally harbor dominant negative mutant p53 (R273H). However, only DBD-XL was active in MDA-MB-468 cells, while p53-XL remains the same low activity as negative control. p53-XL might be sequestered by mutant p53 because both harbor the same TD and could potentially heterotetramerize. Unlike p53-XL, DBD-XL does not contain a TD and is its activity is therefore not impaired by dominant mutant p53 in MDA-MB-468 cells.

DBD fused to XL can overcome dominant negative inhibition *in vitro*, but it was unable to shrink MDA-MB-468 tumors in an orthotopic mouse mode. The dosing regimen might offer an explanation for the treatment failure. While transcriptionally active *wt* p53 can trigger both the extrinsic and intrinsic pathway, mitochondrial DBD solely initiates the intrinsic apoptotic pathway. Due to the different apoptotic profiles, the dose for DBD-XL has to be higher than for *wt* p53. Additionally, we further

optimized mitochondrial targeting of DBD by fusing it to MTS from pro-apoptotic Bak. Anti-apoptotic Bcl-XL needs to be sequestered to release pro-apoptotic Bak or Bax from the inhibitory heterodimer, and allow for pore formation at the mitochondria. However, pro-apoptotic Bak only needs to be activated and not sequestered in order to form pores. In aggressive cancers, anti-apoptotic Bcl-2 protein members such as Bcl-XL, Bcl-2 and Mcl-1 are overexpressed. Therefore, the amount of DBD-XL might not be sufficient to sequester anti-apoptotic Bak, but DBD targeted to Bak might be sufficient to transiently interact with Bak and facilitate its activation and apoptosis.

7.1.4 Chimeric p53 can bypass dominant negative inhibition (Chapter 6)

To bypass dominant negative inhibition of mutant p53, we substituted the tetramerization domain (TD) of p53 with the coiled-coil (CC) domain from BCR. Both oligomerization domains contain a main α- helix that orients in an anti-parallel fashion and a forms dimer of dimers (16, 17). Aside from us, Waterman et al. have substituted the TD with a four-stranded coiled coil. However, their oligomerization domain forms parallel tetramers, instead of anti-parallel as TD, which might explain its low transcriptional and apoptotic activity (18).

To create p53-CC, we replaced most of the C-terminal domain (amino acids 323−393) of *wt* p53 with CC. Thereby we removed two out three nuclear localization signals (3). However, p53-CC still translocates to the nucleus in the same manner as *wt* p53. Next we tested transcriptional and apoptotic activity of p53-CC and demonstrated that p53-CC shows the same apoptosis as *wt* p53 in T47D breast cancer cells which do not exhibit a strong dominant negative effect. Further, we revealed that revealed that p53-CC solely tetramerizes with itself while exogenous *wt* p53 interacts with endogenous p53. To tested apoptotic activity of p53-CC, we overexpressed dominant negative mutant p53 (R175H, R248W, R273H) in p53 null H1373 cells and then in MDA-MB-468 harboring R274H mutant p53. Both

experiments illustrated that p53-CC, unlike *wt* p53, is capable of initiating apoptosis and is therefore not inhibited by mutant p53.

To examine this finding *in vivo* we used an orthotopic xenograft tumor bearing mouse model. Tumors were derived from triple negative MDA-MB-468 cells with dominant negative p53 (19, 20). p53-CC was capable to shrink tumors while *wt* p53 only inhibited tumor growth. We further determined expression levels of adenoviral constructs, measured p21 expression and conducted H&E staining of tumor tissue. Adenovirally delivered p53-CC, *wt* p53 and negative control ZsGreen were highly expressed in tumor tissue. *wt* p53 had higher p21 expression while p53-CC showed higher necrosis (H&E staining). Necrotic potential of p53-CC might contribute to tumor size reduction. p21 is known to cause cell cycle arrest and p21 expression has been linked to minimal tumor regression and early relapse in breast cancer patients (21). Since *wt* p53 initiates p21 expression this might provide an explanation to why *wt* causes inhibition of tumor growth while p53-CC causes tumor shrinking. However, this needs further investigation. We anticipate that p53-CC can be used as an alternative to *wt* p53 for cancer gene therapy, especially in tumors with dominant mutant p53, where *wt* p53 has shown to be inactive.

7.2 Future directions

7.2.1 DBD fused to mitochondrial targeting signal from Bak for ovarian cancer targeting

Previously, we have discovered the minimal domain of p53, its DNA binding domain (DBD), needed for apoptosis (22) and a rationally selected MTS with optimal activity (Chapter 4). We have highlighted that MTSs from the mitochondrial outer membrane (MOM) are optimal for p53-specific activation (14). Using MTSs from pro-apoptotic Bcl-2 family members Bak (23-25) will trigger mitochondrial outer membrane permeabilization (MOMP), resulting in activation of the intrinsic apoptotic pathway.

Previously, we have shown that Bak MTS may be optimal for DBD targeting and apoptosis.

As mentioned in the introduction (Chapter 1), mitochondrial p53 inhibits anti-apoptotic (Bcl-2, Bcl-XL, Mcl-1) (26-28) and activates pro-apoptotic (Bak, Bax) (24, 25) Bcl-2 family members leading to mitochondrial outer membrane permeabilization (MOMP) and resulting in apoptosis. In cancer cells, overexpression of Bcl-2, Bcl-XL and Mcl-1 correlates with more aggressive phenotypes and leads to chemotherapy resistance (29-32). Many agents have been identified to target the anti-apoptotic Bcl-2 family members. These therapeutics cause apoptosis through neutralizing anti-apoptotic proteins at the mitochondria allowing the pro-apoptotic Bcl-2 family members Bak or Bax to homo-oligmomerize initiating apoptosis (33). However, these inhibitors do not target all anti-apoptotic Bcl-2 proteins; in fact most of them (Navitoclax, ABT-199) are selective to Bcl-2 (34). This limits its use since many cancers overexpress Bcl-XL and Mcl-1 (29-32). Therefore, our approach is to directly activate pro-apoptotic Bak by targeting p53 to the mitochondria using Bak's own MTS. p53 activates Bak by disrupting Bak/Mcl-1 and Bak/Bcl-XL complexes (25, 26, 35). We hypothesize that DBD-BakMTS can trigger apoptosis in cancer cells by preferential interaction with Bak (over Mcl-1 or Bcl-XL).

Our data indicate a robust apoptosis from DBD-BakMTS that is entirely dependent on residues in the DBD that directly interact with cellular Bak. We have shown that the minimal domain of p53 (DBD) fused to MTS from pro-apoptotic Bak which is localized at the mitochondrial outer membrane results in apoptosis in a variety of cancer cell lines. Further, we have reported that DBD-BakMTS triggers apoptosis in ovarian cancer cells SKOV-3 while *wt* p53 and p53-CC are incapable of inducing apoptosis in this cell line. Since *wt* p53 and p53-CC mainly cause cell death through transactivating apoptotic genes (36), SKOV-3 might have a defect in p53 transcription machinery. However the exact mechanism why *wt* p53 and p53-CC are inactive in SKOV-3 still needs to be investigated.

Further studies will test DBD-BakMTS for ovarian cancer therapy. Ovarian cancer has shown lack of progress in treatment, since mortality rates of ovarian cancer have not improved over 40 years (37-39). The Cancer Genome Atlas Research network identified a variety of genomic changes in ovarian cancer. While p53 gene mutations occur in more than 96% of ovarian serous tumors, recurrence in mutations in other genes were not noted, or only had a low prevalence (40). Therefore, p53 is an excellent target for ovarian cancer therapy.

The apoptotic activity of DBD-BakMTS will be further tested in ovarian cancer cells, various ovarian cancer cell lines. We hypothesize that ovarian cancer cells with different p53 status will highlight that apoptotic activity of DBD-BakMTS is not dependent on p53 status. Since we already tested SKOV-3 ovarian adenocarcinoma cells from metastatic ascites which are p53 null (41), ovarian cancer cells harboring mutant p53 (OVCAR-3 and Caov-4) (42) and *wt* p53 (A2780) (43) will be tested. Apoptotic activity will be determined by using previously described TMRE-, caspase-9, annexin V and 7-AAD assays.

To explore the effect of DBD-BakMTS on normal cells, BJ normal fibroblasts and immortalized ovarian epithelial cells (IHOEC) will be tested (44). Since DBD-BakMTS is lacking the MBD and C-terminus the DBD-BakMTS is not subject to the p53/MDM-2 degradation pathway. In *wt* p53, E-3 ligase MDM2 binds to the MBD of *wt* p53 which triggers monoubiquitations (45). Then, MDM2 and cofactors (E4 factors, E like molecules) or other E-3 ligases promote polyubiquitination of C-terminal lysines resulting in proteasomal degradation (13). While *wt* p53 is known to be non-toxic to normal cells (46-49), DBD-BakMTS might show some toxicity to normal cells due to the lack of MBD and C-terminus and hence, lack of degradation. If normal cells undergo apoptosis with DBD-BakMTS, cancer specific promoters can be used to prevent this. Cancer specific promoters include survivin (50), unmodified HTERT (51) or ovarian cell-specific OSP-1 promoter (52), which will prevent expression in normal cells and hence apoptosis in these cells. Therefore, the use of these

promoters will ensure expression of DBD-BakMTS mainly in cancer cells and minimize death in normal cells.

Further, the activity of DBD-BakMTS will be tested in a syngeneic orthotopic metastatic mouse model (53). The metastatic ovarian cancer model will be generated by injecting ID8 cells into left ovarian bursa. Prior to initiating treatment, tumors will be grown to approximately a size of 2-2.5cm3. This animal model closely replicates characteristics and hallmarks seen in human ovarian cancer by primary epithelial ovarian tumors, secondary peritoneal metastases and ascites production (53). DBD-BakMTS will be delivered by water soluble lipopolymer (WSLP). Heterogeneity or lack of expression of CAR and integrin co-receptors in ovarian tumors and adenovirus-neutralizing antibodies are major limitations to ovarian cancer adenoviral drug delivery (54). WSLP completed a Phase I clinical trial for ovarian cancer (55). We will intraperitoneal (I.P.) inject plasmid DNA encoding DBD-BakMTS with WSLP into our new syngeneic orthotopic metastatic mouse ovarian cancer model, alone or in combination with carboplatin and paclitaxel. Various studies indicate that I.P. is superior over intravenous (I.V.) delivery (56-58). Higher concentrations of cytotoxic agents can be infused into the peritoneal cavity than would be tolerated systemically. Since the dosing could have been a problem in our breast cancer study with our previously designed mitochondrial construct, we chose I.P. to be able to increase the dosing in the ovarian cancer model. Additionally, I.P. allowed for sustained exposure of tumor implants to antitumor agents while normal tissues, such as bone marrow, are significantly less exposed. Fewell et al. used 10-250ug of WSLP-IL-12 plasmids per injection when using an IP ovarian tumor mouse model (59). Due to the difference in mechanism of action between IL-12 (takes time to induce IFN-α) and p53-MTS (rapid apoptosis expected), we anticipate frequent dosing but a greater effect. Plasmid amount of DBD-BakMTS will be determined first *in vitro* by conducting apoptosis assays in ID8 mouse ovarian cancer cells after that concentration and dosing regime will be optimized in a preliminary animal study.

For future studies we are planning to combine DBD-BakMTS with standard ovarian chemotherapeutics. The combination of carboplatin and paclitaxel are both first line therapy for ovarian cancer but both not completely effective. Platinum resistant cancer recurs in 25% of patients within 6 months (60); platinum requires functional p53 protein for efficient induction of apoptosis, and loss of p53 function enhances resistance to cytotoxic agents (61). We anticipate that DBD delivered to the mitochondria via MTS from Bak will enhance/synergize with standard chemotherapy.

If the animal study is successful for DBD-BakMTS with or without carboplatin and paclitaxel, this work could be beneficial for women diagnosed with late stage (>III) or recurrent high grade serous ovarian cancer and may result in a new clinical trial potent enough to prevent metastatic disease recurrence.

7.2.1 Targeting DBD-Bak for lung cancer therapy

Our p53-based therapeutic approaches may be applicable to other types of cancers as well, including lung cancer which is the leading cause of cancer in the United States. In fact, the overall 5-year survival rate is only about 15% (62). Studies have shown that p53 is mutated in up to 70% of lung cancers (63, 64). Therefore, p53 is an excellent target for lung cancer therapy.

Recently we identified that targeting the DNA binding domain (DBD) of p53 is sufficient (and sometimes more efficient that *wt* p53) in inducing a direct apoptotic effect at the mitochondria in H1373 human non-small cell lung carcinoma cells (Chapter 4). In the future, re-engineered, mitochondrially targeted p53 may be effective against lung cancer. A potential way to deliver mitochondrially targeted p53 would be as a protein formulated as a dry powder for inhalation (65, 66).

wt p53 has been delivered as a protein for oral cancer therapy before and showed inhibition in cancer cell proliferation (67). However, therapeutic levels of *wt* p53 were not maintained for >36 h. This stability problem was mainly due to high degradation

of *wt* p53 via MDM-2/proteasomal pathway (67, 68). Since DBD-Bak does not contain MBD nor the C-terminus, we expected it to be more stable than *wt* p53.

The lung is a good target for drug delivery because drugs can be delivered via inhalation (69, 70). It is wildly known that proteins can be absorbed through the lungs. One example is insulin which was the first peptide approved for inhalation therapy by the U.S. Food and Drug Administration in January 2006 (71). However, Exubera was discontinued in October 2007. The reason for the discontinuation was mainly the high price and insulin related safety concerns. Other insulin delivery alternatives (injectable, pen, etc.) are less costly (72). Potential pulmonary toxicity might occur because of immunogenic and growth-promoting properties of insulin and long-term insulin administration (73). Since DBD-Bak will be only administrate short-term and has completely different pharmacological characteristics than insulin, therefore we do not expect this effect with DBD-Bak protein. One approach is to deliver DBD-Bak as a dry power protein in a similar manner as Exubera using the AERx Pulmonary Drug Delivery System. This system converts large particles (protein agglomerates) into a fine particle aerosol (65). If the lung dysfunction as a result of lung cancer is too severe and the AERx cannot be used, we will deliver the DBD-Bak gene via polymeric non-viral vectors (PEI-PEG, PLL) using jet nebulizers which can be used even when lung function is decreased (74). These vectors can overcome the shear forces created during nebulization while viral vectors and proteins lose their biological activity (75-77). By delivering DBD-Bak specifically to lung cancer cells, side effects will be minimized (78).

Lung cancer is only one other possible type of cancer to target with our mitochondrially targeted p53. Other types of cancers could be targeted as well. This approach highlights mitochondrial targeted DBD again as a "sledgehammer," effective under any circumstances, regardless of genetics or the pathway upon which the cancer develops.

7.3 References

1. Palacios G, Crawford HC, Vaseva A, Moll UM. Mitochondrially targeted wild-type p53 induces apoptosis in a solid human tumor xenograft model. Cell Cycle. 2008 Aug 15;7(16):2584-90.

2. Vaseva AV, Moll UM. The mitochondrial p53 pathway. Biochim Biophys Acta. 2009 May;1787(5):414-20.

3. Shaulsky G, Goldfinger N, Ben-Ze'ev A, Rotter V. Nuclear accumulation of p53 protein is mediated by several nuclear localization signals and plays a role in tumorigenesis. Mol Cell Biol. 1990 Dec;10(12):6565-77.

4. Marchenko ND, Wolff S, Erster S, Becker K, Moll UM. Monoubiquitylation promotes mitochondrial p53 translocation. EMBO J. 2007 Feb 21;26(4):923-34.

5. Marchenko ND, Moll UM. The role of ubiquitination in the direct mitochondrial death program of p53. Cell Cycle. 2007 Jul 15;6(14):1718-23.

6. Costes SV, Daelemans D, Cho EH, Dobbin Z, Pavlakis G, Lockett S. Automatic and quantitative measurement of protein-protein colocalization in live cells. Biophys J. 2004 Jun;86(6):3993-4003.

7. Constance JE, Woessner DW, Matissek KJ, Mossalam M, Lim CS. Enhanced and selective killing of chronic myelogenous leukemia cells with an engineered BCR-ABL binding protein and imatinib. Mol Pharm. 2012 Nov 5;9(11):3318-29.

8. Constance JE, Despres SD, Nishida A, Lim CS. Selective targeting of c-Abl via a cryptic mitochondrial targeting signal activated by cellular redox status in leukemic and breast cancer cells. Pharm Res. 2012 Aug;29(8):2317-28.

9. Rehling P, Brandner K, Pfanner N. Mitochondrial import and the twin-pore translocase. Nat Rev Mol Cell Biol. 2004 Jul;5(7):519-30.

10. Schellenberg B, Wang P, Keeble JA, Rodriguez-Enriquez R, Walker S, Owens TW, et al. Bax exists in a dynamic equilibrium between the cytosol and mitochondria to control apoptotic priming. Mol Cell. 2013 Mar 7;49(5):959-71.

11. Edlich F, Banerjee S, Suzuki M, Cleland MM, Arnoult D, Wang C, et al. Bcl-x(L) retrotranslocates Bax from the mitochondria into the cytosol. Cell. 2011 Apr 1;145(1):104-16.

12. Willis SN, Chen L, Dewson G, Wei A, Naik E, Fletcher JI, et al. Proapoptotic Bak is sequestered by Mcl-1 and Bcl-xL, but not Bcl-2, until displaced by BH3-only proteins. Genes Dev. 2005 Jun 1;19(11):1294-305.

13. Wang X, Jiang X. Mdm2 and MdmX partner to regulate p53. FEBS Lett. 2012 May 21;586(10):1390-6.

14. Mossalam M, Matissek KJ, Okal A, Constance JE, Lim CS. Direct induction of apoptosis using an optimal mitochondrially targeted p53. Mol Pharm. 2012 May 7;9(5):1449-58.

15. Matissek KJ, Mossalam M, Okal A, Lim CS. The DNA Binding Domain of p53 Is Sufficient To Trigger a Potent Apoptotic Response at the Mitochondria. Mol Pharm. 2013 Sep 6.

16. Zhao X, Ghaffari S, Lodish H, Malashkevich VN, Kim PS. Structure of the Bcr-Abl oncoprotein oligomerization domain. Nat Struct Biol. 2002 Feb;9(2):117-20.

17. Jeffrey PD, Gorina S, Pavletich NP. Crystal structure of the tetramerization domain of the p53 tumor suppressor at 1.7 angstroms. Science. 1995 Mar 10;267(5203):1498-502.

18. Waterman MJ, Waterman JL, Halazonetis TD. An engineered four-stranded coiled coil substitutes for the tetramerization domain of wild-type p53 and alleviates transdominant inhibition by tumor-derived p53 mutants. Cancer Res. 1996 Jan 1;56(1):158-63.

19. Gully CP, Zhang F, Chen J, Yeung JA, Velazquez-Torres G, Wang E, et al. Antineoplastic effects of an Aurora B kinase inhibitor in breast cancer. Mol Cancer. 2010;9:42.

20. Zhu W, Wei L, Zhang H, Chen J, Qin X. Oncolytic adenovirus armed with IL-24 inhibits the growth of breast cancer in vitro and in vivo. J Exp Clin Cancer Res. 2012;31:51.

21. Jackson JG, Pant V, Li Q, Chang LL, Quintas-Cardama A, Garza D, et al. p53-mediated senescence impairs the apoptotic response to chemotherapy and clinical outcome in breast cancer. Cancer Cell. 2012 Jun 12;21(6):793-806.

22. Matissek KJ, Mossalam M, Okal A, Lim CS. The DNA binding domain of p53 is sufficient to trigger a potent apoptotic response at the mitochondria. Mol Pharm. 2013 Oct 7;10(10):3592-602.

23. Ferrer PE, Frederick P, Gulbis JM, Dewson G, Kluck RM. Translocation of a Bak C-terminus mutant from cytosol to mitochondria to mediate cytochrome C release: implications for Bak and Bax apoptotic function. PLoS One. 2012;7(3):e31510.

24. Chipuk JE, Kuwana T, Bouchier-Hayes L, Droin NM, Newmeyer DD, Schuler M, et al. Direct activation of Bax by p53 mediates mitochondrial membrane permeabilization and apoptosis. Science. 2004 Feb 13;303(5660):1010-4.

25. Perfettini JL, Kroemer RT, Kroemer G. Fatal liaisons of p53 with Bax and Bak. Nat Cell Biol. 2004 May;6(5):386-8.

26. Leu JI, Dumont P, Hafey M, Murphy ME, George DL. Mitochondrial p53 activates Bak and causes disruption of a Bak-Mcl1 complex. Nat Cell Biol. 2004 May;6(5):443-50.

27. Hagn F, Klein C, Demmer O, Marchenko N, Vaseva A, Moll UM, et al. BclxL changes conformation upon binding to wild-type but not mutant p53 DNA binding domain. J Biol Chem. 2010 Jan 29;285(5):3439-50.

28. Tomita Y, Marchenko N, Erster S, Nemajerova A, Dehner A, Klein C, et al. WT p53, but not tumor-derived mutants, bind to Bcl2 via the DNA binding domain and induce mitochondrial permeabilization. J Biol Chem. 2006 Mar 31;281(13):8600-6.

29. Minn AJ, Rudin CM, Boise LH, Thompson CB. Expression of bcl-xL can confer a multidrug resistance phenotype. Blood. 1995 Sep 1;86(5):1903-10.

30. Perego P, Righetti SC, Supino R, Delia D, Caserini C, Carenini N, et al. Role of apoptosis and apoptosis-related proteins in the cisplatin-resistant phenotype of human tumor cell lines. Apoptosis. 1997;2(6):540-8.

31. Reed JC. Bcl-2-family proteins and hematologic malignancies: history and future prospects. Blood. 2008 Apr 1;111(7):3322-30.

32. Yoshino T, Shiina H, Urakami S, Kikuno N, Yoneda T, Shigeno K, et al. Bcl-2 expression as a predictive marker of hormone-refractory prostate cancer treated with taxane-based chemotherapy. Clin Cancer Res. 2006 Oct 15;12(20 Pt 1):6116-24.

33. Kang MH, Reynolds CP. Bcl-2 inhibitors: targeting mitochondrial apoptotic pathways in cancer therapy. Clin Cancer Res. 2009 Feb 15;15(4):1126-32.

34. Green DR, Walczak H. Apoptosis therapy: driving cancers down the road to ruin. Nat Med. 2013 Feb;19(2):131-3.

35. Bharatham N, Chi SW, Yoon HS. Molecular basis of Bcl-X(L)-p53 interaction: insights from molecular dynamics simulations. PLoS One. 2011;6(10):e26014.

36. Okal A, Mossalam M, Matissek KJ, Dixon AS, Moos PJ, Lim CS. A chimeric p53 evades mutant p53 transdominant inhibition in cancer cells. Mol Pharm. 2013 Oct 7;10(10):3922-33.

37. Howlader N NA, Krapcho M, Garshell J, Neyman N, Altekruse SF, Kosary CL, Yu M, Ruhl J, Tatalovich Z, Cho H, Mariotto A, Lewis DR, Chen HS, Feuer EJ, Cronin KA (eds). SEER Cancer Statistics Review, 1975-2010. National Cancer Institute Bethesda, MD. 2013.

38. Lozano R, Naghavi M, Foreman K, Lim S, Shibuya K, Aboyans V, et al. Global and regional mortality from 235 causes of death for 20 age groups in 1990 and 2010: a systematic analysis for the Global Burden of Disease Study 2010. Lancet. 2012 Dec 15;380(9859):2095-128.

39. Mould T. An overview of current diagnosis and treatment in ovarian cancer. Int J Gynecol Cancer. 2012 May;22 Suppl 1:S2-4.

40. Integrated genomic analyses of ovarian carcinoma. Nature. 2011 Jun 30;474(7353):609-15.

41. Bodner SM, Minna JD, Jensen SM, D'Amico D, Carbone D, Mitsudomi T, et al. Expression of mutant p53 proteins in lung cancer correlates with the class of p53 gene mutation. Oncogene. 1992 Apr;7(4):743-9.

42. Yaginuma Y, Westphal H. Abnormal structure and expression of the p53 gene in human ovarian carcinoma cell lines. Cancer Res. 1992 Aug 1;52(15):4196-9.

43. Astanehe A, Arenillas D, Wasserman WW, Leung PC, Dunn SE, Davies BR, et al. Mechanisms underlying p53 regulation of PIK3CA transcription in ovarian surface epithelium and in ovarian cancer. J Cell Sci. 2008 Mar 1;121(Pt 5):664-74.

44. Sablina AA, Chumakov PM, Kopnin BP. Tumor suppressor p53 and its homologue p73alpha affect cell migration. J Biol Chem. 2003 Jul 25;278(30):27362-71.

45. Li M, Brooks CL, Wu-Baer F, Chen D, Baer R, Gu W. Mono- versus polyubiquitination: differential control of p53 fate by Mdm2. Science. 2003 Dec 12;302(5652):1972-5.

46. Bossi G, Mazzaro G, Porrello A, Crescenzi M, Soddu S, Sacchi A. Wild-type p53 gene transfer is not detrimental to normal cells in vivo: implications for tumor gene therapy. Oncogene. 2004 Jan 15;23(2):418-25.

47. Clayman GL, el-Naggar AK, Roth JA, Zhang WW, Goepfert H, Taylor DL, et al. In vivo molecular therapy with p53 adenovirus for microscopic residual head and neck squamous carcinoma. Cancer Res. 1995 Jan 1;55(1):1-6.

48. Wills KN, Maneval DC, Menzel P, Harris MP, Sutjipto S, Vaillancourt MT, et al. Development and characterization of recombinant adenoviruses encoding human p53 for gene therapy of cancer. Hum Gene Ther. 1994 Sep;5(9):1079-88.

49. Zhang WW, Alemany R, Wang J, Koch PE, Ordonez NG, Roth JA. Safety evaluation of Ad5CMV-p53 in vitro and in vivo. Hum Gene Ther. 1995 Feb;6(2):155-64.

50. Bao R, Connolly DC, Murphy M, Green J, Weinstein JK, Pisarcik DA, et al. Activation of cancer-specific gene expression by the survivin promoter. J Natl Cancer Inst. 2002 Apr 3;94(7):522-8.

51. Tanyi JL, Lapushin R, Eder A, Auersperg N, Tabassam FH, Roth JA, et al. Identification of tissue- and cancer-selective promoters for the introduction of genes into human ovarian cancer cells. Gynecol Oncol. 2002 Jun;85(3):451-8.

52. Bao R, Selvakumaran M, Hamilton TC. Targeted gene therapy of ovarian cancer using an ovarian-specific promoter. Gynecol Oncol. 2002 Feb;84(2):228-34.

53. Cho S, Sun Y, Soisson AP, Dodson MK, Peterson CM, Jarboe EA, et al. Characterization and evaluation of pre-clinical suitability of a syngeneic orthotopic mouse ovarian cancer model. Anticancer Res. 2013 Apr;33(4):1317-24.

54. Zeimet AG, Marth C. Why did p53 gene therapy fail in ovarian cancer? Lancet Oncol. 2003 Jul;4(7):415-22.

55. Anwer K, Kelly FJ, Chu C, Fewell JG, Lewis D, Alvarez RD. Phase I trial of a formulated IL-12 plasmid in combination with carboplatin and docetaxel chemotherapy in the treatment of platinum-sensitive recurrent ovarian cancer. Gynecol Oncol. 2013 Oct;131(1):169-73.

56. Armstrong DK, Bundy B, Wenzel L, Huang HQ, Baergen R, Lele S, et al. Intraperitoneal cisplatin and paclitaxel in ovarian cancer. N Engl J Med. 2006 Jan 5;354(1):34-43.

57. Alberts DS, Liu PY, Hannigan EV, O'Toole R, Williams SD, Young JA, et al. Intraperitoneal cisplatin plus intravenous cyclophosphamide versus intravenous cisplatin plus intravenous cyclophosphamide for stage III ovarian cancer. N Engl J Med. 1996 Dec 26;335(26):1950-5.

58. Markman M, Bundy BN, Alberts DS, Fowler JM, Clark-Pearson DL, Carson LF, et al. Phase III trial of standard-dose intravenous cisplatin plus paclitaxel versus moderately high-dose carboplatin followed by intravenous paclitaxel and intraperitoneal cisplatin in small-volume stage III ovarian carcinoma: an intergroup study of the Gynecologic Oncology Group, Southwestern Oncology Group, and Eastern Cooperative Oncology Group. J Clin Oncol. 2001 Feb 15;19(4):1001-7.

59. Fewell JG, Matar MM, Rice JS, Brunhoeber E, Slobodkin G, Pence C, et al. Treatment of disseminated ovarian cancer using nonviral interleukin-12 gene therapy delivered intraperitoneally. J Gene Med. 2009 Aug;11(8):718-28.

60. Romero I, Bast RC, Jr. Minireview: human ovarian cancer: biology, current management, and paths to personalizing therapy. Endocrinology. 2012 Apr;153(4):1593-602.

61. Reles A, Wen WH, Schmider A, Gee C, Runnebaum IB, Kilian U, et al. Correlation of p53 mutations with resistance to platinum-based chemotherapy and shortened survival in ovarian cancer. Clin Cancer Res. 2001 Oct;7(10):2984-97.

62. Matzke G R WBG PLM, editor. , editor. Pharmacotherapy: A pathophysiological Approach. 7th edition ed: Mc Graw Hhill Medical; 2008.

63. Brambilla E, Brambilla C. p53 and lung cancer. Pathol Biol (Paris). 1997 Dec;45(10):852-63.

64. Vaughan CA, Singh S, Windle B, Yeudall WA, Frum R, Grossman SR, et al. Gain-of-Function Activity of Mutant p53 in Lung Cancer through Up-Regulation of Receptor Protein Tyrosine Kinase Axl. Genes Cancer. 2012 Jul;3(7-8):491-502.

65. Okamoto H, Todo, H., Iida, K., Danjo, K. Dry powders for pulmonary delivery of peptides and proteins. Kona. 2002 71-83.

66. Bosquillon C, Preat V, Vanbever R. Pulmonary delivery of growth hormone using dry powders and visualization of its local fate in rats. J Control Release. 2004 Apr 28;96(2):233-44.

67. Takenobu T, Tomizawa K, Matsushita M, Li ST, Moriwaki A, Lu YF, et al. Development of p53 protein transduction therapy using membrane-permeable peptides and the application to oral cancer cells. Mol Cancer Ther. 2002 Oct;1(12):1043-9.

68. Brooks CL, Gu W. p53 ubiquitination: Mdm2 and beyond. Mol Cell. 2006 Feb 3;21(3):307-15.

69. Davis SS. Delivery of peptide and non-peptide drugs through the respiratory tract. Pharm Sci Technolo Today. 1999 Nov;2(11):450-6.

70. Beck-Broichsitter M, Merkel OM, Kissel T. Controlled pulmonary drug and gene delivery using polymeric nano-carriers. J Control Release. 2012 Jul 20;161(2):214-24.

71. FDA USFaDA. FDA Approves First Ever Inhaled Insulin Combination Product for Treatment of Diabetes. January 27, 2006.

72. Heinemann L. The failure of exubera: are we beating a dead horse? J Diabetes Sci Technol. 2008 May;2(3):518-29.

73. Hsia CC, Raskin P. The diabetic lung: relevance of alveolar microangiopathy for the use of inhaled insulin. Am J Med. 2005 Mar;118(3):205-11.

74. Merkel OM, Zheng M, Debus H, Kissel T. Pulmonary gene delivery using polymeric nonviral vectors. Bioconjug Chem. 2012 Jan 18;23(1):3-20.

75. Kim HW, Park IK, Cho CS, Lee KH, Beck GR, Jr., Colburn NH, et al. Aerosol delivery of glucosylated polyethylenimine/phosphatase and tensin homologue deleted on chromosome 10 complex suppresses Akt downstream pathways in the lung of K-ras null mice. Cancer Res. 2004 Nov 1;64(21):7971-6.

76. Densmore CL, Orson FM, Xu B, Kinsey BM, Waldrep JC, Hua P, et al. Aerosol delivery of robust polyethyleneimine-DNA complexes for gene therapy and genetic immunization. Mol Ther. 2000 Feb;1(2):180-8.

77. Rudolph C, Schillinger U, Ortiz A, Plank C, Golas MM, Sander B, et al. Aerosolized nanogram quantities of plasmid DNA mediate highly efficient gene delivery to mouse airway epithelium. Mol Ther. 2005 Sep;12(3):493-501.

78. Alipour S, Montaseri H, Tafaghodi M. Preparation and characterization of biodegradable paclitaxel loaded alginate microparticles for pulmonary delivery. Colloids Surf B Biointerfaces. 2010 Dec 1;81(2):521-9.

8. Appendix

8.1 Abbreviations

7-AAD	7-Aminoactinomycin D
APAF 1	Apoptotic protease-activating factor 1
BAD	BCL-2 antagonist of cell death
Bak	Bcl-2 antagonist or killer
BakMTS	MTS from Bak
Bax	Bcl-2-associated X protein
BaxMTS	MTS from Bax
Bcl-2	B cell lymphoma 2
Bcr	Breakpoint cluster region
BH	Bcl-2 homology
BID	BH3-interacting domain death agonist
BIK	BCL-2-interacting killer
BIM	BCL-2-interacting mediator of cell death
BMF	BCL-2-interacting mediator of cell death
BNIP3	adenovirus E1B 19 kDa protein-interacting protein 3
CCO	MTS from cytochrome c oxidase
CS	C-segment
DBD	DNA binding domain

E	Nuclear export signal
EMA	European Medicine Agency
FDA	Food and Drug Administration
HAUSP	Herpes virus-associated ubiquitin-specific protease
IMS	Intermembrane space
MBD	MDM2 binding domain
MDM2	Murine double minute 2
MIRA	Mutant p53-dependent induction of rapid apoptosis
MOMP	Mitochondrial outer membrane permeabilization
MTS	Mitochondrial targeting signal
NLS	Nuclear localization signal
OTC	MTS from ornithine transcarbamylase
PAM	Presequence-translocase-associated import-motor
PCC	Pearson’s correlation coefficient
PRD	Proline-rich domain
PRIMA	p53 reactivation and induction of massive apoptosis
REs	p53 response elements
RETRA	Reactivation of transcriptional reporter activity
SFDA	China’s State Food and Drug Administration
SMAC	Second mitochondrial derived activator of caspase

TA	Transactivation domain
TCA	Tricarboxylic acid
TD	Tetramerization domain
TIGAR	*TP53*-induced glycolysis and apoptosis regulator
TIM	Translocase of the inner membrane
TM	Transmembrane
TMRE	Tetramethylrhodamine, ethyl ester
TOM	MTS from translocase of the outer membrane (TOM20)
TUNEL	Terminal deoxynucleotidyl transferase dUTP nick end labeling
XIAP	X-linked inhibitor of apoptosis protein
XL	MTS from Bcl-XL

8.2 Acknowledgments

I am particularly thankful for doing my PhD in Professor Carol Lim's lab. Professor Lim is an incredible mentor, she is extremely smart, kind and carrying. She finds the best in you and inspires those around you. Professor Lim constantly encourages me to become better and she gave me complete creative and intellectual freedom so that I can do things I never thought I can do. I want to thank her so much for all the hours that she spent reviewing my papers and my thesis, for helping me to improve my presentations and for discussing new scientific ideas. On a personal level, Professor Lim always took a personal interest in my well-being. When I first arrived to Salt Lake, she let me stay in her house for a week and even gave me her car for a couple of months. When I am around her, I want to become a better scientist and a better person. She had a major impact in shaping my scientific career, and every single day I am grateful that I am in her lab. All of my scientific accomplishments are due to her support and the collaborative lab environment that she creates. I am proud to know her.

I am very grateful for having Professor Thomas Kissel as my supervisor. He was the one who initially introduced me to the University of Utah and encouraged me to apply for the GPEN program. When preparing for my GPEN time, I spend numerous hours in his office asking for his help and support. And despite his busy schedule, he never turned me down. He was always there to offer his wisdom and input. I am extremely grateful that he agreed to supervise my external dissertation at the University of Utah. I would not have done my PhD without him.

I would like to thank my supervisory committee members, Professor Roland Hartmann, Professor Maike Petersen and Professor Carsten Culmsee for scientific discussion and for reading my thesis. I would like to specifically thank Professor Hartmann for writing the evaluation of my thesis. I would like to thank especially Professor Culmsee for agreeing to be the chair of my committee and for taking time to discuss carrier development planes and my research. I am grateful to Gabriele

Lins for taking the time and effort to help me with all my graduation related questions and problems.

I also would like to thank Professor Margit Janat- Amsbury for training me on animal work and for allowing me to use her equipment in the beginning of our animal studies. A special thanks also to her students Aliyah Almomen and Chieh-Hsiang Yang for their support. I would also like to thank Robert Price for his help with the animal studies.

I would like to thank former and present members of the Lim Lab especially Mohanad Mossalam and Abood Okal for working with me as a team on the p53 project. Mohanad is one of the best teachers I ever had, special thanks to him for his patience and the time he spent with me discussing experiments. Abood and I developed the animal studies together. I am grateful that I got to work with him. His fearless and encouraging attitude made me complete scientific accomplishments I thought I might never be able to do. He was always there reviewing my papers, thesis, for scientific discussion and as a friend. I would also like to thank Ben Bruno, Johathan Constance, Rian Davis, David Woessner, Mudith Kakar, Geoff Miller and Shams Reaz for an amazing time in the Lim Lab with a lot of science talk and a tone of fun. A special thanks to Ben and Abood for all the fun we had during snowboarding. I am filled with joy that we get to work and live together.

I would also like to thank my friends Maren Thomas and Maha Mossalam for their support. Maren for answering all my questions concerning my graduation, for printing and reviewing my thesis and for always being an amazing friend. Maha for listening to my problems, for being the best roommate I can imagine and for giving me a lot of advice.

Foremost, I would like to thank my family, especially my mother. I dedicate this thesis to her. She always puts her children first. I would never be where I am today if it were not for the sacrifices she made, for her constant encouragement, for her positive and stabilizing influence and for her self-less support. I hope that I can

become half as good as a mother that she is to us. I am grateful for my grand-father, who always defended me even when I was wrong, for my grand-mother who was and is an excellent role model for independence and my father who is the most hard-working person I know. My sister Astrid for her countless visits in Salt Lake which made me feel less homesick and for making me travel with her to different places in the US. My brother Stephan who gave me emotional support through the last few months of my PhD and was always able to put a smile on my face. I am incredibly blessed by my family standing behind me every step of the way. I am thankful to God for surrounding me with all these amazing people and giving me the chance to be part of cancer research.

8.3 Declaration/Erklärung

Hiermit versichere ich, dass die vorgelegte Dissertation

“Targeting p53 and its domains for cancer therapy”

von mir selbstständig und ohne unerlaubte Hilfe angefertigt wurde und ich mich keener anderen als der von mir ausdrücklich bezeichneten Quellen und Hilfen bedient habe. Die Dissertation wurde in der jetzigen oder in ähnlicher Form noch an keiner anderen Hochschule eingereicht und hat noch keinen sonstigen Prüfungszwecken gedient.

Salt Lake City, 12. Februar 2014

Karina Matissek

Karina Julia Matissek

30 S 2000E, Suite 105
Salt Lake City, UT 84112
Phone: 801-875-7947
E-mail: Karina.Matissek@utah.edu

Education

Defense date April 7, 2014	**Dr. rer. nat. (PhD)**: "Targeting p53 and its Domains to the Mitochondria for Cancer Gene Therapy" Matriculating out of Department of Pharmaceutics and Biopharmacy, Philipps University, Marburg, Germany Conducting research at University of Utah, Salt Lake City, Utah
Oct 2009	**Master's Degree**: "Nuclear Translocation of Survivin in Breast Cancer Cells'' Martin Luther University Halle-Wittenberg, Halle, Germany
April 2009	**Pharmacy Degree** Philipps University, Marburg, Germany

Experience

Oct 2010-Present

Laboratory of Dr. Carol Lim, University of Utah
Salt Lake City, Utah
Ph.D. Candidate/ Research Assistant

- Extensive experience with recombinant DNA technology, mammalian cell transfection, adenovirus cloning and production, apoptotic assays, immunohistochemistry, flow cytometry, confocal and fluorescence microscopy
- Cell death assay expertise (7-AAD, Annexin V, TUNEL, Colony forming Assay, DNA segmentation, caspase-9 and TMRE assay)
- Human and animal cell culture proficiency (*in vitro*)
- Biosafety Level II certification pathogens (adenovirus and lentivirus)
- IUCAC animal certification to handle and work with mice (*in vivo*): orthotopic tumor generation, tumor size measurement, intratumoral injection and organ harvesting

July 2009- Oct 2010

Stadt-Apotheke Schoemberg
Schoemberg b.B., Germany
Pharmacist

- Dispensed medications to patients
- Patient consultation (drug interactions, side effects and applications)
- Advised physicians about drug interactions, dosing recommendations and side effects
- Compounded and optimized specialty medications
- Trained pharmacy personnel and managed scheduling

Publications

Peer-Reviewed Publications

First Author Publications

- **Matissek K.J.,** Okal, A., Mossalam M., Lim C.S. Delivery of a monomeric p53 subdomain with mitochondrial targeting signals from pro-apoptotic Bak or Bax, Pharm Res., minor revisions.

- **Matissek K.J.,** Mossalam M., Okal A., Lim C.S. The DNA binding domain of p53 is sufficient to trigger a potent apoptotic response at the mitochondria. Mol Pharm. 2013 Oct 7;10(10):3592-602.

- **Matissek K.J.*,** Mossalam M.*** (*co-first authors)** Okal A., Constance J.E., Lim C.S. Direct induction of apoptosis using an optimal mitochondrially targeted p53. Mol Pharm. 2012 May 7;9(5):1449-58.

- **Matissek K.J.,** Bender R.R., Davis J.R., Lim C.S. Choosing Targets for Gene Therapy in the book Targets for Gene Therapy. Intech Open Access Publisher, 2011 July, ISBN 978-953-307-540-2.

Co-Author Publications

- Okal A., Mossalam M., **Matissek K.J.,** Dixon A.S., Moos P.J., Lim C.S. A chimeric p53 evades mutant p53 transdominant inhibition in cancer cells. Mol Pharm. 2013 Oct 7;10(10):3922-33.

- Constance J.E., Woessner D.W., **Matissek K.J.,** Mossalam M., Lim C.S. Enhanced and selective killing of chronic myelogenous leukemia cells with an engineered BCR-ABL binding protein and imatinib. Mol Pharm. 2012 Nov 5;9(11):3318-29.

- Okal A., **Matissek, K.J.,** Matissek S.J., Price R., Salama M., Janát-Amsbury M.M., Lim C.S. Re-engineered p53 activates apoptosis in vivo and causes primary tumor regression in a dominant negative breast cancer xenograft model. submitted to Gene Ther. 2014 Feb 5.

- Okal A., Matissek S.J., **Matissek K.J.,** Cornillie S., Cheatham T. E. III, Lim C.S. Towards Super p53: A Re-engineered Tumor Suppressor with Enhanced Homo-oligomerization and Increased Apoptotic Activity. In preparation, 2014.

Poster Presentations

- **Matissek K.J.,** Mossalam M., Okal A, Lim C.S. Targeting Small Domains of p53 to Mitochondrial Bcl-XL for Cancer Therapy. *American Association for Pharmaceutical Science Rocky Mountain Discussion Group: Perspectives in Translational and Clinical Research;* Salt Lake City, UT, Aug 5, 2013

- **Matissek K.J.,** Mossalam M., Okal A, Lim C.S. Targeting Small Domains of p53 to Mitochondrial Bcl-XL for Cancer Therapy. *American Association for Cancer Research Annual Meeting*; Washington, DC, Apr 6-Apr 10, 2013

- Okal A., Mossalam M., **Matissek K.J.,** Lim C.S. An alternative tetramerization domain of p53 for exclusive homo-oligomerization and potent tumor suppression. *American Association for Cancer Research Annual Meeting*; Washington, DC, Apr 6-Apr 10, 2013

- **Matissek K.J.,** Mossalam M., Okal A., Constance J.E., Lim C.S. Targeting p53 to Mitochondrial Outer Memberane Using the Bcl-XL Signal Causes p53-Specific Apoptosis. *Bioscience Symposium,* Salt Lake City, UT, Sep 25, 2012

- **Matissek K.J.,** Mossalam M., Okal A., Constance J.E., Lim, C.S. Targeting p53 to Mitochondrial Outer Memberane Using the Bcl-XL Signal Causes p53-Specific Apoptosis. *American Association for Cancer Research Annual Meeting*; Chicago, IL, Mar 31-Apr 4, 2012

- Okal A., Mossalam M., **Matissek K.J.,** Lim C.S. Bypassing the Dominant-Negative Effect of Mutant p53 in Breast Cancer Cells. *American Association for Cancer Research Annual Meeting*; Chicago, IL, Mar 31-Apr 4, 2012

- **Matissek K.J.,** Mossalam M., Okal A., and Lim C.S. Direct Induction of Apoptosis Using an Optimal Mitochondrially Targeted p53. *American Association for Pharmaceutical Science*; Washington, DC, Oct 23-27, 2011. Research featured in AAPS Today: "Apoptosis of Cancer Cells Achieved by Targeting Mitochondria?"

Invited Talks

June 27, 2013	**Grand Rounds Lecture to the Department of Obstetrics and Gynecology** University of Utah, School of Medicine, Salt Lake City, UT "Re-Engineering p53 for Effective Treatment of Ovarian Cancer"
May 15, 2013	**Juan Diego High School Summer Research Program** Juan Diego High School, Salt Lake City, UT "Targeting p53 to Pro-Apoptotic Bak Causes Cell Death in Cancer Cells"
Aug 27, 2012	**PHCEU Fall 2012 Seminar Series** University of Utah, College of Pharmacy, Salt Lake City, UT "Mitochondrial Targeting of p53 for Cancer Therapy"
Oct 26, 2009	**Master's Thesis Defense** Martin Luther University Halle-Wittenberg, Halle, Germany "Nuclear Translocation of Survivin in Breast Cancer Cells''

Mentoring

Nov- Dec 2013	**Phong Lu,** graduate student Biological Chemistry Program, University of Utah "Introducing E34K and R55E mutations in p53-CC for breast cancer therapy"
Aug- Oct 2013	**Jennifer Gläsel**, pharmacy student Globalization of Pharmaceutics Education Network (GPEN) Program, Philipps University of Marburg "Targeted Mutations in p53-CC for Ovarian Cancer Therapy''
June-July 2013	**Connor Helgeson**, high school student Juan Diego High School Summer Research Program, Juan Diego High School "Targeting p53 to Pro-Apoptotic Bak Causes Cell Death in Cancer Cells''
Oct 2012- April 2013	**Christian Raab**, pharmacy student Globalization of Pharmaceutics Education Network (GPEN) Program, Philipps University of Marburg "Targeting p53 to Bak and Bax''
April- Aug 2012	**Russell Scow**, pharmacy student PSURF Program University of Utah College of Pharmacy "Targeted Mutations in p53 Enhance Cancer Cell Apoptosis''
Jan - April 2012	**Karen Johnson**, undergraduate researcher ACCESS Program for Women in Science and Mathematics, University of Utah "Residues C176 and N239 are essential for mitochondrial activity of p53''
June -July 2011	**Alex Ikeda**, high school student Juan Diego High School Summer Research Program, Juan Diego High School "Targeting Domains of p53 to the Mitochondria for Cancer Therapy''
Jan - April 2011	**Maha Mossalam**, undergraduate researcher Department of Biology, University of Utah "Targeted Mutations in Mitochondrial p53''

Memberships

Jan 2012- present	Cofounder and member of GSO/GAIN German Table Salt Lake City, Utah
Oct 2010- present	Associate member of American Association of Pharmaceutical Scientists
Oct 201- present	Associate member of American Association for Cancer Research

Internships

Nov 2008- April 2009	**Pharmacy Intern** Eyach Apotheke (pharmacy), Balingen, Germany
April- Oct 2008	**Research Assistant** Department of Pharmaceutics and Pharmaceutical Chemistry, University of Utah, Salt Lake City, Utah

Karina Julia Matissek

March 2005	**Pharmacy Intern** Klinikum am Steinenberg (hospital), Reutlingen, Germany
August 2004	**Pharmacy Intern** Eyach-Apotheke (pharmacy), Balingen, Germany

Language

English, full professional proficiency
German, native
Polish, native
French, basic

References

Carol Sunai Lim, Ph.D.	Associate Professor University of Utah, College of Pharmacy Department of Pharmaceutics and Pharmaceutical Chemistry 30S 2000E Rm 2916, Salt Lake City, 84112, Utah, USA carol.lim@pharm.utah.edu
Prof. Dr. Thomas Kissel	Professor Philipps-Universität Marburg, Faculty of Pharmacy Department of Pharmaceutics and Biopharmacy, Ketzerbach 63, 35037 Marburg, Germany kissel@mailer.uni-marburg.de
Margit-Maria Janat-Amsbury, M.D., Ph.D.	Assistant Professor University of Utah, School of Medicine Department of Obstetrics and Gynecology 30 North 1900 East, Suite 2A200, Office 2A242, Salt Lake City, Utah, 84132, USA margit.janat-amsbury@hsc.utah.edu

1

Choosing Targets for Gene Therapy

Karina J. Matissek, Ruben R. Bender,
James R. Davis and Carol S. Lim
University of Utah
USA

1. Introduction

Gene therapy is often attempted in fatal diseases with no known cure, or after standard therapies have failed. Targeting gene defects includes addressing a single mutation, multiple mutations in several genes, or even addressing missing or extra copies in a particular disease. A defect in one specific gene may impair normal function of the corresponding expressed protein. For example, in X-linked severe combined immunodeficiency (X-SCID), there is a mutation in the IL2 receptor γ gene. Another classic example occurs in thalassemia propagated by a defect in the β-globulin gene. Some diseases are caused by multiple mutations in several genes. For example, some cardiovascular diseases may manifest due to mutations in different chromosomes which are a result of inherited or environmental factors. Before approaching a disease using gene therapy, the key protein(s) and pathways involved in the disease should first be identified. However, in some cases an abnormal gene is formed that results in disease; such is the case for the Bcr-Abl gene. The oncogenic Bcr-Abl protein is the causative agent of chronic myelogenous leukemia (CML) which could be blocked for CML treatment. Genomic sequencing information, microarrays, and biochemical assays can be used to determine up- or down-regulated proteins involved in disease, and will help determine the function of these proteins. In the case of some cancers, the signal transduction pathways for oncogenesis have been mapped out, allowing hub proteins to be identified. Hub proteins are essential proteins that interact with multiple other proteins in signaling cascades. If selected properly, adding back a tumor-suppressing hub protein (such as p53), or blocking an oncogenic hub protein (such as survivin) could halt cancer or alter disease progression. Gene mutations can result in mislocalization of these key proteins which can cause cancer; this mislocalization can be exploited with gene therapy approaches. Further, new types of gene therapy are being developed in our lab to direct proteins to other cellular compartments where their function is altered. This chapter will summarize these and other known targets and also focus on choosing newer targets for gene therapy.

2. Known targets for gene therapy

The general aim of gene therapy is to introduce a well-defined DNA sequence into specific cells. Almost any disease can be targeted with gene therapy by replacing defective genes or imparting a new function. In fact, 85% of clinical trials in gene therapy have been conducted for cancer, cardiovascular diseases and for inherited monogenic diseases. In addition, 6.5%

of clinical trials have been conducted for infectious diseases (mainly HIV). Cancer, cardiovascular diseases and HIV are ideal gene therapy targets because of their enormous prevalence and the associated fatal consequences of these diseases, whereas monogenic disorders reflect the original idea of gene therapy which is replacement of a defective gene. Gene therapy offers a unique opportunity to cure patients with monogenic disorders. One third of clinical trials for monogenic disorders are for cystic fibrosis while about 20% are for SCID (Edelstein et al. 2004). This section highlights the advantages of gene therapy for multifactorial diseases such as cancer, vascular diseases, and HIV and describes the utility of gene therapy for monogenic diseases such as cystic fibrosis, SCID and β-thalassemia.

2.1 Cancer

Cancer was responsible for 7.6 million deaths in 2008 (WHO 2011) and is the largest target for gene therapy clinical trials. The complexity of cancer may make it difficult to bring a product to the market due to the number of genes involved compared to monogenetic disorders. However, gene therapeutics are not designed to correct these mutations by adding an enormous amount of DNA to the cells. Instead, they target critical proteins involved in signaling cascades such as the tumor suppressor p53. For example, the first gene therapy product was Gendicine™, an adenovirus containing the tumor suppressor p53.

The tumor suppressor p53 is mutated in 40% of many types of cancers, and malfunction of p53 is the major contributor for chemotherapy resistance (Goh et al. 2011). Apoptosis can be triggered by transcriptionally active p53 in the nucleus (Taha et al. 2004) as well as by p53-mediated transcriptionally independent mechanisms in the mitochondria (Vaseva et al. 2009). Various animal studies have shown that p53 induces apoptosis even in advanced tumors such as lymphoma and hepatocellular carcinoma (Ventura et al. 2007; Palacios & Moll 2006; Xue et al. 2007).

The first p53 based gene therapy in humans was conducted in 1996. This trial used a retroviral vector containing wild type p53 with an actin promoter for the treatment of non-small cell lung carcinoma. In this study three patients showed tumor regression and three other patients showed tumor growth stabilization (Roth et al. 1996). China was the first country which approved a p53 adenovirus for gene therapy, Gendicine™ SiBiono, in combination with radiotherapy for head and neck squamous cell cancer in 2004 (Shi & Zheng 2009). Gendicine™ is a recombinant serotype 5 adenovirus with the E1 region replaced by the p53 expressing cassette (with a Rous sarcoma virus promoter). The adenovirus particles infect tumor target cells carrying therapeutic p53 (Peng 2005). Clinical trials for Gendicine™ showed that in combination with radiation therapy it caused partial or complete tumor regression (Peng 2005; Xin 2006). There were also some clinical trials for Gendicine™ in advanced liver cancer, lung cancer and other advanced solid tumors (Peng 2005). It should be kept in mind that China's State Food and Drug Administration (SFDA) has different standards for the approval of a cancer drug compared to the U.S. FDA and the European Medicine Agency (EMA). Gendicine™ was approved in China on the basis of tumor shrinkage. The U.S. FDA and the EMA require novel cancer drugs to extend the lifetime of the treated patients (Guo & Xin 2006).

Another p53 product is Oncorine™ from Shanghai SunwayBiotech, an oncolytic virus. Oncorine™ was approved for the treatment of head and neck cancer in China in 2006 (Yu & Fang 2007). It is a replicative adenovirus 2/adenovirus 5 hybrid with deletion in E1B55K and E3B (Raty et al. 2008). This oncolytic virus was expected to infect and lyse cancer cells only and not affect normal cells (Guo et al. 2008). Even though clinical studies showed that it

was not specific for cancer cells, it did, however, kill tumor cells preferentially (Garber 2006). Phase I/II trials showed little dose-limiting toxicity (Lockley et al. 2006) and the combination of Oncorine™ with chemotherapy showed greater tumor shrinkage in patients with head and neck cancer, compared to chemotherapy alone. It should be kept in mind that like Gendicine™, Oncorine™ was also approved by the SFDA based on objective response rate, not on survival (Garber 2006). Nevertheless, all the available data concerning p53 and its proven function as tumor suppressor qualifies it as an adjuvant treatment with radiotherapy or chemotherapy.

Another approach to cancer gene therapy is gene-directed enzyme prodrug therapy (GDEPT). GDEPT transfers an activating transgene into tumor cells followed by systemic treatment with a non-toxic drug which becomes activated only in cells expressing the transgene. Cerepro® is an adenovirus containing a herpes simplex type-1 thymidine kinase transgene under the cytomegalovirus promoter. Cerepro® is under phase I, II and III clinical trials in Europe for malignant glioma, a fatal form of brain cancer. In these clinical trials Cerepro® was injected multiple times into healthy brain tissues of patients following surgical removal of the solid tumor mass. Then the patients were treated with the prodrug ganciclovir, which is converted to its toxic form, deoxyguanosine, by thymidine kinase. This toxic metabolite affects newly dividing cells, thus it prevents new tumors from growing. In phase I and II trials, patients given Cerepro® showed a significant increase in survival. However, after phase III studies, the EMA rejected the marketing application for Cerepro® due to inadequate efficacy (van Putten et al. 2010; Cerepro 2009; Mitchell 2010; Raty et al. 2008). Despite this particular failure, systemic side effects are avoided with the GDEPT concept. The general goal of GDEPT is the improvement of chemotherapy in terms of safety and efficiency using concomitant gene therapy (Edelstein et al. 2004).

2.2 Cardiovascular diseases

Cardiovascular diseases (CVD) encompass disorders of the heart and blood vessels and include hypertension, coronary heart disease, cerebrovascular disease, peripheral vascular disease, heart failure, rheumatic heart disease, congenital heart disease and cardiomyopathies (Chiuve et al. 2006). Cardiovascular diseases are the largest health problem worldwide, claiming 17.1 million lives per year. Despite the complexity of cardiovascular disease, there is great potential for gene therapy especially in ischemia, angiogenesis, hypertension and hypercholesterolemia. Currently there is no gene therapy product on the market for CVD. Nevertheless, several clinical trials have been conducted (Edelstein et al. 2004; Edelstein et al. 2007). Most gene therapies for CVD aim to increase angiogenesis which is a mechanism to overcome ischemia. Ischemia is a condition in which the flow of blood is restricted to parts of the body. The response of the body is to form new blood vessels around the blockage, called angiogenesis, and is triggered by angiogenic proteins such as vascular endothelial growth factor (VEGF), fibroblast growth factor (FGF) and hepatocyte growth factor (HGF) (Abo-Auda & Benza 2003; Kass et al. 1992). The goal of introducing genes coding for these growth factors is to increase the local concentration of these factors to stimulate angiogenesis (Edelstein et al. 2004). Two companies are conducting phase III clinical trials using FGF. Bayer Schering Pharm AG has developed alferminogene tadenovec, which is a replication-deficient human adenovirus serotype 5 which encodes human FGF4. Since myocardial ischemia is linked to coronary artery disease, the therapeutic goal is to improve the reperfusion of ischemic myocardium. Phase IIb/III clinical trials showed that it is well-tolerated; a phase III trial is ongoing to prove its efficacy (Flynn &

O'Brien 2008; CardioVascular BioTherapeutics). Sanofi-Aventis is developing a FGF gene therapy product called riferminogene pecaplasmide or NV1FGF (Riferminogene pecaplasmide 2010). It is a novel pCOR (conditional origin of replication) plasmid-based gene delivery system (Maulik 2009). NV1FGF is injected into muscle cells, and expresses FGF-1. The therapeutic goal is to treat chronic/critical limb ischemia since limb ischemia is linked to peripheral artery disease (Baumgartner et al. 2009). Phase III clinical trials are ongoing in 32 countries (Riferminogene pecaplasmide 2010).
Another gene therapy approach to treat limb ischemia uses HGF. There are several animal studies showing that HGF can trigger formation of new blood vessels (Shigematsu et al. 2010). The injection of the naked HGF gene is well-tolerated as shown in the first clinical trial conducted in Japan (Morishita et al. 2004). Another clinical trial in the U.S. showed that HGF injection increased tissue perfusion compared to placebo (Powell et al. 2008). Lastly, there is also a clinical trial to prove efficacy of HGF gene therapy, using reduction of ulcer size and decrease in rest pain (pain occurring during sleep) as objectives (Shigematsu et al. 2010).

2.3 HIV

The human immunodeficiency virus (HIV) causes acquired immunodeficiency syndrome (AIDS), a severe disease characterized by profound negative effects on the immune system leading to life-threatening opportunistic infections. Although antiretroviral drugs have decreased the morbidity and mortality of HIV infected patients, currently there is no cure. However, new developments in gene therapy have focused on introducing genes encoding RNA or proteins which are capable of interfering with intracellular replication of HIV, so-called intracellular immunization. So far, the approaches range from protein-based strategies such as fusion inhibitors or zinc finger nucleases to RNA-based approaches such as ribozymes, antisense or short hairpin RNA. Currently, a promising target is the chemokine receptor 5 (CCR5) which is needed for fusion of HIV with immune cells. Studies have shown that patients with mutated CCR5 have a higher long-term survival and slower progression of the disease. A homozygous defect in the CCR5 gene, a Δ32 deletion, resulting in a lack of functional CCR5 protein and confers resistance to HIV infection (Liu et al. 1996). An allogeneic stem-cell transplantation of CCR5 defective cells in a patient with HIV infection and acute myeloid leukemia resulted in both a negative HIV plasma viral load and no detection of HIV proviral DNA for more than 3.5 years after treatment (without the use of antiviral drugs). This result has been classified as a cure of HIV (Kitchen et al. 2011, and references therein; Symonds et al. 2010, and references therein).

2.4 Monogenic diseases

Monogenic diseases are prime targets for gene therapy due to their simple single gene mutations. Their disease causing mechanisms are easier to elucidate which is advantageous for choosing a target for gene therapy. In addition, the execution of therapy is more straightforward, since it is easier to transfer single genes into cells instead of several genes. Other important factors are the location and the type of cell in which the gene has to be transferred. Is the cell reachable with existing delivery systems? Is the cell already differentiated or is it a still dividing stem cell? Does gene transfer need to be repeated or is a one-time transfer sufficient? All these questions have to be considered in order to choose the right target for gene therapy, and it must be noted that not every disease caused by single gene mutations can be targeted. Three examples of well-studied diseases and attempts to treat these diseases using gene therapy will be discussed.

2.4.1 Cystic fibrosis

Cystic fibrosis (CF) is a complex inherited disease affecting the lungs and digestive system. The cause of this disease is a defect in the cystic fibrosis transmembrane conductance regulator (CFTR), which is a chloride channel on the apical membrane of respiratory epithelia. This leads to reduced Cl^- and increased Na^+ permeability (Boucher et al. 1988). CF is caused by several different mutations in the CFTR gene located on chromosome 7 (Knowlton et al. 1985). Of the hundreds of mutations that cause CF, the most common mutation, which occurs in approximately 70% of all cases, is the deletion of a phenylalanine residue at amino acid position 508 (ΔF508) (Kerem et al. 1989). CF results in decreased production of pancreatic enzymes leading to malnutrition, and also blocks the lung with unusually viscous mucus leading to life-threatening infections (Cystic Fibrosis Foundation; Wood 1997). It is possible to treat symptoms of CF to improve quality of life but there is no current cure for this disease. Mainstays for symptomatic treatment include enzymatic therapies (pancreatic enzymes and DNAse I) (McPhail et al. 2008), airway clearance and hypertonic saline for improved lung function, use of drugs that enhance Cl^- secretion in airway epithelium (Cloutier et al. 1990) and anti-inflammatories involving ibuprofen or corticosteroids (Flume et al. 2010, and references therein). Despite a clear understanding of genetic links, gene therapy is not yet a standard treatment for CF, as recent attempts to cure patients with CF have not been successful. Moss et al. showed improvement in pulmonary function in a phase II clinical trial with 42 CF patients, of whom 20 received at least one dose of aerosolized adeno-associated serotype 2 virus carrying the CFTR gene. A significant enhancement in FEV_1 (forced expiratory volume per second) was noted after 30 days compared to placebo. Furthermore, this study showed no adverse events demonstrating the safety of adeno-associated vectors (Moss et al. 2004). However, when this same group performed a second, larger phase IIb trial with 102 subjects, there was no significant improvement in FEV1 seen after 30 days compared with placebo (Moss et al. 2007). Expression of CFTR was noted in airway epithelium of 7 individuals with CF after the first administration but the effect lasted only 30 days. The second administration showed decreased expression. Finally, at the third administration, the expression fell to zero (Harvey et al. 1999). In conclusion, there is some indication that gene therapy could be used to cure CF, but no method has shown to be universally applicable. Further research is needed to find the right vector with repeatable administration and subsequent high expression while simultaneously being safe. Gene therapy for CF targets epithelial cells which have a limited life span and do not divide. Because of that, the gene has to be transferred repeatedly into new growing cells, which is problematic since repeated transfections have been ineffective.

2.4.2 Severe combined immunodeficiency

Severe combined immunodeficiency (SCID) is a rare, fatal syndrome with an incidence of 24.3 cases per million live births (Ryser et al. 1988). The disease is characterized clinically by defects in humoral and cellular immunity due to profound deficiencies of T-and B-cell function, and if left untreated usually leads to death in infancy (Buckley et al. 1997). Mutations leading to SCID appear in various genes including Jak-3, adenosine deaminase, IL-7 receptor (Puel et al. 1998), tyrosine phosphatase CD45 (Kung et al. 2000), the interleukin-2 (IL-2) receptor γ chain (IL2-Rγ), the Artemis gene (Kobayashi et al. 2003) and recombinase activating genes 1 or 2 (Schwarz et al. 1996; Buckley et al. 1997, and references therein). The most frequently diagnosed form of SCID is X-SCID, which is characterized by a mutation in the IL2-Rγ gene located on the X chromosome. This disease shows a male

predominance, with a mean age of diagnosis of 6.6 months. The IL2-Rγ chain is a critical component of many cytokine receptors including those for IL-2, -4, -7, -9, -15 and 21, where defects may result in greatly decreased numbers of T and NK cells. The number of B cells is generally normal but their activity is abnormal (Buckley et al. 1997). After maternal antibodies have vanished, the extreme susceptibility to infection due to opportunistic microbes, persistent diarrhea and failure to thrive usually lead to death in the first year of life unless immunologic reconstruction can be achieved.

Hematopoietic stem cell transplantation is the standard of care for all genetic types of SCID with a survival rate of nearly 80% with HLA-identical parental marrow (Antoine et al. 2003). Even with a matched donor, stem cell transplantation may lead to long-term clinical complications (De Ravin & Malech 2009). Thus, other treatments for SCID are needed. An ex vivo gene therapy trial with two X-SCID patients, aged 8 and 11 months, demonstrated that gene therapy has curative potential. Administration of a retroviral vector containing the correct IL2-Rγ gene resulted in T cell counts similar to that of age-matched controls after 105 days. Furthermore, the immune system responded to tetanus toxin and polioviruses within the normal range after primary vaccination. Both patients later showed normal growth and psychomotor development (Cavazzana-Calvo et al. 2000). Other studies confirmed these results (Hacein-Bey-Abina et al. 2002; Thrasher et al. 2005). A separate study of gene therapy for X-SCID with children aged 2.5, 4 and 8 years old showed mixed results. Only the youngest patient experienced benefit from the treatment (Chinen et al. 2007). Another trial with two patients, aged 15 and 20 years old also failed (Thrasher et al. 2005). Despite the variable outcome from these studies, gene therapy may still potentially cure X-SCID and other SCIDs, in particular for younger patients. It is already possible to cure newborn children with this modern technique, if traditional methods like BMT fail. If the safety of gene therapy vectors can be improved to lower the risk of insertional mutagenesis, gene therapy will likely become first-line therapy for to the treatment of X-SCID. In contrast to CF, the presence of accessible stem cells in which the functional gene could be transferred would allow continuous expression of this gene, making X-SCID a good candidate for gene therapy.

2.4.3 β–thalassemia

β–thalassemia syndromes are a group of inherited blood disorders. Thalassemia major is the only transfusion-dependent type of β-thalassemia and manifests itself clinically between 6 and 24 months of life by paleness and failure to thrive. It is marked by reduced (β^+) or absent (β^0) beta globin chain synthesis caused by several different single gene mutations, resulting in reduced hemoglobin in red blood cells (Weatherall 1976). If left untreated, this disease results in growth retardation, pallor, jaundice, poorly developed musculature, skeletal changes and other consequences leading to death during infancy (Cao & Galanello 2010). Blood transfusion is the current standard therapy for β–thalassamia and aims to correct the anemia from reduced hemoglobin (Cao & Galanello 2010). This treatment, however, carries the risk of infection from blood borne diseases such as HIV and hepatitis and as well as the serious side effect of transfusional iron overload which is fatal if untreated. Currently, BMT offers the best chance for curing β-thalassemia in both in children and adults if a HLA identical donor is found, but is limited by complications like graft-versus-host disease or finding suitable donors (Lucarelli & Gaziev 2008).

Gene therapy of human β-thalassemia is still in its infancy and requires the development of efficient, safe and high level gene transfer into target hematopoietic stem cells. It also requires regulation of erythroid lineage-specific expression and therapeutic levels of β-globin expression (Malik & Arumugam 2005). Meeting these requirements may be difficult, but a successful gene therapy trial was achieved in 2007 when an 18 year-old patient was effectively treated using a β-globin-expressing lentiviral vector. The vector was transfected ex vivo into harvested $CD34^+$ cells and then transplanted back into the patient's bone marrow. The patient, who had no HLA-matched donors (making BMT impossible), was treated with high dose chemotherapy with intravenous busulfan to eliminate defective hematopoetic stem cells (HSC) prior to transplantation. This step was critical for the success of this treatment to prevent the defective HSC from diluting the corrected HSC. Three years post-transplant this patient no longer required blood transfusions and showed stable hemoglobin levels. However, mild anemia, compensatory expansion of red-blood-cell precursors in bone marrow, and other safety concerns have been raised (including development of cancers) (Cavazzana-Calvo et al. 2010). Although the long-term prognosis and outcome of gene therapy for β-thalassemia is currently unclear, it still has the same advantage of the presence of accessible stem cells as X-SCID. With this in mind, targeting stem cells may be more successful than differentiated cells, and may be sufficient to cure the disease.

3. Identifying novel targets for gene therapy

Before targeting a disease with gene therapy, the genetic basis of that disease should be identified. Strategies for finding disease genes have greatly improved in the last few years due to the Human Genome Project and the Hap Map Project. The Hap Map Project identifies and catalogs genetic similarities and differences in humans (Human Genome Project; The International Hap Map Consortium 2003) and supplies computerized databases to search through and identify new gene therapy targets (Hap Map Project 2003). To find genes the two most common options are candidate-gene studies and genome-wide studies. Candidate-gene association studies are based on prior biological knowledge of gene function or on significant findings in linkage studies. This method is based on a single polymorphism and haplotypes and compares allele or haplotype frequencies between the case and the control group. Genome-wide studies can be divided into linkage mapping and genome-wide association studies. Genetic linkage mapping studies are used to discover and identify new genes by using genetic and phenotypic data from families. The analysis is conducted without any prior knowledge about genetic basis of disease. Linkage analysis functions by comparing genotype polymorphic markers at known locations in the genome. Genome-wide association studies are the most recent technology. They search the whole genome for single nucleotide polymorphisms (SNPs). Each study can look at hundreds or thousands of SNPs at the same time (for an excellent review see (Hirschhorn & Daly 2005)). The results are plotted into biostatistics algorithms (Nakamura 2009; Hirschhorn & Daly 2005). The proteins identified by genomic methods can be further characterized by standard molecular and biochemical assays. In addition, protein targets have been identified by individual labs using standard molecular and biochemical methods without a priori use of genomic information. With the growing understanding of genes associated with many diseases the future for new gene therapeutics shows promise.

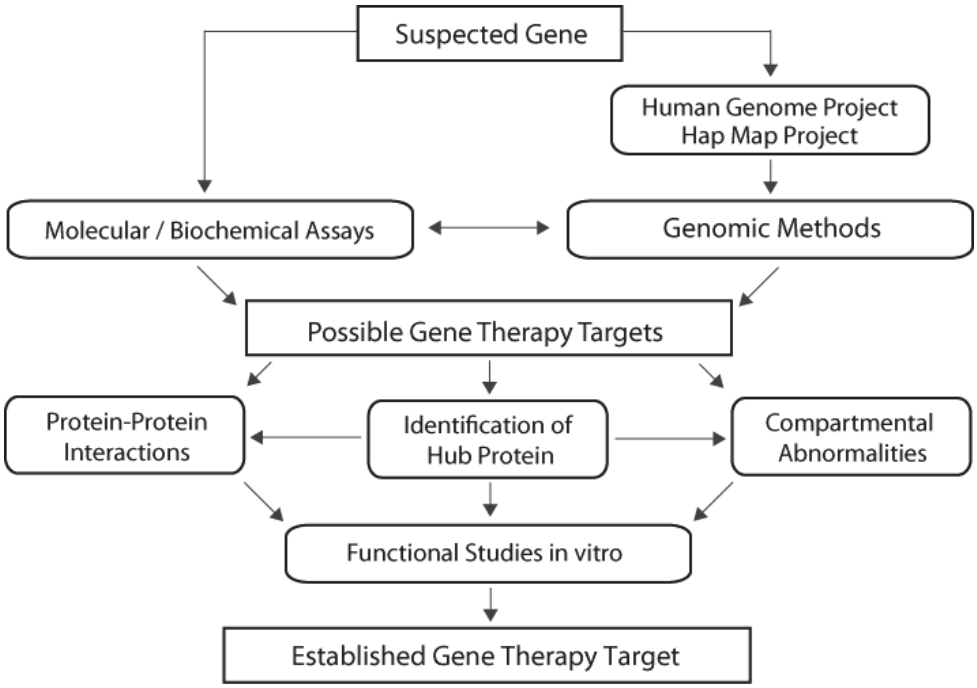

Fig. 1. Finding Novel Gene Therapy Targets. Integration of standard and modern technologies for disease-causing targets for gene therapy.

3.1 Methods to find gene therapy targets

Microarrays lay the groundwork for the methods mentioned above. The two most important advantages of microarrays are their small scale (multi-well plate formats) and ability to detect thousands of different immobilized genes simultaneously (Duggan et al. 1999; Siegmund et al. 2003; NCBI 2007). There are three types of microarray technologies: comparative genomic hybridization, expression analysis and mutation/polymorphism analysis, though the principle remains the same for all. First, the DNA chip corresponding to the DNA of interest is selected. Then, isolated messenger RNA (mRNA) is used as a template to generate complementary DNA (cDNA), with a fluorescent tag. This mixture is incubated with the DNA chip. During this incubation, tagged cDNA can specifically bind to the complementary DNA template on the chip. Afterwards, the hybridized cDNA can be detected with lasers specific to different fluorophores followed by analysis using computational methods (NCBI 2007).

The Human Genome Project and the HapMap project have provided the foundation for candidate gene and genome-wide studies. Using these methods may allow us to draw conclusions between gene abnormalities and diseases. For example, many different studies have been conducted to determine the genes associated with cardiovascular diseases. In fact many CVDs are linked to mutated genes. For example, there is evidence based on genetic linkage analysis that chromosomes 1, 2, 3, 13, 14, 16 and X are involved in myocardial infarction, which is the major killer world-wide. Additionally, myocardial infarction and

stroke are associated with mutations in chromosome 13q12-13 containing the ALOX5AP gene encoding arachidonate 5-lipoxygenase-activating protein. Furthermore, high LDL, low HDL and high triglycerides values are high risk factors for cardiovascular disease, with linkage results located in all autosomes except for 2 and 14 (Arnett et al. 2007, and references therein).

Finding disease-causing genes may not only help to better understand the pathophysiology of the disease, but may improve the diagnosis of the disease by discovery of disease-specific marker genes. Importantly, identification of disease-causing genes will lead to new targets for improved therapeutics. Genome-wide association studies which scan markers across the entire genome can find single mutations causing monogenic disorders as well as different mutations in several genes, which may lead to more gene therapy-based cures for these diseases.

3.2 Hub proteins

Genomic sequencing information, microarrays, and molecular/biochemical assays are tools that can help determine which proteins are responsible for disease. This information can be analyzed to identify hub proteins involved in disease progression. Hub proteins are key proteins that signal to multiple other proteins in transduction cascades. They are highly connected to other proteins with multiple interaction partners. Hub proteins bind with several distinct binding sites to other proteins. Studying the binding interface of cancer-related proteins maybe useful for better understanding of cellular function and biological processes (Keskin & Nussinov 2007; Kim et al. 2006).

3.2.1 Tumor suppressor hub proteins

3.2.1.1 p53

The tumor suppressor p53 is an example of a hub protein involved in cancer which loses the ability to bind different other proteins due to mutations (Shiraishi et al. 2004). It induces transactivation of target genes which are responsible for cell cycle arrest, DNA repair and apoptosis. p53 is mutated in 40% of cancers (Goh et al. 2010). In normal, healthy cells p53 is rapidly degraded via the MDM2 pathway, but when stress signals occur, p53 accumulates dramatically in the cell, allowing it to accomplish its apoptotic functions. p53 stimulates multiple signaling mechanisms which lead to apoptosis: the extrinsic pathway through death receptors and the intrinsic pathway through the mitochondria (Haupt et al. 2003). As a transcription factor it binds to p53-responsive genes, and the expressed proteins trigger apoptosis, G1 arrest, as well as DNA repair through different mechanisms. In addition, p53 translocates to the mitochondria and induces a rapid apoptotic response (Erster et al. 2004; Haupt et al. 2003). Consequently, p53 fulfills the requirements for an ideal hub protein for gene therapy. Indeed, p53 adenovirus has been used for cancer therapy, and was the first gene therapeutic on the market.

3.2.1.2 BRCA1 and BRCA2

Breast cancer susceptibility protein (BRCA)1 and BRCA2 are highly associated with breast and ovarian cancer. The lifetime risk of developing breast cancer for a person carrying mutations in both genes is 82%; mutations in BRCA1 account for 52% and BRCA2 for 23% of all cases. Furthermore, the risk for ovarian cancer is dramatically increased due to mutations in BRCA1 and/or BRCA2. Thus, it is important to identify patients with a probability of

having mutations in these proteins. BRCA1 and BRCA2 regulate cell cycle progression, DNA repair and gene transcription (Metcalfe et al. 2005). Their export into the cytoplasm is associated with apoptosis. In cooperation with cellular partner BARD1 (BRCA1-associated RING domain protein), BRCA1 is able to enter the nucleus and accomplish its role in DNA repair, centrosome regulation and RNA processing (Henderson 2005; Rodriguez et al. 2004). When the sensitive balance between BARD1 and BRCA1 is defective due to cancer-promoting mutations in both, they remain as a dimer which results in nuclear compartmentalization leading to dramatic reduction of their apoptotic activity (Davis et al. 2007; Rodriguez et al. 2004). Silencing BRCA1 expression using RNA-mediated interference, results in increased cytoplasmic levels of BARD1 and causes apoptosis in breast cancer cell lines (Rodriguez et al. 2004). BARD1 translocates to the mitochondria and causes oligomerization of Bax which results in apoptosis (Tembe & Henderson 2007). Therefore, targeting BRCA1 is a viable gene therapy-based approach.

3.2.2 Hub proteins that promote cancer

3.2.2.1 Survivin

In addition to adding back hub tumor suppressors for gene therapy, oncogenic hub proteins can be blocked as well. The oncogene survivin is nearly universally expressed in various types of cancer and is almost undetectable in most adult tissue. Survivin is a unique member of the inhibitor of apoptosis protein (IAP) family and plays a major role as a mitotic regulator (Altieri 2001, and references therein). It is involved in multiple cancer-promoting mechanisms, particularly inhibition of apoptosis. Various parallel pathways, such as intervention in mitochondrial function, inhibition of caspases, and influence on gene expression are responsible for survivin's anti-apoptotic function (Altieri 2008, and references therein). For example, survivin and its binding partners act to prevent caspase activation; activated caspase 9 is required to activate effector caspase 3 and caspase 7, which execute mitochondrial-induced apoptosis (Li & Yuan 2008). Also, a splice variant of survivin, survivin ΔEx-3, translocates to the mitochondria where it interacts with proteins from the Bcl-2 family. These proteins are inhibitors of permeabilization of the mitochondrial outer membrane which is essential for cytochrome c release. Stabilization of Bcl-2 proteins prevents cytochrome c release, thus resulting in the inhibition of caspase 9 and caspase 3 (Altieri 2008, and references therein). Furthermore, survivin's role as a mitotic regulator is related to its inhibition of apoptosis. Survivin expression is upregulated at the G2/M phase to localize to the mitotic apparatus and is downregulated in interphase via ubiquitin-dependent destruction (Li, Ambrosini, et al. 1998; Zhao et al. 2000). High survivin expression was detected in various types of cancers including breast, lung, colon, stomach, esophagus, pancreas, uterus, ovary and liver (Altieri 2008, and references therein). Dramatic overexpression of survivin correlates with more aggressive and invasive clinical phenotypes which means a poor prognosis compared to survivin-negative tumors, an increased rate of recurrence and chemotherapy resistance (Kato et al. 2001; Grossman & Altieri 2001). The differential expression and function of survivin make it an excellent target for cancer therapy (Altieri 2003). There are many gene-based strategies to inhibit survivin in cancer cells, with some in phase I and II clinical trials. One gene-based method uses survivin antisense oligonucleotides to prevent expression in cancer cells. Two phase II trials and one phase I trial by Eli Lilly and Co. are ongoing for relapsed or refractory acute myeloid leukemia, hormone refractory prostate cancer and advanced hepatocellular carcinoma (Ryan

et al. 2009). Furthermore, Alteri et al. created a replication-deficient adenovirus containing a dominant negative survivin mutant where threonine 34 is mutated to alanine. This mutation abrogates phosphorylation of threonine which impairs survivin's ability act as a mitotic regulator, as only phosphorylated survivin is able to localize to the mitotic apparatus (O'Connor et al. 2000). Injection of adenovirus containing survivin mutant triggers apoptosis by cytochrome c release which leads to caspase 3 activation. Alteri et al. demonstrated in several cancer cell lines that this mutant causes apoptosis and confirmed these results in three xenograft breast cancer mice models. Interestingly, this survivin mutant was not able to cause apoptosis in proliferating normal human cells (Mesri et al. 2001).

3.2.2.2 Ras

The RAS supergene family is divided into six subfamilies RAS, RHO, RAB, ARF, RAN and RAD which code for more than 50 structurally related proteins. Their main function is to transmit signals from cell-surface receptors to the cell interior. All proteins have a guanosine triphosphate (GTP) binding motif in common and participate in signaling cascades. The RAS subfamily functions in proliferation and differentiation which makes it a prime target for anti-cancer therapy. The localization of Ras on the cell membrane, and binding to GTP are essential for its function. When Ras binds to GTP, it initiates the signaling pathway for cell proliferation and differentiation. However, when Ras-GTP is hydrolyzed to Ras-GDP by GTPase-activating proteins (GAPs), it is unable to activate its signal transduction pathway. This sensitive regulation process is out of balance in cancer cells due to different mutations in the RAS gene. Most of these mutations occur in the Ras gene itself and in the regulatory proteins of the Ras pathway. These mutations cause Ras to stay in the active Ras-GTP form and prevent conversion into the inactive Ras-GDP form. Mutated Ras protein is hyperactive and triggers cancer development. Hyperactive Ras is associated with different types of solid tumors such as pancreatic, cervical, thyroid, colon, skin, and lung tumors as well as with hematopoietic malignancies such as chronic myelomonocytic leukemia, acute myelogenous leukemia and multiple myeloma to list a few. Ras is an excellent gene therapy target due to its involvement in various cancers (Beaupre & Kurzrock 1999, and references therein). Recently it has been shown that knocking out Ras with an anti-Ras mRNA plasmid-mediated short-hairpin RNA in combination with clinical drug vincristine resulted in inhibition of the growth of human hepatoma HepG2 in vivo (Sun et al. 2009). This illustrates once again that the combination of gene therapy with standard chemotherapy is a promising approach for treatment of cancer.

3.2.2.3 AKT

AKT, a serine/threonine kinase, plays an essential role in oncogenesis. The AKT family consists of three cellular homologues AKT1, AKT2 and AKT3. The encoded proteins have a similar structure consisting of an amino-terminal pleckstrin homology domain, a short α-helical linker and a carboxy-terminal kinase domain. Tissues have different expression levels of the three homologues AKT1, AKT2 and AKT3, which is why it is not surprising that the three different variants of AKT are overexpressed in different types of cancers. For example, AKT1 is overexpressed in gastric cancer and is associated with poor prognosis in breast and prostate cancer; AKT2 is overexpressed in ovarian and pancreatic cancer. AKT3 is overexpressed in estrogen receptor-deficient breast cancer and in androgen-insensitive prostate cancer which implies that AKT3 contributes to aggressive steroid hormone-insensitive cancer. AKT acquires growth signal autonomy and inhibits apoptosis in cancer

cells. It promotes cell survival through its phosphorylation of MDM2, which enhances nuclear accumulation of MDM2. MDM2 inhibits the transcriptional activity of p53 and promotes its degradation by the proteasome (Testa & Bellacosa 2001). AKT gene therapy has been conducted with an aerosol delivery system consisting of nano-sized glucosylated polyethylenimine (GPEI). It has been shown that this aerosol is capable of delivering AKT wild-type and kinase deficient genes into the lung of mice (Tehrani et al. 2007). Dominant negative alleles of AKT directly injected into lung carcinoma cells have also been shown to block cell survival and proliferation (Li, Simpson, et al. 1998).

3.3 Protein-protein interactions

A protein dimer or oligomer is a macromolecular structure formed by two (dimer) or several (oligomer) proteins of either same origin (homo-oligomers) or different origins (hetero-oligomers). For several proteins the formation of oligomers or dimers is essential in order to form functional systems. Both Bcr-Abl and p53 proteins function in the homo-oligomeric form. On the other hand, hemoglobin forms hetero-oligomers consisting of two α and two β subunits to form a functional structure. If one of these subunits is defective or missing, the protein cannot master its tasks leading to diseases such as the previously described β-thalassemia. Mutations in the oligomerization domain can lead to loss of function. Dimer or oligomer formation is governed by non-covalent interactions, including salt bridges, hydrogen bonds and hydrophobic interactions. A common structural motif for dimerization is a coiled coil consisting of usually two to five α-helices that wind around one another like strands of a rope, meshed together like "knobs-into-holes." They contain a characteristic seven-residue sequence repeat (Mason & Arndt 2004; Crick 1952). Coiled coil motifs play an important role in the function of several different proteins ranging from transcription factors such as Jun and Fos which are responsible for cell growth and proliferation (Glover & Harrison 1995) to the oncoprotein Bcr-Abl which leads to cancer (McWhirter et al. 1993). A subgroup of the coiled coil motif is represented by the "leucine zipper", an unusually long α-helix with protruding leucine residues in periodic repetition. The leucine residues from one peptide interact with leucine residues from a second peptide, forming a molecular zipper (Landschulz et al. 1988). Another important dimerization interface for proteins is the helix-loop-helix (HLH) motif. Characterized by two α-helices connected by a short loop, this structure is highly conserved in many diverse organisms. Proteins containing this structure are transcription factors that are only functional as homo- or hetero-dimers (Murre et al. 1994, and references therein). Important HLH family members are myc proteins which play an essential role in cell proliferation, differentiation, cell growth, and apoptosis, but are also involved in development of numerous kinds of cancer (Vita & Henriksson 2006). Finally, another interaction motif is the zinc finger motif, containing several subgroups such as C2H2, Gag knuckle, treble clef, zinc ribbon, Zn2/Cys6, TAZ2 domain like, zinc binding loops and metallothionein (Krishna et al. 2003). The C2H2 zinc finger represents the most prevalent motif and contains a zinc ion coordinated by cysteines and histidines (Wolfe et al. 2000). Although most C2H2 fingers apparently contribute to protein-DNA or protein-RNA interactions, examples for protein-protein interactions also exist. One example is Ikaros, a transcription factor participating in gene silencing and activation in hematopoietic cells. In this protein, dimerization is important for its activity and affinity to DNA (McCarty et al. 2003, and references therein). In addition, more complex oligomerization structures exist. For example, p53 forms a dimer with an antiparallel β-sheet and an antiparallel helix-helix interface. Two dimers associate as a parallel helix-helix to form a tetramer (Jeffrey et al. 1995).

Gene therapy may be used to enhance or inhibit dimerization interfaces. Currently, small molecule drugs are unable to re-establish the ability of proteins to form dimers with the aim of restoring their natural function. In contrast, gene therapy can supply dimerization-capable and functional proteins. On the other hand, if the formation of a dimer is unwanted, it is possible to disrupt the dimerization interface of a disease-causing protein by introducing proteins into the cell which compete for dimerization. Normal dimerization of the disease-causing protein is then blocked, hence stopping the disease.

3.3.1 Homo-oligomerization for apoptotic activity

The classic example of a protein that is only functional as a homo-oligomer is p53. The protein p53 is 393 amino acids long and contains a transactivation domain (amino acids 1-43) and a proline-rich domain (amino acids 61-94), a DNA-binding domain (amino acids 110-286), a tetramerization domain (amino acids 326-355) and a regulatory region (amino acids 363-393) (Chene 2001). As already mentioned, mutations of TP53, the gene encoding for p53, occur in a large proportion of human cancers. Some of these mutations may prevent the formation of tetramers, which lead to loss of p53 function (Vogelstein et al. 2000). Not only does the site-specific binding to DNA depend on oligomerization , but so do a number of post-translational modifications of p53 which are believed to be important regulators of p53 activity (Chene 2001, and references therein). Reintroducing tetramerization-capable p53 using gene therapy may allow treatment of cancers which are caused by mutations in this region of TP53. So far 49 mutations in the tetramerization domain of p53 have been described, even though not all mutations prevent dimerization or tetramerization. Most of these occurring mutants still form tetrameric structures like wild-type p53 but with reduced stability (Kamada et al. 2011).

Another example where protein oligomerization yields functionality occurs with DJ-1. This protein bears cytoprotective functions within cells and protects neurons from stressful stimulants. A L166P mutation in the DJ-1 gene may prevent its ability to homodimerize, and it has been speculated that this can lead to neurodegeneration in autosomal recessive early onset Parkinsonism (Gorner et al. 2007, and references therein). Re-introduction of dimerization-capable DJ-1 with gene therapy is therefore a possible treatment option.

3.3.2 Disruption of disease-causing homo-oligomerization

Like p53, Bcr-Abl is also a protein that functions as a homo-oligomer (dimer of dimers). However, Bcr-Abl derives oncogenic function rather than tumor suppression from oligomerization. Bcr-Abl results from the fusion of the breakpoint cluster region (Bcr) gene on chromosome 22 and the Abelson leukemia oncogene (Abl) on chromosome 9. This results in an abnormal shortened chromosome called the Philadelphia chromosome. Bcr-Abl functions as an oncoprotein leading to increased cell proliferation and inhibition of apoptosis due to the constitutive activation of tyrosine kinase activity and causes 95% of all cases of chronic myeloid leukemia (CML) (Sawyers 1999, and references therein). The oligomerization of Bcr-Abl is essential for the activation of the tyrosine kinase activity of Bcr-Abl (McWhirter et al. 1993). Destroying the ability of Bcr-Abl to form tetramers or using the dimerization domain to disrupt Bcr-Abl activity would be a possible gene therapy approach for CML (Dixon et al. 2009).

Finally, serpins (serine protease inhibitors) such as serpin α1-antitrypsin function aberrantly as oligomers/polymers (Silverman et al. 2001; Lomas & Mahadeva 2002). In fact, the

polymerization of serpin α1-antitrypsin is known to cause hepatocellular carcinoma and liver cirrhosis due to accumulation in the endoplasmatic reticulum of the liver (Lomas & Mahadeva 2002). Disruption of polymerization could also be targeted for gene therapy, using an exogenously added polymerization domain that could compete for binding to serpin α1-antitrypsin.

3.4 Cell compartments

Targeting a gene therapy product to a specific subcellular compartment is another way to overcome disease. There are many diseases associated with protein malfunction in different organelles of the cell (Davis et al. 2007). For example, certain cancers can arise when a protein localizes to the wrong compartment. The typical example is cytoplasmically mislocalized p53. When p53 is in the cytoplasm, it cannot act as tumor suppressor since it is a transcription factor that needs to be in the nucleus in order to function (Kau et al. 2004; Wurzer et al. 2001). In addition to mislocation from the nucleus, the incorrect localization of proteins normally destined for lysosomes, peroxisomes, Golgi apparatus, endoplasmic reticulum (ER) or mitochondria can also lead to disease. Directing gene therapy products to specific subcellular compartments represents not only novel targets but a new way to approach gene therapy (Mossalam et al. 2010).

3.4.1 Lysosomes

Lysosomes degrade unused cellular constituents, receptors and release active enzymes extracellularly and are involved in post-translational maturation of proteins. Dysfunction of lysosomal hydrolases leads to loss of cell growth control and results in chemotherapy resistance as well as high metastatic potential (Castino et al. 2003). Furthermore, lysosome and lysosome-related organelles are associated with Lysosomal Storage Disease (LSD), Alzheimer's disease and development of several types of tumors. LSD is collective term for 40 genetic disorders due to single or multi enzyme deficiency which results in neurodegenerative disorders. Therapy options are limited to BMT and enzyme replacement. The disadvantages of BMT are morbidity and mortality as well as incomplete response to therapy. Enzyme replacement fails because of fast degradation of the enzyme from bloodstream. Due to these limitations, gene therapy represents a potential alternative. Currently, gene therapy is focused on using cargo proteins that deliver proteins to the lysosome. Since clathrin-dependent receptor-mediated endocytosis (RME) is the main transport mechanism for delivery to the lysosome, it is thought that all forms of LSDs can be treated with gene therapy (Bareford & Swaan 2007, and references therein).

3.4.2 Peroxisomes

Peroxisomes are multifunctional organelles which are involved in biochemical and metabolic processes such as oxidation of fatty acids, plasmalogen biosynthesis and glyoxylate detoxification. Malfunction of or defects in peroxisomes are associated with a variety of diseases which can be classified as Zellweger spectrum peroxisome biogenesis disorders or rhizomelic chondrodysplasia punctate. Defects in peroxisome biogenesis proteins (peroxins, encoded by PEX genes) can lead to eye anomalies, extreme hypotension, and hepatomegaly (to name a few), and usually are fatal by age 1-2. In general deficiencies in a single peroxisomal enzyme (PEX) are associated with a variety of diseases. The therapy approaches are focused on protein therapeutics, peroxisomal enzymes and gene therapy.

One possible gene therapy target is the antioxidant enzyme, catalase. A modified catalase molecule was transduced into hypocatalasemic fibroblasts and reduced hydrogen peroxide levels dramatically. This resulted in the restoration of oxidative balance, which may have cytoprotective effects (Terlecky & Koepke 2007). The cytoprotective role of catalase makes it an excellent gene therapy target, because many diseases such as cardiovascular diseases are linked to high hydrogen peroxide levels (Gong et al. 2010).

3.4.3 Proteasome

Targeting the proteasome, the cell's degradation machinery, represents another possible target for gene therapy. The general inhibition of the proteasome is already used for treatment of inflammatory disease and cancer (Nalepa et al. 2006) while the activation of the proteasome can be used for neurodegenerative diseases and cardiac diseases (Dahlmann 2007). Targeting disease-specific components of the ubiquitin-proteasome system provides the possibility for directed therapy approaches (Nalepa et al. 2006). The E3 ubiqitin ligases are important for specificity of proteasomal degradation because they recognize the proteins which should be destroyed (Nalepa et al. 2006). More classical drug targets are the ubiquitin-activation and the actual degradation step which occurs in the proteasome. A new approach suggested by our lab involves capturing oncogenic proteins such as survivin and sending them to the proteasome for degradation. This could be achieved by including a gene therapy construct that has a survivin dimerization domain and a proteasomal degradation domain, capable of capturing endogenous survivin and sending it to the proteasome (Mossalam et al. 2010).

3.4.4 Mitochondria

Mitochondria are essential for production of cellular ATP. The mitochondria consist of the outer membrane, the inner membrane, intermembrane space, cristae and mitochondrial DNA. Mutations in mitochondrial DNA are associated with muscle and central nervous system dysfunction, but only if most of the DNA is mutated. An interesting gene therapy approach is to tag mitochondria targeting signals to endonucleases which are able to degrade the mutated mitochondrial DNA. This mutant DNA contains the T8399G mutation which creates a unique restriction site and allows the restriction enzyme to distinguish between normal DNA and mutated DNA. It provides new therapy options for neuropathy, ataxia and retinitis pigmentosa (Srivastava & Moraes 2001). In addition, the mitochondrion is also essential in cellular apoptosis. Proteins such as p53 can be sent to the mitochondria, eventually resulting in cytochrome c release and apoptosis. Indeed, p53 targeted to the mitochondria has shown to cause apoptosis in different cancer cell lines (Palacios & Moll 2006).

3.4.5 Endoplasmic reticulum

The endoplasmic reticulum (ER) produces almost all cellular lipids, and the majority of proteins are synthesized on the cytosolic surface of the ER. A wide range of diseases occur due to mistakes in protein folding/assembly in the ER such as CF and neurodegenerative diseases. CF is a classic gene therapy target with one single mutation which can be targeted by replacing the defect gene. Unfortunately, all gene therapy approaches for CF have failed thus far. Certain neurodegenerative diseases are affected by mutations in proteins involved in ER assembly. Mutations in Parkin, which is an E3 ligase responsible for ubiquitinylation

and regulation of proteasomal degradation, is associated with juvenile Parkinsonism. The Parkin proteasomal pathway normally degrades Pael-R in dopaminergic neurons. Pael-R accumulates in brain cells when Parkin is mutated (Aridor et al. 2004, and references therein). Adding back functional Parkin would then be a possible gene therapy approach for juvenile Parkinsonism.

3.4.6 Golgi apparatus

In addition to the synthesis of carbohydrates, the Golgi apparatus (GA) sorts as well as dispatch proteins to the ER. SPCA1 is a protein found in the trans-Golgi. When mutations occur in the gene (ATP2C1) encoding SPCA1, a genetic disorder results called Hailey-Hailey disease. These various mutations result in skin lesions which are usually benign and lead only in a few cases into squamous cell carcinoma (Pizzo et al. 2011). Replacing mutated SPCA1 would be a possible gene therapy approach to treat Hailey-Hailey disease.

3.4.7 Nucleus

Many diseases are associated with problems in nuclear import and export. For example, various types of cancers are associated with p53 and FOXO mislocalization in the cytoplasm, while their normal localization is the nucleus. There are several examples of proteins that when mislocalized to different compartments lose their function or may become oncogenic. The control of compartmentalization of key proteins can be used to overcome disease. Besides, tumor suppressors such as p53, cell cycle inhibitors, G-protein coupled receptors and transcription factors can also lose their function when mislocalized (Chinen et al. 2007). $p21^{WAF-1}$ is localized in the nucleus where it accomplishes its function as cell cycle inhibitor. When moved to the cytoplasm, it is associated with tumor progression (Davis et al. 2007; Keeshan et al. 2003). G-protein coupled receptors like rhodopsin, vasopressin V_2, LDL and CFTR all require proper localization for function. For example, rhodopsin is found in the membrane sacs within the rods, and when mislocalized it is confined in the plasma membrane of photoreceptor cell body and causes retinitis pigmentosa (Edwards et al. 2000). Additional transcription factors such as NF-κB and FOXO are both associated with various types of cancer when mislocalized to different compartments. NF-κB is located in the cytoplasm of normal cells whereas nuclear accumulation causes cancer. In contrast FOXO is found in the nucleus of normal cells and cytoplasmic localization results in cancer (Davis et al. 2007, and references therein).

There are several different gene therapy approaches for targeting mislocalized proteins. The standard method is to add back the protein which contains functional localization signals, such as the adenoviral p53 vectors Gendicine™ and Oncorine™. On the other hand, blocking general nuclear import or export machinery has been attempted, but due to the non-specific blockage of import/export, these methods suffer from toxicity. Instead of general inhibition of import/export, the protein itself can be modified. Adding nuclear localization signals (NLS) or nuclear export signals (NES) to the genes encoding mislocalized proteins allows targeting of proteins directly to the desired compartments.

The localization of proteins can be changed by using a protein switch developed in our laboratory (Kakar et al. 2007; Davis et al. 2007). The protein switch is a plasmid encoding a NES, a NLS and a ligand binding domain (LBD) from steroid hormone receptor. The LBD serves as a ligand-inducible nuclear localization switch. The protein switch is cytoplasm in the absence of ligand and translocates to the nucleus when ligand is added. The protein

switch has also been designed to contain dimerization domain that allows capture of an endogenous protein of interest. Upon ligand addition, the protein switch-endogenous protein complex will then translocate to the nucleus. Removal of the endogenous protein from the cytoplasm can result in decrease cytoplasmic signaling or increased apoptotic signaling in the nucleus, with potential use in cancer therapy (Kakar et al. 2007).

4. Conclusions

Some of the major diseases currently targeted by gene therapy include cancer, cardiovascular disease, HIV, and monogenic diseases. Despite many decades of gene therapy research on these diseases, there currently are very few products that have made it to market. The search for new gene therapy targets and improved methods are therefore warranted. The integration of new and standard technologies (genome sequencing, microarrays, improved analysis, and linkage to molecular and biochemical assays) recently have yielded methods to uncover new drivers of cancer (Akavia et al. 2010). In 2008, the NIH started its Undiagnosed Diseases Program. These NIH investigators first try to diagnose an illness by first looking at known genetic markers, followed by standard molecular and biochemical assays. If no candidate genes are revealed, they then use state-of-the-art genetic analyses that can sequence the entire exome (all exons in the human genome) of a patient and their family; high resolution microarrays can genotype the rest of the genome to "bring genomics to the clinic." After comparison to family data and a reference sequence (from the Human Genome Project), the gene causing a particular rare disease may be discovered (Maxmen 2011). Currently patients enrolled in this program are not cured; the candidate gene and corresponding protein are only identified. Small molecule inhibitors of these proteins can take years or decades to screen, therefore making replacement of these defective or mutant genes prime candidates for gene therapy treatment in patients with a rare disease.

Further analysis of the protein can uncover the molecular basis of the disease. Is this protein a hub protein which interacts with many other proteins? What are the protein-protein interactions that govern its activity? Are there any cell compartmentalization abnormalities that promote disease? With this information in mind, more modern gene therapy approaches can be developed. In our laboratory, we have designed a protein switch designed to capture and change location of a harmful protein in a cell. This altered location could be exploited for disease therapy. For example, the Bcr-Abl protein is oncogenic in the cytoplasm, but causes apoptosis when moved to the nucleus (Dixon et al. 2009). A protein switch against Bcr-Abl is being developed in our laboratory that can dimerize to wild type (wt) Bcr-Abl by virtue of a coiled-coil dimerization domain (Mossalam et al. 2010). The protein switch also contains a ligand-inducible domain that can move the protein from the cytoplasm to the nucleus upon the addition of ligand (Kakar et al. 2007). Therefore, after capture, wt Bcr-Abl is dragged to the nucleus, where apoptosis ensues. Understanding the molecular mechanisms that govern protein activity can therefore be used as the next phase in gene therapy, where altered protein location can completely change the function of a protein. Other emerging modern gene therapy-based approaches including anti-gene therapies (antisense, siRNA, ribozymes) and immunotherapy are desired to have a significant impact on disease treatment.

5. References

Abo-Auda, W., and R. L. Benza. 2003. Therapeutic angiogenesis: review of current concepts and future directions. *J Heart Lung Transplant* 22 (4):370-82.

Akavia, U. D., O. Litvin, J. Kim, F. Sanchez-Garcia, D. Kotliar, H. C. Causton, P. Pochanard, E. Mozes, L. A. Garraway, and D. Pe'er. 2010. An integrated approach to uncover drivers of cancer. *Cell* 143 (6):1005-17.

Altieri, D. C. 2001. The molecular basis and potential role of survivin in cancer diagnosis and therapy. *Trends Mol Med* 7 (12):542-7.

Altieri, D. C. 2003. Validating survivin as a cancer therapeutic target. *Nat Rev Cancer* 3 (1):46-54.

Altieri, D. C. 2008. Survivin, cancer networks and pathway-directed drug discovery. *Nat Rev Cancer* 8 (1):61-70.

Antoine, C., S. Muller, A. Cant, M. Cavazzana-Calvo, P. Veys, J. Vossen, A. Fasth, C. Heilmann, N. Wulffraat, R. Seger, S. Blanche, W. Friedrich, M. Abinun, G. Davies, R. Bredius, A. Schulz, P. Landais, and A. Fischer. 2003. Long-term survival and transplantation of haemopoietic stem cells for immunodeficiencies: report of the European experience 1968-99. *Lancet* 361 (9357):553-60.

Aridor, M., A. K. Guzik, A. Bielli, and K. N. Fish. 2004. Endoplasmic reticulum export site formation and function in dendrites. *J Neurosci* 24 (15):3770-6.

Arnett, D. K., A. E. Baird, R. A. Barkley, C. T. Basson, E. Boerwinkle, S. K. Ganesh, D. M. Herrington, Y. Hong, C. Jaquish, D. A. McDermott, and C. J. O'Donnell. 2007. Relevance of genetics and genomics for prevention and treatment of cardiovascular disease: a scientific statement from the American Heart Association Council on Epidemiology and Prevention, the Stroke Council, and the Functional Genomics and Translational Biology Interdisciplinary Working Group. *Circulation* 115 (22):2878-901.

Bareford, L. M., and P. W. Swaan. 2007. Endocytic mechanisms for targeted drug delivery. *Adv Drug Deliv Rev* 59 (8):748-58.

Baumgartner, I., N. Chronos, A. Comerota, T. Henry, J. P. Pasquet, F. Finiels, A. Caron, J. F. Dedieu, R. Pilsudski, and P. Delaere. 2009. Local gene transfer and expression following intramuscular administration of FGF-1 plasmid DNA in patients with critical limb ischemia. *Mol Ther* 17 (5):914-21.

Beaupre, D. M., and R. Kurzrock. 1999. RAS and leukemia: from basic mechanisms to gene-directed therapy. *J Clin Oncol* 17 (3):1071-9.

Boucher, R. C., C. U. Cotton, J. T. Gatzy, M. R. Knowles, and J. R. Yankaskas. 1988. Evidence for reduced Cl- and increased Na+ permeability in cystic fibrosis human primary cell cultures. *J Physiol* 405:77-103.

Buckley, R. H., R. I. Schiff, S. E. Schiff, M. L. Markert, L. W. Williams, T. O. Harville, J. L. Roberts, and J. M. Puck. 1997. Human severe combined immunodeficiency: genetic, phenotypic, and functional diversity in one hundred eight infants. *J Pediatr* 130 (3):378-87.

Cao, A., and R. Galanello. 2010. Beta-thalassemia. *Genet Med* 12 (2):61-76.

CardioVascular BioTherapeutics, Inc. 2011. *Fibroblast Growth Factor-1 (FGF-1) for the Treatment of Coronary Heart Disease (ACORD)* [cited 03/2011 2011]. Available from http://www.clinicaltrials.gov/ct2/show/NCT00117936?term=henry+FGF&rank=1.

Castino, R., M. Demoz, and C. Isidoro. 2003. Destination 'lysosome': a target organelle for tumour cell killing? *J Mol Recognit* 16 (5):337-48.

Cavazzana-Calvo, M., S. Hacein-Bey, G. de Saint Basile, F. Gross, E. Yvon, P. Nusbaum, F. Selz, C. Hue, S. Certain, J. L. Casanova, P. Bousso, F. L. Deist, and A. Fischer. 2000. Gene therapy of human severe combined immunodeficiency (SCID)-X1 disease. *Science* 288 (5466):669-72.

Cavazzana-Calvo, M., E. Payen, O. Negre, G. Wang, K. Hehir, F. Fusil, J. Down, M. Denaro, T. Brady, K. Westerman, R. Cavallesco, B. Gillet-Legrand, L. Caccavelli, R. Sgarra, L. Maouche-Chretien, F. Bernaudin, R. Girot, R. Dorazio, G. J. Mulder, A. Polack, A. Bank, J. Soulier, J. Larghero, N. Kabbara, B. Dalle, B. Gourmel, G. Socie, S. Chretien, N. Cartier, P. Aubourg, A. Fischer, K. Cornetta, F. Galacteros, Y. Beuzard, E. Gluckman, F. Bushman, S. Hacein-Bey-Abina, and P. Leboulch. 2010. Transfusion independence and HMGA2 activation after gene therapy of human beta-thalassaemia. *Nature* 467 (7313):318-22.

Cerepro, EMEA recommendation on. 2009. European Medicines Agency recommendation on Cerepro.

Chene, P. 2001. The role of tetramerization in p53 function. *Oncogene* 20 (21):2611-7.

Chinen, J., J. Davis, S. S. De Ravin, B. N. Hay, A. P. Hsu, G. F. Linton, N. Naumann, E. Y. Nomicos, C. Silvin, J. Ulrick, N. L. Whiting-Theobald, H. L. Malech, and J. M. Puck. 2007. Gene therapy improves immune function in preadolescents with X-linked severe combined immunodeficiency. *Blood* 110 (1):67-73.

Chiuve, S. E., M. L. McCullough, F. M. Sacks, and E. B. Rimm. 2006. Healthy lifestyle factors in the primary prevention of coronary heart disease among men: benefits among users and nonusers of lipid-lowering and antihypertensive medications. *Circulation* 114 (2):160-7.

Cloutier, M. M., L. Guernsey, P. Mattes, and B. Koeppen. 1990. Duramycin enhances chloride secretion in airway epithelium. *Am J Physiol* 259 (3 Pt 1):C450-4.

Consortium, International HapMap. 2003. The International HapMap Project. *Nature* 426 (6968):789-96.

Crick, F. H. 1952. Is alpha-keratin a coiled coil? *Nature* 170 (4334):882-3.

Dahlmann, B. 2007. Role of proteasomes in disease. *BMC Biochem* 8 Suppl 1:S3.

Davis, J. R., M. Kakar, and C. S. Lim. 2007. Controlling protein compartmentalization to overcome disease. *Pharm Res* 24 (1):17-27.

De Ravin, S. S., and H. L. Malech. 2009. Partially corrected X-linked severe combined immunodeficiency: long-term problems and treatment options. *Immunol Res* 43 (1-3):223-42.

Dixon, A. S., M. Kakar, K. M. Schneider, J. E. Constance, B. C. Paullin, and C. S. Lim. 2009. Controlling subcellular localization to alter function: Sending oncogenic Bcr-Abl to the nucleus causes apoptosis. *J Control Release* 140 (3):245-9.

Duggan, D. J., M. Bittner, Y. Chen, P. Meltzer, and J. M. Trent. 1999. Expression profiling using cDNA microarrays. *Nat Genet* 21 (1 Suppl):10-4.

Edelstein, M. L., M. R. Abedi, and J. Wixon. 2007. Gene therapy clinical trials worldwide to 2007--an update. *J Gene Med* 9 (10):833-42.

Edelstein, M. L., M. R. Abedi, J. Wixon, and R. M. Edelstein. 2004. Gene therapy clinical trials worldwide 1989-2004-an overview. *J Gene Med* 6 (6):597-602.

Edwards, S. W., C. M. Tan, and L. E. Limbird. 2000. Localization of G-protein-coupled receptors in health and disease. *Trends Pharmacol Sci* 21 (8):304-8.

Erster, S., M. Mihara, R. H. Kim, O. Petrenko, and U. M. Moll. 2004. In vivo mitochondrial p53 translocation triggers a rapid first wave of cell death in response to DNA damage that can precede p53 target gene activation. *Mol Cell Biol* 24 (15):6728-41.

Flume, P. A., P. J. Mogayzel Jr, K. A. Robinson, R. L. Rosenblatt, L. Quittell, B. C. Marshall, and Committee Clinical Practice Guidelines For Pulmonary Therapies. 2010. Cystic Fibrosis Pulmonary Guidelines: Pulmonary Complications: Hemoptysis and Pneumothorax. *Am J Respir Crit Care Med*.

Flynn, A., and T. O'Brien. 2008. Alferminogene tadenovec, an angiogenic FGF4 gene therapy for coronary artery disease. *IDrugs* 11 (4):283-93.

Foundation, Cystic Fibrosis. 2011. *Cystic Fibrosis Foundation* 2011 [cited 01/18/2011 2011]. Available from http://www.cff.org/.

Garber, K. 2006. China approves world's first oncolytic virus therapy for cancer treatment. *J Natl Cancer Inst* 98 (5):298-300.

Glover, J. N., and S. C. Harrison. 1995. Crystal structure of the heterodimeric bZIP transcription factor c-Fos-c-Jun bound to DNA. *Nature* 373 (6511):257-61.

Goh, A. M., C. R. Coffill, and D. P. Lane. 2010. The role of mutant p53 in human cancer. *J Pathol*.

Goh, A. M., C. R. Coffill, and D. P. Lane. 2011. The role of mutant p53 in human cancer. *J Pathol* 223 (2):116-26.

Gong, G., Y. Qin, W. Huang, S. Zhou, X. Wu, X. Yang, Y. Zhao, and D. Li. 2010. Protective effects of diosgenin in the hyperlipidemic rat model and in human vascular endothelial cells against hydrogen peroxide-induced apoptosis. *Chem Biol Interact* 184 (3):366-75.

Gorner, K., E. Holtorf, J. Waak, T. T. Pham, D. M. Vogt-Weisenhorn, W. Wurst, C. Haass, and P. J. Kahle. 2007. Structural determinants of the C-terminal helix-kink-helix motif essential for protein stability and survival promoting activity of DJ-1. *J Biol Chem* 282 (18):13680-91.

Grossman, D., and D. C. Altieri. 2001. Drug resistance in melanoma: mechanisms, apoptosis, and new potential therapeutic targets. *Cancer Metastasis Rev* 20 (1-2):3-11.

Guo, J., and H. Xin. 2006. Chinese gene therapy. Splicing out the West? *Science* 314 (5803):1232-5.

Guo, Z. S., S. H. Thorne, and D. L. Bartlett. 2008. Oncolytic virotherapy: molecular targets in tumor-selective replication and carrier cell-mediated delivery of oncolytic viruses. *Biochim Biophys Acta* 1785 (2):217-31.

Hacein-Bey-Abina, S., F. Le Deist, F. Carlier, C. Bouneaud, C. Hue, J. P. De Villartay, A. J. Thrasher, N. Wulffraat, R. Sorensen, S. Dupuis-Girod, A. Fischer, E. G. Davies, W. Kuis, L. Leiva, and M. Cavazzana-Calvo. 2002. Sustained correction of X-linked severe combined immunodeficiency by ex vivo gene therapy. *N Engl J Med* 346 (16):1185-93.

Harvey, B. G., P. L. Leopold, N. R. Hackett, T. M. Grasso, P. M. Williams, A. L. Tucker, R. J. Kaner, B. Ferris, I. Gonda, T. D. Sweeney, R. Ramalingam, I. Kovesdi, S. Shak, and R. G. Crystal. 1999. Airway epithelial CFTR mRNA expression in cystic fibrosis patients after repetitive administration of a recombinant adenovirus. *J Clin Invest* 104 (9):1245-55.

Haupt, S., M. Berger, Z. Goldberg, and Y. Haupt. 2003. Apoptosis - the p53 network. *J Cell Sci* 116 (Pt 20):4077-85.

Henderson, B. R. 2005. Regulation of BRCA1, BRCA2 and BARD1 intracellular trafficking. *Bioessays* 27 (9):884-93.

Hirschhorn, J. N., and M. J. Daly. 2005. Genome-wide association studies for common diseases and complex traits. *Nat Rev Genet* 6 (2):95-108.

Jeffrey, P. D., S. Gorina, and N. P. Pavletich. 1995. Crystal structure of the tetramerization domain of the p53 tumor suppressor at 1.7 angstroms. *Science* 267 (5203):1498-502.

Kakar, M., J. R. Davis, S. E. Kern, and C. S. Lim. 2007. Optimizing the protein switch: altering nuclear import and export signals, and ligand binding domain. *J Control Release* 120 (3):220-32.

Kamada, R., T. Nomura, C. W. Anderson, and K. Sakaguchi. 2011. Cancer-associated p53 tetramerization domain mutants: quantitative analysis reveals a low threshold for tumor suppressor inactivation. *J Biol Chem* 286 (1):252-8.

Kass, R. W., M. N. Kotler, and S. Yazdanfar. 1992. Stimulation of coronary collateral growth: current developments in angiogenesis and future clinical applications. *Am Heart J* 123 (2):486-96.

Kato, J., Y. Kuwabara, M. Mitani, N. Shinoda, A. Sato, T. Toyama, A. Mitsui, T. Nishiwaki, S. Moriyama, J. Kudo, and Y. Fujii. 2001. Expression of survivin in esophageal cancer: correlation with the prognosis and response to chemotherapy. *Int J Cancer* 95 (2): 92-5.

Kau, T. R., J. C. Way, and P. A. Silver. 2004. Nuclear transport and cancer: from mechanism to intervention. *Nat Rev Cancer* 4 (2):106-17.

Keeshan, K., T. G. Cotter, and S. L. McKenna. 2003. Bcr-Abl upregulates cytosolic p21WAF-1/CIP-1 by a phosphoinositide-3-kinase (PI3K)-independent pathway. *Br J Haematol* 123 (1):34-44.

Kerem, B., J. M. Rommens, J. A. Buchanan, D. Markiewicz, T. K. Cox, A. Chakravarti, M. Buchwald, and L. C. Tsui. 1989. Identification of the cystic fibrosis gene: genetic analysis. *Science* 245 (4922):1073-80.

Keskin, O., and R. Nussinov. 2007. Similar binding sites and different partners: implications to shared proteins in cellular pathways. *Structure* 15 (3):341-54.

Kim, P. M., L. J. Lu, Y. Xia, and M. B. Gerstein. 2006. Relating three-dimensional structures to protein networks provides evolutionary insights. *Science* 314 (5807):1938-41.

Kitchen, S. G., S. Shimizu, and D. S. An. 2011. Stem cell-based anti-HIV gene therapy. *Virology* 411 (2):260-72.

Knowlton, R. G., O. Cohen-Haguenauer, N. Van Cong, J. Frezal, V. A. Brown, D. Barker, J. C. Braman, J. W. Schumm, L. C. Tsui, M. Buchwald, and et al. 1985. A polymorphic DNA marker linked to cystic fibrosis is located on chromosome 7. *Nature* 318 (6044):380-2.

Kobayashi, N., K. Agematsu, K. Sugita, M. Sako, S. Nonoyama, A. Yachie, S. Kumaki, S. Tsuchiya, H. D. Ochs, Y. Fukushima, and A. Komiyama. 2003. Novel Artemis gene mutations of radiosensitive severe combined immunodeficiency in Japanese families. *Hum Genet* 112 (4):348-52.

Krishna, S. S., I. Majumdar, and N. V. Grishin. 2003. Structural classification of zinc fingers: survey and summary. *Nucleic Acids Res* 31 (2):532-50.

Kung, C., J. T. Pingel, M. Heikinheimo, T. Klemola, K. Varkila, L. I. Yoo, K. Vuopala, M. Poyhonen, M. Uhari, M. Rogers, S. H. Speck, T. Chatila, and M. L. Thomas. 2000. Mutations in the tyrosine phosphatase CD45 gene in a child with severe combined immunodeficiency disease. *Nat Med* 6 (3):343-5.

Landschulz, W. H., P. F. Johnson, and S. L. McKnight. 1988. The leucine zipper: a hypothetical structure common to a new class of DNA binding proteins. *Science* 240 (4860):1759-64.

Li, F., G. Ambrosini, E. Y. Chu, J. Plescia, S. Tognin, P. C. Marchisio, and D. C. Altieri. 1998. Control of apoptosis and mitotic spindle checkpoint by survivin. *Nature* 396 (6711):580-4.

Li, J., L. Simpson, M. Takahashi, C. Miliaresis, M. P. Myers, N. Tonks, and R. Parsons. 1998. The PTEN/MMAC1 tumor suppressor induces cell death that is rescued by the AKT/protein kinase B oncogene. *Cancer Res* 58 (24):5667-72.

Li, J., and J. Yuan. 2008. Caspases in apoptosis and beyond. *Oncogene* 27 (48):6194-206.

Liu, R., W. A. Paxton, S. Choe, D. Ceradini, S. R. Martin, R. Horuk, M. E. MacDonald, H. Stuhlmann, R. A. Koup, and N. R. Landau. 1996. Homozygous defect in HIV-1 coreceptor accounts for resistance of some multiply-exposed individuals to HIV-1 infection. *Cell* 86 (3):367-77.

Lockley, M., M. Fernandez, Y. Wang, N. F. Li, S. Conroy, N. Lemoine, and I. McNeish. 2006. Activity of the adenoviral E1A deletion mutant dl922-947 in ovarian cancer: comparison with E1A wild-type viruses, bioluminescence monitoring, and intraperitoneal delivery in icodextrin. *Cancer Res* 66 (2):989-98.

Lomas, D. A., and R. Mahadeva. 2002. Alpha1-antitrypsin polymerization and the serpinopathies: pathobiology and prospects for therapy. *J Clin Invest* 110 (11):1585-90.

Lomas, David A., and Ravi Mahadeva. 2002. α1-Antitrypsin polymerization and the serpinopathies: pathobiology and prospects for therapy. *The Journal of Clinical Investigation* 110 (11):1585-1590.

Lucarelli, G., and J. Gaziev. 2008. Advances in the allogeneic transplantation for thalassemia. *Blood Rev* 22 (2):53-63.

Malik, P., and P. I. Arumugam. 2005. Gene Therapy for beta-thalassemia. *Hematology Am Soc Hematol Educ Program*:45-50.

Mason, J. M., and K. M. Arndt. 2004. Coiled coil domains: stability, specificity, and biological implications. *Chembiochem* 5 (2):170-6.

Maulik, N. 2009. NV1FGF, a pCOR plasmid-based angiogenic gene therapy for the treatment of intermittent claudication and critical limb ischemia. *Curr Opin Investig Drugs* 10 (3):259-68.

Maxmen, A. 2011. Exome sequencing deciphers rare diseases. *Cell* 144 (5):635-7.

McCarty, A. S., G. Kleiger, D. Eisenberg, and S. T. Smale. 2003. Selective dimerization of a C2H2 zinc finger subfamily. *Mol Cell* 11 (2):459-70.

McPhail, G. L., J. D. Acton, M. C. Fenchel, R. S. Amin, and M. Seid. 2008. Improvements in lung function outcomes in children with cystic fibrosis are associated with better nutrition, fewer chronic pseudomonas aeruginosa infections, and dornase alfa use. *J Pediatr* 153 (6):752-7.

McWhirter, J. R., D. L. Galasso, and J. Y. Wang. 1993. A coiled-coil oligomerization domain of Bcr is essential for the transforming function of Bcr-Abl oncoproteins. *Mol Cell Biol* 13 (12):7587-95.

Mesri, M., N. R. Wall, J. Li, R. W. Kim, and D. C. Altieri. 2001. Cancer gene therapy using a survivin mutant adenovirus. *J Clin Invest* 108 (7):981-90.

Metcalfe, K. A., H. T. Lynch, P. Ghadirian, N. Tung, I. A. Olivotto, W. D. Foulkes, E. Warner, O. Olopade, A. Eisen, B. Weber, J. McLennan, P. Sun, and S. A. Narod. 2005. The risk of ovarian cancer after breast cancer in BRCA1 and BRCA2 carriers. *Gynecol Oncol* 96 (1):222-6.

Mitchell, P. 2010. Ark's gene therapy stumbles at the finish line. *Nat Biotechnol* 28 (3):183-4.

Morishita, R., M. Aoki, N. Hashiya, H. Makino, K. Yamasaki, J. Azuma, Y. Sawa, H. Matsuda, Y. Kaneda, and T. Ogihara. 2004. Safety evaluation of clinical gene therapy using hepatocyte growth factor to treat peripheral arterial disease. *Hypertension* 44 (2):203-9.

Moss, R. B., C. Milla, J. Colombo, F. Accurso, P. L. Zeitlin, J. P. Clancy, L. T. Spencer, J. Pilewski, D. A. Waltz, H. L. Dorkin, T. Ferkol, M. Pian, B. Ramsey, B. J. Carter, D. B. Martin, and A. E. Heald. 2007. Repeated aerosolized AAV-CFTR for treatment of cystic fibrosis: a randomized placebo-controlled phase 2B trial. *Hum Gene Ther* 18 (8):726-32.

Moss, R. B., D. Rodman, L. T. Spencer, M. L. Aitken, P. L. Zeitlin, D. Waltz, C. Milla, A. S. Brody, J. P. Clancy, B. Ramsey, N. Hamblett, and A. E. Heald. 2004. Repeated adeno-associated virus serotype 2 aerosol-mediated cystic fibrosis transmembrane regulator gene transfer to the lungs of patients with cystic fibrosis: a multicenter, double-blind, placebo-controlled trial. *Chest* 125 (2):509-21.

Mossalam, M., A. S. Dixon, and C. S. Lim. 2010. Controlling subcellular delivery to optimize therapeutic effect. *Ther Deliv* 1 (1):169-193.

Murre, C., G. Bain, M. A. van Dijk, I. Engel, B. A. Furnari, M. E. Massari, J. R. Matthews, M. W. Quong, R. R. Rivera, and M. H. Stuiver. 1994. Structure and function of helix-loop-helix proteins. *Biochim Biophys Acta* 1218 (2):129-35.

Nakamura, Y. 2009. DNA variations in human and medical genetics: 25 years of my experience. *J Hum Genet* 54 (1):1-8.

Nalepa, G., M. Rolfe, and J. W. Harper. 2006. Drug discovery in the ubiquitin-proteasome system. *Nat Rev Drug Discov* 5 (7):596-613.

NCBI. 2011. *Microarrays: Chipping away at the Mysteries of science and medicine* 2007 [cited 03/2011 2011]. Available from http://www.ncbi.nlm.nih.gov/About/primer/microarrays.html.

O'Connor, D. S., D. Grossman, J. Plescia, F. Li, H. Zhang, A. Villa, S. Tognin, P. C. Marchisio, and D. C. Altieri. 2000. Regulation of apoptosis at cell division by p34cdc2 phosphorylation of survivin. *Proc Natl Acad Sci U S A* 97 (24):13103-7.

Palacios, G., and U. M. Moll. 2006. Mitochondrially targeted wild-type p53 suppresses growth of mutant p53 lymphomas in vivo. *Oncogene* 25 (45):6133-9.

Peng, Z. 2005. Current status of gendicine in China: recombinant human Ad-p53 agent for treatment of cancers. *Hum Gene Ther* 16 (9):1016-27.

Pizzo, P., V. Lissandron, P. Capitanio, and T. Pozzan. 2011. Ca(2+) signalling in the Golgi apparatus. *Cell Calcium*.

Powell, R. J., M. Simons, F. O. Mendelsohn, G. Daniel, T. D. Henry, M. Koga, R. Morishita, and B. H. Annex. 2008. Results of a double-blind, placebo-controlled study to assess the safety of intramuscular injection of hepatocyte growth factor plasmid to improve limb perfusion in patients with critical limb ischemia. *Circulation* 118 (1):58-65.

Project, Human Genome. 2011. *Human Genome Project* 2011]. Available from http://www.ornl.gov/sci/techresources/Human_Genome/home.shtml.

Project, The International HapMap. 426. *The International HapMap Project* (2003/12/20), Dec 18 2003 [cited 6968 426]. Available from http://www.ncbi.nlm.nih.gov/pubmed/14685227.

Puel, A., S. F. Ziegler, R. H. Buckley, and W. J. Leonard. 1998. Defective IL7R expression in T(-)B(+)NK(+) severe combined immunodeficiency. *Nat Genet* 20 (4):394-7.

Raty, J. K., J. T. Pikkarainen, T. Wirth, and S. Yla-Herttuala. 2008. Gene therapy: the first approved gene-based medicines, molecular mechanisms and clinical indications. *Curr Mol Pharmacol* 1 (1):13-23.

Riferminogene pecaplasmide. 2010. *Am J Cardiovasc Drugs* 10 (5):343-6.

Rodriguez, J. A., S. Schuchner, W. W. Au, M. Fabbro, and B. R. Henderson. 2004. Nuclear-cytoplasmic shuttling of BARD1 contributes to its proapoptotic activity and is regulated by dimerization with BRCA1. *Oncogene* 23 (10):1809-20.

Roth, J. A., D. Nguyen, D. D. Lawrence, B. L. Kemp, C. H. Carrasco, D. Z. Ferson, W. K. Hong, R. Komaki, J. J. Lee, J. C. Nesbitt, K. M. Pisters, J. B. Putnam, R. Schea, D. M. Shin, G. L. Walsh, M. M. Dolormente, C. I. Han, F. D. Martin, N. Yen, K. Xu, L. C. Stephens, T. J. McDonnell, T. Mukhopadhyay, and D. Cai. 1996. Retrovirus-mediated wild-type p53 gene transfer to tumors of patients with lung cancer. *Nat Med* 2 (9):985-91.

Ryan, B. M., N. O'Donovan, and M. J. Duffy. 2009. Survivin: a new target for anti-cancer therapy. *Cancer Treat Rev* 35 (7):553-62.

Ryser, O., A. Morell, and W. H. Hitzig. 1988. Primary immunodeficiencies in Switzerland: first report of the national registry in adults and children. *J Clin Immunol* 8 (6):479-85.

Sawyers, C. L. 1999. Chronic myeloid leukemia. *N Engl J Med* 340 (17):1330-40.

Schwarz, K., G. H. Gauss, L. Ludwig, U. Pannicke, Z. Li, D. Lindner, W. Friedrich, R. A. Seger, T. E. Hansen-Hagge, S. Desiderio, M. R. Lieber, and C. R. Bartram. 1996. RAG mutations in human B cell-negative SCID. *Science* 274 (5284):97-9.

Shi, J., and D. Zheng. 2009. An update on gene therapy in China. *Curr Opin Mol Ther* 11 (5):547-53.

Shigematsu, H., K. Yasuda, T. Iwai, T. Sasajima, S. Ishimaru, Y. Ohashi, T. Yamaguchi, T. Ogihara, and R. Morishita. 2010. Randomized, double-blind, placebo-controlled clinical trial of hepatocyte growth factor plasmid for critical limb ischemia. *Gene Ther* 17 (9):1152-61.

Shiraishi, K., S. Kato, S. Y. Han, W. Liu, K. Otsuka, M. Sakayori, T. Ishida, M. Takeda, R. Kanamaru, N. Ohuchi, and C. Ishioka. 2004. Isolation of temperature-sensitive p53 mutations from a comprehensive missense mutation library. *J Biol Chem* 279 (1):348-55.

Siegmund, K. H., U. E. Steiner, and C. Richert. 2003. ChipCheck--a program predicting total hybridization equilibria for DNA binding to small oligonucleotide microarrays. *J Chem Inf Comput Sci* 43 (6):2153-62.

Silverman, G. A., P. I. Bird, R. W. Carrell, F. C. Church, P. B. Coughlin, P. G. Gettins, J. A. Irving, D. A. Lomas, C. J. Luke, R. W. Moyer, P. A. Pemberton, E. Remold-O'Donnell, G. S. Salvesen, J. Travis, and J. C. Whisstock. 2001. The serpins are an expanding superfamily of structurally similar but functionally diverse proteins. Evolution, mechanism of inhibition, novel functions, and a revised nomenclature. *J Biol Chem* 276 (36):33293-6.

Srivastava, S., and C. T. Moraes. 2001. Manipulating mitochondrial DNA heteroplasmy by a mitochondrially targeted restriction endonuclease. *Hum Mol Genet* 10 (26):3093-9.

Sun, H. X., H. W. He, S. H. Zhang, T. G. Liu, K. H. Ren, Q. Y. He, and R. G. Shao. 2009. Suppression of N-Ras by shRNA-expressing plasmid increases sensitivity of HepG2 cells to vincristine-induced growth inhibition. *Cancer Gene Ther* 16 (9):693-702.

Symonds, G. P., H. A. Johnstone, M. L. Millington, M. P. Boyd, B. P. Burke, and L. R. Breton. 2010. The use of cell-delivered gene therapy for the treatment of HIV/AIDS. *Immunol Res* 48 (1-3):84-98.

Taha, T. A., W. Osta, L. Kozhaya, J. Bielawski, K. R. Johnson, W. E. Gillanders, G. S. Dbaibo, Y. A. Hannun, and L. M. Obeid. 2004. Down-regulation of sphingosine kinase-1 by DNA damage: dependence on proteases and p53. *J Biol Chem* 279 (19):20546-54.

Tehrani, A. M., S. K. Hwang, T. H. Kim, C. S. Cho, J. Hua, W. S. Nah, J. T. Kwon, J. S. Kim, S. H. Chang, K. N. Yu, S. J. Park, D. R. Bhandari, K. H. Lee, G. H. An, G. R. Beck, Jr., and M. H. Cho. 2007. Aerosol delivery of Akt controls protein translation in the lungs of dual luciferase reporter mice. *Gene Ther* 14 (5):451-8.

Tembe, V., and B. R. Henderson. 2007. BARD1 translocation to mitochondria correlates with Bax oligomerization, loss of mitochondrial membrane potential, and apoptosis. *J Biol Chem* 282 (28):20513-22.

Terlecky, S. R., and J. I. Koepke. 2007. Drug delivery to peroxisomes: employing unique trafficking mechanisms to target protein therapeutics. *Adv Drug Deliv Rev* 59 (8):739-47.

Testa, J. R., and A. Bellacosa. 2001. AKT plays a central role in tumorigenesis. *Proc Natl Acad Sci U S A* 98 (20):10983-5.

Thrasher, A. J., S. Hacein-Bey-Abina, H. B. Gaspar, S. Blanche, E. G. Davies, K. Parsley, K. Gilmour, D. King, S. Howe, J. Sinclair, C. Hue, F. Carlier, C. von Kalle, G. de Saint Basile, F. le Deist, A. Fischer, and M. Cavazzana-Calvo. 2005. Failure of SCID-X1 gene therapy in older patients. *Blood* 105 (11):4255-7.

van Putten, E. H., C. M. Dirven, M. J. van den Bent, and M. L. Lamfers. 2010. Sitimagene ceradenovec: a gene-based drug for the treatment of operable high-grade glioma. *Future Oncol* 6 (11):1691-710.

Vaseva, A. V., N. D. Marchenko, and U. M. Moll. 2009. The transcription-independent mitochondrial p53 program is a major contributor to nutlin-induced apoptosis in tumor cells. *Cell Cycle* 8 (11):1711-9.

Ventura, A., D. G. Kirsch, M. E. McLaughlin, D. A. Tuveson, J. Grimm, L. Lintault, J. Newman, E. E. Reczek, R. Weissleder, and T. Jacks. 2007. Restoration of p53 function leads to tumour regression in vivo. *Nature* 445 (7128):661-5.

Vita, M., and M. Henriksson. 2006. The Myc oncoprotein as a therapeutic target for human cancer. *Semin Cancer Biol* 16 (4):318-30.

Vogelstein, B., D. Lane, and A. J. Levine. 2000. Surfing the p53 network. *Nature* 408 (6810):307-10.

Weatherall, D. J. 1976. Molecular pathology of the thalassemia disorders. *West J Med* 124 (5):388-402.

WHO. 2011. *Cancer* 20112011]. Available from http://www.who.int/mediacentre/factsheets/fs297/en/.

Wolfe, S. A., L. Nekludova, and C. O. Pabo. 2000. DNA recognition by Cys2His2 zinc finger proteins. *Annu Rev Biophys Biomol Struct* 29:183-212.

Wood, B. P. 1997. Cystic fibrosis: 1997. *Radiology* 204 (1):1-10.

Wurzer, G., W. Mosgoeller, M. Chabicovsky, C. Cerni, and J. Wesierska-Gadek. 2001. Nuclear Ras: unexpected subcellular distribution of oncogenic forms. *J Cell Biochem Suppl* Suppl 36:1-11.

Xin, H. 2006. Chinese gene therapy. Gendicine's efficacy: hard to translate. *Science* 314 (5803):1233.

Xue, W., L. Zender, C. Miething, R. A. Dickins, E. Hernando, V. Krizhanovsky, C. Cordon-Cardo, and S. W. Lowe. 2007. Senescence and tumour clearance is triggered by p53 restoration in murine liver carcinomas. *Nature* 445 (7128):656-60.

Yu, W., and H. Fang. 2007. Clinical trials with oncolytic adenovirus in China. *Curr Cancer Drug Targets* 7 (2):141-8.

Zhao, J., T. Tenev, L. M. Martins, J. Downward, and N. R. Lemoine. 2000. The ubiquitin-proteasome pathway regulates survivin degradation in a cell cycle-dependent manner. *J Cell Sci* 113 Pt 23:4363-71

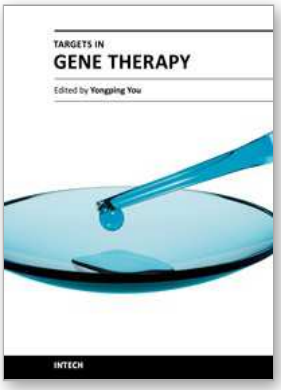

Targets in Gene Therapy

Edited by Prof. Yongping You

ISBN 978-953-307-540-2
Hard cover, 436 pages
Publisher InTech
Published online 23, August, 2011
Published in print edition August, 2011

This book aims at providing an up-to-date report to cover key aspects of existing problems in the emerging field of targets in gene therapy. With the contributions in various disciplines of gene therapy, the book brings together major approaches: Target Strategy in Gene Therapy, Gene Therapy of Cancer and Gene Therapy of Other Diseases. This source enables clinicians and researchers to select and effectively utilize new translational approaches in gene therapy and analyze the developments in target strategy in gene therapy.

How to reference

In order to correctly reference this scholarly work, feel free to copy and paste the following:

Karina J. Matissek, Ruben R. Bender, James R. Davis and Carol S. Lim (2011). Choosing Targets for Gene Therapy, Targets in Gene Therapy, Prof. Yongping You (Ed.), ISBN: 978-953-307-540-2, InTech, Available from: http://www.intechopen.com/books/targets-in-gene-therapy/choosing-targets-for-gene-therapy

INTECH
open science | open minds

InTech Europe
University Campus STeP Ri
Slavka Krautzeka 83/A
51000 Rijeka, Croatia
Phone: +385 (51) 770 447
Fax: +385 (51) 686 166
www.intechopen.com

InTech China
Unit 405, Office Block, Hotel Equatorial Shanghai
No.65, Yan An Road (West), Shanghai, 200040, China
中国上海市延安西路65号上海国际贵都大饭店办公楼405单元
Phone: +86-21-62489820
Fax: +86-21-62489821

Choosing Targets for Gene Therapy in the book Targets for Gene Therapy

Karina J. Matissek, Ruben R. Bender, James R. Davis, Carol S. Lim

InTech Open Access Publisher, July, 2011. ISBN: 978-953-307-540-2

First author contribution:

Manuscript writing: 65%

molecular pharmaceutics

Article

pubs.acs.org/molecularpharmaceutics

Direct Induction of Apoptosis Using an Optimal Mitochondrially Targeted p53

Mohanad Mossalam,[†,‡] Karina J. Matissek,[‡,§] Abood Okal,[†] Jonathan E. Constance,[∥] and Carol S. Lim*[,†]

[†]Department of Pharmaceutics and Pharmaceutical Chemistry, University of Utah, Salt Lake City, Utah 84108, United States

[§]Department of Pharmaceutics and Biopharmacy, Philipps-Universität, 35032 Marburg, Germany

[∥]Department of Pharmacology and Toxicology, University of Utah, Salt Lake City, Utah 84112, United States

Supporting Information

ABSTRACT: Targeting the tumor suppressor p53 to the mitochondria triggers a rapid apoptotic response as efficiently as transcription-dependent p53.[1,2] p53 forms a complex with the antiapoptotic Bcl-XL, which leads to Bak and Bax oligomerization resulting in apoptosis via mitochondrial outer membrane permeabilization.[3,4] Although p53 performs its main role in the mitochondrial outer membrane, it also interacts with different proteins in the mitochondrial inner membrane and matrix.[5,6] To further investigate mitochondrial activity of p53, EGFP-p53 was fused to different mitochondrial targeting signals (MTSs) directing it to the mitochondrial outer membrane ("XL-MTS" from Bcl-XL; "TOM-MTS" from TOM20), the inner membrane ("CCO-MTS" from cytochrome *c* oxidase), or matrix ("OTC-MTS" from ornithine transcarbamylase). Fluorescence microscopy and a p53 reporter dual luciferase assay demonstrated that fusing MTSs to p53 increased mitochondrial localization and nuclear exclusion depending on which MTS was used. To examine if the MTSs initiate mitochondrial damage, we fused each individual MTS to EGFP (a nontoxic protein) as negative controls. We performed caspase-9, TUNEL, annexin-V, and 7-AAD apoptosis assays on T47D breast cancer cells transfected with mitochondrial constructs. Except for EGFP-XL, apoptotic potential was observed in all MTS-EGFP-p53 and MTS-EGFP constructs. In addition, EGFP-p53-XL showed the greatest significant increase in programmed cell death compared to its nontoxic MTS control (EGFP-XL). The apoptotic mechanism for each construct was further investigated using pifithrin-α (an inhibitor of p53 transcriptional activity), pifithrin-μ (a small molecule that reduces binding of p53 to Bcl-2 and Bcl-XL), and overexpressing the antiapoptotic Bcl-XL. Unlike the MTSs from TOM, CCO, and OTC, which showed different apoptotic mechanisms, we conclude that p53 fused to the MTS from Bcl-XL performs its apoptotic potential exclusively through the p53/Bcl-XL specific pathway.

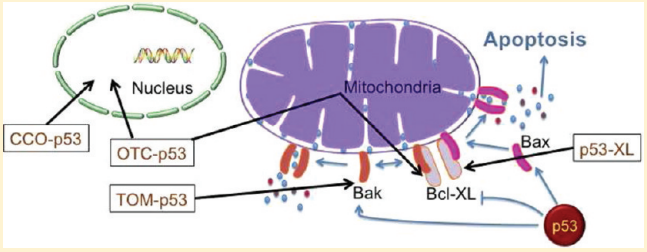

KEYWORDS: *p53, mitochondria, Bcl-XL, apoptosis, pifithrin, T47D*

INTRODUCTION

The tumor suppressor p53 stimulates a wide network of signals involved in DNA repair, cell cycle arrest, senescence, and apoptosis.[7−9] Although most of these effects can be linked to its role as a transcription factor, recent work has clearly demonstrated that p53 can cause apoptosis through its transcription-independent mitochondrial pathway.[3,10] A small but highly reproducible fraction of p53 translocates to the mitochondria at the onset of p53-dependent apoptosis.[10] Translocation of p53 to the mitochondrial outer membrane triggers the release of cytochrome *c* and activation of procaspase-3. The DNA binding domain of p53 (DBD, residues 239−248) forms inhibitory complexes with antiapoptotic Bcl-XL and Bcl-2 proteins (Figure 1), which are located in the mitochondrial outer membrane.[11] This induces oligomerization of Bak and Bax, allowing them to form supramolecular pores.[4,12,13] In addition, p53 activates, directly binds to, and induces oligomerization of Bak and Bax.[4,13,14] The formation of permeability transition pores causes outer membrane rupture and releases cytochrome *c* from the intramembranous space into the cytosol triggering apoptosis via the apoptosome (Figure 1).[15−17] In addition, targeting p53 to the mitochondria triggers apoptosis faster than the transcription-dependent nuclear pathway.[1,2] In most cancer cells, p53 is not able to bind to Bcl-2 proteins due to missense mutations in the DBD of p53, demonstrating the importance of the DBD in mitochondrial apoptosis.[11]

The therapeutic effect of pharmaceutical agents such as p53 may differ depending on their intracellular delivery.[18] Precise compartmentalization and subcompartmentalization of proteins are essential for their biological activity. The majority of endogenous mitochondrial p53 localizes to the outer surface of the mitochondria,[19] which occurs after either DNA damage or hypoxic stress.[10] A detailed mechanism on how p53 translocates

Received: January 12, 2012
Revised: February 21, 2012
Accepted: March 1, 2012
Published: March 1, 2012

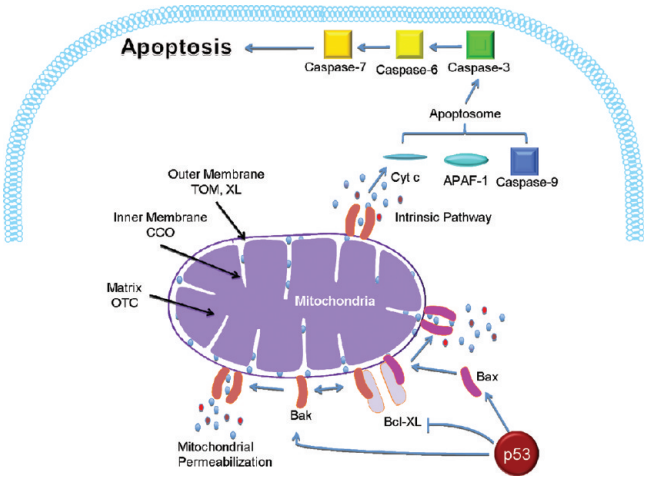

Figure 1. The mitochondrial apoptotic pathway of p53. When p53 is targeted to the mitochondria, it interacts with antiapoptotic Bcl-XL, enables Bax and Bak oligomerization, and activates the intrinsic apoptotic pathway. The apoptosome (cytochrome *c*, APAF-1, and caspase-9) is triggered, leading to apoptosis via activation of caspases-3, -6, and -7. The left side of the diagram indicates the mitochondrial signals (MTSs) used and the different subsections of the mitochondria targeted, including the outer membrane ("XL-MTS" from Bcl-XL; "TOM-MTS" from TOM20), the inner membrane ("CCO-MTS" from cytochrome *c* oxidase), and the matrix ("OTC-MTS" from ornithine transcarbamylase).

into the mitochondria is still under investigation since it is a nuclear protein due to its nuclear localization signals.[20] A study has shown that Bad (Bcl-2 antagonist of cell death) physically interacts with cytoplasmic p53 directing it to the surface of the mitochondria.[21,22] Moll has suggested that p53 is imported via mtHsp70 targeting the membranous compartments.[10] The interaction with mtHsp70 and Hsp60 is increased with the R72P polymorphism in p53 due to elevation in nuclear export of p53.[23] MDM2 protein is responsible for the nuclear exclusion and ubiquitylation of p53. The monoubiquitylated p53 is targeted to the mitochondria under stress, which disrupts the p53/MDM2 complex.[24]

Despite what is known, exogenous mitochondrial targeting of p53 is still under investigation. To improve apoptosis via the p53/Bcl-XL pathway, p53 was delivered to different mitochondrial compartments. In this study, p53 was fused to different mitochondrial targeting signals (MTSs) targeting the mitochondrial outer membrane [MTS from Bcl-XL or MTS from the translocase of the outer membrane (TOM 20)], inner membrane (MTS from cytochrome *c* oxidase subunit VIII), and matrix (MTS from ornithine transcarbamylase) (Figure 1). MTSs (Table 1) are generally thought to form α-helices and are important for their recognition by translocation machineries in the mitochondrial outer (TOM complex) and inner (TIM complex) membranes.[25−28] Since MTSs are mainly found on the amino terminus of mitochondrial proteins,[25] all MTSs used were cloned on the amino terminus except for XL, which is inherently found on the carboxy terminus.[29] XL targets the outer surface of the mitochondria[29−32] while TOM is inserted into the outer membrane;[29] CCO translocates the outer membrane and then becomes imbedded into the inner membrane[33,34] while the OTC crosses both membranes and translocates to the matrix.[3,35] The purpose of this work is to determine the ideal MTS for p53 mitochondrial targeting to induce the intrinsic apoptotic pathway.

MATERIALS AND METHODS

EGFP-p53 Plasmid (pEGFP-p53). The DNA encoding p53 was amplified through PCR from pCMV-p53 wt (a generous gift from Dr. S. J. Baker, Addgene, Cambridge, MA) using the primers 5′-GCGCGCGCGCTCCGGAGCCATGGAGGAGCCG-CAGT-3′ and 5′-GCGCGCGCGCGGTACCTCAGTCTGAGT-CAGGCCCTTCTGTC-3′. This was subcloned into the *Bsp*EI and *Kpn*I restriction enzyme sites in pEGFP-C1 (Clontech, Mountain View, CA).

pOTC-EGFP-p53 Plasmid. An oligonucleotide encoding the mitochondrial targeting signal from OTC (including the Kozak region), 5′-CCGGTCGCCACCATGCTGTTTAATCT-GAGGATCCTGTTAAACAATGCAGCTTTTAGAAATGGT-CACAACTTCATGGTTCGAAATTTTCGGTGTGGA-CAACCACTACAAAATAAAGTGCAGCGA-3′ was annealed to its complementary strand. This was then cloned at the amino terminus of EGFP-p53 at the *Age*I site.

pTOM-EGFP-p53 and pCCO-EGFP-p53 Plasmids. The OTC region from pOTC-EGFP-p53 was replaced with annealed oligonucleotides encoding the mitochondrial targeting signal from the TOM20 complex (TOM) at the *Age*I site, 5′-GATCCCCGGTCGCCACCATGGTGGGTCGGAA-CAGCGCCATCGCCGCCGGTGTATGCGGGGCCCTTTT-CATTGGGTACTGCATCTACTTCGACCGCAAAAGAC-GAAGTGACCCCAACCGA-3′ and its reverse complement, or with oligonucleotides encoding the mitochondrial targeting signal from the cytochrome *c* oxidase (CCO) at the *Age*I site, 5′-CCGGTCGCCACCATGTCCGTCCTGACGCCGCTGCT-GCTGCGGGGCTTGACAGGCTCGGCCCGGCGGCTCC-CAGTGCCGCGCGCCAAGATCCATTCGTTGA-3′ and its reverse complement.

pEGFP-p53-XL Plasmid. The mitochondrial signal from Bcl-XL was fused to the carboxy terminus of EGFP-p53 using the *Bam*HI restriction site as follows. The XL oligonucleotide 5′-AGAAAGGGCCAGGAGAGATTCAACAGATGGTTCCT-GACCGGCATGACCGTGGCCGGCGTGGTGCTGCTGGG-CAGCCTGTTCAGCAGAAAGTGA-3′ was annealed to its complementary strand (with *Bam*HI sticky ends). The p53 stop codon was then mutated (TGA to TTA) in pEGFP-p53-XL using the primers 5′-GAAGGGCCTGACTCAGACTTAGG-TACCGCGGGCCCGGGAT-3′ and the reverse complement.

Table 1. A List of the Mitochondrial Targeting Signals Used in This Paper[a]

protein	compartment	MTS sequence
XL	outer membrane	RKGQERFNRWFLTGMTVAGVVLLGSLFSRK
TOM	outer membrane	MVGRNSAIAAGVCGALFIGYCIYFDRKRRSDPN
CCO	inner membrane	MSVLTPLLLRGLTGSARRLPVPRAKIHSL
OTC	matrix	MLFNLRILLNNAAFRNGHNFMVRNFRCGQPLQNKVQ

[a]TOM and XL target the mitochondrial outer membrane, CCO translocates to the mitochondrial inner membrane, and the OTC localizes to the mitochondrial matrix.

dx.doi.org/10.1021/mp3000259 | *Mol. Pharmaceutics* 2012, 9, 1449−1458

pEGFP Constructs with MTSs. Plasmids encoding OTC-EGFP, TOM-EGFP, CCO-EGFP, and EGFP-XL were constructed using the same oligonucleotides and restriction sites mentioned above but inserted in pEGFP-C1 instead of pEGFP-p53.

pMTS-EGFP-p53NLSmut. Mutations (K319T and K320T) in the nuclear localization signal (NLS) of p53 were introduced in all mitochondrial p53 constructs via QuikChange II XL Site-Directed Mutagenesis Kit (Agilent, Santa Clara, CA) using the primers 5′-CTCTCCCCAGCCAACGACGAAACCACTGG-3′ and its reverse complement.

Cell Lines and Transient Transfections. 1471.1 murine adenocarcinoma cells (gift of G. Hager, NCI, NIH), MCF-7 human breast adenocarcinoma cells (ATCC, Manassas, VA), and T47D human ductal breast epithelial tumor cells (ATCC) were grown as monolayers in DMEM (1471.1) or RPMI (MCF-7 and T47D) (Invitrogen, Carlsbad, CA), supplemented with 10% fetal bovine serum (Invitrogen), 1% penicillin−streptomycin−glutamine (Invitrogen), and 0.1% gentamicin (Invitrogen). In addition, T47D and MCF-7 medium was supplemented with 4 mg/L insulin (Sigma, St. Louis, MO). The cells were maintained in a 5% CO_2 incubator at 37 °C. 7.5×10^4 cells for 1471.1 and 3.0×10^5 cells for MCF-7 and T47D were seeded in 6-well plates (Greiner Bio-One, Monroe, NC) or 2-well live cell chambers (Nalgene Nunc, Rochester, NY). Transfections were carried out 24 h after seeding using Lipofectamine 2000 (Invitrogen) following the manufacturer's recommendations. Unless otherwise indicated, 1 pmol of DNA was transfected per well for all assays.

Mitochondrial Staining, Microscopy, and Image Analysis. Prior to live-cell imaging and mitochondrial staining, medium in live cell chambers was replaced with phenol red-free DMEM (Invitrogen) for 1471.1 cells or phenol red-free RPMI (Invitrogen) for T47D and MCF-7 cells containing 10% charcoal-stripped fetal bovine serum (CS-FBS, Invitrogen). Cells were incubated with 250 nM MitoTracker Red FM (Invitrogen) for 15 min at 37 °C and protected from light. Images were acquired as previously,[36] using an Olympus IX71F fluorescence microscope (Scientific Instrument Company, Aurora, CO) with high-quality narrow band GFP filter (ex, HQ480/20 nm; em, HQ510/20 nm) and HQ:TRITC filter (ex, HQ545/30; em, HQ620/60) from Chroma Technology (Brattleboro, VT) with a 40× PlanApo oil immersion objective (NA 1.00) on an F-View Monochrome CCD camera. Images were analyzed for mitochondrial stain overlap with EGFP fusion constructs using ImageJ software and the JACoP plugin.[37] JACoP was used to generate the colocalization statistic [i.e., Pearson's correlation coefficient (PCC) post Costes' automatic threshold algorithm],[38,39] as we have done before.[40] PCC evaluates correlation between pairs of individual pixels from EGFP and MitoTracker stained cells. The higher the PCC value, the higher the correlation. For increased visual clarity of mitochondrial localization of the EGFP-fused constructs, spatial representations of pixel intensity correlation have been generated using Colocalization Colormap (ImageJ).[41] Microscopy was repeated in triplicate ($n = 3$), and 10 cells were analyzed for each construct.

Luciferase Assay. All constructs (3.5 μg of DNA) were cotransfected with 3.5 μg of p53-Luc Cis-Reporter (encoding for firefly luciferase, Agilent) in T47D and MCF-7 cells. To normalize for transfection efficiency, 0.35 μg of pRL-SV40 plasmid (encoding for renilla luciferase, gift from Dr. Philip Moos, University of Utah) was cotransfected. The Dual-Glo Luciferase Assay System (Promega, Madison, WI) was used to determine firefly luciferase activity and renilla luciferase per manufacturer's instructions. Luciferase activity was detected 24 h after transfection using PlateLumino (Stratec Biomedical Systems, Birkenfeld, Germany). Firefly luciferase values were normalized for renilla luciferase. EGFP-p53 served as a positive control and EGFP as a negative control. The Dual-Glo Luciferase Assay was run three times independently, each in triplicate.

Caspase-9 Assay. T47D cells were probed 19 h after transfection using CaspaLux9-M_2D_2 kit (OncoImmunin, Inc., Gaithersburg, MD) per manufacturer's recommendations. The cells were then suspended in flow cytometry buffer (OncoImmunin, Inc.) and analyzed via the FACSAria-II (BD-BioSciences, University of Utah Core Facility) utilizing 488 nm (for EGFP) and 563 nm (for cleaved caspase 9 substrate) lasers. FACSDiva software was used as an evaluation tool. Only EGFP transfected cells at 507 nm emission were analyzed. All constructs were gated at the same EGFP intensity levels to ensure equal expression of proteins. The samples were detected in the PE (phycoerythrin) channel with the 580 nm emission peak. Each construct was assayed three times ($n = 3$).

TUNEL Assay. T47D cells were prepared 48 h after transfection using In Situ Death Detection Kit, TMR red (Roche, Mannheim, Germany) per the company's protocol. The kit labels the DNA single strand breaks (TUNEL reaction) in apoptotic cells. The FACSAria-II was used to analyze the cells suspended in PBS (Invitrogen). The same FACS settings mentioned above with the caspase-9 assay were used. Only EGFP-positive cells were analyzed for DNA segmentation. Each construct was analyzed three times ($n = 3$).

Annexin-V Assay. At 48 h post transfection, T47D cells were assayed for annexin-V binding. The cells were suspended in 100 μL of annexin binding buffer (Invitrogen) and incubated with 5 μL of annexin−APC (annexin-V conjugated to allophycocyanin, Invitrogen) for 15 min. The incubated cells were then diluted in 400 μL of annexin binding buffer and analyzed using the FACSCanto-II (BD-BioSciences, University of Utah Core Facility) with FACSDiva software. EGFP was excited at 488 nm wavelength and detected at 507 nm. APC was excited with 635 nm laser and detected at 660 nm. Analysis was based on EGFP positive cells. All constructs were gated at the same EGFP intensity levels. Each construct was tested three times ($n = 3$).

7-AAD Assay. T47D and MCF-7 cells were stained with 7-aminoactinomycin D (7-AAD, Invitrogen) according to manufacturer's instructions 48 h after transfection. The samples were analyzed using the FACSCanto-II (BD-BioSciences). Analyzed cells were gated for EGFP (as mentioned in Annexin-V Assay). In addition, EGFP and 7-AAD were excited with the 488 nm laser. EGFP and 7-AAD were detected at 507 and 660 nm, respectively. Each construct was assayed three times ($n = 3$).

Rescue Experiment Using Pifithrin-α. Six hours after transfection, T47D cells were incubated with a previously optimized concentration of 40 μM pifithrin-α (Cayman Chemical, Ann Arbor, MI) for 42 h and compared to transfected cells without pifithrin-α. At the 48 h time point, the 7-AAD assay was performed as above.

Rescue Experiment Using Pifithrin-μ. Six hours after transfection, T47D cells were incubated with a previously optimized concentration of 5 nM pifithrin-μ (Tocris Bioscience, Ellisville, MO) for 42 h and compared to transfected cells without pifithrin-μ. At the 48 h time point, the 7-AAD assay was performed as detailed above.

Rescue Experiment Using Bcl-XL. T47D cells were cotransfected with 1 pmol of MTS constructs and 1 pmol of pBcl-XL (Addgene). After 48 h, cells were pelleted and assayed with 7-AAD as described above.

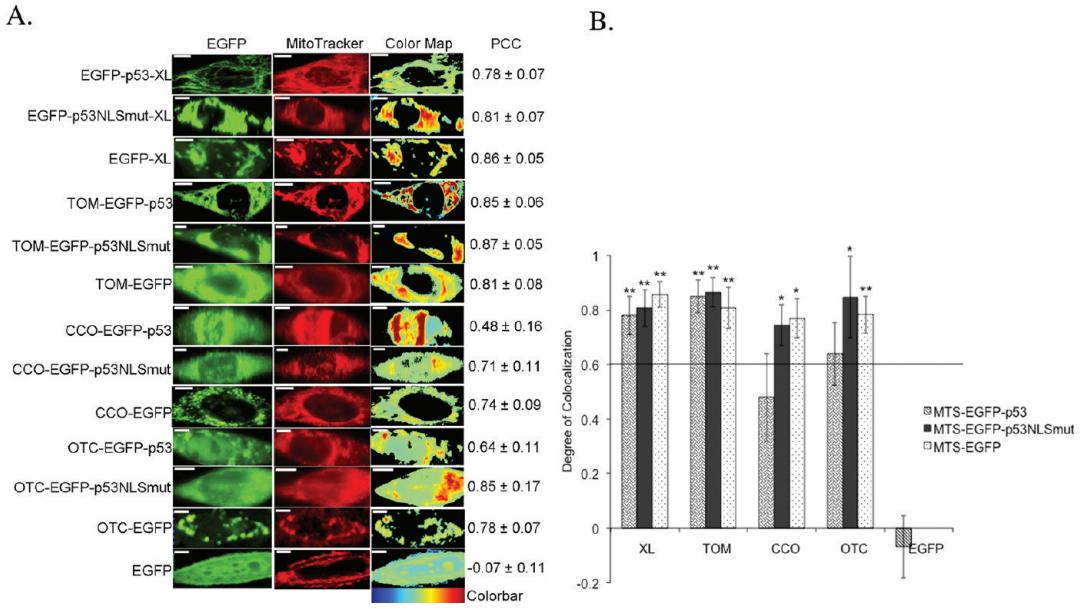

Figure 2. Colocalization of MTS constructs and MitoTracker Red mitochondrial stain in 1471.1 cells. (A) Representative images of MTS-EGFP-p53, MTS-EGFP-p53 NLS mutation, MTS-EGFP, and EGFP-C1 are shown in the left column with images of MitoTracker Red distribution in the middle column. The "EGFP" and "MitoTracker" columns have been false colored green and red, respectively. Enhanced visualization of colocalized pixels is rendered in the "Color Map" column. Warm colors depict pixels with highly correlated intensity and spatial overlap while cool colors are indicative of anticorrelation or random correlation (colorbar for interpretation is shown below column). Corresponding PCC values are shown in the right column. White scale bars are all 10 μm. (B) The degree of colocalization is represented by PCC following Costes' approach.[38,39] All constructs with values higher than 0.6 are considered highly colocalized with mitochondrial stain MitoTracker Red. Statistical analysis was performed by using odds ratio with Pearson's Chi-square. The adjusted odds ratio for PCC value of 0.6 was compared with each sample. *$p < 0.05$, and **$p < 0.01$ comparing odds ratio of lowest value for samples with odds ratio of 1 for PCC of 0.6.

Statistical Analysis. All experiments were repeated in triplicate ($n = 3$). The data were presented as the mean ± standard error. Statistical differences between each MTS-EGFP-p53 and its MTS-EGFP were resolved via unpaired t test using GraphPad Prism software. The MTS-EGFP controls were compared to EGFP by one-way ANOVA with Tukey's post test. The degree of colocalization was analyzed using odds ratio with Pearson's Chi-square. A p value <0.05 was considered significant.

RESULTS

Mitochondrial Localization of MTS-EGFP-p53. Mitochondrial targeting of all constructs was verified using fluorescence microscopy. Figure 2A shows representative 1471.1 cells, which are larger in size, spread well, and are generally easier to visualize versus T47D or MCF-7 cells. However, irrespective of the cell line, similar microscopy results were observed in T47D and MCF-7 cells (data not shown). To better illustrate the colocalization of the EGFP fused constructs, PCC values were generated and graphed for each construct (Figure 2B). PCC values range from +1 to −1; perfect correlation is represented by +1, anticorrelation by −1, and a PCC value of zero denotes random distribution.[37] Following the example of Bolte and Cordelières, a PCC of 0.6 or greater will define colocalization, or cocompartmentalization (Figure 2B).[37,40] Fusing different MTSs to EGFP and p53 showed a high degree of colocalization with the mitochondria. EGFP-C1 served as negative control for colocalization analysis, and as expected, there was no colocalization between EGFP alone and the mitochondria. EGFP and p53 tagged to TOM and XL targeted the mitochondria better than CCO-EGFP-p53 and OTC-EGFP-p53. CCO and OTC were the "weakest" MTSs since there was some nuclear targeting of both CCO-EGFP-p53 and OTC-EGFP-p53. Therefore we mutated K319T and K320T in the nuclear localization signal (NLS) of p53,[20] which resulted in increased mitochondrial targeting for CCO-EGFP-p53 and OTC-EGFP-p53. For easier visualization of colocalization among constructs, a spatial depiction of pixel overlap and intensity correlation are provided in the "Color Map" column (Figure 2A). The Color Map spectrum moves from cold to warm colors as pixel correlation increases.[41]

Testing the Transcriptional Activity of MTS-EGFP-p53. To demonstrate the lack of transcriptional activity of these p53 constructs, a p53 reporter dual luciferase assay was performed in T47D (Figure 3A) and MCF-7 cells (Figure 3B). T47D cells contain a mutation in p53 (in the DBD which renders it inactive) that is also localized in the cytoplasm[42,43] while MCF-7 cells express wild-type p53 mislocalized to the cytoplasm.[44] TOM and XL fused to EGFP-p53 showed no nuclear activity in either cell line. CCO-EGFP-p53 expressed similar transcriptional activity to EGFP-p53 (positive control) in T47D (Figure 3A) and significant activity in MCF-7 (Figure 3B) compared to the EGFP negative control. Introducing NLS mutations (K3319T and K320T) in CCO-EGFP-p53 resulted in major reduction of nuclear activity in both cell lines. OTC-EGFP-p53 showed low transcriptional activity in MCF-7 (Figure 3B) and a significant activation in T47D cells (Figure 3A). Surprisingly, introduction of NLS mutations into OTC-EGFP-p53 did not result in any changes in nuclear activity in either cell line (Figures 3A and 3B).

The Effect of MTS-EGFP-p53 on Early Apoptosis (Caspase-9). In this paper we focused on T47D cells because they are more resistant to apoptosis compared to MCF-7 cells.[45] The apoptotic potential of p53 fused to different MTSs targeting the mitochondrial matrix, outer, and inner membranes was

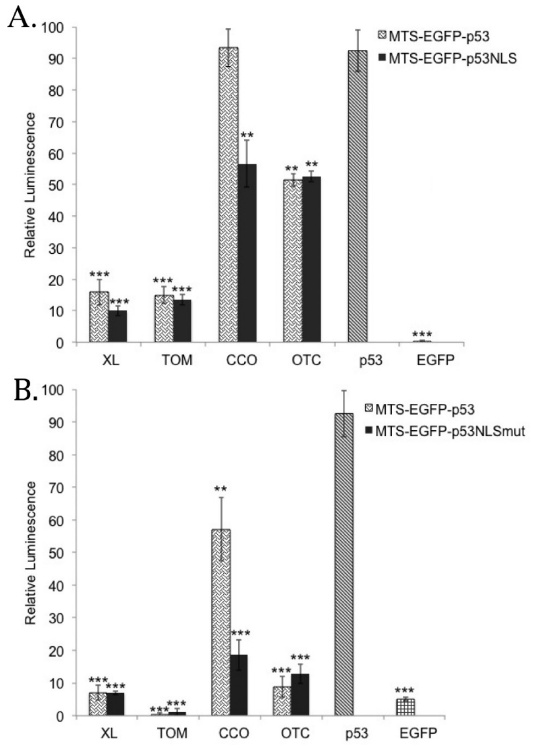

Figure 3. Luciferase assay: All MTS-EGFP-p53 and MTS-EGFP-p53 NLS mutation constructs were tested for their ability to activate a p53 reporter in (A) T47D cells and (B) MCF-7 cells. EGFP-p53 serves as a positive control and EGFP as a negative control. All constructs were corrected to EGFP-p53 control, which is set at 100%. Statistical analysis was performed by using one-way ANOVA with Tukey's post test. $^{**}p < 0.005$ and $^{***}p < 0.0005$ compared to EGFP-p53.

evaluated via caspase-9, TUNEL, annexin-V, and 7-AAD assays. Caspases are a group of proteolytic enzymes that are directly involved in apoptosis by cleaving proteins such as lamin and PARP. Its inactive form procaspase-9 is activated through cytochrome *c* release and APAF-1 which occurs after mitochondrial outer membrane disruption (known as the intrinsic apoptotic pathway).[46] Caspase-9 itself cleaves the peptide sequence LEHD, which was used in the caspase-9 assay to measure the intrinsic apoptotic pathway.[47] Only EGFP-p53-XL ($p < 0.05$) and OTC-EGFP-p53 ($p < 0.05$) were significantly different from their corresponding MTS-EGFP controls as shown in Figure 4.

The Effect of MTS-EGFP-p53 on DNA Fragmentation. Terminal deoxynucleotidyl transferase dUTP nick end labeling (TUNEL) was measured to detect DNA fragmentation by labeling the terminal end of nucleic acids. DNA fragmentation is a hallmark of apoptosis and is generated by caspase cleavage.[48] Figure 5 illustrates that EGFP-p53-XL and CCO-EGFP-p53 are the only constructs that were statistically significant from their control MTS-EGFP. Constructs with mutations in the NLS of p53 did not differ from constructs without mutation (see the Supporting Information: S1). Staurosporine, which activates caspase-3/7 and leads to DNA fragmentation,[45] served as a positive control.

The Effect of MTS-EGFP-p53 on Plasma Membrane. The effects of the mitochondrial constructs were further explored by analyzing externalization of phosphatidylserine and cell membrane rupture. Annexin-V was used to detect the externalization of phosphatidylserine on the cell surface of apoptotic cells

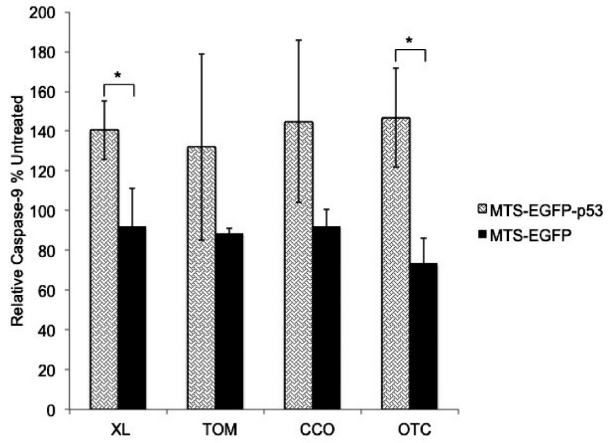

Figure 4. The activation of caspase-9 was analyzed 19 h following transfection of T47D cells. All constructs were corrected to untreated control, which is set at 100%. Statistical analysis was performed by using unpaired *t* test. $^{*}p < 0.05$ for MTS-EGFP-p53 compared to its MTS-EGFP.

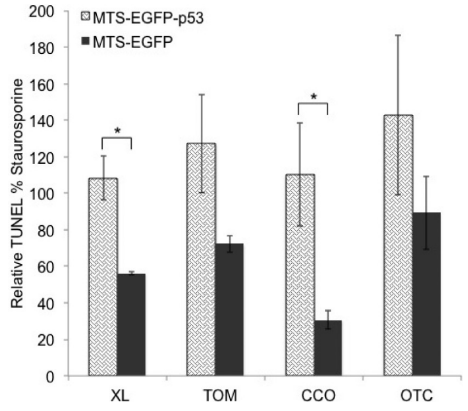

Figure 5. T47D cells were tested 48 h following transfection. DNA fragmentation was analyzed with the TUNEL assay. All constructs were corrected to staurosporine positive control, which is set at 100%. Statistical analysis was performed by unpaired *t* test. $^{*}p < 0.05$ for MTS-EGFP-p53 compared to its MTS-EGFP.

via flow cytometry.[49,50] In the majority of healthy cells, the plasma membrane expresses phosphatidylserine on the cytosolic surface while in apoptotic cells, the phosphatidylserine is transported to the outer surface, which allows labeled annexin-V to bind.[51] All MTS-EGFP-p53 constructs showed a significant effect on inducing apoptosis compared to their corresponding MTS-EGFP controls in T47D cells (Figure 6). In addition, EGFP-XL was the only construct that showed minimal activity similar to the nontoxic EGFP negative control (Figure 6).

To further validate the effect of mitochondrial p53 on late apoptosis, the 7-AAD assay was performed via flow cytometry (Figure 7). The 7-AAD fluorescent marker cannot stain the DNA in healthy cells due to inability to penetrate an intact cell membrane.[52] However, it is able to stain the DNA in apoptotic and necrotic cells because of their disrupted membrane.[53] Similar to annexin-V results, all mitochondrial p53 constructs showed significant 7-AAD intercalation with DNA compared to their MTS-EGFP controls (Figure 7A). In addition, EGFP-XL was the only construct that showed similar activity to EGFP alone (Figure 7A). In a cell line that is less resistant to apoptosis such as MCF-7,[45] EGFP-p53-XL is the only construct that was

dx.doi.org/10.1021/mp3000259 | *Mol. Pharmaceutics* 2012, 9, 1449–1458

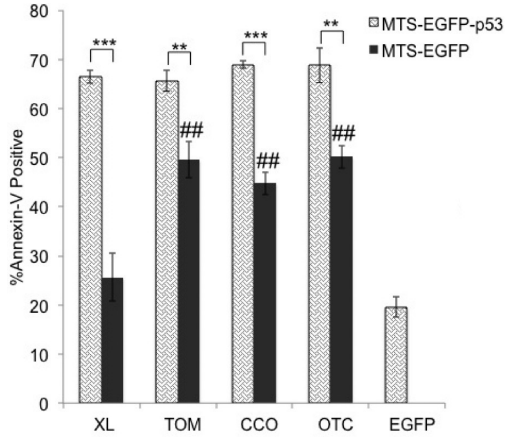

Figure 6. Annexin-V assay was conducted in T47D cells 48 h after transfection. Statistical analysis was performed by one-way ANOVA with Tukey's post test. $^{**}p < 0.005$ and $^{***}p < 0.0005$ comparing MTS-EGFP-p53 to their MTS-EGFP controls. The negative controls (MTS-EGFP) were compared to EGFP-C1 using one-way ANOVA with Tukey's post test $^{\#\#}p < 0.005$.

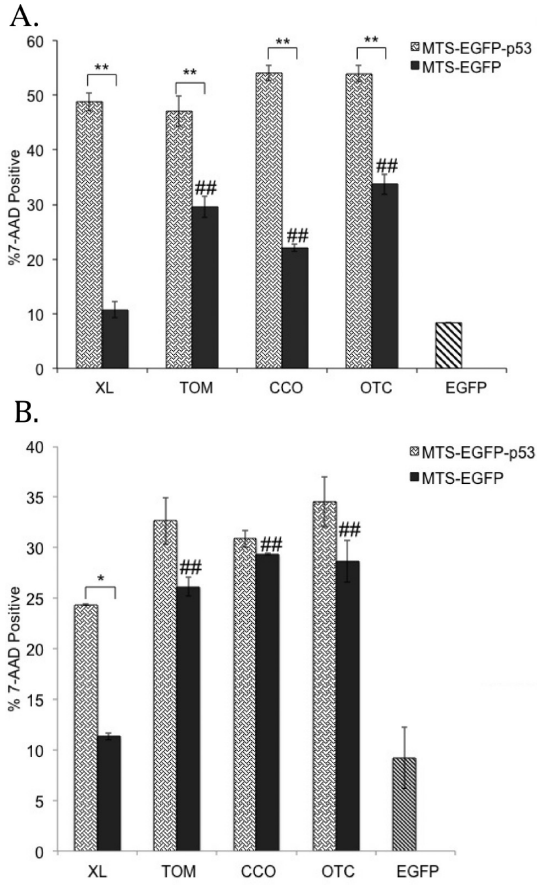

Figure 7. The 7-AAD assay was tested in (A) T47D and (B) MCF-7 cells 48 h after transfection. Statistical analysis was performed by one-way ANOVA with Tukey's post test. $^{*}p < 0.05$, $^{**}p < 0.005$ comparing MTS-EGFP-p53 to their MTS-EGFP controls. The controls (MTS-EGFP) were compared to EGFP-C1 using one-way ANOVA with Tukey's post test $^{\#\#}p < 0.005$.

significantly different from its MTS-EGFP control (Figure 7B). In MCF-7 cells, there was no statistical difference between p53 fused to TOM, CCO, or OTC and their respective MTS-EGFP controls (Figure 7B). Mutating the NLS of p53 in MTS-EGFP-p53 had no effect on 7-AAD permeation in both cell lines except with CCO-EGFP-p53 in T47D (see the Supporting Information: S2). In addition, EGFP-XL showed no activity similar to EGFP alone in MCF-7 (Figure 7B). Similar to annexin-V, EGFP-XL was also the only construct with minimum activity as EGFP alone in T47D cells (Figure 7A).

Investigating the Apoptotic Mechanism. Apoptosis resulting from p53 transcriptional activity of our mitochondrial p53 constructs was examined via a pifithrin-α rescue experiment. Pifithrin-α is a small molecule that inhibits p53-mediated transcriptional activity.[54,55] The effect of pifithrin-α was measured in a 7-AAD assay (Figure 8A). As expected from the

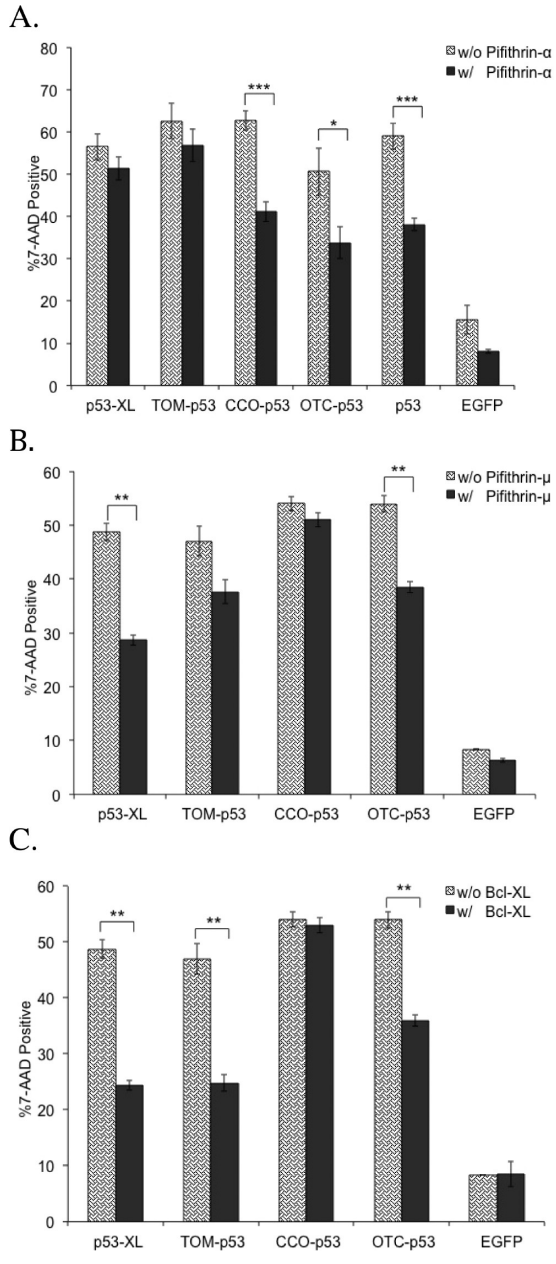

Figure 8. Rescue experiments using (A) pifithrin-α, (B) pifithrin-μ, or (C) Bcl-XL. 7-AAD assay was performed 48 h after transfection in T47D cells. All constructs were fused to EGFP. Statistical analysis was performed by unpaired t test. $^{*}p < 0.05$, $^{**}p < 0.005$, $^{***}p < 0.0005$ comparing treated (with pifithrin-α, pifithrin-μ, or Bcl-XL) to untreated (no drug or Bcl-XL added).

dx.doi.org/10.1021/mp3000259 | Mol. Pharmaceutics 2012, 9, 1449–1458

transcriptional activity data, the apoptotic effect of EGFP-p53 fused to either CCO or OTC was reduced significantly after pifithrin-α treatment. In addition, there was no impact on the apoptotic potential of EGFP-p53 fused to either XL or TOM (Figure 8A).

In order to investigate p53's apoptotic mechanism in the mitochondria, pifithrin-μ was used in a rescue experiment in the 7-AAD assay. Pifithrin-μ is a compound that reduces the binding affinity of p53 to the antiapoptotic proteins, Bcl-2 and Bcl-XL.[56,57] Pifithrin-μ had a significant impact on the apoptotic potential of p53 fused to both XL and OTC (Figure 8B). However, apoptosis caused by p53 fused to either TOM or CCO was not rescued by pifithrin-μ. In addition, all the MTS-EGFP controls were not altered in this rescue experiment (see the Supporting Information: S3A).

The apoptotic mechanism was further explored by overexpression of the antiapoptotic protein, Bcl-XL. The cells were then analyzed in the 7-AAD assay via flow cytometry. Bcl-XL had a significant effect on reducing 7-AAD positive cells treated with EGFP-p53 fused to TOM, XL, and OTC (Figure 8C). Cells treated with EGFP-p53-XL showed the most significant reduction in 7-AAD when cotransfected with Bcl-XL. Meanwhile, Bcl-XL had no effect on cells transfected with CCO-EGFP-p53. In addition, all the MTS-EGFP controls were not altered in this rescue experiment (see the Supporting Information: S3B).

DISCUSSION

The tumor suppressor p53 was targeted with different MTSs in order to investigate its optimal mitochondrially triggered apoptotic pathway. We hypothesized that it might be possible that sending any protein (even EGFP) to mitochondria could be "toxic" to cells by disruption of mitochondrial function. Fusing p53 to MTSs targeting the mitochondrial outer membrane, inner membrane, and matrix did indeed result in apoptosis. However, sending even EGFP to the mitochondrial matrix (OTC), the inner membrane (CCO), or the TOM complex (TOM) perturbed mitochondrial stability as evidenced by the apoptotic assays. Only p53-XL was capable of inducing mitochondrial apoptosis exclusively via mitochondrial p53/Bcl-XL pathway.

Directing EGFP to the matrix and inner membrane via OTC and CCO, respectively, resulted in late stage apoptosis. This shows that fusing EGFP to OTC or CCO has a toxic effect on the mitochondria. We speculate that sending EGFP to the mitochondrial matrix and inner membrane could cause an imbalance in the sensitive mitochondrial system due to import through mitochondrial membranes. On the other hand, targeting EGFP to the mitochondrial outer membrane using TOM and XL shows minimal toxicity with XL but significant toxicity with TOM. Since EGFP-XL is directed toward Bcl-XL[58] on the surface of the outer membrane,[29−31] it is not expected to become imbedded into the mitochondrial membrane. Conversely, the TOM-EGFP may interfere with TOM20 involved in mitochondrial import machinery.[18,59] The TOM complex is responsible for importing proteins across the mitochondrial outer membrane. TOM20 is one of the receptor subunits in the TOM complex.[60,61] Perhaps fusing any protein to the MTS from TOM20 might affect the sensitive import mechanism.

As p53 is a nuclear protein, the MTS fused to it will compete with the protein's nuclear localization signals (NLSs). p53 contains three NLSs; the most active of them is located at residues 305−322.[20] The nuclear import of large proteins is dependent on the availability of a NLS.[62−64] To prevent the nuclear targeting of our constructs, we introduced mutations (K319T and K320T) in the strongest NLS of p53.[20] Colocalization data and p53 transcriptional activity assay showed an increase in mitochondrial targeting and a decrease in p53 nuclear activity after the introduction of the NLS mutations in CCO-p53. According to our colocalization data, CCO-EGFP showed the lowest mitochondrial targeting compared to the other MTS-EGFP (Figure 2). The weak mitochondrial CCO signal explains the high transcriptional activity when fused to p53 without NLS mutations (Figure 3). The strong NLS in p53 competes with the relatively weak MTS from CCO and shifts the distribution to the nucleus. After mutating the strong NLS, the CCO MTS was also in competition with the other weak NLSs in p53,[20] which may explain why the CCO-p53 NLS mutation still showed transcriptional activity (Figure 3). However, the mutations did not have any effect on the mitochondrial targeting or nuclear activity of the TOM, XL, and OTC constructs. EGFP-p53 fused to TOM and XL showed minimal nuclear p53 activity presumably due to their strong mitochondrial signals. Introducing NLS mutations to p53 fused to TOM or XL did not show any reduction on the already low transcriptional activity (Figure 3). On the other hand, OTC-p53 showed significant p53 nuclear activity but was not reduced upon NLS mutation (Figure 3).

In addition, the nuclear activity of MTS-p53 differed between MCF-7 and T47D. These differences might be due to variability in proteins involved with p53 transcriptional activity, mitochondrial shuttling, or number of mitochondria in each cell line. In MCF-7, all MTS-p53 constructs (with or without NLS mutations) showed minimum transcriptional activity except for the CCO-p53, which had half the activity of wild type p53 (Figure 3B). However, in T47D cells all MTS-p53 constructs showed generally higher nuclear activity than in MCF-7, especially CCO-p53, which showed the same nuclear activity as wild type p53. CCO-p53 NLS mutation and OTC-p53 (with and without NLS mutation) showed fifty percent transcriptional activity in T47D (Figure 3A).

Even though the NLS mutations increased mitochondrial targeting of the CCO-p53 construct, it did not have any effect on increasing the apoptotic potential. This was also the case for NLS mutations in all other constructs (see the Supporting Information: S1 and S2). CCO-p53 was significant compared to its CCO-EGFP control in TUNEL, annexin-V, and 7-AAD assays. Since CCO-EGFP showed cytotoxicity, the increase in apoptosis when attached to p53 was likely due to nuclear p53 activity. This is reflected in our luciferase assay (Figure 3) and the rescue experiments with pifithrin-α, pifithrin-μ, and Bcl-XL (Figure 8). The apoptotic activity of CCO-p53 was reduced in the pifithrin-α (an inhibitor of p53 transcriptional activity) rescue experiment. However, it was not rescued by either overexpression with the antiapoptotic Bcl-XL or incubation with pifithrin-μ (an inhibitor of p53 binding to Bcl-2 and Bcl-XL).[56,57] This demonstrates that CCO-p53 does not initiate p53/Bcl-XL specific apoptosis.

OTC-p53 also showed transcriptional activity. In addition, OTC-p53 exhibited significant caspase-9 induction, and late stage apoptosis compared to its cytotoxic OTC-EGFP control. To examine if the increase of activity was due to nuclear or mitochondrial p53, the rescue experiments (with pifithrin-μ and Bcl-XL) were conducted and showed reduction in programmed cell death (Figure 8). This indicates that apoptosis was likely initiated through p53 binding to Bcl-XL and Bcl-2. In addition, the transcriptional activity data demonstrates that OTC-p53 has activity in both the nucleus (rescued by pifithrin-α) and the mitochondria (rescued by pifithrin-μ and Bcl-XL). Even though

Table 2. A Summary of Collected Data and Speculated Mechanism[a]

MTS	XL	TOM	CCO	OTC
mitochondrial compartment	outer surface of outer membrane	outer membrane	inner membrane	matrix
rel MTS strength*	strong	strong	weak	medium/strong
intrinsic mito-toxicity of MTS-EGFP	nontoxic	toxic	toxic	toxic
p53 apoptotic response	caspase-9, TUNEL, annexin-V, and 7-AAD	annexin-V, and 7-AAD	TUNEL, annexin-V, and 7-AAD	caspase-9, annexin-V, and 7-AAD
speculated apoptotic mechanism	may interact with Bcl-XL	may interact with Bak	transcriptional p53	transcriptional p53 and may interact with Bcl-XL

[a]The table compares the four MTSs in mitochondrial localization, strength (*based on colocalization), mitotoxicity of MTS-EGFP, apoptotic response of MTS-p53 compared to MTS-EGFP, and speculated apoptotic mechanism.

OTC directs p53 to the mitochondrial matrix, p53 is still able to interact with Bcl-XL and Bcl-2 proteins on the outer membrane. This could be due to cleavage of the MTS by endopeptidase, which enables p53 to target the outer membrane.[3,10]

Instead of targeting the protein to the matrix and then translocating it to the outer membrane, as was the case for OTC, we fused EGFP-p53 to TOM to *directly* target the outer membrane. Direct targeting of the outer membrane with TOM-p53 was able to initiate apoptosis (annexin-V and 7-AAD) robustly compared to its TOM-EGFP control. Interestingly this increase in apoptosis was only rescued when Bcl-XL was cotransfected but not when pifithrin-α or pifithrin-μ was added (Figure 8). The pifithrin-α rescue experiment indicates that TOM-p53 has no transcriptional activity. We speculate that TOM-EGFP-p53 is binding to proapoptotic Bak and enhancing its oligomerization, which disrupts the mitochondrial outer membrane.[13,14] Bcl-XL forms a heterodimer with Bak and prevents Bak homodimerization.[14,65,66] Therefore, when Bcl-XL is overexpressed, it competes with TOM-p53 in binding with Bak and hence reduces apoptosis. Since pifithrin-μ reduces the binding of p53 to antiapoptotic Bcl-XL and Bcl-2 and has no effect on binding to Bak, it did not show reduction in programmed cell death for TOM-p53.

In an effort to directly target the p53/Bcl-XL pathway, we fused XL to EGFP-p53. Directing p53 to the mitochondria via XL showed significant caspase-9, TUNEL, 7-AAD, and annexin-V activity compared to its EGFP-XL control. This apoptotic response was not due to transcriptional activity of p53 as shown in the luciferase assay data (Figure 3) and the pifithrin-α rescue experiment (Figure 8A). However, the apoptotic response was due to the p53/Bcl-XL pathway. To confirm this interaction, rescue experiments using pifithrin-μ and Bcl-XL were conducted and showed reduction in apoptosis (Figures 8B and 8C). In addition, the EGFP-XL control showed no toxicity compared to the other MTS-EGFP controls especially in MCF-7 cells (Figures 6 and 7). This data demonstrates that sending p53 to a specific protein (Bcl-XL) in the mitochondrial outer membrane causes p53-specific apoptosis. Table 2 is a summary of the results and speculation from this work.

In summary, efficiency in targeting the mitochondria depends on the strength of the MTS. In the case of targeting proteins containing relatively strong NLSs such as p53 (residues 305−322),[20] mitochondrial targeting can best be achieved by using strong MTSs to counter the NLS. In this study, relatively weaker MTSs are not efficient enough to compete with the strong NLS in p53. In addition, protein targeting to the mitochondria disrupts the sensitive balance in the mitochondria, which initiates intrinsic apoptosis. Except for EGFP-XL, all mitochondrial constructs had apoptotic effects. We conclude that p53-XL was the most specific to the p53/Bcl-XL mitochondrial pathway. Our data shows that not all mitochondrial targeting signals are optimal for mitochondrial induction of apoptosis with p53. In conclusion, specific binding of p53 to mitochondrial Bcl-XL (and hence apoptotic activity) is best achieved by directly targeting p53 to Bcl-XL via the XL MTS. This work therefore provides a mechanistic explanation and provides additional speculation toward the understanding of mitochondrial p53 apoptosis. Our future goal is to employ the p53-XL construct as a therapeutic *in vivo* using viral delivery. Ultimately, p53-XL gene therapy is expected to be beneficial for other types of progressive cancers that currently have no effective therapy.

■ ASSOCIATED CONTENT

Supporting Information

Additional figures depicting results from TUNEL assay, 7-AAD assay, and rescue experiment. This material is available free of charge via the Internet at http://pubs.acs.org.

■ AUTHOR INFORMATION

Corresponding Author

*421 Wakara Way Rm 318, Salt Lake City, UT 84108, USA. Fax: 1-801-585-3614. Phone: 1-801-587-9711. E-mail: carol.lim@pharm.utah.edu.

Author Contributions

‡These authors contributed equally to this work thus are referred to as "co-first authors".

Notes

The authors declare no competing financial interest.

■ ACKNOWLEDGMENTS

We acknowledge the use of DNA/Peptide Core and Flow Cytometry Core (NCI Cancer Center Support Grant P30 CA042014, Huntsman Cancer Institute). This work was funded by NIH R01-CA151847. We would like to thank Katharina Opper, Geoff Miller, Andy Dixon, Ben Bruno, Rian Davis, David Woessner, and Shams Reaz for scientific discussions.

■ REFERENCES

(1) Erster, S.; Mihara, M.; Kim, R. H.; Petrenko, O.; Moll, U. M. In vivo mitochondrial p53 translocation triggers a rapid first wave of cell death in response to DNA damage that can precede p53 target gene activation. *Mol. Cell. Biol.* **2004**, *24* (15), 6728−41.

(2) Erster, S.; Moll, U. M. Stress-induced p53 runs a transcription-independent death program. *Biochem. Biophys. Res. Commun.* **2005**, *331* (3), 843−50.

(3) Mihara, M.; Erster, S.; Zaika, A.; Petrenko, O.; Chittenden, T.; Pancoska, P.; Moll, U. M. p53 has a direct apoptogenic role at the mitochondria. *Mol. Cell* **2003**, *11* (3), 577−90.

(4) Chipuk, J. E.; Kuwana, T.; Bouchier-Hayes, L.; Droin, N. M.; Newmeyer, D. D.; Schuler, M.; Green, D. R. Direct activation of Bax

by p53 mediates mitochondrial membrane permeabilization and apoptosis. *Science* **2004**, *303* (5660), 1010−4.
(5) Zhao, Y.; Chaiswing, L.; Velez, J. M.; Batinic-Haberle, I.; Colburn, N. H.; Oberley, T. D.; St. Clair, D. K. p53 translocation to mitochondria precedes its nuclear translocation and targets mitochondrial oxidative defense protein-manganese superoxide dismutase. *Cancer Res.* **2005**, *65* (9), 3745−50.
(6) Canugovi, C.; Maynard, S.; Bayne, A. C.; Sykora, P.; Tian, J.; de Souza-Pinto, N. C.; Croteau, D. L.; Bohr, V. A. The mitochondrial transcription factor A functions in mitochondrial base excision repair. *DNA Repair* **2010**, *9* (10), 1080−9.
(7) Vogelstein, B.; Lane, D.; Levine, A. J. Surfing the p53 network. *Nature* **2000**, *408* (6810), 307−10.
(8) El-Deiry, W. S.; Harper, J. W.; O'Connor, P. M.; Velculescu, V. E.; Canman, C. E.; Jackman, J.; Pietenpol, J. A.; Burrell, M.; Hill, D. E.; Wang, Y.; et al. WAF1/CIP1 is induced in p53-mediated G1 arrest and apoptosis. *Cancer Res.* **1994**, *54* (5), 1169−74.
(9) Harris, S. L.; Levine, A. J. The p53 pathway: positive and negative feedback loops. *Oncogene* **2005**, *24* (17), 2899−908.
(10) Marchenko, N. D.; Zaika, A.; Moll, U. M. Death signal-induced localization of p53 protein to mitochondria. A potential role in apoptotic signaling. *J. Biol. Chem.* **2000**, *275* (21), 16202−12.
(11) Tomita, Y.; Marchenko, N.; Erster, S.; Nemajerova, A.; Dehner, A.; Klein, C.; Pan, H.; Kessler, H.; Pancoska, P.; Moll, U. M. WT p53, but not tumor-derived mutants, bind to Bcl2 via the DNA binding domain and induce mitochondrial permeabilization. *J. Biol. Chem.* **2006**, *281* (13), 8600−6.
(12) Chipuk, J. E.; Maurer, U.; Green, D. R.; Schuler, M. Pharmacologic activation of p53 elicits Bax-dependent apoptosis in the absence of transcription. *Cancer Cell* **2003**, *4* (5), 371−81.
(13) Leu, J. I.; Dumont, P.; Hafey, M.; Murphy, M. E.; George, D. L. Mitochondrial p53 activates Bak and causes disruption of a Bak-Mcl1 complex. *Nat. Cell Biol.* **2004**, *6* (5), 443−50.
(14) Pietsch, E. C.; Leu, J. I.; Frank, A.; Dumont, P.; George, D. L.; Murphy, M. E. The tetramerization domain of p53 is required for efficient BAK oligomerization. *Cancer Biol. Ther.* **2007**, *6* (10), 1576−83.
(15) Green, D. R.; Reed, J. C. Mitochondria and apoptosis. *Science* **1998**, *281* (5381), 1309−12.
(16) Reed, J. C. Cytochrome c: can't live with it--can't live without it. *Cell* **1997**, *91* (5), 559−62.
(17) Green, D. R.; Evan, G. I. A matter of life and death. *Cancer Cell* **2002**, *1* (1), 19−30.
(18) Mossalam, M.; Dixon, A. S.; Lim, C. S. Controlling subcellular delivery to optimize therapeutic effect. *Ther. Delivery* **2010**, *1* (1), 169−93.
(19) Mihara, M.; Moll, U. M. Detection of mitochondrial localization of p53. *Methods Mol. Biol.* **2003**, *234*, 203−9.
(20) Shaulsky, G.; Goldfinger, N.; Ben-Ze'ev, A. Rotter, V. Nuclear accumulation of p53 protein is mediated by several nuclear localization signals and plays a role in tumorigenesis. *Mol. Cell. Biol.* **1990**, *10* (12), 6565−77.
(21) Jiang, P.; Du, W.; Heese, K.; Wu, M. The Bad guy cooperates with good cop p53: Bad is transcriptionally up-regulated by p53 and forms a Bad/p53 complex at the mitochondria to induce apoptosis. *Mol. Cell. Biol.* **2006**, *26* (23), 9071−82.
(22) Sansome, C.; Zaika, A.; Marchenko, N. D.; Moll, U. M. Hypoxia death stimulus induces translocation of p53 protein to mitochondria. Detection by immunofluorescence on whole cells. *FEBS Lett.* **2001**, *488* (3), 110−5.
(23) Dumont, P.; Leu, J. I.; Della Pietra, A. C. 3rd; George, D. L.; Murphy, M. The codon 72 polymorphic variants of p53 have markedly different apoptotic potential. *Nat. Genet.* **2003**, *33* (3), 357−65.
(24) Marchenko, N. D.; Wolff, S.; Erster, S.; Becker, K.; Moll, U. M. Monoubiquitylation promotes mitochondrial p53 translocation. *EMBO J.* **2007**, *26* (4), 923−34.
(25) Von Heijne, G. Mitochondrial targeting sequences may form amphiphilic helices. *EMBO J.* **1986**, *5* (6), 1335−42.
(26) Koehler, C. M. New developments in mitochondrial assembly. *Annu. Rev. Cell Dev. Biol.* **2004**, *20*, 309−35.
(27) Roise, D.; Schatz, G. Mitochondrial presequences. *J. Biol. Chem.* **1988**, *263* (10), 4509−11.
(28) Wiedemann, N.; Frazier, A. E.; Pfanner, N. The protein import machinery of mitochondria. *J. Biol. Chem.* **2004**, *279* (15), 14473−6.
(29) Kaufmann, T.; Schlipf, S.; Sanz, J.; Neubert, K.; Stein, R.; Borner, C. Characterization of the signal that directs Bcl-x(L), but not Bcl-2, to the mitochondrial outer membrane. *J. Cell Biol.* **2003**, *160* (1), 53−64.
(30) Pollack, M.; Leeuwenburgh, C. Apoptosis and aging: role of the mitochondria. *J. Gerontol.* **2001**, *56* (11), B475−82.
(31) Lindsay, J.; Esposti, M. D.; Gilmore, A. P. Bcl-2 proteins and mitochondria--specificity in membrane targeting for death. *Biochim. Biophys. Acta* **2011**, *1813* (4), 532−9.
(32) Rehling, P.; Brandner, K.; Pfanner, N. Mitochondrial import and the twin-pore translocase. *Nat. Rev. Mol. Cell Biol.* **2004**, *5* (7), 519−30.
(33) Power, S. D.; Lochrie, M. A.; Patterson, T. E.; Poyton, R. O. The nuclear-coded subunits of yeast cytochrome c oxidase. II. The amino acid sequence of subunit VIII and a model for its disposition in the inner mitochondrial membrane. *J. Biol. Chem.* **1984**, *259* (10), 6571−4.
(34) Fabrizi, G. M.; Sadlock, J.; Hirano, M.; Mita, S.; Koga, Y.; Rizzuto, R.; Zeviani, M.; Schon, E. A. Differential expression of genes specifying two isoforms of subunit VIa of human cytochrome c oxidase. *Gene* **1992**, *119* (2), 307−12.
(35) Isaya, G.; Fenton, W. A.; Hendrick, J. P.; Furtak, K.; Kalousek, F.; Rosenberg, L. E. Mitochondrial import and processing of mutant human ornithine transcarbamylase precursors in cultured cells. *Mol. Cell. Biol.* **1988**, *8* (12), 5150−8.
(36) Dixon, A. S.; Kakar, M.; Schneider, K. M.; Constance, J. E.; Paullin, B. C.; Lim, C. S. Controlling subcellular localization to alter function: Sending oncogenic Bcr-Abl to the nucleus causes apoptosis. *J. Controlled Release* **2009**, *140* (3), 245−9.
(37) Bolte, S.; Cordelieres, F. P. A guided tour into subcellular colocalization analysis in light microscopy. *J. Microsc.* **2006**, *224* (Part 3), 213−32.
(38) Costes, S. V.; Daelemans, D.; Cho, E. H.; Dobbin, Z.; Pavlakis, G.; Lockett, S. Automatic and quantitative measurement of protein-protein colocalization in live cells. *Biophys. J.* **2004**, *86* (6), 3993−4003.
(39) Adler, J.; Parmryd, I. Quantifying colocalization by correlation: the Pearson correlation coefficient is superior to the Mander's overlap coefficient. *Cytometry, Part A* **2010**, *77* (8), 733−42.
(40) Dixon, A. S.; Miller, G. D.; Bruno, B. J.; Constance, J. E.; Woessner, D. W.; Fidler, T. P.; Robertson, J. C.; Cheatham, T. E.; Lim, C. S. Improved coiled-coil design enhances interaction with bcr-abl and induces apoptosis. *Mol. Pharmaceutics* **2012**, *9* (1), 187−95.
(41) Jaskolski, F.; Mulle, C.; Manzoni, O. J. An automated method to quantify and visualize colocalized fluorescent signals. *J. Neurosci. Methods* **2005**, *146* (1), 42−9.
(42) Schafer, J. M.; Lee, E. S.; O'Regan, R. M.; Yao, K.; Jordan, V. C. Rapid development of tamoxifen-stimulated mutant p53 breast tumors (T47D) in athymic mice. *Clin. Cancer Res.* **2000**, *6* (11), 4373−80.
(43) Alkhalaf, M.; El-Mowafy, A. M. Overexpression of wild-type p53 gene renders MCF-7 breast cancer cells more sensitive to the antiproliferative effect of progesterone. *J. Endocrinol.* **2003**, *179* (1), 55−62.
(44) Takahashi, K.; Sumimoto, H.; Suzuki, K.; Ono, T. Protein synthesis-dependent cytoplasmic translocation of p53 protein after serum stimulation of growth-arrested MCF-7 cells. *Mol. Carcinog.* **1993**, *8* (1), 58−66.
(45) Mooney, L. M.; Al-Sakkaf, K. A.; Brown, B. L.; Dobson, P. R. Apoptotic mechanisms in T47D and MCF-7 human breast cancer cells. *Br. J. Cancer* **2002**, *87* (8), 909−17.
(46) Chowdhury, I.; Tharakan, B.; Bhat, G. K. Caspases - an update. *Comp. Biochem. Physiol., Part B: Biochem. Mol. Biol.* **2008**, *151* (1), 10−27.
(47) Yin, Q.; Park, H. H.; Chung, J. Y.; Lin, S. C.; Lo, Y. C.; da Graca, L. S.; Jiang, X.; Wu, H. Caspase-9 holoenzyme is a specific and optimal procaspase-3 processing machine. *Mol. Cell* **2006**, *22* (2), 259−68.

(48) Loo, D. T.; Rillema, J. R. Measurement of cell death. *Methods Cell Biol.* **1998**, *57*, 251−64.
(49) Koopman, G.; Reutelingsperger, C. P.; Kuijten, G. A.; Keehnen, R. M.; Pals, S. T.; van Oers, M. H. Annexin V for flow cytometric detection of phosphatidylserine expression on B cells undergoing apoptosis. *Blood* **1994**, *84* (5), 1415−20.
(50) Vermes, I.; Haanen, C.; Steffens-Nakken, H.; Reutelingsperger, C. A novel assay for apoptosis. Flow cytometric detection of phosphatidylserine expression on early apoptotic cells using fluorescein labelled Annexin V. *J. Immunol. Methods* **1995**, *184* (1), 39−51.
(51) Metkar, S. S.; Wang, B.; Catalan, E.; Anderluh, G.; Gilbert, R. J.; Pardo, J.; Froelich, C. J. Perforin rapidly induces plasma membrane phospholipid flip-flop. *PLoS One* **2011**, *6* (9), e24286.
(52) Schmid, I.; Krall, W. J.; Uittenbogaart, C. H.; Braun, J.; Giorgi, J. V. Dead cell discrimination with 7-amino-actinomycin D in combination with dual color immunofluorescence in single laser flow cytometry. *Cytometry* **1992**, *13* (2), 204−8.
(53) Serrano, M. J.; Sanchez-Rovira, P.; Algarra, I.; Jaen, A.; Lozano, A.; Gaforio, J. J. Evaluation of a gemcitabine-doxorubicin-paclitaxel combination schedule through flow cytometry assessment of apoptosis extent induced in human breast cancer cell lines. *Jpn. J. Cancer Res.* **2002**, *93* (5), 559−66.
(54) Komarov, P. G.; Komarova, E. A.; Kondratov, R. V.; Christov-Tselkov, K.; Coon, J. S.; Chernov, M. V.; Gudkov, A. V. A chemical inhibitor of p53 that protects mice from the side effects of cancer therapy. *Science* **1999**, *285* (5434), 1733−7.
(55) Liu, X.; Chua, C. C.; Gao, J.; Chen, Z.; Landy, C. L.; Hamdy, R.; Chua, B. H. Pifithrin-alpha protects against doxorubicin-induced apoptosis and acute cardiotoxicity in mice. *Am. J. Physiol.* **2004**, *286* (3), H933−9.
(56) Hagn, F.; Klein, C.; Demmer, O.; Marchenko, N.; Vaseva, A.; Moll, U. M.; Kessler, H. BclxL changes conformation upon binding to wild-type but not mutant p53 DNA binding domain. *J. Biol. Chem.* **2010**, *285* (5), 3439−50.
(57) Strom, E.; Sathe, S.; Komarov, P. G.; Chernova, O. B.; Pavlovska, I.; Shyshynova, I.; Bosykh, D. A.; Burdelya, L. G.; Macklis, R. M.; Skaliter, R.; Komarova, E. A.; Gudkov, A. V. Small-molecule inhibitor of p53 binding to mitochondria protects mice from gamma radiation. *Nat. Chem. Biol.* **2006**, *2* (9), 474−9.
(58) Vaseva, A. V.; Moll, U. M. The mitochondrial p53 pathway. *Biochim. Biophys. Acta* **2009**, *1787* (5), 414−20.
(59) Schmidt, O.; Pfanner, N.; Meisinger, C. Mitochondrial protein import: from proteomics to functional mechanisms. *Nat. Rev. Mol. Cell Biol.* **2010**, *11* (9), 655−67.
(60) Endo, T.; Kohda, D. Functions of outer membrane receptors in mitochondrial protein import. *Biochim. Biophys. Acta* **2002**, *1592* (1), 3−14.
(61) Dolezal, P.; Likic, V.; Tachezy, J.; Lithgow, T. Evolution of the molecular machines for protein import into mitochondria. *Science* **2006**, *313* (5785), 314−8.
(62) Mattaj, I. W.; Englmeier, L. Nucleocytoplasmic transport: the soluble phase. *Annu. Rev. Biochem.* **1998**, *67*, 265−306.
(63) Gorlich, D.; Kutay, U. Transport between the cell nucleus and the cytoplasm. *Annu. Rev. Cell Dev. Biol.* **1999**, *15*, 607−60.
(64) Davis, J. R.; Kakar, M.; Lim, C. S. Controlling protein compartmentalization to overcome disease. *Pharm. Res.* **2007**, *24* (1), 17−27.
(65) Sattler, M.; Liang, H.; Nettesheim, D.; Meadows, R. P.; Harlan, J. E.; Eberstadt, M.; Yoon, H. S.; Shuker, S. B.; Chang, B. S.; Minn, A. J.; Thompson, C. B.; Fesik, S. W. Structure of Bcl-xL-Bak peptide complex: recognition between regulators of apoptosis. *Science* **1997**, *275* (5302), 983−6.
(66) Galluzzi, L.; Morselli, E.; Kepp, O.; Tajeddine, N.; Kroemer, G. Targeting p53 to mitochondria for cancer therapy. *Cell Cycle* **2008**, *7* (13), 1949−55.

NOTE ADDED AFTER ASAP PUBLICATION

This article was published ASAP on March 28, 2012, with errors in the rightmost column of Table 1. The corrected version was published on April 17, 2012.

Title: Direct Induction of Apoptosis Using an Optimal Mitochondrially Targeted p53

Author: Mohanad Mossalam, Karina J. Matissek, Abood Okal, Jonathan E. Constance, and Carol S. Lim

Publication: Molecular Pharmaceutics

Publisher: American Chemical Society

Date: May 1, 2012

PERMISSION/LICENSE IS GRANTED FOR YOUR ORDER AT NO CHARGE

This type of permission/license, instead of the standard Terms & Conditions, is sent to you because no fee is being charged for your order. Please note the following:

- Permission is granted for your request in both print and electronic formats, and translations.
- If figures and/or tables were requested, they may be adapted or used in part.
- Please print this page for your records and send a copy of it to your publisher/graduate school.
- Appropriate credit for the requested material should be given as follows: "Reprinted (adapted) with permission from (COMPLETE REFERENCE CITATION). Copyright (YEAR) American Chemical Society." Insert appropriate information in place of the capitalized words.
- One-time permission is granted only for the use specified in your request. No additional uses are granted (such as derivative works or other editions). For any other uses, please submit a new request.

molecular pharmaceutics

Article

pubs.acs.org/molecularpharmaceutics

The DNA Binding Domain of p53 Is Sufficient To Trigger a Potent Apoptotic Response at the Mitochondria

Karina J. Matissek,[†,‡] Mohanad Mossalam,[†] Abood Okal,[†] and Carol S. Lim*[,†]

[†]Department of Pharmaceutics and Pharmaceutical Chemistry, University of Utah, Utah 84112, United States

[‡]Department of Pharmaceutics and Biopharmacy, Philipps-Universität, D-35032 Marburg, Germany

Supporting Information

ABSTRACT: The tumor suppressor p53 is one of the most studied proteins in human cancer.[1−3] While nuclear p53 has been utilized for cancer gene therapy, mitochondrial targeting of p53 has not been fully exploited to date.[4,5] In response to cellular stress, p53 translocates to the mitochondria and directly interacts with Bcl-2 family proteins including antiapoptotic Bcl-XL and Bcl-2 and proapoptotic Bak and Bax.[6] Antiapoptotic Bcl-XL forms inhibitory complexes with proapoptotic Bak and Bax preventing their homo-oligomerization.[7] Upon translocation to the mitochondria, p53 binds to Bcl-XL, releases Bak and Bax from the inhibitory complex and enhances their homo-oligomerization.[8] Bak and Bax homotetramer formation disrupts the mitochondrial outer membrane, releases antiapoptotic factors such as cytochrome *c* and triggers a rapid apoptotic response mediated by caspase induction.[9] It is still unclear if the MDM2 binding domain (MBD), the proline-rich domain (PRD) and/or DNA binding domain (DBD) of p53 are the domains responsible for interaction with Bcl-XL.[10−17] The purpose of this work is to determine if a smaller functional domain of p53 is capable of inducing apoptosis similarly to full length p53. To explore this question, different domains of p53 (MBD, PRD, DBD) were fused to the mitochondrial targeting signal (MTS) from Bcl-XL to ensure Bcl-XL specific targeting.[18] The designed constructs were tested for apoptotic activity (TUNEL, Annexin-V, and 7-AAD) in 3 different breast cancer cell lines (T47D, MCF-7, MDA-MB-231), in a cervical cancer cell line (HeLa) and in non-small cell lung adenocarcinoma cells H1373. Our results indicate that DBD-XL (p53 DBD fused to the Bcl-XL MTS) reproduces (in T47D cells) or demonstrates increased apoptotic activity (in MCF-7, MDA-MB-231, and HeLa cells) compared to p53-XL (full length p53 fused to Bcl-XL MTS). Additionally, mitochondrial dependent apoptosis assays (TMRE, caspase-9), co-IP and overexpression of Bcl-XL in T47D cells suggest that DBD fused to XL MTS may bind to and inhibit Bcl-XL. Taken together, our data demonstrates for the first time that the DBD of p53 may be the minimally necessary domain for achieving apoptosis at the mitochondria in multiple cell lines. This work highlights the role of small functional domains of p53 as a novel cancer biologic therapy.

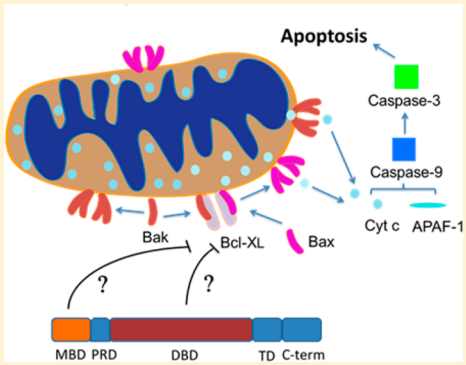

KEYWORDS: *p53, mitochondria, Bcl-XL, apoptosis, DBD, MBD, cancer*

INTRODUCTION

The tumor suppressor p53 is one of the most commonly mutated genes in all cancers.[1−3] Although nuclear-mediated transcriptional activity has been extensively characterized, mitochondrial targeting of p53 has yet to be fully exploited as a therapeutic approach.[4,5] The main advantage of targeting p53 to the mitochondria is its ability to trigger a rapid apoptotic response, while in the nucleus p53 first has to form a tetramer, bind to DNA, and initiate transcription of various apoptotic genes. As a consequence of stress, p53 translocates to the mitochondria and initiates apoptosis through mitochondrial outer membrane permeabilization (MOMP).[6] Mitochondrial p53 directly interacts with anti- and proapoptotic members of the Bcl-2 family of proteins located in the mitochondrial outer membrane. In apoptosis resistant cells, the antiapoptotic members, Bcl-XL, Bcl-2 and Mcl-1 form heterodimers with proapoptotic proteins Bak and Bax, preventing apoptosis.[7] To trigger MOMP, p53 binds to Bcl-XL, Bcl-2 and Mcl-1 and frees proapoptotic Bak and Bax allowing them to oligomerize.[8] Homotetramer formation of Bak and Bax in the mitochondrial outer membrane triggers the release of various proapoptotic proteins such as cytochrome *c*. APAF-1 and cytochrome *c* form the apoptosome and activate caspase-9 that can initiate the caspase cascade resulting in programmed cell death.[9]

It is unclear which domains of p53 are directly responsible for triggering apoptosis at the mitochondria, presumably by interacting with antiapoptotic Bcl-XL.[11−15] The structure of p53 can be divided into amino terminus, DNA binding domain (DBD) and C-terminal region (Figure 1A).[10] The amino terminus consists of the MDM2 binding domain (MBD) and the proline-rich domain (PRD). The C-terminal region

Received: January 25, 2013
Revised: August 13, 2013
Accepted: August 23, 2013
Published: August 23, 2013

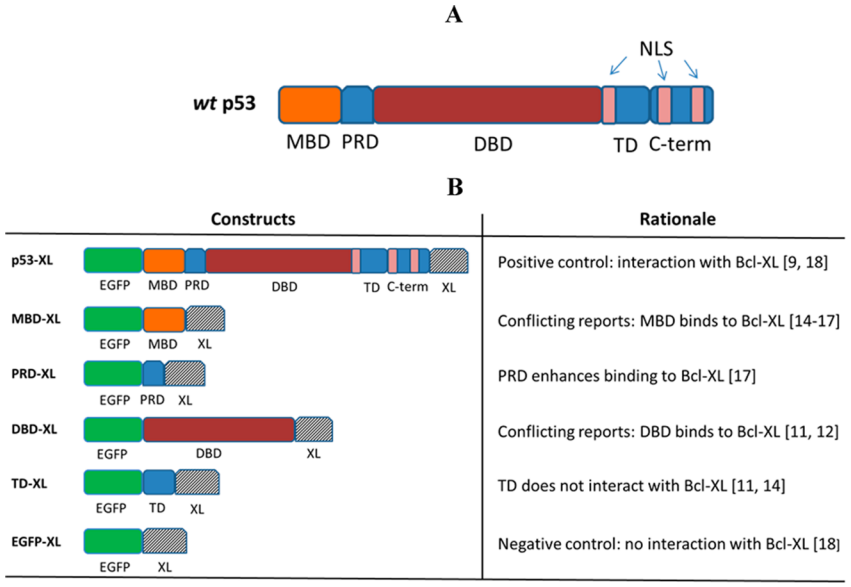

Figure 1. (A) Schematic representation of wild type p53 (wt-p53). The 393 amino acids of p53 are divided into amino terminus, DNA binding domain (DBD), and C-terminal region. The MDM2 binding domain (MBD) and proline-rich domain (PRD) are located in the amino terminus. The tetramerization (TD) domain and the nuclear localization signals (NLSs) are located in the C-terminus. (B) Schematic representation of the main experimental constructs and controls including the rationale for design. p53-XL shows the structure of full length p53 with enhanced green fluorescence protein EGFP on the amino terminus and the MTS from Bcl-XL (XL) on the C-terminus. All the other constructs contain various combinations of the different domains of p53, in addition to EGFP and XL. The negative control (E-XL) consists of only EGFP and XL.

encloses the tetramerization domain (TD) and three nuclear localization signals (NLS) (Figure 1A).[10] It has been reported that the DBD binds to antiapoptotic Bcl-XL in the mitochondrial outer membrane and the PRD functions as an enhancer that improves this binding.[11−13] However, the MBD has been also proposed as a binding partner for Bcl-XL which is enhanced by the PRD.[14−17]

To our knowledge, no one has attempted to target different domains of p53 to the mitochondria. Therefore, the purpose of this study is to determine if a smaller domain of p53 is capable of inducing apoptosis similar to full length p53 when targeted to the mitochondria. This will be achieved by fusing different domains of p53 (MBD, PRD, DBD, TD) to the mitochondrial targeting signal (MTS) from Bcl-XL (abbreviated XL) to ensure mitochondrial targeting (Figure 1B).[18] This information will provide details on which domain is responsible for the rapid apoptotic response at the mitochondria. In addition to answering this mechanistic question, an overall goal is to decrease the size of the p53 construct for gene therapy purposes.

MATERIALS AND METHODS

Cell Lines and Transient Transfections. 1471.1 murine adenocarcinoma cells (gift of G. Hager, NCI, NIH), T47D human ductal breast epithelial tumor cells (ATCC, Manassas, VA), MCF-7 human breast adenocarcinoma cells (ATCC),[18] MDA-MB-231 human breast adenocarcinoma cells (a generous gift from Dr. David Bearss, University of Utah), HeLa human epithelial cervical adenocarcinoma cells (ATCC), and H1373 human non-small lung carcinoma cells (a kind gift from Dr. Andrea Bild, University of Utah) were grown as monolayers in DMEM (1471.1) and RPMI (T47D, MCF-7, MDA-MB-231, HeLa, H1373) (Invitrogen, Carlsbad, CA) supplemented with 10% FBS (Invitrogen), 1% penicillin−streptomycin (Invitrogen), 1% glutamine (Invitrogen) and 0.1% gentamycin (Invitrogen). T47D and MCF-7 cells were additionally supplemented with 4 mg/L insulin (Sigma, St. Louis, MO). Cells were maintained in a 5% CO_2 incubator at 37 °C. 3.0×10^5 cells for T47D and MCF-7 cells, 1.0×10^5 cells for MDA-MB-231 and HeLa, and 2.0×10^5 for H1373 were seeded in 6-well plates (Greiner Bio-One, Monroe, NC). Different amounts of cells were plated to account for varying cell growth rates in order to maximize transfection efficiency. Approximately 24 h after seeding, transfection was performed using 1 pmol of DNA per well and Lipofectamine 2000 (Invitrogen) following the manufacturer's recommendations.

Plasmid Construction. The main plasmids used in this work are depicted in Figure 1B.

pEGFP-p53ΔC-XL (p53ΔC-XL). The DNA encoding p53ΔC (amino acids 1−322), a truncated version of wt-p53 that lacks the C-terminus, was amplified via PCR with the primers 5′-GCGCGCGCGCTCCGGAATGGAGGAGCCGCAGTCA-3′ and 5′-GCGCGCGCGCGGTACCTCATGGTTTCTTC-TTTGGCTGGGG-3′ using previously subcloned pEGFP-p53[18] as the template DNA. p53ΔC was cloned into pEGFP-XL (E-XL)[18] using *Bsp*EI and *Kpn*I sites.

pEGFP-DBD-XL (DBD-XL). The DNA encoding the DBD was amplified via PCR from pEGFP-p53-XL (p53-XL)[18] using 5′-CCGGGCCCGCGGTCCGGAACCTACCAGGGCAGCTA-CG-3′ and 5′-CCGGGCCCGCGGGGTACCTTTCTTGC-GGAGATTCTCTTCCT and cloned into E-XL[18] using *Bsp*EI and *Kpn*I sites.

pEGFP-PRD-DBD-XL (PRD-DBD-XL). The DNA encoding the PRD-DBD was amplified using PCR from p53-XL[18] with the primers 5′-GCGCGCGCGCGGTACCGCTCCCAGAA-TGCCAGAGGC-3′ and 5′-GCGCGCGCGCGGATCCT-TTCTTGCGGAGATTCTCTT and cloned into E-XL[18] at the *Kpn*I and *Bam*HI sites.

pEGFP-TD-XL (TD-XL). The DNA encoding the TD was amplified via PCR from previously subcloned p53-XL[18] using 5′-GCGCGCGCGCGGGATCCGGCTGGATGGAGAAT-ATTTCACCCTTCA-3′ and 5′-GCGCGCGCGCGGGAtCC-

dx.doi.org/10.1021/mp400380s | Mol. Pharmaceutics 2013, 10, 3592−3602

TCACCCAGCCTGGGCATCCTT-3′ and cloned into E-XL[18] at the *Bam*HI site.

pEGFP-MBD-PRD-XL (MBD-PRD-XL). Previously subcloned p53-XL[18] was mutated via site-directed mutagenesis using the QuikChange II XL Site directed Mutagenesis Kit (Agilent, Santa Clara, CA) using 5′-TCCCTTCCCAGAAAAGGTAC-CAGGGCAGCTACGGT-3′ and its reverse complement to introduce an additional *Kpn*I site (mutations underlined). Then the DBD and C-terminus were digested out using *Kpn*I. Additionally, a frame shift mutation was corrected (one base pair deletion) by mutating the cloned plasmid using 5′-TCGAGCTATGGAAACATTTTCAGACCTATGGAAAC-TACTTCCTGAACGGAATTCTG-3′ and its complementary strand via site-directed mutagenesis.

pEGFP-PRD-XL (PRD-XL). MBD-PRD-XL was mutated via site-directed mutagenesis using 5′-TTCACTGAAGACCC-AGGTCCATCCGGAGCTCCCAGAATGCCAGA-3′ and its complementary strand to introduce an additional *Bsp*EI site. The MBD was cut out with *Bsp*EI to create PRD-XL

pEGFP-CC (E-CC). pEGFP-CC was subcloned as before.[19]

pBFP-Bcl-XL (BFP-Bcl-XL). Bcl-XL was digested out from pSFFV-neo-Bcl-XL (gift from Dr. S. Korsmeyer, Addgene, Cambridge, MA) with *Eco*RI and cloned into the *Eco*RI site of the pTagBFP-C vector (Evrogen, Moscow, Russia). A frame shift mutation was conducted (one base pair addition) by mutating the cloned plasmid using 5′-TCTCGAGCTCAAGC-TTCGAATTCATTGGACAATGG-3′ and its complementary strand via site-directed mutagenesis.

Mitochondrial Staining, Microscopy, and Image Analysis. Before live-cell imaging and mitochondrial staining of transfected cells was performed, medium in live cell chambers was replaced with phenol red-free DMEM (Invitrogen) for 1471.1 cells or phenol red-free RPMI (Invitrogen) for T47D and MCF-7 cells containing 10% charcoal stripped fetal bovine serum (CS-FBS, Invitrogen). Cells were incubated with 150 nM MitoTracker Red FM (Invitrogen) for 15 min at 37 °C and protected from light. As previously, images were acquired using an Olympus IX71F fluorescence microscope (Scientific Instrument Company, Aurora, CO) with high quality (HQ) narrow band GFP filter (ex, HQ480/20 nm; em, HQ510/20 nm) and HQ:TRITC filter (ex, HQ545/30; em, HQ620/60) from Chroma Technology (Brattleboro, VT) with a 40× PlanApo oil immersion objective (NA 1.00) on an F-View Monochrome CCD camera.[19−21]

ImageJ software and JACoP plugin were used to analyze images for mitochondrial stain overlap with EGFP fusion constructs.[18,22−24] As previously, JACoP was used to generate the colocalization statistic [i.e., Pearson's correlation coefficient (PCC) with Costes's automatic threshold algorithm].[23−27] PCC evaluates correlation between pairs of individual pixels from EGFP and MitoTracker stained cells. The higher the PCC value, the higher the correlation. According to Costes a PCC value of 0.6 or greater determines colocalization between a cellular compartment and the designed protein.[25] Spatial representations of pixel intensity correlation have been generated using Colocalization Colormap (ImageJ) for increased visual clarity of mitochondrial localization of the EGFP-fused constructs.[28] Microscopy was repeated in triplicate (n = 3), and 10 cells were analyzed for each construct.

7- AAD Assay. Transfected T47D, MCF-7, MDA-MB-231, HeLa and H1373 cells were pelleted and resuspended in 500 μL of PBS (Invitrogen) containing 1 μM 7-aminoactinomycin D (7-AAD) (Invitrogen) for 30 min prior to analysis following the recommended protocol from the manufacturer. The assay was performed 48 h after transfection for T47D,[18] MCF-7[18] and H1373 and 24 h after transfection for MDA-MB-231 and HeLa. Only EGFP positive cells were analyzed by using the FACS Canto-II (BD BioSciences, University of Utah Core Facility) with FACS Diva software. EGFP and 7-AAD were excited with the 488 nm laser, and were detected at 507 and 660 nm, respectively. Independent transfections of each construct were tested three times (n = 3).

Annexin V Assay. 48 h after transfection, T47D cells were pelleted and resuspended in 400 μL of annexin-V binding buffer (Invitrogen) and incubated with 5 μL of annexin-APC (annexin-V conjugated to allophycocyanin, Invitrogen) for 15 min as before.[18] Only transfected cells were analyzed as mentioned in 7-AAD assay. EGFP and APC were excited at 488 and 635 nm wavelengths, respectively, and detected at their corresponding 507 and 660 nm wavelengths. Independent transfections of each construct were tested three times (n = 3).

TUNEL Assay. T47D cells were harvested 48 h after transfection. In situ Death Detection Kit, TMR red (Roche, Mannheim, Germany) was used following the manufacturer's recommendations as before.[18,24] Cells were resuspended in PBS (Invitrogen) and analyzed via the FACSAria-II (BD-Biosciences, University of Utah Core Facility). EGFP and TMR red were excited at 488 and 563 nm, respectively, and FACSDiva software was used to analyze the data. Independent transfections of each construct were tested three times (n = 3).

Colony Forming Assay (CFA). Transfected T47D cells were harvested 24 h post transfection and resuspended in RPMI (Invitrogen) at a concentration of 3.0×10^5 cells/mL. The Cytoselect 96-well Cell Transformation Assay (Cell Biolabs, San Diego, CA) was used following the manufacturer's recommendations. Equal amounts of 1.2% agar solution, 2× DMEM/20% FBS media, and cell suspension (1:1:1) were mixed, and 75 μL of the mixture was added to a 96-well plate containing a solidified base agar layer (50 μL of previously solidified 1.2% agar solution), and allowed to solidify at 4 °C for 15 min. The following steps were performed according to the manufacturer's recommendations. A Spectra Max M2 plate reader (Molecular Devices, Sunnyvale, CA) was used to detect fluorescence using a 485/520 nm filter set. Independent transfections of each construct were tested three times (n = 3).

TMRE Assay. 36 h after transfection T47D cells were incubated with 100 nM tetramethylrhodamine ethyl ester (TMRE) (Invitrogen) for 30 min at 37 °C.[29] T47D cells were pelleted and resuspended in 300 μL of annexin-V binding buffer (1×) (Invitrogen). Only EGFP positive cells were analyzed by using the FACS Canto-II (BD BioSciences, University of Utah Core Facility) with FACS Diva software. EGFP was excited with the 488 nm laser with emission filter 530/35, and TMRE was excited with the 561 nm laser with the emission filter 585/15. Mitochondrial depolarization (loss in TMRE intensity) correlates with an increase in MOMP. Independent transfections of each construct were tested three times (n = 3).

Caspase-9 Assay. T47D cells were probed 48 h after transfection using SR FLICA Caspase-9 Assay Kit (Immunochemistry Technologies, Bloomington, MN).[30,31] Cells were incubated with SR FLICA Caspase-9 reagent for 60 min per the manufacturer's recommendations, pelleted and resuspended in 300 μL of 1× wash buffer (Immunochemistry Technologies). Only EGFP positive cells were analyzed using the FACS Canto-II (BD BioSciences, University of Utah Core Facility) with

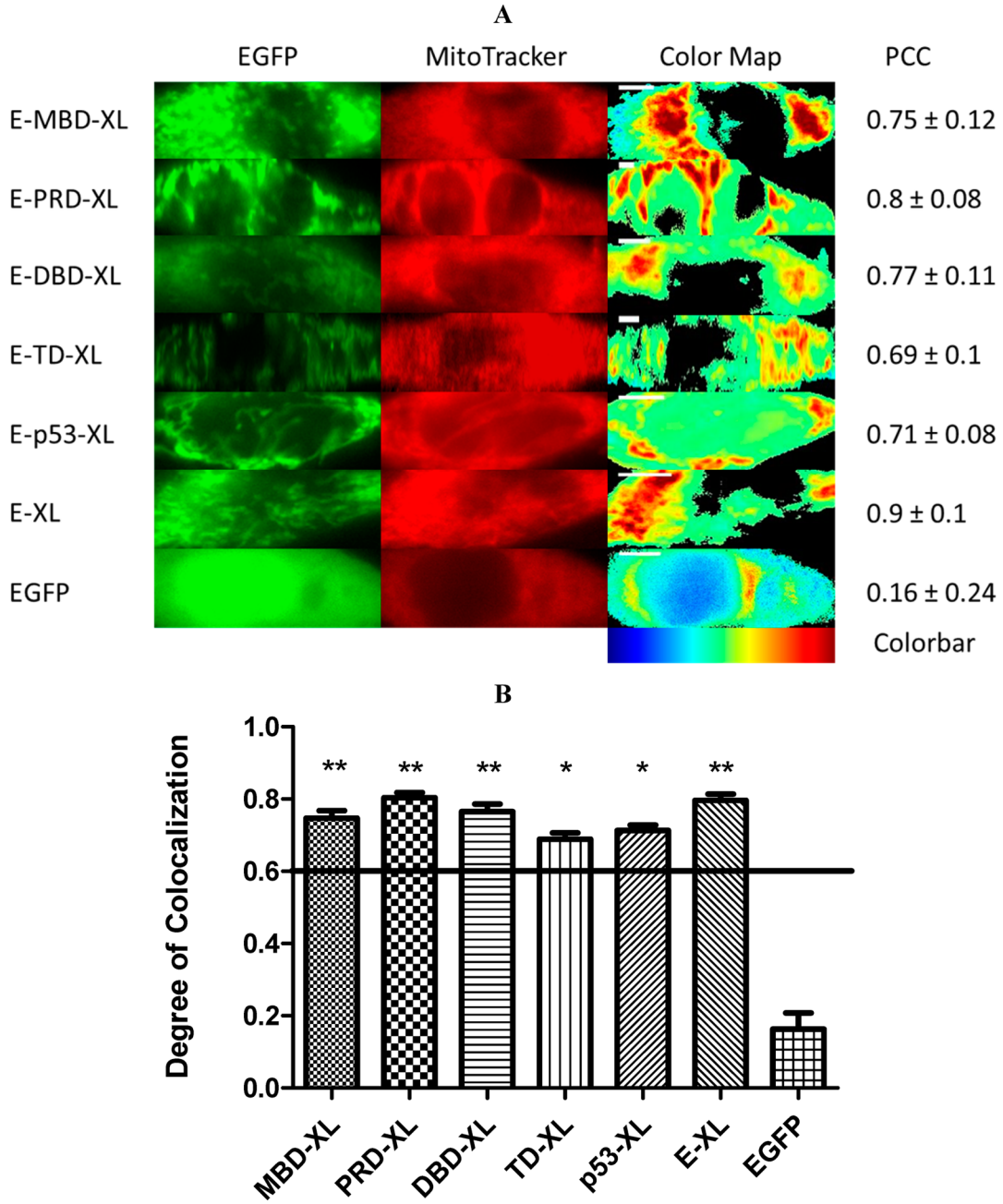

Figure 2. Colocalization of EGFP constructs and MitoTracker Red mitochondrial stain in 1471.1 cells. (A) Representative green fluorescence images of MBD-XL, PRD-XL, DBD-XL, TD-XL, p53-XL, E-XL and EGFP are shown in the left column with images of MitoTracker Red distribution in the middle column. The "EGFP" and "MitoTracker" columns have been false colored green and red, respectively. Enhanced visualization of colocalized pixels is rendered in the "Color Map" column. Warm colors depict pixels with highly correlated intensity and spatial overlap while cool colors are indicative of anticorrelation or random correlation (colorbar for interpretation is shown below column). Corresponding PCC values are shown in the right column. White scale bars are all 10 μm. (B) The degree of colocalization is represented by PCC following Costes's approach. All constructs with values higher than 0.6 are considered highly colocalized with mitochondrial stain MitoTracker Red. Statistical analysis was performed by using odds ratio with Pearson's Chi-square. The adjusted odds ratio for PCC value of 0.6 was compared with each sample. *p < 0.05, and **p < 0.01comparing odds ratio of lowest value for samples with odds ratio of 1 for PCC of 0.6.

FACS Diva software. EGFP and FLICA were excited with the 488 nm (emission filter 530/35) and the 561 laser (emission filter 585/15), respectively. Independent transfections of each construct were tested three times (n = 3).

Co-Immunoprecipitation (Co-IP). Anti-GFP antibody (ab290, Abcam) was coupled to Dynabeads using Dynabeads Antibody Coupling Kit (Invitrogen). 24 h post transfection, T47D cells were prepared using the Dynabeads Co-Immunoprecipitation Kit (Invitrogen). Cell pellets were lysed using extraction buffer B (1 × IP, 100 nM NaCl, 2 mM $MgCl_2$, 1 mM DTT, 1% protease inhibitor). The lysate was incubated for 30 min at 4 °C with 1.5 mg of Dynabeads coupled with anti-GFP antibody, and co-IP was performed per the company's protocol. The final protein complex was denatured, and Western blot was performed[19] by using Bcl-XL antibody (ab 2568, Abcam).

Rescue Experiment Using BFP-Bcl-XL. T47D cells were cotransfected with 1 pmol of EGFP constructs and 1 pmol of

dx.doi.org/10.1021/mp400380s | Mol. Pharmaceutics 2013, 10, 3592−3602

BFP-Bcl-XL (BFP tag is necessary for gating Bcl-XL transfected cells). 48 h after transfection the 7-AAD assay was performed as described above. FACSCanto-II (BD BioSciences, University of Utah Core Facility) and FACSDiva software were used for EGFP and BFP gating. Excitation was set at 488 nm, and detected at 507 and 660 nm for EGFP and 7-AAD, respectively. BFP was excited at 405 nm and detected at 457 nm. Independent transfections of each construct were tested three times (n = 3).

Statistical Analysis. All experiments were conducted in triplicate (n = 3). Statistical significance was determined by one-way analysis of variance (ANOVA) with Tukey's or Bonferroni's post test as indicated in figure legends; Student's t test was used to analyze the rescue experiment data. The degree of colocalization was analyzed using odds ratio with Pearson's Chi-square test. A p value <0.05 was considered significant.

RESULTS

Mitochondrial Localization of Single Domain Constructs. Different domains of p53 (Figure 1B) were fused to the MTS from Bcl-XL (abbreviated XL)[18] and tested for their mitochondrial localization. Mitochondrial targeting of these constructs (Figure 1) was determined by fluorescence microscopy as previously.[18,23,24] Figure 2A illustrates representative 1471.1 cells, which are large in size, spread well, and are optimal for microscopy. However, similar microscopy results were observed in T47D cells (data not shown). Figure 2B shows colocalization of the EGFP fused constructs with mitochondria which were generated using Pearson's correlation coefficient (PCC) following the example of Bolte and Cordelières and graphed for each construct.[22,25,26] PCC values range from +1 (perfect correlation) to −1 (anticorrelation), and a PCC value of zero represents random distribution.[22] Costes et al. have shown that a PCC of 0.6 or greater defines colocalization, or cocompartmentalization (Figure 2B).[25] Figure 2 shows that all designed single domain constructs translocate into the mitochondria, as expected. EGFP served as negative control for colocalization analysis, and there was no colocalization between EGFP alone and the mitochondria. Even though p53 is a nuclear protein containing three nuclear localization signals (NLSs), the XL MTS is strong enough to overcome nuclear targeting and directs p53-XL to the mitochondria (Figure 1 and ref 18).

Screening the Mitochondrial Activity of Different p53 Domains via 7-AAD. To determine if a subdomain of p53 was capable of evoking a similar apoptotic activity as wild type p53, different domains of p53 (Figure 1B) fused to XL and combinations of domains were tested for apoptosis using the 7-AAD viability assay in T47D human breast cancer cells. 7-AAD is a late apoptosis/necrosis assay which allows for distinguishing between apoptotic/necrotic (ruptured plasma membrane) and healthy (intact plasma membrane) cells. If the plasma membrane is disrupted, the 7-AAD dye intercalates with nuclear DNA of apoptotic/necrotic cells.[32,33] Figure 3 demonstrates that all constructs containing DBD (PRD-DBD-XL, DBD-XL, and p53ΔC-XL) are statistically higher than the negative control E-XL. Additionally, these three constructs are not statistically different from p53-XL (positive control), indicating that all constructs containing the DBD show similar apoptotic potential to p53-XL (Figure 3). Further, MBD-XL, MBD-PRD-XL, and PRD-XL are not statistically significant from the negative control E-XL suggesting no apoptotic activity

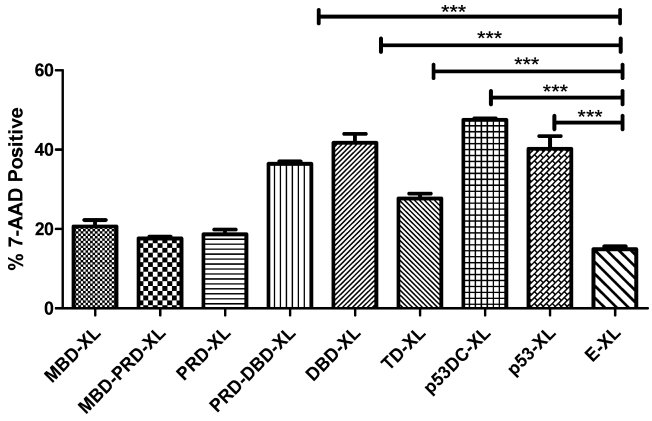

Figure 3. The 7-AAD assay was analyzed in T47D cells 48 h after transfection. Statistical analysis were conducted by one-way ANOVA with Tukey's post test. ***p < 0.001. PRD-DBD-XL, DBD-XL, p53ΔC-XL and p53-XL were not statistically significantly different from each other. MBD-XL, MBD-PRD-XL, PRD-XL, and TD-XL are statistically significantly lower than p53-XL.

(Figure 3). Interestingly, TD-XL is statistically different from the negative controls but is also significantly lower than p53-XL (Figure 3).

Data from Figure 3 illustrate that there is no difference in activity between the single domains (MBD-, PRD-, DBD-, TD; first, third, fifth, sixth bars, respectively) versus combinations of the domains (MBD-PRD, PRD-DBD, p53ΔC; second, fourth, seventh bars, respectively) when fused to XL. Therefore, we proceeded with the single domain constructs (i.e., MBD-XL, PRD-XL, DBD-XL, and TD-XL) for the remaining experiments.

Exploring the Apoptotic Potential of Designed Constructs. To test the apoptotic potential of our designed single domain constructs (Figure 1B), the externalization of phoshatidylserine on the cell surface of apoptotic cells was measured via annexin V staining 48 h after transfection.[18,34] DBD-XL showed a significantly higher apoptotic response than p53-XL (Figure 4A). Additionally, both constructs were significantly higher than the negative control E-XL whereas MBD-XL, PRD-XL and TD-XL were not statistically significantly different from the negative control (Figure 4A).

Further, the fragmentation of nuclear DNA was measured utilizing terminal deoxynucleotidyl transferase dUTP labeling (TUNEL) which tags the terminal end of nucleic acids. DNA fragmentation occurs when a cell is undergoing apoptosis, and the cellular DNA is cleaved by caspases.[35] The TUNEL assay was conducted 48 h after transfection. Figure 4B shows that both p53-XL and DBD-XL have similar activities and are significantly higher than E-XL while MBD-XL, PRD-XL and TD-XL are not statistically different from the negative control.

Testing the Oncogenic Potential. To test the potential of designed constructs to inhibit the transforming ability of cancer cells, a colony forming assay was carried out in T47D cells eight days after treatment. As expected, p53-XL and DBD-XL showed significant decrease in transformative ability of T47D cells represented by fewer colonies (reduction in relative fluorescence units) compared to E-XL (Figure 5). All the other small domain constructs failed to reduce cell proliferation similar to the negative control E-XL.

The Ability of DBD-XL To Induce Late Stage Apoptosis Is Not Cell Line Specific. To ensure that the

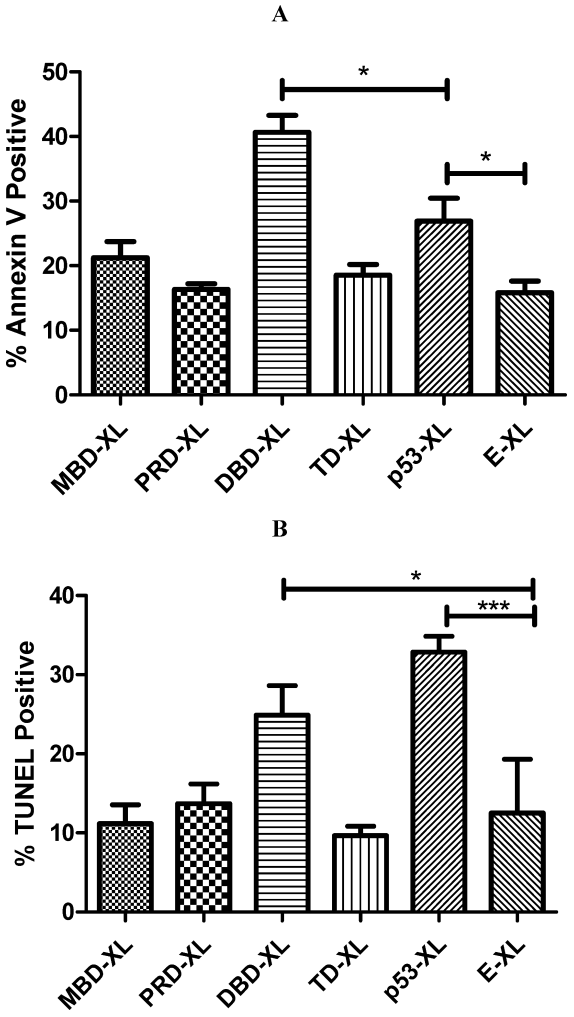

Figure 4. (A) Apoptotic potential was tested in T47D cells 48 h after transfection via annexin V assay. Statistical analysis was performed using one-way ANOVA with Tukey's post test with $*p < 0.05$. (B) Apoptotic potential was tested in T47D cells 48 h after transfection via TUNEL assay. Statistical analysis was performed using one-way ANOVA with Tukey's post test with $*p < 0.05$, $***p < 0.001$. p53-XL and DBD-XL were not statistically significantly different from each other. MBD-XL, PRD-XL, and TD-XL are statistically significantly lower than p53-XL.

ability of DBD-XL to induce apoptosis is not cell line or cancer cell type specific, a 7-AAD assay was conducted in breast cancer cells (MCF-7, MDA-MB-231), cervical adenocarcinoma cells (HeLa) and human non-small cell lung adenocarcinoma cells (H1373). T47D and MDA-MB-231 both express mutant p53, with the mutations restricted to the DBD (L194F in T47D[36] and R280L in MDA-MB-231[37]). These mutations reduce the activity of tumor suppressor activity substantially and cause these cells to be more resistant to apoptosis than MCF-7 and HeLa.[38] Additionally, MCF-7 harbor mislocalized p53 in the cytoplasm,[38] HeLa have endogenous wt-p53[39] and H1373 are p53 null.[40]

Since MDA-MB-231 and HeLa are highly proliferating cells, both cell lines were assayed 24 h after transfection while T47D, MCF-7 and H1373 cells were assayed 48 h post transfection (optimal time points determined empirically).

Interestingly, DBD-XL showed significantly higher apoptotic activity compared to p53-XL in MCF-7 (Figure 6A), MDA-MB-231(Figure 6B) and H1373 (Figure 6D). In HeLa cells, DBD-XL (and PRD-XL) were both statistically significantly different from p53-XL (Figure 5C). These results are consistent with the apoptosis data from T47D cells (Figures 3, 4A, and 4B) and show that DBD-XL is capable of inducing late stage apoptosis in four cell lines which differ in their endogenous p53 status.

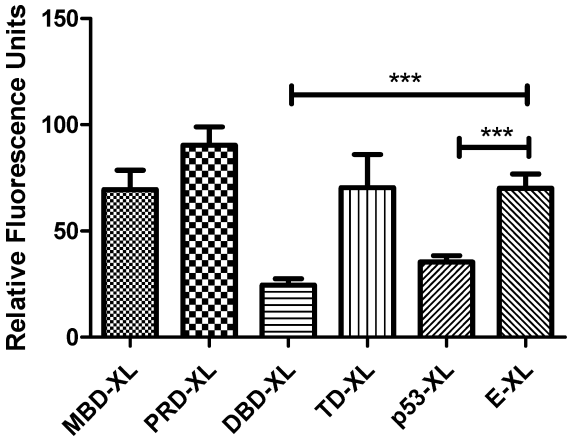

Figure 5. Transformative ability of T47D cells was determined 8 days after transfection of T47D cells via colony forming assay. Statistical analysis was accompanied using one-way ANOVA with Tukey's post test; $***p < 0.001$.

The Apoptotic Activity of DBD-XL Is Triggered via the Mitochondrial/Intrinsic Pathway. To determine that construct-induced apoptotic effects are through the mitochondria, TMRE and caspase-9 assays were performed. The DBD-XL was the only single domain construct that showed apoptotic potential the same as or higher than p53-XL consistently in all tested cell lines. Therefore, we proceeded to investigate only the mechanism for DBD-XL compared to p53-XL for our further studies.

To ensure that DBD-XL causes MOMP in the same manner as p53-XL, the TMRE assay (analogous to the JC-1 assay) was used.[41] TMRE is a cell-permeant, cationic, red-orange fluorescent dye that rapidly accumulates in mitochondria of living cells due to the negative mitochondrial membrane potential ($\Delta\Psi m$) of intact mitochondria compared to cytosol.[29,42,43] Mitochondrial depolarization results in a loss of TMRE from mitochondria and a decrease in mitochondrial fluorescence intensity (FI).[42] The mitochondrial membrane permeabilization (loss of FI) was illustrated as % MOMP induction on the *y*-axis. DBD-XL and p53-XL have similar activity and are significantly higher than E-XL (Figure 7A).

Further, the activation of caspase-9 was measured. Caspase-9 is only triggered through the intrinsic apoptotic pathway. Once cytochrome *c* is released from the mitochondria, caspase-9 is the first effector caspase downstream of cytochrome *c*.[44] Caspase-9 itself cleaves the peptide sequence leucine-glutamic acid-histidine-aspartic acid (LEHD) which is used in the caspase-9 assay to measure the intrinsic apoptotic pathway.[45] DBD-XL and p53-XL show higher caspase-9 activation than E-XL (Figure 7B). However, p53-XL triggers caspase-9 activation significantly more than DBD-XL (Figure 7B). A proposed explanation for this effect will be explained further in the discussion.

Investigating the Apoptotic Mechanism via Co-IP and Overexpression of Bcl-XL. To explore the apoptotic mechanism of our constructs, a co-IP was conducted (Figure

dx.doi.org/10.1021/mp400380s | *Mol. Pharmaceutics* 2013, 10, 3592−3602

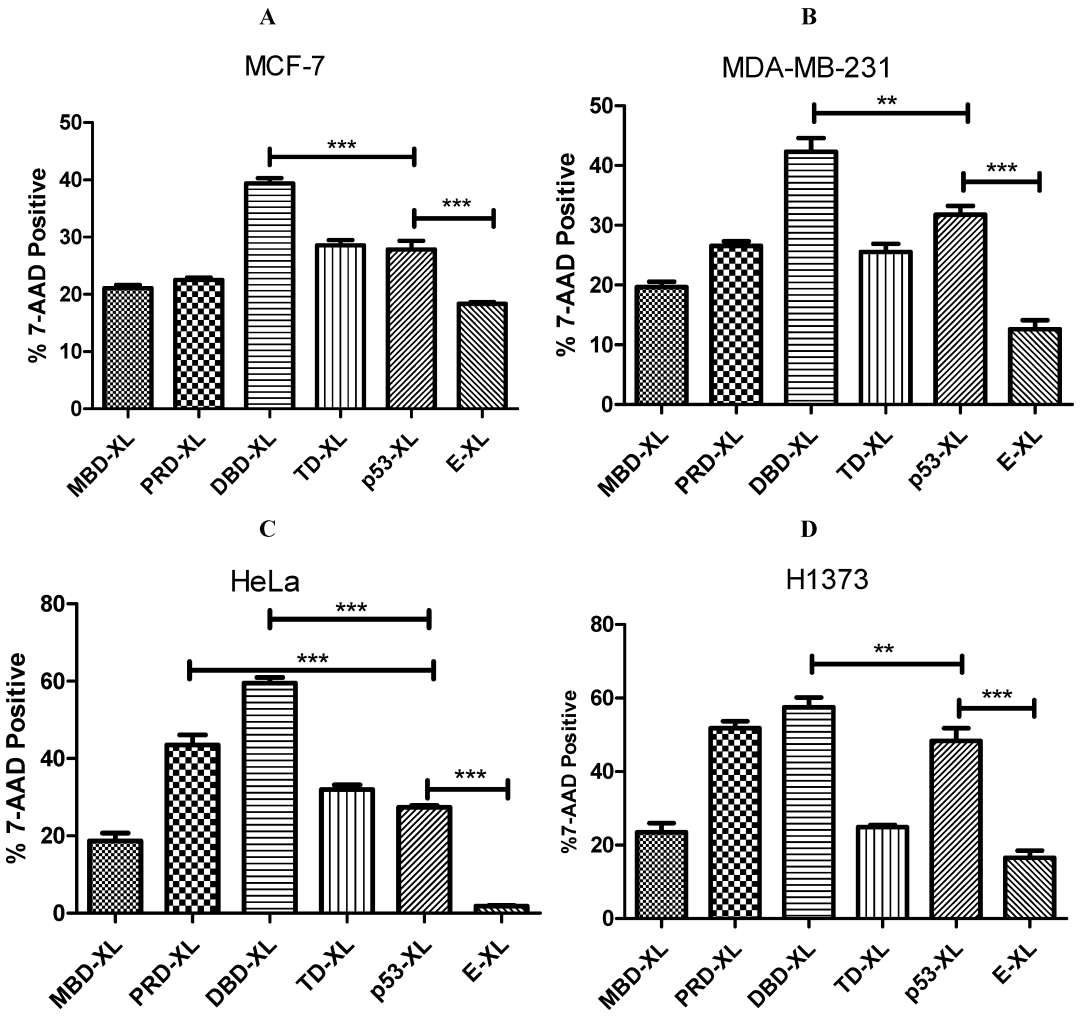

Figure 6. 7-AAD assay was conducted in (A) MCF-7, (B) MDA-MB-231, (C) HeLa and (D) H1373. Statistical analysis was performed using one-way ANOVA with Tukey's post test; $^{**}p < 0.01$ and $^{***}p < 0.001$.

8A). p53-XL, E-XL and E-CC (a negative control that does not contain the XL signal[19]) were transfected into T47D cells. T47D cells express the highest amount of endogenous Bcl-XL protein compared to MCF-7, MDA-MB-231 and HeLa (see Figure S1 in the Supporting Information). Approximately 24 h after transfection, cells were lysed and incubated with anti-GFP antibody. A Western blot was performed against EGFP (which is fused to all the constructs) and against Bcl-XL. Endogenous Bcl-XL (26 kDa) was expected to co-immunoprecipitate with exogenous p53-XL (75 kDa) due to its ability to induce apoptosis, while Bcl-XL should not co-immunoprecipitate with the negative control E-XL. Surprisingly, Bcl-XL co-immunoprecipitated with E-XL (32 kDa) just as p53-XL did (Figure 8A, lane 1 and 2). To address if the binding is due to the mitochondrial targeting signal which was originally taken from the Bcl-XL protein, another negative control E-CC was used, which does not contain a MTS. EGFP (27 kDa) could not be used as a negative control because it is too close in size to Bcl-XL (26 kDa) and would not be distinguishable on the gel. Bcl-XL did not co-immunoprecipitate with E-CC (Figure 8A, lane 3) implying that the binding of E-XL to Bcl-XL was due to the XL mitochondrial targeting signal.

To further explore the apoptotic mechanism of DBD-XL and p53-XL at the mitochondria, Bcl-XL was overexpressed in T47D cells. The apoptotic activity was measured by 7-AAD. Cells transfected with just p53-, DBD-, or E-XL were compared to cells cotransfected with either of these constructs and with BFP-Bcl-XL. It was expected that the apoptotic potential of the constructs that are undergoing apoptosis through the p53/Bcl-XL pathway would be rescued by Bcl-XL overexpression. Indeed, DBD-XL and p53-XL apoptotic activities were significantly reduced when BFP-Bcl-XL was cotransfected (Figure 8B). However, E-XL was not rescued by cotransfection of BFP-Bcl-XL (Figure 8B).

■ DISCUSSION

Our laboratory has previously shown that targeting p53 to antiapoptotic Bcl-XL is best achieved by using the MTS from Bcl-XL.[18] Additionally, we validated that the XL signal is the only MTS that has no inherent toxicity by itself since it is targeting the outer surface of the mitochondrial outer membrane.[18] Mitochondrial targeting of proteins to this region does not disrupt the sensitive balance of the mitochondria as reported with other MTSs.[46−49] As an approach to determine which domain of p53 is capable of inducing apoptosis similar to p53-XL, different domains of p53 were fused to XL. To our knowledge, this is the first attempt to target different domains of p53 to the mitochondria.

Here, we have shown that our designed constructs translocate to the mitochondria (Figure 2) and that any

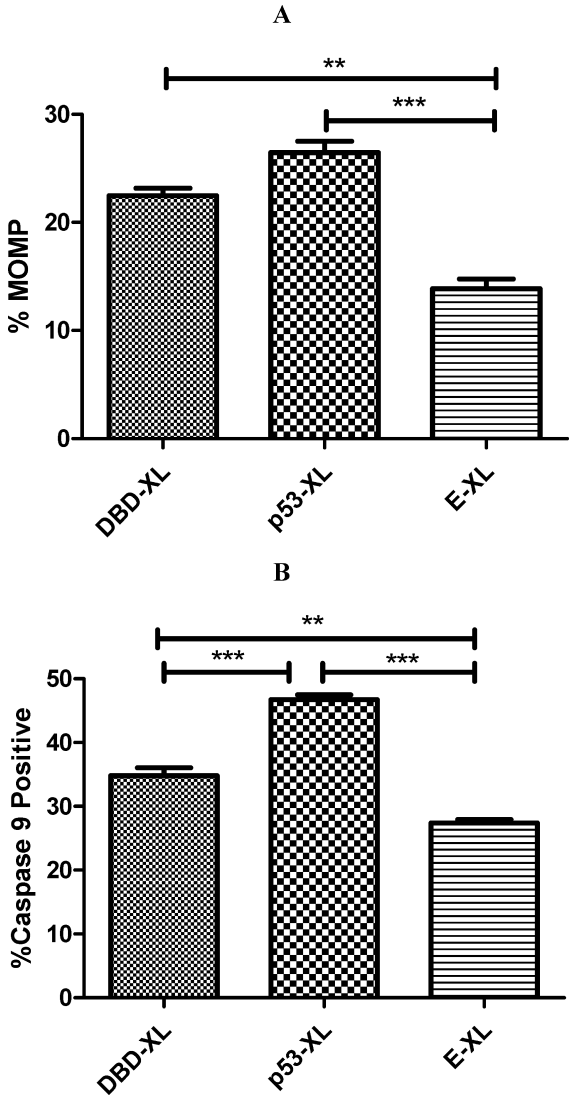

Figure 7. (A) Mitochondrial depolarization correlates with an increase in MOMP (as measured by TMRE). T47D cells were transfected with mitochondrial constructs and assayed using TMRE 36 h post transfection. (B) The activation of caspase-9 was analyzed 48 h following transfection of T47D cells. Statistical analysis was performed by using one-way ANOVA with Bonferroni's post test; $^{**}p < 0.01$ and $^{***}p < 0.001$.

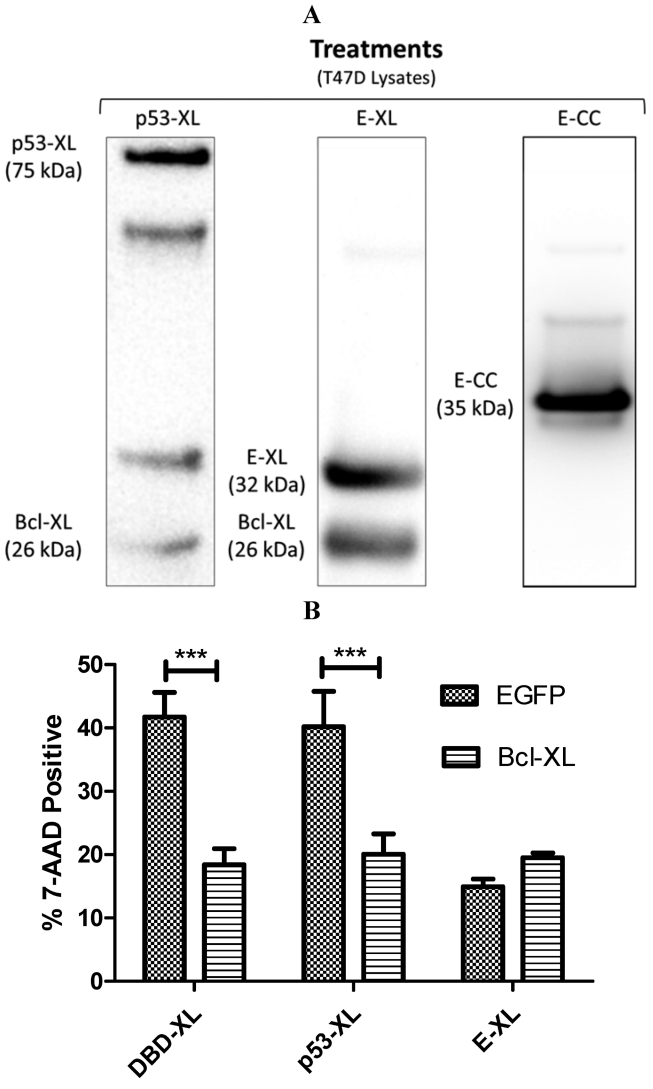

Figure 8. (A) Representative cropped Western blot of protein complexes co-immunoprecipitated using anti-GFP antibody. Lane 1, exogenous p53-XL (75 kDa) which was transfected into T47D cells co-immunoprecipitates with endogenous Bcl-XL (26 kDa). Lane 2, exogenous E-XL (32 kDa) co-immunoprecipitates with exogenous Bcl-XL (26 kDa). Lane 3 exogenous E-CC (35 kDa) fails to co-immunoprecipitate with endogenous Bcl-XL. Unlabeled bands are nonspecific binding. (B) Rescue experiment using Bcl-XL. 7-AAD assay was conducted 48 h post transfection in T47D cells. Statistical analysis was tested via unpaired *t* test; $^{**}p < 0.01$ and $^{***}p < 0.001$.

construct that contains the DBD of p53 is capable of inducing apoptosis similar to wt-p53 (Figure 3). It has been suggested that a combination of different domains of p53 is necessary for its apoptotic function and interaction with Bcl-XL at the mitochondria.[11−13] For instance, the PRD is thought to enhance the binding of p53 to Bcl-XL.[17] However, our data (Figure 3) clearly validates that the DBD region without the PRD region of p53 is sufficient to induce the full mitochondrial apoptotic function of p53. Even though the PRD was reported to enhance the binding of MBD and DBD to Bcl-XL, it did not have any effect on increasing the apoptotic potential. Hence, individual domains of p53 (Figure 1B) instead of combinations of domains were used in the remaining apoptotic assays.

Since the 7-AAD assay (Figure 3) does not distinguish between apoptotic and necrotic cells, early apoptosis assays (annexin V and TUNEL) were conducted to verify that our designed constructs are causing cell death via apoptosis and not necrosis. Indeed, DBD-XL showed the same (Figure 4B) or higher (Figure 4A) apoptotic activity compared to p53-XL in human breast cancer cells (T47D). To further validate the tumor suppressor function of our constructs and their ability to inhibit proliferation, a colony forming assay was conducted. As expected, DBD-XL showed similar reduction in transformative ability as p53-XL in T47D breast carcinoma cells (Figure 5).

To ensure that the increase in apoptotic activity is not cell line, cancer type or p53 status dependent, four different cancer cell lines (MCF-7, MDA-MB-231, HeLa, H1373) were tested. Surprisingly, DBD-XL induces late stage apoptosis significantly higher than p53-XL in all tested cell lines except T47D (Figure 6). The p53/MDM2 pathway might offer an explanation to why DBD-XL shows higher apoptotic activity compared to p53-XL. MDM2, a ubiquitin ligase (E3), binds to the MBD

dx.doi.org/10.1021/mp400380s | *Mol. Pharmaceutics* 2013, 10, 3592−3602

domain of p53 and helps to transfer ubiquitin from E2 to lysine residues on the carboxy terminus of p53. Ubiquinated p53 is dragged to the proteasome for degradation.[50,51] DBD-XL may evade degradation by MDM2 since it lacks the MBD and C-terminal domain, allowing for higher stability and consequently increased apoptotic activity. Hagn et al. showed that the amino acids of p53 responsible for interacting with Bcl-XL are located in the DBD of p53 (Gly117, Ser121, Cys176, His178, Asn239, Met243, Arg248, Gly279, and Arg280) and the contact sites on Bcl-XL are residues Ser18, Tyr22, Ser23, Gln26, and Ser28 in helix 1 and 2, Ile114 between helix 3 and 4, and Val155, Asp156, and Glu158 in helix 5.[11] Consequently, DBD-XL contains the residues important for interaction with Bcl-XL while lacking the domains responsible for degradation.

Alternatively, the antioxidative role of p53 might offer an explanation to why p53-XL shows lower apoptotic activity compared to DBD-XL. In healthy cells, basal p53 expression limits oxidative stress and promotes cell survival.[52] p53 upregulates the expression of genes involved in the oxidative stress survival pathways such as GPX1,[53] SOD2,[53] ALDH4A1,[54] INP1,[55] TIGAR,[56] Hi95[57] and PA26.[57] Even though all designed constructs translocate into the mitochondria (Figure 2), a small fraction could still enter the nucleus. Our previous publication shows that p53-XL retains some residual transcriptional activity.[18] Unlike p53-XL, which contains full length p53, DBD-XL is not capable of transcribing genes because it lacks the TD to form the transcriptionally active tetrameric p53 and the PRD which enhances transcription of various genes. This could provide another explanation why DBD-XL (which does not activate gene expression) shows higher apoptosis than p53-XL (which could upregulate the expression of genes involved in preventing oxidative stress).

Furthermore, the "mitochondrial priming theory" suggests that some cancer cells such as MCF-7 cells are inherently more sensitive to cytotoxic drugs than other cells.[38,58,59] This response correlates with the sensitive balance of anti- and proapoptotic Bcl-2 family members at the mitochondrial outer membrane.[58,59] It is known that T47D,[60] MCF-7,[61,62] MDA-MB-231[62] and HeLa[61] express antiapoptotic Bcl-XL. Therefore, we compared the expression levels of Bcl-XL in T47D,[60] MCF-7,[61,62] MDA-MB-231[62] and HeLa[61] (see Figure S1 in the Supporting Information). Indeed, T47D cells had the highest expression level of Bcl-XL confirming that they are "less primed" and more resistant to apoptosis.

Since the DBD-XL shows similar or higher apoptotic activity (measured by TUNEL, annexin V and 7-AAD) compared to p53-XL consistently in every tested cell line (Figures 3, 4, and 6), we wanted to examine if the effect on cell death is due to a mitochondrial dependent mechanism. DBD-XL triggers more caspase-9 activation than the negative control E-XL (Figure 7B) but surprisingly less caspase-9 induction than p53-XL (Figure 7B). Even though p53-XL caspase activity is higher, this is a transient effect that is not reflected in the more "final" apoptotic assays (Figures 3, 4, and 6). Additionally, a certain threshold of caspase 9 activation achieved by DBD-XL may be sufficient to induce cell death. Furthermore, DBD-XL induces MOMP to the same extent as p53-XL, suggesting that DBD-XL dependent apoptosis occurs through the intrinsic apoptotic pathway and might be through a direct interaction with Bcl-XL (Figure 7A). As described above, p53-XL could possibly be degraded via the proteasome. Once MDM-2, a ubiquitin ligase, binds to the MBD of p53, the C-terminal region of p53 becomes ubiquitinated and p53 is dragged into the proteasome for degradation.[50,51] This could explain why initially p53-XL causes more caspase-9 activation (Figure 7A), but this difference in activity is not reflected in the more "final" apoptosis assays where DBD-XL shows even higher apoptosis activity compared to p53-XL (Figure 6).

In an effort to determine if the apoptotic potential of our designed constructs is due to their interaction with Bcl-XL or if it is independent of the p53/Bcl-XL pathway, we conducted a co-IP and a rescue experiment achieved by overexpressing Bcl-XL. Interestingly, Bcl-XL co-immunoprecipitated with the "negative control" E-XL in the same manner as p53-XL (Figure 8A). We hypothesize that the interaction with Bcl-XL is independent of p53 and it is mainly due to the XL MTS which will directly target every protein that contains XL to Bcl-XL. To investigate this hypothesis, E-CC (a negative control lacking the XL signal) was created. As expected, E-CC did not bind to Bcl-XL (Figure 8A), confirming that the XL signal is responsible for the interaction with Bcl-XL.

To prove indirectly that the apoptotic mechanisms of p53- and DBD-XL are through direct interaction of p53 and DBD with Bcl-XL, a rescue experiment using overexpressed Bcl-XL was conducted. As expected, the apoptotic activity of MBD-, PRD- and E-XL was not altered by Bcl-XL overexpression (see Figure S2 in the Supporting Information). However, DBD-XL and p53-XL (and even TD-XL) demonstrated reduction in apoptotic potential, further demonstrating the necessity of Bcl-XL for apoptosis initiation (Figure 8B; Figure S2 in the Supporting Information). Even though TD-XL showed significantly lower cell death compared to p53-XL, it was still significantly higher than the negative control E-XL, and it was still rescued by Bcl-XL (Figure S2 in the Supporting Information). It could be speculated that TD-XL binds to endogenous, mutant p53 through its TD and drags it to the mitochondria where it potentially interacts with Bcl-XL and triggers marginal apoptosis.[63] Even though endogenous, mutant p53 is transcriptionally inactive in T47D cells due to the presence of the L194F mutation, this mutant p53 could still be active at the mitochondria, since the L194 residue is not involved in the interaction between p53 and Bcl-XL.[11]

In summary, DBD-XL shows the same (T47D) or higher (MCF-7, MDA-MB-231, HeLa, H1373) apoptotic activity compared to p53-XL. Mechanistic studies suggest that DBD-XL may bind and trigger apoptosis similar to p53 through the Bcl-XL dependent pathway. Our data highlights that DBD (about half the size of full length p53) can be used instead of p53 for achieving apoptosis at the mitochondria when fused to the MTS from Bcl-XL. The benefit of decreasing the overall size of p53 by half while still maintaining full apoptotic activity allows for better drug delivery options. The next goal is to use DBD-XL as a therapeutic in vivo using adenoviral drug delivery.

In conclusion, we show for the first time that DBD-XL can be used to trigger a potent, rapid apoptotic response in various cancer cell lines (including breast, cervical and lung carcinomas) with different p53 status, and is an alternative to wt-p53 gene therapy. Importantly, the mechanism of DBD-XL-mediated apoptosis is distinctly different from conventional wild type p53 and represents a novel approach for cancer therapy.

■ ASSOCIATED CONTENT

Supporting Information

Additional figures depicting different endogenous expression levels of Bcl-XL (Figure S1) and rescue experiment including MBD-, PRD-, DBD-, TD-, p53- and E-XL (Figure S2). This material is available free of charge via the Internet at http://pubs.acs.org.

■ AUTHOR INFORMATION

Corresponding Author

*C. S. Lim: 30 South 2000 East, Rm 2916, Salt Lake City, UT 84112, United States; phone, 1-801-587-9711; fax, 1-801-585-3614; e-mail, carol.lim@pharm.utah.edu.

Notes

The authors declare no competing financial interest.

■ ACKNOWLEDGMENTS

We would like to thank Christian Raab, David Woessner, Shams Reaz, Geoff Miller, and Ben Bruno for scientific discussions. We acknowledge the use of DNA/Peptide Core and Flow Cytometry Core (NCI Cancer Center Support Grant P30 CA042014, Huntsman Cancer Institute). Research reported in this publication was supported by the National Cancer Institute of the National Institutes of Health under award number R01-CA151847.

■ REFERENCES

(1) Goh, A. M.; Coffill, C. R.; Lane, D. P. The role of mutant p53 in human cancer. *J. Pathol.* **2011**, *223*, 116−126, DOI: 10.1002/path.2784.

(2) Sherr, C. J. Principles of tumor suppression. *Cell* **2004**, *116*, 235−246, DOI: 10.1016/S0092-8674(03)01075-4.

(3) Martins, C. P.; Brown-Swigart, L.; Evan, G. I. Modeling the therapeutic efficacy of p53 restoration in tumors. *Cell* **2006**, *127*, 1323−1334, DOI: 10.1016/j.cell.2006.12.007.

(4) Xin, H. Chinese gene therapy. Gendicine's efficacy: hard to translate. *Science* **2006**, *314*, 1233 DOI: 10.1126/science.314.5803.1233.

(5) Peng, Z. Current status of gendicine in China: recombinant human Ad-p53 agent for treatment of cancers. *Hum. Gene Ther.* **2005**, *16*, 1016−1027, DOI: 10.1089/hum.2005.16.1016.

(6) Palacios, G.; Crawford, H. C.; Vaseva, A.; Moll, U. M. Mitochondrially targeted wild-type p53 induces apoptosis in a solid human tumor xenograft model. *Cell Cycle* **2008**, *7*, 2584−2590, DOI: 6070.

(7) Fuster, J. J.; Sanz-Gonzalez, S. M.; Moll, U. M.; Andres, V. Classic and novel roles of p53: prospects for anticancer therapy. *Trends Mol. Med.* **2007**, *13*, 192−199, DOI: 10.1016/j.molmed.2007.03.002.

(8) Perfettini, J. L.; Kroemer, R. T.; Kroemer, G. Fatal liaisons of p53 with Bax and Bak. *Nat. Cell Biol.* **2004**, *6*, 386−388, DOI: 10.1038/ncb0504-386ncb0504-386.

(9) Vaseva, A. V.; Moll, U. M. The mitochondrial p53 pathway. *Biochim. Biophys. Acta* **2009**, *1787*, 414−420, DOI: 10.1016/j.bbabio.2008.10.005.

(10) Joerger, A. C.; Fersht, A. R. The tumor suppressor p53: from structures to drug discovery. *Cold Spring Harbor Perspect. Biol.* **2010**, *2*, a000919 DOI: 10.1101/cshperspect.a000919.

(11) Hagn, F.; et al. BclxL changes conformation upon binding to wild-type but not mutant p53 DNA binding domain. *J. Biol. Chem.* **2010**, *285*, 3439−3450, DOI: 10.1074/jbc.M109.065391.

(12) Petros, A. M.; Gunasekera, A.; Xu, N.; Olejniczak, E. T.; Fesik, S. W. Defining the p53 DNA-binding domain/Bcl-x(L)-binding interface using NMR. *FEBS Lett.* **2004**, *559*, 171−174, DOI: 10.1016/S0014-5793(04)00059-6.

(13) Tomita, Y.; et al. WT p53, but not tumor-derived mutants, bind to Bcl2 via the DNA binding domain and induce mitochondrial permeabilization. *J. Biol. Chem.* **2006**, *281*, 8600−8606, DOI: 10.1074/jbc.M507611200.

(14) Bharatham, N.; Chi, S. W.; Yoon, H. S. Molecular basis of Bcl-X(L)-p53 interaction: insights from molecular dynamics simulations. *PLoS One* **2011**, *6*, e26014 DOI: 10.1371/journal.pone.0026014-PONE-D-11-15062.

(15) Chipuk, J. E.; Maurer, U.; Green, D. R.; Schuler, M. Pharmacologic activation of p53 elicits Bax-dependent apoptosis in the absence of transcription. *Cancer Cell* **2003**, *4*, 371−381, DOI: 10.1016/S1535-6108(03)00272-1.

(16) Ha, J. H.; et al. Molecular mimicry-based repositioning of nutlin-3 to anti-apoptotic Bcl-2 family proteins. *J. Am. Chem. Soc.* **2011**, *133*, 1244−1247, DOI: 10.1021/ja109521f.

(17) Xu, H.; Tai, J.; Ye, H.; Kang, C. B.; Yoon, H. S. The N-terminal domain of tumor suppressor p53 is involved in the molecular interaction with the anti-apoptotic protein Bcl-Xl. *Biochem. Biophys. Res. Commun.* **2006**, *341*, 938−944, DOI: 10.1016/j.bbrc.2005.12.227.

(18) Mossalam, M.; Matissek, K. J.; Okal, A.; Constance, J. E.; Lim, C. S. Direct induction of apoptosis using an optimal mitochondrially targeted p53. *Mol. Pharmaceutics* **2012**, *9*, 1449−1458, DOI: 10.1021/mp3000259.

(19) Dixon, A. S.; et al. Disruption of Bcr-Abl coiled coil oligomerization by design. *J. Biol. Chem.* **2011**, *286*, 27751−27760, DOI: 10.1074/jbc.M111.264903.

(20) Dixon, A. S.; et al. Improved coiled-coil design enhances interaction with Bcr-Abl and induces apoptosis. *Mol. Pharmaceutics* **2012**, *9*, 187−195, DOI: 10.1021/mp200461s.

(21) Dixon, A. S.; et al. Controlling subcellular localization to alter function: Sending oncogenic Bcr-Abl to the nucleus causes apoptosis. *J. Controlled Release* **2009**, *140*, 245−249, DOI: 10.1016/j.jconrel.2009.06.026.

(22) Bolte, S.; Cordelieres, F. P. A guided tour into subcellular colocalization analysis in light microscopy. *J. Microsc.* **2006**, *224*, 213−232, DOI: 10.1111/j.1365-2818.2006.01706.x.

(23) Constance, J. E.; Despres, S. D.; Nishida, A.; Lim, C. S. Selective targeting of c-Abl via a cryptic mitochondrial targeting signal activated by cellular redox status in leukemic and breast cancer cells. *Pharm. Res.* **2012**, *29*, 2317−2328, DOI: 10.1007/s11095-012-0758-9.

(24) Constance, J. E.; Woessner, D. W.; Matissek, K. J.; Mossalam, M.; Lim, C. S. Enhanced and selective killing of chronic myelogenous leukemia cells with an engineered BCR-ABL binding protein and imatinib. *Mol. Pharmaceutics* **2012**, *9*, 3318−3329, DOI: 10.1021/mp3003539.

(25) Costes, S. V.; et al. Automatic and quantitative measurement of protein-protein colocalization in live cells. *Biophys. J.* **2004**, *86*, 3993−4003, DOI: 10.1529/biophysj.103.038422.

(26) Adler, J.; Parmryd, I. Quantifying colocalization by correlation: the Pearson correlation coefficient is superior to the Mander's overlap coefficient. *Cytometry, Part A* **2010**, *77*, 733−742, DOI: 10.1002/cyto.a.20896.

(27) Davis, J. R.; Mossalam, M.; Lim, C. S. Controlled access of p53 to the nucleus regulates its proteasomal degradation by MDM2. *Mol. Pharmaceutics* **2013**, *10*, 1340−1349, DOI: 10.1021/mp300543t.

(28) Jaskolski, F.; Mulle, C.; Manzoni, O. J. An automated method to quantify and visualize colocalized fluorescent signals. *J. Neurosci. Methods* **2005**, *146*, 42−49, DOI: 10.1016/j.jneumeth.2005.01.012.

(29) Krohn, A. J.; Wahlbrink, T.; Prehn, J. H. Mitochondrial depolarization is not required for neuronal apoptosis. *J. Neurosci.* **1999**, *19*, 7394−7404.

(30) Grabarek, J.; Amstad, P.; Darzynkiewicz, Z. Use of fluorescently labeled caspase inhibitors as affinity labels to detect activated caspases. *Hum. Cell* **2002**, *15*, 1−12.

(31) Grabarek, J.; Darzynkiewicz, Z. In situ activation of caspases and serine proteases during apoptosis detected by affinity labeling their enzyme active centers with fluorochrome-tagged inhibitors. *Exp. Hematol.* **2002**, *30*, 982−989, DOI: 10.1016/S0301-472X(02)00886-X.

(32) Schmid, I.; Krall, W. J.; Uittenbogaart, C. H.; Braun, J.; Giorgi, J. V. Dead cell discrimination with 7-amino-actinomycin D in

combination with dual color immunofluorescence in single laser flow cytometry. *Cytometry* **1992**, *13*, 204−208, DOI: 10.1002/cyto.990130216.
(33) Serrano, M. J.; et al. Evaluation of a gemcitabine-doxorubicin-paclitaxel combination schedule through flow cytometry assessment of apoptosis extent induced in human breast cancer cell lines. *Jpn. J. Cancer Res.* **2002**, *93*, 559−566.
(34) Vermes, I.; Haanen, C.; Steffens-Nakken, H.; Reutelingsperger, C. A novel assay for apoptosis. Flow cytometric detection of phosphatidylserine expression on early apoptotic cells using fluorescein labelled Annexin V. *J. Immunol. Methods* **1995**, *184*, 39−51, DOI: 10.1016/0022-1759(95)00072-I.
(35) Loo, D. T.; Rillema, J. R. Measurement of cell death. *Methods Cell Biol.* **1998**, *57*, 251−264.
(36) Nigro, J. M.; et al. Mutations in the p53 gene occur in diverse human tumour types. *Nature* **1989**, *342*, 705−708, DOI: 10.1038/342705a0.
(37) Bartek, J.; Iggo, R.; Gannon, J.; Lane, D. P. Genetic and immunochemical analysis of mutant p53 in human breast cancer cell lines. *Oncogene* **1990**, *5*, 893−899.
(38) Mooney, L. M.; Al-Sakkaf, K. A.; Brown, B. L.; Dobson, P. R. Apoptotic mechanisms in T47D and MCF-7 human breast cancer cells. *Br. J. Cancer* **2002**, *87*, 909−917, DOI: 10.1038/sj.bjc.6600541.
(39) Goodrum, F. D.; Ornelles, D. A. p53 status does not determine outcome of E1B 55-kilodalton mutant adenovirus lytic infection. *J. Virol.* **1998**, *72*, 9479−9490.
(40) Bodner, S. M.; et al. Expression of mutant p53 proteins in lung cancer correlates with the class of p53 gene mutation. *Oncogene* **1992**, *7*, 743−749.
(41) Jayaraman, S. Flow cytometric determination of mitochondrial membrane potential changes during apoptosis of T lymphocytic and pancreatic beta cell lines: comparison of tetramethylrhodamineethylester (TMRE), chloromethyl-X-rosamine (H2-CMX-Ros) and MitoTracker Red 580 (MTR580). *J. Immunol. Methods* **2005**, *306*, 68−79, DOI: 10.1016/j.jim.2005.07.024.
(42) O'Reilly, C. M.; Fogarty, K. E.; Drummond, R. M.; Tuft, R. A.; Walsh, J. V., Jr. Quantitative analysis of spontaneous mitochondrial depolarizations. *Biophys. J.* **2003**, *85*, 3350−3357, DOI: 10.1016/S0006-3495(03)74754-7.
(43) Ricci, J. E.; Gottlieb, R. A.; Green, D. R. Caspase-mediated loss of mitochondrial function and generation of reactive oxygen species during apoptosis. *J. Cell Biol.* **2003**, *160*, 65−75, DOI: 10.1083/jcb.200208089jcb.200208089.
(44) Chowdhury, I.; Tharakan, B.; Bhat, G. K. Caspases - an update. *Comp. Biochem. Physiol., Part B: Biochem. Mol. Biol.* **2008**, *151*, 10−27, DOI: 10.1016/j.cbpb.2008.05.010S1096-4959(08)00132-2.
(45) Yin, Q.; et al. Caspase-9 holoenzyme is a specific and optimal procaspase-3 processing machine. *Mol. Cell* **2006**, *22*, 259−268, DOI: 10.1016/j.molcel.2006.03.030.
(46) Mihara, M.; et al. p53 has a direct apoptogenic role at the mitochondria. *Mol. Cell* **2003**, *11*, 577−590, DOI: 10.1016/S1097-2765(03)00050-9.
(47) Power, S. D.; Lochrie, M. A.; Patterson, T. E.; Poyton, R. O. The nuclear-coded subunits of yeast cytochrome c oxidase. II. The amino acid sequence of subunit VIII and a model for its disposition in the inner mitochondrial membrane. *J. Biol. Chem.* **1984**, *259*, 6571−6574.
(48) Mossalam, M.; Dixon, A. S.; Lim, C. S. Controlling subcellular delivery to optimize therapeutic effect. *Ther. Delivery* **2010**, *1*, 169−193.
(49) Schmidt, O.; Pfanner, N.; Meisinger, C. Mitochondrial protein import: from proteomics to functional mechanisms. *Nat. Rev. Mol. Cell Biol.* **2010**, *11*, 655−667, DOI: 10.1038/nrm2959nrm2959.
(50) Nalepa, G.; Rolfe, M.; Harper, J. W. Drug discovery in the ubiquitin-proteasome system. *Nat. Rev. Drug Discovery* **2006**, *5*, 596−613, DOI: 10.1038/nrd2056.
(51) Haupt, Y.; Maya, R.; Kazaz, A.; Oren, M. Mdm2 promotes the rapid degradation of p53. *Nature* **1997**, *387*, 296−299, DOI: 10.1038/387296a0.
(52) Maddocks, O. D.; Vousden, K. H. Metabolic regulation by p53. *J. Mol. Med. (Berlin)* **2011**, *89*, 237−245, DOI: 10.1007/s00109-011-0735-5.
(53) Hussain, S. P.; et al. p53-induced up-regulation of MnSOD and GPx but not catalase increases oxidative stress and apoptosis. *Cancer Res.* **2004**, *64*, 2350−2356.
(54) Yoon, K. A.; Nakamura, Y.; Arakawa, H. Identification of ALDH4 as a p53-inducible gene and its protective role in cellular stresses. *J. Hum. Genet.* **2004**, *49*, 134−140, DOI: 10.1007/s10038-003-0122-3.
(55) Cano, C. E.; et al. Tumor protein 53-induced nuclear protein 1 is a major mediator of p53 antioxidant function. *Cancer Res.* **2009**, *69*, 219−226, DOI: 10.1158/0008-5472.CAN-08-232069/1/219.
(56) Bensaad, K.; et al. TIGAR, a p53-inducible regulator of glycolysis and apoptosis. *Cell* **2006**, *126*, 107−120, DOI: 10.1016/j.cell.2006.05.036.
(57) Budanov, A. V.; Karin, M. p53 target genes sestrin1 and sestrin2 connect genotoxic stress and mTOR signaling. *Cell* **2008**, *134*, 451−460, DOI: 10.1016/j.cell.2008.06.028.
(58) Ni Chonghaile, T.; et al. Pretreatment mitochondrial priming correlates with clinical response to cytotoxic chemotherapy. *Science* **2011**, *334*, 1129−1133, DOI: 10.1126/science.1206727.
(59) Constance, J. E.; Lim, C. S. Targeting malignant mitochondria with therapeutic peptides. *Ther. Delivery* **2012**, *3*, 961−979.
(60) Yamashita, H.; Nishio, M.; Fujii, Y.; Iwase, H. Dominant-negative Stat5 inhibits growth and induces apoptosis in T47D-derived tumors in nude mice. *Cancer Sci.* **2004**, *95*, 662−665.
(61) Shi, J.; Zhou, Y.; Huang, H. C.; Mitchison, T. J. Navitoclax (ABT-263) accelerates apoptosis during drug-induced mitotic arrest by antagonizing Bcl-xL. *Cancer Res.* **2011**, *71*, 4518−4526, DOI: 10.1158/0008-5472.CAN-10-4336.
(62) Li, H.; et al. Liposomes containing (-)-gossypol-enriched cottonseed oil suppress Bcl-2 and Bcl-xL expression in breast cancer cells. *Pharm. Res.* **2011**, *28*, 3256−3264, DOI: 10.1007/s11095-011-0498-2.
(63) Jeffrey, P. D.; Gorina, S.; Pavletich, N. P. Crystal structure of the tetramerization domain of the p53 tumor suppressor at 1.7 angstroms. *Science* **1995**, *267*, 1498−1502.

Title: The DNA Binding Domain of p53 Is Sufficient To Trigger a Potent Apoptotic Response at the Mitochondria

Author: Karina J. Matissek, Mohanad Mossalam, Abood Okal, and Carol S. Lim

Publication: Molecular Pharmaceutics

Publisher: American Chemical Society

Date: Oct 1, 2013

PERMISSION/LICENSE IS GRANTED FOR YOUR ORDER AT NO CHARGE

This type of permission/license, instead of the standard Terms & Conditions, is sent to you because no fee is being charged for your order. Please note the following:

- Permission is granted for your request in both print and electronic formats, and translations.
- If figures and/or tables were requested, they may be adapted or used in part.
- Please print this page for your records and send a copy of it to your publisher/graduate school.
- Appropriate credit for the requested material should be given as follows: "Reprinted (adapted) with permission from (COMPLETE REFERENCE CITATION). Copyright (YEAR) American Chemical Society." Insert appropriate information in place of the capitalized words.
- One-time permission is granted only for the use specified in your request. No additional uses are granted (such as derivative works or other editions). For any other uses, please submit a new request.

molecular pharmaceutics

Article

pubs.acs.org/molecularpharmaceutics

A Chimeric p53 Evades Mutant p53 Transdominant Inhibition in Cancer Cells

Abood Okal,[†] Mohanad Mossalam,[†] Karina J. Matissek,[†,‡] Andrew S. Dixon,[†] Philip J. Moos,[§] and Carol S. Lim*[,†]

[†]Department of Pharmaceutics and Pharmaceutical Chemistry, University of Utah, Salt Lake City, Utah 84112, United States

[‡]Department of Pharmaceutics and Biopharmacy, Philipps-Universität, Biegenstraße 10/12, 35037 Marburg, Germany

[§]Department of Pharmacology and Toxicology, University of Utah, Salt Lake City, Utah 84112, United States

Supporting Information

ABSTRACT: Because of the dominant negative effect of mutant p53, there has been limited success with wild-type (wt) p53 cancer gene therapy. Therefore, an alternative oligomerization domain for p53 was investigated to enhance the utility of p53 for gene therapy. The tetramerization domain of p53 was substituted with the coiled-coil (CC) domain from Bcr (breakpoint cluster region). Our p53 variant (p53-CC) maintains proper nuclear localization in breast cancer cells detected via fluorescence microscopy and shows a similar expression profile of p53 target genes as wt-p53. Additionally, similar tumor suppressor activities of p53-CC and wt-p53 were detected by terminal deoxynucleotidyl transferase dUTP nick end labeling (TUNEL), annexin-V, 7-aminoactinomycin D (7-AAD), and colony-forming assays. Furthermore, p53-CC was found to cause apoptosis in four different cancer cell lines, regardless of endogenous p53 status. Interestingly, the transcriptional activity of p53-CC was higher than wt-p53 in 3 different reporter gene assays. We hypothesized that the higher transcriptional activity of p53-CC over wt-p53 was due to the sequestration of wt-p53 by endogenous mutant p53 found in cancer cells. Co-immunoprecipitation revealed that wt-p53 does indeed interact with endogenous mutant p53 via its tetramerization domain, while p53-CC escapes this interaction. Therefore, we investigated the impact of the presence of a transdominant mutant p53 on tumor suppressor activities of wt-p53 and p53-CC. Overexpression of a potent mutant p53 along with wt-p53 or p53-CC revealed that, unlike wt-p53, p53-CC retains the same level of tumor suppressor activity. Finally, viral transduction of wt-p53 and p53-CC into a breast cancer cell line that harbors a tumor derived transdominant mutant p53 validated that p53-CC indeed evades sequestration and consequent transdominant inhibition by endogenous mutant p53.

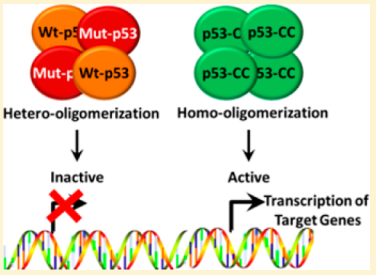

KEYWORDS: *p53, dominant-negative effect, tetramerization domain, coiled-coil, Bcr, breast cancer, tumor suppressor*

INTRODUCTION

The tumor suppressor p53, a 393 amino acid sequence-specific transcription factor, stimulates a wide network of signals including cell cycle arrest, DNA repair, and apoptosis. p53-dependent apoptosis is achieved through two distinct apoptotic signaling pathways: the extrinsic pathway through death receptors and the intrinsic pathway through the mitochondria.[1] While p53 is able to induce apoptosis when targeted to the mitochondria,[2−4] its tumor suppressor function mainly depends on localization to the nucleus and formation of p53 tetramers leading to its function as a transcription factor of several target genes.[5] The p53 protein is commonly divided into three regions: an acidic N-terminal region (codons 1−101), a DNA binding domain (DBD, codons 102−292), and a basic C-terminal region (codons 293−393).[6] The C-terminus contains three nuclear localization signals (NLSs), a nuclear export signal (E), and a tetramerization domain (TD) (Figure 2A). In response to cellular stimuli such as DNA damage and oncogene activation,[7] the murine double minute 2 (MDM2)-p53 degradation pathway is inactivated leading to increased concentration of p53 followed by rapid accumulation in the nucleus, which is essential for regulating cell cycle arrest, DNA repair, senescence, and apoptosis.[8,9]

Current strategies to enhance the anticancer/tumor-suppressor function of p53 are focused on introducing additional wt-p53 to the affected cells or tumor. This treatment modality introduces wt-p53 as a gene into cancer cells using various delivery vehicles. Wild-type p53 is a currently approved gene therapeutic for head and neck cancer in China.[10] While a promising approach, there are significant limitations to the efficacy of this method, namely, the presence of mutations in the endogenous p53 molecule.

The tumor suppressor p53 is inactivated in more than half of all human tumors.[11] Acquisition of missense mutations in the *TP53* gene results in aberrant p53 that is transcriptionally inactive.[12−14] Mutant p53 can also contribute to cancer drug resistance due to its inhibition of wild-type (wt) p53 via a

Received: July 1, 2013
Revised: August 13, 2013
Accepted: August 21, 2013
Published: August 21, 2013

dominant negative effect and the acquisition of gain of function properties.[15] Since p53 binds DNA as a tetramer consisting of a dimer of dimers,[16] when endogenous mutant p53 oligomerizes with exogenous wt-p53, the resulting tetramer is inactive.[17−19] Such heterotetramerization is possible as the TD retains functionality in mutant p53. This dominant negative effect, wherein mutant p53 inactivates therapeutic wt-p53, represents a key problem with using wt-p53 for gene therapy. The dominant negative effect of p53 has shown to be operative *in vivo* using knock-in mice expressing mutant p53.[20]

Because sequestration of wt-p53 into inactive heterotetramers with mutant p53 forms a critical barrier to the efficacy of utilizing p53 for cancer therapy, improvements to advance the efficacy of this therapy even in the presence of p53 mutants is needed.[11] Our approach to bypass the dominant negative effect of tumor-derived p53 is to engineer a p53 variant that relies on a different oligomerization motif to prevent hetero-oligomer formation. To our knowledge, only one attempt has been made to eliminate the dominant negative effect of mutant p53 in heterotetramers via substituting its TD, with marginal success.[21] Whereas the native TD of p53 drives the formation of *antiparallel* tetramers,[21−23] this previous work utilized an oligomerization domain that led to *parallel* tetramer formation which resulted in a significant reduction in p53 function. We recognized that the oligomerization domain from breakpoint cluster region (Bcr) protein, a 72 amino acid coiled-coil (CC), tetramerizes as two dimers of two antiparallel-oriented monomers,[24] in a similar fashion to the TD of wt-p53. This would be a suitable candidate for TD substitution,[22] forming a chimeric p53-Bcr fusion. Table 1 depicts the oligomerization domains for p53 (TD) and the CC domain from Bcr.

Table 1. Comparison of the Native TD from wt-p53 to the CC Domain from Bcr[a]

	TD	CC
Sequence	31 amino acids	72 amino acids
Secondary Structure	Consists of a β strand, a tight turn followed by an α helix	Consists of two α helices
Orientation	Antiparallel	Antiparallel
Tetramer Formation	Dimer of dimers	Dimer of dimers
Structure	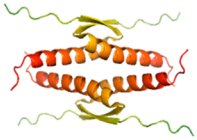	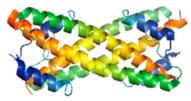

[a]Snapshots were taken with molecular visualization software PyMOL (PyMOL Molecular Graphics System Version 1.5.0.4, Schrödinger, LLC) initiated from the1C26 for p53 TD[22] and 1K1F for Bcr CC[25] PDB structures.

This report demonstrates that our p53 variant, namely, p53-CC, shows higher levels of transcriptional activity in reporter gene assays and exhibits similar tumor suppressor activity compared to wt-p53 in cell lines with varying p53 status. Lastly, we show the ability of p53-CC to circumvent the dominant negative effect in cancer cells harboring a strong transdominant mutant p53. Figure 1 illustrates our hypothesis of bypassing the dominant negative effect with p53-CC (right side), which maintains functional tumor suppressor activity.

MATERIALS AND METHODS

Construction of Plasmids (Figure 2A). To construct pEGFP-p53-CC (p53-CC), a truncated version of wt-p53 that lacks the tetramerization domain (amino acids 1−322) was amplified via PCR with primers 5′-GCGCGCGCGCTCCGGAATGGAGGAGCCGCAGTCA-3′ and 5′-GCGCGCGCGCTCCGGATGGTTTCTTCTTTGGCTGGGGAGA-3′ using the previously cloned pEGFP-p53 (wt-p53) as the template DNA.[4] The PCR product was then subcloned into the BspEI site of pEGFP-CC (CC).[26]

To create pEGFP-p53-ΔTDC (p53-ΔTDC), the same truncated version of wt-p53 (amino acids 1−322) was amplified via PCR with primers 5′-GCGCGCGCGCTCCGGAATGGAGGAGCCGCAGTCA-3′ and 5′-GCGCGCGCGCGGTACCTCATGGTTTCTTCTTTGGCTGGGG-3′ using pEGFP-p53 as the template DNA.[4] The PCR product (insert) was then subcloned into the digested pEGFP-C1 vector (Clontech, Mountain View, CA) at the BspEI and *Kpn*I sites.

To design pTagBFP-mut-p53, wt-p53 was amplified via PCR with primers 5′-GCGCGCGCGCTCCGGAGCCATGGAGGAGCCGCAGT-3′, and 5′-GCGCGCGCGCGGTACCTCAGTCTGAGTCAGGCCCTTCTGTC-3′ using pEGFP-p53 as a template. This insert was then subcloned into the digested pTagBFP-C vector (Evrogen, Moscow, Russia) at the BspEI and *Kpn*I sites. Three hot spot mutations (R175H, R248W, and R273H)[27,28] were then introduced into pTagBFP-p53 via QuikChange II XL Site- Directed Mutagenesis Kit (Agilent, Santa Clara, CA). The following primers were used: for the R175H mutation, 5′-TGACGGAGGTTGTGAGGCACTGCCCCCACCATGAGCGC-3′ and 5′-GCGCTCATGGTGGGGGCAGTGCCTCACAACCTCCGTCA-3′; for R248W, 5′-CTGCATGGGCGGCATGAACTGGAGGCCCATCCTCACCA-3′ and 5′-TGGTGAGGATGGGCCTCCAGTTCATGCCGCCCATGCAG-3′; and for R273H, 5′-GGAACAGCTTTGAGGTGCATGTTTGTGCCTGTCCTGGG-3′ and 5′-CCCAGGACAGGCACAAACATGCACCTCAAAGCTGTTCC-3′.

Cell Lines and Transient Transfection. T47D human ductal breast epithelial tumor cells (ATCC, Manassas, VA), MCF-7 human breast adenocarcinoma cells (ATCC), HeLa human epithelial cervical adenocarcinoma cells (ATCC), H1373 human non-small cell lung carcinoma cells (a kind gift from Dr. Andrea Bild, University of Utah), and MDA-MB-231 human breast adenocarcinoma cells (ATCC) were grown as monolayers in RPMI (Invitrogen, Carlsbad, CA) supplemented with 10% fetal bovine serum (Invitrogen), 1% penicillin−streptomycin−glutamine (Invitrogen), and 0.1% gentamicin (Invitrogen). T47D and MCF-7 were also supplemented with 4 mg/L insulin (Sigma, St. Louis, MO). 1471.1 murine breast adenocarcinoma cells (gift of Dr. Gordon Hager, NCI, NIH), HEK293 human embryonic kidney cells (ATCC), MDA-MB-468 human breast adenocarcinoma cells (ATCC), and 4T1 murine breast carcinoma cells were grown as monolayers in DMEM (Invitrogen) supplemented with 10% fetal bovine serum, 1% penicillin-streptomycin−glutamine, and 0.1% gentamicin. MDA-MB-468 cells were also supplemented with 1% MEM nonessential amino acids (Invitrogen). All cells were incubated in 5% CO_2 at 37 °C. The cells were seeded at a density of 7.5×10^4 cells (for 1471.1, MDA-MB-231, HeLa, and 4T1 cells) and 3.0×10^5 cells (for MCF-7, T47D,

dx.doi.org/10.1021/mp400379c | *Mol. Pharmaceutics* 2013, 10, 3922−3933

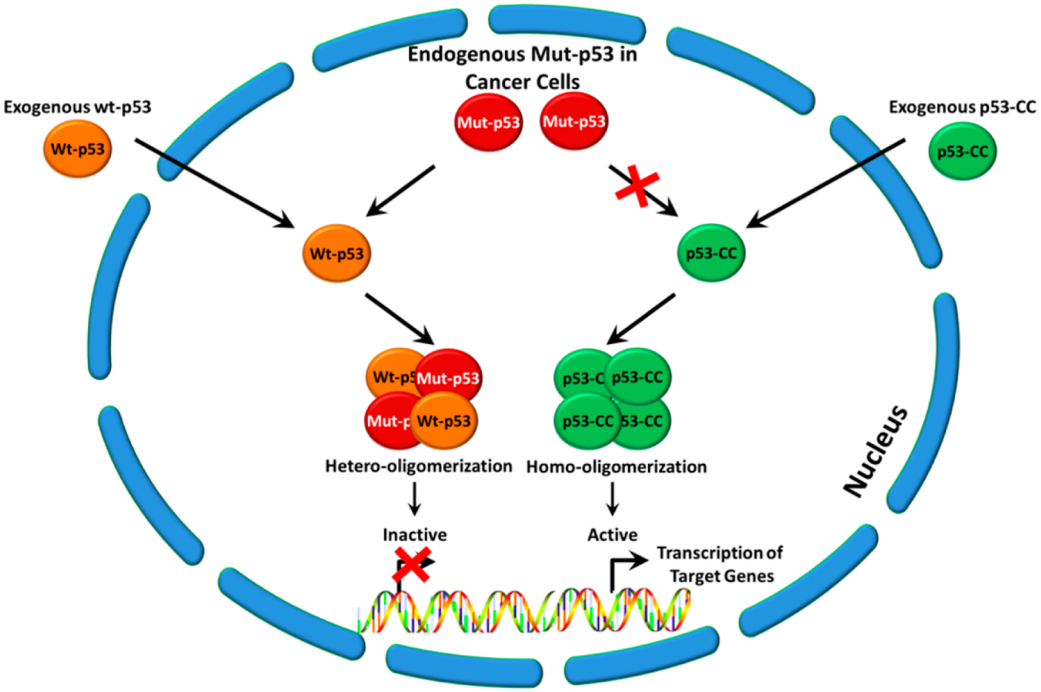

Figure 1. Proposed mechanism of p53-CC activity. Left side of figure: exogenously added wt-p53 can still form heterotetramers with mutant p53 due to the presence of the TD and becomes inactivated. Right side of figure: p53-CC can bypass transdominant inhibition by mutant p53 in cancer cells and still exhibit tumor suppressor activity.

HEK293, MDA-MB-468, and H1373 cells) in 6-well plates (Greiner Bio-One, Monroe, NC). Transfections of 1 pmol DNA were carried out 24 h after seeding using Lipofectamine 2000 (Invitrogen) following the manufacturer's recommendations.[4]

Microscopy. All microscopy was performed using 1471.1 cells due to their ideal microscopic morphology.[4] Twenty-four hours post transfection, media in 2-well live-cell chambers (Nalgene Nunc, Rochester, NY) was replaced with phenol red-free DMEM (Invitrogen). Cells were then incubated with 2 μg/mL Hoechst 33342 nuclear stain (Invitrogen) for 30 min at 37 °C. Images were taken using an Olympus IX71F fluorescence microscope (Scientific Instrument Company, Aurora, CO) with a high-quality narrow band GFP filter (excitation, HQ480/20 nm; emission, HQ510/20 nm) to detect EGFP and cyan GFP v2 filter (excitation HQ436/20 nm, emission HQ480/40 nm, with beam splitter 455dclp) to detect H33342 as previously described.[29]

RT-PCR. Twenty-four hours following transfection of T47D cells, mRNA from cell lysates was isolated using RNeasy Mini Kit (Qiagen, Valencia, CA). cDNA was then obtained using RT^2 First Strand Kit (Qiagen) and mixed with RT SYBR Green qPCR Mastermix (Qiagen). Equal volumes were then aliquoted into a 384-well p53 Signaling Pathway PCR Array (Qiagen). Roche LightCycler 480 was used for real-time PCR cycling. Analysis of the PCR array was performed using the manufacturer's web-based analysis software (http://pcrdataanalysis.sabiosciences.com/pcr/arrayanalysis.php). Genes outside of a 2-fold range were considered to be statistically different per the manufacturer. The PCR array was performed once and used as a screening tool as before.[30−32]

Western Blotting. Twenty-four hours following transfection of T47D cells, EGFP-positive cells were sorted using the FACSAria-II (BD-BioSciences). The 3×10^5 cells were pelleted and resuspended in 200 μL of lysis buffer (62.5 mM Tris-HCl, 2% w/v SDS, 10% glycerol, 1% protease inhibitor). Standard Western blotting procedures[33] were followed using primary antibodies to detect p21/WAF1, Bax, and actin as a loading control. The primary antibodies anti-p21 (ab16767, Abcam, Cambridge, MA), anti-Bax (ab7977, Abcam), antiactin (mouse, ab3280, Abcam), and antiactin (rabbit, ab1801, Abcam) were detected with antirabbit (no. 7074S, Cell Signaling Technology, Danvers, MA) or antimouse (ab6814, Abcam) HRP-conjugated antibodies before the addition of SuperSignal West Pico chemiluminescent substrate (Thermo Scientific, Waltham, MA). Signals were detected using a FluorChem FC2 imager and software (Alpha Innotech, Sanata Clara, CA). Each Western blot was repeated at least three times.

TUNEL Assay. As previously described,[4] T47D cells were prepared 48 h after transfection using an In Situ Death Detection Kit, TMR red (Roche, Mannheim, Germany). Cells were EGFP gated and analyzed using FACSAria-II (BD-BioSciences, University of Utah Core Facility) and FACSDiva software. EGFP and TMR red were excited at 488 and 563 nm wavelengths and detected at 507 and 580 nm, respectively. The terminal deoxynucleotidyl transferase dUTP nick end labeling (TUNEL) assay was repeated three times (n = 3) and analyzed using one-way analysis of variance (ANOVA) with Bonferroni's post hoc test.

Annexin-V Assay. The annexin-V assay was performed as before.[4] Briefly, 48 h post transfection, T47D cells were suspended in 400 μL annexin binding buffer (Invitrogen) and incubated with 5 μL of annexin-APC (annexin-V conjugated to allophycocyanin, Invitrogen) for 15 min. The incubated cells were EGFP gated and analyzed using FACSCanto-II. EGFP and APC were excited at 488 and 635 nm wavelengths and detected at 507 and 660 nm, respectively. Each construct was tested three times (n = 3) and analyzed using one-way ANOVA with Bonferroni's post hoc test.[4]

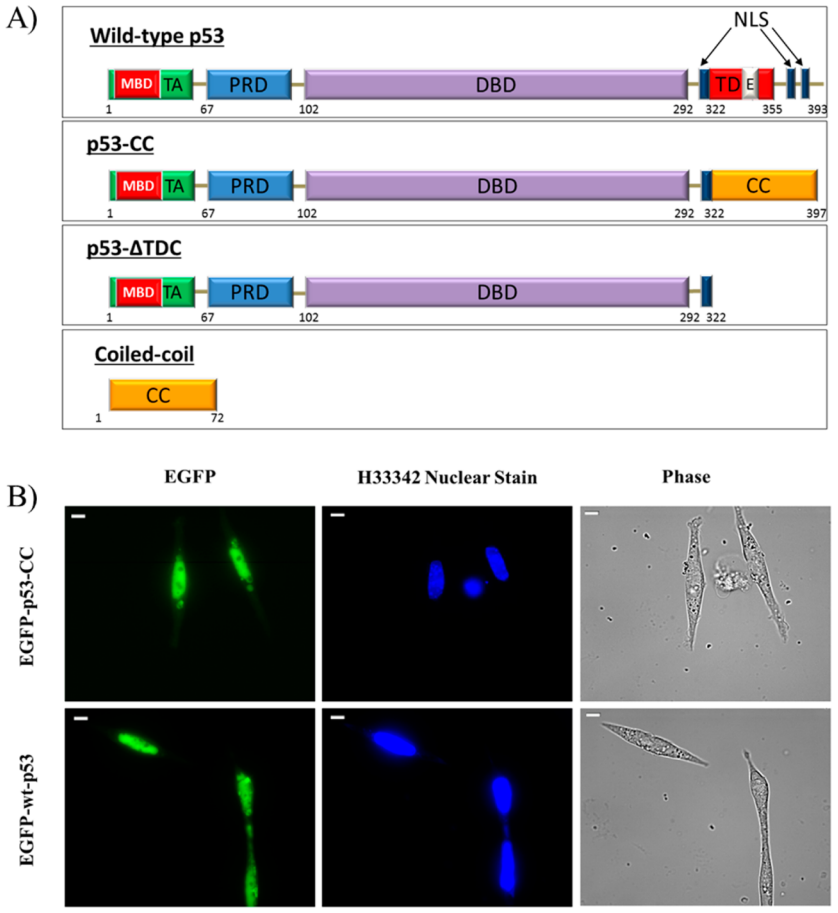

Figure 2. (A) Schematic representation of the experimental constructs and controls. Full length p53 (wt-p53) contains a MDM2 binding domain (MBD), a transactivation domain (TA) in the amino terminus, a proline-rich domain (PRD), a DNA binding domain (DBD), a strong nuclear localization signal (NLS), a tetramerization domain (TD) that also contains a nuclear export signal (E), and a carboxy terminus (C-terminus) that includes two weak NLS's. For p53-CC, the TD and C-terminus were replaced by the coiled-coil (CC) from Bcr. p53-ΔTDC lacks both the TD and the C-terminus. All constructs were fused to EGFP on the N-terminus (not shown in diagram). (B) Representative fluorescence microscopy images of 1471.1 cells confirm exclusive nuclear accumulation of EGFP-p53-CC similar to EGFP-wt-p53. EGFP fluorescence, nuclear staining with H33342, and phase contrast images are shown, left to right. 1471.1 breast cancer cells were chosen for this study due to their optimal microscopy characteristics (elongated morphology and distinguishable subcellular compartments).[4] White scale bars on the top left corners are 10 μm.

7-AAD Assay. As before,[4] following manufacturer's instructions, T47D, MCF-7, H1373, and MDA-MB-468 cells were stained with 7-aminoactinomycin D (7-AAD, Invitrogen) 48 h after transfection. Since HeLa, MDA-MB-231, and 4T1 cells are highly proliferating cells, these cell lines were assayed 24 h post transfection. Cells were analyzed and gated for EGFP (with same fluorescence intensity to ensure equal expression of proteins) using the FACSCanto-II (BD-BioSciences, University of Utah Core Facility) and FACSDiva software. Excitation was set at 488 nm and detected at 507 and 660 nm for EGFP and 7-AAD, respectively. The means from three separate experiments (n = 3) were analyzed using one-way ANOVA with Bonferroni's post hoc test.

Colony Forming Assay (CFA). CFA was carried out using the Cytoselect 96-well cell transformation assay (Cell Biolabs, San Diego, CA). A base agar layer was prepared per manufacturer's directions, and 50 μL was transferred to each well of a clear-bottom 96-well plate. T47D cells were transfected as described above with wt-p53, p53-CC, or CC and harvested 24 h post transfection. The cells were resuspended in RPMI medium (Invitrogen) at a concentration of 3.0×10^5 cells/mL per the manufacturer's instructions. A cell agar layer was then prepared as recommended, and 75 μL of the mixture was transferred to each well of the 96-well plate containing the base agar layer. A portion of 100 μL of complete culture medium was added to each well; plates were then incubated at 37 °C and 5% CO_2 for 7 days. The culture medium was removed, solubilized, and lysed. A sample of 10 μL of cell lysates were then transferred to a new black-bottom 96-well plate. 90 μL of CyQuant GR dye working solution (1:400 in PBS) was added to each well and incubated for 10 min at RT. A Spectra Max M2 plate reader (Molecular Devices, Sunnyvale, CA) was used to detect fluorescence using a 485/520 nm filter set. Independent transfections of each construct were tested three times (n = 3) and analyzed using one-way ANOVA with Bonferroni's post hoc test.

Reporter Gene Assay. A sample of 3.5 μg of construct (wt-p53, p53-CC, CC, or EGFP) was cotransfected with 0.35 μg of pRL-SV40 plasmid encoding for *Renilla* luciferase (Promega, Madison, WI) to normalize for transfection efficiency in T47D cells. In addition to *Renilla* luciferase, constructs were cotransfected with 3.5 μg of p53-Luc Cis-Reporter (Agilent Technologies, Santa Clara, CA),[4] p21/WAF1 reporter (a generous gift from Dr. Bert Vogelstein, Addgene plasmid 16451, Cambridge, MA)[34] or PUMA reporter (from Dr. Vogelstein, Addgene plasmid 16591);[35] all three reporters

dx.doi.org/10.1021/mp400379c | *Mol. Pharmaceutics* 2013, 10, 3922−3933

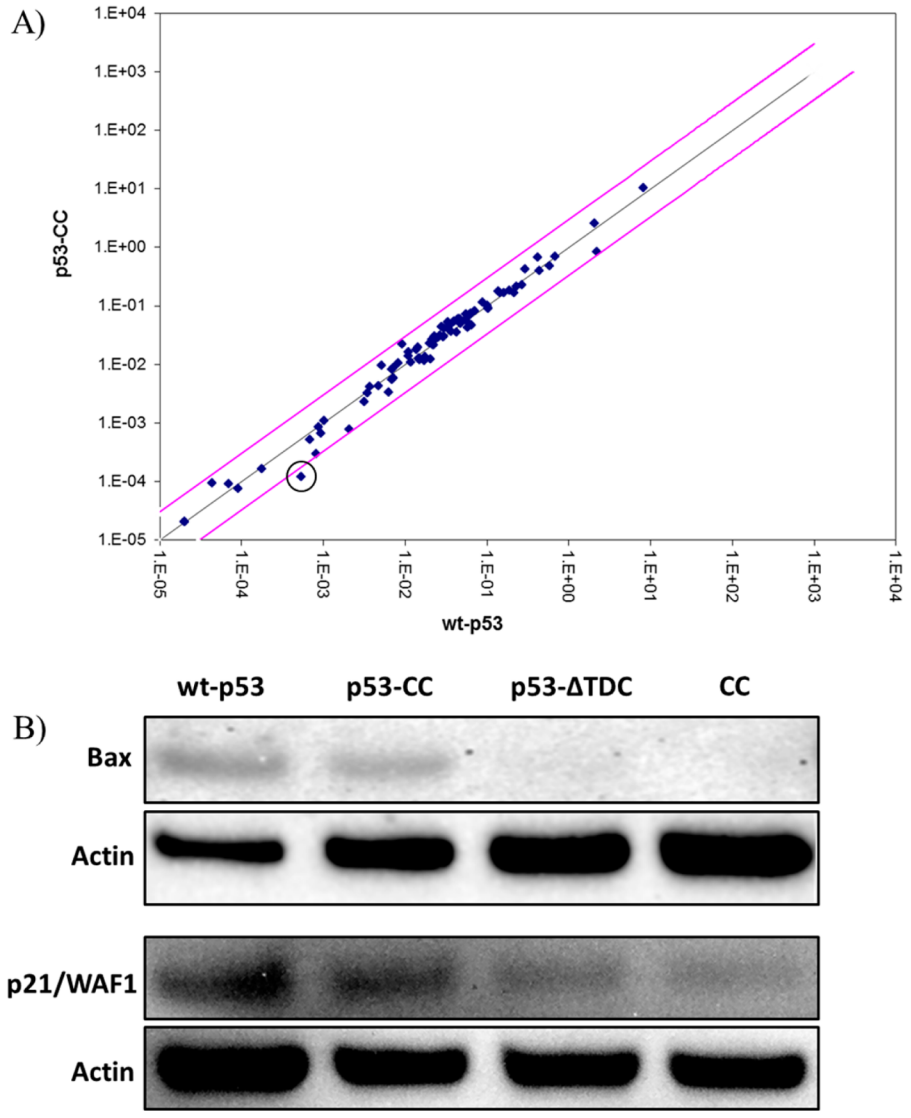

Figure 3. p53-CC is capable of transactivating several p53 target genes. (A) Scatter plot representation of mRNA levels of 84 p53 target genes in T47D cells transfected with wt-p53 or p53-CC. Each dot represents one of the 84 genes assayed in this PCR array. The two magenta lines represent a boundary of 2-fold upregulation or downregulation in mRNA levels. Cells treated with wt-p53 or p53-CC showed similar levels of mRNA for all 84 genes except for one, p53AIP1, which is circled on the scatter plot. (B) Representative cropped Western blots of T47D cell lysates 24 h post transfection with wt-p53, p53-CC, p53-ΔTDC, or CC. Similar levels of Bax and p21/WAF1 protein expression were detected from cells treated with wt-p53 or p53-CC. Each Western blot was repeated at least three times.

encode the firefly luciferase gene. The Dual-Glo Luciferase Assay System (Promega) was used to determine firefly luciferase activity and *Renilla* luciferase per manufacturer's instructions. Luminescence from active luciferase was then detected using PlateLumino (Stratec Biomedical Systems, Birkenfeld, Germany) as previously.[4] *Renilla* luciferase activity was used to normalize the firefly luciferase values. The highest relative luminescence value was set at 100%, and untreated cells were set at 0%. The means from triplicate samples were taken from three independent experiments and analyzed using one-way ANOVA with Bonferroni's post hoc test.

Co-immunoprecipitation (co-IP). The co-IP was performed using Dynabeads co-IP Kit (Invitrogen). T47D cells transfected with either EGFP-wt-p53 or EGFP-p53-CC were collected and weighed out (0.05 g) 20 h post transfection. Anti-GFP antibody (ab290, Abcam) was coupled to magnetic beads using Dynabeads Antibody Coupling Kit (Invitrogen). Approximately 0.2 g of cell pellet was lysed in 1.8 mL of extraction buffer B (1× IP, 100 mM NaCl, 2 mM $MgCl_2$, 1 mM DTT, 1% protease inhibitor). The lysate was incubated for 30 min at 4 °C with 1.5 mg of the Dynabeads coupled with anti-GFP antibody. The immune complexes were then collected by a magnet and washed three times with extraction buffer B and one time with last wash buffer (1× LWB, 0.02% Tween 20). Immune complexes were then eluted using 60 μL of elution buffer. Finally, the eluted complexes were denatured and blotted using anti-p53 antibody HRP-conjugated (sc-126 HRP, Santa Cruz Biotechnology, Santa Cruz, CA).

Overexpression of Mutant p53. H1373 cells were cotransfected with 1 pmol of the transdominant mutant pTagBFP-mut-p53 (R175H, R248W, and R273H)[27,28] and 1 pmol of wt-p53, p53-CC, or CC fused to EGFP. Forty-eight hours post transfection, cells were stained as in the 7-AAD assay above and gated for EGFP and BFP using the FACSCanto-II (BD-BioSciences, University of Utah Core Facility) and FACSDiva software. Excitation for BFP was set

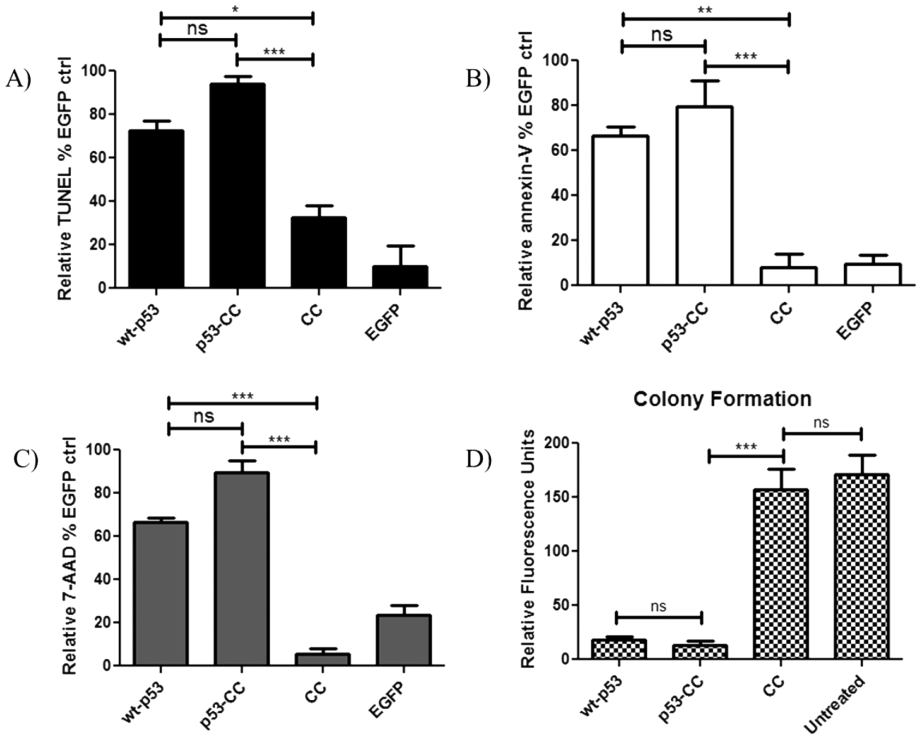

Figure 4. Apoptotic and cell proliferation assays were performed in T47D cells 48 h after transfection. (A) TUNEL assay shows similar apoptotic activity of p53-CC compared to wt-p53. Both p53-CC and wt-p53 demonstrate a significantly higher activity compared to CC negative control. Similar results were obtained from (B) annexin V staining and (C) 7-AAD staining. (D) The colony forming assay shows the transformative ability of T47D cells post treatment with wt-p53, p53-CC, and CC. Cells treated with wt-p53 and p53-CC show significant reduction in transformative ability (oncogenic potential) of T47D cells compared to untreated cells or cells treated with CC. Mean values were analyzed using one-way ANOVA with Bonferroni's post test; * $p < 0.05$, ** $p < 0.01$, and *** $p < 0.001$. Error bars represent standard deviations from at least three independent experiments ($n = 3$).

at 405 nm and detected at 457 nm. The means from three separate experiments ($n = 3$) were analyzed using one-way ANOVA with Bonferroni's post hoc test.

Recombinant Adenovirus Production. Replication-deficient recombinant adenovirus serotype 5 (Ad) constructs were generated using the Adeno-X Adenoviral Expression System 3 (Clontech). Either wt-p53 or p53-CC was inserted into a cassette under the control of the CMV promoter. A separate CMV promoter controls the expression of ZsGreen1 for visualization. The empty virus (vector) was used as a negative control. Wt-p53 and p53-CC were PCR amplified with primers containing 15 base pair homology with a linearized pAdenoX vector (Clontech) based on an In-Fusion HD Cloning Kit (Clontech). Stellar competent cells (Clontech) were transformed with the adenoviral vector plasmids containing our constructs. Viral DNA was then purified, linearized and transfected into HEK293 cells for packaging and amplification. Viral particles were isolated from HEK293 cells by freeze−thawing, purified using an Adeno-X Mega Purification Kit (Clontech), and dialyzed against storage and proper tonicity buffer (2.5% glycerol (w/v), 25 mM NaCl, and 20 mM Tris-HCl, pH 7.4). The viral titer was determined using flow cytometry per the manufacturer's recommendation.

RESULTS

p53-CC Localizes to the Nucleus. Because the nuclear localization of p53 is important for antiapoptotic function, we first chose to investigate if p53-CC also localized to the nucleus. Full length wt-p53 contains three NLSs encoded by amino acids 305−322, 370−376, and 380−386 (Figure 2A, top). Given that p53-CC (illustrated in Figure 2A) lacks most of the C-terminal domain (amino acids 323−393), which contains two NLSs, nuclear accumulation of p53-CC was verified using fluorescence microscopy (Figure 2B). Both wt-p53 and p53-CC were fused to EGFP to enable visualization of the subcellular localization of each protein. Figure 2B shows similar nuclear accumulation of p53-CC and wt-p53 in 1471.1 murine adenocarcinoma cells. CC alone fused to EGFP showed mostly cytoplasmic localization (data not shown). Similar results were obtained in T47D and MCF-7 breast cancer cells (data not shown).

Wt-p53 and p53-CC Show Similar Gene Expression Profiles. After verifying the nuclear localization of p53-CC via fluorescence microscopy, the activity of p53-CC was investigated next. The Human p53 Signaling Pathway RT^2 Profiler PCR Array (Qiagen, Valencia, CA)[32] was used to compare the transcription profiles between wt-p53 and p53-CC in T47D human breast cancer cells. T47D cells contain mutant p53 (a L194F mutation) that does not exhibit a strong transdominant effect.[36] Exogenously added wt-p53 has been shown to be functional in this cell line,[4,33] and hence these cells can be used for comparing wt-p53 activity with p53-CC. The PCR array uses real-time PCR to measure the expression profiles of 84 genes directly related to p53-mediated signal transduction, including genes involved in apoptosis, cell cycle, DNA repair, cell proliferation, and differentiation. Analysis of the PCR array indicated that p53-CC showed a similar expression profile for 83 out of 84 genes compared to wt-p53 (Figure 3A), with the exception of the p53AIP1 gene (circled in black), whose protein product is one of many involved in the intrinsic

apoptotic pathway. A tetramerization-deficient form of p53 (p53-ΔTDC) was included as a negative control in these assays to validate that the activity of p53-CC is due to proper tetramer formation, along with CC (also a negative control). As expected, both p53-ΔTDC and CC had significantly different expression profiles from wt-p53 (Supplementary Figures 1 and 2) in the p53 signaling pathway PCR array.

To verify the array results, the protein expression of two typical genes involved in two different pathways that are directly regulated by p53, Bax and p21/WAF1, were examined by Western blotting. Bax is involved in the p53-dependent intrinsic apoptosis pathway,[1] while p21/WAF1 is involved in cell cycle arrest.[37] Figure 3B shows that T47D cells transfected with wt-p53 (first lane) or p53-CC (second lane) demonstrated overexpression of Bax and p21, while the monomeric form of p53 (p53-ΔTDC, third lane) and the CC (fourth lane) negative controls did not significantly induce expression of the Bax and p21/WAF1. Faint p21/WAF1 bands are observed with negative controls and represent background levels of this protein. Due to its inactivity, p53-ΔTDC was not included in the remaining apoptotic assays.

p53-CC Exhibits Tumor Suppressor Activity. To determine if the similar gene expression profiles between p53-CC and wt-p53 correlate with comparable tumor suppressor activity, the apoptotic potential (TUNEL, annexin V, 7-AAD) and transformative ability (colony formation) were tested in T47D cells. As mentioned before, T47D cells were chosen to compare the activity of p53-CC and wt-p53, since we have shown before that wt-p53 is active in these cells.[4,33]

The TUNEL assay, which measures DNA fragmentation into nucleosomal segments, is a hallmark of apoptosis.[38] Figure 4A shows that p53-CC has a similar ability to induce DNA fragmentation as wt-p53 compared to CC control. Next, the apoptotic potential of p53-CC was also validated in the annexin-V assay, which evaluates the externalization of phosphatidylserine on the cell surface of apoptotic cells.[39,40] Similar levels of annexin-V positive staining were detected between cells transfected with p53-CC and wt-p53 (Figure 4B), and had significantly higher positive staining in cells transfected with CC negative control. The last apoptotic assay tested was the 7-AAD viability assay. In apoptotic or necrotic cells, the plasma membrane is disrupted, allowing intercalation of the 7-AAD stain into DNA in the nucleus of these damaged cells.[41,42] In this assay (Figure 4C), p53-CC maintains the same level of apoptotic activity as wt-p53 and is able to induce higher levels of cell death compared to the control (CC). Finally, the decrease in transformative ability (or oncogenic potential) of cells treated with p53-CC or wt-p53 were tested via a colony forming assay. In this assay, treatment with a tumor suppressor would be expected to reduce the number of cell colonies formed in an agar matrix. Indeed, as shown in Figure 4D, both p53-CC (second bar) and wt-p53 (first bar) significantly reduced the number of colonies formed compared to the negative controls (CC and untreated cells, third and fourth bars, respectively). Overall, these results indicate that p53-CC shows a similar ability to induce statistically significant levels of apoptosis and to reduce oncogenic potential as wt-p53.

To ensure that the potential for p53-CC to induce apoptosis is neither dependent on endogenous p53 status nor cancer cell line specific, p53-CC was tested in several different cell lines. Human epithelial cervical adenocarcinoma cells (HeLa), which express endogenous wt-p53,[43] MDA-MB-231 metastatic triple-negative breast cancer cells harboring mutant p53,[44] MCF-7 breast cancer cells with wild type but mislocalized p53,[45] and H1373 non-small cell lung carcinoma cells that are p53 null[46] (Table 2), were tested in the 7-AAD assay. In all four cell lines, p53-CC and wt-p53 were able to induce similar levels of apoptosis and were higher than the negative control (CC), as shown in Figure 5A–D.

Table 2. Comparison of the Four Different Cell Lines (HeLa, MDA-MB-231, MCF-7, and H1373) in Terms of p53 Status and Cancer Type

cell line	p53 Status	cancer type	ref
HeLa	wild-type	cervical adenocarcinoma	40
MDA-MB-231	mutated (R280K)	triple-negative breast cancer	41
MCF-7	mislocalized to cytoplasm	breast cancer	42
H1373	null	non-small cell lung carcinoma	43

p53-CC Maintains Transcriptional Activity of p53 Target Genes. While p53-CC exhibited similar apoptotic activity as wt-p53, we wanted to determine if p53-CC was capable of activating promoters of p53-dependent target genes. Tetramerization of p53 is a prerequisite to transcriptional activity, thus transcriptional activation will indicate tetramerization ability (of both wt-p53 and p53-CC).[47] The transcriptional activity of p53-CC was tested in T47D cells using three different reporter gene assays. The first was the p53 cis-reporter system, a common reporter for measuring p53 activity, which relies on a synthetic promoter consisting of repeats of the transcription recognition consensus for p53 $(TGCCTGGACT\text{-}TGCCTGG)_{14}$.[48] The second and third reporter systems utilized the binding consensus sequences from p21/WAF1 and PUMA promoters, respectively. p21/WAF1 is a cyclin-dependent kinase inhibitor that mediates p53-dependent G1 cell cycle arrest,[34,37] while PUMA translocates to the mitochondria, deactivates antiapoptotic Bcl-2 and Bcl-XL proteins and induces p53-dependent apoptosis.[49] In all three reporter gene assays, p53-CC showed higher transcriptional activity compared to wt-p53, and both were higher than the negative controls CC and EGFP (Figure 6A–C) in T47D cells.

p53-CC Avoids Interaction with Endogenous p53. We hypothesized that the higher level of transcriptional activity of p53-CC over wt-p53 was due to the possible hetero-oligomerization of wt-p53 with endogenous mutant p53 in this cell line. Therefore, a co-IP assay was performed to determine if exogenously added wt-p53 interacts with mutant p53 present in these cells. To this end, mutant p53 in T47D cells would not be expected to coimmunoprecipitate with p53-CC. Cell lysates transfected with either EGFP-wt-p53 or EGFP-p53-CC were incubated with anti-GFP antibody to selectively immunoprecipitate our fusion EGFP proteins (Figure 6D). Endogenous p53 that could potentially coimmunoprecipitate with either exogenous EGFP-wt-p53 or EGFP-p53-CC was probed using anti-p53 antibody. Figure 6D shows that endogenous p53 (53 kDa) coimmunoprecipitates with exogenous wt-p53 (left lane, 70 kDa) but fails to immunoprecipitate with p53-CC (right lane, 71 kDa). These findings indicate that endogenous p53 interacts directly with exogenous wt-p53, which is presumably due to hetero-oligomerization via their TDs. As expected, p53-CC, which lacks the native TD, evaded binding to endogenous p53. It should be noted that a prominent secondary band is normally

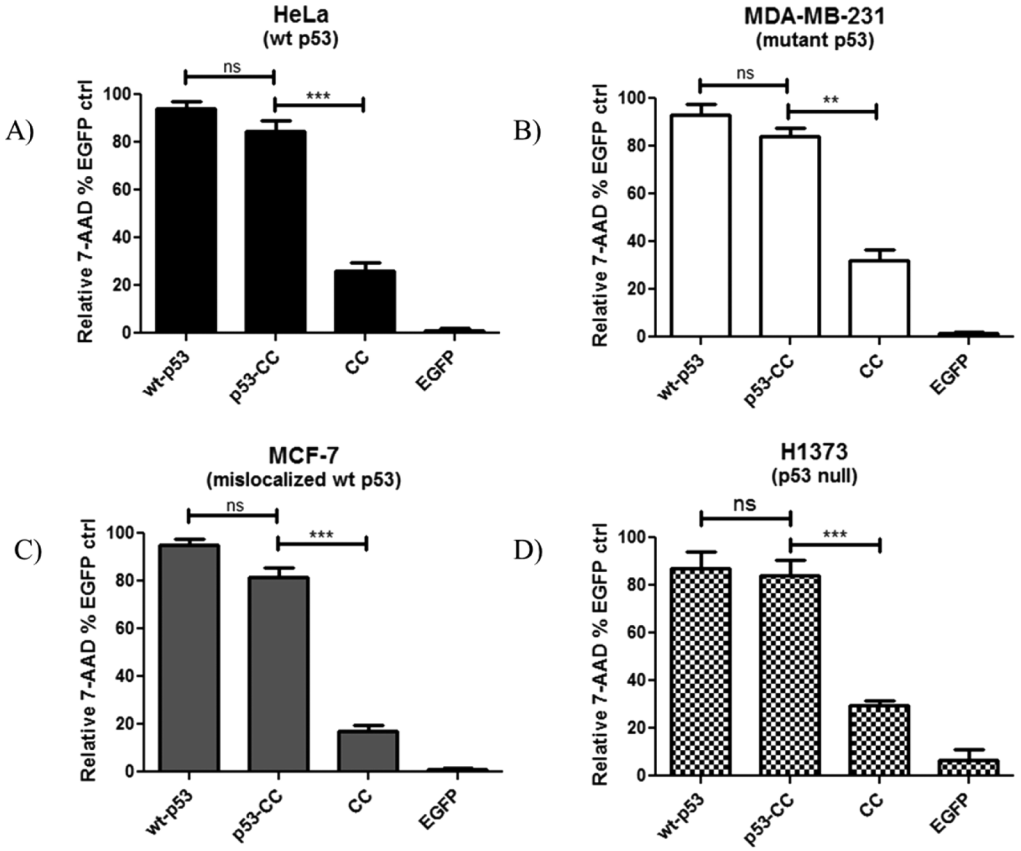

Figure 5. 7-AAD assay conducted in four different cell lines with varying p53 status: (A) Hela, (B) MDA-MB-231, (C) MCF-7, and (D) H1373. In all four cases, p53-CC is capable of inducing cell death in a similar fashion compared to wt-p53, regardless of the endogenous p53 status or the cancer cell line used. Statistical analysis was performed using one-way ANOVA with Bonferroni's post test; $^{**}p < 0.01$ and $^{***}p < 0.001$.

detected by this anti-p53 antibody at about 69 kDa (per Santa Cruz Biotechnology).

Bypassing the Dominant Negative Effect. Since p53-CC did not interact with endogenous wt-p53 in the co-IP assay, the ability of p53-CC to bypass the dominant negative effect was tested, first using overexpression of a dominant negative mutant p53 in H1373 cells (p53 null), and second, in MDA-MB-468 cells that harbor a strong dominant negative p53 mutant.[50] The ability of p53-CC to "rescue" the loss of apoptotic activity induced by an inactive mutant p53 in H1373 (p53 null) cells was tested; Figure 7A shows that, in the absence of the inactive mutant p53 (first three sets of bars), both p53-CC and wt-p53 can similarly induce apoptosis (measured by 7-AAD) compared to the negative CC control. However, when a transdominant mutant p53 is added (bars 4–6), only p53-CC is able to rescue apoptotic activity, while wt-p53 cannot. We engineered this transdominant mutant p53 by combining three hotspot mutations (R175H, R248W, and R273H) that are known to exhibit a dominant negative effect.[27,28] This supports the notion that p53-CC can bypass the dominant negative effect of a transdominant mutant p53. To further investigate this, the ability of p53-CC to induce apoptosis was tested in a cell line known to contain an endogenous strong transdominant mutant form of p53, MDA-MB-468.[51] The endogenous p53 in MDA-MB-468 contains the R273H point mutation that is known to exhibit transdominant inhibition of wt-p53, so exogenous wt-p53 in this case would be expected to have limited activity. MDA-MB-468 cells are resistant to transient transfection with lipofectamine (used in the majority of these studies), so instead, they were transduced with adenovirus (Ad) constructs carrying the wt-p53 or p53-CC as genetic cargo. Figure 7B shows that, indeed, only Ad-p53-CC (second bar) is able to significantly induce apoptotic activity measured by 7-AAD compared to wt-p53 and empty Ad vector (bars 1 and 3, respectively). This suggests that the transdominant effect of endogenous mutant p53 found in MDA-MB-468 cells can be circumvented by using an oligomerization variant of p53, namely, p53-CC. Finally, we also tested adenovirally delivered p53-CC in a p53 null cell line (Figure 7C), where both wt-p53 and p53-CC should be active. Indeed, as shown in Figure 7C, both constructs are active in this cell line. Interestingly, p53-CC is more active than wt-p53 in this particular cell line.

■ DISCUSSION

To summarize, our data show that a version of p53 with an alternative tetramerization domain localizes to the correct subcellular compartment (the nucleus, Figure 2B), and shows a similar gene expression profile as wt-p53 (Figure 3A). Two genes regulated by p53, Bax, and p21/WAF1 also showed similar protein expression levels when induced by p53-CC or wt-p53, as demonstrated by Western blotting (Figure 3B). Tumor suppressor activity, measured apoptotic activity (by TUNEL, annexin V, and 7-AAD) and reduced oncogenic potential (reduced number of colonies), Figure 4A–D, was similar between p53-CC and wt-p53. Importantly, p53-CC was found to induce statistically significant levels of apoptosis in four different cell lines (Figure 5A–D), regardless of p53 status,

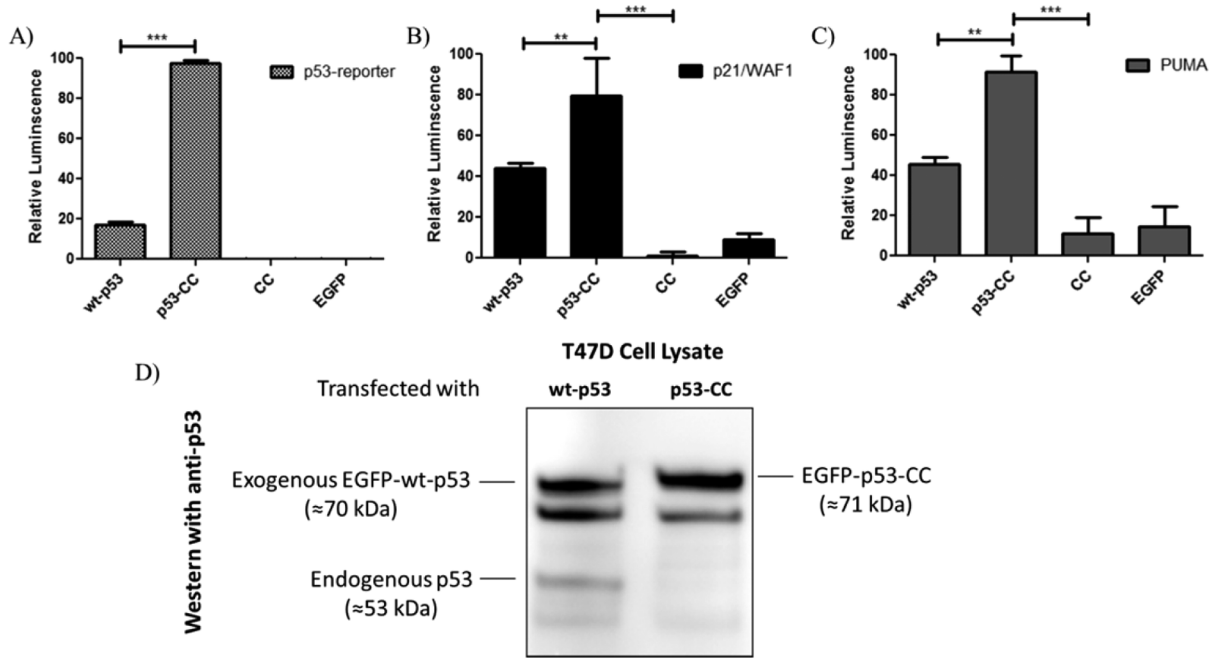

Figure 6. Relative luminescence representing the activation of (A) the p53-cis reporter, (B) the p21/WAF1 reporter, and (C) the PUMA reporter in T47D cells. The ability of p53-CC to transactivate these promoters is higher than wt-p53. In all three cases, 3.5 μg of construct (wt-p53, p53-CC, CC, or EGFP) was cotransfected with 0.35 μg of pRL-SV40 plasmid encoding for *Renilla* luciferase to normalize for transfection efficiency. In addition to *Renilla* luciferase, constructs were cotransfected with 3.5 μg of p53-Luc cis-reporter, p21/WAF1 reporter, or PUMA reporter encoding for firefly luciferase. Mean values were analyzed using one-way ANOVA with Bonferroni's post test; $^{**}p < 0.01$ and $^{***}p < 0.001$. Error bars represent standard deviations from three independent experiments ($n = 3$). (D) Interaction of endogenous p53 with exogenous wt-p53 or p53-CC was investigated in T47D via co-IP. A representative cropped Western blot of protein complexes coimmunoprecipitated using anti-GFP antibody is shown. Left lane, endogenous p53 (53 kDa) coimmunoprecipitates with exogenous EGFP-wt-p53 (70 kDa). Right lane, endogenous p53 fails to coimmunoprecipitate with exogenous EGFP-p53-CC (71 kDa).

indicating that p53-CC activity is not dependent on p53 status, nor is it cell-line specific (see Table 2). The transcriptional activity of p53-CC was tested using three reporter gene assays in Figure 6A–C (a standard p53 reporter gene, a p21/WAF1 reporter involved in cell cycle arrest, and a PUMA reporter involved in apoptosis) and, in all three cases, was higher than wt-p53. In T47D cells, the transcriptional activity of p53-CC was higher than wt-p53 in these reporter gene assays (Figure 6A–C), while the apoptotic activity of p53-CC was similar to wt-p53 (Figure 4A–C). This is not unexpected, since transcriptional activity does not necessarily linearly correlate with apoptotic activity. Transcriptional activity of target genes is a prerequisite step prior to the apoptotic cascade; if a threshold of transcriptional activity is met, the downstream measure of apoptosis may not change significantly. Interestingly, the negative controls (p53ΔTDC and CC) did not have activity in binding nor were able to express apoptotic or cell cycle arrest genes.

A co-IP was performed and showed that p53-CC did not interact with endogenous p53 (Figure 6D). Since there was no interaction between p53-CC and endogenous p53, the ability of p53-CC to bypass the dominant negative effect was tested, first with transdominant mutant p53 overexpression (Figure 7A), and second, in MDA-MB-468 cells that harbor a tumor-derived endogenous transdominant negative p53 mutant (Figure 7B). In both cases, p53-CC appears to not be effected by this endogenous transdominant inhibition. Finally, adenovirally delivered p53-CC was also tested in a p53 null cell line and was active, as expected (Figure 7C).

Mutant p53 retains its tetramerization capability since its TD remains intact and can form inactive p53 tetramers upon the introduction of exogenous wt-p53 in cancer cells (Figure 1, left side). These heterotetramers have a significantly reduced transcriptional activity compared to homotetramers of p53-CC. Such a phenomenon gives rise to a great barrier that limits the utility of p53 for cancer therapy.[11] As an approach to prevent hetero-oligomerization, we investigated swapping the TD with an alternative oligomerization domain (Table 1). The CC from Bcr tetramerizes in a similar fashion as the TD; both form dimers of two antiparallel-oriented monomers.[52] To our knowledge, only one attempt at substituting the TD of p53 to eliminate the dominant negative effect of mutant p53 in heterotetramers has been made, with marginal success.[21] This previous work utilized an oligomerization domain that leads to *parallel* tetramer formation, whereas the native TD of p53 drives the formation of *antiparallel* tetramers.[21−23] This might offer an explanation to the significant reduction in p53 function observed in their published activity assays[21] compared to wt-p53. On the other hand, our results show that p53-CC evades hetero-oligomerization with mutant p53, allowing it to retain the full tumor suppressor function of wt-p53.

Bcr, from which the CC was obtained, is a ubiquitous eukaryotic phosphotransferase protein that may have a role in general cell metabolism. Theoretically, p53-CC could interact with Bcr via its CC domain. While this is a possibility, this may be unlikely due to the compartmentation of Bcr (found in the cytoplasm)[53] vs p53-CC (found in the nucleus, shown in Figure 2B). Bcr-knockout mice still survive; the major defect in these mice was reduced intimal proliferation in low-flow carotid

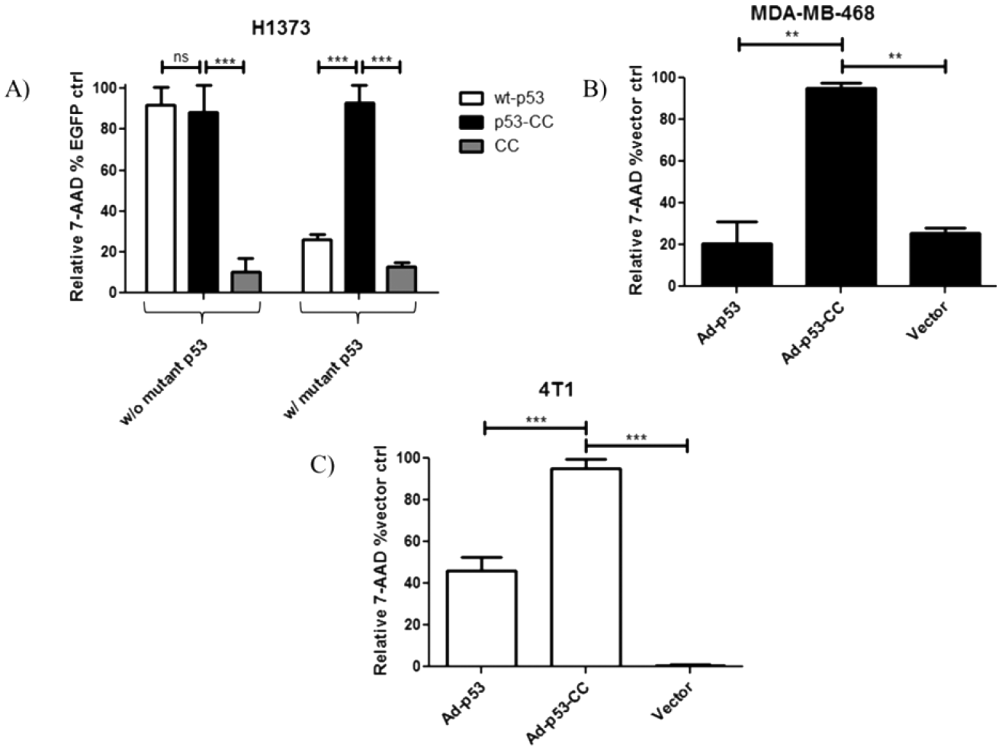

Figure 7. p53-CC circumvention of transdominant inhibition by mutant p53. (A) Overexpression of mutant p53 reduces the activity of exogenous wt-p53 but has no influence on exogenous p53-CC activity. H1373 cells were chosen for this experiment since they are p53 null and hence there will be no additional p53 activity from the cells due to lack of endogenous p53. (B) 7-AAD assay was conducted 48 h post transducing MDA-MB-468 cells, which harbor a potent transdominant mutant p53 (R273H), with adenoviral vectors expressing either wt-p53 or p53-CC with a multiplicity of infection (MOI) of 200. As expected, exogenous wt-p53 (Ad-p53) activity is limited in this cell line due to the presence of endogenous transdominant tumor derived p53. (C) 7-AAD assay was also performed 48 h post transduction of 4T1 cells (MOI 250). Interestingly, p53-CC is more active than wt-p53 in this particular cell line. The adenoviral vector alone was used as a negative control. Mean values were analyzed using one-way ANOVA with Bonferroni's post test; $^{**}p < 0.01$ and $^{***}p < 0.001$. Error bars represent standard deviations from three independent experiments ($n = 3$).

arteries compared to wt mice.[54] Bcr has mostly been studied in the context of chronic myeloid leukemia (CML) where a reciprocal chromosomal translocation with Abl results in the fusion protein Bcr-Abl, the causative agent of CML.[55] The activity of Bcr-Abl is largely due to the constitutive activation of the Abl portion of the molecule.[56] Generally, Bcr may be involved in inflammatory pathways and cell proliferation.[54] We have previously reported that the isolated Bcr coiled-coil does not in itself induce apoptosis.[26] Nevertheless, potential inadvertent interaction with the CC oligomerization domain of Bcr via any introduced p53-CC is currently being addressed in our laboratory by introducing mutations in the CC domain of p53-CC that will disfavor interactions with Bcr-CC.

Besides not interacting with endogenous p53, the elevation in p53-CC transcriptional activity could also be due to a higher stability of the p53-CC tetramer compared to wt-p53 tetramer. We have reported that melting temperature (T_m) for CC is about 83 °C,[26] which is slightly higher than the T_m for TD around 75 °C at physiological pH.[57] In fact, our laboratory has shown previously that CC forms homodimers in thermal denaturation studies.[26] However, further experiments would be needed to definitively prove the biochemical tetramerization of p53-CC.

Our results corroborate our hypothesis that, unlike wt-p53, p53-CC can circumvent transdominant inhibition of mutant p53, illustrating the potential of using p53-CC as an alternative to wt-p53 for cancer gene therapy. Since the dominant negative effect of mutant p53 in cancer cells is currently one of the barriers limiting the use of p53 in cancer gene therapy,[11] our approach offers an alternative to overcome this barrier by swapping the TD of p53 with an alternative oligomerization domain while maintaining the tumor suppressor activity. Our designed p53-CC is expected to cause apoptosis in many types of cancers, especially in tumors with transdominant mutant p53, where wt-p53 has proven to be ineffective. Ultimately, we plan on utilizing the p53-CC construct as a gene therapeutic delivered using an adenoviral vector that could replace the current limited utility of wild-type p53 as a cancer therapeutic.

■ ASSOCIATED CONTENT

Ⓢ Supporting Information

Additional figures depicting p53 signaling pathway PCR array for the controls p53-ΔTDC and CC Figures SI 1 and SI 2. This material is available free of charge via the Internet at http://pubs.acs.org.

■ AUTHOR INFORMATION

Corresponding Author

*Address: 30 South 2000 East, Rm 2916, Salt Lake City, Utah 84112, United States. Phone: 1-801-587-9711. Fax: 1-801-585-3614. E-mail: carol.lim@pharm.utah.edu.

Author Contributions

A.O. and M.M. contributed equally to this work and thus are referred to as "co-first authors".

Notes

The authors declare no competing financial interest.

■ ACKNOWLEDGMENTS

We would like to thank Geoff Miller, Ben Bruno, Rian Davis, David Woessner, Jonathan Constance, and Shams Reaz for scientific discussions. The authors acknowledge the use of DNA/Peptide Core and Flow Cytometry Core (NCI Cancer Center Support Grant P30 CA042014, Huntsman Cancer Institute). Research reported in this publication was supported by the National Cancer Institute of the National Institutes of Health under award number R01-CA151847.

■ REFERENCES

(1) Haupt, S.; Berger, M.; Goldberg, Z.; Haupt, Y. Apoptosis—the p53 network. *J. Cell Sci.* **2003**, *116* (Pt 20), 4077−85.
(2) Marchenko, N. D.; Zaika, A.; Moll, U. M. Death signal-induced localization of p53 protein to mitochondria. A potential role in apoptotic signaling. *J. Biol. Chem.* **2000**, *275* (21), 16202−12.
(3) Mihara, M.; Erster, S.; Zaika, A.; Petrenko, O.; Chittenden, T.; Pancoska, P.; Moll, U. M. p53 has a direct apoptogenic role at the mitochondria. *Mol. Cell* **2003**, *11* (3), 577−90.
(4) Mossalam, M.; Matissek, K. J.; Okal, A.; Constance, J. E.; Lim, C. S. Direct induction of apoptosis using an optimal mitochondrially targeted p53. *Mol. Pharmaceutics* **2012**, *9* (5), 1449−58.
(5) McLure, K. G.; Lee, P. W. How p53 binds DNA as a tetramer. *EMBO J.* **1998**, *17* (12), 3342−50.
(6) Lacroix, M.; Toillon, R. A.; Leclercq, G. p53 and breast cancer, an update. *Endocr. Relat. Cancer* **2006**, *13* (2), 293−325.
(7) Willis, A.; Jung, E. J.; Wakefield, T.; Chen, X. Mutant p53 exerts a dominant negative effect by preventing wild-type p53 from binding to the promoter of its target genes. *Oncogene* **2004**, *23* (13), 2330−2338.
(8) Shaulsky, G.; Goldfinger, N.; Tosky, M. S.; Levine, A. J.; Rotter, V. Nuclear localization is essential for the activity of p53 protein. *Oncogene* **1991**, *6* (11), 2055−65.
(9) Baptiste, N.; Prives, C. p53 in the cytoplasm: a question of overkill? *Cell* **2004**, *116* (4), 487−9.
(10) Peng, Z. Current status of gendicine in China: recombinant human Ad-p53 agent for treatment of cancers. *Human Gene Ther.* **2005**, *16* (9), 1016−27.
(11) de Vries, A.; Flores, E. R.; Miranda, B.; Hsieh, H. M.; van Oostrom, C. T.; Sage, J.; Jacks, T. Targeted point mutations of p53 lead to dominant-negative inhibition of wild-type p53 function. *Proc. Natl. Acad. Sci. U.S.A.* **2002**, *99* (5), 2948−53.
(12) Soussi, T. p53 alterations in human cancer: more questions than answers. *Oncogene* **2007**, *26* (15), 2145−56.
(13) Soussi, T.; Ishioka, C.; Claustres, M.; Beroud, C. Locus-specific mutation databases: pitfalls and good practice based on the p53 experience. *Nat. Rev. Cancer* **2006**, *6* (1), 83−90.
(14) Soussi, T.; Wiman, K. G. Shaping genetic alterations in human cancer: the p53 mutation paradigm. *Cancer Cell* **2007**, *12* (4), 303−12.
(15) Goh, A. M.; Coffill, C. R.; Lane, D. P. The role of mutant p53 in human cancer. *J. Pathol.* **2011**, *223* (2), 116−26.
(16) Weinberg, R. L.; Freund, S. M.; Veprintsev, D. B.; Bycroft, M.; Fersht, A. R. Regulation of DNA binding of p53 by its C-terminal domain. *J. Mol. Biol.* **2004**, *342* (3), 801−11.
(17) Milner, J.; Medcalf, E. A. Cotranslation of activated mutant p53 with wild type drives the wild-type p53 protein into the mutant conformation. *Cell* **1991**, *65* (5), 765−74.
(18) Srivastava, S.; Wang, S.; Tong, Y. A.; Hao, Z. M.; Chang, E. H. Dominant negative effect of a germ-line mutant p53: a step fostering tumorigenesis. *Canc. Res.* **1993**, *53* (19), 4452−5.
(19) Kern, S. E.; Pietenpol, J. A.; Thiagalingam, S.; Seymour, A.; Kinzler, K. W.; Vogelstein, B. Oncogenic forms of p53 inhibit p53-regulated gene expression. *Science* **1992**, *256* (5058), 827−30.
(20) Lee, M. K.; Teoh, W. W.; Phang, B. H.; Tong, W. M.; Wang, Z. Q.; Sabapathy, K. Cell-type, Dose, and Mutation-type Specificity Dictate Mutant p53 Functions In Vivo. *Cancer Cell* **2012**, *22* (6), 751−764.
(21) Waterman, M. J.; Waterman, J. L.; Halazonetis, T. D. An engineered four-stranded coiled coil substitutes for the tetramerization domain of wild-type p53 and alleviates transdominant inhibition by tumor-derived p53 mutants. *Cancer Res.* **1996**, *56* (1), 158−63.
(22) Jeffrey, P. D.; Gorina, S.; Pavletich, N. P. Crystal structure of the tetramerization domain of the p53 tumor suppressor at 1.7 angstroms. *Science* **1995**, *267* (5203), 1498−502.
(23) Lee, W.; Harvey, T. S.; Yin, Y.; Yau, P.; Litchfield, D.; Arrowsmith, C. H. Solution structure of the tetrameric minimum transforming domain of p53. *Nat. Struct. Biol.* **1994**, *1* (12), 877−90.
(24) Wichmann, C.; Becker, Y.; Chen-Wichmann, L.; Vogel, V.; Vojtkova, A.; Herglotz, J.; Moore, S.; Koch, J.; Lausen, J.; Mantele, W.; Gohlke, H.; Grez, M. Dimer-tetramer transition controls RUNX1/ETO leukemogenic activity. *Blood* **2010**, *116* (4), 603−13.
(25) Zhao, X.; Ghaffari, S.; Lodish, H.; Malashkevich, V. N.; Kim, P. S. Structure of the Bcr-Abl oncoprotein oligomerization domain. *Nat. Struct. Biol.* **2002**, *9* (2), 117−20.
(26) Dixon, A. S.; Pendley, S. S.; Bruno, B. J.; Woessner, D. W.; Shimpi, A. A.; Cheatham, T. E., 3rd; Lim, C. S. Disruption of Bcr-Abl coiled coil oligomerization by design. *J. Biol. Chem.* **2011**, *286* (31), 27751−60.
(27) Di Como, C. J.; Gaiddon, C.; Prives, C. p73 function is inhibited by tumor-derived p53 mutants in mammalian cells. *Mol. Cell. Biol.* **1999**, *19* (2), 1438−49.
(28) Dong, P.; Tada, M.; Hamada, J.; Nakamura, A.; Moriuchi, T.; Sakuragi, N. p53 dominant-negative mutant R273H promotes invasion and migration of human endometrial cancer HHUA cells. *Clin. Exp. Metastasis* **2007**, *24* (6), 471−83.
(29) Dixon, A. S.; Kakar, M.; Schneider, K. M.; Constance, J. E.; Paullin, B. C.; Lim, C. S. Controlling subcellular localization to alter function: Sending oncogenic Bcr-Abl to the nucleus causes apoptosis. *J. Controlled Release* **2009**, *140* (3), 245−9.
(30) Barkic, M.; Crnomarkovic, S.; Grabusic, K.; Bogetic, I.; Panic, L.; Tamarut, S.; Cokaric, M.; Jeric, I.; Vidak, S.; Volarevic, S. The p53 tumor suppressor causes congenital malformations in Rpl24-deficient mice and promotes their survival. *Mol. Cell. Biol.* **2009**, *29* (10), 2489−504.
(31) Cutts, B. A.; Sjogren, A. K.; Andersson, K. M.; Wahlstrom, A. M.; Karlsson, C.; Swolin, B.; Bergo, M. O. Nf1 deficiency cooperates with oncogenic K-RAS to induce acute myeloid leukemia in mice. *Blood* **2009**, *114* (17), 3629−32.
(32) Brockschmidt, C.; Hirner, H.; Huber, N.; Eismann, T.; Hillenbrand, A.; Giamas, G.; Radunsky, B.; Ammerpohl, O.; Bohm, B.; Henne-Bruns, D.; Kalthoff, H.; Leithauser, F.; Trauzold, A.; Knippschild, U. Anti-apoptotic and growth-stimulatory functions of CK1 delta and epsilon in ductal adenocarcinoma of the pancreas are inhibited by IC261 in vitro and in vivo. *Gut* **2008**, *57* (6), 799−806.
(33) Reaz, S.; Mossalam, M.; Okal, A.; Lim, C. S. A Single Mutant, A276S of p53, Turns the Switch to Apoptosis. *Mol. Pharmaceutics* **2013**, *10*, 1350−9.
(34) el-Deiry, W. S.; Tokino, T.; Velculescu, V. E.; Levy, D. B.; Parsons, R.; Trent, J. M.; Lin, D.; Mercer, W. E.; Kinzler, K. W.; Vogelstein, B. WAF1, a potential mediator of p53 tumor suppression. *Cell* **1993**, *75* (4), 817−25.
(35) Yu, J.; Zhang, L.; Hwang, P. M.; Kinzler, K. W.; Vogelstein, B. PUMA induces the rapid apoptosis of colorectal cancer cells. *Mol. Cell* **2001**, *7* (3), 673−82.
(36) Tomita, Y.; Marchenko, N.; Erster, S.; Nemajerova, A.; Dehner, A.; Klein, C.; Pan, H.; Kessler, H.; Pancoska, P.; Moll, U. M. WT p53, but not tumor-derived mutants, bind to Bcl2 via the DNA binding domain and induce mitochondrial permeabilization. *J. Biol. Chem.* **2006**, *281* (13), 8600−6.
(37) Waldman, T.; Kinzler, K. W.; Vogelstein, B. p21 is necessary for the p53-mediated G1 arrest in human cancer cells. *Cancer Res.* **1995**, *55* (22), 5187−90.
(38) Loo, D. T.; Rillema, J. R. Measurement of cell death. *Methods Cell Biol.* **1998**, *57*, 251−64.

(39) Koopman, G.; Reutelingsperger, C. P.; Kuijten, G. A.; Keehnen, R. M.; Pals, S. T.; van Oers, M. H. Annexin V for flow cytometric detection of phosphatidylserine expression on B cells undergoing apoptosis. *Blood* **1994**, *84* (5), 1415−20.
(40) Vermes, I.; Haanen, C.; Steffens-Nakken, H.; Reutelingsperger, C. A novel assay for apoptosis. Flow cytometric detection of phosphatidylserine expression on early apoptotic cells using fluorescein labelled Annexin V. *J. Immun. Methods* **1995**, *184* (1), 39−51.
(41) Schmid, I.; Krall, W. J.; Uittenbogaart, C. H.; Braun, J.; Giorgi, J. V. Dead cell discrimination with 7-amino-actinomycin D in combination with dual color immunofluorescence in single laser flow cytometry. *Cytometry* **1992**, *13* (2), 204−8.
(42) Serrano, M. J.; Sanchez-Rovira, P.; Algarra, I.; Jaen, A.; Lozano, A.; Gaforio, J. J. Evaluation of a gemcitabine-doxorubicin-paclitaxel combination schedule through flow cytometry assessment of apoptosis extent induced in human breast cancer cell lines. *Jpn. J. Cancer Res.* **2002**, *93* (5), 559−66.
(43) Goodrum, F. D.; Ornelles, D. A. p53 status does not determine outcome of E1B 55-kilodalton mutant adenovirus lytic infection. *J. Virol.* **1998**, *72* (12), 9479−90.
(44) Bartek, J.; Iggo, R.; Gannon, J.; Lane, D. P. Genetic and immunochemical analysis of mutant p53 in human breast cancer cell lines. *Oncogene* **1990**, *5* (6), 893−9.
(45) Mooney, L. M.; Al-Sakkaf, K. A.; Brown, B. L.; Dobson, P. R. Apoptotic mechanisms in T47D and MCF-7 human breast cancer cells. *Br. J. Cancer* **2002**, *87* (8), 909−17.
(46) Bodner, S. M.; Minna, J. D.; Jensen, S. M.; D'Amico, D.; Carbone, D.; Mitsudomi, T.; Fedorko, J.; Buchhagen, D. L.; Nau, M. M.; Gazdar, A. F.; et al. Expression of mutant p53 proteins in lung cancer correlates with the class of p53 gene mutation. *Oncogene* **1992**, *7* (4), 743−9.
(47) Kawaguchi, T.; Kato, S.; Otsuka, K.; Watanabe, G.; Kumabe, T.; Tominaga, T.; Yoshimoto, T.; Ishioka, C. The relationship among p53 oligomer formation, structure and transcriptional activity using a comprehensive missense mutation library. *Oncogene* **2005**, *24* (46), 6976−81.
(48) Yahagi, N.; Shimano, H.; Matsuzaka, T.; Najima, Y.; Sekiya, M.; Nakagawa, Y.; Ide, T.; Tomita, S.; Okazaki, H.; Tamura, Y.; Iizuka, Y.; Ohashi, K.; Gotoda, T.; Nagai, R.; Kimura, S.; Ishibashi, S.; Osuga, J.; Yamada, N. p53 Activation in adipocytes of obese mice. *J. Biol. Chem.* **2003**, *278* (28), 25395−400.
(49) Brunelle, J. K.; Letai, A. Control of mitochondrial apoptosis by the Bcl-2 family. *J. Cell Sci.* **2009**, *122* (Pt 4), 437−41.
(50) Wang, W.; Cheng, B.; Miao, L.; Mei, Y.; Wu, M. Mutant p53-R273H gains new function in sustained activation of EGFR signaling via suppressing miR-27a expression. *Cell Death Dis.* **2013**, *4*, e574.
(51) Lim, L. Y.; Vidnovic, N.; Ellisen, L. W.; Leong, C. O. Mutant p53 mediates survival of breast cancer cells. *Br. J. Cancer* **2009**, *101* (9), 1606−12.
(52) Taylor, C. M.; Keating, A. E. Orientation and oligomerization specificity of the Bcr coiled-coil oligomerization domain. *Biochemistry* **2005**, *44* (49), 16246−56.
(53) Maru, Y.; Witte, O. N. The BCR gene encodes a novel serine/threonine kinase activity within a single exon. *Cell* **1991**, *67* (3), 459−68.
(54) Alexis, J. D.; Wang, N.; Che, W.; Lerner-Marmarosh, N.; Sahni, A.; Korshunov, V. A.; Zou, Y.; Ding, B.; Yan, C.; Berk, B. C.; Abe, J. Bcr kinase activation by angiotensin II inhibits peroxisome-proliferator-activated receptor gamma transcriptional activity in vascular smooth muscle cells. *Circ. Res.* **2009**, *104* (1), 69−78.
(55) Woessner, D. W.; Lim, C. S.; Deininger, M. W. Development of an effective therapy for chronic myelogenous leukemia. *Cancer J.* **2011**, *17* (6), 477−86.
(56) Melo, J. V.; Barnes, D. J. Chronic myeloid leukaemia as a model of disease evolution in human cancer. *Nat. Rev. Cancer* **2007**, *7* (6), 441−53.
(57) Galea, C.; Bowman, P.; Kriwacki, R. W. Disruption of an intermonomer salt bridge in the p53 tetramerization domain results in an increased propensity to form amyloid fibrils. *Protein Sci.* **2005**, *14* (12), 2993−3003.

molecular pharmaceutics

Article

pubs.acs.org/molecularpharmaceutics

Enhanced and Selective Killing of Chronic Myelogenous Leukemia Cells with an Engineered BCR-ABL Binding Protein and Imatinib

Jonathan E. Constance,[†] David W. Woessner,[†] Karina J. Matissek,[‡] Mohanad Mossalam,[§] and Carol S. Lim*[,§]

[§]Department of Pharmaceutics and Pharmaceutical Chemistry and [†]Department of Pharmacology and Toxicology, College of Pharmacy, University of Utah, Salt Lake City, Utah 84108, United States

[‡]Department of Pharmaceutics and Biopharmacy, Philipps-Universität, Germany

Supporting Information

ABSTRACT: The oncoprotein Bcr-Abl stimulates prosurvival pathways and suppresses apoptosis from its exclusively cytoplasmic locale, but when targeted to the mitochondrial compartment of leukemia cells, Bcr-Abl was potently cytotoxic. Therefore, we designed a protein construct to act as a mitochondrial chaperone to move Bcr-Abl to the mitochondria. The chaperone (i.e., the 43.6 kDa intracellular cryptic escort (iCE)) contains an EGFP tag and two previously characterized motifs: (1) an optimized Bcr-Abl binding motif that interacts with the coiled-coil domain of Bcr (ccmut3; 72 residues), and (2) a cryptic mitochondrial targeting signal (cMTS; 51 residues) that selectively targets the mitochondria in oxidatively stressed cells (i.e., Bcr-Abl positive leukemic cells) via phosphorylation at a key residue (T193) by protein kinase C. While the iCE colocalized with Bcr-Abl, it did not relocalize to the mitochondria. However, the iCE was selectively toxic to Bcr-Abl positive K562 cells as compared to Bcr-Abl negative Cos-7 fibroblasts and 1471.1 murine breast cancer cells. The toxicity of the iCE to leukemic cells was equivalent to 10 μM imatinib at 48 h and the iCE combined with imatinib potentiated cell death beyond imatinib or the iCE alone. Substitution of either the ccmut3 or the cMTS with another Bcr-Abl binding domain (derived from Ras/Rab interaction protein 1 (RIN1; 295 residues)) or MTS (i.e., the canonical IMS derived from Smac/Diablo; 49 residues) did not match the cytotoxicity of the iCE. Additionally, a phosphorylation null mutant of the iCE also abolished the killing effect. The mitochondrial toxicity of Bcr-Abl and the iCE in Bcr-Abl positive K562 leukemia cells was confirmed by flow cytometric analysis of 7-AAD, TUNEL, and annexin-V staining. DNA segmentation and cell viability were assessed by microscopy. Subcellular localization of constructs was determined using confocal microscopy (including statistical colocalization analysis). Overall, the iCE was highly active against K562 leukemia cells and the killing effect was dependent upon both the ccmut3 and functional cMTS domains.

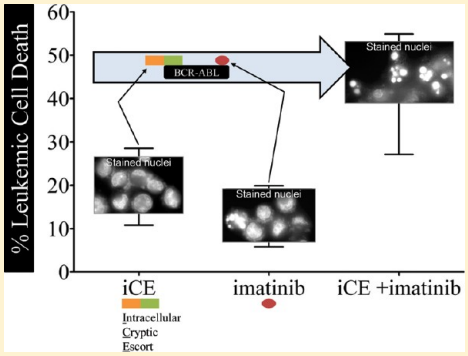

KEYWORDS: *cryptic MTS, Bcr-Abl, Bcr-Abl binding, coiled-coil, molecular chaperone*

INTRODUCTION

The fusion oncoprotein, and constitutively active tyrosine kinase, Bcr-Abl (autoinhibition of c-Abl kinase activity is lost in Bcr-Abl fusion)[1] is the central etiologic agent of chronic myelogenous leukemia (CML) and is exclusively localized in the cytoplasmic space at the plasma membrane primarily through interactions with cytoskeletal actin.[1] Directing a change in Bcr-Abl's subcellular location can change Bcr-Abl from an oncogenic agent into a proapoptotic factor.[2,3]

Normal c-Abl fulfills a terminal role as a proapoptotic factor when targeted to the mitochondria under a variety of cellular insults.[4,5] We previously demonstrated that direct targeting of c-Abl to the mitochondria is toxic to leukemia cells.[6] Therefore, relocalizing Bcr-Abl to the mitochondria would mimic death-directed mitochondrial c-Abl function, which is largely defunct in CML cells.[7,8] In this paper, as with c-Abl,[6] the direct mitochondrial targeting of Bcr-Abl (by fusion to canonical MTSs targeting the mitochondrial matrix,[9] inner mitochondrial membrane,[10] and the intermitochondrial membrane space[11]) was cytotoxic.

In light of this, we designed a small protein, the intracellular cryptic escort (iCE), for the purpose of capturing and translocating Bcr-Abl to the mitochondria. The Bcr-Abl capture motif employed for the iCE was a previously optimized coiled-coil (i.e., the ccmut3)[12] which demonstrated both the ability to bind and, when fused to four nuclear localization signals (NLS), move endogenous Bcr-Abl to the nucleus.[13] The ccmut3 oligomerizes with the coiled-coil domain of the Bcr portion of Bcr-Abl while possessing a reduced affinity for homodimer formation.[12] We paired the ccmut3 with a "cryptic" mitochondrial targeting signal (cMTS) that is activated by phosphorylation (by PKA and/or PKC) in a reactive oxygen species dependent manner.[6]

Received: June 26, 2012
Revised: September 3, 2012
Accepted: September 9, 2012
Published: September 10, 2012

Despite the lack of iCE/Bcr-Abl mitochondrial localization the iCE alone was selectively toxic to Bcr-Abl positive K562 cells to the same degree as 10 μM imatinib at 48 h. The killing capacity of the iCE was ablated by substitution of either the ccmut3 (with the Bcr-Abl binding domain of Ras and Rab interactor 1 (RIN1-BD)[14]) or the cMTS (with the canonical intermitochondrial membrane space targeting sequence (IMS) from Smac/Diablo[11]) in two "mock" iCEs, the RIN-cMTS or the IMS-ccmut3, respectively. The combination of the iCE with imatinib was the most potent inducer of leukemic cell death. This work demonstrates the selective killing of Bcr-Abl positive cells by a designed Bcr-Abl coiled-coil interacting protein where phosphorylation (via PKC and/or PKA) is coincident with the cell death effect.

EXPERIMENTAL SECTION

Subcloning and Construction of Plasmids. pEGFP-Bcr-Abl was constructed as previously described.[3] Bcr-Abl DNA was also cloned into pmCherry-C1 (Clonetech, Mountain View, CA, USA) and pTagBFP-C (Evrogen, Moscow, Russia) at the *Eco*R1 site on both vectors creating pmCherry-Bcr-Abl and pBFP-Bcr-Abl, respectively. The pOTC-EGFP-Bcr-Abl was created using an oligonucleotide encoding the MTS from OTC (incorporating the Kozak sequence), 5′-CCGGTCGCCACCATGCTGTTTAATCTGAGGATCCTGTTAAACAATGCAGCTTTTAGAAATGGTCACAACTTCATGGTTCGAAATTTTCGGTGTGGACAACCACTACAAAATAAAGTGCAGCGA-3′, which was annealed to its complementary strand and subsequently cloned into the *Age*I site of EGFP-Bcr-Abl. The pIMS-EGFP-Bcr-Abl, pIMS-EGFP, and pIMS-EGFP-ccmut3 were made by annealing and ligating four oligonucleotides encoding the Kozak sequence and IMS signal (**1**, (5′-phosphorylated) 5′-CCGGTGCCACCATGAGAAGCGTGTGCAGCCTGTTCAGATACAGACAGAGATTCCCCGTGCTGGCCAACAGCAA-3′; **2**, 5′-GAAGAGATGCTTCAGCGAGCTGATCAAGCCCTGGCACAAGACCGTGCTGACCGGCTTCGGCATGACCCTGTGCGCCGTGCCCATCGGA-3′; **3**, 5′-TGCCACCATGAGAAGCGTGTGCAGCCTGTTCAGATACAGACAGAGATTCCCCGTGCTGGCCAACAGCAAGAAGAG-3′; **4**, (5′ phosphorylated) 5′-ATGCTTCAGCGAGCTGATCAAGCCCTGGCACAAGACCGTGCTGACCGGCTTCGGCATGACCCTGTGCGCCGTGCCCATCAGGACCGG-3′) followed by insertion into the *Age*I site of pEGFP-Bcr-Abl, pEGFP, or pEGFP-ccmut3,[12] respectively. The inner mitochondrial membrane targeting sequence (IMM) was incorporated into the pIMM-EGFP-Bcr-Abl and pIMM-EGFP by annealing the 5′ phosphorylated oligonucleotide encoding the Kozak sequence and IMM signal, 5′-CCGGTCGCCACCATGTCCGTCCTGACGCCGCTGCTGCTGCGGGGCTTGACAGGCTCGGCCCGGCGGCTCCCAGTGCCGCGCGCCAAGATCCATTCGTTGA-3′, with its reverse compliment followed by ligation into the *Age*I site of pEGFP-Bcr-Abl and pEGFP-C1, respectively. The kinase dead mutant of pIMM-EGFP-Bcr-Abl (i.e., pIMM-EGFP-Bcr-Abl-KD) was made using site directed mutagenesis with the primer 5′-CTGACGGTGGCCGTGGCGACCTTGAAGGAGGAC-3′ and its reverse compliment. The pRIN-cMTS construct was made by PCR amplifying the binding domain of the human RIN1 gene (NM_004292, OriGene, Rockville, MD, USA) with the primers 5′-GCGCGCGCGATCTATGGAAAGCCCTGGAGAGTCAGGCGCG-3′ and 5′-GCGCGCGAATTCCCGTACCCCACTGAGCTCTCCCTCCGTAGCAGCTGGC-3′ and inserted into pEGFP-cMTS using the *Bgl*II and *Eco*R1 sites. The murine glutathione *S*-transferase A4-4 [Swiss-Prot: P24472.3] cMTS (N-terminal residues, 172−222)[15] was constructed by annealing four oligonucleotides encoding the cMTS (**1**, (5′-phosphorylated) 5′-AATTCCGCCCCCGTGCTGAGCGACTTCCCCCTGCTGCAGGCCTTCAAGACCAGAATCAGCAACATCCCCACCATCAAGAAGTTCCTGCAGCCC-3′; **2**, 5′-CTGCCGGGCTGCAGGAACTTCTTGATGGTGGGGATGTTGCTGATTCTGGTCTTGAAGGCCTGCAGCAGGGGGAAGTCGCTCAGCACGGGGGCGG-3′; **3**, 5′-GGCAGCCAGAGAAAGCCCCCCCCCGACGGCCCCTACGTGGAGGTGGTGAGAACCGTGCTGAAGTTCGGCGCCGGCTGCTGCCCCGGCTGCTGCTGA-3′; **4**, (5′ phosphorylated) 5′-AATTTCAGCAGCAGCCGGGGCAGCAGCCGGCGCCGAACTTCAGCACGGTTCTCACCACCTCCACGTAGGGGCCGTCGGGGGGGGGCTTTCTCTGG-3′) simultaneously and then inserting the annealed product into the multiple cloning site (MCS) of EGFP-C1 vector (Promega Biotech, Madison, WI), with or without the ccmut3 sequence present, at the *Eco*RI site creating pEGFP-cMTS[6] (cMTS) and pEGFP-ccmut3-cMTS (iCE), respectively. The pEGFP-ccmut3-cMTS null (S189A and T193A) was created using site-directed mutagenesis using primers, 5′-GACCAGAATCGCCAACATCCCCGCCATCAAGAAGTTCCTGCAGCCCGGCAGCCAGAGAA-3′ and its reverse compliment. All constructs were verified by sequence analysis.

Materials. RPMI-1640 medium, MitoTracker Red CM-H_2XRos (MitoTracker CMXros), Hoechst 33342 (cell permeable nuclear stain), 7-aminoactinomycin D (7-AAD; DNA intercalating dye permeable to dying or dead cells), annexin−APC (annexin-V conjugated to allophycocyanin), staurosporine, Lipofectamine LTX with Plus Reagent, trypan blue 0.4%, phosphate-buffered saline (PBS), fetal bovine serum (FBS), and gentamycin were purchased from Invitrogen (Carlsbad, CA). Penicillin−streptomycin−L-glutamine (P-S-G; 100U/mL), DMEM media, and trypsin were purchased from Gibco BRL (Grand Island, NY). The poly-L-lysine (0.01% solution) was purchased from Sigma-Aldrich (St. Louis, MO). Imatinib (CT-IM001) was purchased from ChemieTek (Indianapolis, IN). QuikChange II XL Site-Directed Mutagenesis Kit was purchased from Agilent Technologies (Santa Clara, CA). Cell Line Nucleofector Kit V was purchased from Lonza Group (Basel, Switzerland). Restriction enzymes (*Eco*RI, *Age*I, and *Bgl*II) were purchased from New England Biolabs (Ipswich, MA).

Cell Lines and Culture Conditions. As previously described,[6] K562 cells (nonadherent human chronic myelogenous leukemia cell line), gift from Dr. K. Elenitoba-Johnson, University of Michigan, and Cos-7 (monkey kidney fibroblast adherent cell line; ATCC) were cultured in RPMI 1640 supplemented with 10% FBS, 1% P-S-G, and 0.1% gentamycin. Murine mammary adenocarcinoma 1471.1 cells, (gift from Gordon Hager, PhD, NCI, NIH) were grown as monolayers in DMEM supplemented with 10% FBS, 1% P-S-G, and 0.1% gentamycin. K562 cells were passaged at a density of 0.5×10^5/mL every other day, for ten passages. Cos-7 and 1471.1 cells were passaged at 80% confluency, split 1:10 in fresh media, and discontinued after passage 15. All cells were maintained in a 5% CO_2 incubator at 37 °C.

Expression of Constructs in K562 Leukemia, Cos-7 Fibroblast, and 1471.1 Breast Cancer Cells. Constructs were transiently transfected into K562 cells using the Amaxa Nucleofector II, as described previously.[3] Briefly, 1×10^6 K562 cells (initially seeded at a density of 0.5×10^5 cells/mL) between passages 5 and 10, were pelleted and resuspended in 100 μL of Amaxa Solution V, combined with 2 μg of DNA, and transfected in an Amaxa cuvette under program T-013. Transfected cells were immediately transferred to a 25 cm^2

dx.doi.org/10.1021/mp3003539 | *Mol. Pharmaceutics* 2012, 9, 3318−3329

flask with 7 mL of prewarmed complete RPMI. Transient transfection of 1471.1 and Cos-7 was carried out in two-well live-cell chambers (Lab-Tek chamber slide system, Nalge NUNC International, Naperville, IL) or sterile 6-well tissue culture plates (Greiner CellStar, Greiner Bio-one GmbH) using Lipofectamine LTX as per manufacturers' instructions between passages 3 and 15 in antibiotic free media.

Cell Proliferation. Trypan blue exclusion was used to determine cell proliferation (cell viability)[16] in K562 cells 48 h post-transfection of EGFP-C1, cMTS, ccmut3, cMTS, and iCE, with and without the presence of imatinib (10 μM).

Western Blotting. As previously described,[17] cell lysates were prepared in lysis buffer (62.5 mM Tris-HCl, 2% w/v SDS, 10% glycerol, 50 mM DTT, 0.01% w/v bromophenol blue) followed by standard blotting using antibodies to detect p-Bcr-Abl, p-Crk-L, p-STAT5, and elF4E as the protein loading control. Primary antibody labels (anti-pAbl (Y245), anti-pCrk-L (Y207), and anti-elF4E, Cell Signaling Technology; anti-pSTAT5 (Y694), Abcam) were detected with (#7074, Cell Signaling Technology) secondary antibody prior to the addition of ChemiGlo (AlphaInnotech, Cell Biosciences, Santa Clara, CA, USA) chemiluminescent substrate and detection using a FluorChem FC2 imager (AlphaInnotech).

Mitochondrial Staining. As previously described,[6] aliquots of transfected K562 suspension cells (400 μL) were plated into poly-L-lysine coated 4-well live-cell chambers at least four hours in advance of microscopy. Cells were incubated with MitoTracker Red CM-H_2XRos (K562, 100 nM; Cos-7 and 1471.1, 325 nM) for 45 min at 37 °C and protected from light prior to imaging.

Microscopy. Fluorescent images of K562, Cos-7, and 1471.1 live cells were acquired on an Olympus IX81 FV1000-XY spectral confocal microscope (Imaging Core Facility, University of Utah) equipped with 405 nm diode, 488 nm argon, and 543 nm HeNe lasers using a 60× PlanApo oil immersion objective (NA 1.45) using Olympus FluoView software, as previously described.[6] Excitation and emission filters were as follows: EGFP, 488 nm excitation, emission filter 500−530 nm; MitoTracker Red CM-H_2XRos, 543 nm excitation, emission filter 555−655 nm. Images were collected in sequential line mode with exposure and gain of laser kept constant and below detected pixel saturation for each group of cells. No channel crosstalk was observed. Pixel resolution was kept at 1024 × 1024 (0−2.5-fold digital zoom) with a pixel dwell time of 12.5 μs. Imaging of K562 cells for the analysis of DNA segmentation was acquired on an Olympus IX71F fluorescence microscope (Scientific Instrument Company, Aurora, CO) with a 60× PlanApo oil immersion objective (NA 1.4) on an F-view monochrome CCD camera. K562 cells were stained with the nuclear dye Hoechst 33342 (Invitrogen, Carlsbad, CA) at a concentration of 4 μM.

Image Analysis. Images were analyzed as previously described.[6] Briefly, original images were converted to 8-bit, then stacked as separate channels, and corrected for background noise using ImageJ plugin "BG subtraction from background" in default mode (i.e., mean background intensity outside of cells was subtracted).[18] Image and statistical analysis was performed with JACoP plugin in ImageJ.[19] Pearson's correlation coefficient (PCC) was generated using Costes' automatic threshold algorithm.[20,21] The PCC is dependent upon both the pixel intensity and overlap of signal and has a range of +1 (complete colocalization) to −1 (anticorrelation) with zero correlating with random distribution between comparators.[19] The PCC threshold for defining colocalization (i.e., colocalization due to cocompartmentalization) is 0.6 as per Bolte and Cordelières.[19] Channels have been false-colored (cyan and magenta) using ImageJ LUT for increased visual clarity. Additionally, spatial representation of intensity correlation was included using the Colocalization Colormap ImageJ plugin. "Colormap" displays positively correlated pixels in hot colors and negatively correlated pixels in cold colors that can be visually interpreted using the color scale bar.[22] Identification of segmented nuclei was performed using the nuclear dye H33342 on K562 cells displaying green fluorescence 24 h post transfection.

7-AAD Assay. Flow cytometric assay of cell death was done as previously described.[12] Briefly, K562, Cos-7, or 1471.1 cells were resuspended in 500 μL of ice cold PBS containing 1 μM 7-aminoactinomycin D (7-AAD) for 30 min prior to analysis. Cells that have compromised membrane integrity (late apoptosis/necrosis) are permeable to 7-AAD.[23] Medium from adherent Cos-7 and 1471.1 cells was collected prior to trypsinization of cell monolayer and recombined with the enzymatically released cell population for centrifugation and subsequent resuspension. Analysis and gating was performed on a BD FACSCanto II (Flow Cytometry Core Facility, University of Utah) using BD FACSDiva software (BD Biosciences, Franklin Lakes, NJ). At least three separate experiments ($n \geq 3$) in duplicate were performed. Compensation controls were included with each experiment.

TUNEL Assay. As previously described,[24] detection of DNA strand breaks in the K562 cell line was performed using the In Situ Death Detection Kit, TMR red (Roche, Mannheim, Germany), as per the manufacturers' protocol. Terminal deoxynucleotidyl transferase (TdT) dUTP nick-end labeling (TUNEL) detects cells that have extensive DNA degradation in late stage apoptosis/necrosis.[25] Samples were run on a Becton-Dickinson FACSAria-II (BD-BioSciences, University of Utah Core Facility) using the 488 nm (for EGFP) and 563 nm (TMR red) laser lines with FACSDiva software. Analysis was performed on EGFP positive cells using preset gates. The TMR red positive cells were detected in the PE (phycoerythrin) channel. Each construct was assayed in at least triplicate ($n \geq 3$).

Annexin-V Assay. Annexin-V binding was assessed, as previously described,[24] 48 h post-transfection in K562 cells. Externalized phosphatidylserine in the plasma membrane is indicative of early apoptosis and is bound specifically by annexin V.[26] K562 cells were suspended in 100 μL of annexin binding buffer (Invitrogen) and incubated with 5 μL of annexin-V conjugated to allophycocyanin (annexin−APC, Invitrogen) for 10 min. The incubated cells were then diluted in 400 μL of annexin binding buffer and analyzed using the FACSCanto-II (BD-BioSciences, University of Utah Core Facility) with FACSDiva software. EGFP (excitation 488 nm and emission 507 nm) and APC (excitation 635 nm and emission 660 nm) fluorescence was collected. Analysis was conducted on EGFP-positive cells using preset EGFP gates. Each construct was tested in triplicate ($n = 3$).

Statistics. Data are shown as mean ± SEM, with one-way ANOVA using Tukey's post hoc test or two-way ANOVA using the Bonferroni post-test (as indicated in the figure legends) to compare measurements between experimental data with an N of 3 or greater. Statistical significance was set at $p < 0.05$ (by convention $p < 0.05$ is represented with *; $p < 0.01$ with **; $p < 0.001$ with ***). GraphPad Prism Graph 4 (GraphPad, La Jolla, CA) software was used for generating statistics.

RESULTS

Targeting Bcr-Abl to the Mitochondria Induces Cell Death in K562 Leukemia Cells. Cell death evaluated by flow cytometric analysis of 7-AAD (DNA accessibility) and annexin−APC (phosphatidylserine externalization) staining (Figure 1) showed the toxic consequences of mitochondrially

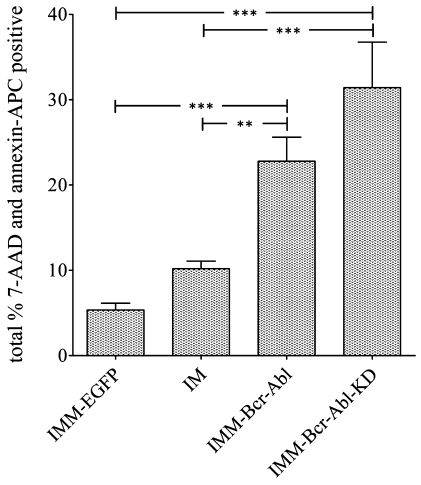

Figure 1. Direct targeting of Bcr-Abl to the mitochondria causes leukemic cell death. Flow cytometric analysis of EGFP positive K562 cells 24 h post-transfection stained with 7-AAD and annexin−APC. Both IMM-Bcr-Abl and the kinase dead version (IMM-Bcr-Abl-KD) displayed higher cell death than imatinib or mitochondrially targeted EGFP (IMM-EGFP). Statistical differences were determined using a one-way ANOVA with Tukey's post hoc test (error bars are ±SEM, $N \geq 4$).

targeted Bcr-Abl (Figure 1, third column) at 24 h post-transfection in K562 cells. DNA segmentation analysis of K562 cells with mitochondrially targeted Bcr-Abl also revealed the same pattern (data not shown). The IMM-Bcr-Abl was created by fusing Bcr-Abl to a canonical mitochondrial targeting signal (MTS; derived from cytochrome *c* oxidase subunit VIII) that is widely used to direct proteins to the mitochondria and the inner mitochondrial membrane in particular (IMM; see Table 1).[10] Interestingly, the kinase dead version (i.e., mutation of a single critical lysine ablates the capacity for kinase activity) of mitochondrially targeted Bcr-Abl (IMM-Bcr-Abl-KD; see Table 1) yields no statistical difference

Table 1. Canonical Mitochondrial Targeting Sequences Used To Target Bcr-Abl to the Mitochondria[a]

construct	target compartment	kinase	reference
OTC-Bcr-Abl	mitochondrial matrix	active	9
IMS-Bcr-Abl	mitochondrial intermembrane space	active	11
IMM-Bcr-Abl	mitochondrial inner membrane	active	10
IMM-Bcr-Abl-KD	mitochondrial inner membrane	inactive	27
IMM-EGFP	mitochondrial inner membrane	N/A	24
E-Bcr-Abl	cytoplasmic (nontargeted)	active	3

[a]MTSs targeting different mitochondrial compartments were fused to Bcr-Abl and tested for cellular toxicity. KD represents a kinase dead version of Bcr-Abl where a so-called "essential lysine" residue is mutated at the ATP binding site, abolishing all kinase activity.[27]

in cell death to that of IMM-Bcr-Abl (compare Figure 1, third and fourth columns). Furthermore, mitochondrially targeted Bcr-Abl and Bcr-Abl-KD (Figure 1, third and fourth columns) significantly induced more cell death as compared to the gold standard of current CML therapy, imatinib (IM; 10 μM) (Figure 1, second column) at 24 h.

In addition to the IMM, Bcr-Abl was also targeted to the mitochondrial matrix (OTC-Bcr-Abl) and IMS (IMS-Bcr-Abl) (Table 1). Figure 2A shows representative images of E-Bcr-Abl or mitochondrially targeted Bcr-Abl in K562 cells compared to MitoTracker CMXros (MitoTracker) dye. The E-Bcr-Abl construct was not associated with the mitochondria (Figure 2A,

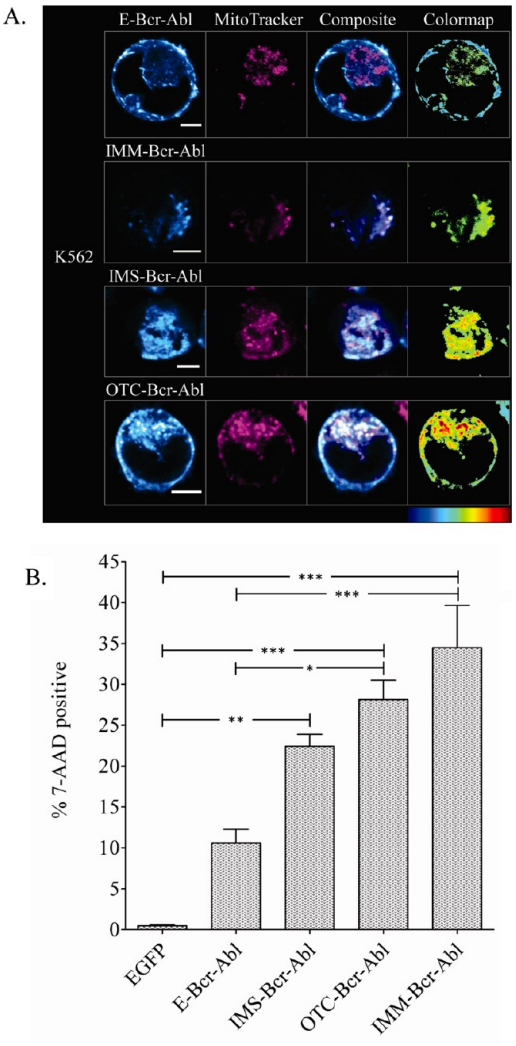

Figure 2. Submitochondrial targeting of Bcr-Abl in K562 leukemia cells. (A) Representative images of E-Bcr-Abl or Bcr-Abl fused to a canonical MTS in K562 cells and compared to MitoTracker CMXros staining. Each of the MTS-Bcr-Abl constructs localizes to the mitochondria while the nontargeted E-Bcr-Abl remains cytosolic. Channel one (EGFP) and channel two (MitoTracker) have been false-colored, cyan and magenta. Colocalized cyan and magenta pixels show as white in merged ("composite" column) images. The "Colormap" (far right column) is a visual representation of pixel correlation both in space and in intensity with positive correlation shown as hot colors and negative correlation in cooler colors and can be interpreted using the color scale bar (shown at bottom of the "Colormap" column). Scale bars are 5 μm. (B) Cell death as determined by 7-AAD staining in K562 cells 48 h post transfection. Statistical differences were determined using a one-way ANOVA with Tukey's post hoc test (error bars are SEM, $N \geq 3$).

compare first column with second, "MitoTracker" column), but each of the mitochondrially targeted Bcr-Abl constructs did

dx.doi.org/10.1021/mp3003539 | *Mol. Pharmaceutics* 2012, 9, 3318−3329

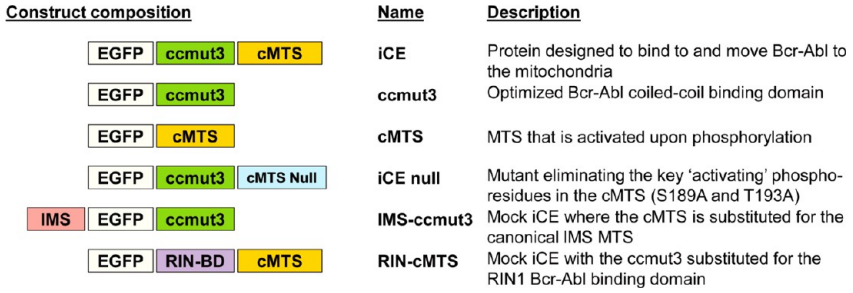

Figure 3. Domain arrangement of constructs. RIN-BD = Abl binding domain from the Ras and Rab interactor 1 (RIN1; binds the SH3/SH2 domains of Bcr-Abl), IMS = intermitochondrial membrane space, ccmut3 = coiled-coil mutation set 3, cMTS = cryptic mitochondrial translocation sequence, Bcr = breakpoint cluster region, Abl = Abelson proto-oncogene, EGFP = enhanced green fluorescent protein. See Figure S2 in the Supporting Information for domain residue sequences.

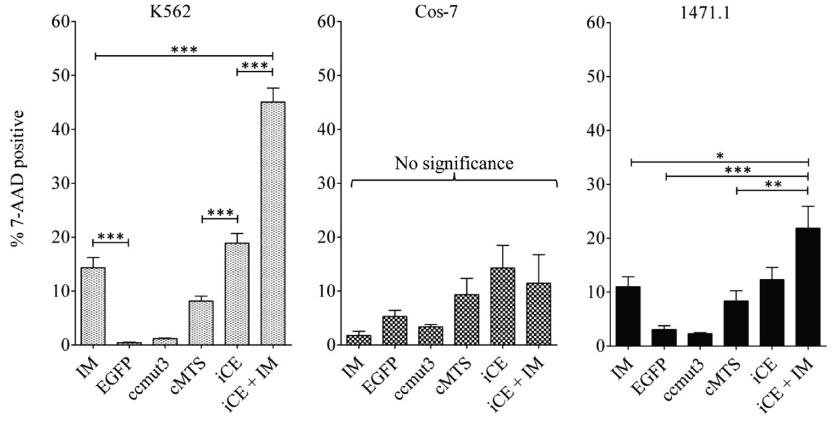

Figure 4. Cell death in Bcr-Abl positive (K562 leukemia) and Bcr-Abl negative (Cos-7 fibroblast and 1471.1 breast cancer) cells 48 h post-transfection or treatment with 10 μM imatinib. Cell death was assessed by flow cytometric analysis of 7-AAD. (A, left) K562 cells. (B, middle) Bcr-Abl negative Cos-7 cells. (C, right) 1471.1 breast cancer cells. One-way ANOVA with Tukey's post-test performed on individual cell types (error bars are SEM, $N \geq 3$).

localize (Figure 2A, second through fourth rows) to the mitochondria. The corresponding EGFP-only constructs (i.e., IMM-EGFP, IMS-EGFP, and OTC-EGFP) were also tested and exhibited mitochondrial localization and low toxicity. Therefore, only data on the IMM-EGFP is shown (Figure 1, IMM-EGFP). We further characterized the effects of targeting Bcr-Abl to the mitochondrial matrix with the OTC MTS in Cos-7 and 1471.1 cells (Figure S1 in the Supporting Information).

In K562 cells, the OTC and the IMM fused Bcr-Abl constructs were significantly more toxic (7-AAD positive) than the nontargeted E-Bcr-Abl (Figure 2B, compare fourth and fifth columns to second column) at 48 h post-transfection. Yet, there was no difference in toxicity between the individual MTS-Bcr-Abl constructs (Figure 2B, compare third, fourth, and fifth columns).

The iCE Exhibits Selective Toxicity to Bcr-Abl Positive K562 Cells. Since Bcr-Abl targeted to the mitochondria is toxic (Figure 1, third column), we designed a bimodal construct (intracellular cryptic escort (iCE)) using a previously characterized cMTS[6] and our optimized Bcr-Abl binding domain, ccmut3[12] (see Figure 3 for description of constructs). The iCE and its component parts (i.e., EGFP, ccmut3, and cMTS; Figure 3) were transfected into Bcr-Abl positive K562 and Bcr-Abl negative Cos-7 and 1471.1 cell lines. The cell death profiles, as measured by flow cytometric analysis of 7-AAD staining, demonstrated a cell type-dependent response to the constructs. The iCE was toxic only in the K562 cell line (Figure 4A, K562, iCE column) as was imatinib (Figure 4A, K562, IM column). There was no significant difference in Cos-7 or 1471.1 between treatment with imatinib or the constructs individually with the exception of 1471.1 cells with the iCE combined with imatinib (Figure 4C, 1471.1, iCE + IM column). This was not evidenced in Cos-7 where the combination of imatinib and the iCE was not toxic (Figure 4B, Cos-7, iCE + IM column). In contrast, within K562 cells imatinib and the iCE were not different from one another (Figure 4A, K562, compare iCE to IM columns) but both were different from the EGFP control and the iCE components (Figure 4A, K562, EGFP, ccmut3, and cMTS columns). The iCE when combined with imatinib (Figure 4A, K562, iCE + IM column) had the greatest killing effect.

Figure 5A includes the components comprising the iCE (i.e., EGFP, ccmut3, and cMTS) combined with imatinib. There was no difference between imatinib alone and the individual components of the iCE combined with imatinib (Figure 5A, compare IM with EGFP+IM, ccmut3 + IM, and cMTS + IM). The cMTS alone was not different from imatinib, however when compared to the iCE alone (Figure 5A, compare cMTS to iCE) the difference was extremely significant ($P < 0.001$). Overall, the iCE + IM was significantly different ($P < 0.001$) in its killing potential when compared to all constructs regardless of imatinib treatment (Figure 5A, compare iCE + IM to EGFP + IM, ccmut3 + IM, and cMTS + IM).

Representative histograms (Figure 5B) from a set of K562 cells transfected and/or treated (imatinib (10 μM) or positive control staurosporine (1 μM)) at 48 h demonstrate the difference in dead cells when the iCE and imatinib are combined

dx.doi.org/10.1021/mp3003539 | Mol. Pharmaceutics 2012, 9, 3318–3329

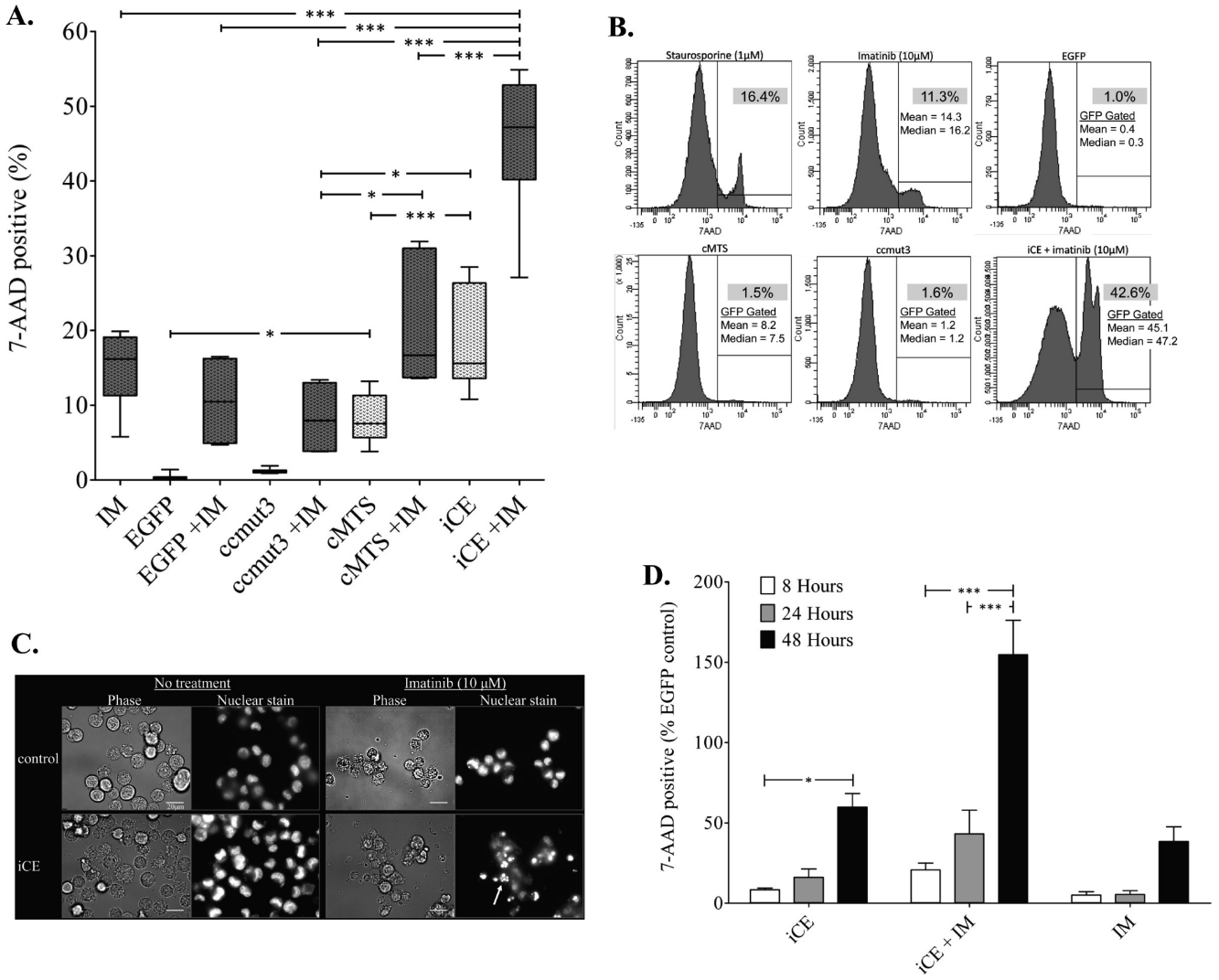

Figure 5. The iCE combined with imatinib is toxic to K562 cells. (A) This figure is an expansion of the data set seen in Figure 4A, K562 (cell death in K562 at 48 h). Box and whisker plot showing percent 7-AAD positive cells 48 h post-transfection and/or treatment with imatinib. The darker shaded boxes (of the box plot) represent the presence of imatinib (10 μM). Statistical differences were determined using one-way ANOVA with Tukey's post hoc test (error bars are SEM, $N \geq 4$). (B) Representative set of flow cytometric histograms displaying cell count on the *y*-axis and 7-AAD intensity on the *x*-axis. The percent 7-AAD positive (as gated) for the sample is listed in the shaded box, and the mean (Figure 4A, K562) and median values (Figure 5A) are listed below. (C) Phase-contrast paired with fluorescent images using the nuclear dye, H33342, at 48 h post-transfection (iCE) or imatinib treatment. Upper left, control K562 cells; lower left, cells transfected with iCE construct; upper right, cells treated with imatinib only; lower right, cells transfected with the iCE and treated with imatinib. White arrow in bottom, rightmost panel indicates a cell with a segmented nucleus. Scale bar is 20 μm. (D) Evaluation of 7-AAD positive K562 cells at 8, 24, and 48 h post-transfection and/or imatinib treatment. Statistical difference was determined for the parameters of time and treatment using two-way ANOVA with Bonferroni post test (error bars are SEM, $N \geq 3$).

(Figure 5B, compare staurosporine or imatinib to iCE + imatinib). The vertical line within the plot is the gate for 7-AAD positive cells for which the percent is listed in the shaded box. As expected, a similar cell death pattern was seen using a different cell permeable nuclear stain (H33342) to identify nuclear segmentation by microscopy[3] (Figure 5C, compare imatinib only (top right set) to iCE + imatinib (lower right set)). The relative health of the cells was revealed by phase contrast as well, where the cells treated with imatinib and the iCE evidence the sequelae of apoptosis/necrosis (e.g., cell shrinkage/swelling and membrane blebbing)[3] in comparison to the untreated control (e.g., round cells with intact membranes) (Figure 5C, compare "Phase" of iCE, "no treatment" and "imatinib" to control, "no treatment"). The combined treatment of imatinib and the iCE increases DNA segmentation (Figure 5C, compare the stained nuclei of the iCE, "no treatment" and "imatinib" to iCE, with "imatinib"). The peak time for iCE + IM killing of K562 is 48 h (Figure 5D) whereas it is later for imatinib alone (10 μM imatinib kills most K562 cells by approximately 72 to 96 h, our unpublished observations).

Cell Viability Decreases and Apoptosis Increases When the iCE Is Combined with Imatinib. Trypan blue exclusion (cell viability), terminal deoxynucleotidyl transferase dUTP nick end labeling (TUNEL), and phosphatidylserine (PS) externalization (annexin-V binding) demonstrated the antileukemic activity of the iCE in K562 cells (Figures 6A, 6B, and 6C, respectively).

Cell viability was significantly decreased for the iCE compared to EGFP and ccmut3 but not the cMTS (Figure 6A, compare

dx.doi.org/10.1021/mp3003539 | *Mol. Pharmaceutics* 2012, 9, 3318−3329

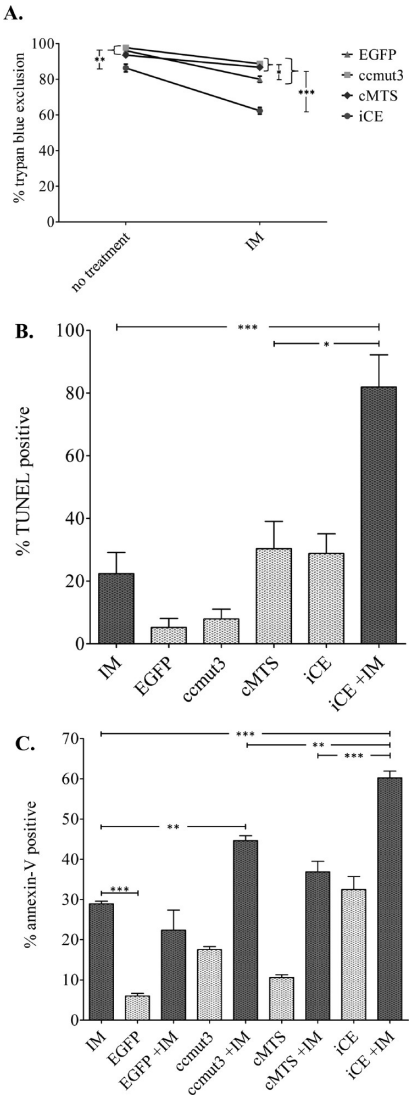

Figure 6. Assessment of cell viability and apoptotic induction in K562 cells. (A) Viability 48 h post-transfection and 24 h after addition of imatinib. One-way ANOVA with Tukey's post hoc test was performed within each treatment type (i.e., "no treatment" and "IM"). (B) Terminal deoxynucleotidyl transferase dUTP nick end labeling (TUNEL) was assessed 48 h post-transfection and/or with imatinib treatment by flow cytometry. (C) Phosphatidylserine externalization detection using annexin−APC and flow cytometric analysis 48 h post-transfection and/or imatinib treatment. Dark shaded columns indicate imatinib treatment. Statistical differences were determined by using one-way ANOVA with Tukey's post hoc test (for all assays here, error bars are SEM, $N \geq 3$).

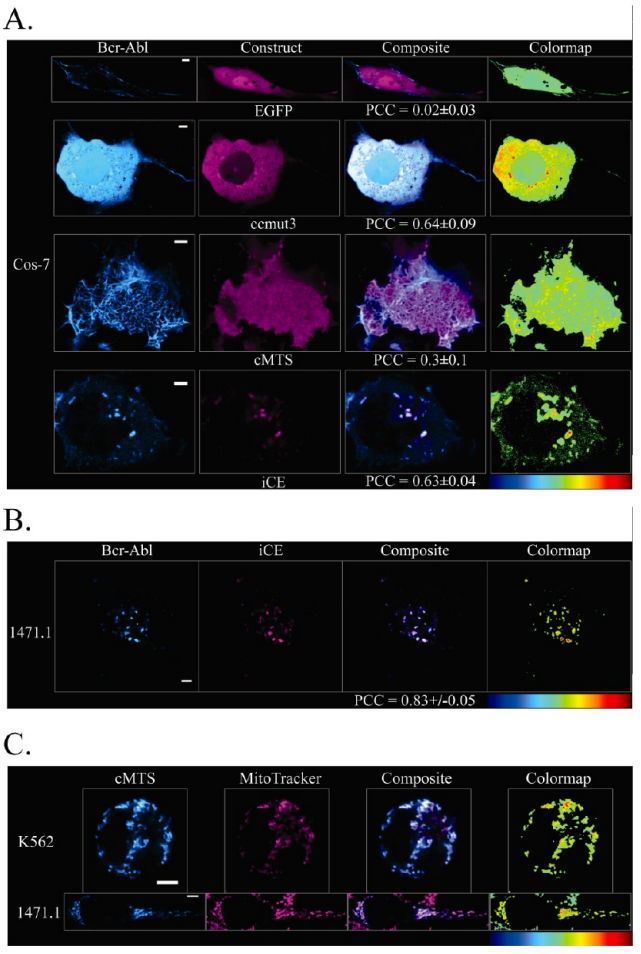

Figure 7. Representative images of exogenous Bcr-Abl coexpressed with the iCE or its individual components and cMTS mitochondrial localization. Scale bars are 5 μm. (A) Comparison of subcellular localization and association between Bcr-Abl (first column, cyan) and the iCE or iCE component parts (second column, magenta) in Cos-7 cells. The PCC values in the "Composite" column represent the degree of colocalization between Bcr-Abl and the given construct. (B) Coexpression of Bcr-Abl (first column, cyan) and the iCE (second column, magenta) in 1471.1 cells with PCC value below the "composite" image. (C) cMTS expression in K562 and 1471.1 cells (first column, cyan) with MitoTracker staining (second column, magenta).

"no treatment", iCE to EGFP and ccmut3 data points). However, the decline in cell viability with imatinib present (Figure 6A, "IM") was extremely significant for the iCE when compared to the other component constructs. The cell viability assessment was completed 48 h post-transfection but 24 h post-addition of imatinib (IM). Reducing the incubation time, for this assay, with imatinib to 24 instead of 48 h allowed better discernment of viable cells (e.g., Figure 5C, bottom row, third column, "Phase" for iCE + imatinib demonstrates the lack of cells with intact plasma membranes). The level of apoptosis as determined by TUNEL and annexin−APC staining (in contrast to 7-AAD staining which detects late-stage necrotic/apoptotic cells)[28] was extremely significant for the combined iCE + IM when compared to IM treated K562 cells (Figure 6B, iCE + IM vs IM; or Figure 6C, compare iCE + IM to ccmut3 + IM and cMTS + IM). Both assays were completed 48 h post-transfection and/or imatinib (10 μM) treatment and analyzed by flow cytometry.

The iCE Colocalizes with Bcr-Abl. Figure 7A shows the cellular localization of the EGFP-tagged iCE or its components (see Figure 3 for domain arrangement of constructs) coexpressed with exogenous Bcr-Abl (labeled with either blue or mCherry fluorescent proteins) in Cos-7 cells. The iCE, like the ccmut3 alone, colocalizes (defined as a Pearson correlation coefficient (PCC) greater than 0.6 as established by Bolte and Cordelières)[19] with Bcr-Abl (Cos-7, Figure 7A, fourth row, PCC = 0.63 ± 0.04; and 1471.1, Figure 7B, PCC = 0.83 ± 0.05). The colocalized iCE/Bcr-Abl exhibits a punctate pattern in both Cos-7 and 1471.1 cells which was different from the typical diffuse pattern of colocalized ccmut3/Bcr-Abl (Figure 7A, compare second row, first column (Bcr-Abl with ccmut3 present) to fourth row, first column (Bcr-Abl with iCE present)).

dx.doi.org/10.1021/mp3003539 | Mol. Pharmaceutics 2012, 9, 3318−3329

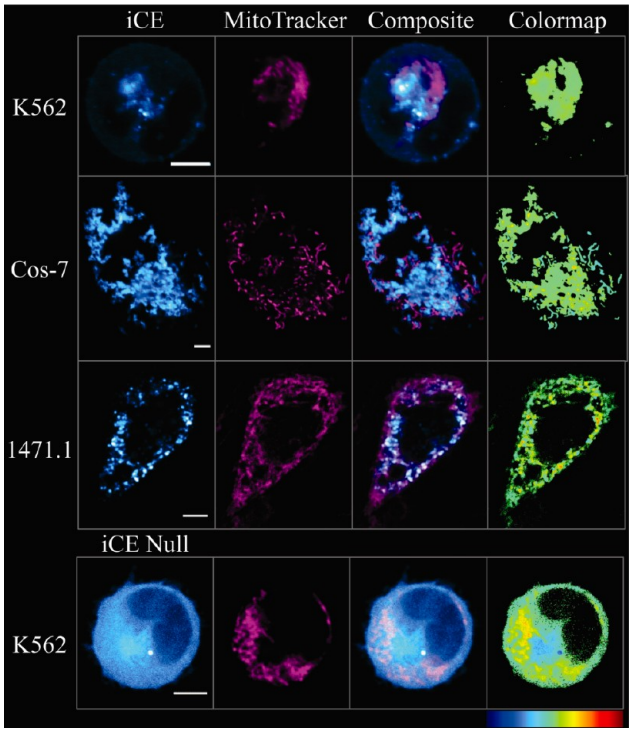

Figure 8. Representative images of the subcellular localization of the iCE (or iCE Null, see Figure 3) in K562, Cos-7, and 1471.1 cells and compared to MitoTracker. The iCE did not localize to the mitochondria of K562, Cos-7 or 1471.1 cells. Scale bars are 5 μm.

The cMTS and EGFP, as expected, do not colocalize with Bcr-Abl in Cos-7 cells (Cos-7: Figure 7A, third row, PCC = 0.3 ± 0.1, for cMTS and Bcr-Abl and Figure 7A, first row, PCC = 0.02 ± 0.03, for EGFP and Bcr-Abl). The cMTS alone localized to the mitochondria (Figure 7C, cMTS in K562 (top) and 1471.1 (bottom) compared to MitoTracker) in K562 and 1471.1 cells with higher oxidative backgrounds but not in the "low ROS" Cos-7 (Figure 7A, third row from top).[6]

The iCE Did Not Associate with the Mitochondria. Unlike the cMTS alone which colocalized with the mitochondria in both K562 and 1471.1 cells[6] (Figure 7C), the iCE remained cytoplasmic in its distribution across all three cell types (Figure 8, compare "iCE" column to "MitoTracker" column, first through third rows). In K562 cells the ccmut3 alone colocalized with Bcr-Abl and the cMTS alone colocalized with the mitochondria (Figure 7C, top), but the iCE did not localize to the mitochondria (Figure 8, first row).

The difference between the iCE and the iCE Null are the S189A and T193A mutations preventing phosphorylation at these sites in the cMTS domain of the iCE Null (Figure 3). Incorporating S189A and T193A mutations (i.e., iCE-Null, see Figure 3) led to a qualitative distribution difference between the iCE (punctate looking) and the diffuse iCE Null (Figure 8, compare "iCE" in the first row with "iCE Null" in the bottom row).

The Toxic Effect of the iCE on K562 Cells Is Lost upon Substitution of the cMTS or the ccmut3 with Another Canonical MTS or Bcr-Abl Binding Domain. When the ccmut3 is substituted for another Bcr-Abl binding domain (i.e., RIN-BD)[14] to create a mock iCE (Figure 3, RIN-cMTS), the cytotoxic effect remains equivalent to the cMTS alone, and the concomitant use of imatinib does not potentiate toxicity beyond that of imatinib alone (Figure 9A, RIN-cMTS and RIN-cMTS + IM columns). Furthermore, substituting the cMTS

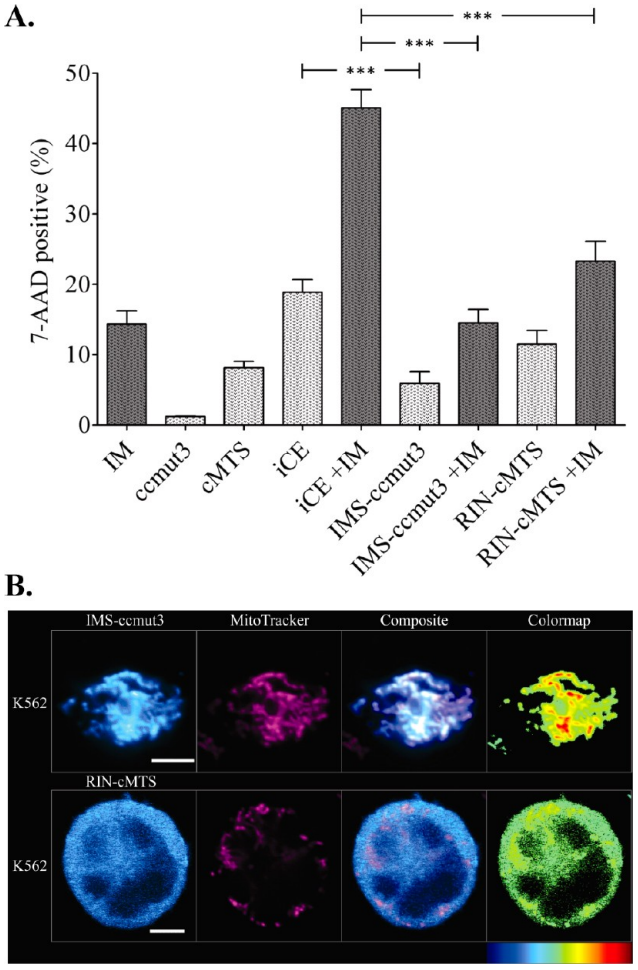

Figure 9. Domain substitution of either the ccmut3 or the cMTS in the iCE. (A) Flow cytometric analysis for 7-AAD was measured 48 h post-transfection and/or treatment. IM, iCE, iCE + IM, ccmut3, and cMTS values are also in Figure 4A. Imatinib is 10 μM. Statistical differences were determined using one-way ANOVA with Tukey's post hoc test (error bars are SEM, $N \geq 3$). (B) Representative images of the subcellular localization of the mock iCE constructs (first column), IMS-ccmut3 (top) and RIN-cMTS (bottom), in K562 cells stained with MitoTracker (second column). Scale bars are 5 μm.

with a canonical IMS MTS,[11] (Figure 3, IMS-ccmut3) diminished toxicity to that of the ccmut3 alone, or upon the addition of imatinib, no more toxicity than imatinib alone (Figure 9A, IMS-ccmut3 and IMS-ccmut3 + IM columns). The mock iCEs localize to different subcellular compartments (Figure 9B, compare top (IMS-ccmut3) and bottom (RIN-cMTS) rows). The IMS-ccmut3 localizes to the mitochondria (Figure 9B, top row, compare "IMS-ccmut3" to "MitoTracker" columns) while the RIN-cMTS remains cytoplasmic (Figure 9B, bottom row, compare "RIN-cMTS" to "MitoTracker" column). The cellular distribution of IMS-ccmut3 (mitochondrial) and RIN-cMTS (cytoplasmic) remained the same in the presence of 10 μM imatinib (data not shown).

The Toxic Effect of the iCE Is Dependent upon the Key Phospho Residues in the cMTS Domain. Incorporating S189A and T193A mutations (i.e., iCE-Null, see Figure 3) into the cMTS domain of the iCE leads to a significant reduction in cell death (i.e., 7-AAD) and apoptosis (e.g., annexin−APC) in K562 cells at 48 h (Figures 10A and C, compare iCE to iCE Null columns). However, this effect is

dx.doi.org/10.1021/mp3003539 | Mol. Pharmaceutics 2012, 9, 3318−3329

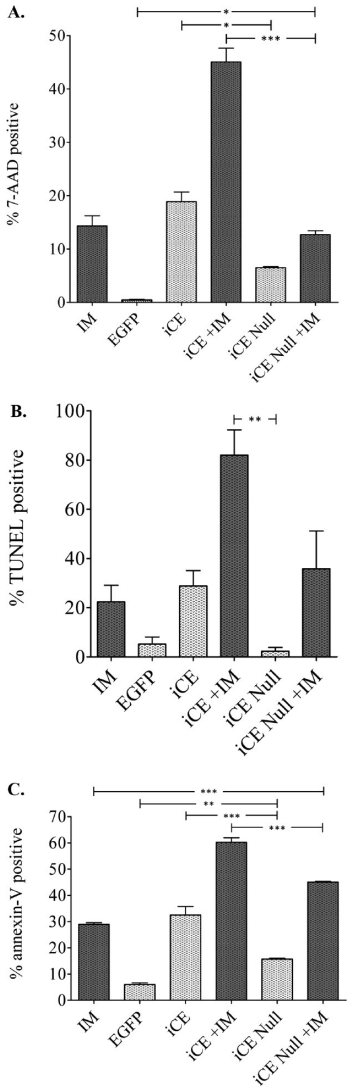

Figure 10. Effect of phospho-residue substitution in the iCE on cell death and apoptosis using flow cytometric analysis at 48 h in K562 cells. Imatinib is 10 μM (indicated by shaded columns). (A) 7-AAD staining. IM, EGFP, iCE, and iCE + IM, values are also in Figure 4A. (B) Apoptosis as measured by TUNEL staining. IM, EGFP, iCE, and iCE + IM, values are also in Figure 6B. (C) Annexin−APC staining. IM, EGFP, iCE, and iCE + IM, values are also in Figure 6C. Statistical difference was determined using one-way ANOVA with Tukey's post hoc test (for all assays here, error bars are SEM, $N \geq 3$).

more pronounced in combination with imatinib (Figures 10A and 10C, compare iCE + IM to iCE Null + IM columns). The trend is similar for TUNEL staining but did not reach statistical significance (Figure 10B).

DISCUSSION

The ubiquitously expressed tyrosine kinase c-Abl has a proapoptotic function at the mitochondria, and we have previously demonstrated that direct targeting of c-Abl to the mitochondria induces K562 leukemia cell death.[6] Based on this we have targeted the constitutively active and oncogenic form of c-Abl (i.e., Bcr-Abl) to the mitochondria. Bcr-Abl is the causative agent for the vast majority of CML cases, and was directed to the mitochondria as a proof of concept that mitochondrial Bcr-Abl could effectively be used to destroy diseased cells. Yet, the mitochondrial substrates(s) and submitochondrial localization of the proapoptotic c-Abl are not known.[5,6] Therefore, in order to investigate the potential antileukemic activity of a "surrogate death-directed c-Abl," in the form of mitochondrial Bcr-Abl, we targeted exogenous Bcr-Abl by fusion with different MTSs to three submitochondrial regions (Table 1). Similar to mitochondrial c-Abl, Bcr-Abl was toxic when targeted to the mitochondria of CML cells (Figure 1, third column). Unlike c-Abl,[29] Bcr-Abl's mitochondrial cytotoxic effect was independent of its kinase activity (Figure 1, fourth column). However, there are instances where the kinase activity of c-Abl is dispensable for the induction of apoptosis (e.g., via p38 MAPK).[30] Overall, the tyrosine kinase-independent killing of CML cells is compelling because it suggests that the strategy of targeting Bcr-Abl to the mitochondria would be compatible with and complementary to current tyrosine kinase inhibitor (TKI) therapy.

This led to an attempt to move endogenous Bcr-Abl by means of a designed chaperone protein (Figure 3, schematic of constructs) to exploit the toxicity of mitochondrial Bcr-Abl. The intracellular cryptic escort (iCE) was constructed for the purpose of binding and translocating endogenous Bcr-Abl to the mitochondria. Both the ccmut3 and cMTS domains which comprise the iCE have been previously characterized.[6,12]

The activation and mitochondrial targeting of the cMTS is limited to cell types with an elevated ROS phenotype.[6] K562 cells exhibit high basal levels of ROS, which is a common pathophysiological feature of malignancy.[31,32] The elevated oxidative stress level leads to an increase in active PKA and PKC which, in turn, phosphorylate (residues S189 (PKA) and/or T193 (PKC)) and thereby "activate" the cMTS to induce mitochondrial translocation in a Hsp70 dependent manner.[6,15] Moreover, the cMTS demonstrated robust and selective mitochondrial targeting when fused to c-Abl (i.e., Abl-cMTS) in K562 cells.[6]

The ccmut3 Bcr-Abl binding protein oligomerizes in an antiparallel orientation with the coiled-coil domain of Bcr-Abl.[12] Dixon et al. demonstrated that the ccmut3 efficiently bound to and translocated Bcr-Abl to the nucleus when fused to four strong nuclear localization signals (NLS).[13] However, cell death from nuclear entrapment or nuclear targeting of Bcr-Abl is less when compared to mitochondrially targeted Bcr-Abl. For instance, K562 cell death assessed by nuclear segmentation analysis 24 h post-transfection with 4NLS-Bcr-Abl or IMM-Bcr-Abl yielded a mean of 12%[3] versus 88%, respectively (data not shown).

Consistent with the cytotoxicity (7-AAD staining) elicited by the direct mitochondrial targeting of Bcr-Abl at 48 h (Figure 2B, third through fifth columns), the iCE also induced cell death (Figure 4A, iCE column) to a similar level within the same time frame. However, subcellular compartmental analysis of confocal images comparing between the mitochondria (stained with MitoTracker) and fluorescent protein tagged iCE and/or Bcr-Abl did not indicate any mitochondrial accumulation of the iCE or iCE/Bcr-Abl (Figure 9, compare iCE column to MitoTracker column, K562 cells). Therefore, the cytoplasmically localized iCE and the mitochondrially targeted Bcr-Abl (MTS-Bcr-Abl) are likely inducing cell death by different mechanisms.

Our experience with NLS (e.g., one NLS was insufficient to move Bcr-Abl but four NLS were sufficient)[3] suggested that perhaps the "strength" of the cMTS (within the iCE) was not sufficient to overcome the cytoplasmic interactions of Bcr-Abl for efficient translocation to the mitochondria. Anticipating that this could happen, we employed imatinib to better facilitate iCE-to-mitochondrial targeting for two reasons. First, imatinib

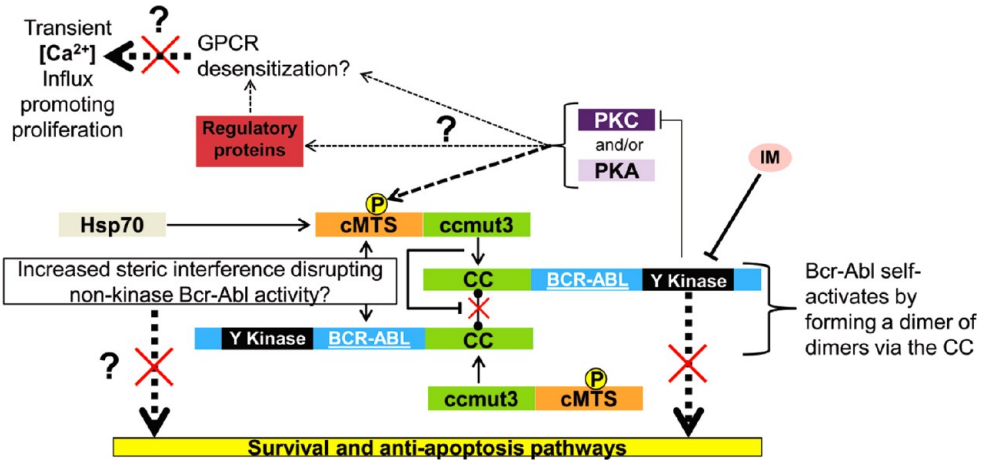

Figure 11. Possible mechanisms for iCE induced toxicity to K562 leukemia cells. With imatinib (IM) present, Bcr-Abl kinase activity is eliminated[1] and the iCE may be potentiating leukemic cell death by altering calcium status and/or blocking kinase-independent oncogenic functions of Bcr-Abl. Bcr-Abl tyrosine kinase (Y kinase) activity stimulates transient calcium influx (which stimulates proliferation) while PKC activation, at the plasma membrane, can have the opposite effect on calcium transients, which has been shown to be toxic to leukemia cells.[36−38] Another cause of iCE enhanced cell death may be through a more complete blockade of Bcr-Abl signaling by steric restriction of kinase-independent pathways.[34,39] Steric effects may be caused by the presence of PKA and/or PKC, a conformational change in the cMTS domain, and/or binding of Hsp70 to the phosphorylated cMTS.[15] iCE toxicity requires interaction with Bcr-Abl via the CC domain and the wild-type cMTS (S/T phospho residues). The ccmut3 competes with Bcr-Abl for oligomerization at the N-terminal portion of the Bcr to Abl fusion at the CC,[12] blocking Bcr-Abl transautophosphorylation.[17].

treatment increases the level of ROS/PKC activity, which in turn stimulates increased mitochondrial localization of the cMTS.[6] Second, imatinib bound Bcr-Abl undergoes a conformational change that decreases its association with actin, freeing Bcr-Abl for relocalization.[33] Yet, even with the addition of 10 μM imatinib the iCE did not localize to the mitochondria in K562 cells.

Moreover, in light of the subcellular distribution of the iCE in Bcr-Abl negative cell types, the iCE was likely not hindered from translocating to the mitochondria due to its interaction with Bcr-Abl. Within the context of the Cos-7 cells (which have low inherent ROS and therefore low mitochondrial accumulation of the cMTS),[6] the iCE was expected to remain cytoplasmic. However, in the Bcr-Abl negative and high ROS 1471.1 cell line the cMTS alone strongly localizes to the mitochondria.[6] Accordingly, without Bcr-Abl to "keep" the iCE cytoplasmic the iCE should localize to the mitochondria in this cell line. This was not the case however, and the iCE did not localize to the mitochondria of 1471.1 cells (Figure 8, third row). This result revealed that the ccmut3 fusion to the cMTS may compromise the capacity for iCE mitochondrial translocation.

Nonetheless, the antileukemic activity caused by the iCE appears to be entirely dependent upon the combination of the ccmut3 and cMTS. Mock "iCE's" substituting either the ccmut3 with RIN-BD (RIN-cMTS; RIN-BD binds SH3/SH2 domains of Bcr-Abl)[14] or the cMTS with the canonical IMS MTS (IMS-ccmut3; IMS targets the intermitochondrial membrane space)[11] failed to restore cell death beyond control levels (Figure 9A). The RIN-cMTS and IMS-ccmut3 results suggest that the toxicity of the iCE is not propagated by either ccmut3 localization to the mitochondria (Figure 9B, top row) or the cMTS remaining bound to Bcr-Abl (at least to the SH2/SH3 domains via RIN-BD, which would put the cMTS domain of the iCE on Bcr-Abl but at a different location) in the cytoplasm (Figure 9B, bottom row). The cytotoxic effect of the iCE is also dependent upon phosphorylation of the cMTS. Mutating the cMTS domain key phospho residues S189A and T193A (iCE Null; Figure 3), which are required for mitochondrial translocation of the cMTS alone,[6] ablates the killing activity of the iCE.

The ccmut3 alone and imatinib, as expected,[12] both reduced the level of phospho-Bcr-Abl and Bcr-Abl substrate phosphorylation (i.e., p-Stat5 and p-Crk-L), but the iCE and iCE Null were unchanged from control in K562 cells (Western blot; data not shown). Therefore, the iCE is not acting as a dominant-negative for Bcr-Abl kinase activity. Yet since the iCE colocalizes with Bcr-Abl, it may be disrupting non-kinase Bcr-Abl survival/antiapoptotic function. For instance, the iCE may hinder (e.g., steric interference) kinase-independent signaling from Bcr-Abl such as Src kinase Hck phosphorylation of the Grb2 binding site on Bcr-Abl or Bcr's RhoGEF activity.[34,35]

Alternatively, it may be possible that the ccmut3 (binding in an antiparallel coiled-coil)[17] positions the cMTS where the phosphorylation of the S189 and/or T193 is central to the mechanism for cell death induction. In K562 cells only phosphorylation of the T193 is critical for mitochondrial translocation function of the cMTS whereas S189 is not.[6] Perhaps the cytotoxic nature of the iCE is also primarily a function of PKC phosphorylation. Although beyond the scope of this paper, a negative feedback coupling of PKC and Bcr-Abl involving transient calcium influx may play a role in the essential nature of cMTS phospho residues, and T193 in particular. Increased transient calcium influx can stimulate cellular proliferation while, conversely, blocking calcium influx via PKC activation is toxic to Ph^+ leukemia cells.[36] Inhibition of Bcr-Abl activity with imatinib relieves negative regulation of PKC and thereby diminishes intracellular calcium flux.[36] Perhaps increased stimulation or altered localization of PKC (due to the presence of the iCE) could further diminish transient calcium influx. A fascinating possibility that connects calcium homeostasis and iCE toxicity is depicted in Figure 11.

In this report, we demonstrate that direct targeting of Bcr-Abl to the mitochondria elicits cell death induction in a cell

dx.doi.org/10.1021/mp3003539 | Mol. Pharmaceutics 2012, 9, 3318−3329

type specific and kinase-independent manner. Additionally, we attempted to harness Bcr-Abl's mitochondrial death induction activity with the use of a designed protein chaperone (i.e., iCE) in order to restore the defunct apoptotic avenue of "mitochondrial death-directed c-Abl" in CML cells. Though the iCE bound to Bcr-Abl, the iCE/Bcr-Abl complex did not translocate to the mitochondria. However, the iCE combined with imatinib treatment was potently antileukemic as measured by 7-AAD (late apoptosis/necrosis), TUNEL (apoptosis/necrosis), annexin-V (apoptosis), and trypan blue exclusion assay (cell viability).

■ ASSOCIATED CONTENT

Supporting Information

Figures depicting Bcr-Abl targeted to the mitochondria of K562, Cos-7, and 1471.1 cells and residue sequences for the construct domains. This material is available free of charge via the Internet at http://pubs.acs.org.

■ AUTHOR INFORMATION

Corresponding Author

*Dept. of Pharmaceutics and Pharmaceutical Chemistry, College of Pharmacy, University of Utah, 421 Wakara Way, Rm. 318, Salt Lake City, UT 84108. Phone: 801-581-7120. Fax: 801-585-3614. E-mail: Carol.Lim@pharm.utah.edu.

Notes

The authors declare no competing financial interest.

■ ACKNOWLEDGMENTS

We acknowledge the use of the University of Utah, School of Medicine, Cell Imaging Facility and would like to thank the Director, Chris Rodesch, PhD, for scientific discussions. We would also like to thank Dr. Andy Dixon, J. Rian Davis, Ben Bruno, and Geoff Miller for scientific discussions. The Core Facilities described in this project were supported by Award Number P30CA042014 from the National Cancer Institute. The content is solely the responsibility of the authors and does not necessarily represent the official views of the National Cancer Institute or the National Institutes of Health. This work was funded by NIH R01-CA129528 and by an AFPE Pre-Doctoral Fellowship (J.E.C.). This work was supported in part by a grant to University of Utah from the Howard Hughes Medical Institute through the Med into Grad Initiative (D.W.W.).

■ REFERENCES

(1) Hantschel, O.; Wiesner, S.; Guttler, T.; Mackereth, C. D.; Rix, L. L.; Mikes, Z.; Dehne, J.; Gorlich, D.; Sattler, M.; Superti-Furga, G. Structural basis for the cytoskeletal association of Bcr-Abl/c-Abl. *Mol. Cell* **2005**, *19* (4), 461−73.

(2) Vigneri, P.; Wang, J. Y. Induction of apoptosis in chronic myelogenous leukemia cells through nuclear entrapment of BCR-ABL tyrosine kinase. *Nat. Med.* **2001**, *7* (2), 228−34.

(3) Dixon, A. S.; Kakar, M.; Schneider, K. M.; Constance, J. E.; Paullin, B. C.; Lim, C. S. Controlling subcellular localization to alter function: Sending oncogenic Bcr-Abl to the nucleus causes apoptosis. *J. Controlled Release* **2009**, *140* (3), 245−9.

(4) Qi, X.; Mochly-Rosen, D. The PKCdelta -Abl complex communicates ER stress to the mitochondria - an essential step in subsequent apoptosis. *J. Cell Sci.* **2008**, *121* (Part 6), 804−13.

(5) Kumar, S.; Bharti, A.; Mishra, N. C.; Raina, D.; Kharbanda, S.; Saxena, S.; Kufe, D. Targeting of the c-Abl tyrosine kinase to mitochondria in the necrotic cell death response to oxidative stress. *J. Biol. Chem.* **2001**, *276* (20), 17281−5.

(6) Constance, J. E.; Despres, S. D.; Nishida, A.; Lim, C. S. Selective Targeting of c-Abl via a Cryptic Mitochondrial Targeting Signal Activated by Cellular Redox Status in Leukemic and Breast Cancer Cells. *Pharm. Res.* **2012**, *29* (8), 2317−28.

(7) Gupta, M.; Milani, L.; Hermansson, M.; Simonsson, B.; Markevarn, B.; Syvanen, A. C.; Barbany, G. Expression of BCR-ABL1 oncogene relative to ABL1 gene changes overtime in chronic myeloid leukemia. *Biochem. Biophys. Res. Commun.* **2008**, *366* (3), 848−51.

(8) Mancini, M.; Veljkovic, N.; Corradi, V.; Zuffa, E.; Corrado, P.; Pagnotta, E.; Martinelli, G.; Barbieri, E.; Santucci, M. A. 14−3-3 ligand prevents nuclear import of c-ABL protein in chronic myeloid leukemia. *Traffic* **2009**, *10* (6), 637−47.

(9) Isaya, G.; Fenton, W. A.; Hendrick, J. P.; Furtak, K.; Kalousek, F.; Rosenberg, L. E. Mitochondrial import and processing of mutant human ornithine transcarbamylase precursors in cultured cells. *Mol. Cell. Biol.* **1988**, *8* (12), 5150−8.

(10) Rizzuto, R.; Simpson, A. W.; Brini, M.; Pozzan, T. Rapid changes of mitochondrial Ca2+ revealed by specifically targeted recombinant aequorin. *Nature* **1992**, *358* (6384), 325−7.

(11) Ozawa, T.; Natori, Y.; Sako, Y.; Kuroiwa, H.; Kuroiwa, T.; Umezawa, Y. A minimal peptide sequence that targets fluorescent and functional proteins into the mitochondrial intermembrane space. *ACS Chem. Biol.* **2007**, *2* (3), 176−86.

(12) Dixon, A. S.; Miller, G. D.; Bruno, B. J.; Constance, J. E.; Woessner, D. W.; Fidler, T. P.; Robertson, J. C.; Cheatham, T. E.; Lim, C. S. Improved coiled-coil design enhances interaction with Bcr-Abl and induces apoptosis. *Mol. Pharmaceutics* **2012**, *9* (1), 187−95.

(13) Dixon, A. S.; Constance, J. E.; Tanaka, T.; Rabbitts, T. H.; Lim, C. S. Changing the Subcellular Location of the Oncoprotein Bcr-Abl Using Rationally Designed Capture Motifs. *Pharm. Res.* **2011**, *29* (4), 1098−109.

(14) Afar, D. E.; Han, L.; McLaughlin, J.; Wong, S.; Dhaka, A.; Parmar, K.; Rosenberg, N.; Witte, O. N.; Colicelli, J. Regulation of the oncogenic activity of BCR-ABL by a tightly bound substrate protein RIN1. *Immunity* **1997**, *6* (6), 773−82.

(15) Robin, M. A.; Prabu, S. K.; Raza, H.; Anandatheerthavarada, H. K.; Avadhani, N. G. Phosphorylation enhances mitochondrial targeting of GSTA4−4 through increased affinity for binding to cytoplasmic Hsp70. *J. Biol. Chem.* **2003**, *278* (21), 18960−70.

(16) Strober, W. Trypan blue exclusion test of cell viability. *Curr. Protoc. Immunol.* **2001**, *Appendix 3*, Appendix 3B.

(17) Dixon, A. S.; Pendley, S. S.; Bruno, B. J.; Woessner, D. W.; Shimpi, A. A.; Cheatham, T. E., 3rd; Lim, C. S. Disruption of Bcr-Abl coiled coil oligomerization by design. *J. Biol. Chem.* **2011**, *286* (31), 27751−60.

(18) Rasband, W. S. *Available at* www.uhnres.utoronto.ca/facilities/wcif/imagej/image_intensity_proce.htm#intensity_BG, 2004.

(19) Bolte, S.; Cordelieres, F. P. A guided tour into subcellular colocalization analysis in light microscopy. *J. Microsc.* **2006**, *224* (Part 3), 213−32.

(20) Costes, S. V.; Daelemans, D.; Cho, E. H.; Dobbin, Z.; Pavlakis, G.; Lockett, S. Automatic and quantitative measurement of protein-protein colocalization in live cells. *Biophys. J.* **2004**, *86* (6), 3993−4003.

(21) Barlow, A. L.; Macleod, A.; Noppen, S.; Sanderson, J.; Guerin, C. J. Colocalization analysis in fluorescence micrographs: verification of a more accurate calculation of pearson's correlation coefficient. *Microsc. Microanal.* **2010**, *16* (6), 710−24.

(22) Jaskolski, F.; Mulle, C.; Manzoni, O. J. An automated method to quantify and visualize colocalized fluorescent signals. *J. Neurosci. Methods* **2005**, *146* (1), 42−9.

(23) Lecoeur, H.; de Oliveira-Pinto, L. M.; Gougeon, M. L. Multiparametric flow cytometric analysis of biochemical and functional events associated with apoptosis and oncosis using the 7-amino-actinomycin D assay. *J. Immunol. Methods* **2002**, *265* (1−2), 81−96.

(24) Mossalam, M.; Matissek, K. J.; Okal, A.; Constance, J. E.; Lim, C. S. Direct Induction of Apoptosis Using an Optimal Mitochondrially Targeted p53. *Mol. Pharmaceutics* **2012**, *9* (5), 1449−58.

(25) Kyrylkova, K.; Kyryachenko, S.; Leid, M.; Kioussi, C. Detection of Apoptosis by TUNEL Assay. *Methods Mol. Biol.* **2012**, *887*, 41−7.
(26) van Engeland, M.; Nieland, L. J.; Ramaekers, F. C.; Schutte, B.; Reutelingsperger, C. P. Annexin V-affinity assay: a review on an apoptosis detection system based on phosphatidylserine exposure. *Cytometry* **1998**, *31* (1), 1−9.
(27) Zhang, X.; Ren, R. Bcr-Abl efficiently induces a myeloproliferative disease and production of excess interleukin-3 and granulocyte-macrophage colony-stimulating factor in mice: a novel model for chronic myelogenous leukemia. *Blood* **1998**, *92* (10), 3829−40.
(28) Kroemer, G.; Galluzzi, L.; Vandenabeele, P.; Abrams, J.; Alnemri, E. S.; Baehrecke, E. H.; Blagosklonny, M. V.; El-Deiry, W. S.; Golstein, P.; Green, D. R.; Hengartner, M.; Knight, R. A.; Kumar, S.; Lipton, S. A.; Malorni, W.; Nunez, G.; Peter, M. E.; Tschopp, J.; Yuan, J.; Piacentini, M.; Zhivotovsky, B.; Melino, G. Classification of cell death: recommendations of the Nomenclature Committee on Cell Death 2009. *Cell Death Differ.* **2009**, *16* (1), 3−11.
(29) Kumar, S.; Mishra, N.; Raina, D.; Saxena, S.; Kufe, D. Abrogation of the cell death response to oxidative stress by the c-Abl tyrosine kinase inhibitor STI571. *Mol. Pharmacol.* **2003**, *63* (2), 276−82.
(30) Galan-Moya, E. M.; Hernandez-Losa, J.; Aceves Luquero, C. I.; de la Cruz-Morcillo, M. A.; Ramirez-Castillejo, C.; Callejas-Valera, J. L.; Arriaga, A.; Aranburo, A. F.; Ramon y Cajal, S.; Silvio Gutkind, J.; Sanchez-Prieto, R. c-Abl activates p38 MAPK independently of its tyrosine kinase activity: Implications in cisplatin-based therapy. *Int. J. Cancer* **2008**, *122* (2), 289−97.
(31) Ralph, S. J.; Rodriguez-Enriquez, S.; Neuzil, J.; Saavedra, E.; Moreno-Sanchez, R. The causes of cancer revisited: "mitochondrial malignancy" and ROS-induced oncogenic transformation - why mitochondria are targets for cancer therapy. *Mol. Aspects Med.* **2010**, *31* (2), 145−70.
(32) Sattler, M.; Verma, S.; Shrikhande, G.; Byrne, C. H.; Pride, Y. B.; Winkler, T.; Greenfield, E. A.; Salgia, R.; Griffin, J. D. The BCR/ABL tyrosine kinase induces production of reactive oxygen species in hematopoietic cells. *J. Biol. Chem.* **2000**, *275* (32), 24273−8.
(33) Preyer, M.; Vigneri, P.; Wang, J. Y. Interplay between kinase domain autophosphorylation and F-actin binding domain in regulating imatinib sensitivity and nuclear import of BCR-ABL. *PLoS One* **2011**, *6* (2), e17020.
(34) Warmuth, M.; Bergmann, M.; Priess, A.; Hauslmann, K.; Emmerich, B.; Hallek, M. The Src family kinase Hck interacts with Bcr-Abl by a kinase-independent mechanism and phosphorylates the Grb2-binding site of Bcr. *J. Biol. Chem.* **1997**, *272* (52), 33260−70.
(35) Vigil, D.; Cherfils, J.; Rossman, K. L.; Der, C. J. Ras superfamily GEFs and GAPs: validated and tractable targets for cancer therapy? *Nat. Rev. Cancer* **2010**, *10* (12), 842−57.
(36) Vichalkovski, A.; Kotevic, I.; Gebhardt, N.; Kaderli, R.; Porzig, H. Tyrosine kinase modulation of protein kinase C activity regulates G protein-linked Ca2+ signaling in leukemic hematopoietic cells. *Cell Calcium* **2006**, *39* (6), 517−28.
(37) Pellicano, F.; Copland, M.; Jorgensen, H. G.; Mountford, J.; Leber, B.; Holyoake, T. L. BMS-214662 induces mitochondrial apoptosis in chronic myeloid leukemia (CML) stem/progenitor cells, including CD34 + 38- cells, through activation of protein kinase Cbeta. *Blood* **2009**, *114* (19), 4186−96.
(38) Robert, G.; Ben Sahra, I.; Puissant, A.; Colosetti, P.; Belhacene, N.; Gounon, P.; Hofman, P.; Bost, F.; Cassuto, J. P.; Auberger, P. Acadesine kills chronic myelogenous leukemia (CML) cells through PKC-dependent induction of autophagic cell death. *PLoS One* **2009**, *4* (11), e7889.
(39) Wertheim, J. A.; Forsythe, K.; Druker, B. J.; Hammer, D.; Boettiger, D.; Pear, W. S. BCR-ABL-induced adhesion defects are tyrosine kinase-independent. *Blood* **2002**, *99* (11), 4122−30.

Enhanced and Selective Killing of Chronic Myelogenous Leukemia Cells with and Engineered BCR-ABL Binding Protein and Imatinib

Jonathan E. Constance, David W. Woessner, Karina J. Matissek, Mohanad Mossalam, Carol S. Lim

Molecular Pharmaceutics, September 10, 2012

Co-first author contribution:

Research design: 10%

Experimental work: 15%

Data analysis and evaluation: 15%

Manuscript writing: 5%

Title: Enhanced and Selective Killing of Chronic Myelogenous Leukemia Cells with an Engineered BCR-ABL Binding Protein and Imatinib

Author: Jonathan E. Constance, David W. Woessner, Karina J. Matissek, Mohanad Mossalam, and Carol S. Lim

Publication: Molecular Pharmaceutics

Publisher: American Chemical Society

Date: Nov 1, 2012

PERMISSION/LICENSE IS GRANTED FOR YOUR ORDER AT NO CHARGE

This type of permission/license, instead of the standard Terms & Conditions, is sent to you because no fee is being charged for your order. Please note the following:

- Permission is granted for your request in both print and electronic formats, and translations.
- If figures and/or tables were requested, they may be adapted or used in part.
- Please print this page for your records and send a copy of it to your publisher/graduate school.
- Appropriate credit for the requested material should be given as follows: "Reprinted (adapted) with permission from (COMPLETE REFERENCE CITATION). Copyright (YEAR) American Chemical Society." Insert appropriate information in place of the capitalized words.
- One-time permission is granted only for the use specified in your request. No additional uses are granted (such as derivative works or other editions). For any other uses, please submit a new request.